DISS. ETH NO. 22701

Studies on the catalysis derived from dinuclear palladium species of oxidation state (I)

A thesis submitted to attain the degree of

DOCTOR OF SCIENCES of ETH ZURICH

(Dr. sc. ETH Zurich)

presented by

Marialuisa Aufiero

Dottore in Chimica, Università "La Sapienza" in Rome

born on *05.05.1986*
Citizen of Italy

accepted on the recommendation of
Prof. Dr. Jeffrey W. Bode, examiner
Prof. Dr. Franziska Schoenebeck, co-examiner

Zürich 2015

Dedicated to my family and to all the people

who shared this wonderful experience with me

Acknowledgements

Selected publications derived from this Thesis:

1.   "Reactivity and Stability of Dinuclear Pd(I) Complexes: Studies on the Active Catalytic Species, Insights into Precatalyst Activation and Deactivation, and Application in Highly Selective Cross-Coupling Reactions" - F. Proutiere, M. Aufiero, F. Schoenebeck, *J. Am. Chem. Soc.* **2012**, *134*, 606−612.

2.   "Redox Reactions in Palladium Catalysis: On the Accelerating and/or Inhibiting Effects of Copper and Silver Salt Additives in Cross-Coupling Chemistry Involving Electron-rich Phosphine Ligands" - M. Aufiero, F. Proutiere, F. Schoenebeck, *Angew. Chem.* **2012**, *124*, 7338−7342; *Angew. Chem. Int. Ed.* **2012**, *51*, 7226−7230. (Selected as **very important paper (VIP)** & **highlighted** in *Chimia* and *Angew. Chemie*)

3.   "Combining the Reactivity Properties of PCy_3 and $PtBu_3$ into a Single Ligand: $P(iPr)(tBu)_2$. Reaction via Mono- or Bisphosphine Pd(0) centers and Pd(I) Dimer Formation", F. Proutiere, E. Lyngvi, M. Aufiero, I. A. Sanhueza, F. Schoenebeck, *Organometallics* **2014**, *33*, 6879.

4.   "Highly Efficient $C-SeCF_3$ Coupling of Aryl Iodides Enabled by an Air-Stable Dinuclear Pd(I) Catalyst", M. Aufiero, T. Sperger, A. S. Tsang, F. Schoenebeck, *Angew. Chem. Int. Ed.* DOI: 10.1002/anie.201503388

Selected poster presentations

1.   Marialuisa Aufiero, Franziska Schoenebeck:
Insight on the Influence of Copper Additives in Pd(0) Catalysis
14th Belgian Organic Synthesis Symposium, Boss XIV,
Louvain-la-Neuve, Belgium, July 13-18, 2014

2.   Marialuisa Aufiero, Franziska Schoenebeck:
Insight on the Influence of Copper Additives in Pd(0) Catalysis
5th Münster Symposium On Cooperative Effects In Chemistry
Westfälische Wilhelms-Universität Münster, Münster Germany, May 9-2014

3.   Marialuisa Aufiero, Franziska Schoenebeck :
Effect of Copper Salts on Palladium Catalysis.
7th Dorothy Crowfoot Hodgkin Symposium,
Uni Irchel, Zürich, October 8-2012

Selected oral presentations

1.   M. Aufiero, F. Schoenebeck:
On the role of Copper Additives in Palladium Catalysis".
Aachen-Groeningen Organic Chemistry Symposium (Agocs 2013)
RWTH Aachen, June 13-2012

Table of Contents

Abbreviations

°C	degree(s) Celsius	dppp	1,3-(diphenyl-phosphino)propane
δ	chemical shift in ppm (delta)	e.g	exempli gratia
ΔG	Gibbs free energy	EHMO	Extended Hückel Molecular Orbital
ν	wavenumbers (nu)	equiv	equivalents
π	p-orbitals (pi)	Et_2O	diethylether
Å	Angstrom(s)	FBIP	bis-imidazoline bis-palladacycles
Ac	acetyl		
Ad	adamantly	Fc	ferrocene
AIM	atoms in molucules	g	grams
Ar	generic aromatic group	GC-MS	gas chromato-graphy-mass spectroscopy
atm	atmosphere		
BDE	bond dissociation energy	h	hour(s)
Bn	benzyl group	hfac	Hexafluoroacetylacetone
br	broad	HOMO	highest occupied molecular orbital
Calcd.	calculated for		
CAS+DDCI	complete active space + difference dedicated configuration interaction	HppH	1,5,7-Triaza-bicyclo[4.4.0]dec-5-ene
		HRMS	high resolution mass spectroscopy
CASSCF	complete active space self-consistent filed	Hz	Hertz
		i.e	id est
c.f	confer	i.s	internal standard
CH_2Cl_2	dichloromethane	*i*Pr	iso-propyl
cod	1,5, cyclooctadiene	*J*	coupling constant in Hertz
COSY	Correlation SpectroscopY	L	litre(s)
CPCM	conductor polarized continuum model	LHMDS	lithium bis(trimethyl-silyl)amide
Cy	cyclohexyl	LiNCy2	lithium bis(tricycle-hexyl)amide
d	doublet		
dba	dibenzylideneacetone	LUMO	lowest unoccupied molecular orbital
dcpe	1,2-(diciclohexeyl phosphino)ethane		
		M	mega, molar
dd	doublet of doublets	m	metre, mille, multiplet
Dfmpe	1,2-(ditrifluoromethyl phosphino)ethane	m.p	melting point
		m/*z*	mass-to-charge ratio
DFT	density functional theory	Me	methyl
dma	bis(diphenyl-arsino)methane	meo-mop	2-(diphenylphosphino)-2′-methoxy-1,1′-binaphthyl
DMF	*N,N*-dimethylforamide		
DMSO	dimethylsulphoxide	min	minute(s)
dmpm	1,1-(dimethyl-phosphino)methane	MMLCT	metal-metal to ligand charge transfer
		mol	mole(s)
DOSY	Diffusion Ordered SpectroscopY	NMR	nuclear magnetic resonance
dotpm	1,1-(di-*o*-tolyl-phosphino)methane	NOESY	Nuclear Overhauser Effect Spectroscopy
		OTf	trifluoromethanesulfonate
dppa	1,2-bis(diphenyl-phosphino)amine	Ph	phenyl
dppe	1,2-(diphenyl-phosphino)ethane	ppm	parts per million
		py	pyridine
dppm	1,1-(diphenyl-phosphino)methane	pz	pyrazol-1-y

q	quartet	TDDFT	time-dependent density functional theory
Qphos	1,2,3,4,5-Pentaphenyl-1′-(di-*tert*-butylphosphino)ferrocene	THF	tetrahydrofuran
		TLC	thin layer chromatography
r.t	room temperature	TMEDA	tetramethylethylene-diamine
R	unspecified alkyl group		
s	singlet	TMS	trimethylsilyl, tetramethylsilane
t	triplet		
*t*Bu	*tert*-butyl		

Summary

The use of bulky-ligands in combination with Pd(0) and Pd(II) sources in cross-coupling reaction has become a common strategy for the coupling of challenging substrates, such as non-activated aryl chlorides. The success of these ligands is presumed to be due to their ability to generate a monoligated 12-electron Pd(0)L species that undergoes facile oxidative addition. In the last decades, particular attention has be directed towards the synthesis of new Pd-based catalysts that could easily facilitate the release of this very active species (Pd(0)L), among these catalysts Pd(I)-Pd(I) dimers had caught the attention of many research groups. Some of these Pd(I) dimers were shown to be particularly good precatalyst in the cross-coupling reactions with aryl halides but the mechanism that leads to their activation is not well understood.

Part of this thesis was devoted to the understanding of additives effect onto Pd(0) chemistry. We discovered that exposure of a series of Pd(0) commonly used in cross-coupling reactions to $CuBr_n$ (n=1, 2) and CuI led to the complete or partial comsumption of the Pd(0) precursor and the formation of new species. A combined spectroscopical and crystallographic study allowed us to gain insight into the possible products formed, and oxidation of higher oxidation states of Pd, such as I and II, was observed for almost all of all the Pd(0) complexes tested. Particular focus was directed into the reaction of $Pd(0)(PtBu_3)_2$ with $CuBr_n$ (n=1, 2) and CuI additives: two different Pd(I)-Pd(I) dimers were obtained with bromides and iodides bridges respectively.
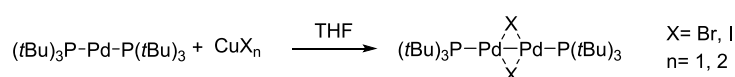
Scheme A: Formation of Pd(I) dimer from reaction of $Pd(PtBu_3)_2$ and copper additives.

This discovery led us to investigate the possible effects of dimer formation in Sonogashira and Suzuki cross-coupling reactions. The *in situ* formation of these two dimers dramatically influenced the rate of $Pd(0)(PtBu_3)_2$. A parasite oligomerisation reaction of the alkyne did not allow the normal Sonogashira coupling with aryl chlorides to occur. In the case of Suzuki coupling an increase in the yields was observed in the presence of $CuBr_n$ salts, whilst inhibition was observed in the presence of CuI salt, due to the higher stability of the Pd(I) dimer formed.
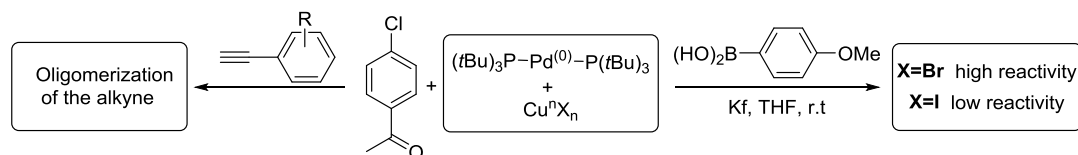
*Scheme **B***: Effect of copper additives onto Pd(0)(PtBu$_3$)$_2$ in: Sonogashira reactions (left); in Suzuki reactions (right)

The effect of other metal additives onto Pd(0)(PtBu$_3$)$_2$ was subsequently investigated. Pd(I) dimer formation was observed also in the presence of AgBr, AgI, FeBr$_3$ and AuBr$_3$, additives that are commonly use in combination with Pd(0) sources and were shown to increase the rate of reactions.

Part of this thesis work was then devoted to the understanding of the possible mechanism of activation of [Pd(μ-X)PtBu$_3$]$_2$ (X= Br, I) dimers. A detailed mechanistic study was performed to investigate the possible reasons for the high activity shown by the [Pd(μ-Br)PtBu$_3$]$_2$. The catalysis shown by this system was consistent with a Pd(PtBu$_3$) as active catalytic species. Further investigation allowed us to identify a nucleophilic-assisted disproportionation as a likely mechanism for the activation of [Pd(μ-Br)PtBu$_3$]$_2$. The effect of different nucleophiles onto [Pd(μ-Br)PtBu$_3$]$_2$ was tested and a minimum value of nucleophilic power was set: 10.5, under this value no activation was observed. The same study was extended to [Pd(μ-I)PtBu$_3$]$_2$. We found out that stronger nucleophiles are required for its activation (N= 16.1, according to the Mayr's scale), consistent with the higher stability shown by this dimer. For the first time we were able to activate and use this precatalyst in Suzuki cross-coupling reactions under both aerobic and anaerobic conditions.
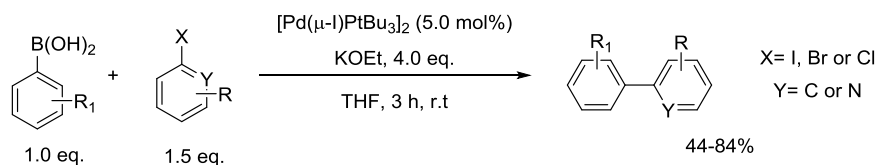
*Scheme **C***: Suzuki cross-coupling reactions catalysed by [Pd(μ-I)PtBu$_3$]$_2$ under both aerobic and anaerobic conditions.

Lastly, part of this thesis was devoted at developing direct catalysis at these dinuclear Pd(I) sites. We succeeded in the development of the first Pd(I)-catalysed C-Se bond formation. Extensive substrate scope was investigated and the reaction was shown to be tolerant to a

wide range of functional groups, including unprotected amines and anilines. Good yields were achieved under really mild conditions.
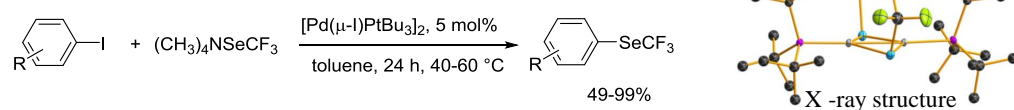
*Scheme **D***: Trifluoromethylselenolation catalysed by the *in situ* formed $[Pd(\mu\text{-}SeCF_3)PtBu_3]_2$. X-ray structure of the Pd(I) dimer $[Pd(\mu\text{-}SeCF_3)PtBu_3]_2$.

A combination of spectroscopic and computational studies allowed us to gain more insight into the possible mechanism of the transformation that does not exclude a direct dimer catalysis as a possible pathway.

Riassunto

L'uso di ligandi con elevato ingombro sterico in combinazione con fonti di Pd(0) e Pd(II) in reazioni di cross-coupling è diventata una comune strategia per l'accoppiamento di cloruri arilici non attivati, generalmente considerati substrati difficili da accoppiare. Il successo legato all'uso di questi ligandi si pensa essere dovuto alla loro presunta abilità di generare un complesso Pd(0)L monoligato avente 12 elettroni. La formazione di questo complesso monoligato favorisce l'ossidazione riduttiva. Negli ultimi decenni particolare attenzione è stata diretta allo sviluppo di catalizzatori al Pd che possano facilmente rilasciare in soluzione questa specie monoligata e molto attiva Pd(0)L. Tra i vari catalizzatori proposti, i dimeri al palladium hanno attirato l'attenzione di molti gruppi di ricerca. Alcuni di questi dimeri al Pd sono stati dimostrati essere degli ottimi precatalizzatori nelle reazioni di cross-coupling con alogenuri arilici, tuttavia il meccanismo di reazione resta tuttora sconosciuto.

Parte di questa tesi è stata dedicata allo studio dell'effetto che i sali di rame ed argento hanno sulla reattività dei complessi di Pd(0). Abbiamo scoperto che l'esposizione di diversi complessi di Pd(0) a sali di $CuBr_n$ (n=1, 2) e CuI porta al consumo totale o parziale del complesso di Pd(0) e alla formazione di nuove specie. Una combinazione di studi spettroscopici e cristallografici, ci ha permesso di risalire alla natura di queste nuove specie e ossidazione del complesso di Pd(0) a più alti stati di ossidazione, come I e II, è stata osservata per quasi tutti i complessi presi in esame. Particolare attenzione è stata rivolta alla reazione del complesso $Pd(0)(PtBu_3)_2$ con additivi come $CuBr_n$ (n=1, 2) oppure CuI. In questo caso, infatti, abbiamo osservato la formazione di Pd(I)-Pd(I) dimeri aventi ponti di bromuri e ioduri rispettivamente.

$$(tBu)_3P-Pd-P(tBu)_3 + CuX_n \quad \xrightarrow{\text{THF}} \quad (tBu)_3P-Pd\overset{X}{\underset{X}{\diagup\diagdown}}Pd-P(tBu)_3 \qquad \begin{matrix} X= Br, I \\ n= 1, 2 \end{matrix}$$
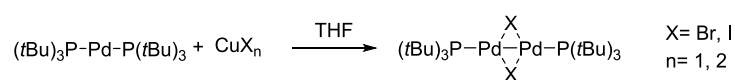
Schema A: Formazione di dimeri di Pd(I) dovuti alla reazione di $Pd(PtBu_3)_2$ con additivi al rame.

Spronati da questa scoperta, abbiamo investigato il possibile effetto di questa trasformazione nelle reazioni di Sonogashira e Suzuki cross-coupling. Abbiamo scoperto che la formazione *in situ* di questi dimeri ha una forte influenza sulla reattività di $Pd(0)(PtBu_3)_2$. La reazione di Sonogashira è totalmente inibita a causa di una reazione di

polimerizzazione degli alchini arilici. Nel caso della reazione di Suzuki un incremento delle rese è stato osservato in presenza di sali di $CuBr_n$ (n=1, 2), mentre è stata osservata inibizione in presenza di CuI, probabilmente dovuta alla maggiore stabilità di questo dimero.
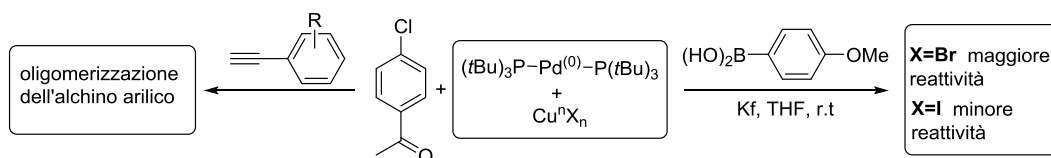
Schema B: Effetto dei Sali di rame sul $Pd(PtBu_3)_2$ nelle reazioni di Sonogashira (sinistra); nelle reazioni di Suzuki (destra)

Successivamente abbiamo anche investigato l'effetto di altri additivi comunemente usati in combinazione con Pd(0) come: AgBr, AgI, $FeBr_3$ e $AuBr_3$. La formazioni di questi due dimeri è stata osservata anche in presenza di questi sali ossidanti. Questa scoperta potrebbe spiegare alcuni degli effetti benefici che sono stati riscontranti nell'utilizzo di questi sali in combinazione con fonti di Pd(0).

Parte di questo lavoro di tesi è stato dedicato alla compresione del meccanismo di attivazione di questi dimeri $[Pd(\mu\text{-}X)PtBu_3]_2$ (X= Br, I). Un dettagliato studio meccanicistico è stato effettuato per capire il motivo dell'elevata reattività mostrata dal dimero $[Pd(\mu\text{-}Br)PtBu_3]_2$. La reattività mostrata da questo dimero è consistente quella mostrata dal complesso monoligato $Pd(PtBu_3)$ come specie catalitica attiva. Maggiori esperimenti ci hanno permesso di identificare come possibile meccanismo di attivazione un disproporzionamento assistito da nucleofili. L'effetto di diversi nucleofili sul dimero $[Pd(\mu\text{-}Br)PtBu_3]_2$ è stato poi testato. In questo modo è stato possibilire stabilire un minimo valore di nucleofilicità al di sotto del quale non si ha attivazione, valore stimato a 10.5. Lo stesso studio è stato poi esteso al dimero $[Pd(\mu\text{-}I)PtBu_3]_2$. Anche in questo caso è stato possibile stabilire un valore minimo di nucleofilicità di 16.0 (secondo la scala sviluppata da Mayr's), al di sotto di questo valore non è possibile avere attivazione. Il fatto che un maggiore potere nucleofilo sia richiesto per l'attivazione del dimero $[Pd(\mu\text{-}I)PtBu_3]_2$ è in accordo con la sua maggiore stabilità rispetto all'analogo bromo-dimero. Per la prima volta abbiamo dimostrato che è possibile attivare anche il dimero $[Pd(\mu\text{-}I)PtBu_3]_2$ e come ulteriore conferma lo abbiamo utilizzato come precatalizzatore nelle reazioni di Suzuki sia in presenza che in assenza di ossigeno.
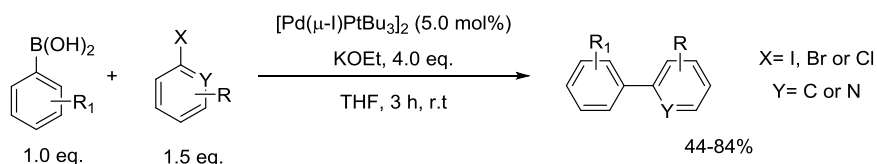
Schema C: Reazioni di Suzuki coupling catalizzate dal dimero [Pd(μ-I)PtBu$_3$]$_2$ in assenza ed in presenza di ossigeno.

Infine, parte di questo lavoro di tesi è stato dedicato allo svilluppo di una catalisi direttamente derivate dall'uso di questi dimeri. Siamo stati in grado di sviluppare la prima reazione che porta alla formazione nuovi legami C-Se catalizzata direttamente da questi dimeri. La reazione è stata effettuata su numerosi ioduri arilici e si è dimostrata essere tollerante ad un gran numero di gruppi funzionali, comprese amine ed aniline non protette. Buone rese sono state ottenute in condizioni molto blande.
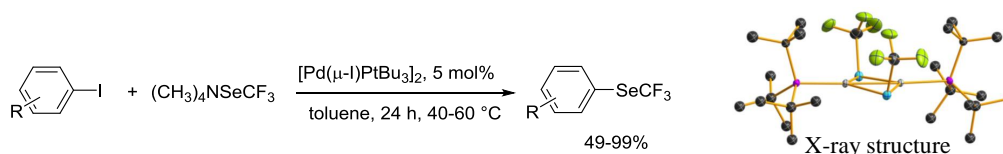
Scheme D: Trifluorometilselenolazione catalizzata da [Pd(μ-SeCF$_3$)PtBu$_3$]$_2$ (destra). Struttura ai raggi X del dimero [Pd(μ-SeCF$_3$)PtBu$_3$]$_2$.

Inoltre una combinazione di studi spettroscopici e computazionali ci ha permesso di aquisire un quadro più chiaro per quanto riguarda il possibile meccanismo di questa trasformazione. Lo studio non ha escluso la possibilità di avere catalisi derivante direttamente dall'utilizzo di questi dimeri.

Chapter 1. Introduction

Chapter 1: Introduction

The advent of transition metal-catalysed reactions opened the way to a large number of new reactions that were not possible to achieve with the previously known standard organic chemistry methodologies. Progress has been made in the field of polymer chemistry and one of the most famous examples are the Ziegler-Natta catalysts for the polymerisation of ethylene and propylene.[1] The method gave, for the first time, the opportunity of controlling the stereochemistry of polymers allowing the synthesis of isotactic (where all the stereogenic centers are in the same configuration) and syndiotactic (where the stereogenic centers have an alternate configuration) polypropylene.[2] This discovery lead the two chemists receiving the Nobel prize in 1963[3] and until then the method has been used in industry for the synthesis of large amount of plastic materials.

Of particular importance is also the Wacker-Hoechst process, it represents the first example of an organometallic reaction being performed on an industrial scale. The $PdCl_4^{2+}$-catalysed process allows the conversion of alkenes into aldehydes using oxygen as oxidant[4] and $CuCl_2$ as co-oxidant.[5]

Among all of the chemical transformations palladium-catalysed cross-coupling reactions of organo-halides with organometallic reagents have a very important role for the formation of C-C and C-heteroatom bonds. The introduction of cross-coupling reactions in organic synthesis dramatically changed the preparation of very complex molecules and supramolecular entities.[6] They have found particular use in pharmaceutical, agricultural and polymer chemistry due to the scope, the ease of carrying out procedures and the very high conversions.[7-10] A recognition of the high importance of cross-coupling reactions came in 2010 when Richard F. Heck, Ei-ichi Negishi and Akira Suzuki were jointly awarded the Nobel Prize in Chemistry "for palladium-catalyzed cross couplings in organic synthesis".[11,12]

1.2 Pd(0)/Pd(II) cycles in cross-coupling reactions

Group 10 of the periodic table has a crucial role in transition metal-catalysed cross-coupling reactions and among them palladium is the most widely used. Despite it being isoelectronic with nickel and platinum, palladium adopts a different electronic configuration. Instead of the $d^9 s^1$ and $d^8 s^2$ configurations adopted by the platinum and

nickel respectively, it instead has a $d^{10} s^0$. This allows palladium to show unique activity in comparison to the other members of the group. For example, theoretical studies have shown that for particular ligand systems reductive elimination from Pt(II)-complexes has a lower driving force compared to the one of Pd(II)-complexes, (*Scheme 1*).

$$Pt(PH_3)_2(CH_3)_2 \longrightarrow Pt(PH_3)_2 + H_3C{-}CH_3 \qquad \Delta G = \text{-11.3 Kcal/mol} \qquad (1)$$

$$Pd(PH_3)_2(CH_3)_2 \longrightarrow Pd(PH_3)_2 + H_3C{-}CH_3 \qquad \Delta G = \text{-45.8 Kcal/mol} \qquad (2)$$
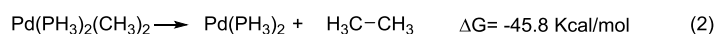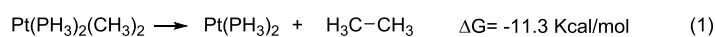
Scheme 1: Calculated ΔG for C-C reductive elimination from platinum(II) (1), and palladium(II) (2).[13]

Many studies have been performed to gain an insight into the possible mechanism of cross-coupling reactions.[14-17] The mechanism of cross-coupling reactions generally involves a Pd(0)/Pd(II) cycle that can be divided in three major steps: *(i)* oxidative addition (red); *(ii)* transmetallation (green); and the final step of *(iii)* reductive elimination (blue) that allows the regeneration of the catalyst, (*Figure 1*).
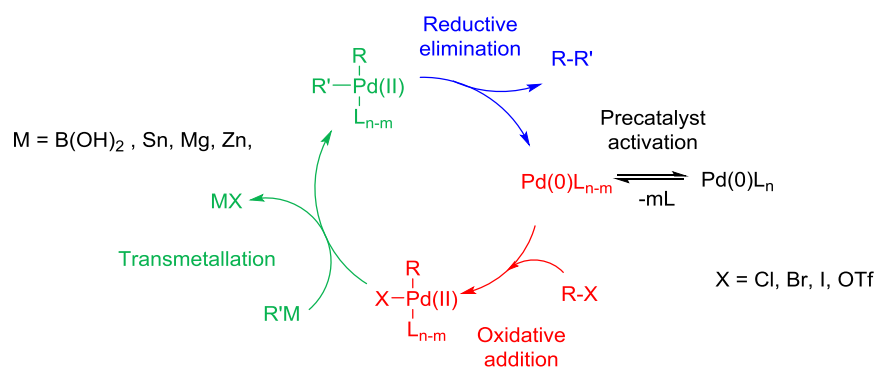
Figure 1: General catalytic cycle for Pd-catalysed coupling reactions.

1.2.1 The oxidative addition step

The oxidative addition of an aryl (pseudo)halide onto the pre-formed catalytic active species (14- or 12-electrons Pd(0)L_{n-m}) with cleavage of the C-X bond and formation of an L_{n-m}Pd(II)RX species is generally the first step of the cycle in cross-coupling reactions.[18] The choice of ligand, solvent, C-X, temperature and the presence of additives can dramatically influence the outcome of the reaction especially in terms of selectivity at this stage of the process.[19-24] For example if several C-X bonds are present in the molecule an

appropriate choice of ligand, the Pd(0) source or the polarity of the solvent can dramatically alter the outcome of the reaction.[25-27] An excellent example of how the ligand can affect the selectivity of coupling reactions was reported by Hayashi *et al.* in 1997, (*Scheme 2*).[28]
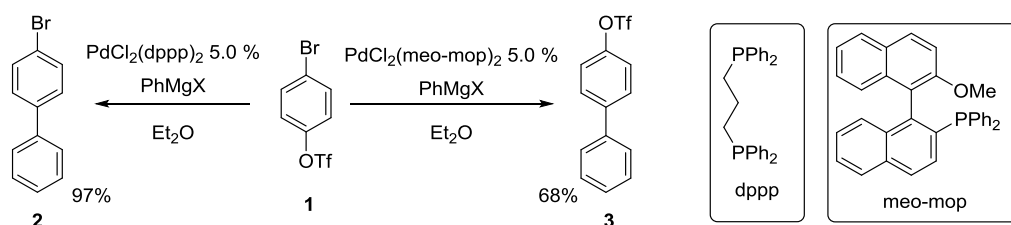
Scheme 2: Example of chemoselective Kumada cross-coupling.[28]

As illustrated in *Scheme 2*, the change in the catalyst system completely changes the chemoselectivity of the Kumada coupling. The system $PdCl_2(dppp)_2$ preferentially gives aryl triflate addition so that compound **2** is obtained in 97% yield as the major product of the reaction. However, when $PdCl_2(meo-mop)_2$ is used there is exclusively aryl bromide addition and compound **3** is formed as the only product in 68% yield. Brown *et al.* investigated the possible reasons that could control the selectivity.[29] They tested the arylbromotriflate **1** also in other cross-coupling reactions: Stille, Negishi and Suzuki. The Stille and Negishi gave results consistent with what reported by Hayashi: bromide addition was exclusively observed in the presence of $PdCl_2(meo-mop)_2$, which was presumed to operate as a monophosphine catalyst, and triflate addition was predominantly observed when $PdCl_2(dppp)_2$ was used as a precatalyst. However, for the Suzuki coupling reaction the outcome of the study showed that bromide addition was observed in the presence of both catalysts. Brown *et al.* proposed as a possible explanation a direct implication of the boronic acid in the catalytic cycle.

Another example of how the ligand system can influence the outcome of the reaction was reported by Fu *et al.*[30]
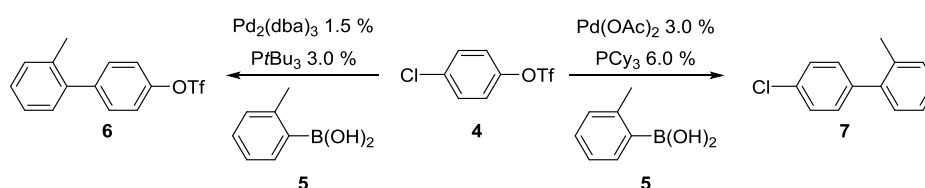
Scheme 3: Example of chemoselective Suzuki cross-coupling.[30]

Again, the change in the catalyst system completely changes the chemoselectivity of the reaction, as illustrated in *Scheme 3*. The system $Pd_2(dba)_3/PtBu_3$ preferentially gave only chloride addition so that compound **3** is obtained in 95% yield as the only product of the reaction. However when $Pd(OAc)_2/PCy_3$ is used there is exclusively aryl triflate addition and compound **4** is formed as the only product in 87% yield. A computational study performed by Schoenebeck and Houk contributed to understand the different reactivity observed with the two systems.[31] The ligation onto the Pd catalyst was found to be the key to control the chemoselectivity of the process. $Pd(PCy_3)_2$ was shown to react *via* a bisligated Pd species under the condition employed. In fact for this system, the triflate addition onto this system was found to be 4.3 kcal/mol lower than that of Cl. In the case of the bisligated Pd species a strong HOMO-LUMO interaction favours the addition of the triflate, whilst for the monoligated Pd species Cl insertion is favoured due a lower C-Cl BDE compared to that of C-O.

Another important parameter that should always be considered is the solvent. The polarity of the solvent can affect the formation and the nature of the active catalytic species. An excellent example of chemoselectivity arising from solvent polarity was reported previously by our group. Through a combination of experimental and computational studies it was possible to understand the reason for the different chemoselectivity observed for compound **4** in THF and CH_3CN (*Scheme 4*).[25,32] This work represent the first evidence for the intermediacy of an anionic Pd species in catalysis.
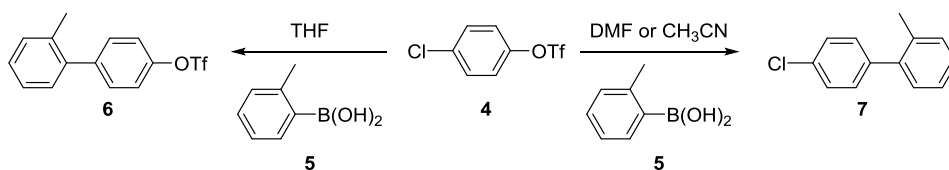
Scheme 4: Solvent effect on the chemoselectivity of Suzuki cross-coupling.[25,32]

In the presence of $Pd_2(dba)_3/PtBu_3$ Cl-addition is exclusively observed in THF, however in the presence of a polar solvent such as CH_3CN a selectivity change is observed, and triflate addition product **7** is obtained as the only product. A combination of experimental and computational studies revealed that in polar solvent the anionic $[Pd(PtBu_3)X]^-$ species, where X is either $ArB(OH)_2$ or F^-, is responsible for the change of chemoselectivity, whilst in non polar solvent the active species is a neutral $Pd(0)PtBu_3$ species. The possibility of

switching the selectivity of a reaction just by changing one parameter in the reaction conditions is a powerful tool in the hands of organic chemists for the design of new complex molecules.

1.2.2 The transmetallation step

In the transmetallation step the X group of the $L_{n-m}Pd(II)(R)(X)$ complex generated in the oxidative addition is replaced with an organic group from an appropriate coupling partner. Many organometallic coupling partners have been shown to undergo transmetallation with the Pd(II) complex and according to the reagent used the coupling has a different name. Suzuki-Miyaura for organoboron (R-B(OH)$_2$),[33] Negishi for organozinc (R-Zn-Br),[34] Heck for di-substituted alkenes (RHC=CH),[35] Sonogashira for alkynes (H≡─R)[36], Hiyama for organosilicon (RR^{I}R^{II}SiAr)[37,38], Buchwald-Hartwig for amines (RR^{I}NH)[39-41], Kumada for organomagnesium (RMgBr)[42], Stille for organotin (Bu$_3$SnR),[43,44] (*Figure 2*).
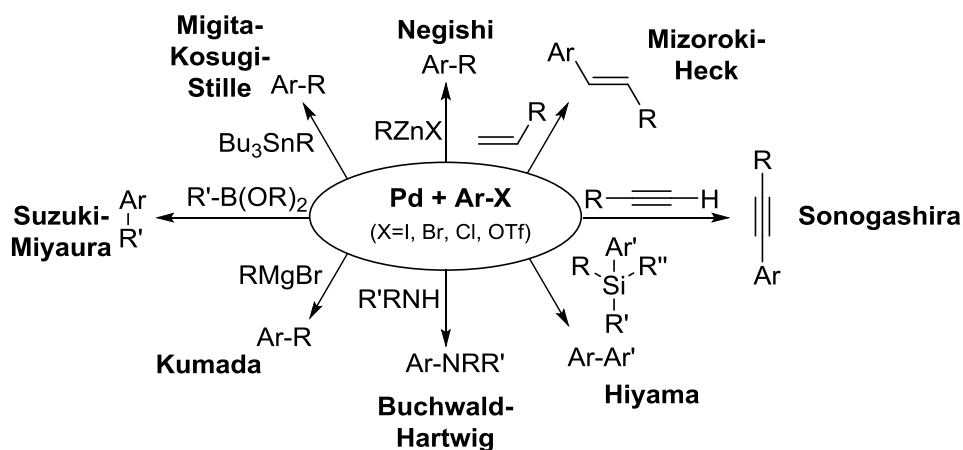
Figure 2: Different types of Pd-catalysed cross-coupling reactions.

Transmetallation is usually an irreversible step due to thermodynamic reasons, and of the three steps the transmetallation has been the least studied. However, it has been reported that the inorganic base plays a crucial role in the transmetallation step of Suzuki-Miyaura reaction. In 2002 Miyaura proposed two different pathways for the transmetallation step in Suzuki-Miyaura cross-coupling reactions.[45] In **pathway a** the X group of the oxidative

addition complex **8** is substituted with the the $^-$OR group of the base to generate the alkoxy-palladium complex **9** which undergoes transmetallation with the neutral reagent **10** to give dialkyl-palladium complex **13** *via* intermediate **11**. In **pathway b** the oxidative addition complex **8** undergoes direct transmetallation with the four-coordinate boron reagent **12**, formed upon reaction of the inorganic base with **10**, to form the dialkyl-palladium complex **13**, (*Scheme 5*).
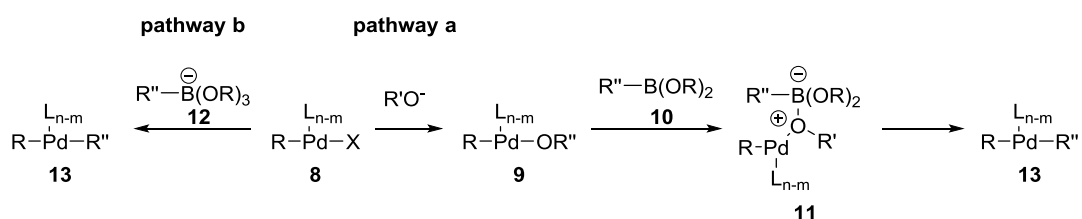
Scheme 5: Pathways proposed by Miyaura for the base-assisted transmetallation step.[45]

Miyaura concluded that the coupling of bis(pinacolate)diboron ester with aryl, 1-alkenyl and allyl halides/triflates in the presence of KOAc proceeds by **pathway a**. However the possibility for the reaction to proceed *via* one of the two pathways depends on many factors such as the boron source, the Pd source, the nature of the base and its counterion.

The work of Lloyd-Jones,[46] Amatore and Jutand[47] and that of Hartwig[48] have given the possiblility of a better understanding of the possible mechanism for transmetallation. In 2010, Lloyd-Jones *et al.* reported a study on the reactivity of boronic acids ($RB(OH)_2$) *vs* potassium trifluoro borates (RBF_3K), (*Scheme 6*).[46]
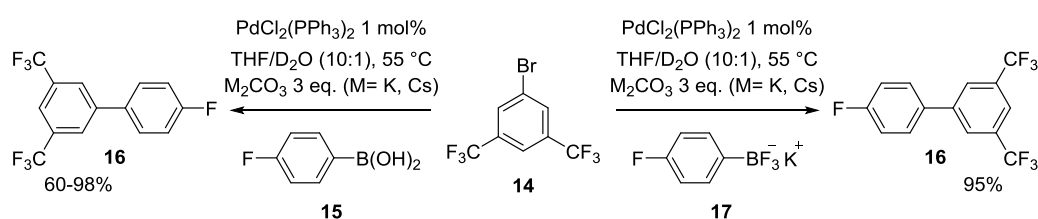
Scheme 6: Susuki coupling reaction of bromide **14** with boronic acid **15** (left). Suzuki coupling reaction of bromide **14** with potassium trifluoro borate **17** (right).[46]

The reactions performed in the presence of the trifluoro borate **17** gave high conversions and formation of side products variable from 0.1 to 2% also under aerobic conditions, whilst the reactions in the presence of boronic acid **15** gave very variable conversions with

formation of side products variable from 2 to 40%. These results could have led to the conclusion that the potassium trifluoro borate could be the transmetallating agent. However, a combination of ^{19}F and ^{11}B spectroscopic together with the use of labelled D-**15** and D-**17** showed that the active transmetallating species is the boronic acid **15**. The potassium trifluoro borate was shown to slowly hydrolise under the applied reaction conditions to generate the boronic acid **15**. The reason for the enhanced catalysis observed in the presence of potassium trifluoro borate was explained to be due: *(i)* the ability of F^- of reducing $PdCl_2(PPh3)_2$ to $Pd(PPh_3)_2$ avoiding the 2-stage transmetallation/reduction that usually generate $Pd(PPh_3)_2$ and homocoupling product from the boronic acid; *(ii)* ability of F^- to destroy the tetrahydrofuran-2-hydroperoxide, which could be generated from oxygen trace amounts present in the unit cell of the boronic acid or potassium trifluoro borate. This peroxo-complex is responsible of the oxidation of the boronic acid into phenol.

Amatore and Jutand studied the transmetallation step with combination of electrochemical and spectroscopic experiments.[47] *Trans*-[*o*-CN-PhPdBr(PPh$_3$)$_2$] **20**, Ph-B(OH)$_2$ **19**, *n*Bu$_4$NOH as an $^-$OH source and DMF as solvent have been chosen as standard system for this study. They observed that *(i)* the reaction of *trans*-[*o*-CN-PhPdBr(PPh$_3$)$_2$] **20** with Ph-B(OH)$_2$ **19** in the absence of a base did not give any product, even with the addition of an excess of PPh$_3$. A drastically change was observed upon addition of the base to the reaction mixture. *(ii)* The increase in the concentration of Br^- in solution caused a decrease in the rate of the reaction, confirming the possibility for the reaction to proceed *via* intermediate **18**. *(iii)* The presence of a very high excess of the base also caused a decreases in the rate of reaction excluding the possibility of a transmetallation step involving **18** and **21**, *(iv)* The reaction of **20** with **21** in the presence of an excess of bromide salts does not lead to the formation of the desired product **22**, (*Scheme 7*)
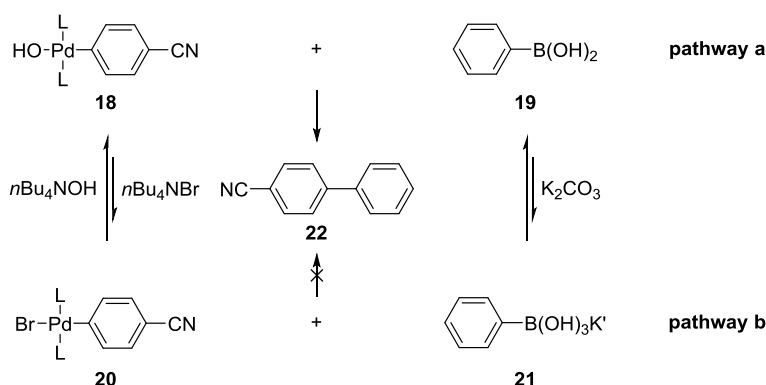
Scheme 7: Possible scenarios for the transmetallation step investigated by Amatore and Jutand.[46]

Their experimental results are consistent with a transmetallation process proceeding *via* **pathway a** and with a direct involvement of the boronic acid **19** as transmetallating agent as previously reported by Lloyd-Jones *et al.*[46,49] In addition, they identified three distinct roles of the base in the catalytic cycle: the first role concerns the formation of the Pd-OH species, which was proposed to be the active catalytic species of the transformation; the second role concerns the formation of the unreactive $R-B(OH)_3^-$, that explain why an excess of the base should be avoid; in the third role the base facilitates the reductive elimination step *via* coordination of the tetra-coordinate Pd(II) complex to generate a penta-coordinate Pd complex as shown in *Scheme 8*.

$$\underset{\underset{L}{|}}{\overset{\overset{L}{|}}{Ar-Pd-Ar}} \quad \xrightarrow{^-OH} \quad \left[\underset{\underset{OH}{|}}{\overset{\overset{Ar}{|}}{Ar-Pd}}{\overset{\cdots L}{\underset{L}{\diagdown}}} \right]^- \quad \xrightarrow[\textbf{Fast}]{+\,L} \quad Ar-Ar \;+\; PdL_3 \;+\; {}^-OH$$
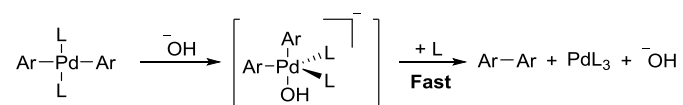
Scheme 8: Hydroxide-assisted reductive elimination, as proposed by Amatore and Jutand.[47]

In a following study Amatore and Jutand investigate the effect of F^- in Suzuki cross-coupling reaction using a combined spectroscopic and cyclic voltammetric studies.[50] They demonstrated that the reaction of aryl boronic acid with a preformed PhPd(II)FL$_2$ complex led to the same Pd(II)complex obtained from the transmetallation of aryl boronic acid with PhPd(II)OHL$_2$. The F^- was shown to have the same three roles of $^-$OH, two positive and one negative: *(i)* it promotes the formation of the Pd-F specie responsible for the trasmetallation with aryl boronic acid; *(ii)* it can react with aryl boronic acids to form the unreactive fluoroborates; *(iii)* it facilitates the trasmetallation step by coordinating the tetra-coordinate Pd(II) complex to generate a penta-coordinate complex, that undergoes faster reductive elimination.

^{31}P-NMR spectroscopy was used by Hartwig *et al*. to measure the rate of stoichiometric transmetallation of complex **18** and **20** (see *Scheme* 7) with *p*-tolylboronic acid and the corresponding trihydroxyboronate respectively.[48] The transmetallation of **18** with neutral boronic acids was found to be four orders of magnitude faster than the reaction of **20** with trihydroxyboronates. Moreover complex **18** undergoes fast transmetallation with stoichiometric amounts of neopentyl glycol or catechol esters of *p*-fluorephenyl boronic acid even at −55 °C.

These studies are consistent with a transmetallation step proceeding *via* **pathway a** for the systems taking into account, but do not exclude that for other systems transmetallation could proceed *via* **pathway b**.

1.2.3 The reductive elimination step

The reductive elimination represents the product forming step: two covalent ligands at the metal centre couple to generate the product and regenerate the active catalytic species. The metal centre goes from an oxidation state of *n+2* to *n*. Mechanicistically it can be seen as the reverse process of the oxidative addition and as for the oxidative addition many factors can have an impact: steric properties, electronic properties and bite angle[51,52] of the ligand; coordination number of the metal centre;[53] geometry of the complex;[54] and also the type of bond that has to be formed.[55] These parameters can dramatically influence and change the outcome of the reaction.[56] An interesting example of how bite angle can influence the rate of the reductive elimination was described by Brown *et al.* in 1994.[51] In their work Brown *et al.* studied the thermal decomposition of three different Pd(II)-complexes bearing bidentates ligands with increasing bite angle, (*Figure 3*).
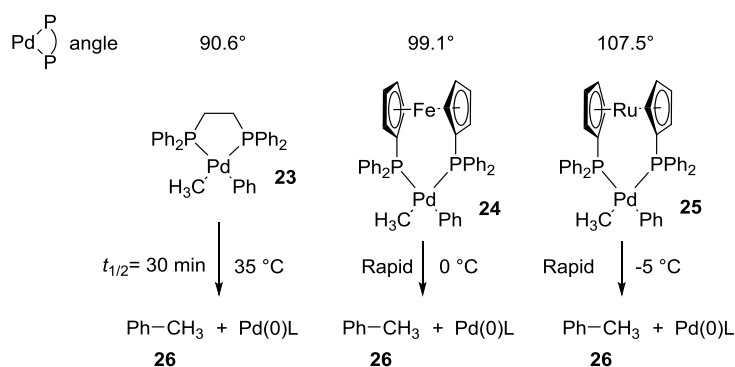
Figure 3: Reductive elimination of Pd(II)-complexes with different bite angles.[51]

As illustrated in *Figure 3* the increase in the bite angle between complex **23** and **24** results in an increase in the rate of reductive elimination to give product **26** and the respective Pd(0)L. On the basis of this observation it could be argued that the bigger the bite angle the faster the reductive elimination process. Although this is true in many cases, there are also other aspects that together with the bite angle can affect the rate of reductive elimination.

In the case of the Pd(II)-complexes **24** and **25**, despite the increase in the bite angle, there is not a significant increase in the rate of reductive elimination. Brown *et al.* proposed also an explanation for this behaviour: the stable conformation of these Pd(0) complexes is where the ligand is linear (L) so in order to promote the reductive elimination process the metallocene-type ligand has to bend (B) as illustrated in *Figure 4:*
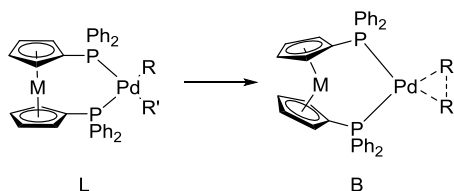
Figure 4: Distortion of the metallocene-type ligands to favour the reductive elimination process.[51]

Ruthenocene-type ligands are slightly more rigid than ferrocene-type ligands which results in a higher energy to distort the ruthenocene-type ligand to the geometry of the reductive elimination TS.

Examples of how the electronic properties of the ligands attached to the Pd centre and those of the substituents on the coupling substrates can influence the reductive elimination step was reported by Hartwig *et al.*[57] Pd-amido complexes are usually unstable due to their propensity to undergo β-hydrogen elimination rather than reductive elimination.[58] Moreover, the presence of the electronegative N could cause an additional decrease in the reactivity of these Pd(II) complexes towards reductive elimination.[59,60] Hartwig *et al.* reported the synthesis and studies of the stoichiometric reductive eliminations of monomeric and dimeric Pd(II)-amido complexes with a series of different ligands as reported in *Scheme 9.*
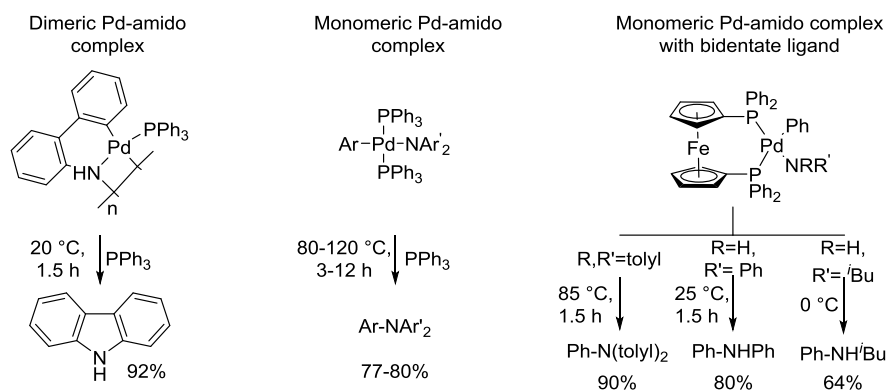
Scheme 9: Reductive elimination from a dimeric Pd-amido complex (left); reductive elimination from monomeric Pd-amido complexes (middle); reductive elimination from monomeric Pd-amido complexes bearing a bidentate ligand (right).[57]

The reductive elimination from the dimeric Pd-amino complex was shown to proceed at room temperature giving 92% yield in less than 2 hours. Higher temperature and prolonged reaction times were necessary to reductive eliminate the substituted amine from monomeric Pd-amido complexes. The PPh_3 was necessary for the reactions to proceed, in fact in the absence of extra ligand only 20 % of product formation was observed for both monomeric and dimeric amido complexes. Different scenario can be observed in the case of Pd-amido complex bearing a bidentate ligand. In this case the rate of reductive elimination depends on the nature of the substituent on the amino group: the higher the pK_a of the group attached, the faster the reductive elimination. The reductive elimination of Ph-N(tolyl)$_2$ required high temperatures (85 °C) to occur and within 1 hour 90% of product was formed. A lower temperature (25 °C) was necessary for the reductive elimination of Ph-NHPh in the same reaction time, whilst the reductive elimination of Ph-NH*i*Bu was so fast that at 0 °C 64 % of product was formed within minutes.

In later works, the study of the reductive elimination to form C-X bonds was also extended to arylpalladium arenethiolate[61] and arylpalladium phenoxides.[52] Electron rich substituent on the S atom were shown to undergo faster reductive elimination compared to electron poor substituents, same electronic effect was described by Buchwald *et al.* for arylpalladium phenoxides.[62] Moreover, reductive elimination of aryl sulphites was shown to be faster than the reductive elimination of aryl amines,[61] whilst the reductive elimination from arylpalladium anilide complexes was shown to be faster than that of arylpalladium phenoxide complexes. These experiments allowed not only a better understanding of the reductive elimination process, but they allowed also to set a scale of reactivity of C-X bonds towards reductive elimination: C-S >C-N > C-O.[52]

1.3 Pd(I)-Pd(I): classification, synthesis, structure, bond features and reactivity

Pd(0)/Pd(II) are the most stable and well known oxidation states of palladium. Many studies have been performed to elucidate the mechanism of reactions involving these, in order to design more efficient catalyst systems. In recent decades the attention of some groups has shifted to other oxidation states of palladium such as Pd(I) and Pd(III) but little is known about their role in catalysis.

Pd(I) is predominantly found in a dimeric form, although clusters based on Pd(I) units are also known.[63,64] Typically these Pd(I) dimers have a σ-bond between the two palladium

centres. In their review of 2002 Kurosawa and Murahashi summarised all of the characteristics (Pd-Pd bond distance, geometries and reactivity) of Pd(I)-Pd(I) dimers known at that time.[65] Pd(I)-Pd(I) dimers were divided in two main categories *(i)* corner-sharing and *(ii)* edge-sharing as well as a further three intermediate subcategories *(iii)* rigid bridging support, *(iv)* allyl bridging support and *(v)* single atom bridge, (*Figure 5*).
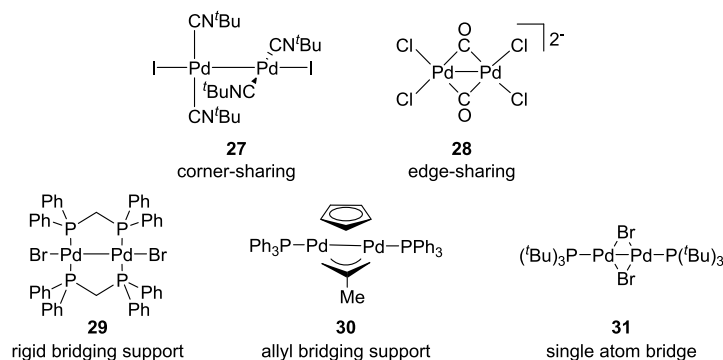
Figure 5: Examples of the five different categories of Pd(I)-Pd(I) dimers.

1.3.1 Corner-sharing Pd(I) dimers: synthesis, structure and bond features

Corner-sharing dimers are characterised by Pd atoms bonded to each other only through the Pd-Pd bond without any additional bridging ligand. The first example of a corner-sharing dimer was reported by Balch and Eisenberg in 1975.[66] The dimer **32a** was obtained by mixing $Na_2(PdCl_4)$ with an excess of methyl isocyanide in an aqueous solution for 18 hours. Precipitation with NH_4PF_6 gave the complex $[Pd_2(CH_3CN)_6][PF_6]_2$ **32a** in 80% yield. The structure was confirmed by X-ray analysis: the two Pd atoms both adopt a square-planar geometry in which one coordination site is occupied by the other Pd-atom. The Pd-Pd bond length is 2.53 Å. The dihedral angle between the two coordination planes is 86.2°. The bond length of the two "axial" Pd-C bonds is shorter than that of the four other "equatorial" Pd-C bonds 1.96 *vs* 2.05 Å respectively.
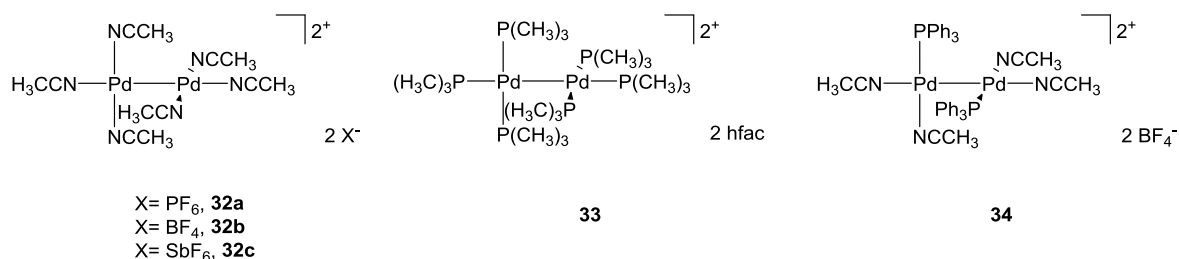
Figure 6: First examples of Pd(I)-Pd(I) corner-sharing.

In 1994, Girolami *et al.* reported the first synthesis of complex **33** (*Figure 6*) *via* the comproportionation reaction of Pd(0)(PMe$_3$)$_4$ and Pd(II)(hfac)$_2$ followed by recrystallisation in Et$_2$O/ CH$_2$Cl$_2$.[67] In this case the structure was also confirmed by X-ray analysis: two square-planar Pd atoms joined by a Pd-Pd bond, where the Pd-Pd distance is 2.60 Å, slightly longer than the one found for complex **32a**. The Pd-P distance of the "axial" P(CH$_3$)$_3$ groups which is slightly shorter than the one of the "equatorial" P(CH$_3$)$_3$ groups, ranging from 2.33 to 2.35, vs 2.37 Å for **32a**. The two square-planar planes are orthogonal to each other avoiding steric repulsions between the P(CH$_3$)$_3$ groups giving a dihedral angle between the two planes of 89.0°.

In 2000 the group of Kurosawa showed that it is possible and easy to substitute the CH$_3$CN ligands of complex **32b** with alternative ligands such as PPh$_3$.[68] This gave access to a series of new Pd(I)-Pd(I) dimers. Mixing complex **32b** with 2 equivalents of PPh$_3$ in CH$_2$Cl$_2$ leads to the quantitative formation of complex **34**, (*Scheme 10*).

32b   **34**
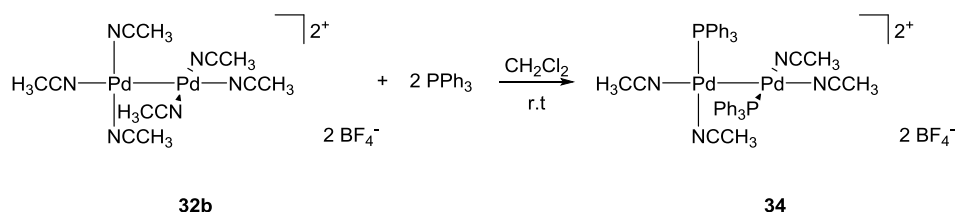
Scheme 10: Synthesis of complex **34** from complex **32b** and PPh$_3$.[68]

Interestingly, EHMO calculations performed by Harvey (P.D) and Murtaza on the [Pd$_2$(CH$_3$CN)$_4$Cl$_2$] complex showed that these dimers do not show the same trend observed for other M$_2$ σ-bonds. The contribution to the σ-bond in M-M complexes usually arises almost entirely from the d$_{z^2+z^2}$ orbital overlap. However in corner-sharing complexes the bond is mainly created by the interaction of two d$_{x+y}$ orbitals, (*Figure 7*). The reason for the different behaviour is due to the fact that the two square-planar metal complex interacts *via* a side-by side fashion rather than the usual face-to face one.[69]

$$d_{z^2+d_{z^2}} \qquad d_{xy+d_{xy}}$$
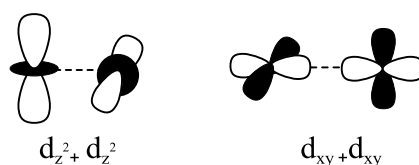
Figure 7: Side-by-side interaction between d$_{z^2+z^2}$ (left) and d$_{xy+d_{xy}}$ (right) orbitals.[69]

A borderline example of a corner-sharing dimer is represented by a Pd-Pd complexes bearing a pincer ligand. The first evidence of the formation of a Pd(I) complex containing a pincer ligand was described by Ozerov *et al.* in 2007.[70] They reported that exposure of complex **35** to sunlight or artificial UV light (λ= 350 nm) generates Pd(I) dimer **36** through homolytic cleavage of the Pd-C bond followed by dimerisation, (*Scheme 11*).
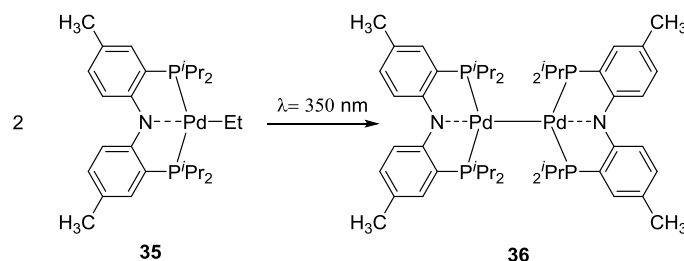
Scheme 11: Synthesis of Pd(I) dimer **36** from homocoupling of complex **35**.[70]

X-ray analysis of complex **36** showed that the two Pd atoms adopt a distorted square-planar geometry where the dihedral N-Pd-Pd-N angle is 31°, the Pd-Pd bond length is 2.57 Å, the Pd-P bond lengths are in the range of 2.29-2.31 Å and the Pd-N bond lengths are in the range of 2.12-2.21 Å. In 2011 Ozerov *et al.* reported the synthesis and the crystal structure of a two more Pd(I) dimers bearing pincer ligands **37** and **38**, (*Figure 8*).[71]
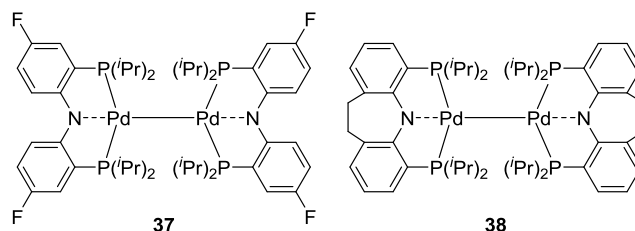
Figure 8: Examples of Pd(I) dimers bearing pincer ligands.[71]

The X-ray analysis shows that in these other two complexes the two Pd atoms also adopt a distorted square-planar geometry, but the extent of this distortion is lower for complex **37**. The molecule is completely symmetric, the N-Pd-Pd-N lies in the plane and all the Pd-P and Pd-N bonds are equivalent. The Pd-Pd bond length is elongated compare to that of the other two dimers, as shown in *Table 1*.

Table 1 Selected bond distances for Pd(I) dimers **36-38**.[71]

Bonds	Pd(I) dimer **36** (Å)	Pd(I) dimer **37** (Å)	Pd(I) dimer **38** (Å)
Pd-Pd	2.57	2.72	2.58
Pd-P$_{min}$	2.29	2.31	2.27
Pd-P$_{max}$	2.31		2.30
Pd-N$_{min}$	2.12	2.16	2.18
Pd-N$_{max}$	2.21		2.20

1.3.2 Corner-sharing Pd(I) dimers:reactivity

Due to the lability of their ligands, the corner-sharing Pd(I) dimer **32a** and Pd(I) dimer **32b** have been mainly used as building blocks for the synthesis of more "robust" dimers.[72] However, despite thier high lability compared to the other categories of dimers, Pd(I) dimer **32a** has found application in the oligomerization of alkynes, whilst[73] Pd(I) dimer **32b** was shown to be an efficient catalyst/precatalyst for the photoinduced carbonylation of aryl iodides to generate carboxylic acid esters, (*Scheme 12*).[74]
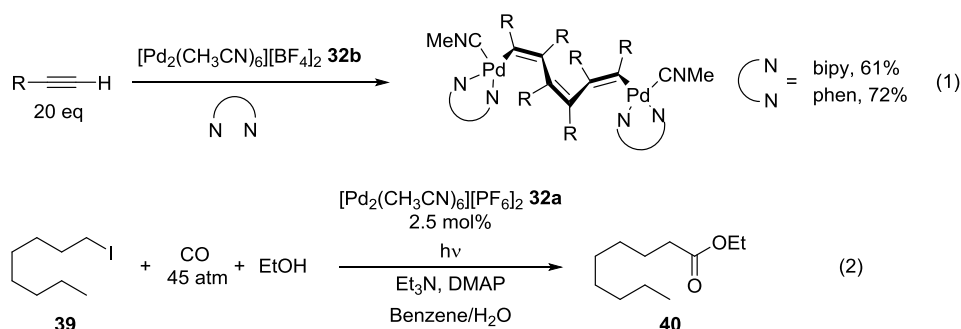
Scheme 12: Use of Pd(I) dimer **32b** in the oligomerization of alkynes (top);[73] use of Pd(I) dimer **32a** as a catalyst/precatalyst (bottom).[74]

[Pd$_2$(CH$_3$CN)$_6$][SbF$_6$]$_2$ **32c** was employed by Hor *et al.* in combination with different monodentate and bidentated ligands for the Suzuki coupling of aryl bromides and chlorides, giving from good to excellent yields, (*Scheme 13*).[75]
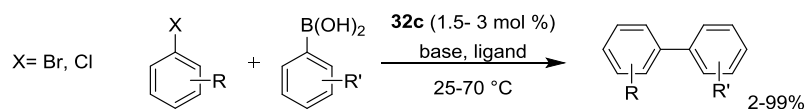
Scheme 13: Use of Pd(I) dimer **32c** as a precatalyst in the Suzuki cross coupling of aryl bromides and chlorides.[75]

Ozerov *et al.* used stoichiometric amount of pincer dimers **36** and **37** to cleave H-Y bonds (Y= OH, NH_2 or H) of small molecules. Thermolysis of these compounds in the presence of a small molecule such as H_2, H_2O or NH_3 generated a series of monomeric Pd(II) complexes. The photoinduced reaction with oxygen generated two different products depending on the amount of oxygen present in solution. Low concentrations of oxygen favoured the formation of a Pd(II) bridging peroxide dimer, whilst high concentration of oxygen favoured the formation of a superoxide Pd(II) monomer, (*Scheme 14*).[71]
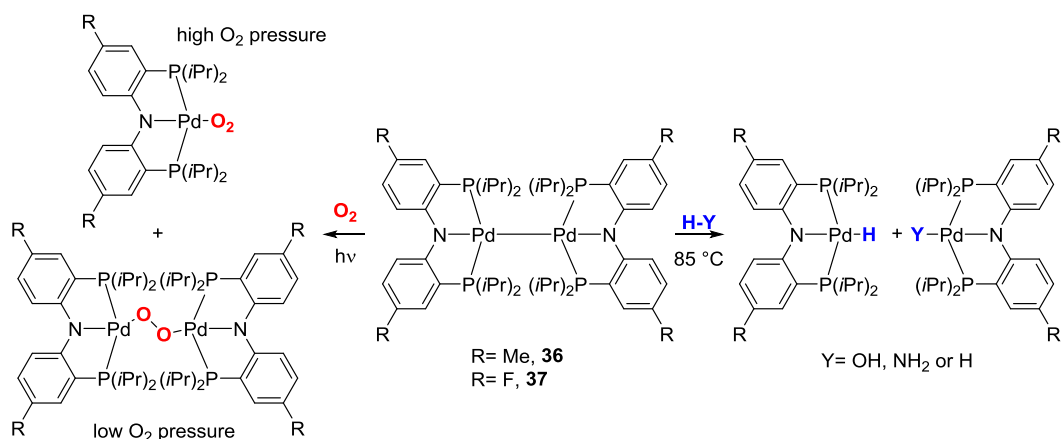
Scheme 14: Use of Pd(I) dimers bearing pincer ligands.[71]

1.3.3 Edge-sharing Pd(I) dimers: synthesis, structure and bond features

Edge-sharing Pd(I) dimers are characterised by two Pd atoms bonded to each other not only by a Pd-Pd σ-bond, but also through two bridging groups. The first reported example of a Pd-(I) edge-sharing dimer **28** dates from 1942 when Gelman and Meilakh suggested a dimeric structure for the green-yellow compound $NH_4(PdCl_2CO)$, obtained after reaction of $PdCl_4^{2-}$ with CO in concentrated HCl.[76] The proposal of the two Russian chemists was confirmed by Goggin and Mink in 1974 through IR spectroscopy[77] and subsequently Goggin obtained the final confirmation by X-ray analysis in 1981.[78] The crystal structure of dianionic compound **28** revealed that Pd-Pd bond length is 2.70 Å, Pd-C 1.99 Å and the one of Pd-C 2.37 Å. The Pd-C moieties are planar with a Pd-C-Pd angle of 85.2°.

Another example of an edge-sharing Pd(I) dimer was presented by Kobayashi *et al.* in 1994. The dimer $Pd_2[HB(pz)_3]_2[\mu-2,4,6-(CH_3)_3C_6H_2NC]_2$ **41** was obtained by mixing $Pd_2Cl_2(2,4,6-(CH_3)_3C_6H_2NC)_4$ with $Na[HB(pz)_3]$.[79]
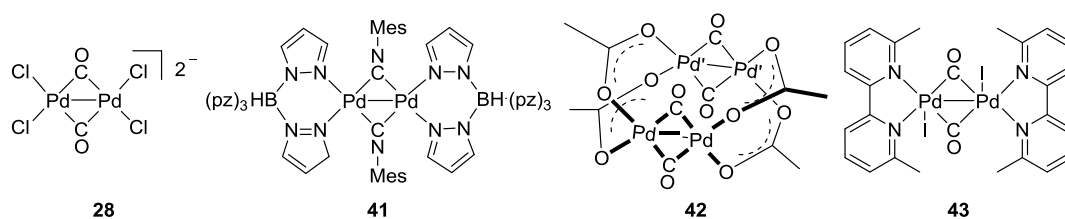
Figure 9: Examples of edge-sharing Pd(I) dimers.

The structure incorporates two Pd atoms bridged by two isocyanides, the Pd-C core is planar and the $HB(pz)_3$ ligand coordinates to the metal in an asymmetrical tridentate manner. The Pd-Pd and the Pd-L bond lengths are reported in *Table 2*.

Complex **42** was synthesised by Struchkov *et al.* in 1978 by stirring $Pd(OAc)_2$ in glacial acetic acid under a CO atmosphere. Pd(I) dimer **42** was obtained as a yellow solid in 80% yield.[80] X-ray analysis confirmed the Pd_4 structure where two $[Pd_2(CO)]_2^+$ fragments are connected by two acetate bridges.

Pd(II) dimers containing chelating nitrogen ligands can be reduced by CO to metallic palladium. The reaction proceeds through the formation of a CO-adduct. In 2011 Ragaini and Casati reported the synthesis, isolation and X-ray crystal structure of the CO-adduct resulting in Pd(I) dimer **43**.[81] The formation of dimer **43** was proposed to happen *via* a comproportionation reaction of unreacted $Pd(II)(Bipy)I_2(CO)$ and the unstable $Pd(0)(Bipy)_2$ (formed after reduction of Pd(II) by CO and trace amounts of water). The structure of this dimer differs quite a lot from other members of the family: there are five coordinating groups per Pd atom (two CO, two chelating bipyridine and one iodide). The bond lengths are reported in *Table 2*.

Table 2: Selected bond distances for Pd(I) dimers **28**, **41, 42** and **43**.

Bonds	Pd(I) dimer **28** (Å)	Pd(I) dimer **41** (Å)	Pd(I) dimer **42** (Å)	Pd(I) dimer **43** (Å)
Pd-Pd	2.70	2.76	2.66	2.67
Pd-L$_{edge}$	1.99	1.95		1.91
				2.14
Pd-L$_{ancillary}$	2.37	1.24		2.20
				2.38

As shown in *Table 2* the four dimers exhibit similar Pd-Pd bond lengths and similar Pd-L$_{edge}$ bond distances. The only dichotomy is represented by Pd(I) dimer **43** due to its pentacoordination instead of the tetracoordination mode adopted by the other three dimers.

A theoretical study on complex **28** and analogous Pd(I) dimers was presented by Kalck *et al.* in 2006.[82] Both DFT and highly correlated ab-initio methods were performed to elucidate both the nature of the Pd(I)-Pd(I) bond and that of the diamagnetism observed for complex **28**. CASSCF and CAS+DDCI calculations were performed on the d_{xy} orbitals bearing the two electrons to try to explain the diamagnetism of these complexes. As a results it was shown that the delocalisation along the CO ligand causes the pairing of the two electrons. Moreover, the corresponding HOMO exhibits a nonbonding character between the d_{xy} atomic orbitals of the two Pd atoms but a bonding interaction between the d_{xy} and the π^* orbital of the CO ligand. These results are in agreement with the Hartree-Fock calculations performed by Fenske, (*Figure 10*).[83]
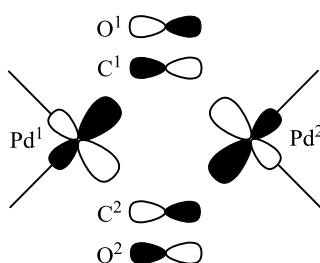
Figure 10: Representation of the HOMO of complex **28**.[82]

1.3.4 Pd(I) dimers bearing rigid bridging ligand: synthesis, structure and bond features

Rigid bridging ligands are good at stabilising weak Pd-Pd bonds. The first Pd(I) dimer belonging to this class of complexes was synthesised by Penfold, Colton *et al.* in 1973.[84] Complex **46** was obtained by mixing [Pd(CO)Cl]$_2$ **44a** and dma **45** in CH$_2$Cl$_2$ under an N$_2$ atmosphere as illustrated in *Scheme 15*.
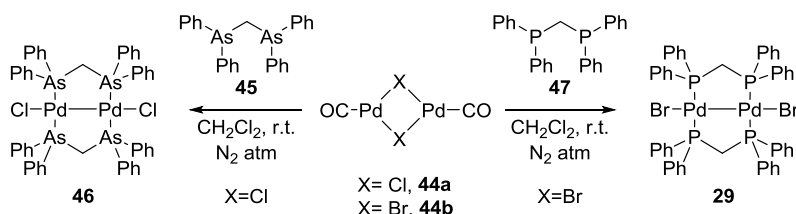
Scheme 15: Synthesis of [Pd(dma)Cl]$_2$ **46** from dma **45** and Pd(I) dimer **44a** (left);[84] synthesis of Pd(I) dimer **29** from Pd(I) dimer **44b** and dppm **47** (right).[85]

The assigned structure of the Pd(I)-Pd(I) motif in the molecule was supported by further research by the same group of chemists in 1976, when they synthsised a Pd(I)-bromo dimer bearing the bidentate phosphine dppm **47**.[85] The analogous procedure to the synthesis of [Pd(dma)Cl]$_2$ **46** was followed, but this time recrystallisation in CH$_2$Cl$_2$/hexane furnished crystals of [Pd(dppm)Br]$_2$ **29** which were suitable for X-ray analysis. The crystal structures showed two Pd atoms bonded to each other through two dppm ligands, the Pd-Pd distance is 2.70 Å and the Pd-P bond lengths are in the range of 2.28-2.29 Å. The two palladium atoms adopts a square planar geometry so that the Pd-P-P-Pd and the Br-Pd-Pd-Br motifs are almost planar. An improved method for the synthesis of Pd(I) dimer **48** was reported by Balch in 1978.[86] In this, the formation of Pd(I) dimer **48** is proposed to occur *via* the comproportionation of Pd(II)Cl$_2$(CNPh)$_2$ and Pd(0)$_2$(dba)$_3$·(CH$_3$Cl). The Pd(I)-bromo dimer **29** analogue is then obtained by mixing the Pd(I)-chloro dimer **48** with an excess of NaBr in CH$_2$Cl$_2$, (*Scheme 16*).
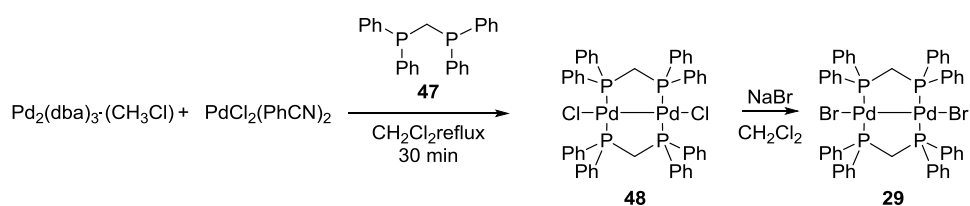
Scheme 16: Synthesis of [Pd(dppm)Br]$_2$ **29** by comproprotionation of Pd(0) and Pd(II) followed by halide exchange.[86]

The ability of complex **29** to insert small molecules such as CO into the Pd-Pd bond caught the attention of many groups. A number of derivatives have been synthesised and characterised by X-ray analysis, (*Figure 11*). Complexes **49**,[87] **50**[88,89] and **51**[90] still present the same dppm core as the Pd(I) dimer **29**. Pd(I) dimers **52** and **53** exhibit a different bidantate ligand, in the Pd(I) dimer **52** the dppm ligands were substituted by dppa, instead in complex **53** the phenyl groups of dppa are substituted with phenoxy ones.[91] In Pd(I) dimer **54** the dppm ligands were substituted with dmpm ones. [92]
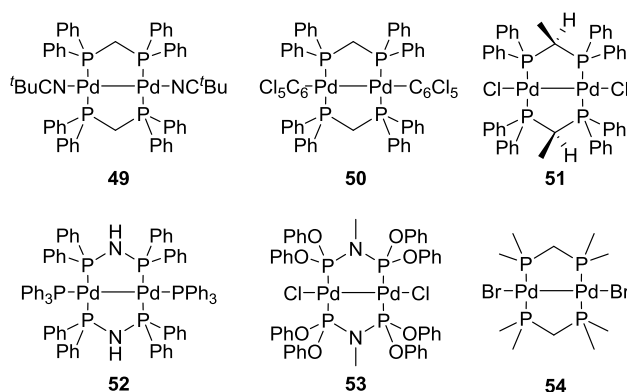
Figure 11: Examples of Pd(I) derivatives of complex **29**.

The change in the nature of the ligand does not influence the geometries of the Pd centres, in all the complexes **49**-**54** the Pd atoms adopt a distorted square planar geometry. The Pd-P and Pd-Pd bond lengths seem to not be influenced by the change in the nature of the ligand, although Pd(I) dimer **52** exhibits a more elongated Pd-Pd bond length compared to the rest of analogous dimers, (*Table 3*).

Table 3: Selected bond distances for Pd(I) dimers **49-54**.

Bonds	Pd(I) dimer **49** (Å)	Pd(I) dimer **50** (Å)	Pd(I) dimer **51** (Å)	Pd(I) dimer **52** (Å)	Pd(I) dimer **53** (Å)	Pd(I) dimer **54** (Å)
Pd-Pd	2.62	2.67	2.57	2.81	2.62	2.60
Pd-P$_{min}$	2.27	2.27	2.29	2.29	2.24	2.27
Pd-P$_{max}$	2.31	2.32	2.32	2.31	2.27	2.29

A series of mixed P-N ligands have been also used for the synthesis of Pd(I) dimeric species. These Pd(I) dimers are usually prepared using a comproportionation reaction between appropriate Pd(II) and Pd(0) complexes.[93,94] The presence of an asymmetric bidentate ligand allows them to exist in two different geometrical isomers: H-H (head-to-head) and H-T (head-to-tail) as shown in *Scheme 17*.
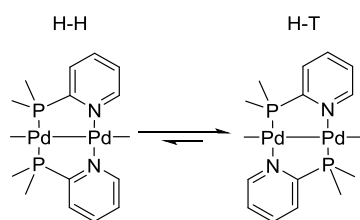
Scheme 17: Isomerisation reaction between H-H and H-T geometrical forms.

The H-H isomers are usually not stable for Pd(I) dimers, although examples of H-H geometries have been reported for Pd(I)-Pt(I) and Pt(I)-Pt(I).[94] One of the few examples of H-H isomers bearing a Pd-Pd bond, complex **55**, was isolated by Bensenyei *et al.* in 2006.[95] They observed that the H-H isomers (kinetic product) is the first one to be formed in solution when the Pd(II) and the Pd(0) source are mixed, although the less stable H-H isomer is fast converted to the more stable H-T isomer (thermodynamic product) in solution. As a consequences, short reaction times and very dilute solutions were shown to favour the formation and isolation of the H-H isomer. In *Figure 12* are reported some examples of H-T complexes with P-N ligand: Pd(I) dimers **56**[96,97], **57**[98] and **58**.[99]
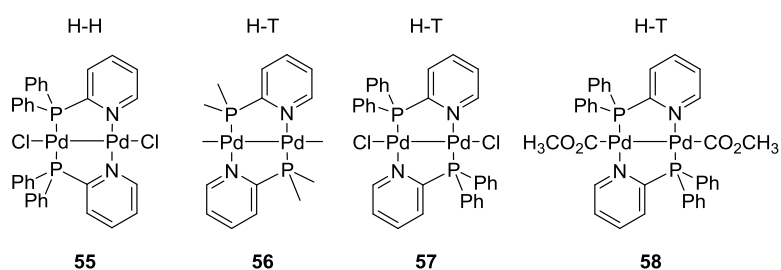
Figure 12: Examples of mixed P-N ligands in Pd(I) dimers.

The geometry adopted by the two Pd atoms is the same for all of the four complexes: distorted square planar. The Pd-Pd bond lengths do not seem to be affect by the change of geometry (H-H *vs* H-T) or by the different substitution on the ligand as illustrated in *Table 4*. However, different bond lengths are observed for the Pd-N and Pd-P bonds for the two geometrical isomers: the H-H isomer exhibits shorter Pd-N and Pd-P bond lengths. On the contrary, the presence of different substituents on the phosphine or in the ancillary ligand for the H-T complexes **55**-**58** does not cause any change in the bond lengths.

Table 4: Selected bond distances for Pd(I) dimers **55**-**58**.

Bonds	Pd(I) dimer **55** (Å)	Pd(I) dimer **56** (Å)	Pd(I) dimer **57** (Å)	Pd(I) dimer **58** (Å)
Pd-Pd	2.56	2.58	2.61	2.58
Pd-N$_{min}$	2.04	2.14	2.11	2.11
Pd-N$_{max}$	2.04	2.16	2.14	2.12
Pd-P$_{min}$	2.28	2.19	2.19	2.19
Pd-P$_{max}$	2.28	2.20	2.20	2.20

The Pd(I) dimers in **59**[100] and **60**[101] represent a borderline example of Pd(I) dimers bearing bridging rigid ligands. One of the two bidentate bridging ligands has been substituted by a single atom bridging ligand, (*Figure 13*).
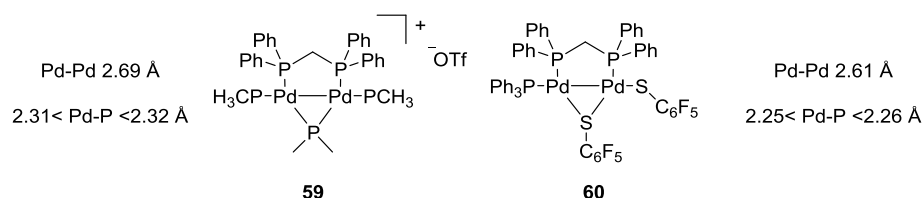
Figure 13: Examples of Pd(I) dimers with a single bidentate ligand.

Due to this asymmetric coordination, the square planar coordination adopted by the two Pd atoms is bigger than in the case Pd(I) dimers bearing two bridging rigid ligands.

1.3.5 Pd(I) dimers bearing rigid bridging ligand: reactivity

The high flexibility of the bridging bidentate ligands confers special characteristics to this family. Small molecules can be inserted into the Pd-Pd bond, which only marginally changes the geometry and the stability of these structures, whilst leaving the Pd_2L_4 core intact. The resulting complexes can be divided into two main categories: A-frame complexes with a single atom inserted into the Pd-Pd bond and A-frame complexes with two atoms inserted into the Pd-Pd bond.[102,103] The insertion usually does not change the formal oxidation state of the two Pd centres, (*Figure 14*).
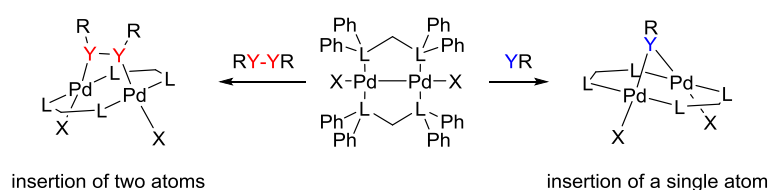
Figure 14: Possible insertion modes of small molecules in Pd-Pd bonds of Pd(I) dimers bridging rigid ligands.[103]

The first example of insertion into the Pd-Pd bond of this types of dimer was reported by Balch *et al.* in 1977.[104] When Pd(I) dimers **29** and **48** were exposed to an over-pressure of

CO, Pd dimers of composition [Pd(dppm)X]$_2$(CO) **C** were obtained, although the binding of CO to the metal was found to be reversible. Insertion into the Pd-Pd bond was also observed when isocyanides were mixed with dimers **29** and **48**, but this time the coordination/insertion was not reversible. X-ray analysis of the RCN-inserted Pd(I) dimer **D** confirmed the presence of the dimeric structure, but the Pd-Pd distance of 3.21 Å (very close to the combined van der Waals radii)[105] is too long to consider the two Pd atoms bonded to each other. The coordination geometry of the two Pd atoms is of distorted square planar complexes with two positions occupied by the P atoms in a *trans* relationship and the last two by the C atoms of the bridging CH$_3$CN molecule and also by the C atom of a non-bridging CH$_3$CN molecule. Encouraged by the possibility of inserting small molecules into the Pd-Pd bond, many groups shifted their attention onto finding new strategies and molecules for this reaction. In 1978, Rattray showed that aryldiazonium salts can be also inserted into the Pd-Pd bond generating type **E** complexes.[106] In the case of this dimer the diazonium salts did not do oxidative addition onto the Pd centres, therefore it was not observe loss of N$_2$ that generally follows the oxidative addition step of aryldiazonium salts onto Pd(0).[107]
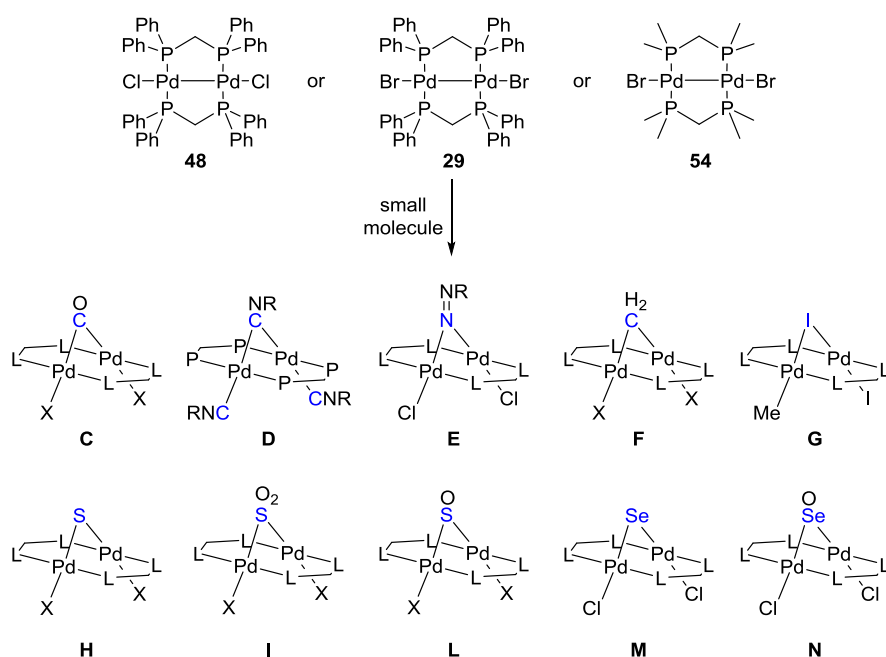
Figure 15: Examples of A-frame Pd dimer-insertion complexes with a single bridging atom resulting from the insertion of small molecules into the Pd-Pd bond of Pd(I) dimer **29**, Pd(I) dimer **48** or Pd(I) dimer **54**.

Pd dimers such as **F** are generated by oxidative addition of CH_2I_2 onto $Pd_2(dppm)_3$. Further protonation of the resulting complex **F** with TFA or HBF_4 allows the formation of complexes of type **G**.[108] Complexes with a sulphur bridge (**H**) can be prepared by reaction of **29** and **48** with elemental S[109] or H_2S,[110] whilst oxidation of complex **H** with peracids or H_2O_2 generates complexes **I** and **L**.[111] However, an alternative and direct way to synthesise complexes of type **I** is to bubble SO_2 through a solution containing Pd(I) dimers **29** and **48**. Reaction of Pd(I) dimer **29** with H_2Se gives the corresponding A-Frame μ-Se dimers. The higher acidity of H_2Se compared to H_2S results in the substitution of one or both of the Cl ions with SeH. Reaction of grey Se with Pd(I) dimer **29** gives the corresponding μ-Se dimer **M** without exchange of the two Cl ions. Further oxidation of **M**-type dimers with *t*BuOOH gives the **N**-type dimers. Reaction of Pd(I) dimer **54** or its Cl-analogues with Br_2 or Cl_2 respectively gives the face-to-face Pd(II) dimer **O**, whilst the reaction of the I-analogue with I_2 generates Pd(II) complexes of type **P**, (*Figure 16*).[112]
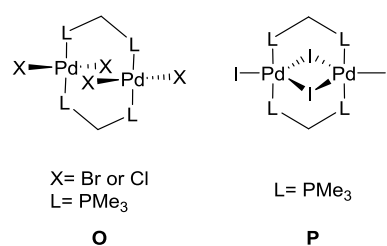
Figure 16: Pd(II) dimer generated from the addition of X_2 to Pd(I) dimer **54** and the Cl- and Br-analogues.[112]

The insertion of small molecules into the Pd-Pd bond is not limited to a single atom but there are also examples of insertion of two atoms. Reaction of Pd(I) dimers with acetylene that is bearing electron-withdrawing groups such as -CF_3 and –CO_2CH_3 gives complexes of types **Q** and **R**[113] respectively, as illustrated in *Figure 17*.
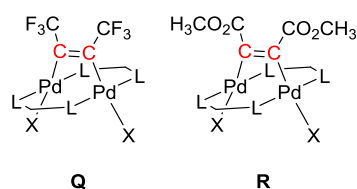
Figure 17: Examples of insertion of two C atoms into the Pd-Pd bond.[113]

Pd(I) dimers **22** and **39** do not react with acetylenes that do not possess electron-withdrawing groups.[114]

An interesting example of dinuclear reductive elimination using this category of Pd(I) dimers was reported by Stille in 1985.[115] Reaction of Pd(I) dimer **48** with 1 equivalent of trimethylaluminium gave the intermediate **61** which could not be isolated. Reaction with ethanol at −78 °C generated complex **62** that at ambient temperature spontaneously reductively eliminates CH_4, as shown in *Scheme 18*.
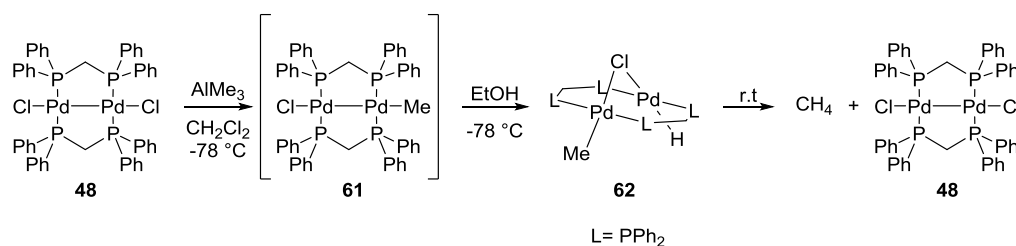
Scheme 18: Example of dinuclear intramolecular reductive elimination.[115]

1.3.6 Pd(I) dimers bearing bridging allyl ligands

Pd(I) dimers belonging to this category have a common feature: the coordination to the Pd-Pd involves only the three C atoms of the allylic moiety, although there are some cases with a different coordination mode at the Pd centres.

Pd(I) dimers bearing bridging allyl ligands are the most studied class of Pd(I) dimers in the last decades. The interest surrounding these dimers is mainly due to the fact that some of them have been shown to be efficient precatalysts in cross-coupling reactions.[116,117] Allyl Pd(I) dimers can be divided into two main categories: *(a)* Pd(I) dimers bearing two bridging allyl ligands, *(b)* Pd(I) dimers bearing a single bridging allyl ligand and one bridging halide, CO_2 or SR ligand, (*Figure 18*).
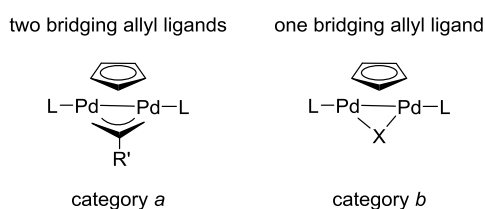
Figure 18: Representation of the two categories of Pd(I) bridging allyl ligands.

The two categories present different reactivity towards electrophiles such as CO_2, HCl or MeI. Pd(I) dimers bearing two bridging allyl groups react with CO_2 whilst Pd(I) bearing only one bridging allyl group does not react at all with electrophiles.[118] To understand the reason for the different reactivity of the two categories of Pd(I) dimers, DFT calculations were performed by Hazari *et al.* on category *a* and *b* employing the hybrid functional M06-2X along with the LANL2DZ basis set for Pd and the 6-31G++(d,p) basis set for all other atoms. The results show that for category *b* the HOMO of the Pd(I) dimers is located at the central atom of the allyl group and along the two Pd atoms. For category *a* the HOMO is located on the terminal C of the allyl ligand as a consequence of an out-of-phase combination of the π_2 orbitals of the bridging allyl ligand and the Pd 5_p orbitals. This interaction is responsible for the nucleophilic behaviour of Pd(I) dimers belonging to category *a*. These results were also confirmed by Wang, Green and Hazari in 2012.[119]

1.3.6.1 Pd(I) dimers bearing two bridging allyl ligands: synthesis, structure and bond features

The first well-characterised Pd(I) dimers of this family were presented by the group of Allegra in 1965.[120] The Pd(I) dimer **63** was simply formed by reaction of $AlCl_3$, Al metal and $PdCl_2$ in refluxing benzene. In 1970 the same group showed that in the presence of substoichiometric amounts of the $AlCl_3$, Pd(I) dimer **64** is formed instead of **63**, (*Scheme 19*).[121]
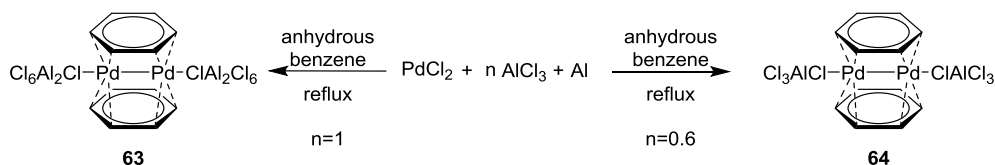
Scheme 19: First synthesis of Pd-Pd dimers bearing π ligands.[121]

X-ray analysis of the two dimers reveals some differences between the two structures, especially in the orientation of the two benzene rings. In the case of complex **64** the two rings are not symmetrically attached to the Pd-Pd moiety,[121] as illustrated in *Figure 19*.

$Cl_6Al_2Cl-Pd\overline{\quad\quad}Pd-ClAl_2Cl_6$ $\quad\quad$ $Cl_3AlCl-Pd\overline{\quad\quad}Pd-ClAlCl_3$

63 $\quad\quad\quad\quad\quad\quad\quad\quad\quad\quad\quad\quad$ **64**

Figure 19: View from the side of Pd(I) dimer **63** and Pd(I) dimer **64**.

Despite the differences in the coordination of the two unsaturated molecules these dimers exhibit the same Pd-Pd bond length of 2.57 Å, the same Pd-Cl bond lengths of 2.45 Å and Pd-C bond lengths in the range of 2.20-2.25 Å.

Five different types **I-V** of Pd(I) dimers with two allyl bridges have been synthesised and characterised since 1975, (*Figure 20*).

Figure 20: Classification of Pd(I) dimers bearing two bridging allyl ligands.

The first Pd(I) dimers of type **I** were reported by Werner *et al.* in 1975.[122] The scope of the reaction was subsequently extended to other allyl bridging and other phophines ligands in 1977.[123] These Pd dimers with oxidation state +1 were obtained from the reaction of Pd(II) with an appropriate ligand as shown in *Scheme 20*.

Scheme 20: First synthesis of type **I** Pd(I) dimers bearing two bridging allyl ligands.[123]

The crystal structures of compounds **54** and **55** both show two dimeric Pd(I) complexes with Pd-Pd bond lengths of 2.68 and 2.69 Å respectively, as well as an almost linear P-Pd-Pd-P group (176°) for complex **65** but a slightly more distorted Pd-Pd-P (166.9° and 173.2°) plane for compound **66**. The Pd-P bond lengths are 2.30 and 2.21 Å respectively.

The allyl bridging ligand binds through all three C centres to the Pd-Pd system with the central carbon showing bonding interactions with each of the metals. In these structures it is not clear how the cyclopentadiene (Cp) moiety is coordinated to the metal. Werner later suggested, based on the analysis of the solid state structure, that the Cp group is trihapto-bonded to the Pd-Pd and not pentahapto-bonded. Cp therefore binds only through the three carbons, there is no interection between the Pd-Pd bond and the other two aromatic C atoms. The two bridging groups adopt a *syn* arrangement, as reported in *Figure 21*.[124]
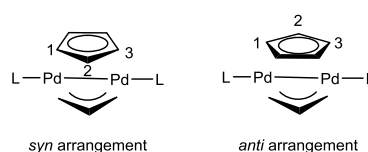
Figure 21: Representation of the two possible arrangements for the two bridging ligand: *syn* (left) and *anti* (right). The numbers refer to the 3 C atoms responsible for the binding of the Cp moiety to the Pd-Pd bond.

A series of improved strategies have been developed in the last 38 years.[125,126] The main contributions have been made by Werner *et al.*[127] and Hazari *et al.*[128,129] for the synthesis of more sensitive Pd(I) dimers bearing different allyl and cyclopentadienyl moieties, (*Scheme 21*).
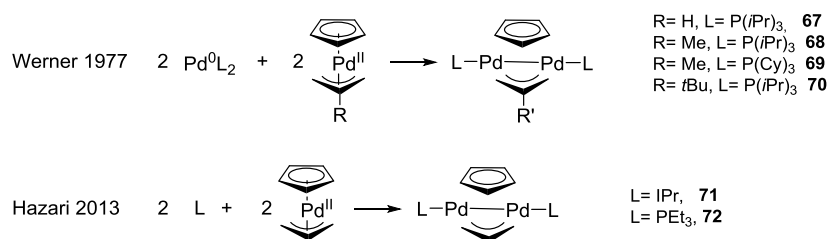
Scheme 21: Reported methodologies for the syntheses of Pd(I) dimers bearing a Cp and an allylic bridges.

Werner made a large contribution to the development of methodologies for the synthesis of this class of dimers. He is also the pioneer in the field of the type **II** Pd(I) dimers. Between 1977 and 1979 he reported the first syntheses of Pd-Pd moieties coordinated in a sandwich-like fashion by two symmetrical allyl groups *via* a comproportionation reaction of Pd(II) **73** and Pd(0)L$_2$.[127,130] An alternative and more efficient route for the synthesis of type **II** Pd(I) dimers was reported by Hazari *et al.* in 2011, (*Scheme 22*).[131]
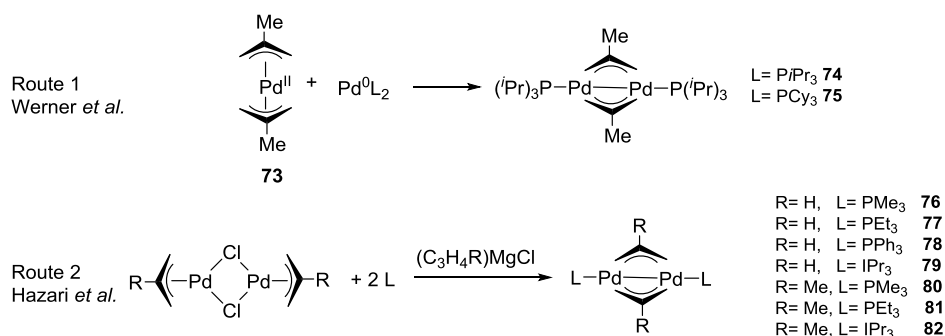
Scheme 22: First syntheses of type **II** Pd(I) dimers.[127,130,131]

Other contributions to the library of type **II** Pd(I) dimers have been reported by Turner *et al.*,[132] Jolly *et al.*,[133,134] Hazari *et al.*[118,128] and Wang, Hazari, Green,[119] following one of the two synthetic routes (1 or 2), as reported in *Figure 22*.
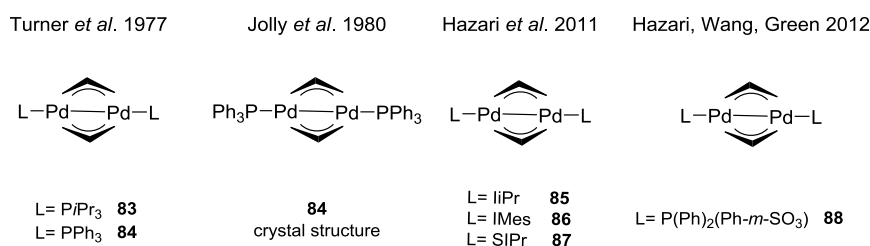
Figure 22: Examples Pd(I) dimer of type **II**.

X-ray analysis of compounds **83**, **84** and **85** showed that L-Pd-Pd-L is not linear, with a L-Pd-Pd angle in the range of 147-152°, 147-155° and 144-149° and Pd-Pd bond lengths of 2.72, 2.77 and 2.70 Å respectively. The two allyl bridges adopt a *syn* arrangement and the coordination to the Pd-Pd moiety involves all three C atoms, although only the central carbon atom is bonded to both Pd-atoms.

As well as these first two classes of Pd(I) dimers, Werner was also a pioneer in the preparation of type **III** Pd(I) dimers.[135-137] Pd(I) dimers **89**-**95** were obtained by mixing $(Cl(L)Pd(II))_2(\mu\text{-}CH_3COO)_2$ and TlC_5H_5 in benzene. In 2013 Hazari *et al.* reported a new methodology for the synthesis of type **III** Pd(I) dimers. Pd(I) dimer **99** was obtained by mixing $(\eta^3\text{-Ind})Pd(IPr)Cl$ **96** and lithium indenyl **97** to a THF solution containing $(\eta^1\text{-Cp})(\eta^5\text{-Cp})Pd(IPr)$ **98**,[129] the two procedures are illustrated in *Scheme 23*.

Scheme 23: Methodologies reported for the synthesis of type **III** Pd(I) dimers.

For complexes **92** and **99** X-ray analysis revealed that the nature of the ancillary ligand does not change the main structural features of type **III** Pd(I) dimers. The P-Pd-Pd motif is almost planar at 175.45° and 173.77° respectively. Interestingly, in both crystal structures the two Cp moieties are in an *anti* arrangement parallel to each other.

Table 5: Selected bond distances for Pd(I) dimers **92** and **99**.

Bonds	Pd(I) dimer **92** (Å)	Pd(I) dimer **99** (Å)
Pd-Pd	2.67	2.68
Pd-C$_{min}$	2.17	2.15
Pd-C$_{max}$	2.22	2.19

The synthesis and X-ray analysis of type **IV** Pd(I) dimers was described for the first time by Yamamoto *et al*. in 1993.[138] Compounds **100-102** were obtained by reaction of PdCl$_2$(RCN)$_2$ with lithium indenyl **97** in benzene, (*Scheme 24*).

Scheme 24: First synthesis of type **IV** Pd(I) dimers.[138]

The crystal structures of complexes **100** and **101** showed the two Pd-Pd atoms with two bridging indenyl ligands and two ancillary isocyanide ligands. The planes of the two indenyl ligands are not parallel to each other but instead are wedge-shaped and in a *syn* arrangement. The dihedral angle between the two indenyl planes is 66.5°. Another

interesting characteristic of these indenenyl ligands is that the coordination to the Pd-Pd only involves the three allylic carbons of the five-membered ring, and the Pd-C distances to the phenyl moiety are too long to be considered bonds.

Table 6: Selected bond distances for Pd(I) dimers **100** and **101**.

Bonds	Pd(I) dimer **100** (Å)	Pd(I) dimer **101** (Å)
Pd-Pd	2.65	2.66
Pd-C_{CNR}	1.95	1.95
	1.97	1.96
Pd-C_{In}	2.17	2.16
	2.20	2.19

In 2013 Hazari reported an alternative methodology for the synthesis of a new type **IV** Pd(I) dimer. Pd(II) dimer **103** was first mixed with IPr ligand, and lithium indenyl **97** was subsequently added to the reaction mixture, (*Scheme 25*).[129]
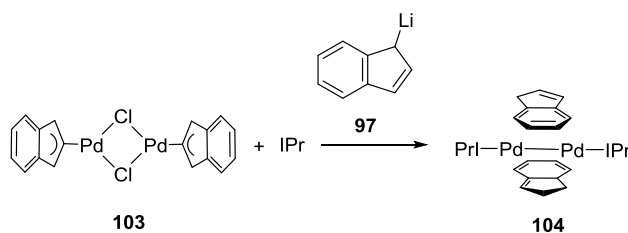
Scheme 25: Alternative synthesis of a type **IV** Pd(I) dimer as developed by Hazari *et al.*[129]

Complex **104** has also been characterised by X-ray analysis and surprisingly the two bridging indenyl groups adopt an *anti* conformation, probably due to the high steric demand of the IPr ligand. As a consequence of the steric hindrance of the NHC ligand the Pd-Pd bond length (2.69 Å) is longer than in dimers **100** and **101**. Also, in this case the coordination to the Pd-Pd bond does not occur *via* the aromatic ring. Attempts to prepare Pd-Pd complexes bearing PPh$_3$ and PEt$_3$ as ancillary ligands were unsuccessful with both methodologies.

Type **V** Pd(I) dimers also called "sandwich" complexes, represent a borderline example of *category a* complexes. Usually for bridging allyl dimers the coordination to the Pd-Pd bond only involves three C atoms of allyl, Cp and indenyl ligands. In the case of type **V**

Pd(I) dimers coordination to the two metals usually involves four C atoms of the aromatic system. It is actually this extended coordination that allows these systems to form the otherwise unstable Pd(I)-Pd(I) bond. Most of the examples reported of this type of Pd(I) dimers are cases of complexes being isolated unexpectedly as intermediates of other transformations. For example, in a work performed by Pfeffer in 1989,[139] an attempt to show that it was possible to selectively form heterocyclic compounds by the reaction of cyclopalladated complexes with internal alkynes, Pd(I) dimer **107** was isolated from the reaction mixture, (*Scheme 26*).
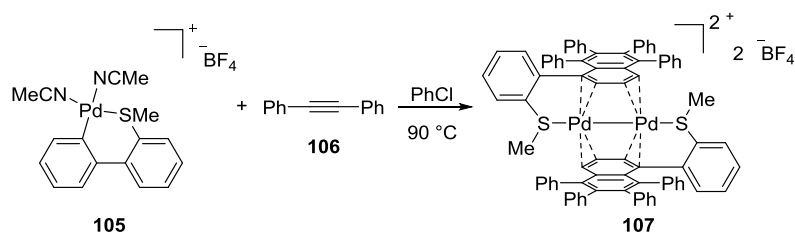
Scheme 26: Synthesis of complex **107** by reaction of the cyclopalladated complex **105** with alkyne **106**.[139]

The X-ray structure of Pd(I) dimer **107** exhibits a Pd-Pd bond (2.26 Å) which is μ-η^4-coordinated by the two substituted naphthyl rings. The two groups adopt an *anti* arrangement.

Other examples of these type **V** Pd(I) dimers were reported by Kloo *et al*. who described the synthesis of the first Pd-Ga complexes with aromatic rings as bridging ligands.[140-142] Also, in 2005 Barder *et al*. reported a Pd-Pd "sandwich" complex with Buchwald's ligand X-phos.[143] In 2013, Agapie *et al*. reported the synthesis of dipalladium complexes with terphenyl diphosphine ligands, which are able to coordinate different aromatic molecules at the bridge position.[144] Murahashi meanwhile reported a series of Pd(I) dimers coordinated by pyrroles and indoles,[145] as illustrated in *Figure 23*.
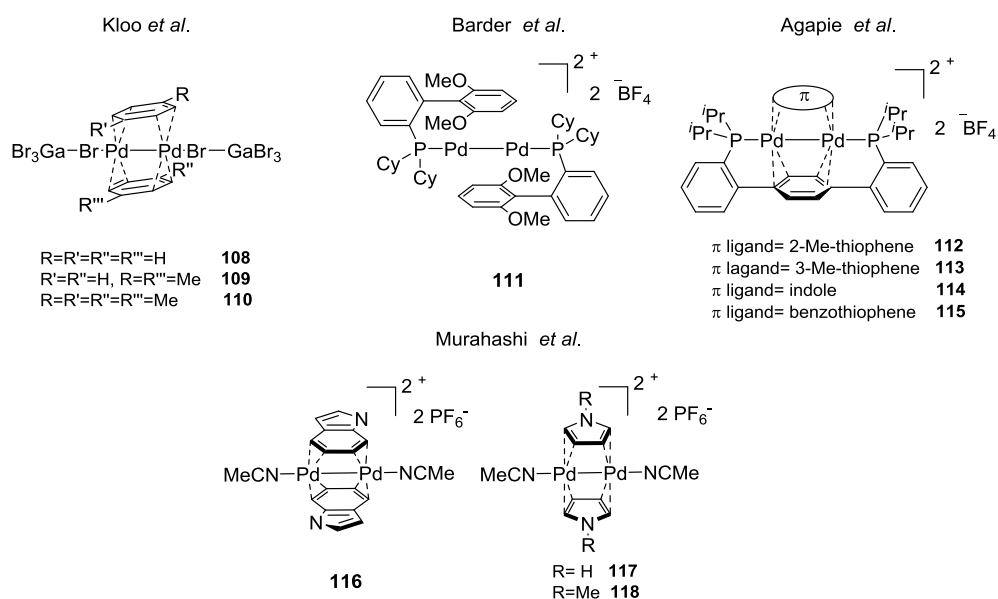
Figure 23: Examples of Pd(I) dimers type **V**.

All the compounds shown in *Figure 23* were suitable for X-ray analysis. Pd-Pd bond lengths are, as expected, quite different due to the presence of different bridging and ancillary ligands, as illustrated in *Table 7*.

Table 7: Selected Pd-Pd bond leangths for complexes **108-118**

Pd(I) dimer	Pd-Pd bond length (Å)	Pd(I) dimer	Pd-Pd bond length (Å)
108	2.57	**114**	2.71
109	2.60	**115**	2.72
110	2.58	**116**	2.58
111	2.70	**117**	2.48
112	2.71	**118**	2.48
113	2.69		

The bridging ligands in these complexes are mostly η^4-coordinated to the Pd-Pd moiety. However, complexes **112** and **115** exhibit a μ-η^3-coordination mode which is very similar to those of the Cp and indenyl systems. The coordination for non-symmetric systems, such as **109**, **116**, **117** and **118**, tends to follow an *anti* arrangement.

1.3.6.2 Pd(I) dimers bearing two bridging allyl ligands: reactivity

In the previous section summary of the synthetic routes for the preparation of categoriy *a* of Pd(I) dimers has been presented. The next section will deal with their role in transition-metal mediated transformations and in catalysis.

Pd(I) dimers belonging to category *a* behave as nucleophiles due to the previously described out-of-phase combination of the π_2 orbitals of the bridging allyl ligand and the Pd 5_p orbitals. Werner *et al.* were responsible for exploring the reactivity of these Pd(I) dimer towards different types of molecules. These Pd(I) dimers can mainly undergo two different types of reactions: *a)* reactions in which the bimetallic system is split into two monomeric units and *b)* reaction in which the Pd-Pd bond stays intact.[137,146] The reaction with MeI and I_2 causes the cleavage of the Pd-Pd bond to generate two monomeric complexes, whilst the reaction with HCl only causes the scission of the Pd-Pd for dimers bearing ancillary phosphine ligands. Instead, carboxylic acids and thiols react with these Pd(I) dimers, displacing one of the two bridging allyl molecules to form Pd(I) dimers with one bridging allyl and one bridging carboxylate or thiolate ligand, as illustrated in *Scheme 27*.
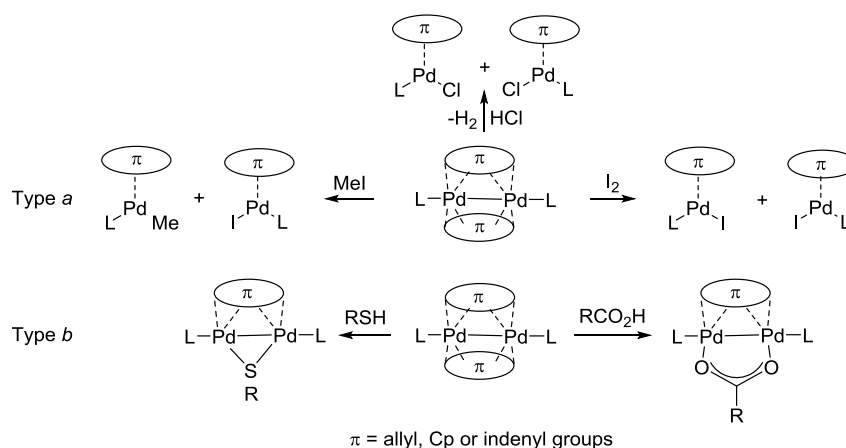
Scheme 27: Example of type *a* and type *b* reactions involving category *a* Pd(I) dimers.

An interesting feature concerning type *b* reactions is that in the presence of type **I** Pd(I) dimer with one bridging allyl and one Cp ligand, the reaction with carboxylic acids and thiols always results in the loss of the Cp molecule, (*Scheme 28*).
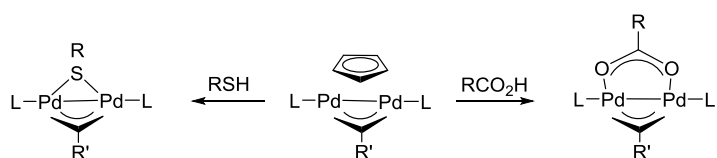
Scheme 28: Reaction of type **I** Pd(I) dimers with carboxylic acid and thiols.

Type **II** Pd(I) dimers were the first dimers containing allyl bridging ligands to show direct reactivity of the allyl ligand with CO_2 to form a bridging carboxylate. Hazari *et al.* showed that the rate of insertion of CO_2 is dependent on the nature of the R group of the allyl moiety (2-methylallyl react faster than the non-substituted allyl) and on the nature of the ancillary ligand (the insertion with NHC ligand is faster than the insertion in the presence of phosphine ligand). The insertion of CO_2 is only possible on one of the two allylic groups, the second insertion does not even occur at elevated pressure of CO_2, (*Scheme 29*).[116,131]
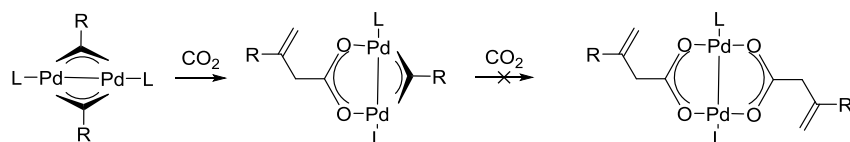
Scheme 29: Reaction of type **II** Pd(I) dimers with CO_2.[116]

Some mechanistic hypotheses have been posed, but the mechanism of insertion of CO_2 remains unclear. One hypothesis concerns the possibility of the bridging allyl moiety to open and to attack the CO_2, whilst an alternative pathway for species bearing weakly coordinated ligands could involve the dimer splitting into both a Pd(0) and Pd(II) species, the latter of which can react with CO_2 before recombining with the Pd(0) species to form monocarboxylated bridged dimers.

Hazari *et al.* showed that type **II** Pd(I) dimers **119-121** are efficient catalysts for the carboxylation of allylstannanes and allylboranes, (*Scheme 30*).[131]

Y= *n*Bu₃Sn, Me₃Sn or (pinacol)B

L= IiPr   85
L= IMes   86
L= SIPr   87
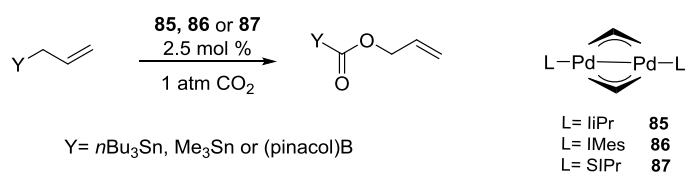
Scheme 30: Carboxylation of allylstannanes and allylboranes with type **II** Pd(I) dimer bearing NHC ancillary ligands.[131]

In the previous sections we have shown that Pd(I)-dimers are mainly used in stoichiometric amount. The example reported by Hazari *et al.* is one of the first examples of use of a Pd(I) dimers in catalysis, although it is not clear if this dimer act as a catalyst or as a precatalyst. In the first case this would represent one of the prime example of direct catalysis by a Pd(I) dimer.

Most of the reactions of category *a* concern the transformation of these dimers in category *b* Pd(I)dimers.

1.3.6.3 Pd(I) dimers bearing a single allyl bridge ligand: synthesis, structure and bond features.

This category is characterised by the presence of a single allyl bridging ligand. Discoveries of these Pd-Pd complexes is usually made in parallel to that of the analogous Pd(I) dimers with two bridging allyl ligands. Most of the compounds can be prepared by simple reaction of category *a* dimers with appropriate compounds, such as carboxylic acids. The first step of the transformation requires the protonation of the allylic group, followed by reaction of the carboxylate with the Pd-Pd moiety.
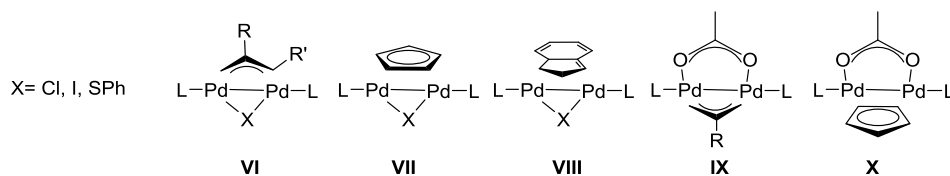
Figure 24: Examples of the five different types of Pd(I) dimers bearing a single bridging allyl ligand.

The first to introduce type **VI** Pd(I) dimers with one bridging halide were Kobayashi *et al.* in 1972.[147] They reported the synthesis and crystal structure of $[(\mu\text{-}C_3H_5)(\mu\text{-I})Pd_2(PPh_3)_2]$ **120** from the reaction of $[(\eta\text{-2-}CH_3\text{-}C_3H_5)(\mu\text{-I})Pd]_2$ **119** and an excess of PPh_3. Other methodologies for the synthesis of halide-bridged Pd(I) dimers were reported by Werner *et al.* in 1977 where a Pd(I) dimer was generated *via* comproportionation of $[(\eta\text{-2-}CH_3\text{-}C_3H_5)(\mu\text{-X})Pd]_2$ and $Pd(0)L_2$,[127] and by Hazari *et al.* in 2011 where the type **VI** Pd(I) dimer was obtained by reaction of HCl with type **II** Pd(I) dimers.[118]
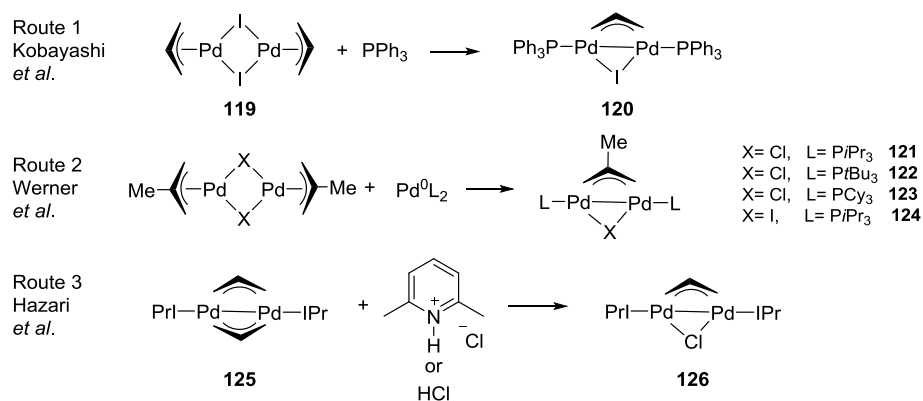
Scheme 31: Reported routes for the synthesis of type **VI** Pd(I) dimers with bridging halides.

Important contributions to the library of type **VI** Pd(I) dimers were reported by Sieler *et al.* in 1987 which described an analogue of complex **120** with bridging Cl instead of I.[148] Milstein *et al.*,[149] Shauganessy and Colacot,[150] and Green, Hazari and Wang[119] described three different Pd(I) dimers bearing asymmetric phosphine as ancillary ligands, whilst Kurosawa *et al.*[151] and Hazary *et al.*[117] reported Pd(I) dimers with different substituents on the allylic system, (*Figure 25*).
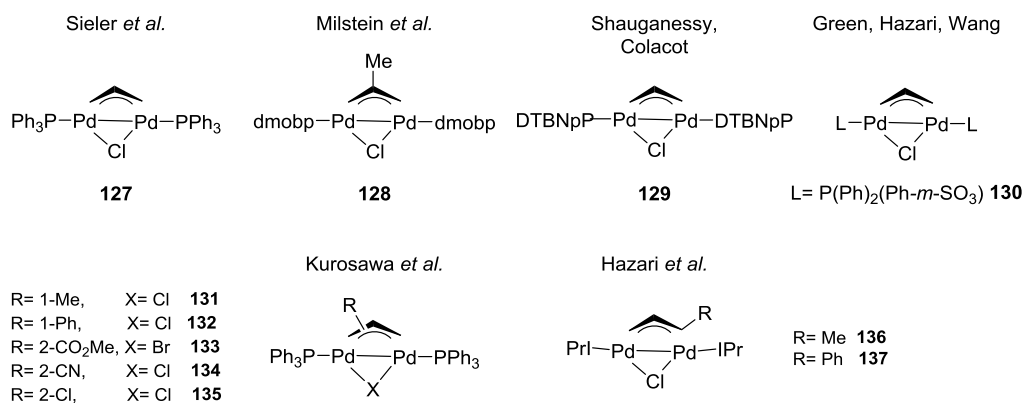
Figure 25: Examples of reported type **VI** Pd(I) dimers bearing a bridging chloride ligand.

X-ray analysis of these Pd(I) dimers reveals that the Pd-Pd and Pd-L bond lengths are very similar for complexes bearing ancillary phosphine ligands and slightly shorter values are observed in the case of Pd(I) dimers bearing NHC ancillary ligands.

Parallel to the development of type **VI** Pd(I) dimers with one bridging halide ligand there was also interest in developing Pd-Pd complexes with different bridging groups such as

SR, OR and SeR. Yamamoto *et al.* reported that allyl thiols can react with: 1) Pd(0)L$_2$ species generating a Pd(II) complexes that can comproportionate with unreacted Pd(0)L$_2$ or 2) *in situ* generated Pd(0) complex **142** to give Pd(I) dimeric species.[152-155] In 1995 Kurosawa *et al.* proposed an alternative methodology for the synthesis of these Pd(I) dimers bearing one bridging thiol or selenol, as illustrated in *Scheme 32* equiv (3).[151,156]
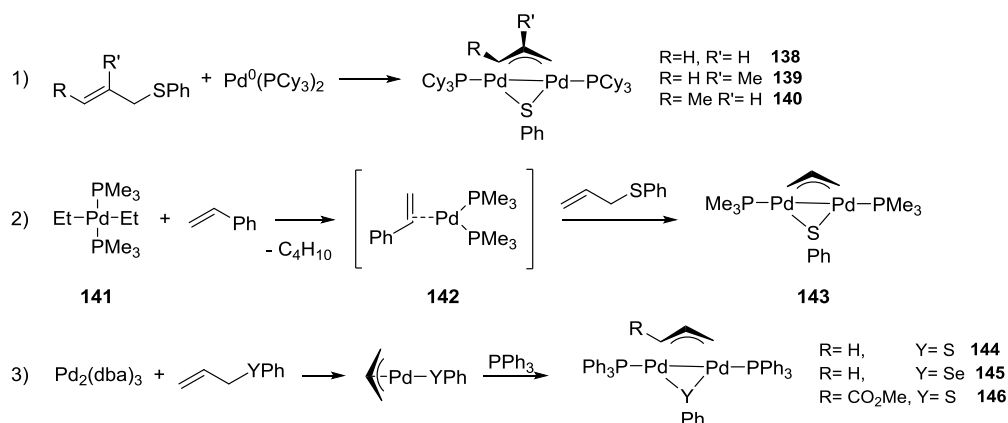
Scheme 32: First reported syntheses of Pd(I) dimers bearing bridging thiol and selenol ligands.

X-ray analyses of complexes **143** and **146** show that the Pd-Pd and the Pd-P bond lengths and the Pd-P ones are very similar to the ones reported for bridging halides complexes.

The first methodologies for the preparation of **VII** Pd(I) dimers type were described by Turner *et al.* in 1975-77.[157] They reported that monomeric Pd(II)-complex **A** reacts with reducing agents to give Pd(I) dimers **147-151**. Later, Werner *et al.* reported that: *a)* the reaction of type **III** Pd(I) dimers with a specific class of substrates can generate a variety of type **VII** Pd(I) dimers[136] and *b)* comproportionation of Pd(II) complex **155** with Pd(0)L$_2$ generates Pd(I) dimers with single bridging halides.[158,159] (*Scheme 33*).
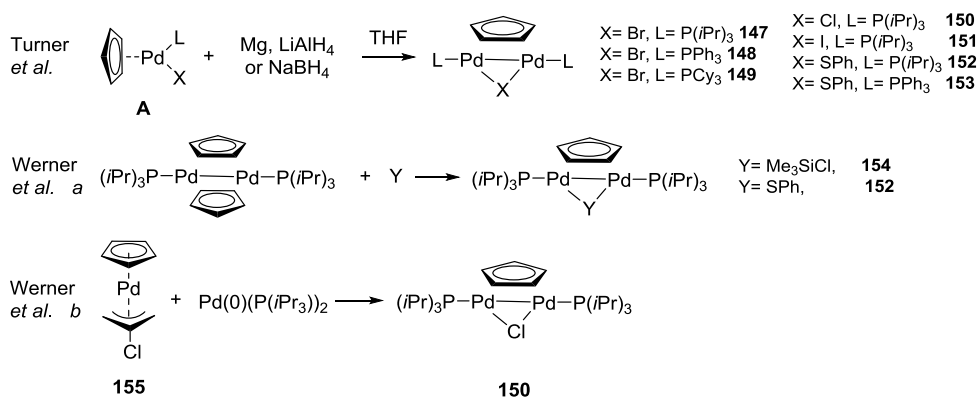
Scheme 33: Reported syntheses of type **VII** Pd(I) dimers.

The only crystal structure available for these Pd(I) dimers is of compound **147**. The structure shows a Pd-Pd complex with two ancillary *i*-propyl ligands and the bridging positions are occupied by a Cp group and a Br atom. The P-Pd-Pd-P plane is almost linear and the Pd-Pd bond length is 2.61 Å.

The first synthetic methodologies for type **VIII** Pd(I) dimers were reported in 2006 by Zargarian *et al.*, more than 30 years later than the allyl and Cp analogues. Pd(I) dimers **156** and **157** where first isolated by chance as products of decomposition of the monomeric complex **B**, and subsequently different methods for their preparation were proposed by Zargarian *et al*, (*Scheme 34*).[160]
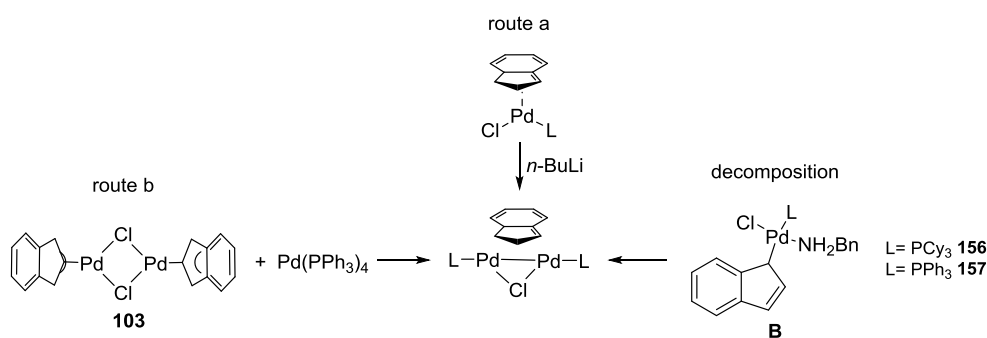
Scheme 34: Methodologies for the synthesis of type **VIII** Pd(I) dimers as reported by Zargarian *et al*.[160]

X-ray analysis of the two dimers showed that the structure of these complexes is very similar to that of the type **IV** dimers, in terms of the bonding of the indenyl ligands (μ-η^3-coordination) and the Pd-Pd bond length (2.60 Å).

The first examples of type **IX** Pd(I) dimers were reported by Werner *et al*. They proposed two possible methodologies for the synthesis of these dimers: a) *via* a comproportionation reaction of Pd(II) and Pd(0)L$_2$ species;[161] b) *via* reaction of type **I** Pd(I) dimers and carboxylic acids.[137] In 1981 Yamamoto *et al*. reported that formation of type **IX** Pd(I) dimers can occur *via* the addition of phosphine ligand to the monomeric Pd(II) complex **163**.[162] A particularly interesting example of formation of these carboxylated-bridge dimers was reported by Hazari *et al*. in 2011.[118,131] They showed that it is possible to insert CO_2 directly into the allyl moiety, as shown in *Scheme 35*.
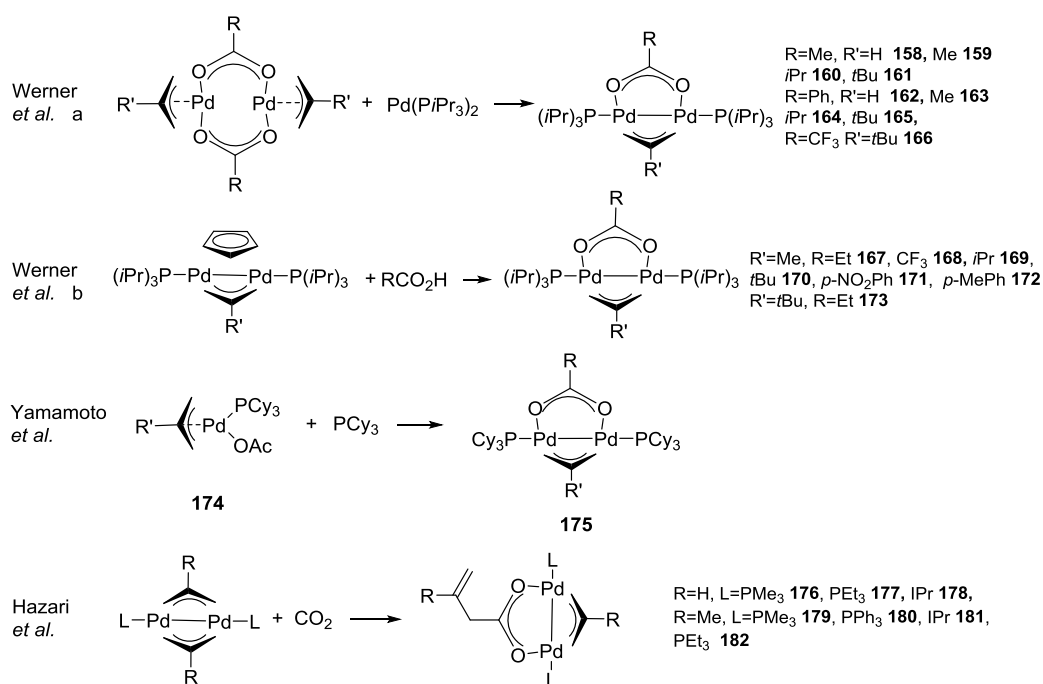
Scheme 35: Reported syntheses of type **IX** Pd(I) dimers.

X-ray analysis of dimers **177-179** showed that the carboxylic groups are μ-η^2-coordinated to the two Pd atoms through the two terminal oxygen atoms, and the substituents on the carboxylate moiety are oriented in the opposite direction compared to the bridging allyl ligand. The P-Pd-Pd planes are almost planar and the Pd-Pd bond lengths are 2.66, 2.64 and 2.63 Å respectively.

The final type of Pd(I) dimers were synthesised by Werner *et al.* by simply mixing type **III** Pd(I) dimers with carboxylic acids, as shown in *Scheme 36*.[136,137]
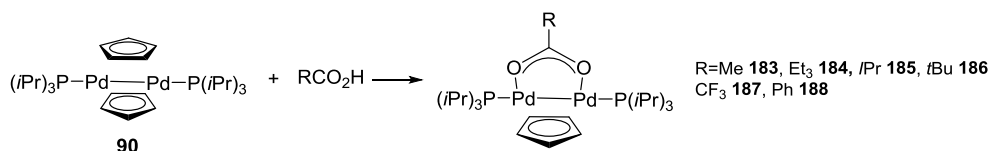
Scheme 36: Reported synthesis of type **X** Pd(I) dimers.

1.3.6.4 Pd(I) dimers bearing a single allyl-bridge ligand: reactivity.

Category *b* Pd(I) dimer bearing a single allyl-bridge ligand have found widespread use as precatalysts in cross-coupling reactions. The reason for the success of these dimers as

precatalysts is presumably due to their easy of formation of the real active catalytic species of the reaction a 12-electron Pd(0)L,[163] although the mechanism that leads to its formation is still not clear.

One of the first examples of the use of category *b* Pd(I) dimers in catalysis was reported by Milstein in 2004.[149] Pd(I) dimer **128** was employed in Suzuki cross-coupling reactions of aryl chlorides and phenyl boronic acids. At 40 °C the rate of reaction for Pd(I) dimer **128** is higher compared to the one of the Pd(0)L$_2$ **192** analogue, as shown in *Scheme 37*.
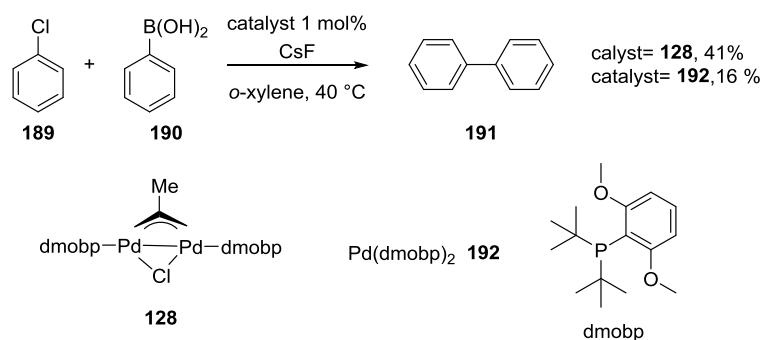
Scheme 37: Suzuki coupling of chlorotoluene **189** with phenylboronic acid **190** as reported by Milstein *et al.*[149]

The reason for this enhanced reactivity of the Pd(I) was hypothesised to be due to the ease for this catalyst to form the 12-electron Pd(0)L species compared to Pd(0)L$_2$, where the dissociation of the ligand is a high energy process.

Subsequently, Denmark *et al.* reported the use of Pd(I) dimer **122** for the coupling of five-membered heterocyclic silanolates with aryl bromides. The reaction proceeds smoothly in toluene at 50 °C giving good to excellent yields and a broad reaction scope.[164,165] Moore *et al.* also gave their contribution to the use of Pd(I) dimer **122** in cross-coupling reactions. The precatalyst was used for the coupling of aryl bromides and iodides with alkynes in the presence of ZnBr$_2$ to form *m*-phenylene ethynylene oligomers, or for the Sonogashira coupling of phenylacetylene and aryl bromides in the presence of ZnCl$_2$.[166,167]
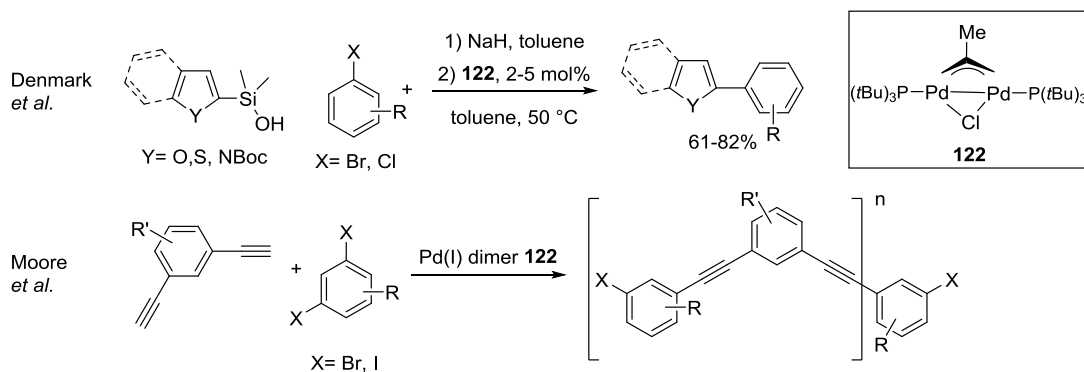
Scheme 38: Use of Pd(I) dimer as precatalyst, as reported by Denmark *et al.* (top), and by Moore *et al.* (bottom).[164,166]

In 2010 Shaughnessy and Colacot reported the use of Pd(I) dimer **129** for the α-arylation of propiophenone with aryl bromides and chlorides.[150]
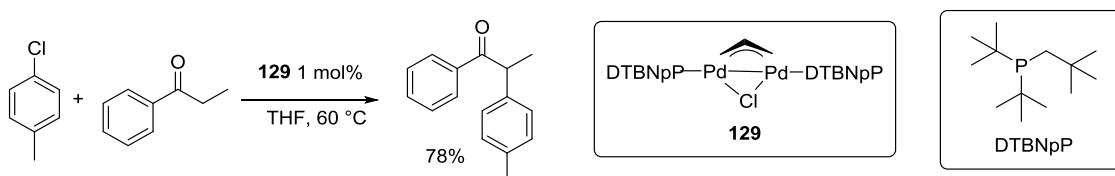
Scheme 39: α-arylation of propiophenone with 4-chlorotoluene in the presence of Pd(I) dimer **129**, as reported by Shaughnessy and Colacot.[150]

1.3.7 Pd(I) dimers with single atom bridges: synthesis, structure and bond features.

The last category of this big family of Pd(I) dimers is represented by Pd(I) dimers bearing two bridging single atom ligands. This category is not as broad as the one of bridging allyl dimers and the limitation is mainly due to the electronic and especially steric properties of the ligand as described in more detail later in this chapter. Despite this, it represents one of the most utilised and studied categories of Pd(I) dimers due to the great efficiency of these dimers to act as precatalysts in a series of cross-coupling reactions.[168]

The first synthesis of these type of dimers was reported by Mingos *et al.* in 1996.[169,170] Crystals of complexes **31** and **193** were obtained by reaction of $Pd_2(dba)_3$, $PtBu_3$ and the corresponding haloform CHX_3, as illustrated in *Scheme 40*.

$$Pd_2(dba)_3 \quad + \quad 2 \;\; P t Bu_3 \quad + \quad 1/2 \;\; CHX_3 \quad \longrightarrow \quad (tBu)_3P-Pd\overset{X}{\underset{X}{\diamond}}Pd-P(tBu)_3 \quad \begin{matrix} X= Br \;\; \mathbf{31} \\ X= I \;\;\; \mathbf{193} \end{matrix}$$
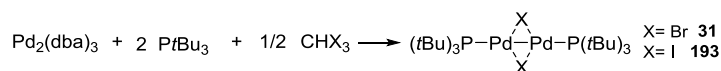
Scheme 40: Synthesis of the first Pd(I) dimers with two single atoms bridges.[169]

The X-ray structures of the two complexes show Pd-Pd dimers with two bridging Br or I ligands with very acute Pd-X-Pd angles (63.8° and 62.4° respectively). The Pd atoms adopt a trigonal coordination geometry instead of the usual square planar, and Pd-Pd bond lengths are 2.62 and 2.70 Å respectively.

The two procedures were subsequently used by Hartwig *et al.*[171] and Vilar *et al.*[172] for the synthesis of new complexes: [PdBr[P(1-Ad)(tBu)_2]]_2 **195** and [PdI[P(Ph)(tBu)_2]]_2 **197**, (*Figure 26*).
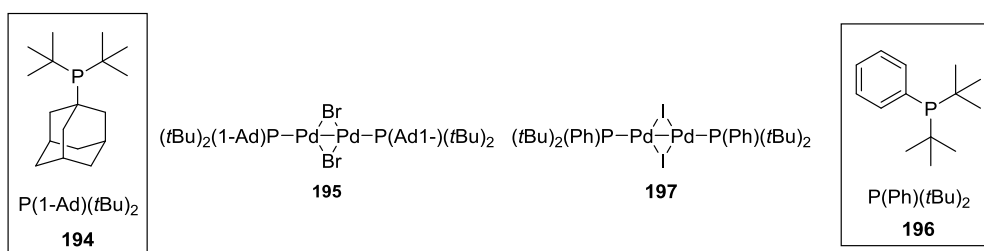
Figure 26: Examples of Pd(I) dimers bridged by two single atoms.

An interesting study on the factors (bulkiness of the ligand and ability of the halide to stabilise a bridge structure) that can influence the formation of Pd(I) dimer with two single atoms was reported by Vilar *et al.* in 2006.[172] In the attempt to synthesise new dimers with different ancillary ligands they found out that when [P(Ph)(tBu)_2] **196** is used as ligand, two completely different structural Pd(I) dimers can be obtained depending on the halide. The reaction of Pd[P(Ph)(tBu)]_2 **198** with Pd(COD)Br_2 does not give the expected Pd(I) with two Br atoms occupying the bridging positions but instead gives Pd(I) dimer **199** with the two Br atoms occupying the ancillary positions and the two phosphine ligands bridging such that P is bound to one Pd and the other Pd atom interacts through μ-η^2-coordination at the phenyl ring. The reaction of Pd[P(Ph)(tBu)]_2 **198** with CHI_3 instead gives the expected single atoms bridges dimer **197**, (*Scheme 41*).
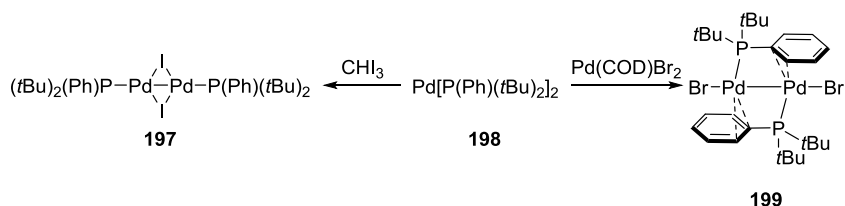
Scheme 41: Synthesis of dimers **197** and **199** by Pd[P(Ph)(*t*Bu)]$_2$ **198**.[172]

A detailed survey of the potential energy surface shows that for Br the µ-halide bridged-geometry is less stable than the bridged phosphine one (ΔE = 2.2 kcal mol^{-1}), whilst a different outcome was found for I (ΔE = –4.4 kcal mol^{-1}). They proposed that the switch between the two isomers is probably due to steric interactions between the phosphine ligand and the halide.

1.3.8 Pd(I) dimers with single atom bridges: reactivity.

Pd(I) dimers **31** and **193** were reported by Mingos and Vilar to react with a number of small molecules such as CO, H$_2$, alkynes and nitriles to give a series of Pd$_4$ clusters; monomeric Pd hydride complexes; polymers; and corner sharing dimers, respectively.[169,173] Interestingly, Pd(I) dimer **193** was found to be less reactive than the Br-analogue **31**.[174] Pd(I) dimer **31** can also react with oxygen to generate the oxo-complex **200**, formed after O=O bond scission, intramolecular C-H activation and C-O bond formation. This compound decomposes rapidly in solution, although it is slower in the solid state, giving cyclopalladated Pd(I) dimer **201**,[175] as illustrated in *Scheme 42*. Pd(I) dimer **193** was also exposed to oxygen but no oxo-complex intermediate was detected. This confirms once again the higher stability of this dimer in comparison to the Br-analogue **31**.
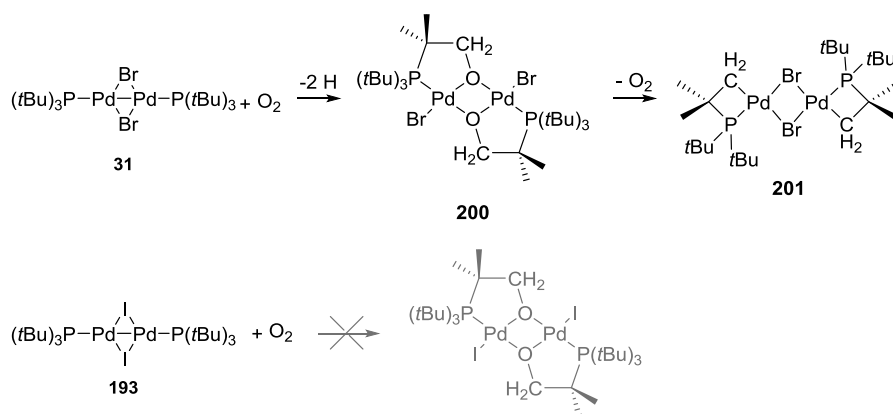
Scheme 42: Reaction of Pd(I) dimer **31** and Pd(I) dimer **193** with O$_2$.[175]

This category of Pd(I) dimers has found widespread use for their ability to react as precatalysts in cross coupling reactions. As in the case of the Pd(I) allyl and Cl bridging dimers, the reason for this success could be due to the ability of these precatalysts to generate a 12-electron Pd(0)L complex, which is presumed being the real active catalytic species. The mechanism of the formation of the monoligated Pd(PtBu$_3$) species is still not clear. Many catalysts bearing bulky phosphine and NHC ligands, including Pd(I) dimers **195** and **197**, have been specifically designed to have a Pd:ligand ratio of 1:1 in order to form unsaturated Pd(0)L species that readily undergo oxidative addition.[31,176-183]

The first use of Pd(I) dimers **31** and **195** as a source of Pd(0)L in cross-coupling reactions was reported by Hartwig *et al.* in 2002. These catalysts were used in both the amination reaction of aryl chlorides and bromides and also the Suzuki coupling of hindered aryl bromides, (*Scheme 43*).[171]
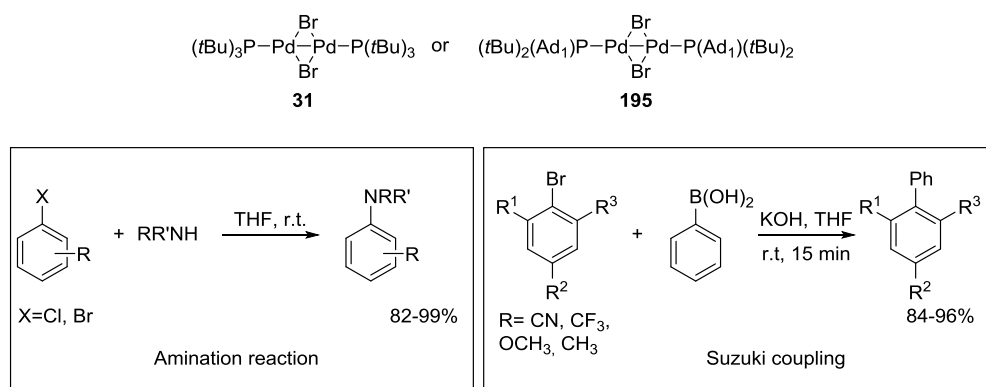
Scheme 43: Example of an amination reaction and a Suzuki coupling where Pd(I) dimers **31** and **195** are used as precatalysts.[171]

The potential shown by Pd(I) dimer **31** to act as a precatalyst in the formation of C-N and C-C bonds drove many groups to explore its application in various coupling reactions as summarised in *Scheme 44*. Prashad *et al.* have used this commercially available dimer **31** for the synthesis of challenging substrates such as hindered N-alkyl-substituted diarylamines. The rate of reaction of this catalyst was shown to be superior to that of other catalyst systems such as Pd(OAc)$_2$ and binap; Xantphos; DPEphos; or P*t*Bu$_3$.[184] In 2007 Huang *et al.* used this catalyst for the α-vinylation of carbonyl compounds with vinyl bromides, tosylates and triflates, in the presence of LHMDS as base.[185] Also in this case the performance of dimer **31** has been shown to be superior to the combination of Pd$_2$(dba)$_3$ with Qphos; Xphos; Sphos; or Xantphos. Hartwig *et al.* also reported the successful use of this catalyst in the Reformatsky reaction of vinyl and aryl bromides with zinc enolates of amides to form α-vinyl or aryl amides.[186] Subsequently the scope of the reaction was increased to also include zinc enolates of esters with aryl bromides bearing a wide range of functional groups, for the formation of α-aryl esters.[187] For the majority of the substrates the zinc enolates are formed *in situ* from α-bromo amides or esters and the reaction can be carried out at ambient temperature. Hartwig *et al.* also presented the α-arylation of esters using aryl bromides and chlorides in the presence of an alkali base such as LiNCy$_2$ and NaHMDS.[188,189]
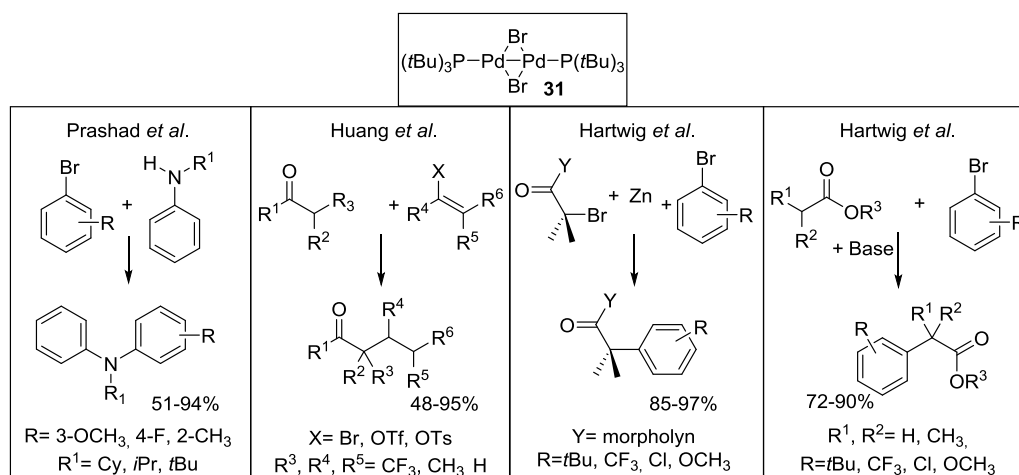
Scheme 44: Examples of reactions where Pd(I) dimer **31** is used as precatalyst.

A successful example of C-S bond formation using Pd(I) dimer **31** as precatalyst was reported by Stambuli *et al.* in 2009.[190] In general, strategies for the formation of C-S bonds using Pd-based catalysts fail due to the facile displacement of the bulky phosphine ligand

by the thiolate group. In this reaction Zn plays a special role: due to its very high affinity for sulphur, Zn coordinates to thiols better than Pd, therefore avoiding coordination of the thiols to the Pd. The organo-Zn can then undergo facile trasmetallation with the LPd(II)(Ph)(X) complex formed upon oxidative addition of the aryl halide to the Pd. The coupling of alkyl thiols proceeds smoothly at ambient temperature, however higher temperatures are required for the coupling of aryl thiols.

Ryberg *et al.* reported a cyanation reaction of aryl bromides in the presence of Pd(I) dimer **31** as precatalyst. The reaction requires the use of $Zn(CN)_2$ as the cyanide source and can be carried out on a 10 kg scale.[191]

Bercot and Caille described the diasteroselective α-arylation of 4-substituted cyclohexyl esters with aryl halides and pseudo-halides. The reaction proceeds smoothly at ambient temperature in the presence of strong Li-bases.[192] Recently Gooßen *et al.* described the use of Pd(I) dimer **31** as a precatalyst in the conversion of allylic esters into enol esters.[193] Transition metal-mediated isomerisation of allyl esters is not a thermodynamically favoured process due to the possibility of the metal inserting into the C-O bond of the esters to form stable carboxylate bridged complexes. Pd(I) dimer **31** was shown to easily isomerise allylic esters and the catalyst does not undergo side reactions such as cleavaging of the C-O bond of the resulting product.
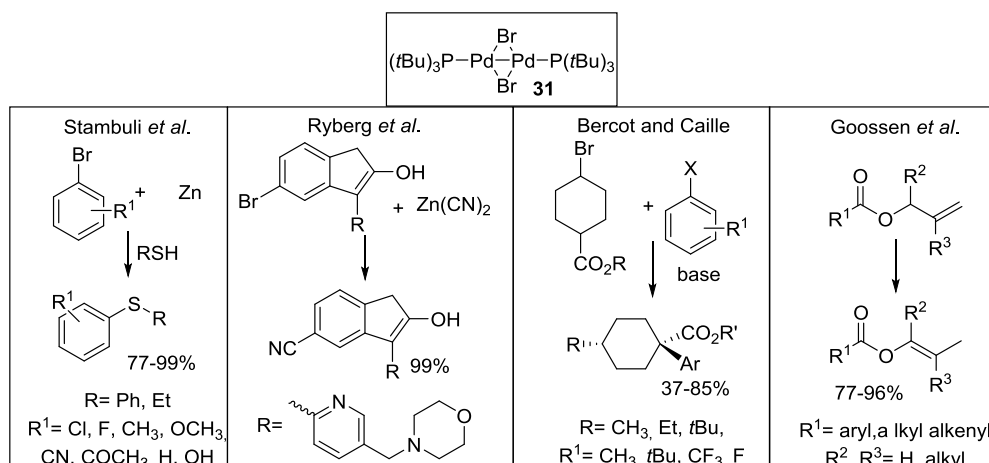
Scheme 45: Other xamples of reactions where Pd(I) dimer **31** is used as precatalyst.

Presumably, due to its higher stability Pd(I) dimer **193** has not found broad applicability in catalysis in comparison to the Br-analogue **31**. The only example in which this dimer is as used as catalyst/precatalyst was reported by Vilar *et al.* in 2011 for the aminocarbonylation

of aryl bromides and iodides.[194] The use of this catalyst allowed the aminocarbonylation reaction to be completed in less than 10 minutes at 150°C. Same result was not possible to achieve with other catalytic system such as Pd(PPh)$_4$ or Pd(PtBu$_3$)$_2$ (46% vs 88%) , whilst similar conversions could be achieved using Pd(I) dimer **31**, (*Scheme 46*).
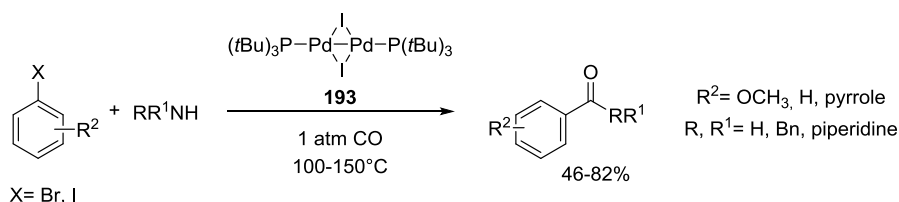
Scheme 46: Aminocarbonylation reaction of aryl halide in the presence of Pd(I) dimer **193**.[194]

In all the previous example Pd(I) dimers **31** and **193** exhibited high potential as precatalysts in many different transformations.

1.4 Other oxidation states of Pd-Pd dimers

1.4.1 Pd(0)-Pd(0) dimers

There are few examples in the literature of Pd(0)-Pd(0) dimers due to the fact that d^{10} centres have a closed filled shell and the generation of the d^{10}-d^{10} needs special requirements. However, if there are unfilled orbitals on one Pd atom which are close enough in energy to filled orbitals on another Pd atom, then this can generate a bonding interaction between the two centres if the overlap between the two orbitals is great enough. There is the possibility for these systems to undergo a rearrangement in the MOs so that some bonding and antibonding MOs can be converted into other bonding and antibonding MOs. Extended Hückel calculations using Pt$_2$(PH$_3$)$_4$ as a model concluded that in this system the bond is generated from the overlap of a vacant p orbital of one Pt atom and a filled d orbital of the other Pt atom.[195]

The first example of this category of dimers was reported in the early 1970s by Stern *et al.*, in which they described the synthesis and properties of Pd$_2$(dppm)$_3$ **203**, as well as its potential as a catalyst in the hydrogenation of olefins.[196] Complex **203** was synthesised by

mixing $(PPh_3)_2Pd_2Cl_2$ with $Ph_2PCH_2PPh_2$ **47**, followed by reduction with hydrazine, (*Scheme 47*).
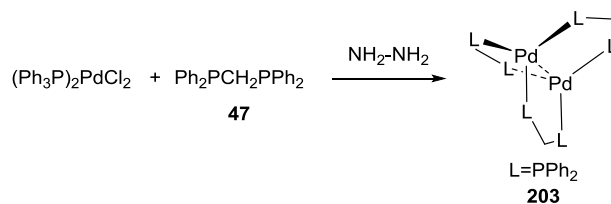
Scheme 47: Synthesis of Pd(0) dimer **203** from $(PPh_3)_2Pd_2Cl_2$ and phosphine ligand **47**.[196]

The crystal structure of complex **203** was reported almost 20 years later by Eisenberg *et al.* It exhibits two trigonally coordinated Pd(0) atoms bridged by three dppm ligands. The Pd-Pd bond length is 2.96 Å, which is long compared to the ones reported for Pd(I) dimers.[197] In addition to its use as hydrogenation catalyst, Pd(0) dimer **203** was also used as a building block for the formation of Pd(I) dimers and A-frame complexes, as shown in *Scheme 48*.[103,108,198]
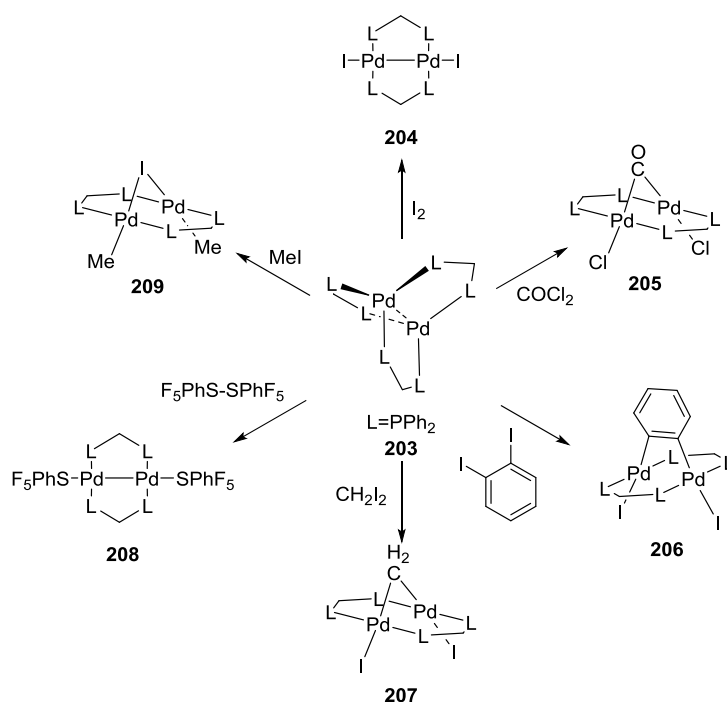
Scheme 48: Examples of reactions involving the Pd(0) dimer **203**.

In 1993 Fink *et* al. reported that irradiation of complex **210** with UV light of wavelength 254 nm readily generates Pd(0) dimer **211**, which showed high sensitivity towards aerobic conditions, (*Scheme 49*).[199]
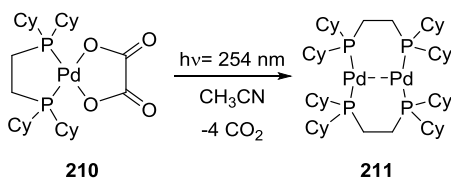
Scheme 49: Photoinduced formation of Pd(0) dimer **211**.[199]

The solid structure of complex **211** exhibits two bonded Pd atoms separated by a distance of 2.76 Å, shorter than that Pd$_2$(dppm)$_3$ **203**. In solution, complex **211** is not very stable and it exists in equilibrium with its monomeric monoligated Pd(0) form. The existence of this equilibrium is supported by the fact that it reacts with small molecules to generate mainly complexes containing only one palladium centre, as illustrated in *Scheme 50*.[199]
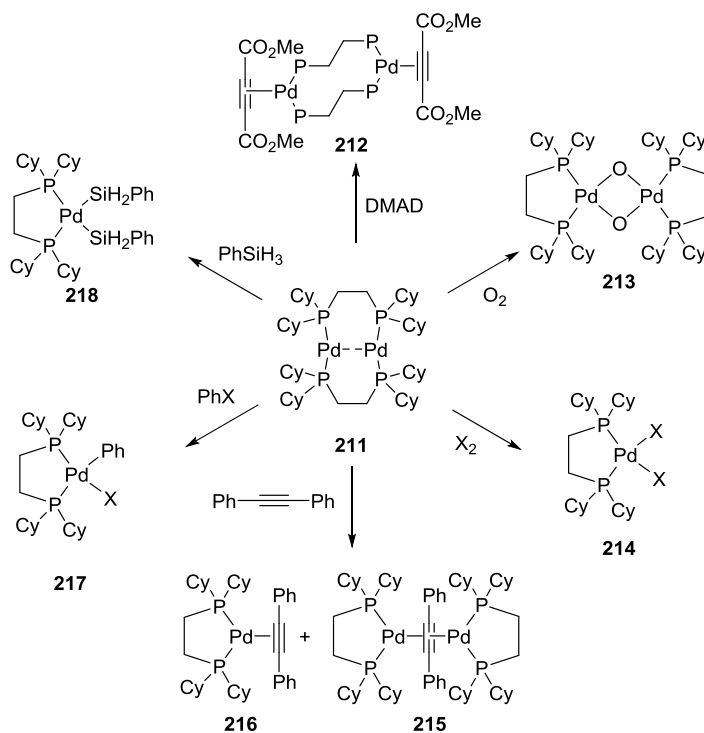
Scheme 50: Examples of reactions involving Pd(0) **211**.[199]

The possibility of having an equilibrium between the monomeric and dimeric forms inspired Fink *et al.* to explore the possibility of forming mixed phosphine Pd(0) dimer. Dimer **211** was mixed with the *i*Pr-analogue **219**, which was synthesised in the same way as **211**, to obtain the mixed phosphine Pd(0) dimer **220**, (*Scheme 51*).[200]
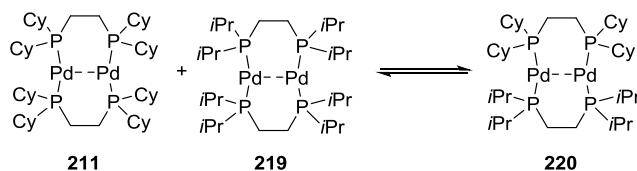
Scheme 51: Synthesis of mixed phosphine Pd(0) dimer **220** from dimer **211** and **219**.[200]

In 1999 Pörschke *et al.* reported two examples of a Pd(0) dimer: **223** and **224**. Complex **223** was also characterised by X-ray diffraction and it represents one of the first examples of the structure elucidation of a bimetallic Pd-complex coordinating a single molecule of CO. Pd-complex **221** reacts with an excess of CO to generate the Pd-dicarbonyl complex **222**. Application of vacuum to this compound allows the removal of one molecule of CO and the formation of Pd(0) complex **223**. In solution complex **223** slowly loses CO to generate the other Pd(0) dimer, **224**, (*Scheme 52*).[201]
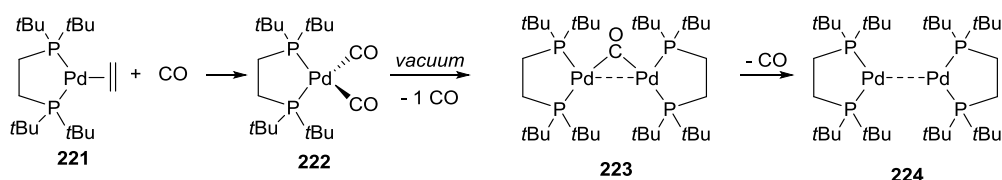
Scheme 52: Formation of Pd(0) dimers **223** and **224**.[201]

The solid structure of complex **223** shows a coplanar P-Pd-Pd-P plane with a Pd-Pd distance of 2.74 Å, which again is short compared to the one of Pd(0) dimer **203**, but in accordance with the one of dimer **211**.

A few years later, Fink *et al.* reported another example of a Pd(0) dimer, this time bearing dppm ligands.[202] Reacting (tmeda)PdMe$_2$ complex **225** in the presence of bidentate ligands such as **226** forms the air stable and very strained dimethyl Pd-complex **227**. This complex reductively eliminates ethane at 65 °C to give the Pd(0) dimer **228**, (*Scheme 53*).
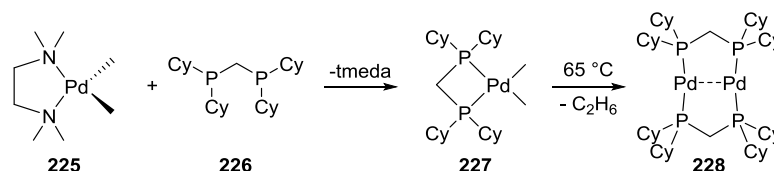
Scheme 53: Synthesis of Pd(0) dimer **228** from Pd(II) **225** and bidentate phosphine **226**.[202]

The X-ray structure of Pd(0) dimer **228** shows that the two bidentate ligands are twisted relative to each other at an angle of approximately 45°. The Pd-Pd bond distance is 2.86 Å, which is slightly longer than the dcpe analogue **211**. An analogous Pd(0) dimer with dotpm instead of dcpe was reported by Shelby *at al.* in 2010. The solid structure of complex **230** shows two Pd(0) atoms separated by a distance of 2.86 Å. Each Pd atoms is tri-coordinated with two dotpm ligands and the third coordination site is occupied by the other Pd(0) atom.[203] The P atoms are not in the same plane but instead twisted with an angle of 13.8° to minimise the steric interactions between the *o*-tolyl groups. The complex is synthesised by reduction of Pd(II) complex **229** with *n*-BuLi, and can easily undergo oxidative addition with C-Cl bonds. As illustrated in *Scheme 54*, this complex undergoes facile oxidative addition of CH_2Cl_2 to form the A-frame complex **231**.
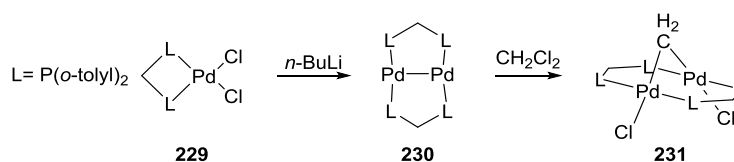
Scheme 54: Synthesis and reactivity of complex **230**.[203]

Yamamoto and Itoh reported an example of a Pd(0) dimer bearing alkenyl ligands.[204] The structure of complex **234** was confirmed by X-ray analysis and shows two Pd(0) atoms tetracoordinated with two benzoquinone ligands and one norbornene ligand each. The fourth coordination site is occupied by the bond with the other Pd(0) atoms, with a Pd-Pd bond length of 2.94 Å. Each *p*-benzoquinone is η^2-coordinated to each of the Pd atoms, whereas the norbornene ligand is η^2-coordinated to only one Pd atom. The Pd(0) dimer **234** was obtained by mixing $Pd_2(dba)_3$ with an excess of *p*-benzoquinone **232** and norbornene **233**, as illustrated in *Scheme 55*.

Pd₂(dba)₃ + **232** + **233** → **234**
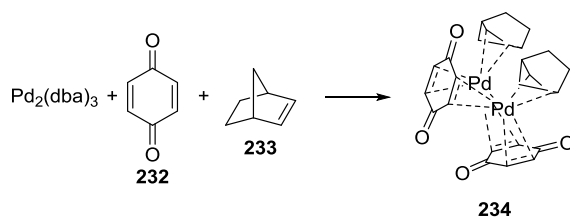
Scheme 55: Synthesis of Pd(0) dimer **234**.[204]

1.4.2 Pd(II)-Pd(II) dimers

Examples of d^8-d^8 Pd dimers are rare in the chemistry literature. The electronic configuration of the palladium in these dimers ($\sigma^2\pi^4\delta^2\delta^{*2}\pi^{*4}\sigma^{*2}$) suggests that the complexes should not have a metal-metal bond due to the cancellation of the four filled bonding orbitals with the four filled antibonding orbitals.[205] However, as in the case of Pd(0) dimers, the possibility to rearrange some of the MOs to generate new bonding and antibonding MOs allows the formation of Pd-Pd bond interaction. Some examples of Pd(II) dimers **235**,[206] **236**,[207] **237**,[208] **238**[209] and **239**[210,211] have been reported between late 1970s and early 1980s, (*Figure 27*).

| **235** | **236** | **237** | **238** | **239** |
| 2.94 Å | 2.56 Å | 2.74 Å | 2.55 Å | 2.82 Å |
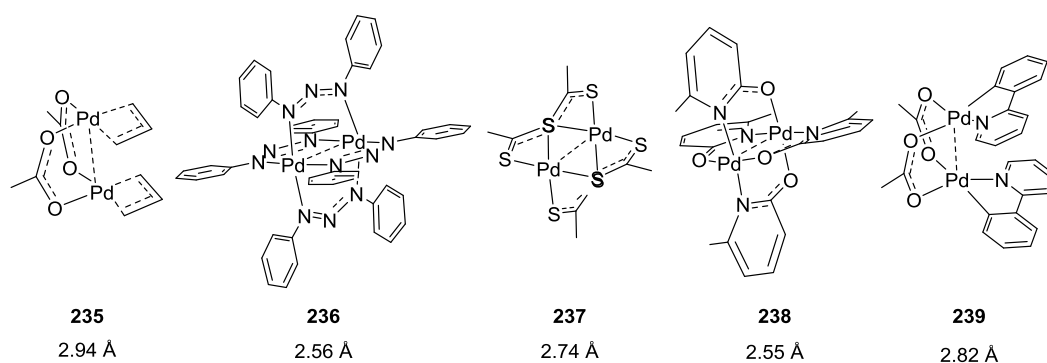
Figure 27: Early examples of Pd(II) dimers and their respective Pd-Pd bond lengths.

The complexes present Pd-Pd bond distances which are smaller than the sum of the van der Waals radii of 3.26 Å,[105] but unfortunately the lack of appropriate physical data for these complexes did not give any information about the presence of a Pd-Pd bond. Theoretical studies have also shown mixed results. In 1988 Cotton *et al.* reported that there is no-bonding between the two Pd atoms based on SCF-Xα-SW calculations using

$[Pd(NH_2CH_2NH_2)_2]_2$ as a model compound.[205] On the contrary Che *et al.* reported that weak and attractive Pd-Pd interactions in the ground state can be calculated at the MP2 level of theory on the model compound $[\textit{trans}\text{-}Pd(CN)_2(PH_3)_2]_2$.[212] A few years later Zhang *et al.* reported the same results using $[Pd_2(CN)_4(PH_2CH_2PH_2)_2]$ as a model compound, also at the MP2 level of theory and with TDDFT.[213]

A crystal structure analysis combined with photophysical, electrochemical, DFT and AIM computational studies reported by Gray *et al.* on systems **239** and the analogous Pd(II) derivatives **240**-**242** allowed to gain more insight into the nature of the Pd(II)-Pd(II) bond interaction, (*Figure 28*).[211]

239   **240**   **241**   **242**
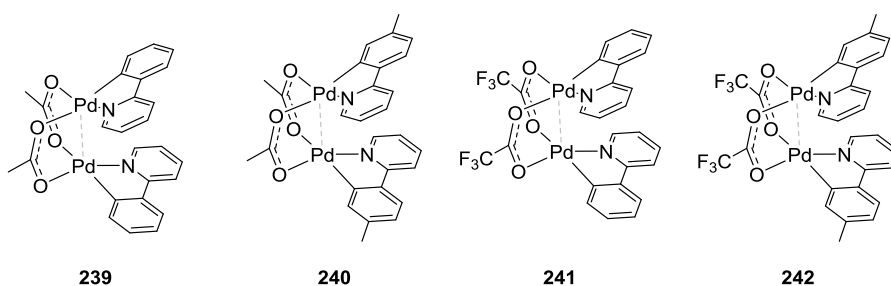
Figure 28: Pd(II) dimers used by Gray *et al.* in their study.[211]

The decision to study these systems was due to the fact that these complexes do not adopt a planar geometry but rather an open "clamshell" one, with the two acetate bridges perpendicular to the Pd-Pd bond. The reason for this different geometry was believed to be a consequence of both the π-stacking interactions between the two phenylpyridine ligands and also the d^8-d^8 bond interactions. Complexes **243** and **244** were used as reference for the electrochemistry and photophysics experiments, the Pd-Pd bond distance of complex **243** (of 3.64) is too long to show d^8-d^8 interactions, (*Figure 29*).

243   **244**
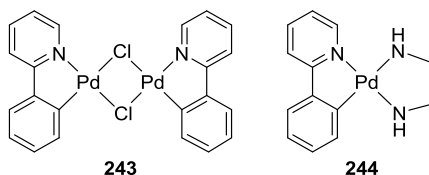
Figure 29: [(2-Phenylpyridine)Pd(μ-Cl)]$_2$ **243** and [(2-phenylpyridine)-Pd(en)][Cl] **244**.[211]

Cyclic voltammetric experiments concluded that the nature of the substituent on the acetate units strongly influence the oxidation potential of the complexes (380 mV for **242** *vs* 1180 mV for **244**). The oxidation potential of **239** and **240** is lower than that of complex **243**. Absorption profiles for complexes **239-242** showed intense absorption bands at wavelengths shorter than 350 nm, attributed to the π–π^* intraligand transitions, the visible absorptions are instead assigned to [dσ^*(Pd$_2$)–π^*(ppy)] MMLTC. The emission spectra exhibit a broad absorption around 740 nm attributed to the MMLCT. This band is not present in the spectra of **243** and **244**. DFT calculations showed that the HOMO is an antibonding combination of mainly Pd d$_{z^2}$ orbitals, small contributions due to symmetry-allowed mixing are also coming from the 5s and 5p$_z$ orbitals. The LUMO and other orbitals close in energy are located on the 2-phenylpyridine rings and possess mainly ligand character. A Pd-Pd bond order of 0.11 was calculated for Pd(II) dimer **239**, supporting the presence of bonding interactions between the two Pd centres, albeit very weak. The AIM analysis furnished additional support for the presence of a bonding interaction between the two Pd atoms. For both complexes **239** and **241** it was found that there are critical points centered in between the two Pd atoms. This work supported the hypothesis of existence of a d^8-d^8 bond interactions between the two Pd(II) centres, although they are very weak. Other examples of Pd(II) dimers showing pronounced d^8-d^8 bond interactions were reported by Hazary *et al.*, in which they described the synthesis of the "clamshell"-like Pd(II) dimer **245** bearing a pyrophosphate ligand and two bipyridines;[214] and by Mirica *et al.*, where they reported a special Pd(II) dimer **246**, this dimer does not exhibit any bridging ligand but the two Pd atoms are bonded together exclusively through the Pd(II)-Pd(II) bond.[215] Also Peters *et al.* reported a borderline example in Pd(II) dimer **247** which bears a monomeric FBIP ligand where the very weak d^8-d^8 interactions contribute to the bending of the Cp moieties, (*Figure 30*).[216]

245	**246**	**247**
Pd-Pd= 3.04 Å	Pd-Pd= 3.11 Å	Pd-Pd= 3.16 Å
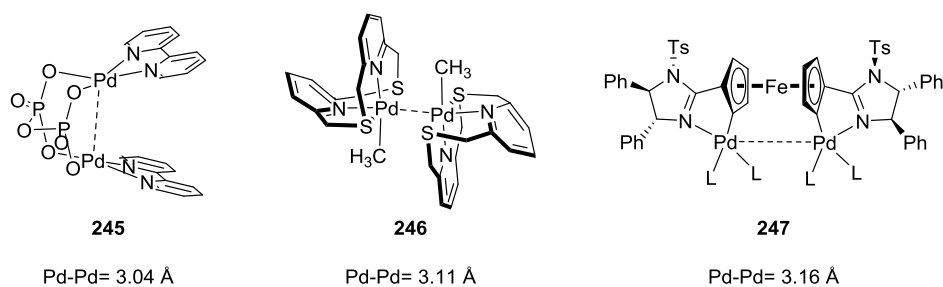
Figure 30: Examples of Pd(II) dimers with d^8-d^8 bonding interactions.

One of the most interesting features shown by some Pd(II) dimers is the way that they can undergo oxidative addition. The two electrons are not transferred to a single metal centre, but instead are shared between the two Pd centres, allowing the formation of Pd(III) dimers instead of a Pd(II)/Pd(IV) dimer.[217] The possibility of having single electron transfer for these Pd(II)-Pd(II) dimers was demonstrating by Bear *et al.* Complex **248** was shown to undergo a reversible one electron oxidation to generate the cation-radical $[Pd^{II}/Pd^{III}(\mu\text{-dpb})_4]^+$.[218]

248
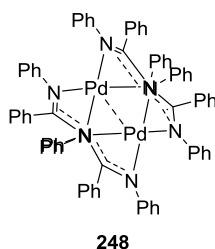
Figure 31: Pd(II) dimer **248** utilised by Bear *et al.* for cyclic voltammetric studies.[218]

The first example of bimetallic oxidative addition was reported by Cotton *et al.* in 1998.[219] Complex **249** was synthesised by mixing Pd(OAc)$_2$ and LiHpp in THF. The resulting complex **249** was treated with PhI(Cl)$_2$ to generate the Pd(III) dimer **250**, (*Scheme 56*).

249
Pd-Pd 2.55 Å

250
Pd-Pd 2.39 Å
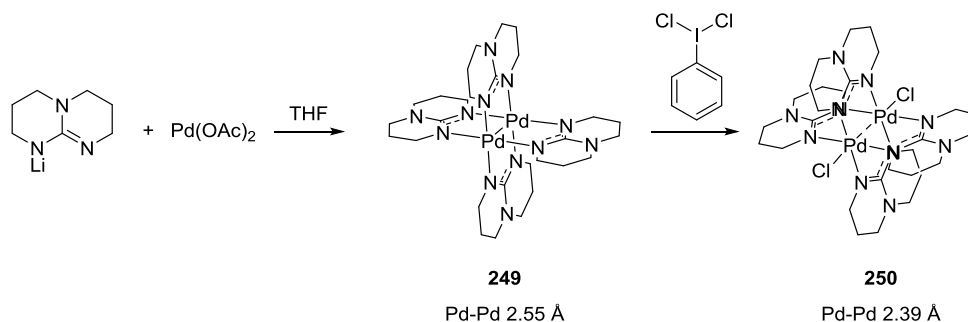
Scheme 56: First example of bimetallic oxidative addition onto a Pd(II) dimer.[219]

This one electron oxidation on both Pd atoms gave access to a series of Pd(III) dimers that could not be synthesised otherwise. Pd(II) dimer **251** was obtained by mixing Pd(OAc)$_2$ and 2-phenylpyridine in a mixture of CH$_2$Cl$_2$ and acetic acid. Pd(II) dimer **252** was obtained in a similar manner mixing Pd(OAc)$_2$ and benzo[*h*]quinoline in methanol. Reaction of these two Pd(II) dimers with oxidising agents such as hypervalent iodine

reagents and Br_2 gave access to the corresponding Pd(III) dimers **252** and **254**-**256**, (*Scheme 57*).
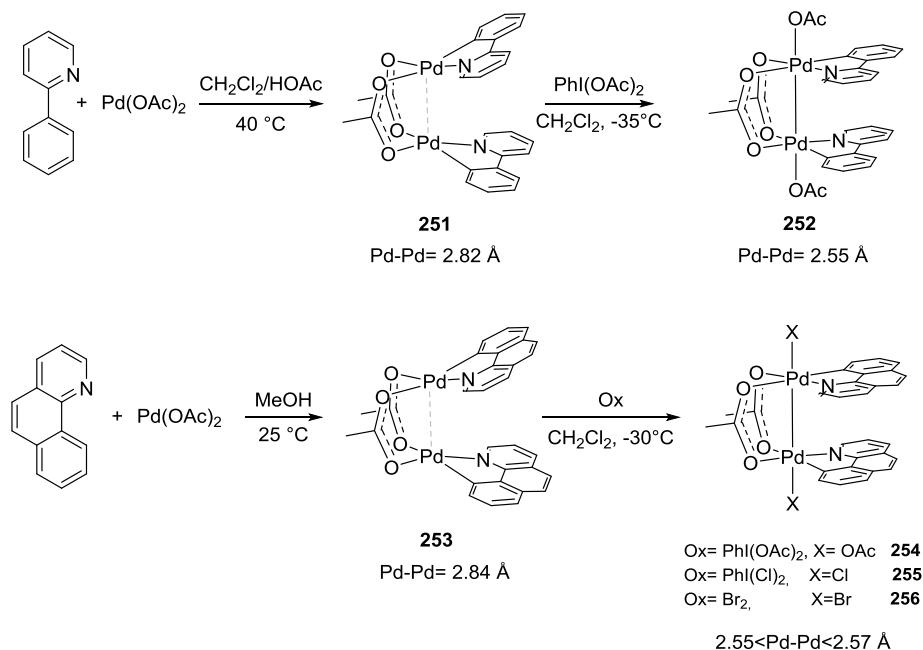
Scheme 57: Syntheses of Pd(II) dimers **252** and **253** and their further reaction with oxidising agents.[220,221]

The coordination of the Pd centres changes from square planar for the Pd(II) dimers to octahedral for the Pd(III) dimers. The Pd-Pd bond distances of Pd(II) are longer than the one of Pd(III) dimers, indicating a stronger bond interaction.

1.4.3 Pd(III)-Pd(III) dimers

Characterised examples of Pd(III)-Pd(III) dimers are rare. The first well characterised dimer was reported by Cotton *et al.* in 1998 (*Scheme* 55). Pd(III) dimer **250** was synthesised by single electron oxidation of the two Pd atoms of the Pd(II) complex **249** using PhI(Cl)$_2$ as an oxidant. Other examples were reported by Cotton *et al.* in 2006 and by Lahuerta *et al.* in 2008. Pd(III) dimers **258a-c**[222] and **259**[223] where obtained by treatment of the corresponding Pd(II) dimers with hypervalent iodine reagents or Br_2 (*Scheme 58*).
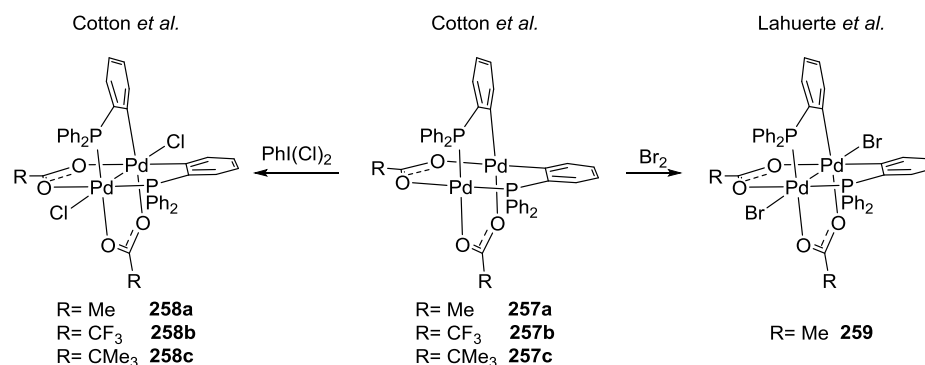
Scheme 58: Examples of Pd(III) dimers obtained by single electron oxidation of the corresponding Pd(II) dimers.[223]

In addition, these Pd(III) dimers were shown by Lahuerta *et al.* to be good catalysts for the diboration-oxidation and diboration-arylation of alkenes, (*Scheme 59*).[223]
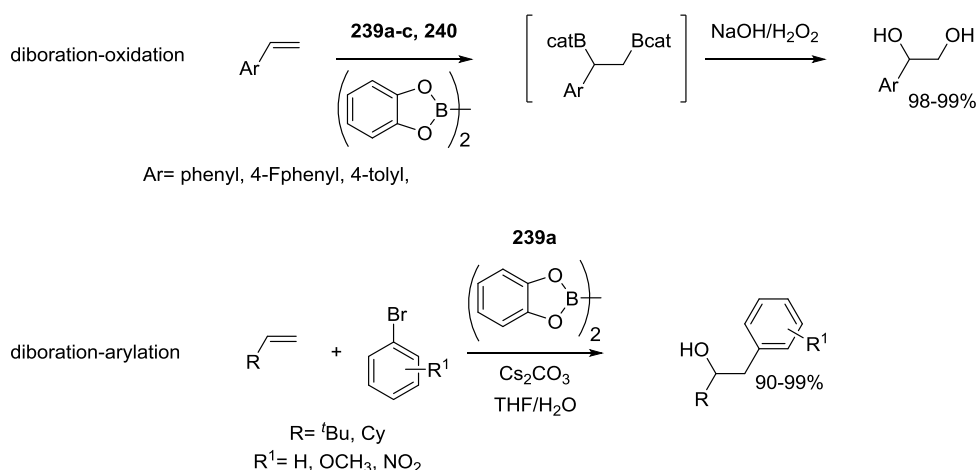
Scheme 59: Diboration-oxidation and diboration-arylation reaction catalysed by Pd(III) dimers **258a-c** and **259**.[223]

In 2009 Ritter *et al.* reported four new examples of Pd(III) dimers, **252** and **254-256**, as illustrated in *Scheme 56*. These dimers where shown to be important intermediates in the C-H functionalisation of 2-phenylpyridine and benzo[*h*]quinoline.[220,221]

It was proposed that when Pd(III) dimer **255** is warmed up to 23 °C, bimetallic reductive elimination occurs to afford Cl-functionalised benzo[*h*]quinoline **260** in 96% yield and Pd(II) species **261**, that upon reaction with free benzo[*h*]quinoline regenerates the Pd(II) dimer **253**, (*Scheme 60*).
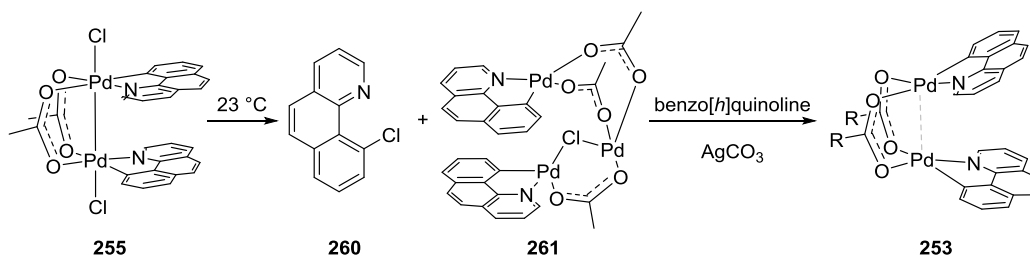
Scheme 60: First example of bimetallic reductive elimination involving a Pd(III) dimer.[221]

This example indicates that C-H oxidative functionalisation could occur *via* a Pd(II)/Pd(III) redox cycle involving bimetallic systems instead of the well established Pd(II)/Pd(IV) one, where a monomeric Pd(IV) species is thought to be responsible for the reductive elimination.[224] A combined experimental and computational study at the M06L level of theory was performed by Ritter *et al.* to gain more insight into the mechanism of the reductive elimination. There were two questions being investigated: 1) whether reductive elimination occurs *via* a monomeric or bimetallic complex ; 2) if the reductive elimination is from a bimetallic complex, then does it involve both Pd centres.[225] DFT calculations performed on Pd(III) dimer **255** clearly showed that reductive elimination occurs *via* a bimetallic system. The presence of the second metal lowers the activation barrier of the reductive elimination by approximately 30 kacl/mol compared to the monometallic pathway. Experimental studies reinforced the hypothesis of reductive elimination occurring from a bimetallic system. Pd(III) dimer **262** was mixed with Pd(III) dimer **255**. If Pd-Pd cleavage is faster than reductive elimination then the scrambled Pd(III) dimer **263** should be observed. However, no Pd(III) dimer **263** was observed upon mixing the two Pd(III) dimers, (*Scheme 61*).
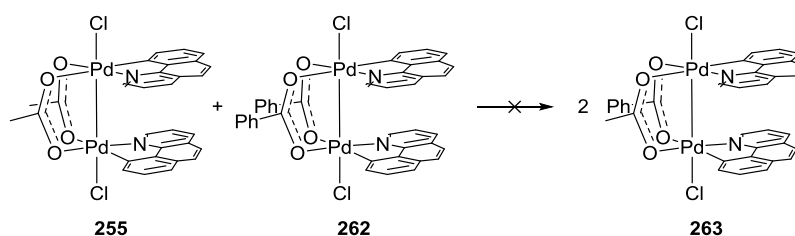
Scheme 61: Possible scrambling reaction between Pd(III) dimer **255** and **262** to generate Pd(III) dimer **263**.[225]

In addition, the more robust Pd(III) dimer **264** was shown to decompose 1500 times slower than complex **255**. However, comparison of the rate of reductive elimination at 35 °C of the two Pd(III) dimers showed that reductive elimination for complex **264** is only 16 times slower than that of complex **255**. This result also excludes the possibility of having Pd-Pd dimer cleavage prior to reductive elimination, (*Figure 32*).

264
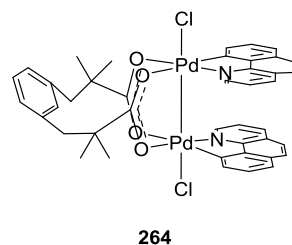
Figure 32: Pd(III) dimer **264**.[225]

These results lend strong support to the hypothesis of reductive elimination occurring from a bimetallic complex. Other computational studies were performed to gain more insight into the reductive elimination. Electron binding energies of the 4s core electrons of both Pd centres were calculated to clarify the contribution of each metal centre to the reductive elimination process. Three scenarios where explored: *(i)* reductive elimination where the second Pd acts as a spectator *via* a dinuclear Pd(I)/Pd(III) mixed valence complex; *(ii)* splitting of the Pd(III)-Pd(III) bond to generate a Pd(II)/Pd(IV) mixed valence complex prior to reductive elimination from the Pd(IV) centre; *(iii)* simultaneous redox participation from both Pd centres for the reductive elimination process. Decrease of the electron bonding energy was only observed in the case of *(iii)*, confirming the synergism of the two Pd centres in the reductive elimination process.

C-H oxidising functionalisation involving Pd(III) intermediates was also observed for other apical substituents on the Pd(III) moiety, such as Pd(III) dimers **254** and **256** as well as Pd(III) dimer **252**, (*Scheme 62*).[226]
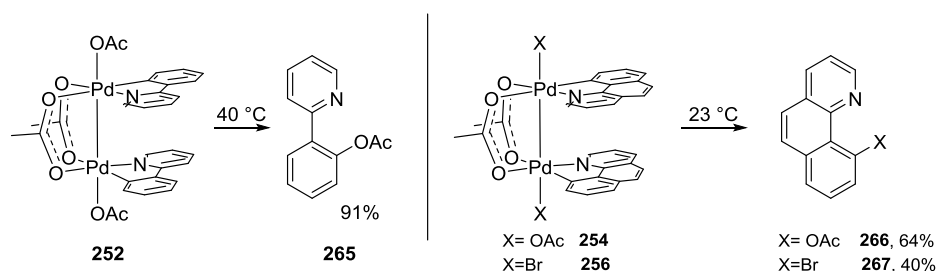
Scheme 62: Further examples of bimetallic reductive elimination.[226]

In 2010 Canty *et al.* performed DFT studies at the M06L and LANL2TZ (for Pd) level of theory to study the effect of the apical ligands in the reductive elimination of Pd(III) dimers of structure X-Pd-Pd-Y.[227] In the study, Y=Cl (weak σ donor ligand) was kept constant and different X groups were examined to understand if the electronic nature of this group can favour the dissociation of the Cl ligand (model b) and as a consequence allow a Pd(II)/Pd(IV) redox cycle, (*Scheme 63*).

model a   model b
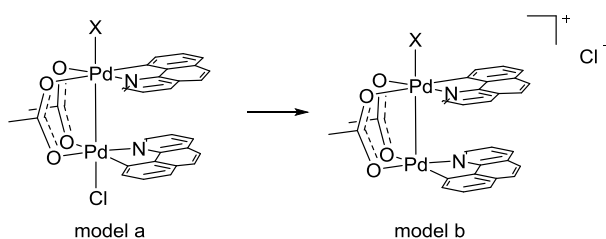
Scheme 63: Dissociation of the Cl ligand promoted by the X ligand.[227]

The X ligand was shown to have a crucial role in the dissociation of the Y ligand. Strong σ donors, such as $SiMe_3$, Me or Ph, cause an impairment in the Pd-Pd and Pd-Cl bonds allowing the dissociation of Cl^-. An increase of the d_{z^2} population is observed in the presence of strong σ donor ligands, which leads the Pd centre to prefer a Pd(II)-like arrangement. However, when X is a weak σ donor ligand, such as OAc, Br and Cl, model a is favoured and dissociation does not occur, supporting the proposal of Ritter. The polarity of the solvent also plays an important contribution: polar solvents favour the dissociated model b.

1.5 Aims and objectives

The design of Pd-precatalyst bearing bulky ligands has been a very active field in recent years. The use of bulky phosphine ligands in cross-coupling reactions allowed the coupling of most challenging substrates such as aryl chlorides and triflates. Bulky ligands are presumed to favour a monoligated 12-electron Pd(0)L as active catalytic species that undergoes facile oxidative addition. Moreover, the use of additives such as Cu and Ag salts has been shown, in most of the cases, to have a beneficial effect in cross-coupling reactions. The first part of this study will be focused on the understanding of these effects

first on Pd(P*t*Bu$_3$)$_2$ and then on other Pd(0)L$_2$ *via* NMR spectroscopy and X-ray crystallography. New Pd(I) and Pd(II) species have been identified and characterised.

We have shown in this introductory parts, that Pd(I)-Pd(I) complexes are usually used as precatalyst in cross-coupling reactions, however little is know about the possible mechanism that leads to their activation. The second part of this work is mainly focused on gaining more insights into the possible mechanism of activations of two of these Pd(I) dimers: Pd(I)-bromo dimer **31** and its iodo-analogues **193**. The possible mechanism of activation has been explored together with the additives that allows the *in situ* formation of the Pd(0)P*t*Bu$_3$ species.

In the literature there are no examples of direct reactivity of Pd(I)-dimer with aryl halides. The high reactivity of these Pd(I) dimer is generally presumed to be due to the generation of a monoligated Pd(0)L species that undergoes facile oxidative addition. On one hand, this approach allows the coupling of challenging substrates, such as aryl chlorides, on the other hand half of the Pd used in the reaction is not utilised in the catalytic cycle. The possibility of a direct dimer catalysis would be from an economical point of view, very appealing. The last part of this thesis was focused on the synthesis of new Pd(I) dimers and their use as catalysts in reaction of C-heteroatoms formation.

Chapter 2. Additive effect on Pd(0) complexes

The following results have been the subject of a publication.[258] F. Proutière contributed to the investigations of Cu, Pd and Ag salt additives on the reactivity of Pd(PtBu$_3$)$_2$ and he performed the synthesis of Pd(0)[P(iPr)(tBu)$_2$]$_2$. M. C. Nielsen performed the synthesis of Pd(0)(dfmpe)$_2$. The crystal structures reported in this chapter were solved by Dr B. Schweizer, Dr M. D Wörle and Dr N. Trapp, whilst M. Solar took care of the data collection.

Chapter 2: Introduction

Additives in Pd-catalysed cross-coupling reactions have frequently been shown to have a beneficial effect on the reactivity of the Pd(0) catalysis.[228-232] The combination of palladium and copper is one of the most utilised, for examples in Sonogashira reaction,[233] although a "copper effect" has also been observed in Suzuki[234,235] and Stille[230,232,236] coupling reactions. Increasing is also the number of cross-coupling reactions where Pd(0) catalysis benefits from the presence of the salts of the other two members of group 11 of the periodic table: Ag and Au.[237-241]

The precise role of Cu salts (or other additives) in the catalytic cycle, in particular in the Sonogashira coupling, is still not well understood.[242] Over the years several proposals have been given to the role of copper in the catalytic cycle but two are the main ones: *i*) In the widely-accepted mechanism for the Sonogashira reaction the presence of copper invokes a synergism of copper and palladium cycles. The Cu(I) salt (CuI and CuBr are the most utilised) is supposed to play an important role in the transmetallation step through the formation of organo-copper species[243] that undergo faster exchange with the X group (that can be an iodide, a bromide, a chloride or a triflate) in the LPd(II)(R)(X) shown in *Scheme 64*. Accelerating effect are observed especially in the presence of aryl iodide and activated aryl bromides, where oxidative addition is usually not the rate limiting step.[240,244,245]
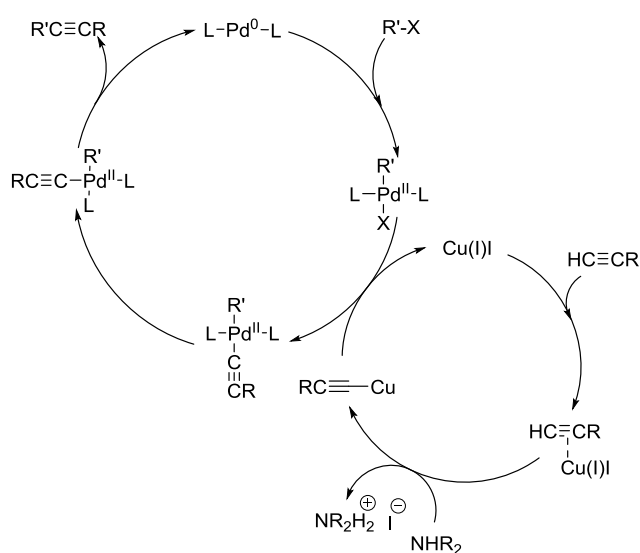
Scheme 64: General accepted mechanism for Sonogashira coupling reaction.[8]

2) Farina *et al.* and Espinet *et al.* gave a good contribution in the understanding of the "copper effect" in the Stille coupling. They suggested that, in the case of ligand dissociation prior to oxidative addition, copper can act as a free ligand scavenger, when PPh₃ is used as a ligand. This coordination reduces the "autoretardation" phenomenon observed in the presence of free ligand in the transmetallation step.[230,236]

Aryl chlorides are usually difficult substrates for cross-coupling reactions, due to the fact that oxidative addition for this compounds is very challenging and represents very often the rate limiting step of the cycle. Examples employing the cheap aryl chlorides analogues in Sonogashira coupling are rare, compared to aryl bromides and iodides, and very often bulky ligands in combination with Pd and Cu sources are needed to allow the coupling.[246-249]

Despite the large number of examples where Pd catalysis benefits of the presence of copper, one of the limitations concerning the use of Cu additives in the presence of alkynes is the formation of homocoupling product of the alkyne. This side reaction is even more pronounced in presence of oxygen (Glaser coupling, Hay coupling).[250] The necessity to avoid the homocoupling of the terminal alkyne, led to development of large number of Cu free Sonogashira coupling reactions, number that is still increasing.[251-254] In the case of aryl chlorides, particularly successful is the combination of Pd and bulky ligands.[255,256] One interesting example of copper free Sonogashira reaction of aryl chlorides in presence of a bulky monodentate ligands (Xphos) was reported by Buchwald *et al.* in 2003.[257]

R= CH₃, OCH₃, CN, *n*Bu, CO₂CH₃
R¹= *t*Bu, SiEt, Cyclohexenyl, Ph
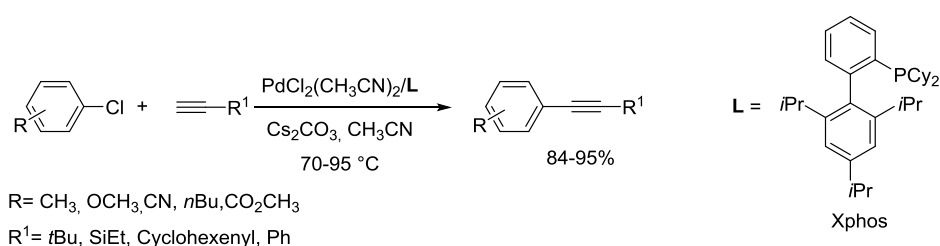
Scheme 65: Sonogashira-type coupling of aryl chlorides and alkyl and aryl alkynes reported by Buchwald *et al.*[257]

The reaction in the absence of copper additives proceeded smoothly under mild conditions, even for very challenging substrates such as electron rich aryl chlorides and alkyl acetylenes. However, the addition of CuI dramatically decreased the yield of the reaction, and it was observed that the higher the concentration of CuI, the greater the suppression of the coupling process. In addition, they performed the coupling of 4-chloroanisole and

*t*butylacetylene in the presence of different Cu salts of oxidation state +1 and +2 (copper(I) chloride, cupper phelylacetylide, Cu(II) *i*butirate). The results obtained not only showed that the Sonogashira coupling was suppressed but also the alkyne was consumed in a side reaction, most probably oligomerisation.

The example reported by Buchwald *et al.* showed that despite the large use of additives in cross-coupling reactions, especially in the Sonogashira coupling where a synergism between Cu and Pd cycles is generally assumed, the actual role of Cu in the reaction mechanism is still not well understood. In particular, there are no reports on the effect of Cu additives on the active species. Herein we will show that in the presence of Cu additives the Pd catalyst is rapidly consumed and new species arise. The effect of additives and of the ligand attached to the Pd(0) on the formation of these new species/disappearance of the Pd(0) were studied in depth. The role of the newly formed species in catalysis were examined with the goal to gain fundamental understanding of the role of the additive and related accelerating or inhibiting effects derived from the change of the active catalytic species. The study was also extended to Ag, Au and Fe salt additives, that are frequently used in substitution of copper additives in cross-coupling reactions, as well as other oxidizing salts.

2.2 Investigation into the effects of copper additives on Pd(0)(P*t*Bu$_3$)$_2$ 268

2.2.1 Investigation into the effects of Cu^{n}Br$_n$ on Pd(0)(PtBu$_3$)$_2$ 268

Our group is interested in understanding the mechanism of reactions employing both computational and experimental approaches. As part of my studies, particular focus was given to those reactions utilising palladium sources in cross-coupling reactions. The large dichotomy of results obtaining employing Cu salts, in particular the inhibiting effect described by Buchwald *et al.*, led us to further investigate the role of copper in the catalytic cycle, in particular the possibility for Cu salts not only to form organo-copper species that facilitate the transmetallation step or to act as ligand scavenger, but also the possibility of having an influence on the normal Pd(0) catalysis. Pd(0)(P*t*Bu$_3$)$_2$ **268**, very often use in Suzuki coupling reaction as a source of monoligated Pd(P*t*Bu$_3$), was chosen as suitable Pd(0) source to explore the effect of Cu salts on Pd(0) catalysis. Complex **268** was exposed to CuBr$_2$ in THF without the presence of any coupling partners to see if the copper can

react with the Pd(0) forming new phosphorus-containing species. The reaction was monitored by ^{31}P-NMR spectroscopy over time. After 15 minutes of exposure the signal of Pd(0) **268** at 85.5 ppm in the ^{31}P-NMR spectrum of the reaction mixture had disappeared and new phosphorous-containing species appeared at 87.2 ppm and 57.0 ppm, (*Figure 33*).[258]
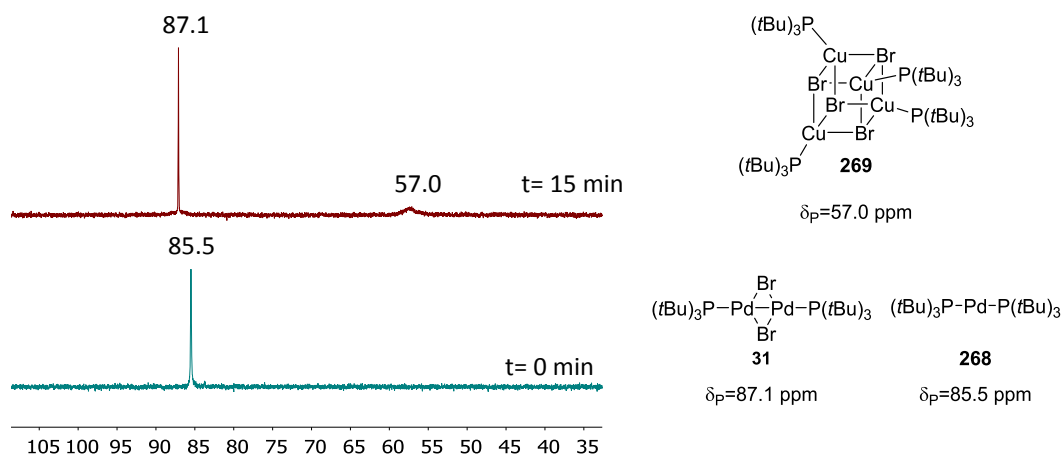
Figure 33: ^{31}P-NMR spectroscopic analysis of the reaction of Pd(0)(P*t*Bu$_3$)$_2$ **268** and CuBr$_2$ at t=0 min (green); reaction of Pd(0)(P*t*Bu$_3$)$_2$ **268** and CuBr$_2$ after 15 minutes (red). (Chemical shift in ppm referenced to trimethoxyphosphine oxide as an internal standard).

Recrystallisation of the reaction mixture from toluene:acetone 1:2 led to the formation of two different types of crystals: one dark green and the other one colourless. To our surprise, the dark green crystals were those of the known Pd(I)-bromo-dimer **31**, whilst the colourless ones corresponded to the Cu(I)-bromo cubane **269**.[259] This transformation occurred *via* a RedOx reaction: Cu(II) is reduced to Cu(I) and Pd(0) is oxidised to Pd(I), (*Scheme 66*).
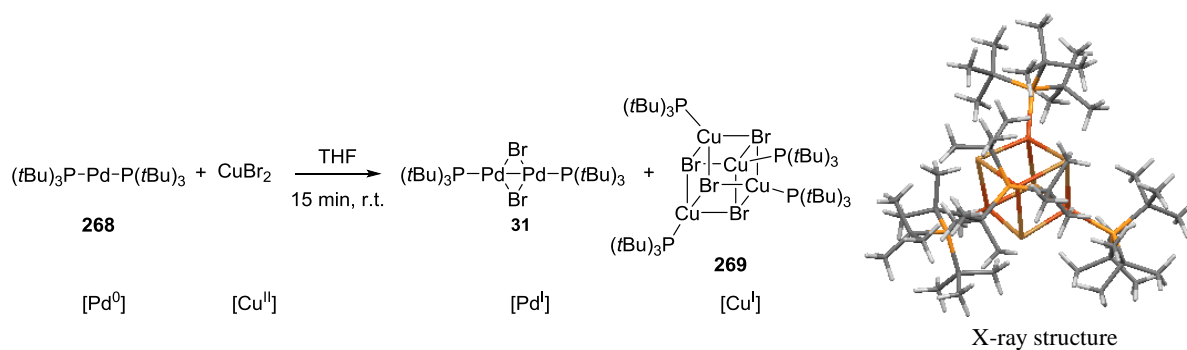
Scheme 66: Formation of Pd(I)-bromo-dimer **31** and Cu(I)-cubane **269** from Pd(0) **268** and CuBr$_2$ (left). Crystal structure of Cu-cubane **269** (right).[258]

As Cu(I) salts are the most utilised in catalysis, Pd(0)(PtBu$_3$)$_2$ **268** was also exposed to commercial CuBr in THF. In this case the the reaction also gives formation of Pd(I)bromo-dimer **31** and the Cu(I) cubane **269**. It was hypothesised that this phenomenon could be due to disproportionation of Cu(I) in Cu(II), which is responsible for the RedOx reaction, and Cu(0), (*Figure 34*).
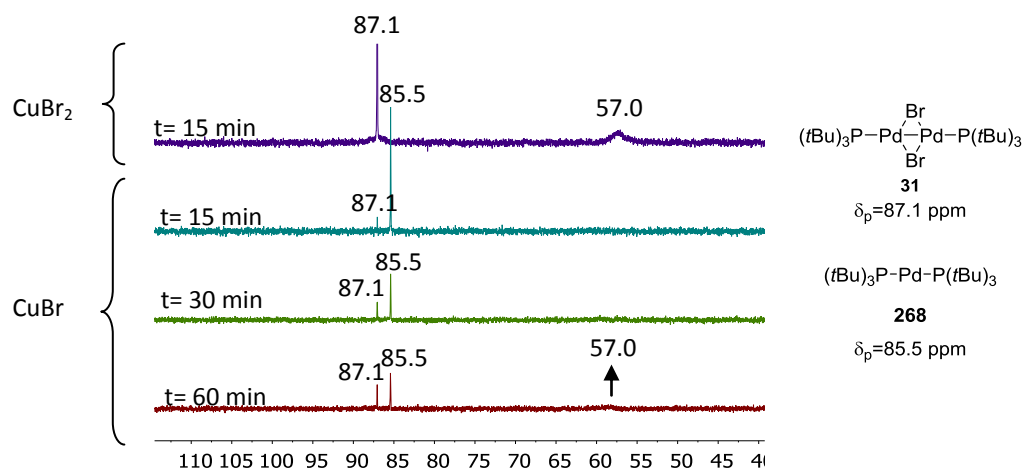
Figure 34: ^{31}P-NMR spectroscopic analysis of the reaction of Pd(0)(PtBu$_3$)$_2$ **268** with: CuBr after 15 minutes (light blue), CuBr after 30 minutes (green); CuBr after 60 minutes (red) and CuBr$_2$ after 15 minutes (dark blue). (Chemical shifts in ppm referenced to trimethoxyphosphine oxide as an internal standard)

The formation of the Pd(I)bromo-dimer **31** was unexpected and could, at least in part, explain some of the beneficial effects of the addition of Cu additives on reaction with Pd(0) **268**. As previously discussed in section 1.3.7, Pd(I)bromo-dimer **31** was first synthesised by Vilar and Mingos in 1996[169] and has shown efficient use by Hartwig *et al.* in the amination reaction and Suzuki reaction of aryl bromides at room temperature[171] and by Prashad *et al.* in the amination reaction of aryl bromides and chlorides.[184]

2.2.2 Investigation into the effects of CuI on Pd(0)(PtBu₃)₂ 268

CuI is probably one the most utilised sources of Cu in cross-coupling reactions. Similarly to Cu(I) and Cu(II) bromide salts, Pd(PtBu$_3$)$_2$ **268** was exposed to 1 equivalent of CuI in THF. The reaction was monitored by ^{31}P-NMR. No change was observed within the first 30 minutes of exposure but a new species at 102.5 ppm, which would correspond to the

Pd(I)iodo-dimer **193** could be detected after 1 hour of reaction time. However, even after 3 hours the major species in solution was still the Pd(0) species **268** at 85.5 ppm, (*Figure 35*).
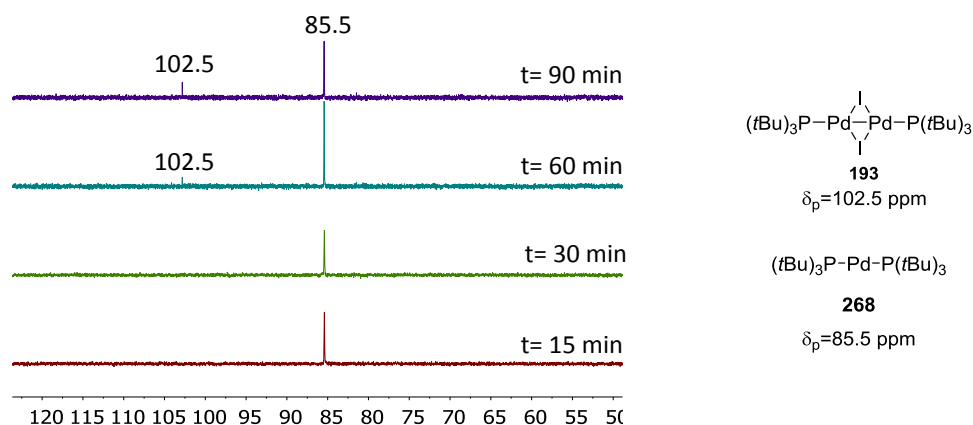
Figure 35: ^{31}P-NMR spectroscopic analysis of the reaction of Pd(0)(PtBu$_3$)$_2$ **268** with CuI after: 15 minutes (red), 30 minutes (green); 60 minutes (light blue) and 90 minutes (dark blue). (Chemical shifts in ppm referenced to trimethoxyphosphine oxide as an internal standard).

Also in this case, as in the case of CuBr, the use of one equivalent of CuI does not lead at the full conversion of the Pd(0) **268** to Pd(I) dimer **193**, even after prolonged exposure the major species in the ^{31}P-NMR spectrum of the reaction mixture corresponds to the Pd(0) **268**. In the presence of CuI, as in the case of CuBr, the occurrence of a RedOx reaction led to the formation of Pd(I)-iodo-dimer **193**, (*Scheme 67*).
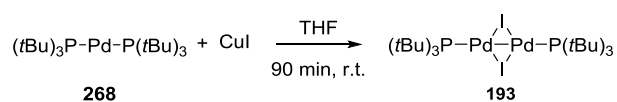
Scheme 67: Formation of Pd(I)iodo-dimer **193** from Pd(0) **268** and CuI.[258]

2.3 Investigation into the effects of Cu salts and Pd salts on other Pd(0)L$_2$ complexes

In the previous section we explored the effect of Cu salts on Pd(0)(PtBu$_3$)$_2$ **268**. A redox reaction took place that led to the formation of the Pd(I)bromo-dimer **31** in the case of Cu^{n}Br$_n$ (n=1, 2) salts, and of Pd(I)iodo-dimer **193** in the case of CuI. The possibility that redox reactions could also be occurring in the presence of other Pd(0)L$_2$ species led us to investigate the effect of Cu salts and also Pd salts on commonly used Pd(0)L$_2$ complexes.

These complexes were first synthesised according to reported literature procedures and then exposed to $CuBr_2$, CuI, $PdBr_2$ and PdI_2 salts.

2.3.1 Investigation into the effect of Cu and Pd salts on Pd(PCy$_3$)$_2$ 270

Use of bulky ligands such as PtBu$_3$ and PCy$_3$ allows the Suzuki coupling of challenging substrates including aryl chlorides and triflates.[30] Despite the presence of a bulky tricyclohexyl group, oxidative addition onto Pd(0)(PCy$_3$)$_2$ **270** is presumed to proceed directly on the bisligated complex, whilst in the case of Pd(0)(PtBu$_3$)$_2$ **268** ligand dissociation is presumed to happen prior to oxidative addition.[260,261] The reaction of Pd(0) **270** and copper salts was followed by ^{31}P-NMR to see if the small differences in the steric and electronic properties can influence a RedOx reaction of the Pd(0) complex **270** with the Cu salts.

Before proceeding with the redox reaction, Pd(0)(PCy$_3$)$_2$ was synthesised following the procedure reported by Osakada in 2005, (*Scheme 68*).[262]
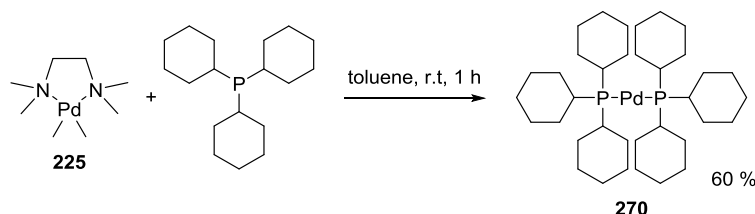
Scheme 68: Formation of Pd(PCy$_3$)$_2$ **270** from Pd(Me)$_2$(tmeda) **225** and tricyclohexylphosphine.[262]

An alternative way to synthesise Pd(PCy$_3$)$_2$ **270** from the less expensive Pd$_2$(dba)$_3$ and PCy$_3$ was also explored. The reaction performed in THF gave a brown precipitate after 1 hour that was filtered and washed with ether to remove the excess of dba. The solid obtained was then dried under reduced pressure. Suitable crystals for X-ray analysis were obtained. However, unfortunately the crystals obtained were not of the desired product **270** but of the already reported (dba)Pd(PCy$_3$)$_2$ **271** complex, where a molecule of dba is still coordinated to the Pd(0) core, (*Scheme 69*).[263]
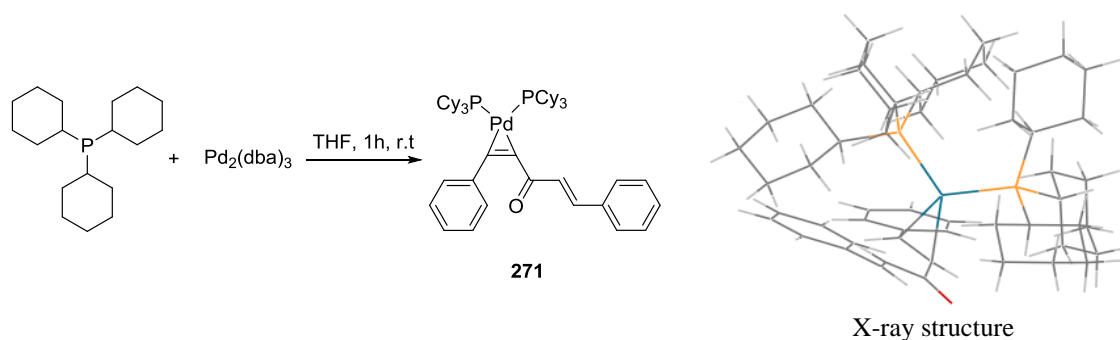
X-ray structure

Scheme 69: Alternative attempted synthesis Pd(PCy$_3$)$_2$ **270** from Pd$_2$(dba)$_3$ and tricyclohexylphosphine (left). Crystal structure of the (dba)Pd(PCy$_3$)$_2$ **271** (right).[264]

The Pd(PCy$_3$)$_2$ **270** obtained in the reaction in *Scheme 68* was exposed to 1 equivalent of CuBr$_2$. After 15 minutes it was already possible to detect a new species at 25 ppm, although the main the peak was still that of Pd(PCy$_3$)$_2$ **270** at 39.5 ppm. After 30 minutes the reaction appeared to have reached an equilibrium and no more Pd(PCy$_3$)$_2$ **270** was converted into the species at 25.0 ppm. The ^{31}P-NMR spectra after 30 minutes and after 1 hour of reaction time did not substantially change, (*Figure 36*).
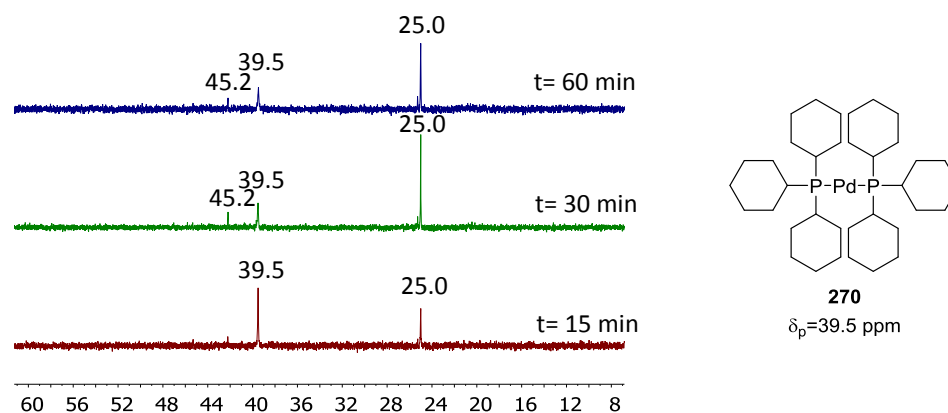
Figure 36: ^{31}P-NMR spectroscopic analysis of the reaction of Pd(PCy$_3$)$_2$ **270** (39.5 ppm) and CuBr$_2$ after: 15 minutes (red), 30 minutes (green); 60 minutes (blue). (Chemical shifts in ppm referenced to trimethoxyphosphine oxide as an internal standard).

Attempts to obtain suitable crystals for X-ray analysis failed and it was not possible to isolate a Cu(I) complex that could confirm the occurrence of a RedOx reaction. However a ^{31}P-NMR study of the reaction performed at a higher concentration showed the presence of a broad signal at 19 ppm that was not possible to observe before. A complex of composition [Cu(PCy$_3$)Br]$_2$ was previously reported by Healy in 2002,[265] but unfortunately

only the solid state ^{31}P CPMAS NMR spectrum was reported for this compound making comparison difficult.
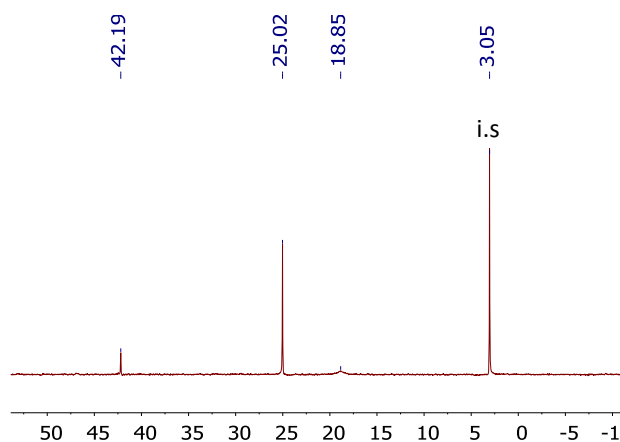
Figure 37: ^{31}P-NMR spectrum of the more concentrated reaction of Pd(PCy$_3$)$_2$ **270** (39.5 ppm) and CuBr$_2$ after 20 minutes. (Chemical shifts in ppm referenced to trimethoxyphosphine oxide as an internal standard).

In the case of Pd(0)(PtBu$_3$)$_2$ **268** its reaction with CuBr$_2$ afforded Pd(I)bromo dimer **31** and Cu-cubane **269**, whilst Pd(I)bromo-dimer **31** could be exclusively obtained by changing the bromide source to PdBr$_2$. The same approach was used in the case of Pd(PCy$_3$)$_2$ **270** in order to achieve a pure sample of possible Pd(I)dimer that would facilitate the crystallization step. Pd(PCy$_3$)$_2$ **270** was exposed to 1 equivalent of PdBr$_2$. The reaction after 20 minutes showed poor conversion, but after 1 hour the major species observed in the ^{31}P-NMR spectrum was the one at 25 ppm, in agreement with what was already observed with CuBr$_2$, (*Figure 38*).
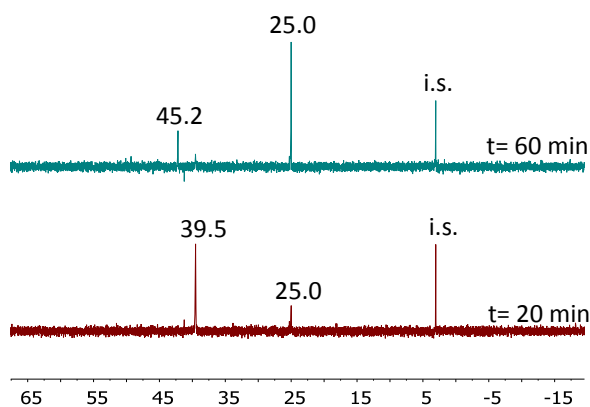
Figure 38: ^{31}P-NMR spectroscopic analysis of the reaction of Pd(PCy$_3$)$_2$ **270** (39.5 ppm) and PdBr$_2$ after: 20 minutes (red), 60 minutes (green). (Chemical shifts in ppm referenced to trimethoxyphosphine oxide as an internal standard).

After removal of the solvent and washing the solid obtained with hexane to remove the traces of unreacted Pd(PCy$_3$)$_2$ **270**, suitable crystals for X-ray diffraction were obtained in CH$_2$Cl$_2$ at –35 °C. To our surprise, the structure obtained was dimeric, but in this case a new Pd(II) dimer was obtained instead of the presumed Pd(I)-Pd(I) dimer. Evidently small changes in the steric properties of the ligand had resulted in dramatic changes in the reactivity and transformations of the two Pd(0) complexes **268** and **270**, (*Scheme 70*).
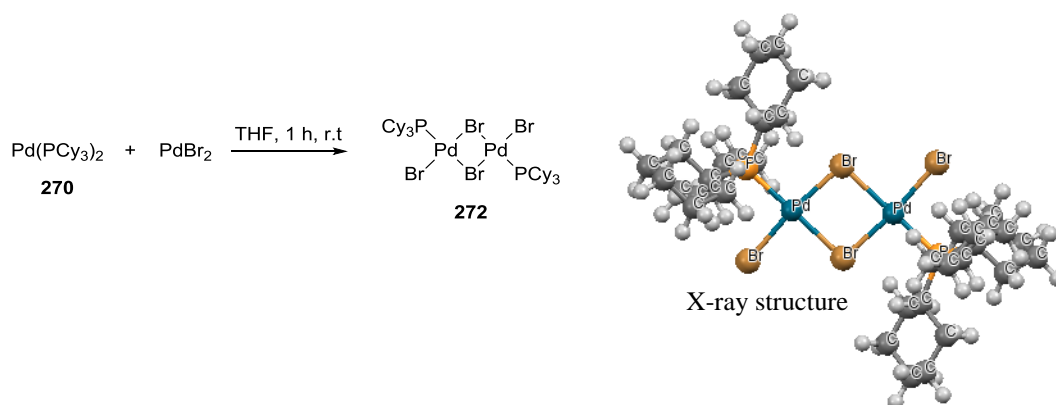
Scheme 70: Synthesis of [PdBr$_2$(PCy$_3$)]$_2$ **272** from Pd(PCy$_3$)$_2$ **270** and PdBr$_2$ (left). Crystal structure of the Pd(PCy$_3$)$_2$Br$_2$ **272** (right).

However, it is worth to mention that a dark precipitate in the presence of both CuBr$_2$ and PdBr$_2$ salts was formed. This phenomenon does not exclude the hypothesis of the formation of a very unstable Pd(I) dimer, which immediately disproportionate into a Pd(II) monomer and a monoligated Pd(0). This monoligated Pd(0) species can then lose the ligand and precipitate as Pd-black or take another ligand to form Pd(0) **270**, (*Scheme 71*).
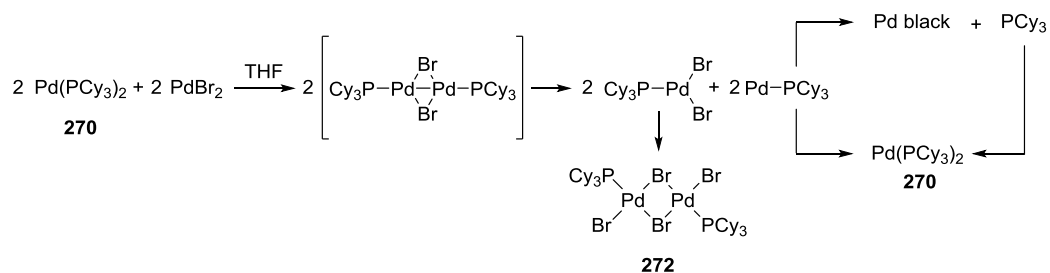
Scheme 71: Proposed mechanism for the formation of the Pd(II) complex **272** *via* an unstable Pd(I) intermediate.

A control experiment was then performed to support our hypothesis that the chemical shift at 25 ppm as being due to [PdBr$_2$(PCy$_3$)]$_2$ **272**. PdBr$_2$ was added to a THF solution containing 1 equivalent of PCy$_3$ and after 3 hours the only P-containing species in solution

had a chemical shift of 25 ppm, supporting our hypothesis. However, it was not possible to identify the species at 45.2 ppm

After the interesting results obtained with the bromide salts, the influence of CuI was also examined. As in the formation of $[PdBr_2(PCy_3)]_2$ **272**, $Pd(PCy_3)_2$ **270** was exposed to 1 equivalent of CuI and the reaction was monitored by ^{31}P-NMR spectroscopy. After 30 minutes a new species appeared in the ^{31}P-NMR spectrum, but the major species was still $Pd(PCy_3)_2$ **270**. After 1 hour the spectrum showed a substantial change in the species present in the reaction mixture. $Pd(PCy_3)_2$ **270** was no longer present in solution, with the major peak now being the one at 26.4 ppm, that presumably corresponds to the $[PdI_2(PCy_3)]_2$ **273**, the iodo-analogue of $[PdBr_2(PCy_3)]_2$ **272**. In this case a control experiment was also performed to support the hypothesis that the chemical shift at 26 ppm is the one that we have assigned to $[PdI_2(PCy_3)]_2$ **273**. PdI_2 was added to a THF solution containing 1 equivalent of PCy_3 and after 30 minutes of exposure the only P-containing species was at 26 ppm, supporting our hypothesis. Two additional small peaks were also present, one corresponding to the free phosphine PCy_3 and the other one to an unidentified species at 45.2 ppm, that was also present in the spectrum of the reaction with $CuBr_2$, (*Figure 39*).
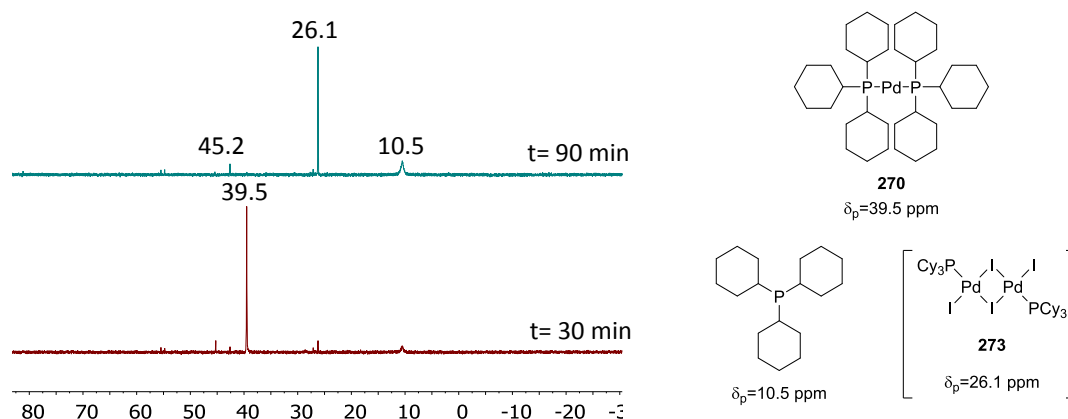
Figure 39: ^{31}P-NMR spectroscopic analysis of the reaction of $Pd(PCy_3)_2$ **270** (39.5 ppm) and CuI after: 30 minutes (red), 90 minutes (green). (Chemical shifts in ppm referenced to trimethoxyphosphine oxide as an internal standard).

After recrystallisation two different types of solids were detected: one was dark brown but not crystalline, and the other was light brown and gave suitable crystals for X-ray analysis, (*Scheme 72*).
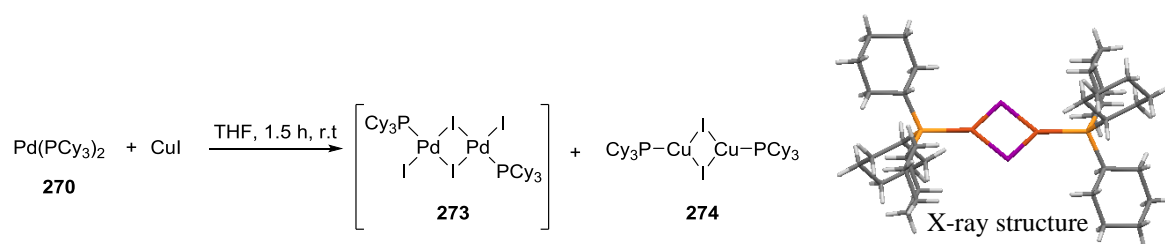
Scheme 72: Reaction between $Pd(PCy_3)_2$ **270** and CuI (left). Crystal structure of one of the products, $[CuI(PCy_3)]_2$ **274** (right).

The X-ray analysis revealed the presence of the Cu-dimer **274** in the reaction mixture, similar to the Cu-Cubane **269** obtained in the reaction of $Pd(PtBu_3)_2$ **268** and $CuBr_2$. We can exclude that the species at 45.2 ppm could be assigned to a Pd(I) dimer because the same species was observed also in the reaction with $CuBr_2$ and $PdBr_2$.

2.3.2 Investigation into the effect of Cu and Pd salts on $Pd[P(iPr)(tBu)_2]_2$ 276

The results obtained from exposing Cu salts to two of the most utilised $Pd(0)L_2$ complexes in cross-coupling reactions confirmed that the role of the copper in the catalytic cycle is more complex than was previously thought. In addition, the steric properties of the ligand influences the product that is formed: Pd(I) dimer *vs* Pd(II) dimer or monomer. We decided to further investigate this and extend the study to $P(iPr)(tBu)_2$ **275**. This ligand, in fact, should have intermediate properties (cone angle,[266] steric hindrance, nucleophilicity, reactivity) compared to $PtBu_3$ and PCy_3. As described in the previous paragraphs, $PtBu_3$ has been shown to involve a monoligated metal complex in oxidative addition to ArCl, whilst PCy_3 undergoes oxidative addition of 4-chlorophenyl trifluoromethanesulfonate through a bisligated metal complex.[31] This difference in the ligation state results in a different reactivity of the two systems. An example of this was presented by Fu *et al*. in the reaction of 4-chlorophenyl trifluoromethanesulfonate **4** with 2-tolylboronic acid **5**. While $PtBu_3$ favours the Cl-addition product, PCy_3 favours the triflate-addition one (see *Scheme 3* and *Scheme 4* in Chapter 1).[30,31]

Synthesis of the $Pd[P(iPr)(tBu)_2]_2$ **276** was performed by Proutière from our group. The $P(iPr)(tBu)_2$ **275** was prepared according to Iwazaki's procedure with isopropyl magnesium chloride and $(tBu)_2PCl$ in presence of CuCl.[267] Subsequently ligand **275** was used in the presence of the tmeda comple **225** to form the $Pd[P(iPr)(tBu)_2]_2$ **276**.[32,268]

As part of my work, Pd[P(iPr)(tBu)$_2$]$_2$ **276** was first exposed to Pd(II) salts in order to facilitate the isolation of a pure Pd-containing product. The reaction with PdBr$_2$ generated two new species in the ^{31}P-NMR spectrum, one at 72.5 ppm that we assumed belonged to the Pd(I)bromo dimer **277**[269] and another species at 53 ppm that we could not identify, but we can exclude a belonging to the free ligand that has a chemical shift of 46.2 ppm, (*Scheme 73*).
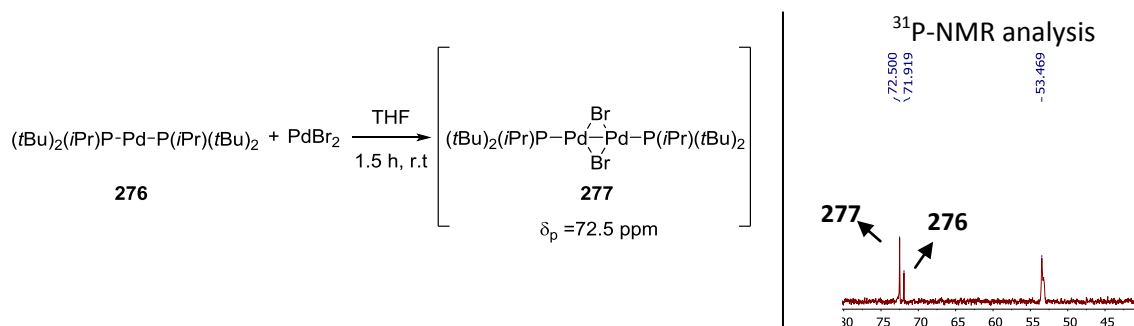
Scheme 73: Reaction between Pd[P(iPr)(tBu)$_2$]$_2$ **276** and CuBr$_2$ (left). ^{31}P-NMR spectroscopic analysis of the reaction mixture (right). (Chemical shifts in ppm referenced to trimethoxyphosphine oxide as an internal standard).

Prolonged exposure of Pd[P(iPr)(tBu)$_2$]$_2$ **276** did not improve the conversion and the crystals obtained from the reaction mixture were not suitable for X-ray analysis. This may be due to fast decomposition of the Pd(I)-dimer **277** in solution.

In the case of the PtBu$_3$ ligand, the Pd(I)-iodo dimer **193** is more stable than the bromide analogue **31** both in solution and in the solid state. Pd[P(iPr)(tBu)$_2$]$_2$ **276** was exposed to 1 equivalent of PdI$_2$ for 1.5 hours in THF. The spectrum of the reaction mixture after 1.5 hour only showed a single species at 88.9 ppm. Recrystallisation of the reaction mixture gave dark purple crystals of Pd(I)-dimer **278** (*Scheme 74*), which were suitable for X-ray analysis.
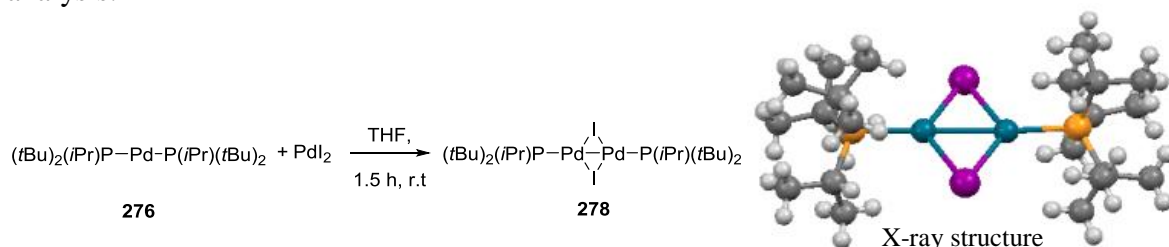
Scheme 74: Reaction between Pd[P(iPr)(tBu)$_2$]$_2$ **276** and PdI$_2$ (left). Crystal structure of the novel Pd(I)-dimer **278** (right).

The structural confirmation of the formation of Pd(I) dimer **278** led us to further explore the effect of CuI on Pd[P(*i*Pr)(*t*Bu)$_2$]$_2$ **276**. One equivalent of CuI was added to a THF solution containing the Pd(0) species **276**. After 1.5 hours the reaction was analysed by ^{31}P-NMR and Pd(I)-dimer **278** was found to be present in solution together with unreacted Pd(0) complex **276** (the major species in solution) and a peak at 42.7 ppm. This could correspond to the cubane complex, which would remove CuI from the reaction mixture, in an analogous manner to the reaction of Pd(P*t*Bu$_3$)$_2$ **268** and CuI, explaining the poor conversions observed. Therefore, in the presence of oxidising salts, P(*i*Pr)(*t*Bu)$_2$ **275** behaves like P*t*Bu$_3$ resulting in the formation, at least in the presence of iodide salts, of Pd(I) dimeric structures.

2.3.3 Investigation into the effect of Cu salts on Pd(dppm)$_2$ 279

As described in Chapter one, the use of dppm ligand in combination with a Pd(0) and a Pd(II) sources can generate Pd(I) dimeric species bearing the dppm as a bridging ligand. We were interested to explore the influence of Cu salts also with this type of ligand, in order to verify whether oxidation is occurring and in case which kind of complexes are formed.

For the synthesis of Pd(dppm)$_2$ **279**, the same procedure as described for Pd(PCy$_3$)$_2$ **270** was followed. Two equivalent of dppm ligand were mixed with 1 equivalent of Pd(Me)$_2$(tmeda) **225** in a toluene solution for 1 hour. This gave predominatly a single species at 13.1 ppm as shown in *Scheme 75*.
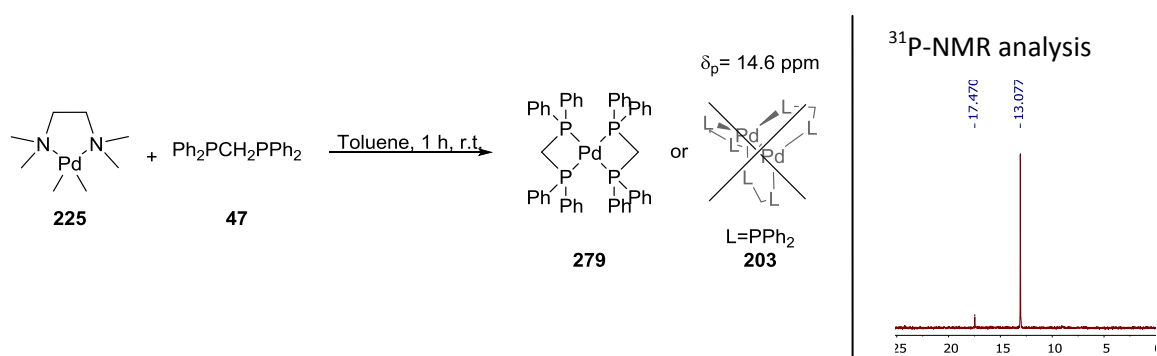
Scheme 75: Formation of Pd(dppm)$_2$ **279** from Pd(Me)$_2$(tmeda) **225** and dppm (left). ^{31}P-NMR spectroscopic analysis of the reaction mixture (right). (Chemical shifts in ppm referenced to trimethoxyphosphine oxide as an internal standard).

The dimeric complex $Pd_2(dppm)_3$ has previously been reported.[198] However, we excluded the possibility of formation of this Pd(0) complex because it has a δ_p= 14.6 ppm. Also, the use of the tmeda complex **225**, at least in the cases of PCy_3 and $P(iPr)(tBu)_2$ **275** reported before, usually furnishes Pd(0) complexes bearing only two phosphine ligands. Complex **279** was previously reported by Denise *et al.* by reduction of $Pd(dppm)Cl_2$ with $NaBH_4$, but unfortunately no spectroscopic data were reported.[270]

As described in the introduction, this type of ligand has been used for the synthesis of Pd(I) dimers bearing rigid bridging ligands. For example, the synthesis of the Pd(I)-bromo dimer **29** required two synthetic steps: in the first step the chloro-analogue **48** was prepared through comproportionation of $Pd(II)Cl_2(CNPh)_2$ and $Pd(0)_2(dba)_3\cdot(CH_3Cl)$. The Pd(I)Br **29** analogue was then obtained by mixing the Pd(I)Cl dimer **48** with an excess of NaBr in CH_2Cl_2, (*Scheme 16*).[86]
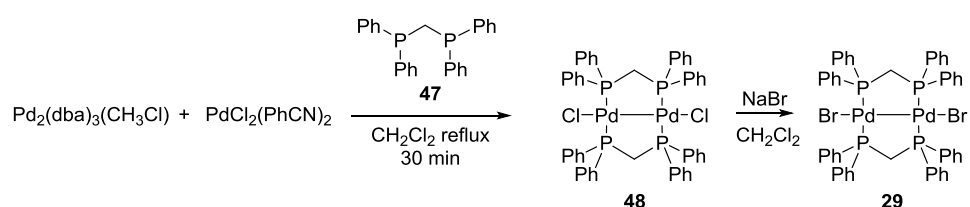
Scheme 16: Synthesis of [Pd(dppm)Br]$_2$ **29** by comproprotionation of Pd(0) and Pd(II) followed by halide exchange.[86]

From our previous work we considered that a RedOx reaction between $Pd(dppm)_2$ **279** and $CuBr_2$ should furnish the Pd(I)bromo dimer **29**. To verify our hypothesis Pd(0) complex **279** was exposed to 1 equivalent of $CuBr_2$. After 1 hour reaction time the Pd(0) complex **279** was fully consumed and new peaks appeared in the ^{31}P-NMR spectrum of the reaction mixture: one at −5 ppm, corresponding to the Pd(I)-dimer **29**,[271] another at 17.5 ppm, and a third broad peak at −16.2 ppm. The species at 17.5 ppm was already present in trace amounts in the ^{31}P-NMR spectrum of the starting material and it increased its intensity after reaction with $CuBr_2$. A control experiment to investigate the identity of the species at −16.2 ppm was carried out: a THF solution containing dppm **47** was exposed to $CuBr_2$. After 1 hour the reaction mixture was analysed by ^{31}P-NMR spectroscopy and the species at −16.2 pmm was one of the three species present in solution. A similar chemical shift (−16.4 ppm) was reported by Tatsumi in 1998 for the complex $[Cu_3(dppm)_3Br_2]Br$ **280**, and the signal was also broad and of low intensity as in this case.[272]
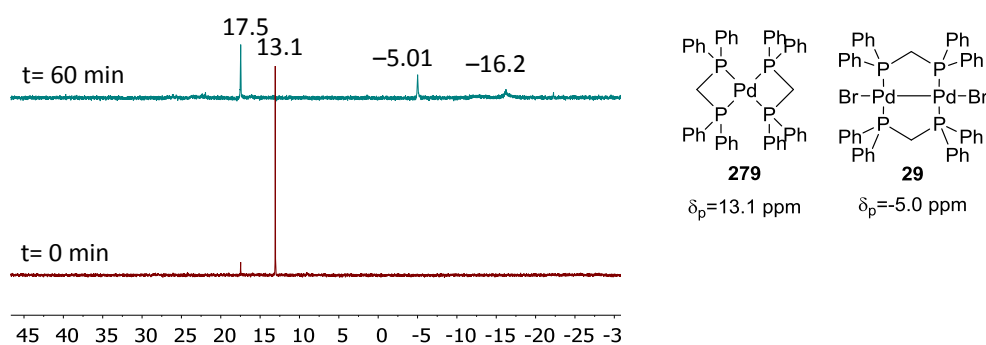
Figure 40: ^{31}P-NMR spectroscopic analysis of the reaction of Pd(dppm)$_2$ **279** (13.1 ppm) with CuBr$_2$ after: 0 minutes (red), 60 minutes (green). (Chemical shifts in ppm referenced to trimethoxyphosphine oxide as an internal standard)

In this case a RedOx reaction must be responsible for converting the Pd(0) into Pd(I) and the Cu(II) into Cu(I). This time the halide is not in the bridging position due to the presence of a chelating diphosphine ligand. Interestingly, similar results were obtained by just mixing Pd$_2$(dba)$_3$·CH$_3$Cl, dppm **47** and CuBr$_2$ in CH$_2$Cl$_2$ for 30 minutes, (*Scheme 76*).
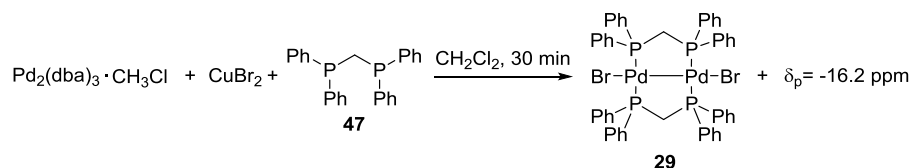
Scheme 76: One pot synthesis of [Pd(dppm)Br]$_2$ **29** from Pd$_2$(dba)$_3$·CH$_3$Cl, dppm **47** and CuBr$_2$.

In a way similar to that reported for the synthesis of Pd(I)-bromo dimer **29**, treatment of the chloro-dimer **48** with NaI or KI gave the corresponding iodo-analogue **281** (δ_p= −10.3 ppm), (*Scheme 77*).[271]
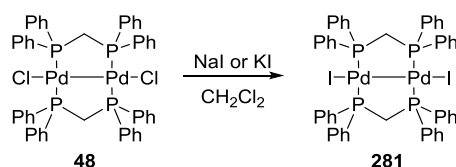
Scheme 77: Synthesis of Pd(I)-dimer **281** *via* halide exchange reaction between Pd(I)-dimer **48** and NaI or KI.[271]

In an analogous manner to before with CuBr$_2$, CuI was added to a THF solution containing Pd(0) complex **279**. After 3 hours of stirring at ambient temperature, the reaction was analysed by ^{31}P-NMR spectroscopy. To our surprise, the spectrum did not show any traces of the Pd(I)-dimer **281**, (*Figure 41*). However, Pd(0) complex **279** is completely converted into a new species at −25 ppm, A possible explanation for this behaviour could be due to the intrinsic lower reactivity of CuI towards reduction compared to the CuBr$_2$. In the case of Pd(PtBu$_3$)$_2$ **268**, the reaction with CuBr$_2$ is complete within 15 minutes, whilst in the presence of CuI the new product only started to form after approximately 1 hour.
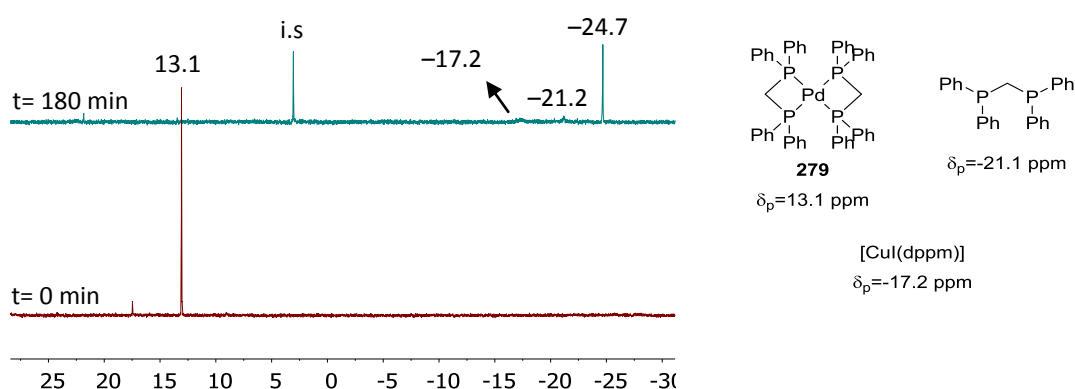
Figure 41: ^{31}P-NMR spectroscopic analysis of the reaction of Pd(dppm)$_2$ **279** (13.1 ppm) and CuI after: 0 minutes (red), 180 minutes (green). (Chemical shifts in ppm referred to trimethoxyphosphine oxide as an internal standard)

To gain more insight into the identity of the new species a control experiment was undertaken. CuI was added to a THF solution containing dppm **47**. Unfortunately, this time the reaction only confirmed the presence of a Cu complex with the dppm ligand at −17 ppm, probably due to [Cu$_3$(dppm)$_3$I$_2$] **282**. This complex first was reported by Pettinari *et al.* and was obtained by reaction of dppm and CuI in CH$_3$CN, (*Scheme 78*).[273]
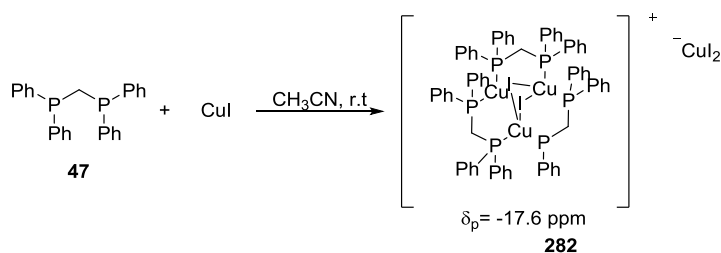
Scheme 78: Synthesis of complex [Cu$_3$(dppm)$_3$I$_2$] **282**, as reported by Pettinari.[273]

Unfortunately, it was not possible to establish the identity of the species at −25 ppm.

2.3.4 Investigation into the effect of Cu salts on Pd(dppe)₂ 283

Pd(0)(dppe)$_2$ **283** was prepared according to the reported procedure of Bäckvall.[274,275] Pd$_2$(dba)$_3$·CH$_3$Cl was added to a solution of dppe in benzene and it was then stirred for 1 hour at ambient temperature. After purification a yellow solid was obtained, (*Scheme 79*).
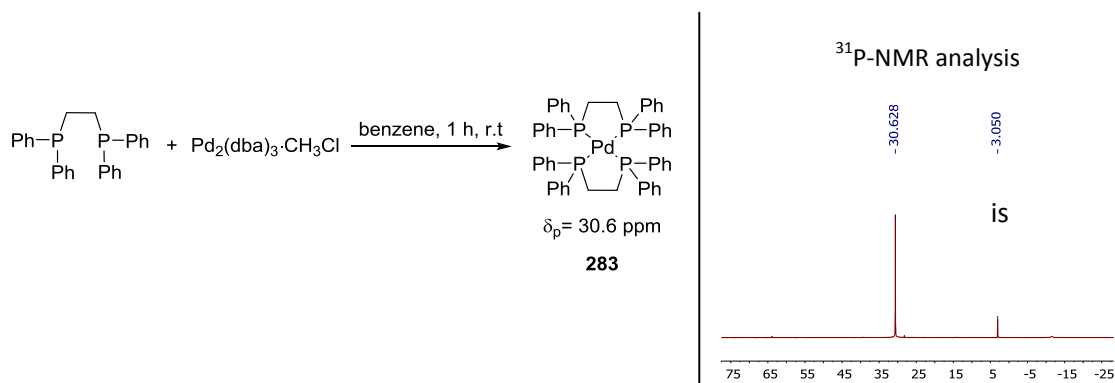
Scheme 79: Synthesis of Pd(dppe)$_2$ **283** from Pd$_2$(dba)$_3$·CH$_3$Cl and dppe (left). ^{31}P-NMR analysis of the reaction mixture. (Chemical shifts in ppm referenced to trimethoxyphosphine oxide as an internal standard)

Exposure of the obtained Pd(0) complex **283** to CuBr$_2$ did not results in substantial changes in the ^{31}P-NMR spectrum of the reaction mixture, even after 24 hours, (*Scheme 80*).
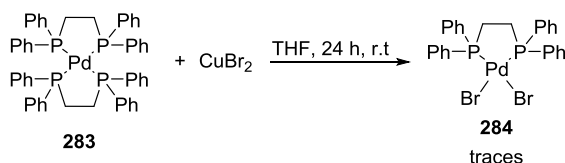
Scheme 80: Reaction between Pd(dppe)$_2$ **283** and CuBr$_2$.

Traces of the Pd(dppe)Br$_2$ **284** (δ_p= 64.0)[276] could be detected after 1 hour of exposure. However, the increase in the intensity of the peak of free dppe in the reaction mixture over time suggests that something is actually happening between the Pd(0) complex and the CuBr$_2$, but the lack of structural and spectroscopic data did not allow us to determine whether this phenomenon is due to occurrence of an oxidation process, (*Figure 42*).
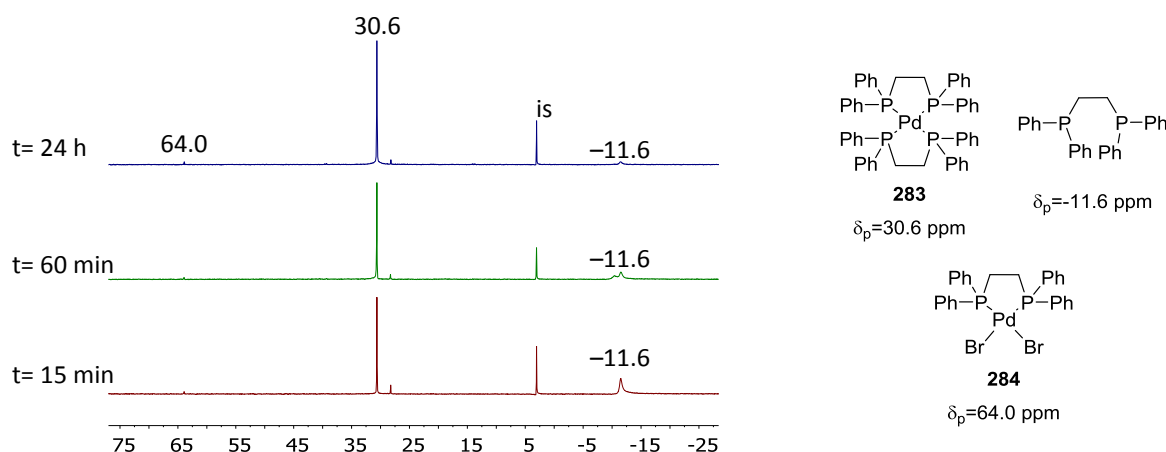
Figure 42: ^{31}P-NMR spectroscopic analysis of the reaction of Pd(dppe)$_2$ **283** (30.6 ppm) and CuBr$_2$ after: 15 min (red), 60 min (green) and 24 h (blue). (Chemical shifts in ppm referenced to trimethoxyphosphine oxide as an internal standard).

The use of CuI was not attempt because previously its reaction with Pd(0) complexes has been slow compared to that of CuBr$_2$ salts.

2.3.5 Investigation into the effect of Cu and Pd salts on Pd(dfmpe)$_2$ 286

In 2014 our group reported the synthesis of a new perfluoroalkyl diphosphine ligand, dfmpe **285**.[277] This ligand, that was successfully used to promote the ArCF$_3$ reductive elimination from (dfmpe)Pd(II)(Ar)(CF$_3$), was also used in this study to investigate the effect of Cu and Pd salts on its stability.

Pd(0)(dfmpe)$_2$ **286** was prepared by Nielsen, a member of our group, using Pd$_2$(dba)$_3$ as the palladium source together with 2 equivalents of ligand **285** with benzene as solvent.[277] The new Pd(0) complex **286** was characterised both spectroscopically and structurally (X-ray analysis), (*Scheme 81*).
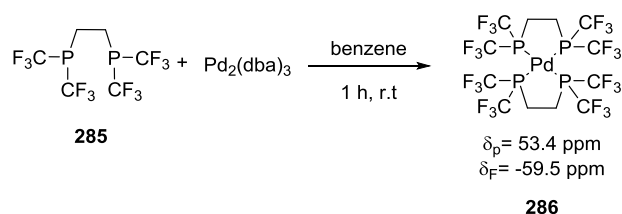
Scheme 81: Synthesis of Pd(dfmpe)$_2$ **286** from Pd$_2$(dba)$_3$ and dfmpe **285**. (Chemical shifts in ppm referenced to trimethoxyphosphine oxide for ^{31}P and 4,4'-difluorobiphenyl for ^{19}F as an internal standards).

Pd(dfmpe)$_2$ **286** was exposed to 1 equivalent of CuBr$_2$. After 1 hour of reaction a new doublet formed in the ^{19}F-NMR spectrum along with a heptuplet in the ^{31}P-NMR spectrum. Prolonged exposure slightly improved the conversion. However, it was the addition of an excess of CuBr$_2$ that drove the reaction to completion, (*Figure 43*).
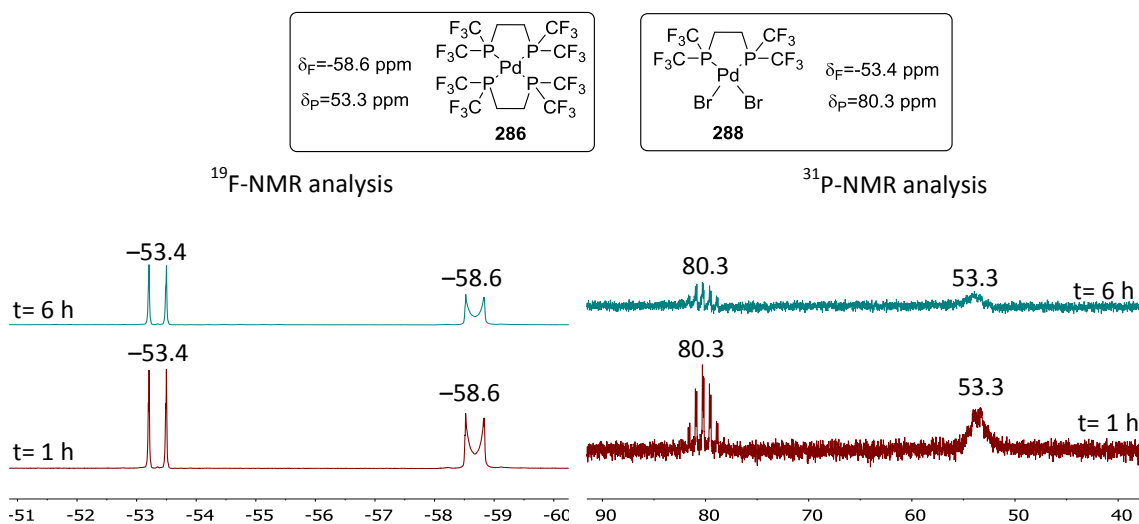
Figure 43: ^{19}F-NMR spectroscopic analysis of the reaction of Pd(dfmpe)$_2$ **286** (–58.6 ppm) and CuBr$_2$ after: 1 hour (red) and 6 hours (green) (left); ^{31}P-NMR spectroscopic analysis of the reaction of Pd(dfmpe)$_2$ **286** (53.3 ppm) and CuBr$_2$ after: 1 hour (red) and 6 hours (green). (Chemical shifts in ppm referenced to trimethoxyphosphine oxide for ^{31}P and 4,4'-difluorobiphenyl for ^{19}F as an internal standards).

To gain more insight into the possible composition of the new species formed, Pd(dfmpe)$_2$ **286** was exposed to 1 equivalent of PdBr$_2$ in dioxane at 60 °C . The same new species was formed after 4 hours (δ_F= –53.4 and δ_P= 80.3 ppm). Again, prolonged reaction time did not improve the conversion and addition of 1 equivalent of PdBr$_2$ allowed the reaction to go to completion.

In a separate experiment Nielsen exposed Pd(dfmpe)$_2$ **286** to I$_2$ in a THF solution at ambient temperature. Recrystallisation of the reaction mixture furnished suitable crystals for X-ray analysis corresponding the iodide-Pd(II) complex **287**, (*Scheme 82*).
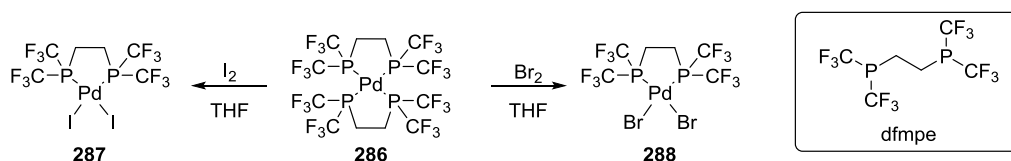
Scheme 82: Reaction of Pd(dfmpe)$_2$ **286** with Br$_2$ and I$_2$ perfomed by Nielsen.

Same procedure was also followed with Br_2. Based on the results obtained with I_2, it was assumed that the reaction with Br_2 gave the same analogous Pd(II) monomeric complex **288**. Interestingly, the reaction with Br_2 gave the same ^{19}F and ^{31}P-NMR spectra that were obtained for the reaction of Pd(dfmpe)$_2$ **286** with PdBr$_2$ and CuBr$_2$ salts.

The formation of a dark precipitate at the bottom of the reaction flask could be due to a reaction similar to the one we have observed already for Pd(PCy$_3$)$_2$ **270**, as shown in *Scheme 83*.
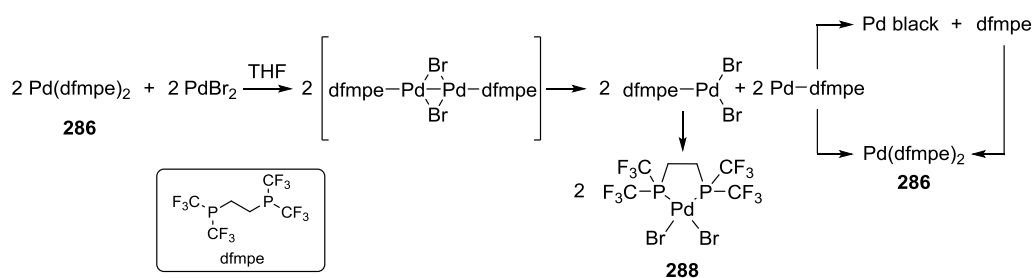
Scheme 83: Possible mechanism for the formation of the Pd(II) species **288**.

In the proposed mechanism, we hypothesised the formation of an unstable Pd(I) dimer that undergoes fast disproportionation in a Pd(II) species (in this case Pd(II) **288**) and a monoligated Pd(0) species. The so formed monoligated Pd(0) species can: *(i)* lose the ligand and precipitate as Pd black or *(ii)* gain one ligand and reform Pd(dfmpe)$_2$ **286**.

As described in section *2.3.3*, the reaction of dppm ligand **47** with Pd(II)Cl$_2$(CNPh)$_2$ and Pd(0)$_2$(dba)$_3$·CH$_3$Cl afforded the Pd(I)chloro-dimer **48**. The same approach was attempted with dfmpe **275** with the aim of possibly obtaining a Pd(I)chloro-dimer. Pd(II)Cl$_2$(CNPh)$_2$ and Pd(0)$_2$(dba)$_3$·CH$_3$Cl were added to a CH$_2$Cl$_2$ solution of dfmpe **275**. The solution was allowed to stir for 1 hour at room temperature and was then analysed by ^{19}F and ^{31}P-NMR. The spectra showed the formation of two species, one corresponding to Pd(dfmpe)$_2$ **286**, and the other new ($\delta_F = -53.4$ and $\delta_P = 80.3$ ppm), (*Scheme 84*).
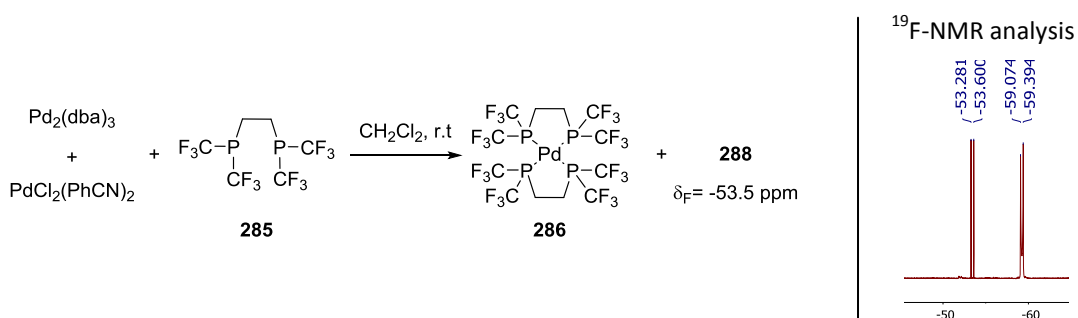
Scheme 84: Reaction between dfmpe **285**, Pd$_2$(dba)$_3$·CH$_3$Cl and Pd(II)Cl$_2$(CNPh)$_2$ (left). ^{19}F-NMR spectroscopic analysis of the reaction mixture (right). (Chemical shifts in ppm referenced to 4,4'-difluorobiphenyl as an internal standards).

To identify this species a control experiment was undertaken. Dfmpe **285** was mixed with Pd(II)Cl$_2$(CNPh)$_2$ in CH$_2$Cl$_2$ for 30 minutes at ambient temperature. The reaction was analysed by ^{19}F-NMR spectroscopy. There were three doublets present in solution: the first one at −59.6 ppm, the second one at −53.5 ppm and the third one ar −52.0 ppm, (*Scheme 85*).
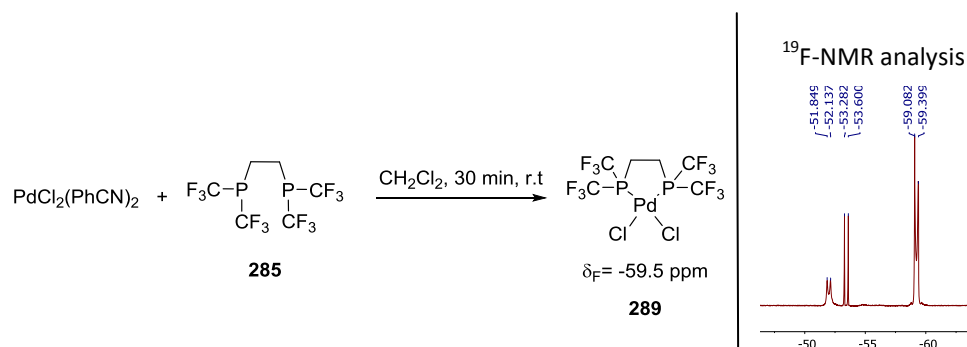
Scheme 85: Reaction between dfmpe **285** and Pd(II)Cl$_2$(CNPh)$_2$ (left). ^{19}F-NMR spectroscopic analysis of the reaction mixture (right). (Chemical shifts in ppm referenced to 4,4'-difluorobiphenyl as an internal standard).

The species at −59.6 ppm has a chemical shift very close to the Pd(II) species **288**. So based on the results obtained with the bromide analogue, it was assumed that this species corresponded to the Pd(II) complex **289**.

An oxidation reaction after exposure to Cu and Pd salts leads to the formation of Pd(II) monomers in this case. Analysis of the reaction between Pd(0) **286** and Pd(II) could let think of a simple ligand exchange between the Pd(0) and the Pd(II) moieties. However, the fact that the same transformation occurs in the presence of Cu supports the oxidation pathway. Formation of a Pd(I) dimeric species could be, in this case, disfavoured both by

steric also electronic repulsions, due to the presence of the two electron withdrawing CF_3 groups in the ligand **285**.

2.3.6 Investigation into the effect of Cu and Pd salts on Pd[Qphos]₂ 292

In 1999 Hartwig *et al.* reported the first synthesis of a phosphine ligand containing a ferrocene moiety **290** and its use in C-O bond formation.[278] This ligand was prepared by addition of P(P*t*Bu)₂Cl to a THF solution containing ferrocene and *tert*-butyllithium. The combination of ligand **290** and Pd₂(dba)₃ allowed the coupling of electron rich aryl halides (iodides, bromides and chlorides) with aryl phenoxide with *tert*-butoxide as base. One year later, while investigating how the catalyst structure can influence the reactivity in order to try to improve the conversions, they found that subjection of an excess of ligand to PhCl in the presence of NaO*t*Bu and catalytic amounts of Pd(OAc)₂ gave quantitative conversion of ligand **290** into a new ferrocene-based ligand: Qphos **291**, (*Scheme 86*). The combination of ligand **291** and Pd₂(dba)₃ also allowed the coupling of electron rich aryl halides and phenoxides at room temperature.[279]
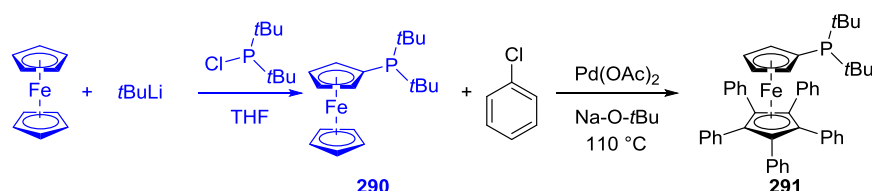
Scheme 86: Synthesis of ligand **290** from ferrocene and (*t*Bu)₂PdCl in the presence of *t*BuLi (left, blue). And reactions of ligand **290** with chlorobenzene to afford Qphos **291** (right, black).

This ligand first designed for the formation of C-O now has wide use; in combination with Pd(OAc)₂, Pd₂(dba)₃ or in the form of Pd(Qphos)₂ **292**, it is an efficient catalyst/precatalyst for various coupling reactions for the formation of both C-C (Suzuki coupling,[280] Reformatsky reaction,[186,281,282] Heck reaction,[283] arylation of dicarbonyl compounds[284,285] and C-N (amination) bonds.[280,286]

Due to its wide-spread use in catalysis, we decided to investigate what happen to the Pd(Qphos)₂ **292** when the catalyst/precatalyst is exposed to Cu and Pd salts. The complex

was prepared following the procedure reported by Hartwig: where Qphos **291** is added to Pd(dba)$_2$ at 60 °C, (*Scheme 87*).[279]
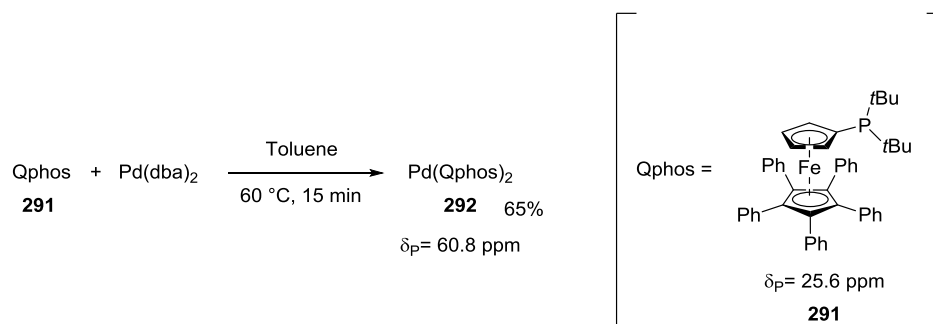
Scheme 87: Synthesis of Pd(Qphos)$_2$ **292** from Qphos **291** and Pd$_2$(dba)$_3$.[279]

Pd(Qphos)$_2$ **292** was subjected to one equivalent of CuBr$_2$ in a THF solution. The reaction was monitored by ^{31}P-NMR spectroscopy. After 15 minutes Pd(0) **292** was completely consumed and two new species were formed: one with a sharp signal at 64.7 ppm, possibly corresponding to an oxidised form of the Pd(0) **292**, based on what we observed with other bulky ligands such as PtBu$_3$ and P(iPr)(tBu)$_2$ **275**, and one broad signal at 38.3 ppm, (*Scheme 88*).
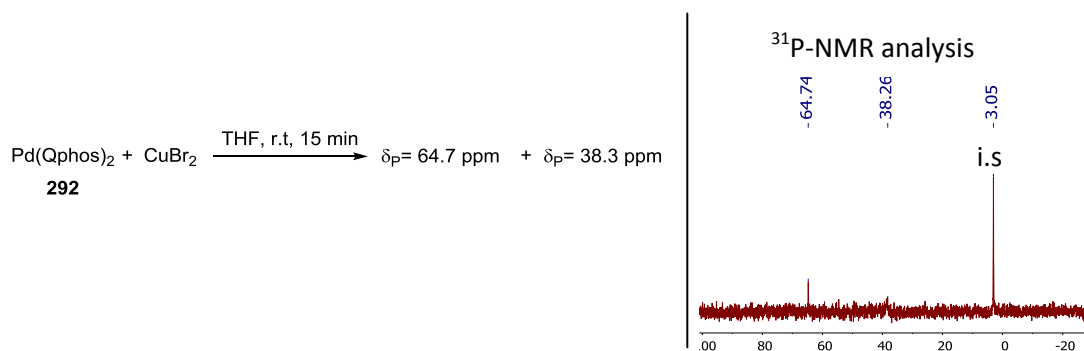
Scheme 88: Reaction between Pd(Qphos)$_2$ **292** and CuBr$_2$ (left). ^{31}P-NMR spectroscopic analysis of the reaction mixture (right). (Chemical shifts in ppm referenced to trimethoxyphosphine oxide as an internal standard).

Qphos **291** was subsequently exposed to PdBr$_2$ and to CuBr as a control experiment. In the first instance we wanted to verify if the new species formed at 64.7 ppm could be due to a Pd(II) monomer or dimer as well as to verify if the broad signal at 38.3 ppm could be assigned to a Cu(I) complex with the phosphine ligand. This would support a hypothesis of the occurrence of a RedOx reaction. The reaction with PdBr$_2$ did not introduce any changes in the ^{31}P-NMR spectrum of the ligand, excluding the possibility that the species

at 64.7 ppm could be due to a monomeric or dimeric Pd(II) species. Interstingly, the reaction with CuBr gave the same broad peak obtained in the spectrum of the reaction shown in *Scheme 86*, supporting the hypothesis of a RedOx reaction occurring.

To gain more information about the nature of the species at 64.7 ppm, Pd(Qphos)$_2$ **292** was exposed to 1 equivalent of PdBr$_2$. After 4 hours the reaction mixture was analysed by ^{31}P-NMR spectroscopy: the main species was still Pd(0) **292**, but in the spectrum the signal at 64.7 ppm, already obtained in the reaction with CuBr$_2$, was observable, (*Figure 44*).
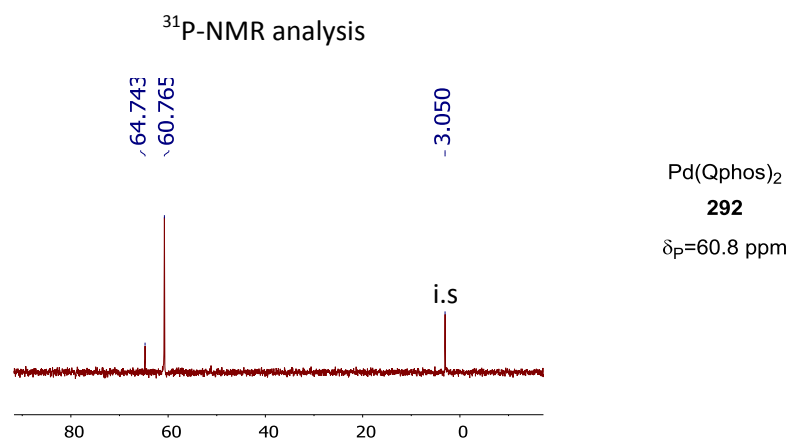
Figure 44: ^{31}P-NMR spectroscopic analysis of the reaction of Pd(Qphos)$_2$ **292** with PdBr$_2$. (Chemical shifts in ppm referred to trimethoxyphosphine oxide as an internal standard).

Unfortunately attempts to grow crystals for X-ray analysis was unsuccessful, however, the formation of the same species in the presence of different oxidants was observed as in the case of PtBu$_3$ and P(iPr)(tBu)$_2$. This could suggest Pd(I) dimer formation.

One last attempt was made employing PdI$_2$ as both an oxidant and an iodide source. The Pd(I) dimer with bridging iodides are usually more stable and easier to handle in air. Pd(Qphos)$_2$ **292** was subjected to one equivalent of PdI$_2$ and the solution analysed by ^{31}P-NMR spectroscopy after 4 hour of reaction time. The peak corresponding to the Pd(0) species **292** had disappeared and a new species had formed at 79.9 ppm, which could correspond to a new Pd(I)-dimer **294**, (*Figure 45*).
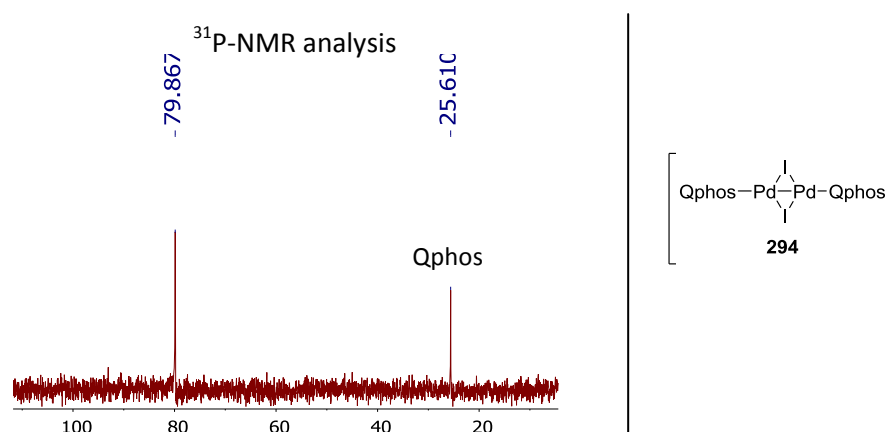
Figure 45: ^{31}P-NMR spectroscopic analysis of the reaction of Pd(Qphos)$_2$ **292** with PdI$_2$ (left) possible structure of the new species at 79.9 ppm (right). (Chemical shifts in ppm referenced to trimethoxyphosphine oxide as an internal standard).

2.3.7 Investigation into the effect of Cu salts on Pd(PPh$_3$)$_4$ 296

Pd(PPh$_3$)$_4$ **296** is one of the most utilised and most studied sources of Pd(0) in cross-coupling reactions.[287-294] This complex was first synthesised in 1957 by Malatesia and Angoletta by reduction of (PPh$_3$)$_2$PdCl$_2$ **295** using hydrazine in the presence of an excess of PPh$_3$ and it can be isolated as an air-stable bright yellow solid.[295] Many variation in the first synthesis have been reported over the years, (*Scheme 89*).[296,297]

$$2 \text{ (PPh}_3)_2\text{PdCl}_2 + 4 \text{ PPh}_3 + 5 \text{ H}_2\text{N-NH}_2 \longrightarrow 2 \text{ Pd(PPh}_3)_4 + 4 \text{ H}_2\text{N-NH}_2\text{HCl} + \text{N}_2$$

295 **296**
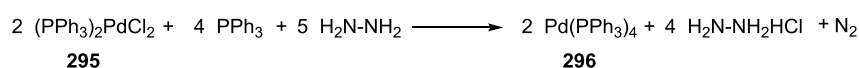
Scheme 89: First synthesis of Pd(PPh$_3$)$_4$ reported by Malatesia and Angoletta.[295]

The behaviour of this precatalyst in solution has been extensively studied. Malatesia and Angoletta observed that in solvents such as benzene, complex **296** dissociates into Pd(PPh$_3$)$_3$ **297** and Pd(PPh$_3$)$_2$ **298** and free PPh$_3$ ligand. This observation was also reported by Tolman *et al.* in 1972 and by Mann, who through a ^{31}P-NMR spectroscopic study of the complex in solution showed that the predominant species is Pd(PPh$_3$)$_3$ **297**, (*Scheme 90*).[298]

$$\text{Pd(PPh}_3)_4 \rightleftharpoons \text{PPh}_3 + \text{Pd(PPh}_3)_3 \rightleftharpoons \text{PPh}_3 + \text{Pd(PPh}_3)_2$$

296 **297** **298**
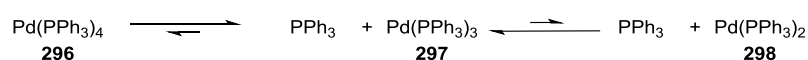
Scheme 90: Behaviour of Pd(PPh$_3$)$_4$ **296** in solution.[298]

Oxidative addition onto the species arising from Pd(PPh$_3$)$_4$ **296** has been exhaustively studied over the years.[291,299,300] The first example of a well-characterised oxidative addition complex upon oxidative addition of aryl halides was reported by Fitton *et al.* in the late 1960's, (*Scheme 91*).[301,302]
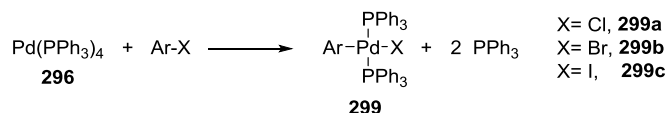
Scheme 91: Oxidative addition complexes from Pd(PPh$_3$)$_4$ **296**, as reported by Fitton *et al.*[302]

The first kinetic data were reported almost 15 years later by Fauvarque and Pflüge.[303] The two chemists showed that oxidative addition of aryl iodides proceeds via a fast dissociation of a ligand from Pd(PPh$_3$)$_3$ **297** to afford complex Pd(PPh$_3$)$_2$ **298**, that slowly undergoes oxidative addition. In 1991, a kinetic study performed by Amatore and Jutand later supported the hypothesis of Fauvarque and Pflüger, that Pd(PPh$_3$)$_3$ **297** is not directly involved in the oxidative addition despite it being the main species in solution.[304] However, they reported that the second ligand dissociation is a particularly slow process. In fact, when Pd(PPh$_3$)$_3$X$_2$ **300** (X=Cl, Br) is directly reduced in solution to generate Pd(PPh$_3$)$_2$ **298** *in situ* the rate of reaction substantially increases, but not as much as expected. They also observed that the nature of the halides X plays an important role and it is not just a spectator. In the case of X=Cl, three Pd(0) species **301a-c** are present in solution, whilst when X=Br only two Pd(0) species **302b-c** are present in solution. This experiment showed that the bromides ligands have lower bridging ability to the Pd(0) formed compared to the chlorides ligands, (*Scheme 92*).[304]
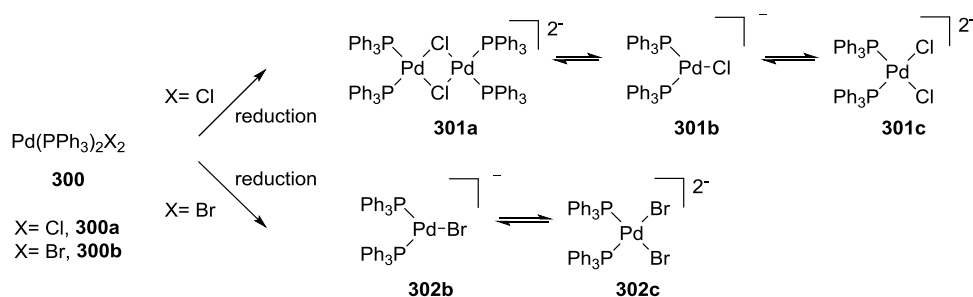
Scheme 92: *In situ* reduction of Pd(PPh$_3$)$_3$X$_2$ **300** reported by Amatore and Jutand.[304]

According to Amatore and Jutand the coordination of the counterion Cl or Br to the Pd(0) could explain why the rate of oxidative addition of aryl iodides onto $Pd(PPh_3)_2$ **298**, which is formed *in situ* upon reduction of $Pd(PPh)_3X_2$ **300**, were not as high as expected compared to reaction in the presence of $Pd(PPh_3)_4$ **296**.

The role of Cu additives as ligand scavengers in cross-coupling reactions, in particular the Stille coupling, was explored by Farina *et al.*[230] However, the possible effect of Cu salts as oxidants on the chemistry of $Pd(PPh_3)_4$ **296** has not been explored to date. We decided to expose $Pd(0)L_4$ complex **296** to Cu^nBr_n (n=1, 2) and CuI salts.

Exposure of $Pd(PPh_3)_4$ **296** to 1 equivalent of $CuBr_2$ was monitored by ^{31}P-NMR spectroscopy. After 15 minutes of reaction time the spectrum showed a broad peak approximately at 22 ppm which corresponds to the $Pd(PPh_3)_3$ **297**, according to the data reported by Mann,[298] and a small broad peak at −6 ppm corresponding to the free PPh_3. After 2.5 hours the reaction was analysed again and two new species had formed, although the main peak was still the one of $Pd(PPh_3)_3$ **297**. There was one new peak at 24 ppm, the chemical shift of which is in agreement with that reported for $Pd(PPh_3)_2Br_2$ **300a** complex,[305,306] and another doublet at 10 ppm which identity was not identified, (*Scheme 93*).
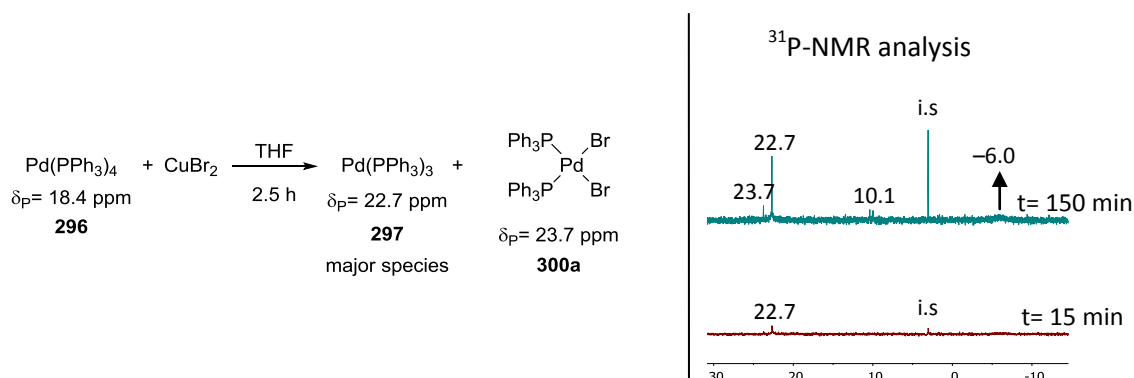
Scheme 93: Reaction of $Pd(PPh_3)_4$ **296** with $CuBr_2$ (left); ^{31}P-NMR spectroscopic analysis of the reaction mixture (right). (Chemical shifts in ppm referenced to trimethoxyphosphine oxide as an internal standard).

The same study was repeated with 2 equivalents of CuBr, since Cu(I) salts are the most utilised as co-catalysts in cross-coupling reactions. The reaction mixture was analysed after 2 hours of exposure by ^{31}P-NMR spectroscopy. In this case we could observe an increase in the relative concentration of the species at 10.1 and 23.7 ppm, and the formation of a new species at 24 ppm. A control experiment where PPh_3 and CuBr where mixed led to the

formation of the same Cu(I) species which therefore could be $(PPh_3)_2CuBr$ monomer, (*Figure 46*).[307]
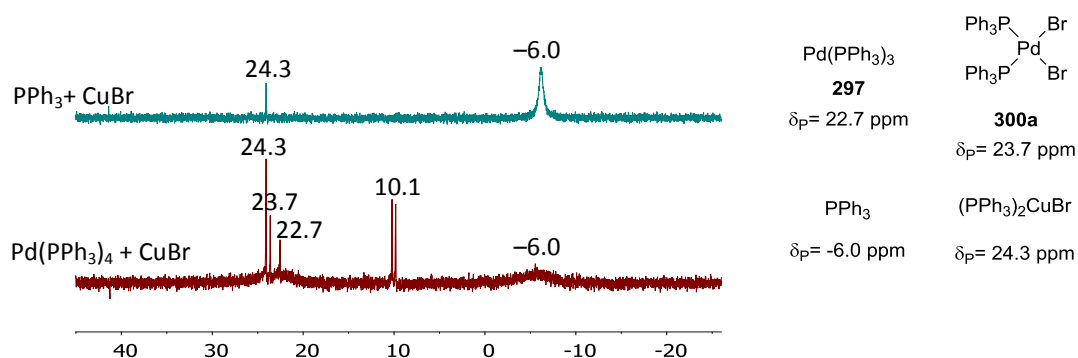
Figure 46: ^{31}P-NMR spectroscopic analysis of the reaction of $Pd(PPh_3)_4$ **296** and 2 equivalents of CuBr after 2 hours (red); reaction between PPh_3 (–6.0 ppm) and CuBr (green). (Chemical shifts in ppm referenced to trimethoxyphosphine oxide as an internal standard).

The formation of Pd(II) species **300a** as well as a Cu(I) complex implies that in this case the Cu salts also acted as an oxidant.

The same approach was also used for CuI. A slight excess of CuI was added to a THF solution containing $Pd(PPh_3)_4$ **296**. The solution turned from yellow to blue within 15 minutes with formation of a precipitate that was not soluble in organic solvents. Analysis of the reaction mixture after 1 hours by ^{31}P-NMR spectroscopy showed an ill-defined spectrum, probably due to the low concentration of the species remaining in solution or due to the high concentration of solid particle formed. A very broad and small peak of $Pd(PPh_3)_3$ **297** could be observable at 23 ppm as well as a sharp peak at 13 ppm, which is agreement with that reported for $Pd(PPh_3)_2I_2$ **303**.[305] Broad signals around 11 ppm could also be observed, (*Scheme 94*).
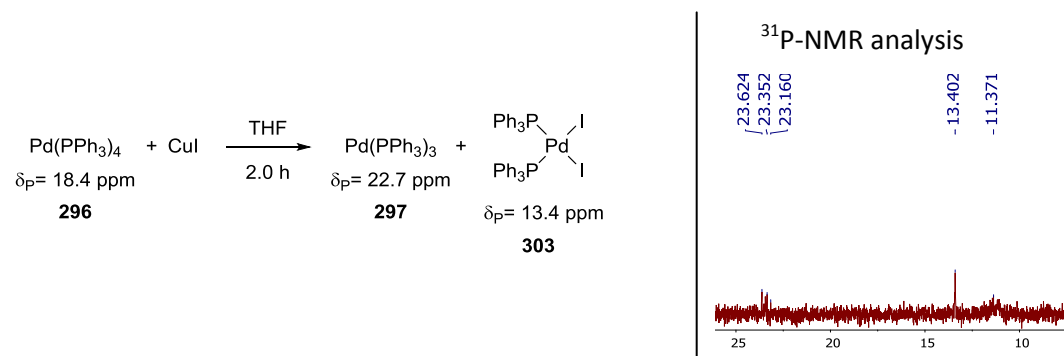
Scheme 94: Reaction of $Pd(PPh_3)_4$ **296** with CuI (left); ^{31}P-NMR spectroscopic analysis of the reaction mixture (right). (Chemical shifts in ppm referenced to trimethoxyphosphine oxide as an internal standard).

As in the case of Cu^nBr_n salts, also in the presence of CuI oxidation products could be observed upon reaction of Pd(0) **296** and Cu(I).

2.3.8 Investigation into the effect of Cu and Pd salts on Pd(Cy-JohnPhos)$_2$ 305

The use of bulky phosphine ligands in cross-coupling reactions has opened the possibility to also use of challenging substrates such as aryl chlorides and triflates as coupling partners, which was not previously possible using less bulky ligands. The interests of many research groups still lies in the development of ligands able to give high conversions in a range of cross-coupling reactions. In particular, attention has been focused on the development of ligand systems that could favour the formation a monoligated 12-electron Pd(0)L species, for the ease it can undergo oxidative addition.[31] In 1998, Buchwald *et al.* reported the first use in catalysis of monodentate, bulky dialkylbiarylphosphines in combination with Pd(0) sources for amination reaction, Suzuki couplings and the arylation of ketones using aryl chlorides and bromides, (*Scheme 95*).[176]
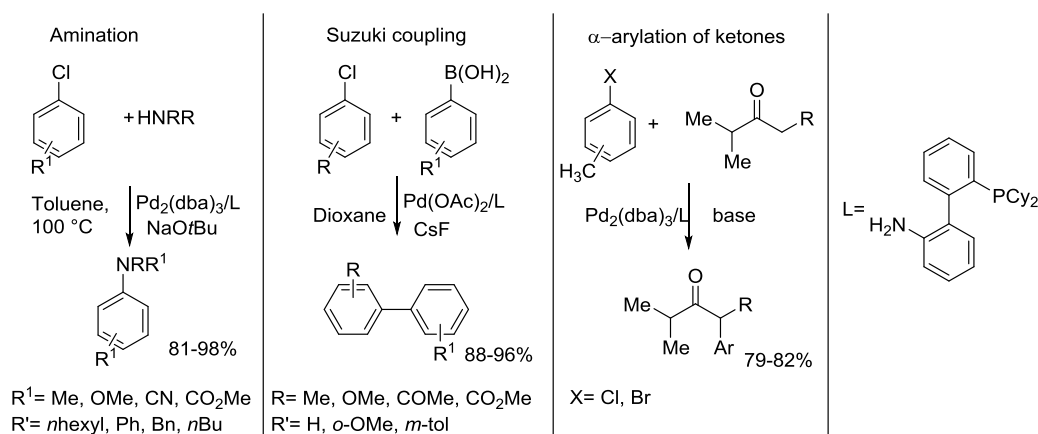
Scheme 95: First use of a monodentate dialkylbiarylphosphine in cross-coupling reactions as reported by Buchwald *et al.*[176]

In 2001, the same group reported an improved methodology for the synthesis of functionalised bialkylbiarylphosphines for use as ligand. Before the synthesis of this type of ligands required four synthetic steps and the overall yields were very low (less than 30%).[308] The reaction of an organo magnesium or organo lithium compound with an *in situ* generated benzyne along with a catalytic amount of CuCl, followed by addition of an appropriate chlorophosphine, allowed the one-pot synthesis of sterically-hindered biarylphosphines, (*Scheme 96*).
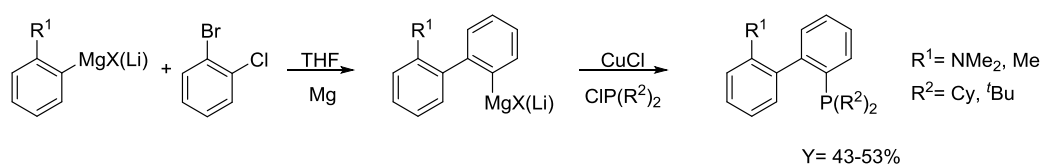
Scheme 96: One-pot synthesis of diarylbiarylphosphines as reported by Buchwald *et al.*[308]

This new methodology provided valuable contribution to increasing the scope of this family ligands. It has been possible to understand of their mechanism of reaction, allowing the design of tune ligands according to specific needs: 1) substitution in ortho-position of the phosphine bearing ring enhances the rate of reductive elimination (green); 2) the lower ring helps to prevent oxidation of the phosphine by O_2 and favours the reductive elimination, as well as its substitution in the 2-, 4-, 6-positions increases the stability and therefore the concentration of Pd(0)L in solution (red); 3) alkyl groups on the P increase the rate of oxidative addition, and the larger their size, the faster the rate of reductive elimination (pink), (*Figure 47*).[309]
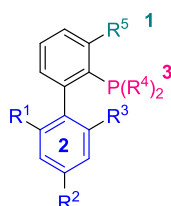
Figure 47: Structural features and related influence in catalysis of diarylbiarylphosphines.[309]

These ligands are currently use as efficient catalyst systems in combination with Pd(0) for a wide range of cross-coupling reactions for both C-C and C-X bond formation.[309-314] The great success and their widespread use as ligand in catalysis intrigued us to further explore the behaviour of one member of the family in the presence of Cu and Pd salts: Cy-JohnPhos **304**.[315]

Pd(Cy-JohnPhos)$_2$ **305** was prepared following the same procedure utilised for the synthesis of Pd(PCy$_3$)$_2$ **270**, using tmeda-Pd(II) **225** and 2 equivalent of Cy-JohnPhos **304**, (*Scheme 97*).
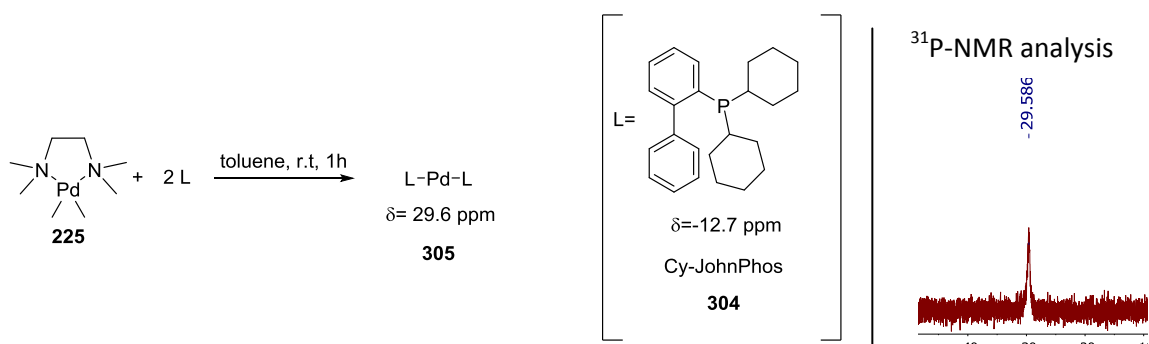
Scheme 97: Synthesis of Pd(Cy-JohnPhos)$_2$ **305** from Pd(Me)$_2$(tmeda) **225** and L=Cy-JohnPhos **304** (left). ^{31}P-NMR spectroscopic analysis of the reaction mixture (right). (Chemical shifts in ppm referenced to trimethoxyphosphine oxide as an internal standard).

After isolation, the off-yellow complex **305** was first subjected to CuBr$_2$ and the reaction was monitored by ^{31}P-NMR spectroscopy. After the first 5 minutes a precipitate had formed at the bottom of the round-bottomed flask. Interestingly, the peak corresponding to our internal standard at 3.05 ppm had disappeared, whilst the peak of the starting material had decreased considerably in intensity. After prolonged time the spectrum was fully consisting by noice. Similar results were obtained in the presence of PdBr$_2$ and CuI: the starting material was fully consumed over time and several peaks of very low intensity had formed in both spectra. The structural analysis of the solution was not possible because the solids obtained in the presence of the three salts were not crystalline.

For this ligand both spectroscopic and crystallographic analyses were inconclusive. However, consumption of the Pd(0) complex was observed for all of three salts.

2.4 Investigation on the effects of Cu salts on Sonogashira coupling

In the introductory section it was described that a large number of metal additives is used in combination with palladium sources in the Sonogashira couplings. For this reason our interested became directed into investigating the effects of Cu salts on the Sonogashira coupling reaction. Pd(0)(P*t*Bu$_3$)$_2$ **268** was utilised as catalysts/precatalyst in our study due to our prior gained knowledge of this system and the possible products it may form. All the reactions were performed in the absence of oxygen to avoid the occurrence of Glaser or Hay couplings.

Table 8: Sonogashira coupling of 4-chloroacetophenone **306** with 3,3-dimethyl-1-butyne **307** in the presence of different catalyst systems.
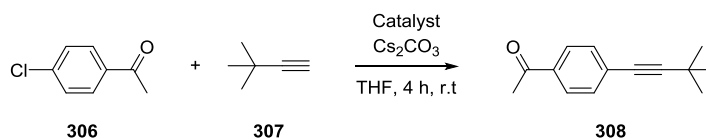
Entry	Catalyst	Temperature (°C)	^{1}H-NMR Yield **308** (%)[a]
1	Pd(PtBu$_3$)$_2$ **268**	r.t	-
2	Pd(I)-Br-dimer **31**	r.t	-
3	Pd(I)-Br-dimer **31**	30	-

General conditions: **306** 1.0 equiv, **307** 1.0 equiv, Cs$_2$CO$_3$ 2.6 equiv, catalyst load 5 mol% for Pd(PtBu$_3$)$_2$ **268** and 2.5 mol % for Pd(I)-Br-dimer **31**, THF M=0.4. a) Yields are calculated from the ^{1}H-NMR spectrum using 1,4-dioxane as an internal standard.

The first test was done employing 3,3-dimethyl-1-butyne **307** together with 4-chloroacetophenone **306**, (*Table 8*). The reaction after 4 hours at room temperature did not show any trace of the product in the ^{1}H-NMR spectrum and GC-MS chromatogram. Increase the temperature to 30 °C did not help the reaction. Further increase was not possible due to the low boiling point of the alkyne (32-33 °C). We therefore decided to use a different alkyne with a higher boiling point: phenylacetylene **309**. In some examples we also explored using a homogeneous base, such as NH(iPr)$_2$, because the solubility of Cs$_2$CO$_3$ in THF is very low (most of it did not dissolve over the reaction time), (*Table 9*).

Table 9: Sonogashira coupling of 4-chloroacetophenone **306** and phenylacetylene **309** in the presence of different catalyst systems.
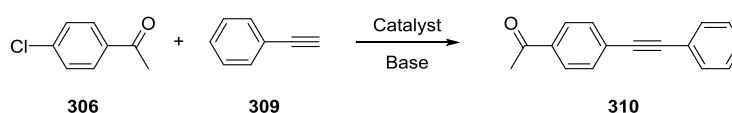
Entry	Catalyst	Base	Time (h)	Solvent	Temperature (°C)	^{1}H-NMR Yield **310** (%)[a]
1	Pd(I)-Br-dimer **31**	Cs$_2$CO$_3$	4	THF	55	0
2	Pd(I)-Br-dimer **31**	Cs$_2$CO$_3$	2	THF/CH$_3$CN	50	13
3	Pd(I)-Br-dimer **31**	NH(iPr)$_2$	2	THF	50	5
4	Pd(I)-Br-dimer **31**	NH(iPr)$_2$	4	THF	50	17
5	Pd(PtBu$_3$)$_2$ **268**	NH(iPr)$_2$	4	THF	50	7

General conditions: **306** 1.0 equiv, **309** 1.0 equiv, base 2.6 equiv for C$_2$CO$_3$ and 4.5 equiv for NH(iPr)$_2$, catalyst load 5 mol% for Pd(PtBu$_3$)$_2$ **268** and 2.5 mol % for Pd(I)-Br-dimer **31**, THF M=0.4. a) Yields are calculated from the ^{1}H-NMR spectrum using 1,4-dioxane as an internal standard.

As already observed, the low solubility of Cs$_2$CO$_3$ in THF does not allowed the reaction to proceed. Addition of CH$_3$CN as co-solvent allowed the formation of the product **310**,

although in very low amount (see Entries 1 and 2). The use of NH(*i*Pr)$_2$ as base and prolonged reaction times allowed the formation of the product in up to 17% yields. The use of Pd(0)(P*t*Bu$_3$)$_2$ **268** as catalyst/precatalyst did not improve the yields. Interestingly, analysis of the species formed in the GC-MS chromatogram of the reaction in Entry 4 revealed that no alkyne was left in the reaction mixture, whilst new species had formed corresponding to the dimer and trimer of the phenylacetylene (see *Figure 48*). Polymerisation in the presence of Pd-(I) dimer **31** was not observed before. Analysis of the GC-MS chromatogram of the reaction in Entry 5 showed that a large amount of alkyne was left in the reaction mixture in this case, although traces of dimer and trimer of the phenylacetylene were also present in solution.
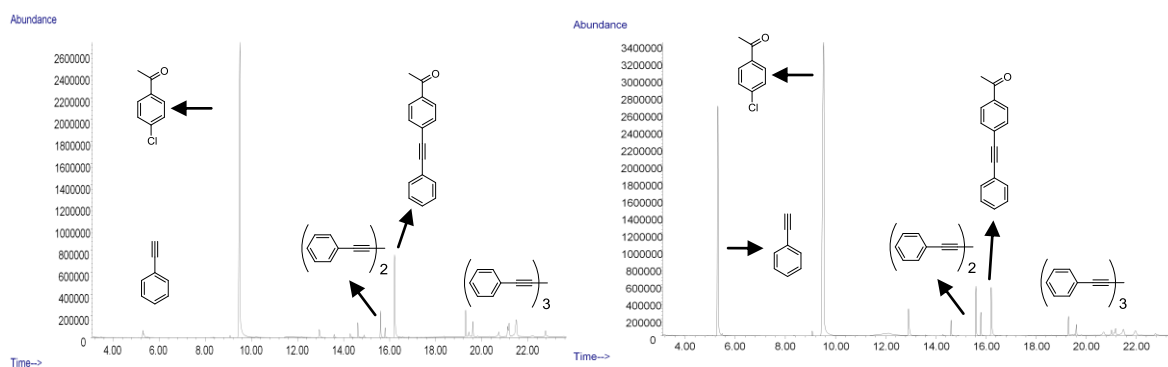
Figure 48: Comparison between the GC-MS chromatograms of the reactions in Entry 4 (left) Entry 5 (right).

An additional study was carried out to verify whether the polymerisation process is due to direct Pd(I)-dimer catalysis or just to the fact that Pd(I)-bromo dimer **31** is presumed to form the 12-electron monoligated species Pd(P*t*Bu$_3$) faster than Pd(0)(P*t*Bu$_3$)$_2$ **268**. Three different systems were examined: Pd(I)-bromo dimer **31**, Pd(0)(P*t*Bu$_3$)$_2$ **268** and the Pd$_2$(dba)$_3$/P*t*Bu$_3$ 1:1 system. The amount of alkyne remaining was determined by calibrated GC-MS analysis using 1,3,5-tri-*tert*-butylbenzene as internal standard, (*Table 10*).

Table 10: Quantitative study of the remaining alkyne in the Sonogashira coupling reaction of 4-chloroacephenone **306** and phenylacetylene **309** with different Pd sources.
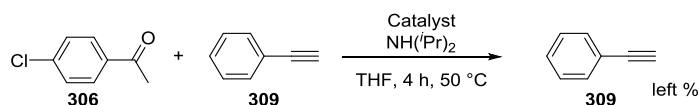
Entry	Catalyst	Alkyne left GC-MS Yield (%)[a]
1	Pd(I)-Br-dimer **31**	1
2	Pd(0)(P*t*Bu$_3$)$_2$ **268**	47
3	Pd$_2$(dba)$_3$/P*t*Bu$_3$	69

General conditions: **306** 1.0 equiv, **309** 1.0 equiv, NH(*i*Pr)$_2$ 4.5 equiv, catalyst load 5 mol% for Pd(P*t*Bu$_3$)$_2$ **268** and 2.5 mol % for Pd(I)-Br-dimer **31** and Pd$_2$(dba)$_3$, solvent 0.4 M. a) Yields are calculated by calibrated GC-MS using 1,3,5-tri-*tert*-butylbenzene as an internal standard.

The outcome of the study showed that the consumption of the alkyne is faster in the presence of the Pd(I) dimer **31** (see *Table 10*), supporting the hypothesis that the polymerization process could be directly catalysed by the Pd(I)-bromo dimer **31** and not due to the formation of the monoligated Pd(P*t*Bu$_3$) complex, as in the case of the Pd$_2$(dba)$_3$/P*t*Bu$_3$ 1:1 system, where the monoligated species should be formed due to the ideal ratio Pd:P of 1:1, the amount of alkyne left in solution is considerably high. If the process is directly catalysed by the Pd(I) dimer **31**, similar results should be also achieved in the presence of the more stable Pd(I)-iodo dimer **193**. To verify this, Pd(I)-bromo dimer **31** and Pd(I)-iodo dimer **193** were used in the presence of 4-methoxyphenylacetylene **311** or phenylacetylene **309**. The use of a different alkyne was in order to see if the polymerization process can be affected by the substituent on the benzene ring. We tested the reaction at two different temperatures and in the case of Pd(I)-bromo dimer **31**, the reaction was also performed in the presence of Cs$_2$CO$_3$.

Table 11: Effect of the temperature and the base on the polymerization reaction of 4-methoxyphenylacetylene **311** or phenylacetylene **309**.
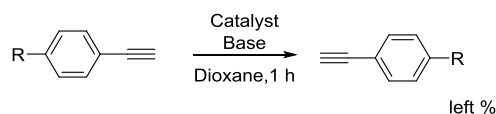
Entry	Catalyst	Base	Temperature (°C)	Alkyne remaining (%)[a]	R
1	Pd(I)-Br-dimer **31**	Cs_2CO_3	r.t	64	OCH_3
2	Pd(I)-Br-dimer **31**	Cs_2CO_3	55	24	OCH_3
3	Pd(I)-Br-dimer **31**	$NH(iPr)_2$	r.t	38	OCH_3
4	Pd(I)-Br-dimer **31**	$NH(iPr)_2$	55	1	OCH_3
5	Pd(I)-I-dimer **193**	$NH(iPr)_2$	r.t	60	OCH_3
6	Pd(I)-I-dimer **193**	$NH(iPr)_2$	55	22	OCH_3
7	Pd(I)-Br-dimer **31**	$NH(iPr)_2$	55	9	H
8	Pd(0)(PtBu$_3$)$_2$ **268**	$NH(iPr)_2$	55	57	H
9	Pd(I)-I-dimer **193**	$NH(iPr)_2$	55	30	H

General conditions: **alkyne** 1.0 equiv, base 2.6 equiv for C_2CO_3 and 4.5 equiv for $NH(iPr)_2$, catalyst load 5 mol% for Pd(PtBu$_3$)$_2$ **268** and 2.5 mol % for Pd(I)-dimers **31** and **193**, solvent 0.4 M. a)Yields are calculated by calibrated GC-MS using 1,3,5-tri-*tert*-butylbenzene as an internal standard.

The study showed that the polymerisation process is favoured at high temperature (Entry 1 *vs* Entry 2, Entry 3 *vs* Entry 4, Entry 5 *vs* Entry 6). The polymerisation is faster in the presence of a homogeneous base both at ambient temperature and at 55 °C (Entry 1 *vs* Entry 3, Entry 2 *vs* Entry 4). Consumption of the alkyne is also observed in the presence of the Pd(I)-iodo dimer **193**, although the process is slower compared to the Pd(I)-bromo dimer **31** (Entry 4 *vs* Entry 6, Entry 7 *vs* entry 9). The conditions that favour the Sonogashira coupling also seem to favour also the polymerisation of the alkyne, in the presence of both Pd(I)-dimers **31** and **193**. Analysis of the reaction mixture of Entry 4 by ^{31}P-NMR spectroscopy after 45 minutes at 50 °C showed that the only peak in the spectrum is Pd(0) **268** at 85.5 ppm. However, in the case of Pd(I)-I-dimer **193** (Entry 6) the ^{31}P-NMR spectrum consisted of several peaks the major one belonged to the dimer **193**, and another one to the Pd(0) **268**, whilst the others are signals are currently unknown, (*Figure 49*).
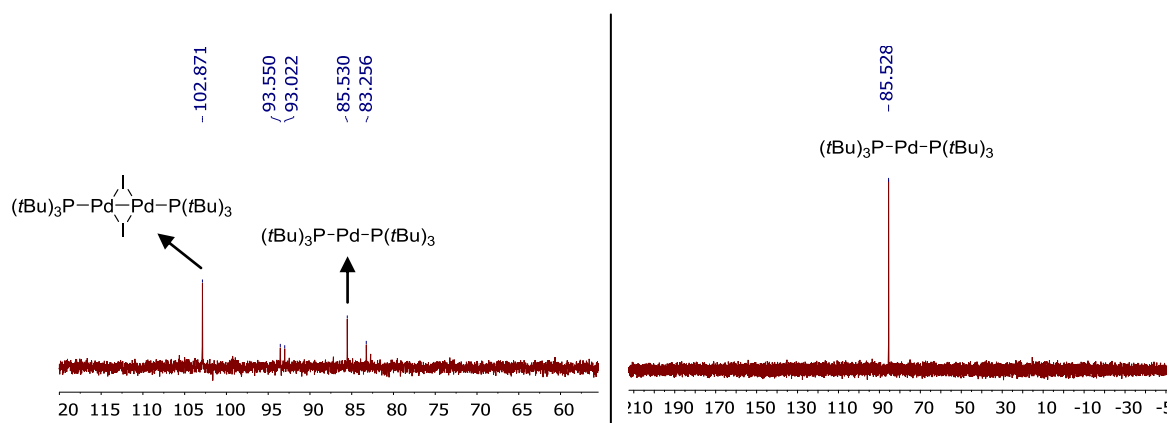
Figure 49: ^{31}P-NMR analysis of the reaction between Pd(I)-iodo-dimer **193** (102.9 ppm) and 4-methoxyphenylacetylene **311** at 50 °C (left). ^{31}P-NMR analysis of the reaction between Pd(I)-bromo-dimer **31** (87.1 ppm) and 4-methoxyphenylacetylene **311** at 50 °C (right). (Chemical shifts in ppm referenced to trimethoxyphosphine oxide as an internal standard).

An additional ^{31}P-NMR study was performed to verify if the formation of the Pd(0) complex **268** at 85.5 ppm is due to the presence of the base or to the polymerisation reaction. Pd(I) dimers **31** and **193** were exposed to an excess of NH(*i*Pr)$_2$ at 50 °C and the reactions were analysed using ^{31}P-NMR spectroscopy, (*Figure 50*).
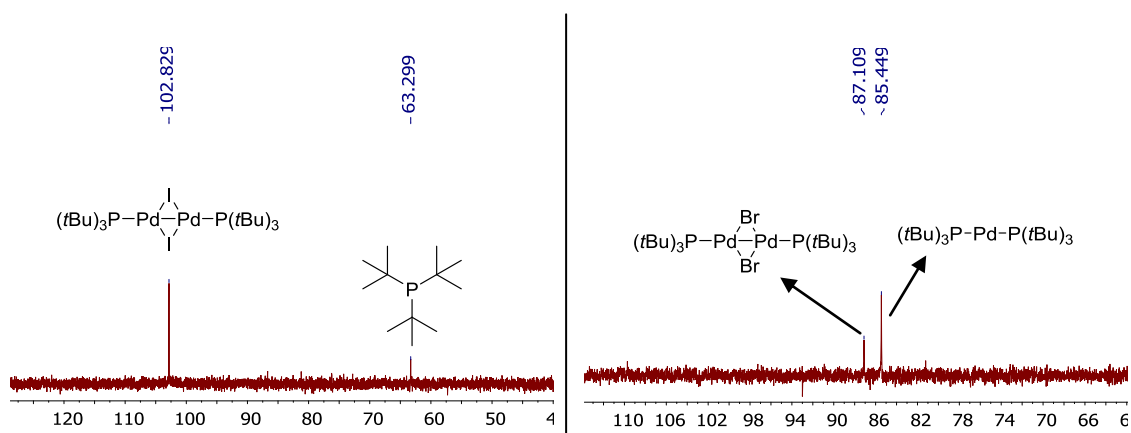
Figure 50: ^{31}P-NMR spectrum of the reaction between Pd(I)-iodo-dimer **193** (102.5 ppm) and NH(*i*Pr)$_2$ at 50 °C (left). ^{31}P-NMR spectrum of the reaction between Pd(I)-bromo-dimer **31** (87.1 ppm) and NH(*i*Pr)$_2$ at 50 °C (right). (Chemical shifts in ppm referenced to trimethoxyphosphine oxide as an internal standard).

The study showed that for Pd(I)-bromo dimer **31** the presence of the base led to the formation of the Pd(0)(P*t*Bu$_3$)$_2$ **268** (see Chapter 3), whilst in the case of the Pd(I)-iodo dimer **193** the presence of free phosphine suggested that something was happening to the Pd(I) dimer that could be either decomposition of the dimer in the presence of base or coordination of the alkyne. The species encountered previously at 93 and 83 ppm are not

present in the ^{31}PNMR spectrum, suggesting that they could be alkyne-adducts with the Pd(I)-iodo dimer **193**. The results obtained with these studies are consistent with a polymerisation process directly catalysed by the two dimers.

We have shown that in the presence of Pd-(I) dimers **31** and **193** a polymerisation reaction can take place before the expected Sonogashira coupling, whilst in the presence of Pd(0)(PtBu$_3$)$_2$ **268** the polymerisation reaction is very slow (see *Table 10* and *11*). Addition of CuBr$_n$ (n=1 or 2) and CuI salts to the Pd(0)(PtBu$_3$)$_2$ **268** should affect both the amount of alkyne left in solution (due to the formation of the Pd(I) dimers **31** or **193**) and the product formation (the formation of the organo-Cu species should facilitate the transmetallation step). Different salts were tested in the presence of Pd(0)(PtBu$_3$)$_2$ **268**, and these results are summarised in *Table 12*

Table 12: Sonogashira coupling of 4-chloroacetophenone **306** and phenylacetylene **309** or 4-methoxyphenylacetylene **311** in the presence of different catalyst systems.
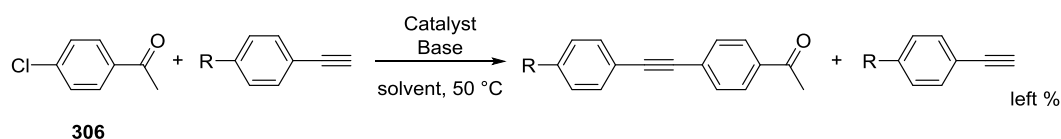
Entry	Catalyst	R	Base	solvent	Time (h)	^{1}H-NMR yield (%)[a]	Alkyne remaining (%)[b]
1	Pd(PtBu$_3$)$_2$ **268**	OCH$_3$	NH(iPr)$_2$	Dioxane	1	-	81
2	CuBr /Pd(PtBu$_3$)$_2$ **268**$_2$	OCH$_3$	NH(iPr)$_2$	Dioxane	1	5	23
3	CuI /Pd(PtBu$_3$)$_2$ **268**	OCH$_3$	NH(iPr)$_2$	Dioxane	1	-	21
4	Pd(I)-Br-dimer **31**	OCH$_3$	NH(iPr)$_2$	Dioxane	1	5	2
5	Pd(I)-I-dimer **193**	OCH$_3$	NH(iPr)$_2$	Dioxane	1	1	26
6	CuBr /Pd(PtBu$_3$)$_2$ **268**	OCH$_3$	Cs$_2$CO$_3$	CH$_3$CN	5	-	10
7	CuI /Pd(PtBu$_3$)$_2$ **268**	OCH$_3$	Cs$_2$CO$_3$	CH$_3$CN	5	-	25
8	CuBr/ Pd(I)-Br-dimer **31**	OCH$_3$	Cs$_2$CO$_3$	CH$_3$CN	5	-	15
9	CuI /Pd(PtBu$_3$)$_2$ **268**	OCH$_3$	KOEt	THF	5	-	63
10	CuI	H	NH(iPr)$_2$	THF	5	-	80

General conditions: **306** 1.0 equiv, **alkyne** 1.0 equiv, base 2.6 equiv for C$_2$CO$_3$ and 4.5 equiv for NH(iPr)$_2$, Cu additives 5 mol %, catalyst load 5 mol% for Pd(PtBu$_3$)$_2$ **268** and 2.5 mol % for Pd(I)-dimers **31** and **193**, solvent 0.4 M. a) Yields are calculated from the ^{1}H-NMR spectrum using 1,4-dioxane as an internal standard. b) the amount of remaining alkyne is calculated by calibrated GC-MS using 1,3,5-tri-*tert*-butylbenzene as an internal standard.

The study clearly shows that in the presence of Cu additives the amount of alkyne left in the reaction mixture is lower than in the absence of additives, (Entry 1 *vs* Entries 2-3). Oligomerisation is observed in the presence of NH(iPr)$_2$ and Cs$_2$CO$_3$, but it is partially inhibited in the presence of KOEt (Entries 3,7 *vs* Entry 9) (see chapter 3 for explanation).

The oligomerisation in the presence of Pd(I)-iodo dimer **193** has the same rate as oligomerisation in the presence of the Pd(P*t*Bu$_3$)$_2$ **268**/CuI catalyst system (Entry 3 *vs* Entry 5), whilst oligomerisation in the presence of Pd(I)-bromo dimer **31** is faster than in the presence of the Pd(P*t*Bu$_3$)$_2$ **268**/CuBr$_2$ catalyst system.

In conclusion we have shown that the Sonogashira coupling of aryl chloride in the presence of Pd(I)-iodo **193** and Pd(I)-bromo **31** dimers is inhibited by the occurrence of competing oligomerisation reaction. The reaction is directly catalysed by the two dimers and not by the Pd(0)(P*t*Bu$_3$) **268** that can be easily generated in the case of Pd(I)-bromo dimer **31**. The oligomerisation reaction is very slow in the presence of Pd(P*t*Bu$_3$)$_2$ **268**, but increases when CuBr and CuI salts are used as co-catalyst, consistent with *in situ* formation of Pd(I) dimers **193** and **31**. The occurrence of Glaser or Hay coupling in the presence of copper additives can be ruled out because all reactions were performed under oxygen and moisture free conditions.

2.5 Investigation into the effects of additives on Pd(0)(P*t*Bu$_3$)$_2$ 268

2.5.1 Investigation into the effect of Cu^{n}Br$_n$ and CuI salts on Suzuki coupling

In the previous section we have shown that in Sonogashira coupling the *in situ* formation of Pd(I)-dimers **31** and **193** from reaction of Pd(P*t*Bu$_3$)$_2$ **268** with CuBr or CuI salts is responsible for an oligomerisation reaction that consumes the alkyne, decreasing the amount of coupling with aryl chlorides.

The possible implications for the formation of Pd(I) dimers **31** and **193** from Pd(P*t*Bu$_3$)$_2$ **268** in the presence of CuBr and CuI respectively, in the Suzuki coupling, have been explored by Proutière. The studies were carried out using the reaction of 4-chloroacetophenone **306** with 4-methoxyphenylboronic acid **312** in the presence of KF as base, (*Scheme 98*).
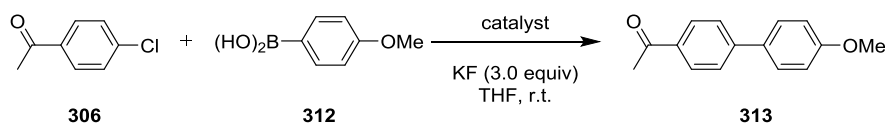
Scheme 98: Suzuki-type reaction of 4-chloroacetophenone **306** and 4-methoxyphenylboronic acid **312**, used for our studies.[258]

Different catalyst systems were studied: Pd(I)-bromo dimer **31**, Pd(PtBu$_3$)$_2$ **268** and Pd(I)-iodo dimer **193**, both in the presence and in the absence of Cu additives. Pd(I)-bromo-dimer **31** gave almost full conversion within 1 hour whilst the corresponding Pd(0) complex **268** gave very poor conversion in the same reaction time. Pd(I)-iodo dimer **193** did not give any product formation. A considerable increase in the reactivity was observed when CuBr$_2$ was used as an additive in the presence of Pd(0) complex **268**. This is consistent with formation of Pd(I)-bromo-dimer **31** *in situ* under normal reaction conditions. The same reaction profile and conversion was observed in the presence of CuBr. A consistent decrease in the reactivity of the Pd(0)(PtBu$_3$)$_2$ **268** can be observed in the presence of CuI. However, this decrease in the reactivity cannot be explained solely by the formation of the Pd(I)-iodo-dimer **193** because the ^{31}P-NMR study reported in *Figure 35* clearly shows that this dimer is only present in trace amounts after 1 hour of exposure of Pd(0)(PtBu$_3$)$_2$ **268** to CuI. A possible alternative explanation for this behaviour could be the presence of iodide in solution. Inhibition of aminations reaction in the presence of iodide sources was also observed by Hartwig *et al.* in 2008,[316] and by Buchwald in 2009.[317] The effect of the addition of NaI on the initial rate of reaction between aniline and 4-bromoanisole was studied using calorimetry. Saturation was reached after just 10% of added NaI. The explanation given by Buchwald *et al.* was that iodide can interfere with amine binding to the Pd by competitive formation of complexes **315a-b** after the oxidative addition step. Alternatively the iodide could bind to the Pd(II) complex after transmetallation and form complex **315c**, that inhibits the reductive elimination step, (*Scheme 99*).
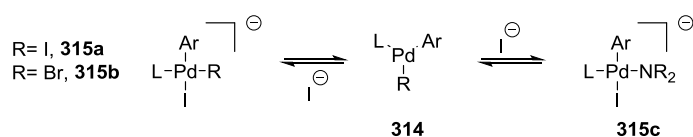
Scheme 99: Iodide inhibition pathways proposed by Buchwald *et al.*[317]

The effect of iodide salts on the Suzuki cross-coupling reaction of 4-chloro- or iodo-acetophenone with 4-methoxyphenylboronic acid **312** in the presence of KF as base and using Pd$_2$(dba)$_3$/PtBu$_3$ was further investigated as part of my studies, (*Table 13*).

Table 13: Effect of different salts on the reactivity of the $Pd_2(dba)_3$/$PtBu_3$ catalytic system.
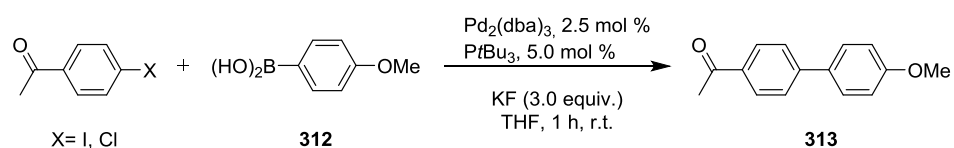
Entry	X	Additive	Equiv	Yield **313** %
1	Cl	absence	-	48
2	Cl	KI	3.0	10
3	Cl	KI	0.05	12
4	Cl	KBr	3.0	45
5	I	absence	-	77
6	I	KI	0.05	50
7	Cl	CsI	0.05	13
8	Cl	NaI	0.05	8

General conditions: aryl halide 1.00 equiv, **312** 1.05 equiv, KF 3.00 equiv, $PtBu_3$ 5 mol %, $Pd_2(dba)_3$ 2.5 mol %, THF 0.45 M. Yields are calculated from the ^{1}H-NMR spectrum using 1,4-dioxane as an internal standard.

Reaction in the presence of additives proceeds smoothly, giving almost 50% product formation within 1 hour (Entry 1). The addition of KI caused a dramatic decrease in the reactivity of the $Pd_2(dba)_3$/$PtBu_3$ system whether in catalytic amounts or in excess (Entries 2 and 3). However, the addition of an excess of KBr did not have the same inhibitory effect, and the reaction gave a similar outcome to the reaction in the absence of additives, (Entry 4 *vs* Entry 1).
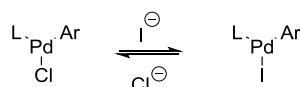
Scheme 100: Possible halide exchange on the Pd(II) oxidative addition complex.

The possibility for the free I^- to exchange with Cl^- after oxidative addition therefore disfavouring the transmetallation step was also explored. Addition of KI to the reaction of 4-iodoacetophenone with 4-methoxyphenylboronic acid **312** also caused a decrease in the reactivity, making less likely the possibility of interference in the transmetallation step (Entry 5 *vs* Entry 6). The effect of the counter-ion was then explored. The highest inhibition is observed for NaI, maybe due to the higher solubility of this salt compared to

KI and CsI (Entry 3, 7 and 8).[318] ^{31}P-NMR Analysis of the reaction mixture only shows a single phosphine containing species in solution, corresponding to the Pd(0)(PtBu$_3$)$_2$ **268**. In 2012, Ananikov and Zalesskiy reported a study on the behavior is solution of the Pd$_2$(dba)$_3$ complex and on how to determine its purity.[319] With the help of combined DOSY, 2D COSY and 2D NOESY NMR analyses the two chemists were able to identify, in the ^{1}H-NMR spectrum of the complex, three characteristic peaks that could help to determine the purity of the Pd$_2$(dba)$_3$: *(i)* a signal approximately at 5.3 ppm corresponding to an olefinic group of the major isomer of Pd$_2$(dba)$_3$; *(i)* a second signal approximately at 5.5 ppm corresponding to an olefinic group of the minor isomers of Pd$_2$(dba)$_3$; *(iii)* a third signal approximately at 7.7 ppm corresponding to free dba. Having this in mind, a ^{1}H-NMR was performed to investigate the effect of KI onto the Pd$_2$(dba)$_3$. In *Figure 51* are shown the ^{1}H-NMR spectrum of Pd$_2$(dba)$_3$ in the absence of KI and the ^{1}H-NMR of the Pd$_2$(dba)$_3$ after 10 minutes from the addition of KI.
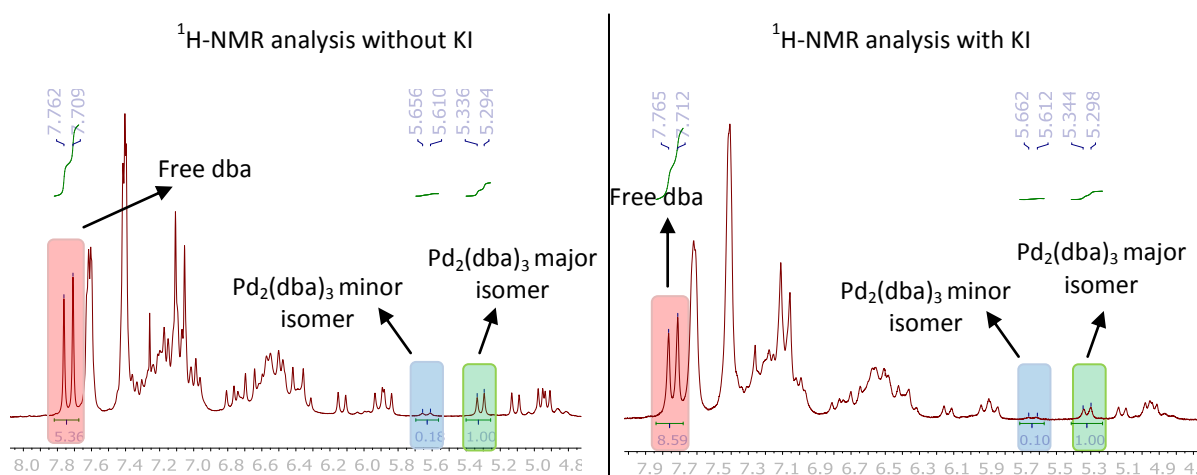
Figure 51: ^{1}H-NMR spectroscopic study of Pd$_2$(dba)$_3$ in absence of KI: the red peaks correspond to the free dba, the green peaks to the major isomer of the Pd$_2$(dba)$_3$ and the blue one to the minor isomer of the Pd$_2$(dba)$_3$ (left). ^{1}H-NMR spectroscopic study of the Pd$_2$(dba)$_3$ in presence of KI: the red peaks correspond to the free dba, the green peaks to the major isomer of the Pd$_2$(dba)$_3$ and the blue one to the minor isomer of the Pd$_2$(dba).

The presence of KI caused a general broadening of the peaks, the signals showed a higher overlapping especially the two of the free dba around 7.6 and 7.8 ppm. This phenomenon made the integration difficult. However, the ^{1}H-NMR analysis of the reaction mixture after 10 minutes from the addition of KI showed a decrease in the intensity of the peak of the minor isomer of Pd$_2$(dba)$_3$ and a slight increase of the concentration of the free dba. A possible reason for the decrease in the rate of reaction observed for the Pd$_2$(dba)$_3$/PtBu$_3$

system in the presence of KI could be due to coordination of the I^- to: *(i)* Pd$_2$(dba)$_3$, that can cause a decrease in the rate of formation of the monoligated Pd(PtBu$_3$) species; *(ii)* monoligated Pd(PtBu$_3$) species decreasing the rate of oxidative addition of aryl halides onto the Pd(0).

Another interesting behaviour emerged from the study performed by Proutière of our group: the reactivity of the Pd(I)-bromo-dimer **31** dramatically decreased in the presence of Cu-cubane **269** (from 87 to 38 %). As part of my work, the possibility of an equilibrium between the Cu-cubane **269** and its monomer, that could combine with Pd(0)PtBu$_3$ to form a mixed Pd-Cu dimer **316**, was explored, (*Scheme 101*).
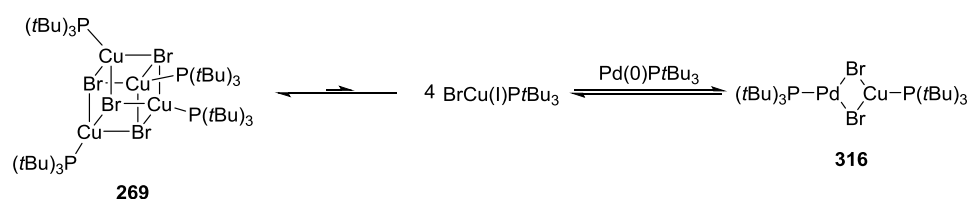
Scheme 101: Possible equilibrium between Cu-cubane **269** and its monomeric form (left); and formation of the mixed Pd-Cu dimer **316**.

Recrystallisation of the reaction mixture containing Pd(I)-bromo dimer **31** and Cu-cubane **269** was attemped in different solvent mixtures. An attempt in toluene:acetone 2:1 gave two type of crystals: a dark green crystals, which were expected to correspond to Pd(I)-bromo dimer **31**, and colourless crystals corresponding to the Cu-cubane **269**. However, the X-ray analysis of the dark green crystals revealed some anomalies in the unit cell, which was calculated to contain 63% Pd and 37% Cu. Unfortunately, it was not possible to determine if this ratio is due to the co-existence of Pd-Pd dimer **31** and Cu-Cu dimer units, or to the presence of Pd-Pd dimer **31** and the mixed Pd-Cu species **316**. However, the absence of symmetry in the unit cell is consistent with the co-existence of Pd-Pd dimer **31** and the mixed Pd-Cu dimer **316**, (*Figure 52*).
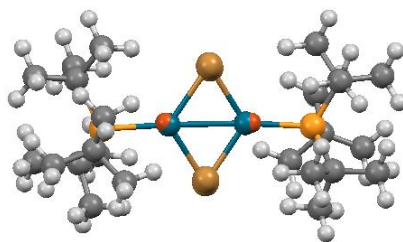
Figure 52: X-ray structure obtained by recrystallisation of the reaction mixture containing Pd(I)-bromo dimer **31** and Cu-cubane **269**. The half orange sphere represents Cu, whilst the blue one represents the Pd present in the unit cell.

The study by Proutière showed that on one hand the presence of Cu(I) and Cu(II) salts is beneficial for the reaction through the *in situ* formation of Pd(I)-bromo dimer **31**, whilst on the other hand the concomitant formation of the Cu-cubane **269** is somehow responsible for the lower rate of reaction compared to that of Pd(I)-bromo dimer **31**. As part of my studies I also explored the possibility of having an optimal concentration of Cu salts that allows the formation of dimer **31** but not the one of Cu-cubane **269**. Pd(P*t*Bu₃)₂ **268** was exposed to different concentrations of CuBr₂ using the reaction reported in *Table 14*.

Table 14: Suzuki-type reaction of 4-chloroacetophenone **306** and 4-methoxyphenylboronic acid **312** in the presence of different concentrations of CuBr₂.
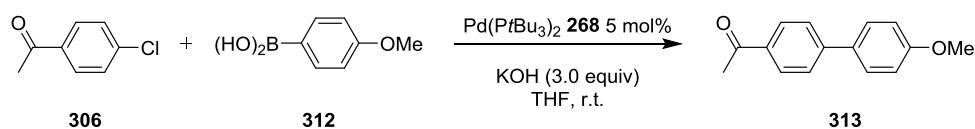
Entry	CuBr$_2$ (mol%)	^{1}H-NMR yield **313** (%)
1	-	12
2	2.5	82
3	4.5	72
4	5.0	61
5	50.0	5

General conditions: **306** 1.0 equiv; **312** 1.1 equiv; Pd(P*t*Bu₃)₂ **268** 5 mol%, KF 3.0 equiv; THF 0.45 M. Yields are calculated from the ^{1}H-NMR spectrum using 1,4-dioxane as an internal standard.

The reaction of Pd(0) **268** in the presence of KOH as base (Entry 1) gave the same poor outcome as the reaction in the presence of KF observed by Proutière.[32,258] The addition of 2.5 mol % of CuBr₂ consistently improved the conversion and within 1 hour the reaction gave 82% yield (Entry 2). Increasing of the number of equivalents of CuBr₂, relative to Pd complex, resulted in a decrease in the yield, the more the equivalents of CuBr₂ the lower

the yield (Entries 3-4). In the presence of 10 equivalents of $CuBr_2$ the yield decreased dramatically to 5 % (Entry 5).

The study showed that the effect of Cu salts can be beneficial within a certain range of concentrations, whilst an excess of the salts can dramatically decrease the yields. Therefore we have successfully identified an ideal concentration of $CuBr_2$ in this particular transformation in which the inhibitory effect of the Cu-cubane **269** can be minimised.

2.5.2 Investigation into the effect of Ag and Au salts on Pd(0)(PtBu₃)₂ 268

In the previous sections **2.1-2.4** we studied the effect of Cu additives on different Pd(0) systems, for almost all of the systems, Pd(0) was oxidised either to Pd(I) or Pd(II). This led us to question whether it is only an effect of Cu salts or could it be extended to other member of group 11: Ag or Au? Some gold, but in particular silver additives, have been used in cross-coupling reactions in place of Cu additives.[237-239,320-323] For example in the Sonogashira coupling reactions to avoid the formation of the homocoupling product from the alkyne catalysed in the presence of Cu and O_2. We decided to explore the behaviour of Pd(P*t*Bu₃)₂ **268** in the presence of Ag and Au salts, with and without coupling partners, as we did previously with $CuBr_2$, CuBr and CuI salts.

2.5.2.1 Investigation on the effect of Ag salts on Pd(0)(PtBu₃)₂ 268.

The reaction of Pd(P*t*Bu₃)₂ **268** with $CuBr_2$ led to the complete formation of Pd(I)-bromo dimer **31** within 15 minutes, whilst the reaction was shown to be slower and not quantitative in the presence of 1 equivalent of CuBr. In a similar way, 1 equivalent of AgBr was added to a THF solution containing Pd(P*t*Bu₃)₂ **268** and the reaction was monitored by ^{31}P-NMR spectroscopy over time, (*Figure 53*).
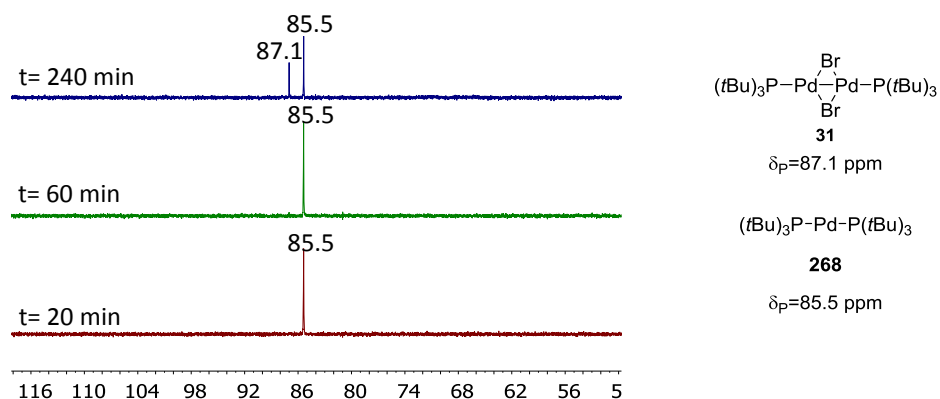
Figure 53: ^{31}P-NMR spectroscopic analysis of the reaction of Pd(P*t*Bu₃)₂ **268** (85.5 ppm) and AgBr after: 20 minutes (red), 60 minutes (green) and 240 minutes (blue). (Chemical shifts in ppm referenced to trimethoxyphosphine oxide as an internal standard).

In the first 2 hours the ^{31}P-NMR spectrum of the reaction mixture showed a single species at 85.5 ppm corresponding to Pd(0) **268**. However, after 4 hours of exposure it was possible to observe formation of Pd(I)-bromo dimer **31**. Recrystallisation of the reaction mixture from a toluene:acetone 1:3 gave two type of crystals: one dark green corresponding to Pd(I)-bromo dimer **31**, and the other one colourless, that X-ray analysis confirmed to belong to Ag-cubane **317**, a new cubane-structured complex, (*Scheme 102*).
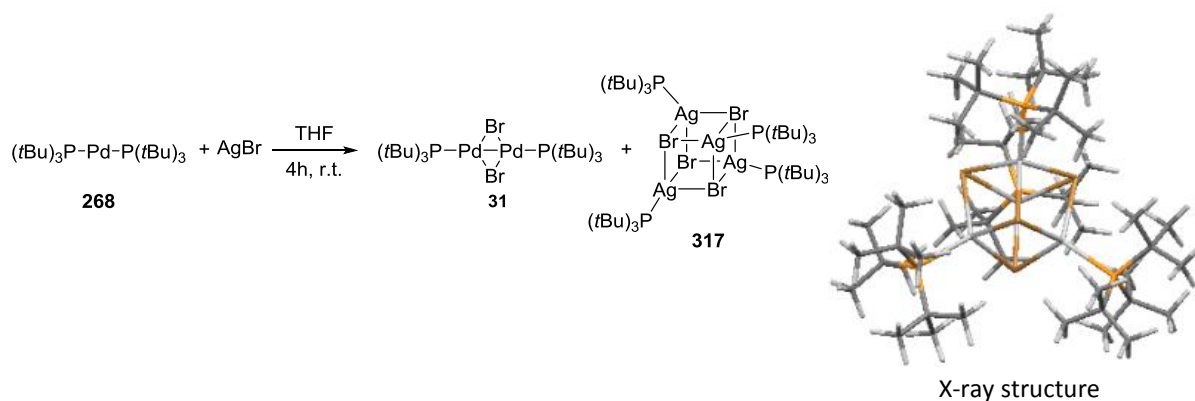
Scheme 102: Formation of Pd(I)-bromo-dimer **31** and Ag-cubane **317** from Pd(0) **268** and AgBr (left). Crystal structure of the novel Ag-cubane **317** (right).[258]

The reaction was also repeated in the absence of light, to rule out any possible light induced radical mechanism for the formation of the Pd(I)-bromo dimer **31**. Dimer **31** was also formed under this condition. After having established the formation of the Pd(I) upon exposure of Pd(0) **268** to AgBr, we tested the catalyst system in the Suzuki reaction of

4-chloroacetophenone **306** and 4-methoxyphenylboronic acid **312** in the presence of KF as base, (*Table 15*).

Table 15: Suzuki-type reaction of 4-chloroacetophenone **306** and 4-methoxyphenylboronic acid **312** both in the presence and absence of AgBr.
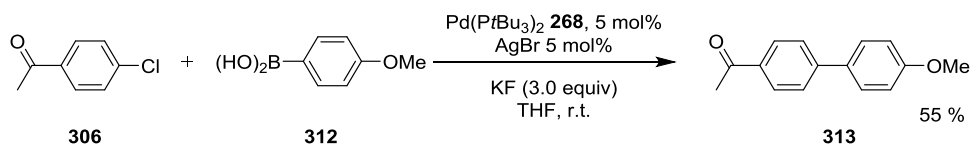
Entry	Additive	Time (h)	Yield **313** (%)
1	AgBr	1	55
2	-	1	11

General conditions: **306** 1.00 equiv; **312** 1.05 equiv; KF 3.0 equiv; THF 0.45 M. Yields are calculated from the ^{1}H-NMR spectrum using 1,4-dioxane as an internal standard.

The presence of AgBr in the reaction mixture was beneficial to the rate of reaction (see *Table 15*), with the yield improving from 11% to 55% (Entry 1 *vs* Entry 2).

In the case of Cu, the use of CuI led to the formation of the less reactive Pd(I)-iodo dimer **193**.[258] In order to see if AgI also has the same effect on Pd(0)(P*t*Bu$_3$)$_2$ **268**, 1 equivalent of AgI was added to a solution containing the Pd(0) complex **268** and the reaction was monitored by ^{31}P-NMR spectroscopy, (*Scheme 103*).
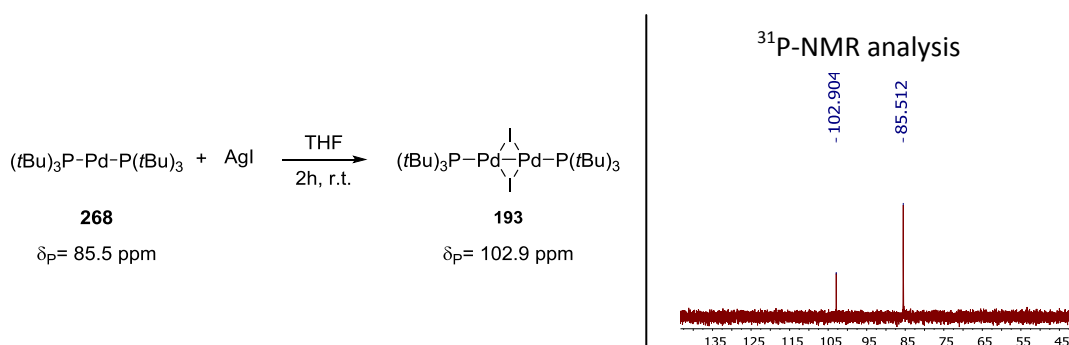
Scheme 103: Reaction of Pd(P*t*Bu$_3$)$_2$ **268** with AgI (left). ^{31}P-NMR spectroscopic analysis of the reaction mixture (right). (Chemical shifts in ppm referenced to trimethoxyphosphine oxide as an internal standard).

After 2 hours of reaction time the peak of the Pd(I)-iodo dimer **193** was present, but the major species in solution was still Pd(0) **268**, as in the case of CuI.

2.5.2.2 Investigation into the effect of Au salts on Pd(0)(PtBu$_3$)$_2$ 268

The observation of Pd(I)-bromo dimer **31** formation in the presence of Cu and Ag salts, led us to further investigate also effect of Au salts on Pd(0) **268**. As for the other two cases, 1 equivalent of AuBr$_3$ was added to a THF solution containing Pd(PtBu$_3$)$_2$ **268** and the reaction was monitored by ^{31}P-NMR spectroscopy, (*Scheme 104*).
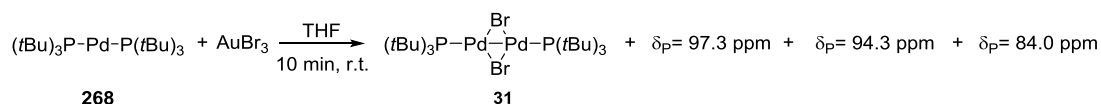
Scheme 104: Reaction of Pd(PtBu$_3$)$_2$ **268** with AuBr$_3$. (Chemical shifts in ppm referenced to trimethoxyphosphine oxide as an internal standard).

After 10 minutes of exposure, all of the Pd(0) **268** was consumed and 4 new species were formed: one at 87.1 ppm corresponding to dimer **31**, and 3 other species at 97.3, 92.3 and 84.0 ppm. The species at 97.3 ppm has a chemical shift very similar to the [(PtBu$_3$)$_2$Au](Br$_3$)(Br$_2$) complex reported by Schimidbaur *et al.*[324] It is possible that in our case the counterion may be simple Br$^-$ **318**. The peak at 94.3 ppm was also obtained by reaction of AuBr$_3$ with PtBu$_3$, which we therefore hypothesise to be the monomeric (PtBu$_3$)AuBr$_3$ **319**.
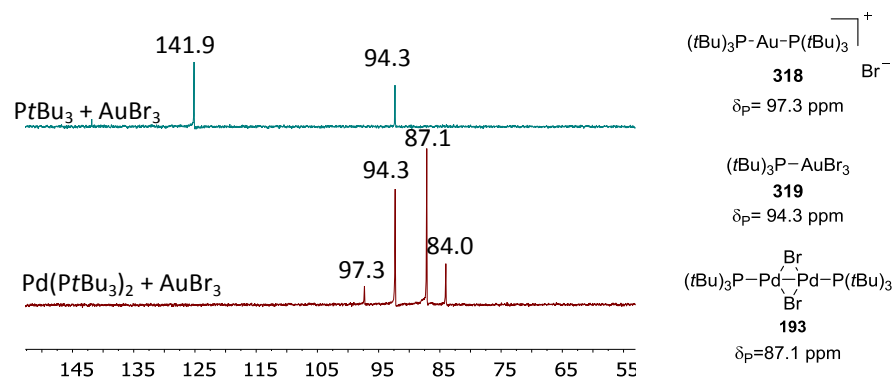
Figure 54: ^{31}P-NMR spectroscopic analysis of the reaction of Pd(PtBu$_3$)$_2$ **268** (85.5 ppm) and AuBr$_3$ after 10 minutes (green), ^{31}P-NMR spectroscopic analysis of the reaction of PtBu$_3$ (63.3 ppm) and AuBr$_3$ (red). (Chemical shifts in ppm referenced to trimethoxyphosphine oxide as an internal standard).

The identity of the species at 84.0 ppm is still unknown.

As the formation of the dimer **31** has been proven to occur under stoichiometric conditions (by reaction of Pd(P*t*Bu$_3$)$_2$ **268** with AuBr$_3$) in the absence of coupling partners, the logical next step was to test the reactivity of this catalyst system in the Suzuki cross-coupling reaction of 4-chloroacetophenone **306** and 4-methoxyphenylboronic acid **312** in the presence of KF as base (*Table 16*).

Table 16: Suzuki-type reaction of 4-chloroacetophenone **306** and 4-methoxyphenylboronic acid **312** both in the presence and absence of AuBr$_3$.
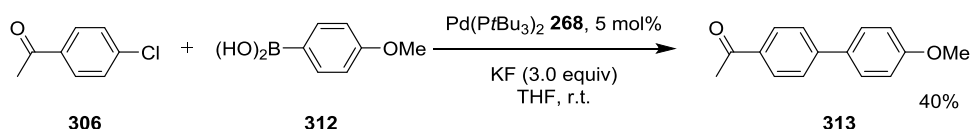
Entry	Additive	Time (h)	Yield **313** (%)
1	AuBr$_3$	1	40
2	-	1	11

General conditions: **306** 1.00 equiv; **312** 1.05 equiv; KF 3.0 equiv; THF 0.45 M. Yields are calculated from the ^{1}H-NMR spectrum using 1,4-dioxane as an internal standard.

Reaction in the presence of AuBr$_3$ increased the yield of product formation compared to the reaction in the absence of additives, as in the case of CuBr and AgBr salts (see *Table 16* Entry 1 *vs* Entry 2).

2.5.3 Investigation into the effect of other salts on Pd(0)(PtBu$_3$)$_2$ 268.

In the previous sections we have shown that the occurrence of a RedOx reaction between Cu, Ag and Au salts leads to oxidation of Pd(0)(P*t*Bu$_3$)$_2$ **268** to Pd(I) dimer **31**. We started to investigate the effects of several other additives commonly employed in cross-coupling reactions on Pd(0)(P*t*Bu$_3$)$_2$ **268**, to see if it was possible to observe a correlation between the reduction potential of the additive and the ability to oxidise the Pd(0) in **268** to Pd(I).

The selected salts were first tested in the absence of coupling partners and in the presence of only Pd(0)(P*t*Bu$_3$)$_2$ **268**. In this case the reaction was monitored by ^{31}P-NMR spectroscopy at different time points to see if new phosphine-containing species were formed. Subsequently, the new catalyst system was tested in the Suzuki coupling reaction of 4-chloroacetophenone **306** and 4-methoxyphenylboronic acid **312**. The results obtained are summarised in *Table 17*.

Table 17: Effect of commonly used additives in cross-coupling reactions on Pd(PtBu$_3$)$_2$ **268**: (1) in the absence of coupling partners; (2) in the Suzuki coupling reaction of 4-chloroacetophenone **306** and 4-methoxyphenylboronic acid **312**.
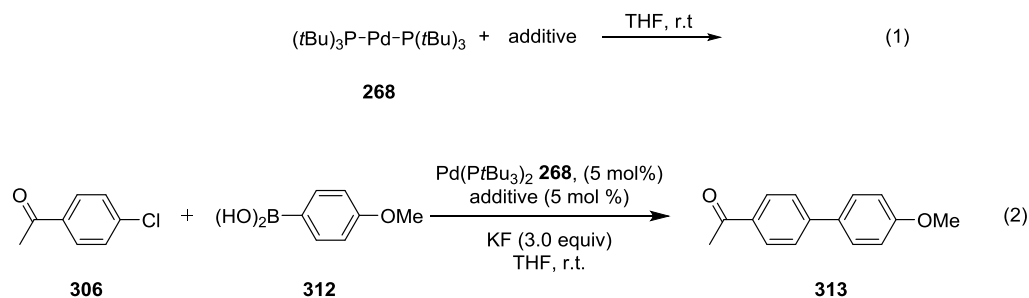
Entry	Additive	New peaks in the ^{31}P-NMR spectrum (ppm)[a]	Yield **313** (%)[b]	Reduction potential (eV)[c]
1	ZnBr$_2$	-	7	–0.76
2	ZnCl$_2$	-	10	–0.76
3	FeBr$_2$	-	3	–0.44
4	FeCl$_2$	-	2	–0.44
5	CoCl$_2$	-	11	–0.28
6	NiCl$_2$	-	5	–0.26
7	NiBr$_2$	-	10	–0.26
8[d]	-	reference	12	
9	Cu(OTf)$_2$	49, –13	37	–0.22
10	SnBr$_2$	63, 49	-	–0.14
11	AgBr	87	53	0.07
12	CuCl$_2$	83, 62, –10	60	0.15
13	CuBr$_2$	87, 57	52	0.15
14	CuF$_2$	-	16	0.15
15	CuI	102	5	0.52
16	CuBr	87 and 57	52	0.52
17	Ag$_2$O	-	74	0.34
18	FeBr$_3$	87	40	0.77
19	AgF	-	24	0.78
20	AuBr$_3$	97, 94, 87 and 84	40	1.40

a) General conditions for the NMR study: Pd(PtBu$_3$)$_2$ **268** 0.04 mmol, additive 0.04 mmol, THF 0.04 M. b) General conditions for the Suzuki coupling: **306** 1.00 equiv; **312** 1.05 equiv; KF 3.0 equiv; THF 0.45 M. Yields are calculated from the ^{1}H-NMR spectrum using 1,4-dioxane as an internal standard. c) The additives are arranged in ascending order of the reduction potential (*E*°, 298 K, 100.325kPa (1 atm), [1 M], reference electrode: standard hydrogen electrode).[325] d) We took as reference the signal obtained from the ^{31}P-NMR spectrum of Pd(PtBu$_3$)$_2$ **268**.

For very negative reduction potentials no new phosphine-containing species were formed (see Entries 1-7, red zone). The reactions using Zn-based additives gave similar conversions (see Entry 1 and 2) to that of only Pd(0) **268**. Almost complete inhibition can be observed in the presence of Fe(II) additives (see Entries 3 and 4), whilst no effect can be observed in the presence of the Co salt (see Entry 5) and Ni(II) salts (see Entries 6 and 7). Changes to the ^{31}P-NMR spectrum of the reaction mixture and also increases in the yields of the Suzuki couplings were observed when additives with a reduction potential higher than –0.22 eV were employed (see Entries 9-20, blue zone). In the case of Cu(OTf)$_2$ the

catalyst system gave a higher conversion compared to the reference (11% vs 37%) and after one 1 hour the peak of the Pd(0) **268** had disappeared and new species had formed in the ^{31}P-NMR of the reaction mixture: one at 48.8 ppm most probably due to the formation of HPd(PtBu$_3$)$_2$OTf **320** (the same peak was observed when Pd(0)(PtBu$_3$)$_2$ **268** was exposed to 1 equivalent of triflic acid (*Figure 55*). The second species at −12.9 ppm could be due to the formation of the cyclopalladate complex **321**, similar products (HPd(PtBu$_3$)$_2$Cl **322** and cyclopalladated) were observed by Proutière by reaction of Pd(0)(PtBu$_3$)$_2$ **268** with HCl.[32]
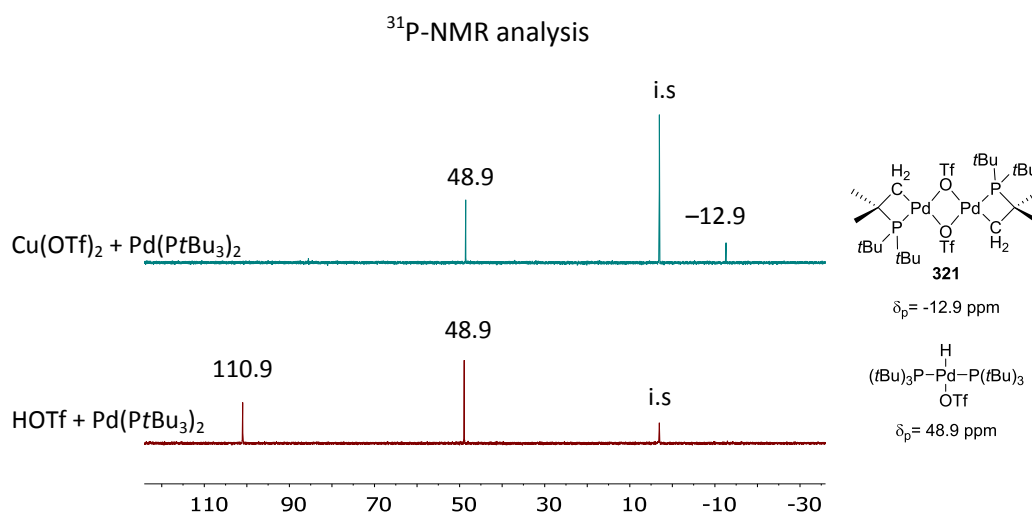
Figure 55: ^{31}P-NMR spectroscopic analysis of the reaction between Pd(PtBu$_3$)$_2$ **268** and Cu(OTf)$_2$ (red), and ^{31}P-NMR spectroscopic analysis of the reaction of Pd(PtBu$_3$)$_2$ **268** with HOTf (green). (Chemical shifts in ppm referenced to trimethoxyphosphine oxide as an internal standard).

The reaction in the presence of SnBr$_2$ did not give any product formation and the Pd(0)(PtBu$_3$)$_2$ **268** disappeared from the reaction mixture within the first 10 minutes to form free phosphine and a new species at 48.6 ppm, whom nature is still not known. The reaction with CuCl$_2$ gave a higher conversion compared to the reference reaction in the Suzuki coupling of 4-chloroacetophenone **306** and 4-methoxyphenylboronic acid **312**. We hypothesised that the species (see Entry 12) at 82.7 could be due to the formation of an HCl complex HPd(PtBu$_3$)$_2$Cl **322** due to HCl impurities in the CuCl$_2$. Three additional experiments were perfomed: *(i)* 1 equivalent of HCl was added to a solution containing Pd(0)(PtBu$_3$)$_2$ **268**; *(ii)* 1 equivalent of 2,6-di-*tert*-butylpyridine was added to a THF solution containing the CuCl$_2$ and after 1 hour of stirring Pd(0)(PtBu$_3$)$_2$ **268** was added with the aim of neutralising possible traces of HCl; *(iii)* 1 equivalent of Hünig base was added to a THF solution containing the CuCl$_2$ and after 1 hour of stirring Pd(0)(PtBu$_3$)$_2$

268 was added with the aim of neutralising possible traces of HCl. The results of these three experiment are demonstrated in *Figure 56*.
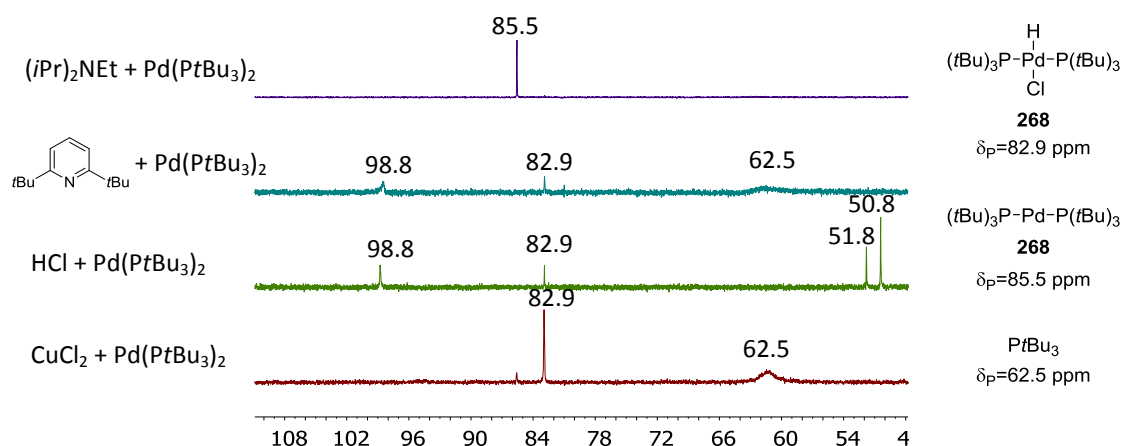
Figure 56: ^{31}P-NMR spectroscopic analysis of the reaction of Pd(PtBu$_3$)$_2$ **268** (85.5 ppm) and CuCl$_2$ after 15 minutes (red); ^{31}P-NMR spectroscopic analysis of the reaction of Pd(PtBu$_3$)$_2$ **268** (85.5 ppm) and HCl after 10 minutes (green); ^{31}P-NMR spectroscopic analysis of the reaction of Pd(PtBu$_3$)$_2$ **268** (85.5 ppm), 2,6-di-*tert*-butylpyridine and CuCl$_2$ after 10 minutes (light blue); and ^{31}P-NMR spectroscopic analysis of the reaction of Pd(PtBu$_3$)$_2$ **268** (85.5 ppm), Hünig base and CuCl$_2$ after 30 minutes (purple). (Chemical shifts in ppm referenced to trimethoxyphosphine oxide as an internal standard).

After 10 minutes of exposure of Pd(0)(PtBu$_3$)$_2$ **268** to HCl new species had appeared in the ^{31}P-NMR spectrum of the reaction mixture and the peak of the Pd(0)(PtBu$_3$)$_2$ **268** had disappeared, showing a ^{31}P-NMR spectrum similar to the one obtained by reaction Pd(0)(PtBu$_3$)$_2$ **268** and CuCl$_2$. This experiment strongly supports the presence of HCl impurities in the CuCl$_2$. Exposure of CuCl$_2$ to 2,6-di-*tert*-butylpyridine for 1 hour before the addition of the Pd(0) **268** did not prevent the formation of the HCl-complex **317**, whilst exposure of CuCl$_2$ to Hünig base prior to the addition of Pd(0)(PtBu$_3$)$_2$ **268** did prevent the formation of the HCl complex **322**, showing that the exposure of Pd(0)(PtBu$_3$)$_2$ **268** to CuCl$_2$ does not cause any apparent change in the ^{31}P-NMR spectrum of the reaction mixture. This could be due partially to poor ability of Cl$^-$ to stabilise a dimeric structure as in the case of Br$^-$ and I$^-$. However, a large improvement in the reactivity can be observed (60% *vs* 11%, see Entry 12 *vs* Entry 8). The same trend was observed when Pd(0)(PtBu$_3$)$_2$ **268** was exposed to CuF$_2$, AgF and Ag$_2$O: no visible changes can be observed in the ^{31}P-NMR, but the yields of reaction increased considerably (see Entries 14, 17 and 19). The salts in these cases could act as ligand scavengers facilitating the formation of the monoligated Pd(0)(PtBu$_3$) species from Pd(0)(PtBu$_3$)$_2$ **268**, which is usually the rate

determining step of the coupling. One interesting discovery was made in the presence of $FeBr_3$ where exposure of $Pd(0)(PtBu_3)_2$ **268** to this salt generated Pd(I) dimer **31** within 10 minutes of reaction time, (*Scheme 105*).
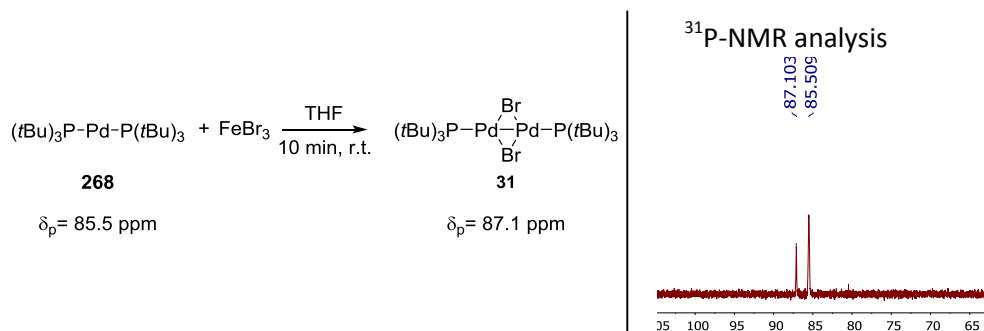
Scheme 105: Reaction of $Pd(PtBu_3)_2$ **268** with $FeBr_3$ (left). ^{31}P-NMR spectroscopic analysis of the reaction mixture. (Chemical shifts in ppm referenced to trimethoxyphosphine oxide as an internal standard).

In the case of Fe(II) additives almost complete inhibition of the Suzuki coupling reaction in equation (2) was observed, whilst in the case of $FeBr_3$ an increase in the yield of the reaction was observed. Buchwald and Bolm reported that Cu impurities can be present in some salts such as $FeCl_3$.[326,327] To eliminate this possibility, $FeBr_3$ and $PtBu_3$ were used as catalyst system for the Suzuki coupling reaction reported above, in the absence of $Pd(0)(PtBu_3)_2$ **268**. The outcome of the reaction clearly showed that the catalysis is not due to impurities in the $FeBr_3$, but to the combination of the salt with the Pd(0) **268**, as no product formation was observed in the absence of $Pd(0)(PtBu_3)_2$ **268**. The same procedure was repeated for $CuBr_2$, where it was used as a catalyst together with $PtBu_3$ in the Suzuki coupling reported above. Again, in this case no product formation was observed.

2.6 Conclusions

In this chapter the role of copper in the presence of different Pd(0) systems has been explored through spectroscopic and crystallographic studies. Oxidation of the Pd(0) to higher oxidation states of Pd (I and II) have been observed. This discovery introduce an additional role of the copper as an oxidant in the catalytic cycle not only of Sonogashira reaction but also in other cross-coupling reactions. In particular for $Pd(0)(PtBu_3)_2$ **268**, the *in situ* formation of Pd(I)-bromo dimer **31** and Pd(I)-iodo dimer **193** in the Sonogashira

coupling led to the occurrence of an oligomerisation side-reaction that consumed the alkyne, hindering the coupling with aryl chlorides. In the case of Suzuki coupling, beneficial effects in catalysis could be observed in the presence of Cu^nBr_n (n=1, 2) due to the formation of highly reactive Pd(I)-bromo dimer **31**, whilst inhibition of the coupling has been observed in the presence of CuI due to the formation of the less reactive Pd(I)-iodo dimer **193**.

The oxidation reaction has also been explored for the other two members of group 11 of the periodic table and similar results were obtained: $Pd(0)(PtBu_3)_2$ **268** was oxidised to Pd(I)-bromo dimer **31** or Pd(I)-iodo dimer **193** according to the nature of the counterion utilised. In addition a direct correlation between the reduction potential of the additive and the formation of the Pd(I) dimers has been observed. For $Pd(0)(PtBu_3)_2$ **268** additives with a reduction potential higher than –0.22 eV can result in formation of Pd(I) dimers if the counterion is Br^- or I^-. Beneficial effects in the Suzuki coupling reaction have also been observed for those additives with a reduction potential higher than –0.22 eV, but with counterions that are unable to bridge Pd(I) centres.

Chapter 3. Study of the mechanism of Pd(I) dimers activation

This work was inspired by the observation done by F. Proutière of our group that when Pd(I)-bromo dimer **31** was subjected to a THF solution containing KF, water and boronic acid within 20 minutes its complete comsumption was observed and Pd(0)(PtBu$_3$)$_2$ **268** was formed. The crystal structure reported in this chapter was solved by Dr N. Trapp, whilst M. Solar took care of the data collection.

Chapter 3: Introduction

In Chaper 2 it was demonstrated that Pd(I) dimers can form when Pd(0)L$_2$ complexes bearing certain phosphine ligands, such as PtBu$_3$, are exposed to Cu salts or another oxidant with an appropriate oxidation potential. For Pd(PtBu$_3$)$_2$ **268** we have identified the lower value of oxidation potential necessary to induce oxidation. Below this value the additive does not react with the Pd(0) and it is possible to observe catalysis derived directly from this Pd(0) complex. We showed that the formation of Pd(I)-bromo dimer **31** in the presence of oxidants substantially increases the yield of reaction in the Suzuki coupling of 4-chloroacetophenone **306** and 4-methoxyphenylboronic acid **312**. It was speculated that the increase in the reactivity can be attributed to an easier formation of 12-electron monoligated Pd(0)PtBu$_3$ from Pd(I)-bromo dimer **31** compared to from Pd(PtBu$_3$)$_2$ **268** itself.[30,328] However, the potential mechanism of activation to provide Pd(0) species from the Pd(I) dimer is unknown. Many hypotheses have been posed,[150,171,329] and the most probable seems to be: disproportionation; reduction by substrate or base; homolytic cleavage of the Pd-Pd bond; or direct dimer catalysis, (*Scheme 106*).
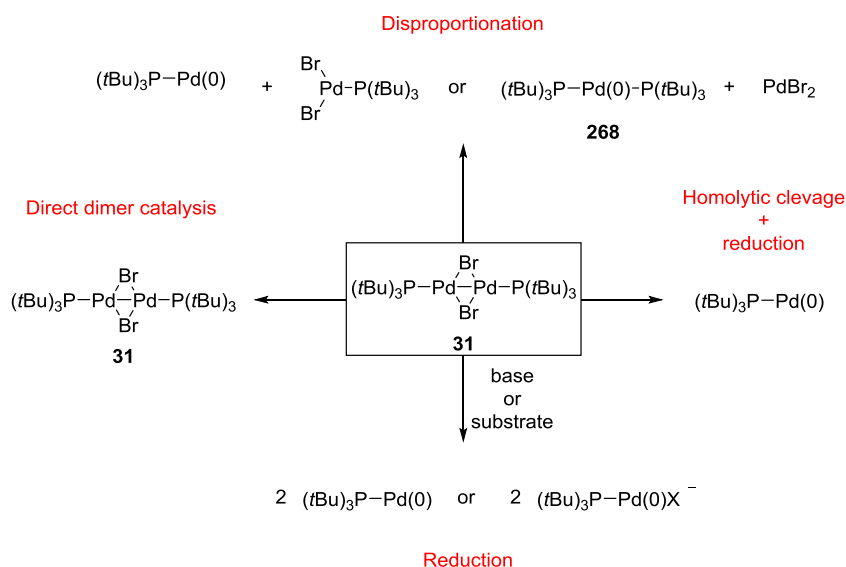
Scheme 106: Possible ways of generating the monoligated Pd(0)(PtBu$_3$) from the Pd(I)-bromo dimer **31**.[330]

Hartwig *et al.* speculated about the possibility for Pd(I) dimer **31** to form the active species by disproportionation to form Pd(0)PtBu$_3$ and Br$_2$Pd(II)PtBu$_3$, or by reduction *via* the action of either a base or a substrate.[171,331] The hypothesis of disproportionation was also

suggested by Shaughnessy and Colacot for the generation of the monoligated complex Pd(0)(DTBNpP) from the allyl bridged Pd(I) dimer **129**.[150]
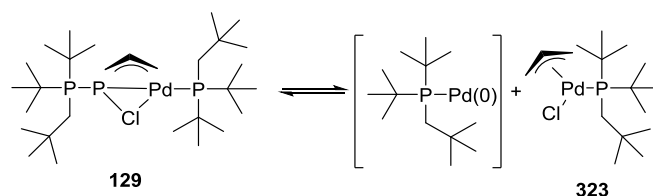
Scheme 107: Disproportionation reaction suggested by Shaughnessy and Colacot for the formation of Pd(0)(DTBNpP) from the allyl bridged Pd(I) dimer **129**.[150]

The monoligated Pd(0)(DTBNpP) was never isolated nor seen spectroscopically, as in the case of the P*t*Bu$_3$ analogue.

Another potential way of generating the Pd(0)P*t*Bu$_3$ could be homolytic cleavage of the Pd-Pd bond followed by reduction. The homolytic Pd-Pd bond cleavage of a series of Pd-Pd complexes bearing the bridging bidentate dppm ligand and different ancillary ligands (I, Br, Cl, NCO) was calculated, using a UV/vis spectrophotometric study, to be between 90-120 kJ/mol (21-29 kcal/mol).[332] The energies calculated by James *et al.* for these Pd(I) dimers are adequate enough to consider homolytic cleavage, followed by reduction, as a possible pathway for the formation of the monoligated Pd(P*t*Bu$_3$).

A complete bimetallic catalytic cycle for the Suzuki cross-coupling of aryl bromides with Pd(I) dimer **324** was suggested by Bera *et al.*[329] In the cycle proposed, and shown in *Figure 57*, oxidative addition occurs across the bimetallic system, followed by transmetallation and bimetallic reductive elimination. However, they did not report any direct evidence, neither spectroscopic nor crystallographic, that could support the proposed bimetallic mechanism.
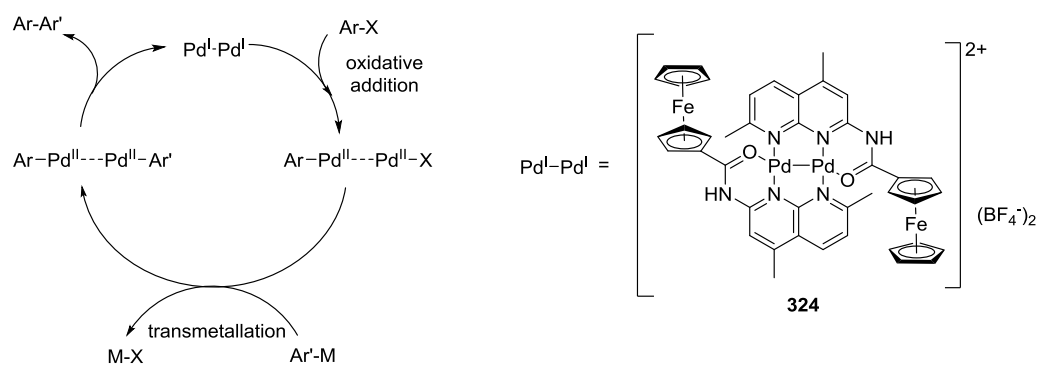
Figure 57: Bimetallic cross-coupling reaction cycle as proposed by Bera *et al.* for dimer **324**.[329]

One of the first studies to support the hypothesis of formation of the monoligated Pd(0)(P*t*Bu$_3$) from Pd(I)-bromo dimer **31** was reported by Proutière, Schoenebeck and myself in 2011.[330] To demonstrate whether monoligated Pd(P*t*Bu$_3$) species could be formed from Pd(I)-bromo dimer **31** Suzuki coupling of 4-chlorophenyl triflate **4** with 2-methylphenylboronic acid **5** was used as a reactivity probe. In a previous work was it shown that in the presence of the Pd$_2$(dba)$_3$/P*t*Bu$_3$ 1:1 system Cl-addition is exclusively observed in THF, whilst in the presence of a polar solvents such as CH$_3$CN, a selectivity change is observed and triflate addition is obtained exclusively. The change of selectivity was shown to be due to the formation of an anionic [Pd(P*t*Bu$_3$)X]⁻ active species, where X is either Ar-B(OH)$_2$ or F⁻,in polar solvents, whilst in non-polar solvent the active species was predominantly Pd(P*t*Bu$_3$), (*Scheme 108*).[25]
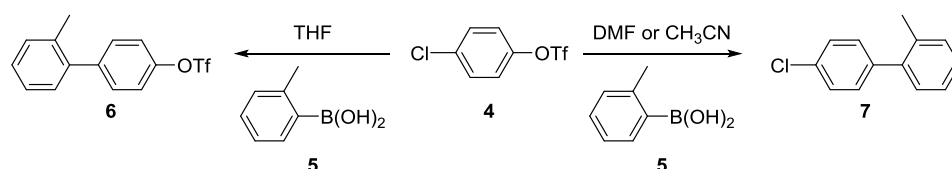
Scheme 108: Suzuki coupling reaction used by Schoenebeck *et al*. to support the formation of Pd(0)(P*t*Bu$_3$) in the presence of Pd(I)-bromo dimer **31** as precatalyst.[25]

Pd(I)-bromo dimer **31** was used as precatalyst in the reaction shown in *Scheme 108*, both in polar and non-polar solvents. Cl-addition was observed in non-polar solvents with good conversions (yields: 76% in the presence of KF and 82% in the presence of KOH), whilst OTf-addition was observed in CH$_3$CN, again with high yields (76% in the presence of KF and 82% in the presence of KOH). These results are consistent with what was observed before for the Pd$_2$(dba)$_3$/P*t*Bu$_3$ 1:1 system. In polar solvents the active species is likely an anionic [Pd(P*t*Bu$_3$)X]⁻, whilst in non-polar solvents the active species is likely to be instead a monoligated neutral Pd(P*t*Bu$_3$). The four possible ways of generating the monoligated Pd(*t*Bu$_3$) species, shown before in *Scheme 106*, were subsequently investigated through a series of experimental and computational studies. Homolytic cleavage was ruled out both computationally and experimentally. The use of radical traps did not infer the presence of radicals in solution and computations on the oxidative addition of 4-chlorophenyl trifluoromethanesulfonate **4** predicted C-Cl addition for a Pd(I) radical both in polar and apolar solvents, in contrast with the experimental findings. Direct disproportionation was shown to be disfavoured due to a very high energetic penalty (38.1 kcal/mol), whilst no evidence of direct dimer catalysis was found. Among all the possible pathways explored,

reduction catalysed by a base or the boronic acids, appeared to be the most plausible pathway. In fact, it was observed that exposure of Pd(I)-bromo dimer **31** to a mixture containing water, boronic acid and KF led to the formation of Pd(PtBu$_3$)$_2$ **268**. Formation of the Pd(PtBu$_3$)$_2$ **268** can be observed after 5 minutes of exposure and is complete within 20 minutes. The formation of the Pd(0) complex **268** was slower or not observed when one of the three components was missing. In addition, formation of a black precipitate, presumably Pd black, was observed when Pd(I)-bromo dimer **31** was exposed to these three components.

The lack of a clear picture about the possible mechanism that leads to the formation of Pd(PtBu$_3$) from Pd(I)-bromo-dimer **31** combined with the observation that Pd(I)-iodo dimer **193** and Pd(I)-bromo dimer **31** show different reactivity, despite the similarity in the structure, led us to further explore the possibility of intermediacy of an external stimuli, such as a base or a nucleophile, for their activation. Herein we will show our mechanistic proposal of a nucleophile-assisted disproportionation as a likely pathway for the activation of these two dimers, supported by a spectroscopic and crystallographic study. The two dimers were subjected to different nucleophiles, either charged or neutral, according to an increasing nucleophilic power (set according to the Mayr's scale). A linear correlation between the nucleophilic power and the stability of the two dimers was observed and a minimum N-value for their activation was determined. This value was consistently higher for the Pd(I)-iodo dimer **193**. The identification of a minimum N-value for the activation of Pd(I)-dimers **193** and **31** allowed us to define a range for the nucleophilic power where the dimer is stable in its dimeric form and can be use as a catalyst (direct dimer catalysis), as it will be shown in Chapter 4. Above the set N-value, the dimer reacts with the nucleophile and the monoligated Pd(PtBu$_3$) is formed, allowing the use of these dimers as precatalysts in cross-coupling reactions. In particular, the air stability of the Pd(I)-iodo dimer **193** allowed the use and handling of this complex also in the presence of oxygen, as it will be shown in the following chapter.

3.2 Pd(I) dimers activation

3.2.1 Insight on the nucleophile-assisted mechanism of activation for Pd(I)-bromo dimer 31

Hartwig *et al.* and Vilar *et al.*[333,334] reported that when Pd(I)-bromo-dimer **31** was exposed to NaO*t*Bu, formation of Pd(P*t*Bu$_3$)$_2$ **268** was observed. Proutière observed that formation of Pd(P*t*Bu$_3$)$_2$ **268** from Pd(I)-bromo dimer **31** was also observed in the presence of KOH and water.[32] However, the observation of a black precipitate, that was attributed to Pd black, led us to further explore the nature of this precipitate and the mechanism that led to its formation. Direct disproportionation was shown to be a very high energy process and was excluded as a possible way to generate monoligated Pd(P*t*Bu$_3$), but the possibility of a base- or nucleophile-assisted disproportionation was not previously considered. In *Scheme 109* and *Scheme 111* are illustrated the proposed mechanisms for the activation of Pd(I)-bromo dimer **31**, with both charged nucleophiles and neutral nucleophiles, respectively.

Scheme 109: Proposed activation mechanism in the presence of charged nucleophiles.

We hypothesised that in the presence of an excess of charged nucleophile the two bridging bromine atoms could be substituted by two nucleophiles to generate a new Pd(I)-dimer. If the nucleophile is not good in stabilising the bridging structure, this dimer will undergo facile disproportionation to form the monoligated Pd(P*t*Bu$_3$) and a Pd(II) species. Release of one ligand from the Pd(II) complex and recombination with Pd(P*t*Bu$_3$) will form the Pd(P*t*Bu$_3$)$_2$ **268** that we observe when Pd(I)-bromo dimer **31** is used as precatalyst in the presence of base/nucleophiles.

Halide exchange was observed when Pd(I)-bromo dimer **31** was exposed to an excess of KI. After 18 hours the Pd(I)-bromo dimer **31** was fully converted into its iodide-analogue **193**, (*Scheme 110*).

Scheme 110: Formation of Pd(I)-iodo dimer **193** from Pd(I)-bromo dimer **31** and KI.

In the case of neutral nucleophiles, such as phophine compounds, an alternative mechanism can be proposed (*Scheme 111*).

Scheme 111: Proposed activation mechanism in the presence of neutral nucleophiles.

In this case the nucleophile does not substitute the bridging bromide, as in the case of the charged nucleophiles, but the substitution concerns the P*t*Bu₃. In this way a new Pd(I)-bromo dimer is formed. This new dimer will then undergo disproportionation in a Pd(0) and a Pd(II) species if its steric and electronic cannot stibilise a Pd(I) dimeric structure, as in the case of P*t*Bu₃.

As part of my study, the effect of different oxygen-based bases as well as a range of other nucleophiles on Pd(I)-bromo dimer **31** was explored in order to gain more insight into the possible mechanism that leads to its activation. Particular focus was given to the isolation of the Pd(II) species that would firmly support our mechanistic proposal.

3.2.1.1: Effect of oxygen-based nuclepophiles on Pd(I)-bromo dimer **31**

To begin with, the reaction of Pd(I)-bromo dimer **31** with 20 equivalents of KOH was repeated in the in the absence of boronic acids. Proutière showed that Pd(I)-bromo dimer **31** was fully converted in Pd(P*t*Bu₃)₃ **268** within 20 minutes, when the dimer is subjected to a THF solution of KF, water and boronic acids. This reaction in the absence of boronic acid is slower than expected and after 20 minutes only a small portion of Pd(I)-bromo dimer **31** had been converted into the Pd(P*t*Bu₃)₂ **268**. After 1 hour the main species in the

^{31}P-NMR spectrum was still represented by the Pd(I)-bromo dimer **31**, at 87 ppm, (*Scheme 112*).
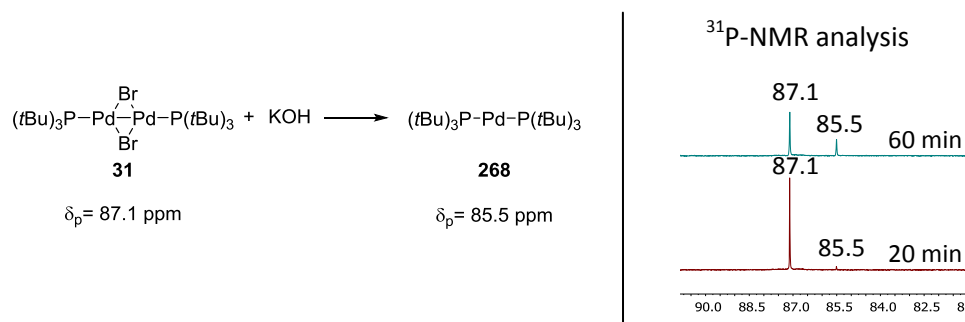
Scheme 112: Reaction between Pd(I)-bromo dimer **31** and KOH in the presence of water (left). ^{31}P-NMR spectroscopic analysis of the reaction mixture after 20 minutes (red) and after 60 minutes (green) (right). (Chemical shifts in ppm referenced to trimethoxyphosphine oxide as an internal standard).

In this case a black precipitate, that could be either PdO or Pd black, was also formed. Unfortunately, it consisted of a fine amorphous powder which was not suitable for X-ray analysis. Attempts to dissolve it in polar solvents such as methanol and DMF to recrystallise it were not successful. We decided to use different oxygen-containing bases in the hope of obtaining a crystalline Pd(II) species. For this purpose, Pd(I)-bromo dimer **31** was exposed to a further two oxygen-based bases, KOEt and KO*t*Bu, again in the presence of water. Formation of Pd(P*t*Bu$_3$)$_2$ **268** can be observed and its formation was considerably faster. Almost all of Pd(I)-bromo dimer **31** was fully converted into Pd(P*t*Bu$_3$)$_2$ **268** within 20 minutes (82%) in the presence of KOEt, whilst the reaction of Pd(I)-bromo dimer **31** and KO*t*Bu was complete after just 5 minutes, (*Scheme 113*).[335]
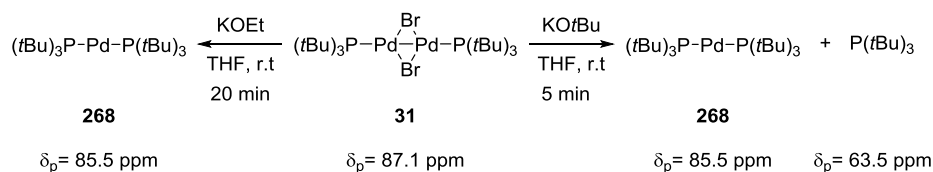
Scheme 113: Reaction between Pd(I)-bromo dimer **31** and KOEt and KO*t*Bu in the presence of water.[336]

Significant amounts of black precipitate was formed in the course of the reaction with both KO*t*Bu and KOEt, but unfortunately it was not crystalline and therefore was unsuitable for X-ray analysis.

The formation of Pd(PtBu$_3$)$_2$ **268** from Pd(I)-bromo dimer **31** was found to have different rates in the presence of the three different bases. We decided to investigate the possibility of this influencing the outcome of the reaction where Pd(I)-bromo dimer **31** is used as precatalyst. Reactivity tests were performed using the three bases in the Suzuki cross-coupling reaction of 4-chloroacetophenone **306** with 4-methoxyphenylboronic acid **312**. We expected that the higher the rate of formation of Pd(PtBu$_3$)$_2$ **268**, the lower the conversion. This is because the ligand loss from the Pd(II) and its recombination with the reactive monoligated Pd(PtBu$_3$) is faster. The results obtained are summarised in *Table 18*.

Table 18: Suzuki cross-coupling reaction of 4-chloroacetophenone **306** with 4-methoxyphenylboronic acid **312** in the presence of three different bases
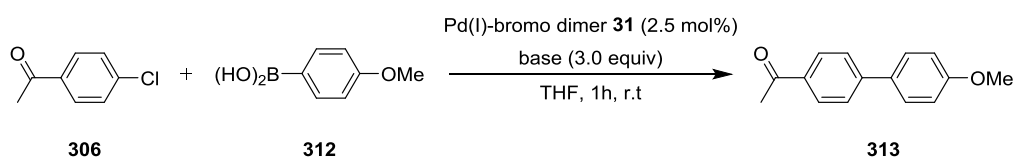
Entry	Base	Yield **313** (%)[a]
1	KOH	87
2	KOEt	40
3	KOtBu	8

a) Yield reported according to calibrated ^{1}H-NMR analysis using dioxane as an internal standard.

The results obtained were consistent with our hypothesis: the faster the formation of Pd(PtBu$_3$)$_2$ **268**, the lower the conversion. This may be due to there being a lower concentration of the monoligated Pd(PtBu$_3$) which is presumed to be responsible for the catalysis.

3.2.1.2: Effect of hppH 325 on Pd(I)-bromo dimer 31

We have previously shown that strong nucleophiles/base, such as KOEt and KOtBu are able to activate Pd(I)-bromo dimer **31**. Unfortunately, it was not possible in the presence of these nucleophiles/bases to isolate a Pd(II) species that could firmly support our mechanistic hypothesis. We decided therefore to investigate also the effect of other nucleophiles on Pd(I)-bromo dimer **31**, in the hope of obtaining a crystalline Pd(II) structure to support our hypothesis. HppH was chosen as suitable candidate for the obtainment of a possibly crystalline Pd(II) complex. Exposure of Pd(I)-bromo dimer **31** to

hppH **325** gave full conversion of the Pd(I)-dimer **31** into Pd(P*t*Bu₃)₂ **268** within 20 minutes. The formation of Pd(0) complex **268** could also be observed visibly, with the dark green colour of the Pd(I)-bromo dimer **31** turning bright yellow after approximately 10 minutes, confirming that Pd(I)-bromo dimer **31** was no longer present in solution, (*Scheme 114*).
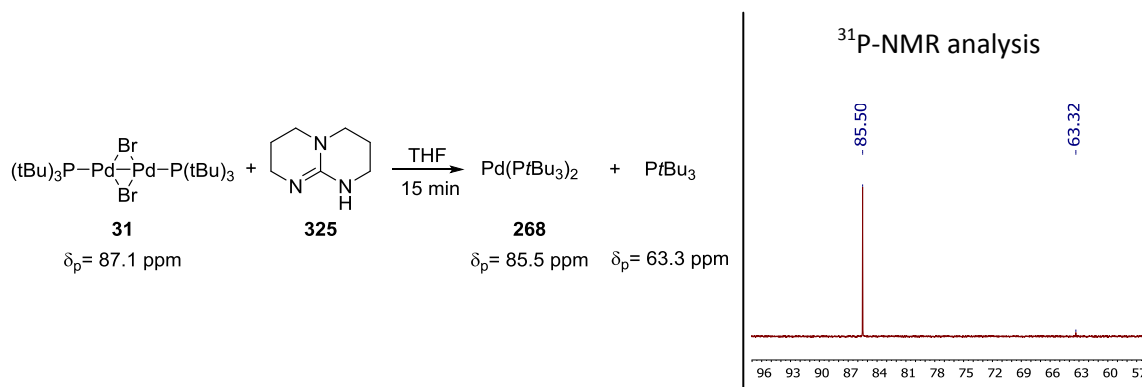
Scheme 114: Reaction between Pd(I)-bromo dimer **31** and hppH **325** (left). ³¹P-NMR spectroscopic analysis of the reaction mixture (right). (Chemical shifts in ppm referenced to trimethoxyphosphine oxide as an internal standard).

After 20 minutes a bright yellow precipitate started to form in the reaction mixture, but unfortunately it was not crystalline and could not be analysed by X-ray diffraction. The effect of hppH on Pd(I)-bromo dimer **31** catalysis was then tested in the Suzuki coupling of 4-chloroacetophenone **306** with 4-methoxyphenylboronic acid **312**, as previously performed for the O-containing bases.

Table 19: Suzuki cross-coupling reaction of 4-chloroacetophenone **306** with 4-methoxyphenylboronic acid **312** in the presence of hppH **325**.
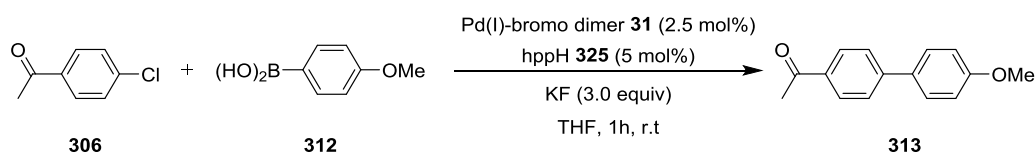
Entry	Time of premixing (min)[b]	Yield **313**[a] (%)
1	0	55
2	10	57

a) Yield reported according to calibrated ¹H-NMR analysis using dioxane as an internal standard. b) Pd(I)-bromo dimer **31** and hppH **325** were separately mixed in a THF solution before being added to the reaction mixture.

The results summarised in *Table 19* clearly show that even in the presence of a catalytic amount of hppH the reactivity of Pd(I)-bromo dimer **31** is lower than in the absence of the

nucleophile (82% *vs* 55%). Premixing of the Pd(I)-bromo dimer **31** and based did not further decrease the yield.

3.2.1.3: Effect of PCy₃ on Pd(I)-bromo dimer 31

We next decided to use a P-based nucleophile in the hope of forming Pd(II) species that would be more soluble in the reaction medium than the O- and N-based ones, therefore allowing detection by ^{31}P-NMR spectroscopy. PCy₃ was previously used in the oxidation project (see Chapter 2), so we had familiarity with the possible Pd(0) and Pd(II) complexes that could be formed in solution. As with the previous studies, Pd(I)-bromo dimer **31** was exposed to a THF solution containing two equivalents of PCy₃ and the reaction was monitored by ^{31}P-NMR spectroscopy over time. The ^{31}P-NMR spectrum of the reaction mixture after 30 minutes of exposure presented several species, all of them familiar to us, whilst Pd(I)-bromo dimer **31** was no longer present in the reaction mixture. There were two major species in solution at 85.6 and 25.0 ppm, corresponding to Pd(PtBu₃)₂ **268** and to [PdBr₂(PCy₃)] **272** (this structure was also also confirmed by X-ray analysis), as well as two minor species at 39.7 and 63.3 ppm, corresponding to the Pd(PCy₃)₂ **270** and to the free PtBu₃, respectively (*Figure 58*).
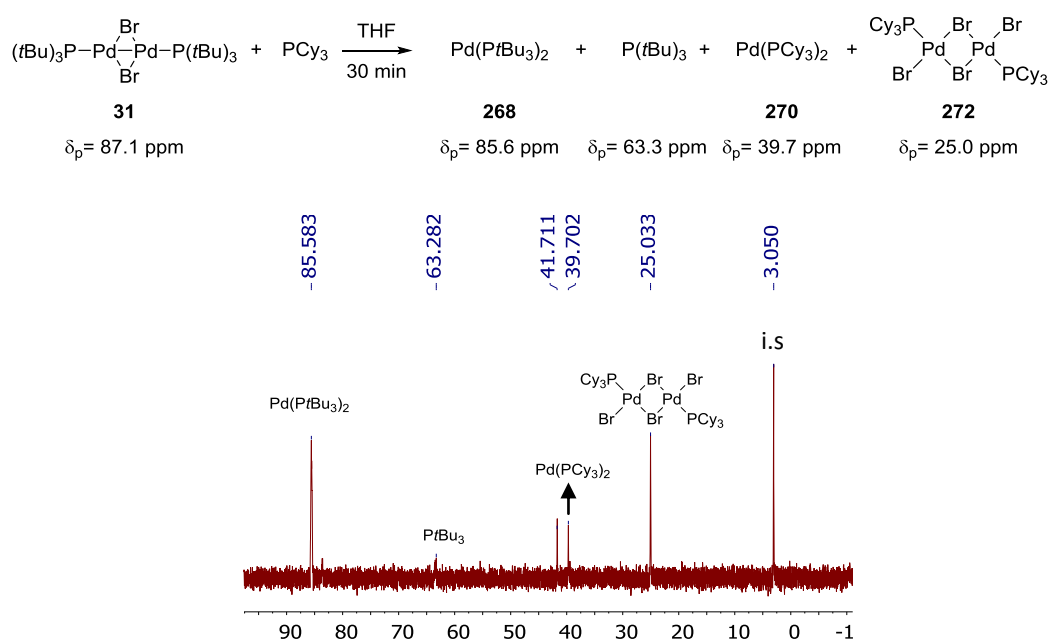
Figure 58: ^{31}P-NMR analysis of the reaction between Pd(I)-bromo dimer **31** and PCy₃. (Chemical shifts in ppm referenced to trimethoxyphosphine oxide as an internal standard).

The formation of the Pd(II) species upon exposure of Pd(I)-bromo dimer **31** to the P-based nucleophile PCy$_3$ supports our mechanistic hypothesis that the formation of the active species is due to a nucleophile-assisted disproportionation.

3.2.1.4: Effect of PEt$_3$ on Pd(I)-bromo dimer **31**

According to the Mayr's N value, the nucleophilicities and their donating power to the metal of the PCy$_3$ and PtBu$_3$ are comparable,[337] and this could explain the formation of Pd(PCy$_3$)$_2$ **270**. We decided to test a different, stronger, P-based nucleophile: PEt$_3$. Pd(I)-bromo dimer **31** was exposed to 2 equivalents of PEt$_3$ and within 15 minutes the solution turned from very dark green to bright yellow. After a prolonged reaction time the solution remained clear and no precipitate was formed unlike the case of hppH. ^{31}P-NMR spectroscopy confirmed the complete consumption of Pd(I)-bromo dimer **31** and showed the formation of two species at 85.5 (Pd(PtBu$_3$)$_2$ **268**) and at 15.1 ppm (most probably PEt$_2$PdBr$_2$ **326**), (*Scheme 115*).
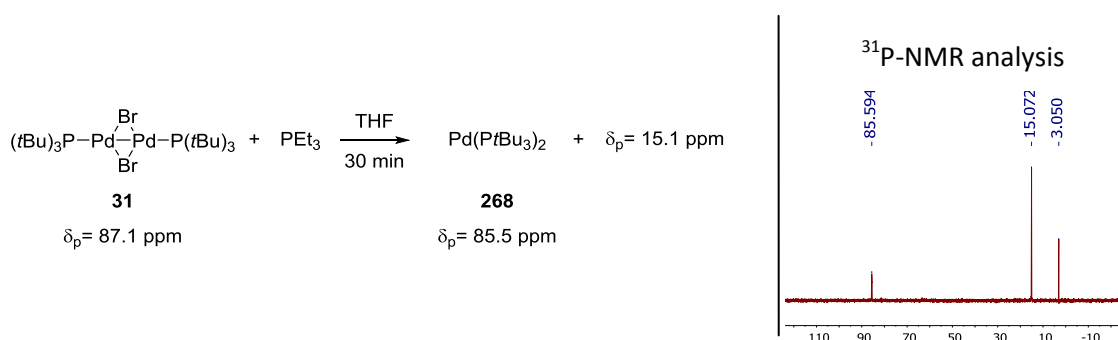
Scheme 115: Reaction between Pd(I)-bromo dimer **31** and PEt$_3$ (left). ^{31}P-NMR spectroscopic analysis of the reaction mixture (right). (Chemical shifts in ppm referenced to trimethoxyphosphine oxide as an internal standard).

After recrystallisation from CH$_2$Cl$_2$ suitable crystals for X-ray analysis were obtained, and the structural analysis confirmed that the species at 15.1 ppm corresponds to the novel Pd(II) complex **326**, (*Figure 59*).
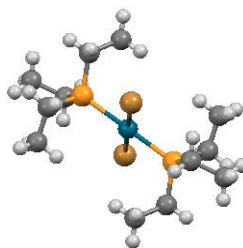
Figure 59: X-ray structure of complex **326** obtained after recrystallisation of the reaction mixture reported in *Scheme 115*. (The blue sphere represent the Pd(II), the golden ones the two bromide atoms and the light orange ones the two phosphorous atoms).

The precatalyst system Pd(I)-bromo dimer **31**/PEt$_3$ was also tried in the Suzuki coupling of 4-chloroacetophenone **306** with 4-methoxyphenylboronic acid **312** in order to test the effect of the presence of a soluble Pd(II) species on the catalysis of Pd(I)-bromo dimer **31**, the results are summarised in *Table 20*.

Table 20: Suzuki cross-coupling reaction of 4-chloroacetophenone **306** with 4-methoxyphenylboronic acid **312** in the presence of PEt$_3$.
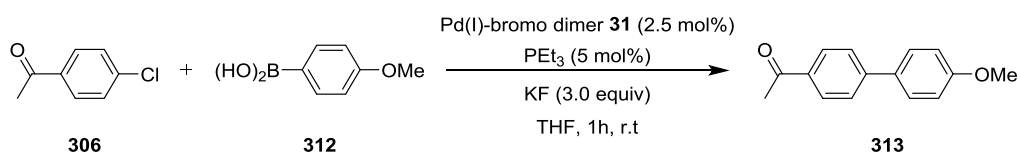
Entry	Time of premixing (min)[b]	Yield **313**[a] (%)
1	0	18
2	10	0

a) Yield reported according to calibrated ^{1}H-NMR analysis using dioxane as an internal standard. b) Pd(I)-bromo dimer **31** and PEt$_3$ were separately mixed in a THF solution before being added to the reaction mixture.

The presence of PEt$_3$ dramatically decreased the rate of reaction of Pd(I)-bromo dimer **31**. Complete inhibition was observed when the Pd(I)-bromo dimer **31** and PEt$_3$ were pre-mixed for 10 minutes before being added to the reaction mixture. In the latter case the solution containing the precatalyst mixture was light green when it was added to the reactants, meaning that most of the Pd(I)-bromo dimer **31** was already converted into Pd(0) **268** before the addition. The presence of PEt$_3$ not only completely inhibited the Pd(I)-bromo dimer **31** catalysis, but also that of Pd(PtBu$_3$)$_2$ **268**.

3.2.1.5: Effect of KF on Pd(I)-bromo dimer 31

In section **3.1** it was briefly described that the combination of water, KF and boronic acid led to the formation of Pd(PtBu$_3$)$_2$ **268** from Pd(I)-bromo dimer **31** within 20 minutes.[32] However, the effect of KF on Pd(I)-bromo dimer **31** in the absence of any other additive was not explored. KF was added to a THF solution containing Pd(I)-bromo dimer **31** and the reaction was monitored by ^{31}P-NMR spectroscopy over time. The spectra after 20 minutes and 1 hour did not show any traces of Pd(PtBu$_3$)$_2$ **268** and the only peak is the one at 87.1 ppm, which corresponds to the Pd(I)-bromo dimer **31**. The formation of Pd(0) **268** in the presence of KF, boronic acid and water could be due to the reaction of the KF with the boronic acid, which generate a molecule of ⁻OH responsible for the activation of the Pd(I)-bromo dimer **31**, as illustrated in *Scheme 116*. In the absence of boronic acid the formation of the ⁻OH is not possible and therefore activation cannot be achieved.
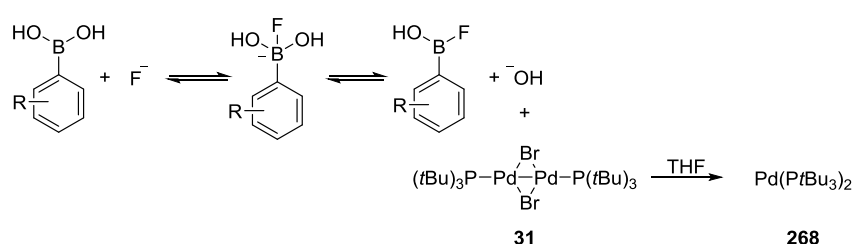
Scheme 116: Formation of ⁻OH from arylboronic acid and KF (top). Activation of Pd(I)-bromo dimer **31** by ⁻OH (bottom).

3.2.1.6: Effect of Diethyl 1,4-dihydro-2,6-dimethyl-3,5-pyridinedicarboxylate (Hantzsch ester) 327 on Pd(I)-bromo dimer 31

According to the nucleophilicity scale reported by Mayr *et al.*, the Hantzsch ester **327** (*Figure 60*) has an N value of 9.0, which is in between that of KF and KOH.[338,339] In this case, due the low N value calculated by Mayr *et al.*, we should not observe more than a trace of formation of Pd(PtBu$_3$)$_2$ **268**. Pd(I)-bromo dimer **31** was added to a THF solution containing an excess of the Hantzsch ester **327** and the reaction ws monitored by ^{31}P-NMR spectroscopy over time.
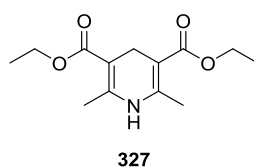
Figure 60: Hantzsch ester **327**.

The spectra after 20 minutes and 1 hour showed a single peak corresponding to Pd(I)-bromo dimer **31**. Even after a prolonged reaction time no new peaks had formed, confirming that the nucleophilicity of ester **327** is not high enough to promote the activation of Pd(I)-bromo dimer **31**. For N values below that of KOH (10.5) we did not observe formation of Pd(P*t*Bu$_3$)$_2$ **268**, and therefore there was no dimer activation. For N values above 10.5 there should be activation and we should therefore observe Pd(P*t*Bu$_3$)$_2$ **268**.

3.2.1.7: Effect of 1-Pyrrolidino-1-cyclopentene *328* on Pd(I)-bromo dimer *31*

After the previous observations, we decided to try a different N-based nucleophile with an N value of 15.9 in between that of PCy$_3$ and PEt$_3$.[340] We have previously defined the lowest value of N in which we should observe activation followed by formation of Pd(P*t*Bu$_3$)$_2$ **268** to be 10.5. In the case of 1-Pyrrolidino-1-cyclopentene **328** which has an N value of 15.1 we should therefore observe formation of the Pd(0) **268**. As in the previous studies, Pd(I)-bromo dimer **31** was added to a THF solution containing the nucleophile and the reaction was monitored over time by ^{31}P-NMR spectroscopy, (*Scheme 117*).
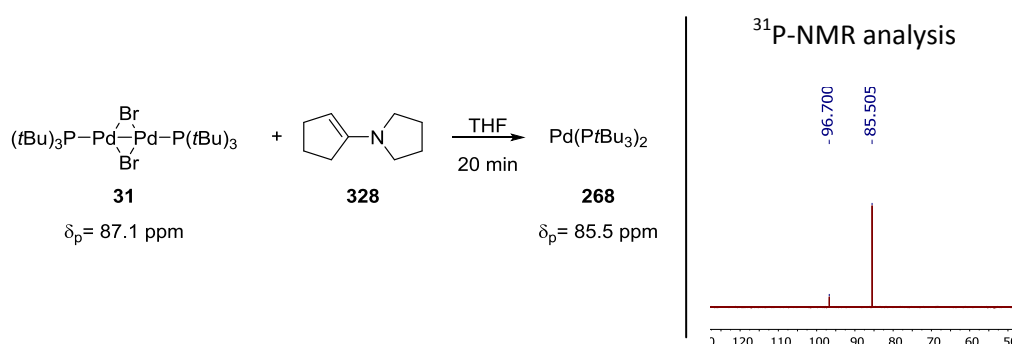
Scheme 117: Reaction between Pd(I)-bromo dimer **31** and 1-pyrrolidino-1-cyclopentene **328** (left). ^{31}P-NMR spectroscopic analysis of the reaction mixture (right). (Chemical shifts in ppm referenced to trimethoxyphosphine oxide as an internal standard).

Pd(I)-bromo dimer **31** was fully converted into Pd(P*t*Bu$_3$)$_2$ **268** within 20 minutes. Traces of formation of a new species at 96.7 ppm could also be observed in the ^{31}P-NMR spectrum of the reaction mixture, but the nature of this species is still unknown.

*3.2.1.8: Development of a nucleophilicity vs activation reactivity scale for Pd(I)-bromo dimer **31***

In this section we have shown that a nucleophile-assisted disproportionation could be a possible pathway for the activation of Pd(I)-bromo dimer **31**. The Pd(II) complexes hypothesised in our mechanism have been observed and characterised with two nucleophiles: PCy_3 and PEt_3. Moreover, we have observed a direct correlation between the nucleophilic value (N) of the nucleophile and its ability to generate $Pd(PtBu_3)_2$ **268** from Pd(I)-bromo dimer **31**. We have shown that for N values lower than 10.5 the formation of Pd(0) **268** was not observed which means that no activation took place, whilst for N values higher than 10.5 formation of $Pd(PtBu_3)_2$ **268** can be observed. In addition, we observed that the higher the rate of formation of $Pd(PtBu_3)_2$ **268**, the lower the yield of the Suzuki coupling of 4-chloroacetophenone **306** with 4-methoxyphenylboronic acid **312**.

A quantitative ^{31}P-NMR study was also performed to check for any loss, such as precipitates, of phosphine ligand during the reaction. We decided to perform the reaction in the presence of a fixed concentration of nucleophile (20 equivalents) and Pd(I)-bromo dimer **31** (1 equivalent) for all of the nucleophiles. All reactions assessed after 20 minutes. The results are summarised in *Table 21*.

Table 21: Quantitative analysis of the reaction between Pd(I)-bromo dimer **31** and different nucleophiles.
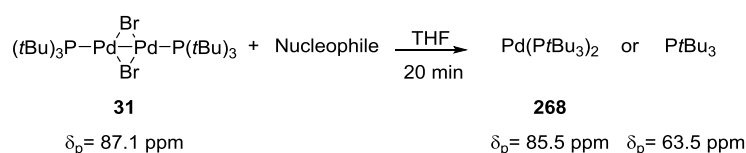
Entry	Nucleophile	N value[337-340]	Pd(I)-bromo dimer **31** left (%)	Pd(PtBu₃)₂ **268** formed (%)	PtBu₃ formed (%)	Other peaks/(%)
1	KF	<9.0	67	0	0	N/A
2	Hantzsch ester **327**	9.0	82	0	0	N/A
3	KOH	10.5	64	25	0	N/A
4	PCy_3	14.7	0	24	64	N/A
5	1-Pyrrolidino-1cyclopentene **328**	15.9	0	73	0	17
6	PEt_3	≈16.0	0	0	93	N/A
7[a]	KOEt	16.1	11	82	0	N/A
8	hppH **325**	16.2	0	88	4	N/A
9[a]	KOtBu	>18.0	0	50	13	N/A

Conditions: Pd(I)-bromo dimer **31** 1 equiv, nucleophile 20 equiv, THF 0.4 M, internal standard trimethoxyphosphine oxide 3.5 equiv, 1 drop of water; For the NMR study was chosen a pulse angle of 45°, a relaxtion time of 10s and a total number of scans of 250. a) in this case triphenylphosphine oxide was used as internal standard.

The quantitative study did not show a dramatic loss of phosphine during the course of the reaction, with less than 10 % for the majority of the cases (see Entries 2-8). However, in the case of KF and KO*t*Bu the loss is higher than 30%. In the latter case this could be due to the addition of the THF to the two solids giving rise to a very exothermic reaction. *Table 21* has been divided into two part: in the red part the Pd(I)-bromo dimer **31** is the major species in solution and the nucleophile is evidently not strong enough to promote its activation, whilst in the blue part the nucleophiles with an N value high enough to promote activation are listed.
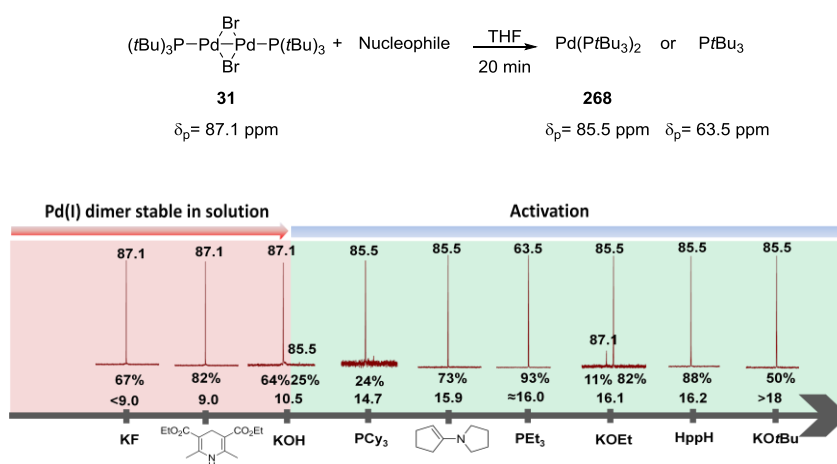
Figure 61: Effect of different nucleophile with an increasing N value on Pd(I)-bromo dimer **31**. The ^{31}P-NMR quantitative analyses was done using trimethoxyphosphine oxide or triphenyl oxide as internal standards.

3.2.2 Insight on the nucleophile-assisted mechanism of activation for Pd(I)-iodo dimer 193

After exploring the impact of nucleophiles on Pd(I)-bromo dimer **31**, we decided it would be interesting to also explore the effect of different nucleophiles on the iodide analogue of Pd(I)-bromo dimer **31,** Pd(I)-iodo dimer **193**. In 2012, our group showed that Pd(I)-iodo dimer **193** is not a good precatalyst in the Suzuki coupling of 4-chloroacetophenone **306** with 4-methoxyphenylboronic acid **312**.[330] It was shown that in the presence of Pd(I)-bromo dimer **31** with KF as base, 82 % of product formation was obtained within 1 hour, whilst in the presence of Pd(I)-iodo dimer **193** no product was formed.

As in the case of Pd(I)-bromo dimer **31**, Pd(I)-iodo dimer **193** was also exposed to different nucleophiles according to an increasing value of N.

3.2.2.1: Effect of weak nucleophiles on Pd(I)-iodo dimer 193

The reactivity of Pd(I)-iodo dimer **193** was explored with a class of weak nucleophiles such as KF, Hantsch ester **327** and KOH. In the case of Pd(I)-bromo dimer **31**, activation could be observed in the presence of KOH as nucleophile. Due to its higher stability, the Pd(I)-iodo dimer **193** should not react with KOH, and therefore with nucleophiles weaker than KOH, to give Pd(P*t*Bu$_3$) or Pd(P*t*Bu$_3$)$_2$ **268**. Pd(I)-iodo dimer **193** was exposed to the three different nucleophiles in THF as solvent. The three reaction were monitored by ^{31}P-NMR spectroscopy over time, (*Scheme 118*).
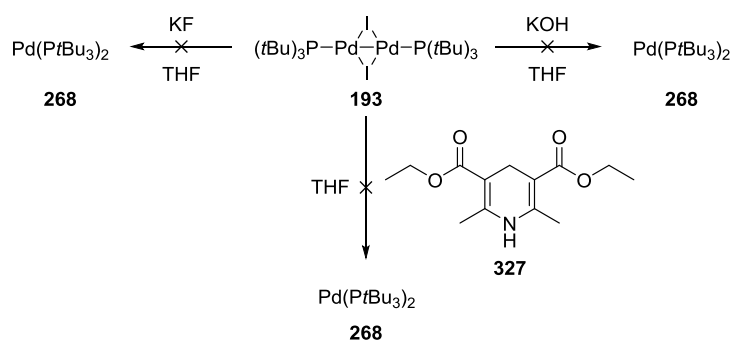
Scheme 118: Reaction of Pd(I)-iodo dimer **193** with weak nucleophiles.

Even after a prolonged reaction time of 24 hours, no changes could be observed either in the ^{31}P-NMR spectra or in the colour of all of the three solutions, with them remaining dark purple. This results are consistent with that previously reported by our group: in the presence of both KF and KOH, Pd(I)-iodo dimer **193** does not give any product in Suzuki coupling reactions because the monoligated Pd(P*t*Bu$_3$) cannot be generated.[258]

3.2.2.2: Effect of PCy$_3$ on Pd(I)-iodo dimer 193

Exposure of Pd(I)-iodo dimer **31** to PCy$_3$ had led to the formation of Pd(P*t*Bu$_3$)$_2$ **268** and Pd(II) complex **272**, that had provided the first support to our mechanistic hypothesis. Pd(I)-iodo dimer **193** was also added to a THF solution containing PCy$_3$ and the reaction was monitired by ^{31}P-NMR spectroscopy over time. After 1 hour of exposure the ^{31}P-NMR analysis showed complete consumption of Pd(I)-iodo dimer **193** and formation of Pd(P*t*Bu$_3$)$_2$ **268** as well as a species at 26.1 ppm, which could be due to Pd(II) iodo

complex **273** (see Chapter 2 section *2.3.1*), PtBu$_3$, PCy$_3$ and two unknown species at 84.1 and 45.4 ppm, (*Scheme 119*).
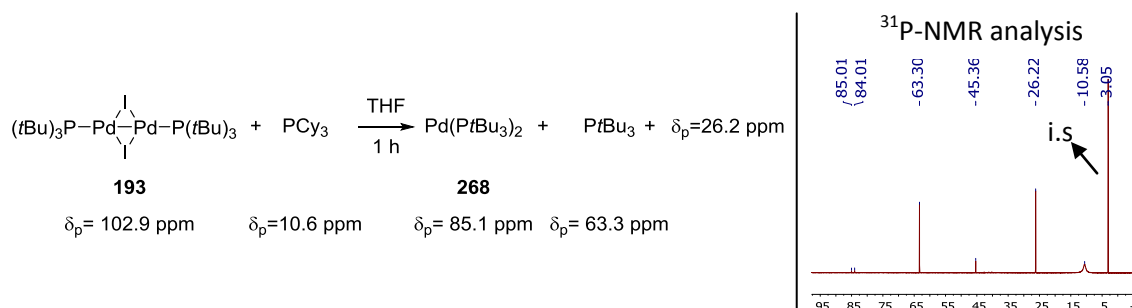
Scheme 119: Reaction between Pd(I)-iodo dimer **193** and PCy$_3$ (left). ^{31}P-NMR spectroscopic analysis of the reaction mixture after 60 minutes (right). (Chemical shifts in ppm referenced to trimethoxyphosphine oxide as an internal standard).

The reaction of Pd(I)-iodo dimer **193** with PCy$_3$ gave the free PtBu$_3$ ligand as well as Pd(II) iodo complex **273**. However, the formation of these new species could be partially due to both a high N value and the very high affinity of Pd towards phosphine-containing compounds.

3.2.2.3: Effect of 1-Pyrrolidino-1-cyclopentene **328** on Pd(I)-iodo dimer **193**

This nucleophile has an N value higher than the one of PCy$_3$, so if the activation observed in the case of PCy$_3$ is only due to the nucleophilic power of the phosphine, we should also observe formation of Pd(PtBu$_3$)$_2$ **268** when Pd(I)-iodo dimer **193** is exposed to compound **328**. Pd(I)-iodo dimer **193** was added to a THF solution containing nucleophile **328** and the reaction was monitored over time by ^{31}P-NMR spectroscopy. The reaction with 1-Pyrrolidino-1-cyclopentene **328** did not promote the activation of Pd(I)-iodo dimer **193** as was evident from Pd(0) **268** not being formed. This experiment showed that in the case of phosphine ligands an additional effect could be responsible for the activation, most probably the very high affinity of Pd for phosphine compounds.[341]

3.2.2.4: Effect of PEt$_3$ on Pd(I)-iodo dimer 193

Pd(I)-iodo dimer **193** was exposed to an excess of PEt$_3$ and after 1 hour of reaction time the solution was analysed by ^{31}P-NMR spectroscopy, (*Scheme 120*).
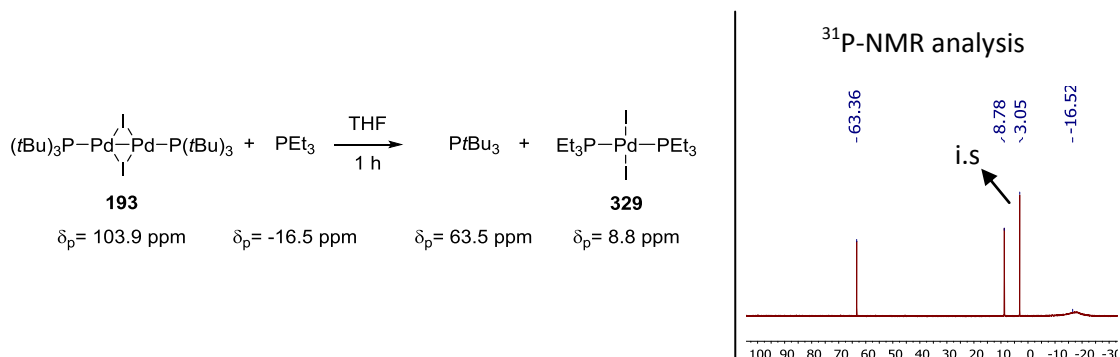
Scheme 120: Reaction between Pd(I)-iodo dimer **193** and PEt$_3$ (left). ^{31}P-NMR spectroscopic analysis of the reaction mixture (right). (Chemical shifts in ppm referenced to trimethoxyphosphine oxide as an internal standard).

In the case of this phosphine we also observed formation of Pd(PtBu$_3$)$_2$ **268** in the ^{31}P-NMR spectrum, as well as formation of another species at 8.8 ppm, which could be Pd(II) complex **329**, by comparison with previous reactions.

3.2.2.5: Effect of KOEt on Pd(I)-iodo dimer 193

As previously described, exposure of Pd(I)-bromo dimer **31** to KOEt led to the formation of Pd(PtBu$_3$)$_2$ **268** within 20 minutes. The use of KOEt as base instead of KF in the Suzuki coupling of 4-chloroacetophenone **306** with 4-methoxyphenylboronic acid **312** resulted in a decrease in the reactivity of Pd(I)-bromo dimer **31**. The yield in the presence of the ethoxide base decreased from 87% to 40% due to the fast formation of Pd(PtBu$_3$)$_2$ **268**. On the contrary, the use of Pd(I)-iodo dimer **193** as precatalyst in the presence of KF as base did not give any conversion in the same transformation. To verify whether Pd(I)-iodo dimer **193** could be activated in the presence of a stronger O-based base we exposed Pd(I)-iodo dimer **193** to 4 equivalents of KOEt with THF as solvent, (see *Scheme 121*).
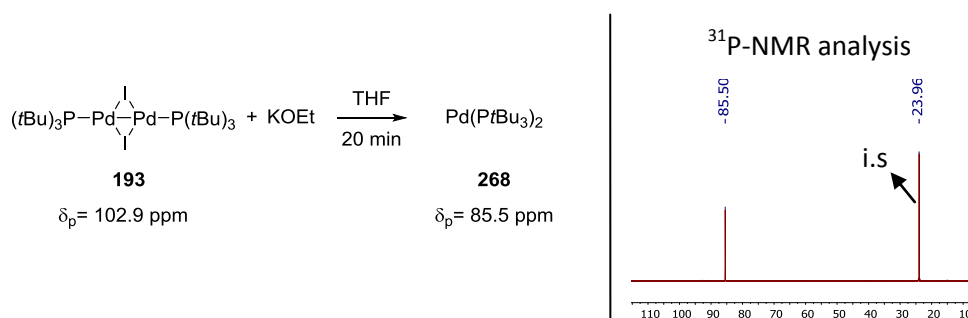
Scheme 121: Reaction between Pd(I)-iodo dimer **193** and KOEt (left). ^{31}P-NMR spectroscopic analysis of the reaction mixture (right). (Chemical shifts in ppm referenced to triphenylphosphine oxide as an internal standard).

After 20 minutes of exposure we could observe formation of Pd(PtBu$_3$)$_2$ **268** in the ^{31}P-NMR spectrum of the reaction mixture. The same precatalyst/base system was tested in the Suzuki coupling of 4-chloroacetophenone **306** with 4-methoxyphenylboronic acid **312** to verify whether the formation of Pd(PtBu$_3$)$_2$ **268** resulted in the formation of product, which would be consistent with our hypothesis that the process that leads to activation of Pd(I)-iodo dimer **193** is also the same process by which Pd(PtBu$_3$)$_2$ **268** is formed. The reaction was carried out both in the presence and absence of water, as the majority of Suzuki coupling reactions require the presence of water to allow the coupling, (see *Table 22*).

Table 22: Suzuki cross-coupling reaction of 4-chloroacetophenone **306** with 4-methoxyphenylboronic acid **312** in the presence of KOEt
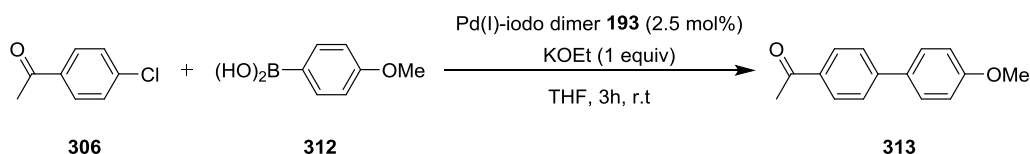
Entry	Presence of water	Yield **313** (%)[a]
1	yes	0
2	no	30

a) Yield reported according to calibrated ^{1}H-NMR analysis using dioxane as an internal standard.

The absence of water is crucial for the success of the reaction. In fact, no conversion was observed when water was present and the solution remained deep purple even after 3 hours, indicating that Pd(I)-iodo dimer **193** was still present. In the case of the reaction in the absence of water we decided to prolong the reaction time from one to three hours,

because in the first hour we did not notice a colour change of the solution. A substantial colour change from deep purple to brown was then observed after the second hour. After three hours of reaction time the product **313** was formed in 30% yield. This represents the first example of a successful application of Pd(I)-iodo dimer **193** as a precatalyst in a Suzuki cross-coupling reactions.

3.2.2.6: Effect of hppH **325** on Pd(I)-iodo dimer **193**

The use of KOEt as nucleophile for the first time allowed the activation of Pd(I)-iodo dimer **193** and its use as a precatalyst in a Suzuki cross-coupling reactions. We have observed that the coupling reaction is slow in the presence of KOEt and in the first hour almost no product was formed. We hypothesised that the use of a stronger nucleophile could be beneficial for the rate of reaction. We first exposed Pd(I)-iodo dimer **193** to an excess of hppH **325** in the absence of any coupling partner and the reaction was monitored by ^{31}P-NMR spectroscopy (see *Scheme 122*), and subsequently we used the same precatalyst system in the Suzuki coupling of 4-chloroacetophenone **306** with 4-methoxyphenylboronic acid **312**, (see *Table 22*).
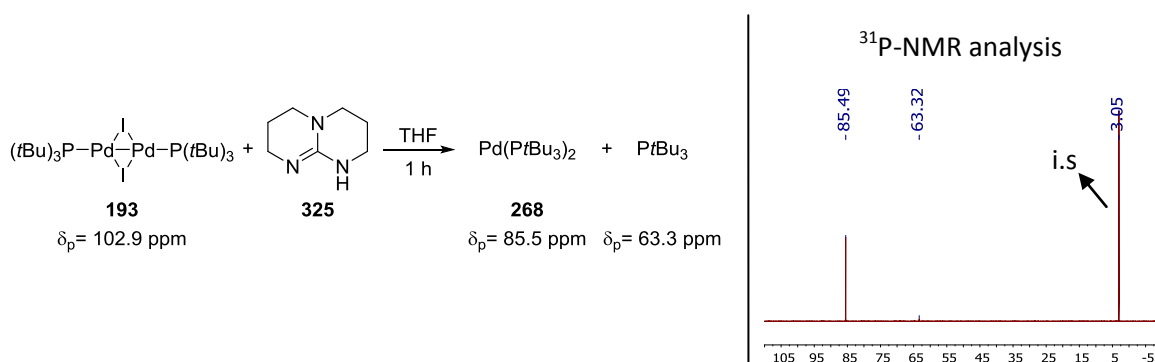
Scheme 122: Reaction between Pd(I)-iodo dimer **193** and hppH **325** (left). ^{31}P-NMR spectroscopic analysis of the reaction mixture (right). (Chemical shifts in ppm referenced to trimethoxyphosphine oxide as an internal standard).

As expected, according to the Mayr's scale the use of a strong nucleophile, led to the formation of Pd(P*t*Bu$_3$)$_2$ **268** within 1 hour of exposure. This allowed us to test the new precatalyst system in the Suzuki cross-coupling of the aryl chloride.

Table 23: Suzuki cross-coupling reaction of 4-chloroacetophenone **306** with 4-methoxyphenylboronic acid **312** in the presence of hppH **325**
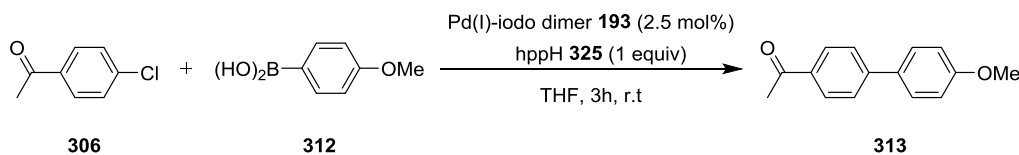
Entry	Presence of water	Yield **313** (%)[a]
1	yes	0
2	no	0

a) Yield reported according to calibrated ^{1}H-NMR analysis using dioxane as an internal standard.

To our surprise the reaction did not show any conversion either in the presence or absence of water. A decrease in the reactivity was also observed when Pd(I)-bromo dimer **31** was used as a precatalyst in the presence of this base/nucleophile. This could be due to the presence of a stable Pd(II) species formed in solution upon activation that facilitate the formation of the Pd(0)(PtBu$_3$)$_2$ **268**. In the case of Pd(I)-iodo dimer **193** the presence of iodides in solution, formed upon activation could also be responsible for the inhibition, (see Chapter 2).

3.2.2.7: Effect of KOtBu on Pd(I)-iodo dimer **193**

After the use of the stronger nucleophile hppH had not show any conversion in the Suzuki coupling reaction, we decided to test the effect of the even stronger nucleophile KOtBu on Pd(I)-iodo dimer **193**, first in the absence of coupling partners (see *Scheme 123*) and afterwards in their presence, (see *Table 23*).
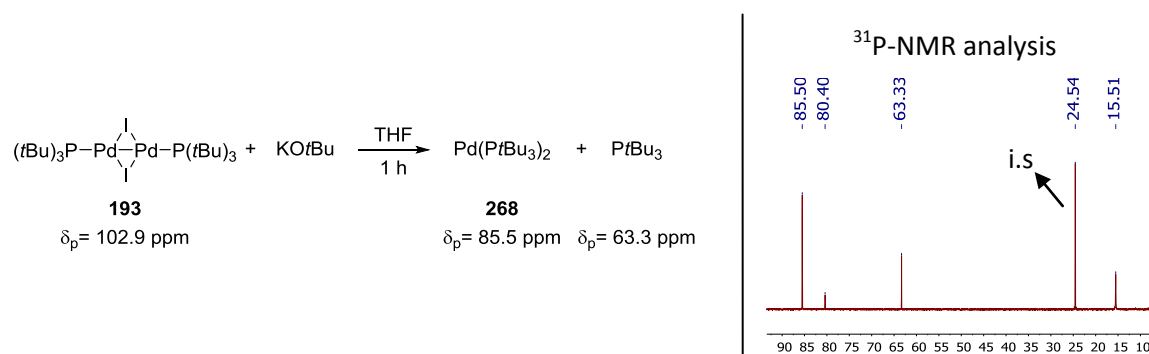
Scheme 123: Reaction between Pd(I)-iodo dimer **193** and KOtBu (left). ^{31}P-NMR spectroscopic analysis of the reaction mixture (right). (Chemical shifts in ppm referenced to triphenylphosphine oxide as an internal standard).

As in the case of Pd(I)-bromo dimer **31**, the reaction of Pd(I)-iodo dimer **193**, was very exothermic and dimer **193** was completely converted into Pd(PtBu$_3$)$_2$ **268** within 20 minutes. The KOtBu is so nucleophilic that the internal standard also reacted with it generating the species at 15 ppm. The precatalyst system was used in the Suzuki coupling of 4-chloroacetophenone **306** with 4-methoxyphenylboronic acid **312** both in the presence and absence of water.

Table 24: Suzuki cross-coupling reaction of 4-chloroacetophenone **306** with 4-methoxyphenylboronic acid **312** in the presence of KOtBu
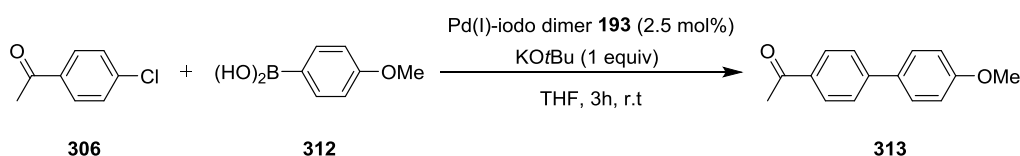
Entry	Presence of water	Yield **313** (%)[a]
1	yes	0
2	no	9

a) Yield reported according to calibrated ^{1}H-NMR analysis using dioxane as an internal standard.

The use of water in this case, as in the case of KOEt, also inhibits the reaction, most probably due to the formation KOH in solution, as illustrated in *Scheme 124*:

$$KOR \; + \; H_2O \; \rightleftharpoons \; HOR \; + \; KOH$$

Scheme 124: Formation of KOH from water in the presence of strong bases.

Surprisingly, the reaction in the absence of water also did not give good conversion. There was only 9% formation of product after 3 hours of reaction. The results showed that KOtBu is a too strong nucleophile to be used as a base for Suzuki cross-coupling reactions when Pd(I)-iodo dimer **193** is used as precatalyst.

3.2.2.8: Development of a nucleophilicity vs activation reactivity scale for Pd(I)-iodo dimer 193

Before testing the Pd(I)-iodo dimer **193** as a precatalyst in the Suzuki coupling of different aryl halides, we performed a quantitative ^{31}P-NMR study to verify whether or not a loss phosphine-containing products could occur in the course of the reaction, for example as

precipitates. The results are summarised in *Table 25*, and as in the case of Pd(I)-bromo dimer **31** the table had been divided into two parts: a red part where the nucleophile is not strong enough to promote the activation; and a blue part where the power of the nucleophile is enough to promote the activation.

Table 25: Quantitative analysis of the reaction between Pd(I)-iodo dimer **193** and different nucleophiles.

$$(t\text{Bu})_3\text{P}-\text{Pd}\overset{\text{I}}{\underset{\text{I}}{-}}\text{Pd}-\text{P}(t\text{Bu})_3 \ + \ \text{Nucleophile} \ \xrightarrow[\text{1h}]{\text{THF}} \ \text{Pd}(\text{P}t\text{Bu}_3)_2 \quad \text{or} \quad \text{P}t\text{Bu}_3$$

	193			**268**	
	δ_p= 102.5 ppm			δ_p= 85.5 ppm	δ_p= 63.5 ppm
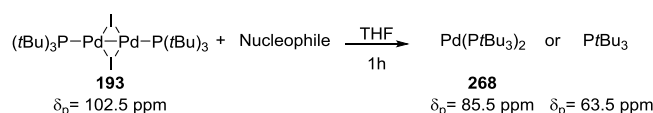
Entry	Nucleophile	N value[337-340]	Pd(I)-iodo dimer **193** left (%)	Pd(PtBu$_3$)$_2$ **268** formed (%)	PtBu$_3$ formed (%)	Other peaks/(%)
1	KF	<9.0	82	0	0	N/A
2	Hantzsch ester **327**	9.0	99	0	0	N/A
3	KOH	10.5	81	0	0	N/A
4	PCy$_3$	14.7	0	0	98	N/A
5	1-Pyrrolidino-1cyclopentene **328**	15.9	87	0	0	N/A
6	PEt$_3$	≈16.0	0	0	99	N/A
7[a]	KOEt	16.1	11	87	0	N/A
8	hppH **325**	16.2	0	97	4	N/A
9[a]	KOtBu	>18.0	0	75	25	N/A

Conditions: Pd(I)-iodo dimer **193** 1 equiv, nucleophile 20 equiv, THF 0.4 M, internal standard trimethoxyphosphine oxide 3.5 equiv, 1 drop of water; For the NMR study was chosen a pulse angle of 45°, a relaxtion time of 10s and a total number of scans of 250. a) in this case triphenylphosphine oxide was used as internal standard.

The quantitative study showed that in the case of Pd(I)-iodo dimer **193** no substantial loss of phosphine ligand can be observed, especially for the nucleophiles which promote the activation (see Entries 7-9). We were able to assign a limit value of N, corresponding to 16.0: below this value the Pd(I)-iodo dimer **193** does not react with the nucleophile whilst above this value it is possible to observe activity of the dimer **193**. However, an exception is presented by P-based nucleophiles. For these nucleophiles an additional effect appears to be responsible for the observed transformation of Pd(I)-iodo dimer **193** into Pd(PtBu$_3$)$_2$ **268** or free PtBu$_3$.
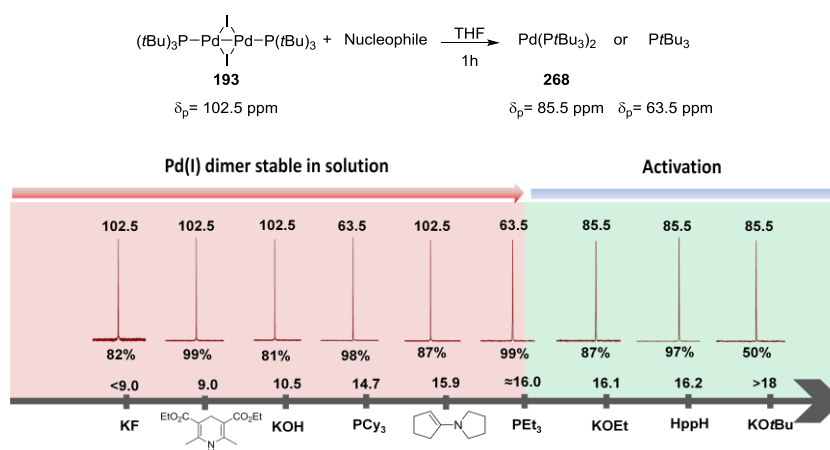
Figure 62: Effect of different nucleophile with an increasing N value on Pd(I)-iodo dimer **193**. The ^{31}P-NMR quantitative analyses was done using trimethoxyphosphine oxide or triphenyl oxide as internal standards.

3.3 Proof of mechanism: First demonstration of activity of Pd(I) dimer 193 in catalysis

Having demonstrated the first reactivity of Pd(I)-iodo dimer **193** as precatalyst in Suzuki coupling we decided to further explore the use of Pd(I)-iodo dimer **193** in the Suzuki cross-coupling reactions of aryl iodides, bromides and chlorides, to investigate the possible scope

3.3.1 Suzuki coupling of aryl iodides catalysed by Pd(I)-iodo dimer 193

The activity of Pd(I)-iodo dimer **193** as a precatalyst was explored for a series of aryl iodides and aryl boronic acids. The results obtained are summarised in *Tables 26*, *Table 27* and *Table 28*.

Table 26: Suzuki cross-coupling of aryl iodides with 2-methylphenylboronic acid **5**, with Pd(I)-iodo dimer **193** as a precatalyst.
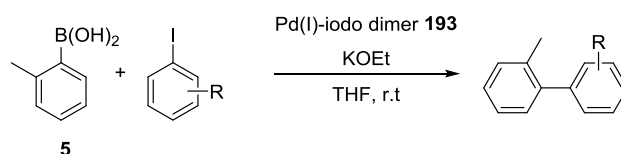
Entry	R	Catalyst load (mol%)	Base (equiv)	Time (h)	Yield (%)[a]
1	4-CH$_3$	1.0	3.3	1.5	76
2	4-CH$_3$	1.0	4.0	1.5	70
3	4-CH$_3$	1.0	4.0	3.0	73
4	4-OCH$_3$	1.0	4.0	1.5	76
5	4-OCH$_3$	1.0	4.0	3.0	84
6	H	1.0	4.0	3.0	80
7	4-CN	1.0	4.0	3.0	96
8	4-NO$_2$	1.0	4.0	1.5	81
9	4-NO$_2$	1.0	4.0	3.0	87
10	4-OCH$_3$	2.5	4.0	3.0	87
11	H	2.5	4.0	3.0	80

a) Yield reported according to calibrated ^{1}H-NMR analysis using dioxane as an internal standard

The use of Pd(I)-iodo dimer **193** as precatalyst gave good conversions both with electron-withdrawing and electron-donating groups (Entries 3, 5, 6, 7 and 9). Slightly higher yields can be obtained with prolonged reaction times (compare Entries 2 and 3, Entries 4 and 5, Entries 8 and 9) or by increasing the catalyst load (compare Entries 5 and 10 and Entries 6 and 11).

Table 27: Suzuki cross-coupling of aryl iodides with phenylboronic acid **330**, with Pd(I)-iodo dimer **193** as a precatalyst.
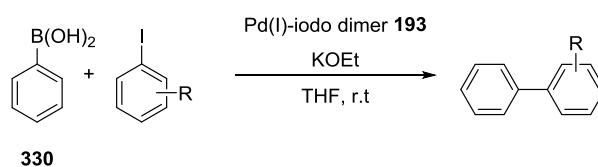
Entry	R	Catalyst load (mol%)	Base (equiv)	Time (h)	Yield (%)[a]
1	4-CH$_3$	1.0	4.0	3.0	65
2	4-OCH$_3$	1.0	4.0	3.0	56
3	H	1.0	4.0	3.0	40

a) Yield reported according to calibrated ^{1}H-NMR analysis using dioxane as an internal standard

The coupling of phenylboronic acids **330** with aryl iodides also gave good yields, although lower compared to the ones obtained with 2-methylphenylboronic acid **5**.

Table 28: Suzuki cross-coupling reaction of aryl iodides with 4-methoxyphenylboronic acid **312**, with Pd(I)-iodo dimer **193** as a precatalyst.
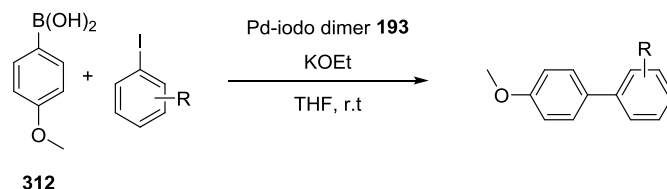
Entry	R	Catalyst load (mol%)	Base (equiv)	Time (h)	Yield (%)[a]
1	4-CH$_3$	1.0	4.0	3.0	69
2	4-OCH$_3$	1.0	4.0	3.0	45
3	4-OCH$_3$	1.0	4.0	3.0	84
4	H	1.0	4.0	1.5	88
5	H	1.0	4.0	3.0	93
6	4-CN	1.0	4.0	3.0	95
7	4-NO$_2$	1.0	4.0	3.0	96
8	4-F	2.5	4.0	3.0	90
9	H	2.5	4.0	3.0	90

a) Yield reported according to calibrated ^{1}H-NMR analysis using dioxane as an internal standard

The use of Pd(I)-iodo dimer **193** as precatalyst allowed the reactions to proceed in good yields. Prolonged reaction times and increasing the catalyst loading did not substantially improve the conversions.

For the first time we have shown that Pd(I)-iodo dimer **193** can be used as an efficient precatalyst in the Suzuki coupling of aryl iodides and good yields are obtained both with electron-withdrawing and electron-donating groups. An additional study was performed to compare the reactivity of dimer **193** with that of the Pd$_2$(dba)$_3$/PtBu$_3$ (0.5/1.1) system, using KF as base, as reported by Fu *et al.* in 2000.[30] The two precatalyst systems were tested in the presence of aryl iodides bearing electron-withdrawing, electron-donating and electron-neutral groups. The results are summarised in *Table 29*.

Table 29: Suzuki cross-coupling reaction of aryl iodides in presence of Pd(I)-iodo dimer **193** or Pd$_2$(dba)$_3$/PtBu$_3$ as precatalysts.
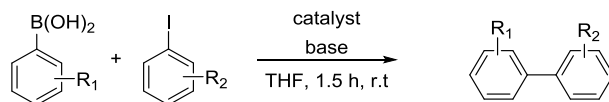
Entry	R$_1$	R$_2$	Catalyst/(mol) %	Base (equiv)	Yield (%)[a]
1	2-CH$_3$	4-CH$_3$	Pd$_2$(dba)$_3$/PtBu$_3$/(0.5/1.1)	KF (3.3)	49
2	2-CH$_3$	4-CH$_3$	Pd(I)-iodo dimer **193**/(1.0)	KOEt (3.3)	76
3	2-CH$_3$	4-CH$_3$	Pd$_2$(dba)$_3$/PtBu$_3$/(0.5/1.1)	KF (4.0)	37
4	2-CH$_3$	4-CH$_3$	Pd(I)-iodo dimer **193**/(1.0)	KOEt (4.0)	70
5	4-OCH$_3$	H	Pd$_2$(dba)$_3$/PtBu$_3$/(0.5/1.1)	KF (4.0)	45
6	4-OCH$_3$	H	Pd(I)-iodo dimer **193**/(1.0)	KOEt (4.0)	88
7	4-CH$_3$	4-NO$_2$	Pd$_2$(dba)$_3$/PtBu$_3$/(0.5/1.1)	KF (4.0)	43
8	2-CH$_3$	4-NO$_2$	Pd(I)-iodo dimer **193**/(1.0)	KOEt (4.0)	81
9	2-CH$_3$	4-OCH$_3$	Pd$_2$(dba)$_3$/PtBu$_3$/(0.5/1.1)	KF (4.0)	45
10	2-CH$_3$	4-OCH$_3$	Pd(I)-iodo dimer **193**/(1.0)	KOEt (4.0)	76

a) Yield reported according to calibrated ^{1}H-NMR analysis using dioxane as an internal standard

We were expecting similar reactivity of the two precatalyst systems due to the fact that they should form the same active species: the monoligated Pd(PtBu$_3$) species. Surprisingly, the reaction in which the Pd$_2$(dba)$_3$/PtBu$_3$ 0.5/1.1 system is used as precatalyst showed considerably lower yields compared to the reaction in which Pd(I)-iodo dimer **193** is used as precatalyst. This led us to investigate the reasons for this decrease in the reactivity observed in the presence of the Pd$_2$(dba)$_3$/PtBu$_3$ (0.5/1.1) system. The Suzuki coupling of both aryl iodides with electron-donating and electron-withdrawing groups with 2-methylphenylboronic acid **5** in the presence of the Pd$_2$(dba)$_3$/PtBu$_3$ (0.5/1.1) system was followed by ^{31}P-NMR spectroscopy, (see *Figure 63*).
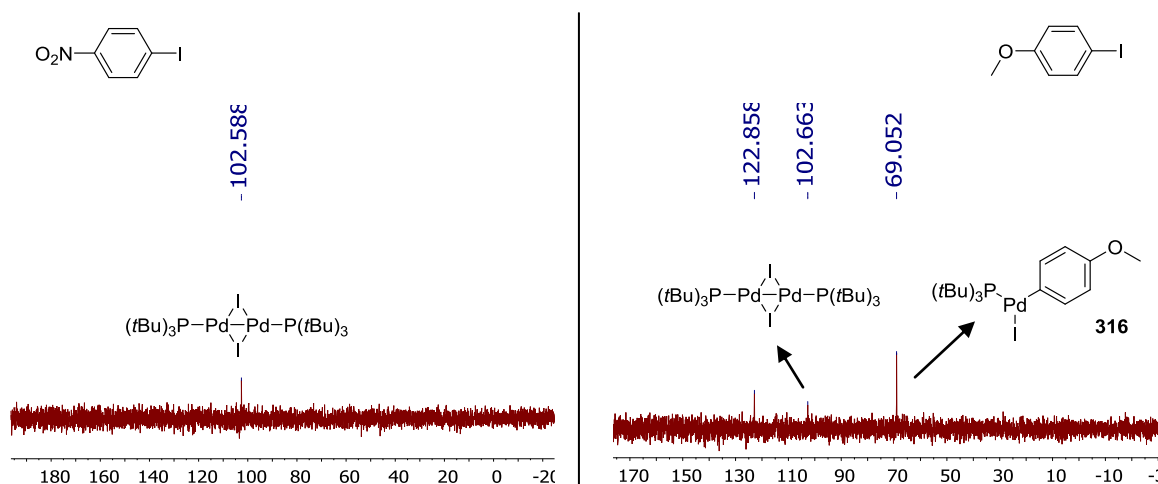
Figure 63: ^{31}P-NMR analysis sof the Suzuki coupling of 2-methylboronic acid **312** with: 1-iodo-4-nitrobenzene (left) and 1-iodo-4-methoxybenzene (right). (Chemical shifts in ppm referenced to triphenylphosphine oxide as an internal standard)

The ^{31}P-NMR analysis of the reaction mixture after 30 minutes provided an interesting outcome. In both reactions it is possible to detect the formation of Pd(I)-iodo dimer **193**. The formation of Pd(I) dimers in the presence of Pd(II) oxidative addition products was also observed by Proutiere of our group.[32] It was shown that these Pd(I)-dimers are formed upon reductive elimination of biaryl from a dimeric Pd(II) complex (see *Scheme 125*). However, similar observation of biaryl formation upon oxidative addition of aryl halides to Pd(P*t*Bu₃)₂ was reported by Hartwig *et al.*, although they did not furnish an explanation for this phenomenon.[342]
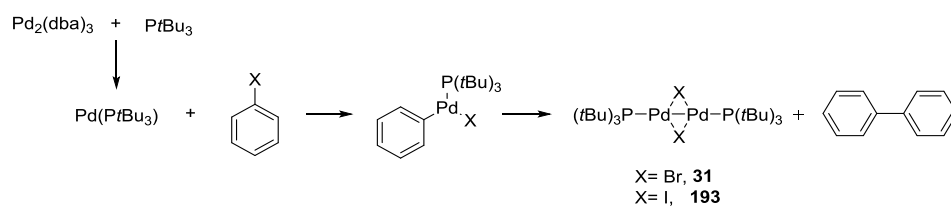
Scheme 125: Formation of Pd-dimers and biaryl from Pd(II) oxidative addition complexes.[32]

According to this, we should observe biaryl formation together with the formation of Pd(I)-iodo dimer **193**. The GC-MS analysis of the two reaction mixtures did not show any trace of biaryl side product, although this is probably due to the very low catalyst loading (if the reaction is complete we should expect 1% of biaryl formation). We decided to repeat the reaction of 1-iodo-4-nitrobenzene with a higher catalyst loading (increased from 0.5/1.1 to 5/11 mol%), (*Figure 64*).
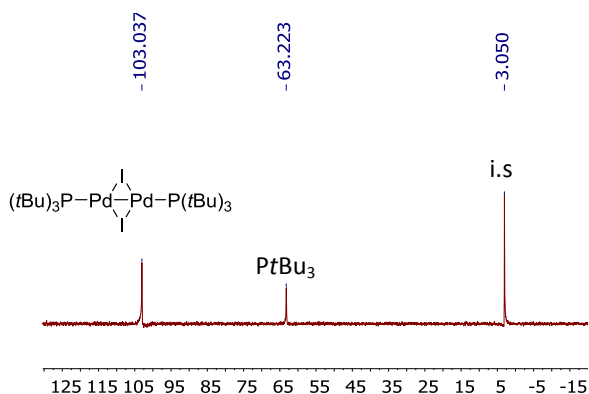
Figure 64: ^{31}P-NMR analysis of the Suzuki coupling of 2-methylboronic acid **5** with 1-iodo-4-nitrobenzene. (Chemical shifts in ppm referenced to trimethoxyphosphine oxide as an internal standard).

The increase of the catalyst loading allowed an increase in the intensity of the P-containing compounds in the ^{31}P-NMR spectrum of the reaction mixture. The peaks of Pd(I)-iodo

dimer **193**, together with the free PtBu$_3$ ligand are now clear signals. This time the presence of the biaryl was detected in the ^{1}H-NMR spectrum of the reaction mixture.

The formation of Pd(I)-iodo dimer **193** could explain the decrease in the reactivity observed when the Pd$_2$(dba)$_3$/PtBu$_3$ (0.5/1.1) system is used in the presence of KF as base. In the previous section we have shown that KF is not a strong nucleophile and it is not able to promote the activation of Pd(I)-iodo dimer **193**, so its formation could remove active catalytic species from the reaction mixture that cannot be further activated by the KF. To verify this hypothesis we performed the same reaction shown in *Table 29*, but this time in the presence of KOEt as base instead of KF. If our hypothesis is correct we should observe an increase in the yields of the reaction, due to the ability of KOEt to activate the Pd(I)-iodo dimer **193** formed in solution.

Table 30: Suzuki cross-coupling reaction of aryl iodides in the presence of Pd$_2$(dba)$_3$/PtBu$_3$ system as precatalyst and in the presence of KOEt as base.
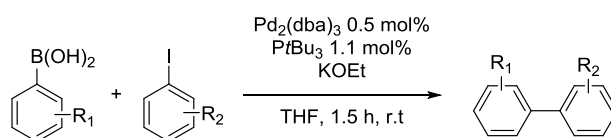
Entry	R$_1$	R$_2$	KOEt (Equiv)	Yield with KOEt (%)[a]	Yield with KF (%)[a]
1	2-CH$_3$	4-CH$_3$	3.3	87	49
2	2-CH$_3$	4-CH$_3$	4.0	77	37
3	4-OCH$_3$	H	4.0	97	45
4	2-CH$_3$	4-NO$_2$	4.0	89	43
5	2-CH$_3$	4-OCH$_3$	4.0	80	45

a) Yield reported according to calibrated ^{1}H-NMR analysis using dioxane as an internal standard

The use of KOEt as a base considerably increased the yields for all of the substrates tested. Inhibition due to the use of iodides in cross-coupling reactions has also been observed by other groups, as discussed in Chapter 2. In this case the use of aryl iodides caused the formation of the stable Pd(I)-iodo dimer **193**, that has been shown to be inactive in the presence of KF as base. The use of the right base/nucleophile allowed us to overcome this and reach good conversions when employing aryl iodides as substrates.

3.3.2 Suzuki coupling of aryl bromides and chlorides catalysed by Pd(I)-iodo dimer 193

In the previous section we showed that good conversions can be achieved using Pd(I)-iodo dimer **193** as precatalyst in the Suzuki coupling of aryls iodides in the presence of KOEt as base. We decided to further explore the reactivity of this dimer with aryl bromides and aryl chlorides. The latter are usually challenging substrates in Suzuki cross-coupling reactions compared to iodide and bromide analogues. The results obtained are summarised in the tables below. A higher catalyst loading has been used, because in the case of aryl iodides improved conversions were obtained employing 2.5 mol% of catalyst instead of 1 mol%.

Table 31: Suzuki cross-coupling reaction of aryl bromides and 2-methylphenylboronic acid **5**, with Pd(I)-iodo dimer **193** as a precatalyst.
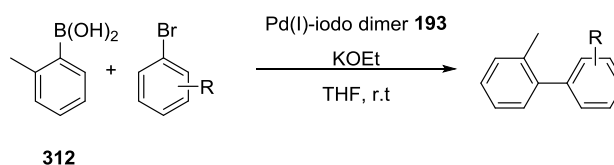
Entry	R	Catalyst loading (%)	Base (equiv)	Time (h)	Yield (%)[a]
1	4-OCH$_3$	2.5	4.0	3.0	83
2	2-CH$_3$	2.5	4.0	3.0	56
3	H	2.5	4.0	3.0	81
4	4-F	2.5	4.0	3.0	83
5	4-CH$_3$	2.5	4.0	3.0	75

a) Yield reported according to calibrated ^{1}H-NMR analysis using dioxane as an internal standard

Table 32: Suzuki cross-coupling reaction of aryl bromides and phenylboronic acid **330**, with Pd(I)-iodo dimer **193** as a precatalyst.
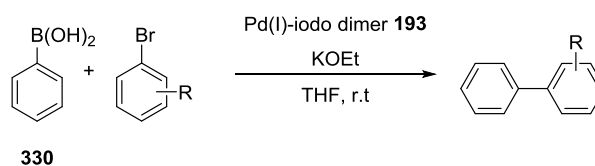
Entry	R	Catalyst loading (%)	Base (equiv)	Time (h)	Yield (%)[a]
1	2-CH$_3$	1.0	4.0	3.0	67
2	4-OCH$_3$	1.0	4.0	3.0	59

a) Yield reported according to calibrated ^{1}H-NMR analysis using dioxane as an internal standard

Table 33: Suzuki cross-coupling reaction of aryl bromides with 4-methoxyphenyl boronic acid **312**, with Pd(I)-iodo dimer **193** as a precatalyst.
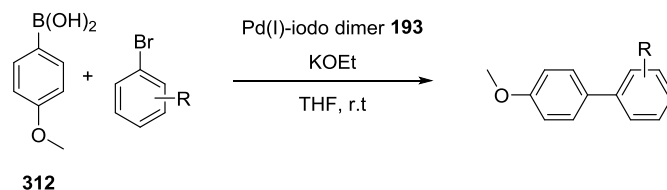
Entry	R	Catalyst loading (%)	Base (equiv)	Time (h)	Yield (%)[a]
1	4-OCH$_3$	2.5	4.0	3.0	83
2	4-CH$_3$	2.5	4.0	3.0	95
3	2-CH$_3$	2.5	4.0	3.0	95
4	H	2.5	4.0	3.0	94
5	4-F	2.5	4.0	1.0	86

a) Yield reported according to calibrated ^{1}H-NMR analysis using dioxane as an internal standard

Table 34: Suzuki cross-coupling reaction of aryl chlorides with 4-methoxyphenyl boronic acid **312**, with Pd(I)-iodo dimer **193** as a precatalyst.
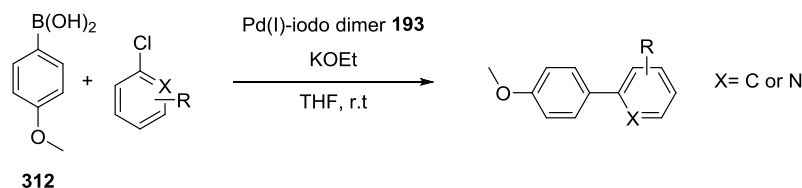
Entry	X	R	Catalyst loading (%)	Base (equiv)	Time (h)	Yield (%)
1	C	4-COCH$_3$	2.5	4.0	3.0	65
2	N	2-CH$_3$	2.5	4.0	3.0	38
3	C	4-CF$_3$	2.5	4.0	3.0	63
4	C	4-CH$_3$	2.5	4.0	3.0	6
5	C	4-F	2.5	4.0	1.0	3

a) Yield reported according to calibrated ^{1}H-NMR analysis using dioxane as an internal standard

The results obtained employing aryl bromides, shown in *Tables 31, 32* and *33*, are similar to those obtained with aryl iodides for both electron-withdrawing and electron-donating groups. In the case of aryl chlorides good yields can only be achieved with activated substrates (see Entries 1-3), whilst a considerably decrease in the reactivity can be observed when non-activated substrates are employed (compare Entries 4-5 of *Table 34* with Entries 2 and 5 of *Table 33*).

3.3.3 Suzuki coupling of aryl halides catalysed by Pd(I)-iodo dimer 193 under aerobic conditions

In the previous sections we have shown that with the use of an appropriate nucleophile/base it is possible to activate the very stable Pd(I)-iodo dimer **193** in Suzuki cross-coupling reactions. A minimum value of the nucleophilic power for this has been determined: above this value there is activation and below this value the Pd(I)-iodo dimer **193** is stable and can be present is solution in its dimeric form. The efficiency of this precatalyst, although reasonable when aryl bromides and iodides are employed, remains very low towards aryl chlorides compared to that of Pd(I)-bromo dimer **31**. Our interest for the use of Pd(I)-iodo dimer **193** as a catalyst was partially to support our mechanistic proposal, but also due to the very high stability of this dimer towards oxygen, both in the solid state and in solution. In general, there are two main limitations regarding the use of Pd catalyst under aerobic conditions: one is represented by the fact that phosphine ligands, in particular electron rich ones, are easily oxidised to phosphine oxide by O_2, that consequently reduces the binding interaction with the Pd leading to its decomposition and formation of Pd black. The second limitation concerns a homocoupling reaction between two molecules of boronic acid. A possible mechanism for this oxidative coupling was proposed by Moreno-Mañas *et al*. in 1996. It was shown that the oxidative coupling is favoured by the presence of electron-donating groups on the aryl ring of the boronic acid, and is accelerated in the presence of oxygen.[343,344]

The stability of Pd(I)-iodo dimer **193** in air has allowed the ability to overcome at least one of the two problems related to the use of a Pd catalyst bearing electron rich phosphines under aerobic conditions. We decide to test this precatalyst in the Suzuki coupling of 4-bromotoluene **331** with 2-methylphenylboronic acid **5** under aerobic conditions. The use of non-anhydrous THF as solvent did not give any conversion. The addition of the solvent was apparently followed by an exothermic acid-base reaction between the KOEt base and the water present in the THF and as a consequence no product was formed. The use of anhydrous THF was necessary in order to have the sufficient amount of KOEt in solution to activate the Pd(I)-iodo-dimer **193**. We decided to use the same conditions used as in the case of Entry 5 *Table 30*, (*Scheme 126*).

Scheme 126: Suzuki cross-coupling reaction of 4-bromotoluene **331** with 2-methylphenylboronic acid **5** under aerobic conditions. Conditions: 2.5 mol% catalyst load, 3 h reaction time and 4.0 equiv of base.

The reaction performed under aerobic conditions gave a lower yield compared to the reaction performed under oxygen-free conditions (75 *vs* 51 %). In addition, 6% of homocoupling product was formed as side product. A screening of the optimum reaction conditions was required in order to increase the yields of reaction and limit the formation of the homocoupling products derived from two molecule of boronic acids. The results are summarised in *Table 35*.

Table 35: Suzuki cross-coupling reaction of 4-bromotoluene **331** with 2-methylphenylboronic acid **5** under aerobic conditions.

Entry	Catalyst loading (mol%)	Additive	Equiv of base	Time (h)	Yield **332** (%)[b]	Yield **333** (%)[b]
1	2.5	TMAF/ 2 equiv	2.0	3.0	4	2
2	2.5	0.2 mL of EtOH	4.0	3.0	49	6
3	2.5	1 mL of EtOH	4.0	3.0	8	2
4	1.0	Ag$_2$O	4.0	3.0	34	14
5	2.5	Molecular sieves	4.0	3.0	15	3
6	2.5	Molecular sieves	2.0	3.0	27	13
7	1.0	FeBr$_3$/0.5 mol%	4.0	3.0	30	10
8	2.5	FeBr$_3$/2.5 mol%	4.0	4.0	55	12
9	2.5	FeBr$_3$/1.3 mol%	8.0	3.0	71	7
10	2.5	-	6.0	3.0	31	-
11	2.5	-	4.0	3.0	59	5
12[a]	2.5	-	4.0	3.0	31	7
13	5.0	-	4.0	3.0	86	4

a) In this case the base reagent was old. b) Yield reported according to calibrated ^{1}H-NMR analysis using dioxane as an internal standard

The reaction was performed in the presence of several additives and different equivalents of base and catalyst loading. The use of ethanol, Ag_2O and molecular sieves not only lowered the yields but also increased the formation of the biaryl side product **333** (see Entries 2-6). A substantial improvement could be observed in the presence of $FeBr_3$ as additive (see Entries 7-9). This may be due to reaction between the Fe and O_2, with good results being obtained in the presence of catalytic amount of $FeBr_3$ and 8 equivalents of base (see Entry 9). However, the best result was obtained employing 5 mol% of catalyst load and 4.0 equivalents of base (see Entry 13). It is important to note that the quality of the base also has an important role. We performed two different experiments: one using 4 equivalents of an old base, that most probably was already partially hydrolysed, and one using a base from a new bottle that was stored under a nitrogen atmosphere (see Entries 11 and 12). The reaction gave markedly different outcomes, with lower yields being obtained in the presence of the old base, whilst the quantity of homocoupling product **333** remained the same.

After finding the optimal reaction conditions we proceeded to investigate the scope of the reaction.

Table 36: Suzuki cross-coupling reactions using Pd(I)-iodo dimer **193** as a precatalyst under oxygen and oxygen-free conditions.
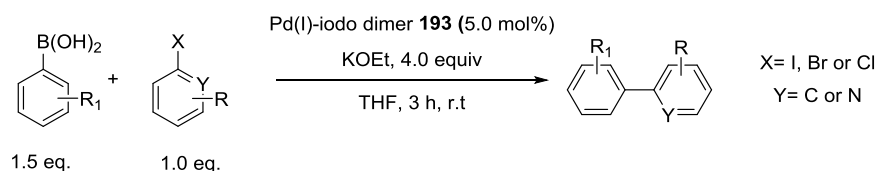
Entry	Boronic acid	Aryl halide	Anaerobic yield (%)	Aerobic yield (%)
1	O⟨⟩B(OH)$_2$	I⟨⟩CN	78	76
2	⟨⟩B(OH)$_2$	I⟨⟩NO$_2$	66	71
3	⟨⟩B(OH)$_2$	I⟨⟩O	53	54
4	O⟨⟩B(OH)$_2$	I⟨⟩	43	43
5	⟨⟩B(OH)$_2$	Br⟨⟩F	76	82
6	O⟨⟩B(OH)$_2$	Cl⟨⟩	44	45
7	⟨⟩B(OH)$_2$	Cl⟨N⟩	82	84
8	O⟨⟩B(OH)$_2$	Br⟨⟩CN	72	70

169

The Suzuki coupling of aryl iodides, bromides and chlorides was performed under both oxygen and oxygen-free conditions in order to compare the reactivity of the Pd(I)-iodo dimer **193** under both conditions. The results are illustrated in *Table 36* and the yields reported are isolated yields.

The use of Pd(I)-iodo dimer **193** as a precatalyst gave good to excellent isolated yields whether the reaction was performed inside or outside the glovebox. The formation of the small amount of homocoupling product derived from the oxidative coupling of two molecules of boronic acid evidently does not influence the outcome of the reaction, as the yields are very similar. Lower conversions are observed in the presence of electron-donating groups on the phenyl ring of the aryl iodides (compare Entries 1-2 with 3-4), whilst the low yields observed in the case of 4-chloroacetophenone **306** in Entry 6 are caused by problems in the purification due to the starting material and product having a similar R_f.

3.4 Conclusions

In this chapter we have proposed possible nucleophile-assisted disproportionation pathways for the activation of Pd(I)-bromo dimer **31** and Pd(I)-iodo dimer **193**, for both charged and neutral nucleophiles. For each dimer we have identified a lower value of N above which the dimer reacts with the nucleophile. In addition, we have shown for the first time that in the presence of the right nucleophile/base the very stable Pd(I)-iodo dimer **193** can also be used as a precatalyst in the Suzuki coupling of aryl iodides, bromides and chlorides. The presence of oxygen does not influence the outcome of the reaction, with similar yields being obtained both under oxygen and moisture free conditions as well as in the presence of oxygen. This allows this coupling to be performed outside the glovebox without the necessity of degassing the reactants. However, dry THF and fresh KOEt are required to achieve good levels of product formation.

Chapter 4. Pd(I)-catalysed trifluoromethylselenolation of aryl halides

The following results have been the subject of a publication.[345] A. Tsang, of our group, performed the synthesis of the $(CH_3)_4NSeCF_3$ salt. The crystal structure reported in this chapter was solved by Dr M. D. Wörle and Dr N. Trapp, whilst M. Solar took care of the data collection.

Chapter 4: Introduction

Multi-metal catalysis is ubiquitous in nature, recrystallisation of several enzymes revealed that almost one third of them, called metallo-enzymes, contains metals, such as Mg, Fe, Ca, Cu and Mo.[346] The synergism between two or more metal center is supposed to be responsible for the particular reactivity of these metallo-enzymes. However, examples of applications of multi-metal centers are not common in homogeneus catalysis, where the use of well-defined monomeric metal centers is ubiquitous, especially for Pd complexes. As shown in Chapter 1, most of the Pd(I)-Pd(I) dimers reported have found broad use as precursors of more reactive monoligated "Pd(0)L" species. In the previous chapter we have shown how the Pd(I)-bromo dimer **31** and Pd(I)-iodo dimer **193** are activated and this allowed us to identify the conditions under which these dimers can remain stable in solution. With the objective to explore novel catalysis modes, with potentially new reactivities, and making use of the air-stability of Pd(I)-iodo dimer **193** as a practically highly interesting feature, the possibility for direct reactivity and catalysis involving Pd(I) dimers was explored in the following chapter. The first use of Pd(I) dimers as a catalyst in reaction of I/Br exchange was previously shown by our group.[347-348] The group showed for the first time that: *(i)* oxidative addition of aryl iodides can occur directly on Pd(I)-bromo dimer **31**; *(ii)* the exchange is likely directly catalysed by the Pd(I)-dimer **31** (first example of dinuclear catalysis). Herein we will present the first catalytic protocol for the synthesis of Ar-SeCF$_3$ compounds, involving Pd(I) dimeric species as catalysts. Simultaneously to the developments of Ar-SeCF$_3$ coupling presented herein, SCF$_3$ coupling was also developed in our group by G. Yin, I. Kalvet and F. Schoenebeck. They showed that the reaction of Pd(I)-iodo dimer **193** with $(CH_3)_4NSCF_3$ salt led to the formation of a novel Pd(I) dimer: $[Pd(\mu\text{-}SCF_3)PtBu_3]_2$. This dimer, formed *in situ* from Pd(I)-iodo dimer **193** and $(CH_3)_4NSCF_3$ salt, was then used as a catalyst for the trifluoromethylthiolation of aryl halides.[349] The presence of the CF$_3$ group makes the SCF$_3$ and SeCF$_3$ medicinally attractive groups. In the last decades, compounds containing OCF$_3$ or SCF$_3$ groups have found widespread use in both pharmaceutical and agrochemical research, as antibiotics, antihypertensives, insecticides, fungicides as well as having many other applications.[350] The use of SeCF$_3$ compounds is less developed due to the lack of synthetic procedures that do not make use of toxic intermediates or stoichiometric amounts of transition metals.

The introduction of F atoms or F-containing groups in general have been shown to improve the metabolic stability of drugs against oxidation, especially against oxidising enzymes

present in the liver. Moreover, fluorine-containing groups increase the lipophilicity of the compound generally without affecting its solubility, which is usually decreased by the increase of the lipophilicity.[351] There are numerous procedures available for the introduction of OCF_3[352-354] or SCF_3[314,355-357] groups into an organic molecule, however there are few procedures for the introduction of the $SeCF_3$ moiety, even though the $SeCF_3$ has been shown to have similar properties (Hammet constant, Taft parameters and nucleophilicity) as the SCF_3 group.[358,359] All of the procedures reported to date make use of unstable, toxic reagents, or stoichiometric amounts of metal compounds. One of the first reported procedures for the introduction of $SeCF_3$ to organic molecules dates from 1985 and was described by Ruppert.[360] PhSeCF$_3$ **336** was prepared by reaction of the unstable PhSeCl **334** with salt **335** (*Scheme 127*). In the same year Yagupolskii *et al.* reported the formation of $ArSeCF_3$ from the reaction of aryl iodides with $CuSeCF_3$.[361] A few years later, in 1990, Umemoto and Ishihara described the synthesis of $ArSeCF_3$ **338** by reduction of 2-selenocyanatobiphenyl **337** with $NaBH_4$, followed by reaction with CF_3I,[362] as illustrated in *Scheme 127*.
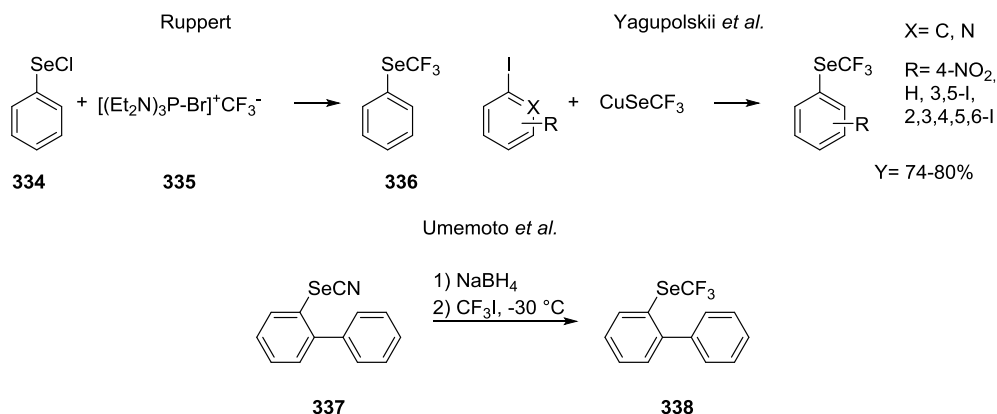
Scheme 127: Synthesis of PhSeCF$_3$ **336** reported by Ruppert (top left),[360] synthesis of ArSeCF$_3$ reported by Yagupolskii *et al.* (top right),[361] and synthesis of ArSeCF$_3$ **338** reported by Umemoto *et al.* (bottom).[362]

These first procedures suffered from very limited reaction scope. New methodologies were reported by Langlois *et al.* at the end of the 1990s.[363] In 1996, they reported the use of diselenites in combination with TMSCF$_3$ as the CF$_3$ source and TBAF as a F$^-$ source for the formation of PhSeCF$_3$ **336**. However, in this case the reaction scope was still very limited. One year later, the same group reported a different methodology for the preparation of ArSeCF$_3$ compounds using cyano-compounds as precursors together with

TMSCF$_3$ and TBAF.[364] However, this still did not provide a great improvement in the reaction scope.
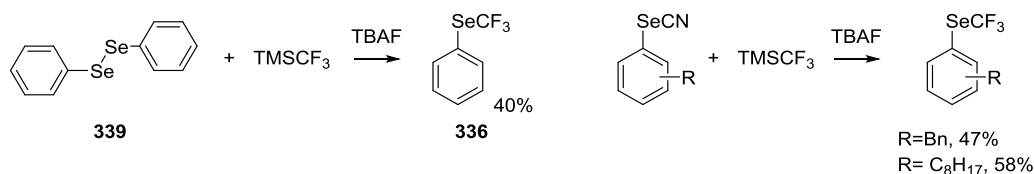
Scheme 128: Synthesis of PhSeCF$_3$ **336** from diselenite reported by Langlois *et al.* in 1996 (left),[363] synthesis of ArSeCF$_3$ reported by Langlois *et al.* in 1997 (right).[364]

In 2004, Dolbier *et al.* reported the synthesis of PhSeCF$_3$ **336** from diphenyl diselenite **339** and TDAE/CF$_3$I.[356] However, the main contribution to the increase in the reaction scope was provided by Weng *et al.* In 2014, they reported the use of the dimeric [Cu(bpy)SeCF$_3$]$_2$ **340** for the introduction of SeCF$_3$ onto aromatic moieties using aryl bromides and iodides as coupling partners.[365] The reaction is tolerant to a wide-range of functional groups, but it requires stoichiometric amounts of the Cu dimer **340**. A few months later, an improved methodology was reported by the same group, where Cu dimer **340** is formed *in situ* from CuI and phenanthroline and is used in a catalytic amount. The reaction also requires stoichiometric amounts of Ag$_2$CO$_3$ to proceed, (*Scheme 129*).[366]
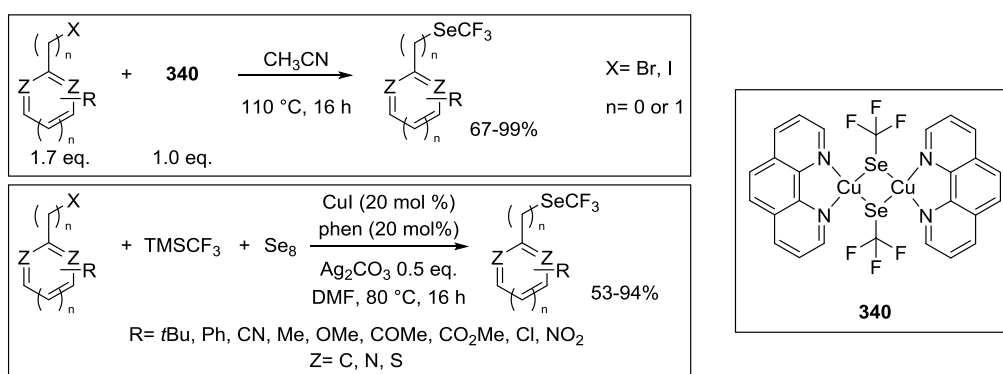
Scheme 129: synthesis of ArSeCF$_3$ reported by Weng *et al.* with stoichiometric amounts of [Cu(bpy)SeCF$_3$]$_2$ **340** (top left),[365] synthesis of ArSeCF$_3$ reported by Weng *et al.* with catalytic amounts of [Cu(bpy)SeCF$_3$]$_2$ **340** (bottom left),[366] [Cu(bpy)SeCF$_3$]$_2$ **340** (right).

4.2 Synthesis of Pd(I) dimers with SeR bridges

In the previous chapters, we have demonstrated that Pd(I)-bromo dimer **31** and Pd(I)-iodo dimer **193** can be readily formed from Pd(PtBu$_3$)$_2$ **268** by reaction with salts with an appropriate oxidation potential and with counterions able to stabilise the dimeric bridged-structure (such as Br or I). In turn, these dimers can be converted back to Pd(0) complex **268** by reaction with nucleophiles with an appropriate N value. This chapter, instead is devoted to exploring the potential of reacting directly at the dimer and to exploring the potential of dinuclear Pd(I) catalysis.

In chapter 3, we demonstrated how Pd(I)-bromo dimer **31** and Pd(I)-iodo dimer **193** can react with charged nucleophiles to form a new Pd(I) bridged dimer. Depending on the ability of the nucleophile to stabilise a bridging structure, the dimer can subsequently be isolated as a dimer, or it may fragment into Pd(0) and Pd(II) as illustrated in *Scheme 130*.
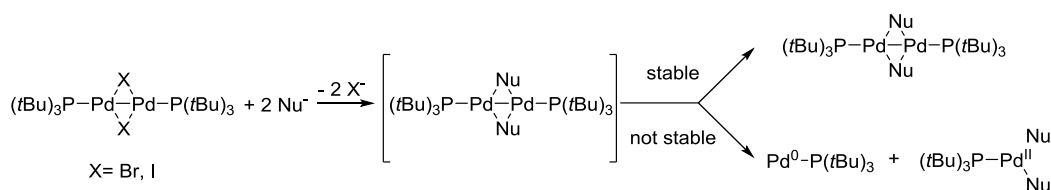
Scheme 130: Reaction of Pd(I)-bromo dimer **31** and Pd(I)-iodo dimer **193** with nucleophiles.

For most of the nucleophiles previously explored the disproportionation reaction occurred due the high instability of the Pd-(I) dimers derived. We considered the possibility of using Se-based nucleophile, which were not explored before, both for the formation of novel SeR Pd(I) dimers and possibly for the development of a novel, convenient way to prepare ArSeR compounds.

4.2.1 Synthesis of Pd(I) dimers with SePh bridges

The first nucleophile investigated was the benzeneselenol **341**. The Se-H bond of PhSeH **341** is very acidic (pK_a=5.9)[367] and this allows its deprotonation with bases such as $^-$OH or NaH to generate the corresponding phenyl selenolate ion **342**. However, PhSeH **341** is

sensitive to oxygen and readily forms diphenyl selenide **339** in its presence. The formation of diphenyl selenides is even faster in the presence of phenyl selenolate ion **342** and this made the formation and use of phenyl selenolate **342** under oxygen free conditions necessary, (*Scheme 131*).
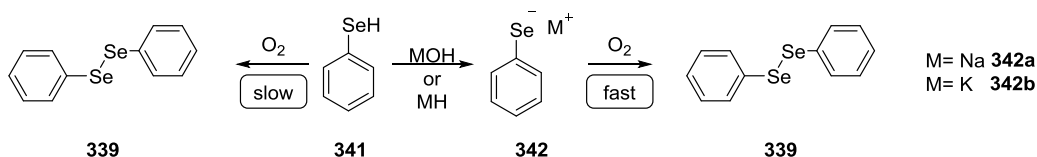
Scheme 131: Formation of phenyl selenolate ion **342** from phenyl selenol **341**, and their reactivity towards oxygen.[367]

We wanted to combine this with our Pd(I)-dimer chemistry in an effort to form the corresponding Pd(I)-dimer. A Pd-(I) dimer bearing a single SePh bridging ligand **145** has previously been reported by Kurosawa *et al.* and was obtained by oxidative addition of allyl phenyl selenide **343** to Pd$_2$(dba)$_3$, followed by reaction with PPh$_3$.[151,156] However, this dimer did not find any application in catalysis.
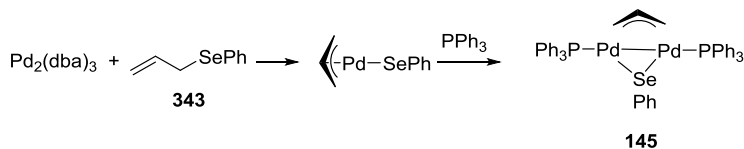
Scheme 13: Synthesis of Pd(I) dimer **145** reported by Kurosawa *et al.*[156]

The synthesis of a Pd-(I) dimer bearing two bridging SePh groups has not been reported. Pd(I)-iodo dimer **193** was exposed to an excess of PhSeH **341** in the presence of KOH as base. The choice of using KOH was for practical reasons: it does not fragment dimer **193** and the observation of any change in solution should therefore only be due to the reaction between the dimer and the selenolate **342**. The solution turned orange after a few minutes and an orange precipitate was formed. Unfortunately, the ^{31}P-NMR spectroscopic analysis of the reaction mixture did not show the presence of any phosphine, indicating that the phenyl selenolate **342b** may be too strong a nucleophile. Moreover the precipitate formed is not soluble in organic solvents.
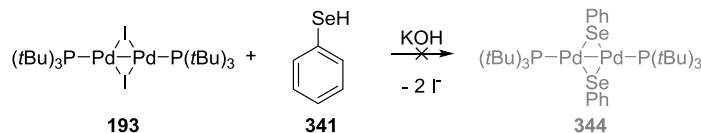
Scheme 132: Attempted synthesis of Pd(I) dimer **344** from Pd(I)-iodo dimer **193** and phenyl selenide **341**.

Despite these results we decided to test the Pd(I)-iodo dimer **193** for the SePh functionalisation of aryl iodides. We first tried to run the reaction in the presence of 1 equivalent of PhSeH **341**, 1 equivalent of KOH to deprotonate the PhSeH **341** and 5 mol % of Pd(I)-iodo dimer **193**. The reaction turned dark orange within 1 hour, meaning that the Pd(I)-iodo dimer **193** was no longer present in the reaction mixture. GC-MS chromatographic analysis of the reaction mixture after 1 hour did not show any trace of the product, only starting material and PhSePh generated in the GC-MS machine due to the very high temperatures. We left the reaction under stir for an additional 23 hours, but also in this case no product was detected.
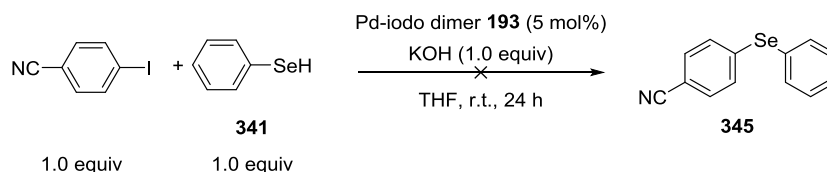
Scheme 132: Attempted coupling of aryl iodides and phenyl selenolate **341**, catalysed by Pd-iodo dimer **193**.

As already observed in the stoichiometric reaction, phenyl selenolate **342b** is a strong nucleophile and it leads to the complete decomposition of the Pd(I)-iodo **193** dimer within 1 hour. We decided to add the nucleophile to the reaction mixure dropwise in order to keep its concentration low. Addition to the THF solution containing the aryl iodide, KOH and 5 mol% of Pd(I)-iodo dimer **193** was carried out over 10 hours and the reaction mixture was left to stir at ambient temperature for an additional 14 hours. In this case the coupling was also unsuccessful and only traces of the product **345** could be detected in the GC-MS chromatographic analysis of the reaction mixture after 24 hours. A final attempt involved adding the pre-formed phenyl selenolate **342b** dropwise to the THF solution containing the aryl iodide and the Pd(I)-iodo dimer **193**. The phenyl selenolate was prepared by addition

of phenyl selenol **341** to a THF solution containing an excess of NaH. The addition of the phenyl selenolate **342b** was carried out over 10 hours and the solution was left to stir for an additional 14 hours. As in the previous case, the GC-MS analysis only showed traces of the product. We decided to not further explore this functionalisation, especially because the ^{31}P-NMR spectroscopic studies were shown to not be promising.

4.2.1 Synthesis of the first Pd(I) dimers with SeCF$_3$ bridges

The use of selenolates as nucleophile was shown to be unsuccessful, both for the synthesis of new Pd(I) dimer and also for the SePh functionalisation of aryl halides. The reason may be due to the strong nucleophilicity of the ⁻SePh anion **342**. As the ⁻SeCF$_3$ group is a weaker nucleophile compared to ⁻SePh **342**, due to the presence of three electron-withdrawing fluorine atoms, we considered that this nucleophile could be amenable for the formation of a new SeCF$_3$ containing dimer, even possibly for further SeCF$_3$ functionalisation of organic molecules. We chose the (CH$_3$)$_4$NSeCF$_3$ salt **346**[357] as the ⁻SeCF$_3$ source, as this salt was previously used by Tyrra and Naumann for the successful synthesis of L$_2$Pt(II)SeCF$_3$ complexes.[368]

Pd(I)-iodo dimer **193** was added to a toluene solution containing 2 equivalents of (CH$_3$)$_4$NSeCF$_3$ salt **346**, previously prepared according to a modified procedure reported by Tyrra *et al.*[357] and the reaction was monitored by ^{31}P and ^{19}F-NMR spectroscopy over time, (*Scheme 133*).
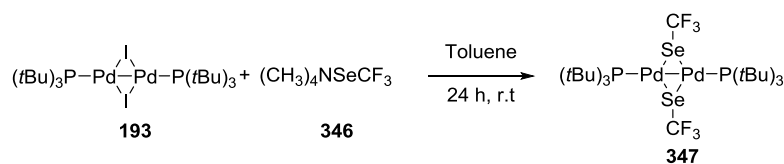
Scheme 133: Synthesis of Pd(I) dimer **347** from Pd(I)-iodo dimer **193** and (CH$_3$)$_4$NSeCF$_3$ salt **346**.

After the first 30 minutes a new species could be detected in both the ^{31}P (δ_P=101.4 ppm) and ^{19}F NMR (δ_F=−26.2 ppm) spectra. After 2 hours the Pd(I)-iodo-dimer **193** (δ_p=102.3 ppm) was fully consumed and a species was formed in the ^{31}P-NMR spectrum (δ_P= 101.4 ppm) and a single species in the ^{19}F-NMR spectrum (δ_F=−26.2 ppm). After 5 hours the concentration of the species at 101.4 ppm in the ^{31}P-NMR spectrum had increased its

concentration, whilst a new, small peak had formed in the ^{19}F-NMR spectrum at −24.5 ppm. After 24 hours the ^{31}P and ^{19}F-NMR spectroscopic analysis of the reaction mixture revealed the formation of one single species for both nuclei (δ_P= 99.1 ppm; δ_F= −24.5 ppm), (*Figure 65*).
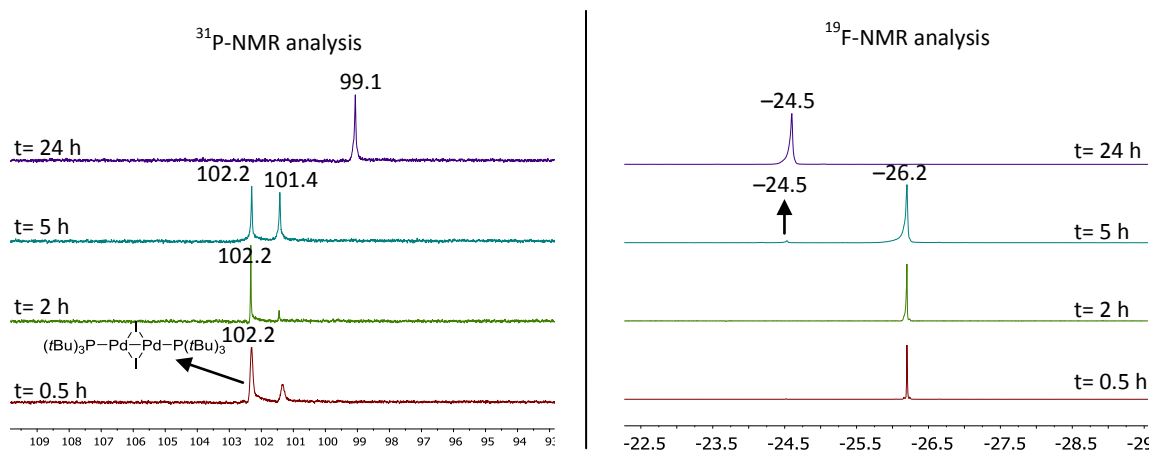
Figure 65: ^{31}P-NMR spectroscopic analysis of the reaction of Pd(I)-iodo dimer **193** (102.3 ppm) and (CH$_3$)$_4$NSeCF$_3$ salt **346** after: 0.5 hours (red); 2 hours (green); 5 hours (light blue) and 24 hours (purple) (left). ^{19}F-NMR spectroscopic analysis of the reaction of Pd(I)-iodo dimer **193** and (CH$_3$)$_4$NSeCF$_3$ salt **346** after: 0.5 hours (red); 2 hours (green); 5 hours (light blue) and 24 hours (purple) (right); (Chemical shifts in ppm referenced to trimethoxyphosphine oxide for ^{31}P and 4,4'-difluorobiphenyl for ^{19}F as internal standards).

The solution containing the new species was filtered to remove precipitates and unreacted (CH$_3$)$_4$NSeCF$_3$ salt **346**. The solvent was then removed and the dark brown solid obtained recrystallised, which gave suitable crystal for X-ray analysis, (*Figure 66*).
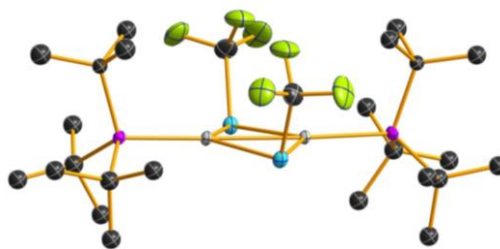
Figure 66: Crystal structure of the Pd(I)-SeCF$_3$ dimer **347**.

The X-ray crystallographic analysis confirmed the formation of a Pd(I) dimeric structure with a Pd-Pd bond length of 2.6073(3) Å, which is slightly shorter than the one of the Pd(I)-iodo precursor **193**[170] but is consistent with being Pd(I)-Pd(I) bond.[65] The angle Pd-Se-Pd of 57.907° is small compared to the one reported for the Pd(I)-iodo dimer **193** of

62.4°.[170] The two SeCF$_3$ groups adopt a *syn* conformation as can be observed in *Figure 66*. The formation of this new dimer is likely slow due to the low solubility of the (CH$_3$)$_4$NSeCF$_3$ salt **346** in toluene, so the ⁻SeCF$_3$ is only released to react with the Pd(I)-iodo dimer **193**.

To investigate the nature of the intermediate species formed during the course of the reaction a control experiment was carried out: Pd(I)-iodo dimer **193** was added to a toluene solution containing the Pd(I)-SeCF$_3$ dimer **347**. The reaction was left to stir for 2 hours and was then analysed through ^{31}P and ^{19}F-NMR spectroscopy, (*Figure 67*).
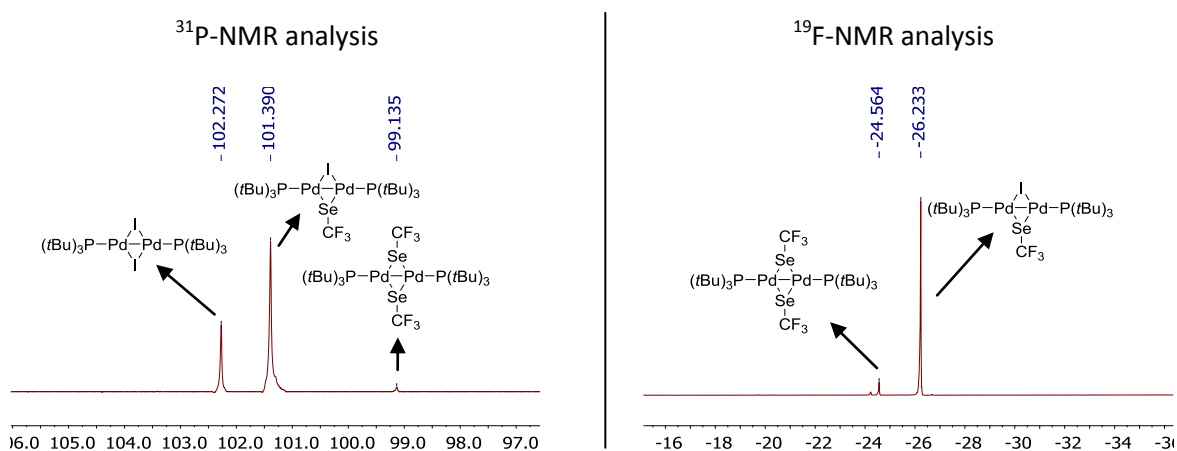
Figure 67: ^{31}P-NMR spectroscopic analysis of the reaction of Pd(I)-iodo dimer **193** and Pd(I)-SeCF$_3$ dimer **347** after 2 hours (left). ^{19}F-NMR spectroscopic analysis of the reaction of Pd(I)-iodo dimer **193** and Pd(I)-SeCF$_3$ dimer **347** after 2 hours (right); (Chemical shifts in ppm referenced to trimethoxyphosphine oxide for ^{31}P and 4,4'-difluorobiphenyl for ^{19}F as internal standards).

The outcome of the experiment suggested that one of the intermediate species observed in the ^{31}P-NMR spectra belonged to the mixed Pd(I)-I-Se dimer **348**, (*Scheme 134*).
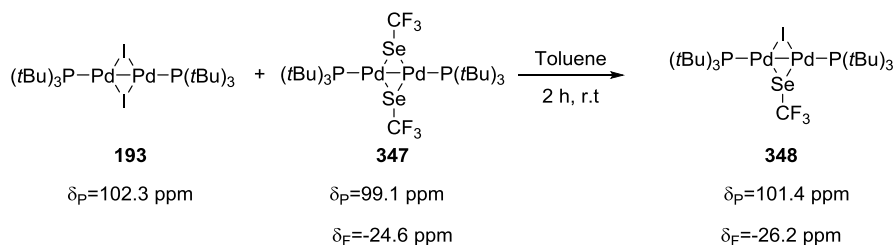
Scheme 134: Reaction between Pd(I)-iodo dimer **193** and Pd(I)-SeCF$_3$ dimer **347**.

4.3 Development of dinuclear Pd(I)-catalysed SeCF$_3$-functionalisation of aryl halides

4.3.1 Use of Pd(I)-iodo dimer 193 as precatalyst in the SeCF$_3$ functionalisation of aryl halides

A large number of Pd(I) dimers have been reported in the literature (see Chapter 1), but for most of them they did not find a suitable use in catalysis. In the previous section we reported the synthesis and characterisation of a novel Pd(I) dimer bearing SeCF$_3$ bridging ligands. In this section we will now explore its application in catalysis, in particular for the SeCF$_3$ functionalisation of aromatic compounds. Aryl iodides have been shown to be excellent coupling partners for the SeCF$_3$[365,366] and also more general SeR[369] functionalisation of aromatic compounds. We decided to test the new Pd(I)-SeCF$_3$ dimer **347**, to be generated *in situ* from Pd(I)-iodo dimer **193** and the (CH$_3$)$_4$NSeCF$_3$ salt **346**, for the SeCF$_3$ functionalisation of aryl iodides. The first experiments were performed using stoichiometric amounts of catalyst with aryl iodides bearing both electron-withdrawing (1-iodo-4-nitrobenzene) and electron-donating (1-iodo-4methylbenzene) groups. Toluene was chosen as solvent because both Pd(I)-iodo dimer **193** and the *in situ* formed Pd(I)-SeCF$_3$ dimer **347** are soluble in this reaction medium, (*Scheme 135*) .
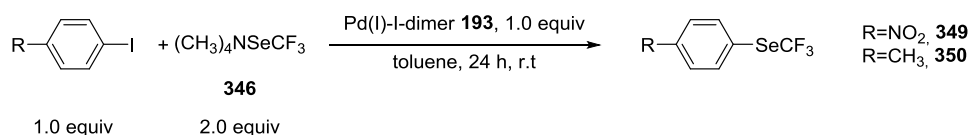
Scheme 135: SeCF$_3$ functionalisation of aryl iodides using stoichiometric amounts of Pd(I)-iodo dimer **193**.

The GC-MS analysis of the two reaction mixtures showed full consumption of the starting material, and the desired product was the only species present in solution for both aryl iodides.

The promising results obtained with the stoichiometric reactions led as to also explore the catalytic transformation. We used 4-iodobiphenyl to test the effect of solvents, catalyst loading and amount of (CH$_3$)$_4$NSeCF$_3$ salt **346**. The results are summarised in *Table 37*.

Table 37: Screening of the reaction conditions for the SeCF$_3$ functionalisation of 4-iodobiphenyl.
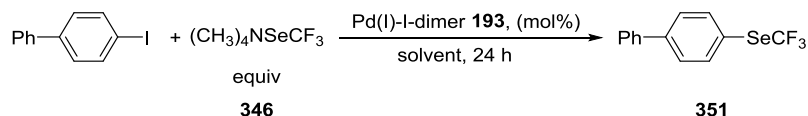
Entry	Pd(I)-iodo dimer 193 loading (%)	(CH$_3$)$_4$NSeCF$_3$ 346 (equiv)	Temperature (°C)	Solvent	351 Yield (%)[a]
1	1.0	1.5	r.t	Toluene	15
2	1.0	1.5	r.t	THF	5
3	1.0	1.5	40	Toluene	55
4	1.0	1.5	40	THF	10
5	1.0	1.5	40	DMSO	Traces
6	1.0	1.5	40	DMF	Traces
7	1.0	1.5	40	CH$_3$CN	Traces
8	1.0	1.5	60	Toluene	20
9	5.0	1.5	40	Toluene	80
10	5.0	2.0	40	Toluene	99

a) Yields reported according to the ratio between product and starting material in the GC-MS chromatogram. The two compounds were the only species present in it.

The reactions performed at ambient temperature did not give good conversions, with only 5% of product formation being observed in the case of THF as solvent (see Entry 2), with a slightly better conversion in the presence of toluene as solvent (see Entry 1). A further screening of the solvents was carried out at higher temperature (40 °C), in which case the highest product formation was also observed in the presence of toluene as solvent (compare Entries 3-7). Further increase of the temperature caused a decrease in the conversion, whilst increase of both the Pd(I)-iodo dimer **193** loading and also the number of the equivalents of (CH$_3$)$_4$NSeCF$_3$ salt **346** used allowed full convertion of 4-iodobiphenyl to the SeCF$_3$ product **351**, (see Entry 10)**.**

After having found the optimal conditions for the coupling we proceeded with screening substrates for the functionalisation to investigate the scope. Aryl iodides, bromides and chlorides with both electron-withdrawing and electron-donating groups were tested under the optimised conditions.

Table 38: Screening of aryl halides for the SeCF$_3$ functionalisation.
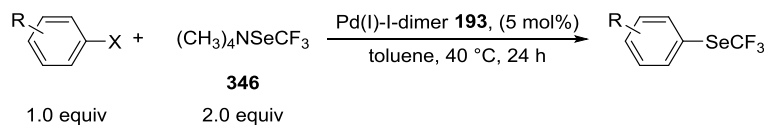
Entry	X	R	GC-MS yields (%)[a]
1	I	4-CN	30
2	I	4-NO$_2$	20
3	I	4-CH$_3$	99
4	I	4-OCH$_3$	99
5	I	4-Ph	99
6	Br	4-CN	12
7	Br	4-CH$_3$	40
8	Cl	4-CN	0

a) Yields reported according to the ratio between product and starting material in the GC-MS chromatogram. The two compounds were the only species present in it.

Interestingly, the reaction with electron-withdrawing groups as substituent on the aryl iodide did not give very high conversions, whilst in the reaction with electron-donating substituents the starting materials are fully converted into the SeCF$_3$ products (compare Entries 1-2 *vs* Entries 3-5). This was unexpected because usually aryl halides with electron-withdrawing groups are better substrates for cross-coupling reactions due to the ease at which they undergo oxidative addition compared to aryl halides with electron-donating groups. The same phenomenon can be observed when aryl bromides are used as coupling partners, where lower conversions are obtained in the presence of electron-withdrawing groups (compare Entries 6 *vs* 7). However, the conversions observed using aryl bromides are also considerably low compared to those obtained employing the iodide analogues (compare Entries 1 *vs* 6, 3 *vs* 7). Aryl chlorides are not reactive under the applied reaction conditions (Entry 8).

We decided to further investigate the phenomenon related to the poor conversions obtained when using aryl halides with electron-withdrawing substituents, using 1-iodo-4-nitrobenzene as the test substrate.

Table 39: Screening of the reaction conditions for the SeCF$_3$ functionalisation of 1-iodo-4-nitrobenzene. The yields reported refer to GC-MS yields.

$$O_2N-\langle\text{benzene}\rangle-I \quad + \quad (CH_3)_4NSeCF_3 \xrightarrow[\text{toluene, 24 h}]{\text{Pd(I)-dimer (5 mol\%)}} O_2N-\langle\text{benzene}\rangle-SeCF_3$$

| | 1.0 equiv | | 2.0 equiv **346** | | | **349** |
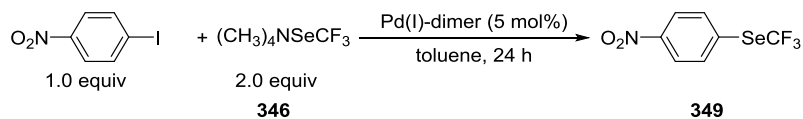
Entry	Catalyst	Temperature (°C)	Impurity in the ^{19}F-NMR spectrum of **346** (%)	Color of **346**	**349** Yield (%)
1	Pd(I)-I dimer **193**	60	2	Light green	25
2	Pd(I)-I dimer **193**	r.t	2	Light green	2
3	Pd(I)-I dimer **193**	80	2	Light green	15
4	Pd(I)-I dimer **193**	40	2	Light green	12
5	Pd(I)-I dimer **193**	60	20	green	7
6	Pd(I)-Br dimer **31**	60	2	Light green	8
7	Pd(I)-I dimer **193**	50	2	Light green	10
8	Pd(I)-I dimer **193**	75	2	Light green	12
9	Pd(I)-Br dimer **31**	50	2	Light green	8
10	Pd(I)-Br dimer **31**	75	2	Light green	9
11	Pd(I)-I dimer **193**	60	Not detectable	Off-white	75

a) Yields reported according to the ratio between product and starting material in the GC-MS chromatogram. The two compounds were the only species present in it.

The screening of the optimal conditions for the coupling of aryl iodides bearing electron-withdrawing groups revealed that slightly higher conversions can be achieved by increasing the temperature from 40 °C to 60 °C. The use of the Pd(I)-bromo dimer **31** as precatalyst slightly decrease the yields of reaction (compare Entries 1 *vs* 6). However, the main parameter responsible for a successful coupling appears to be the purity of the (CH$_3$)$_4$NSeCF$_3$ salt **346**. In the synthesis of the (CH$_3$)$_4$NSeCF$_3$ salt **346** the TMSCF$_3$ decomposed over time, generating an intense green side-product which was very difficult to remove without considerably lowering the yield of the salt. We performed two control experiments to eliminate the possibility of this impurity of being responsible for the catalysis observed. The reaction of 4-iodobiphenyl and (CH$_3$)$_4$NSeCF$_3$ salt **346** was performed *(i)* in the absence of Pd(I)-iodo dimer **193** and *(ii)* in the presence of Pd(I)-iodo dimer **193** and an excess of the impurity (in this case the colour of the (CH$_3$)$_4$NSeCF$_3$ salt **346** was dark green). In the first case no product formation was observed, whilst in the second case the yield was considerably lower compared to the reaction where only traces of the impurity were present (25% *vs* 99). In addition, it should be noted that in the coupling of the (CH$_3$)$_4$NSeCF$_3$ salt **346** with aryl iodides bearing electron-donating groups,

the presence of traces of this impurity (light green colouration of the $(CH_3)_4NSeCF_3$ salt **346**) did not influence the outcome of the reaction.

After this finding we decided to perform the coupling using pure $(CH_3)_4NSeCF_3$ salt **346** and to use a higher temperature (60 °C) for the coupling of aryl iodides bearing electron-withdrawing groups. The results are summarised in the tables below.

Table 40: SeCF_3 functionalisation of aryl halides bearing electron-donating groups, catalysed by Pd(I)-iodo dimer **193**.
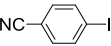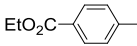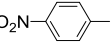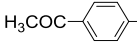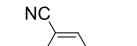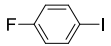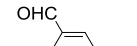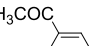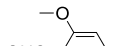
Entry	Aryl halide	GC-MS yields (%)[b]	isolated yield (%)	Entry	Aryl halide	GC-MS yields (%)[b]	isolated yield (%)
1	Ph—◯—I	99	96	6	◻N—◯—I	99	83
2	—◯—I	99	84	7	O◻N—◯—I	99	80
3	O—◯—I	99	96	8	◯—I	60	-
4	tBu—◯—I	99	80	9	nBu—◯—I	95	75(97)[a]
5	Ph◯—I	99	99	10	O—◯—I	99	59(90)[a]

a) The numbers in parenthesis refer to ^{19}F-NMR yields using as an internal standard 4,4'-difluorobiphenyl. b) Yields reported according to the ratio between product and starting material in the GC-MS chromatogram. The two compounds were the only species present in it.

The reaction gives the product in good to excellent yields, even when the substitution is in the ortho position (see Entries 5 and 10). The purification is often difficult, as in most of the cases the product has the same R_f value as the catalyst, even in very apolar solvents such as pentane. For some substrates more than one column was required to obtaine a pure product. In addition, some of the compounds are volatile, especially those with CH_3 and OCH_3 substituents, and the complete removal of the solvents also resulted in loss of product (see Entries 2, 3 and 10). Despite that, the isolated yields are still frequently over 90% and the reaction uses mild conditions.

Table 41: SeCF₃ functionalisation of aryl halides bearing electron-withdrawing groups, catalysed by Pd(I)-iodo dimer **193**.

Entry	Aryl halide	GC-MS yields (%)[a]	isolated yield (%)	Entry	Aryl halide	GC-MS yields (%)[a]	isolated yield (%)
1	NC–C₆H₄–I	99	96	6	EtO₂C–C₆H₄–I	55	-
2	O₂N–C₆H₄–I	99	84	7	H₃COC–C₆H₄–I	50	-
3	I–C₆H₄–I	40	-	8	NC-meta-C₆H₄–I	99	90
4	F–C₆H₄–I	0	-	9	OHC-meta-C₆H₄–I	80	49
5	H₃COC-meta-C₆H₄–I	75	48	10	(–O, OHC)–C₆H₃–I	30	-
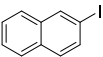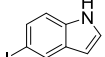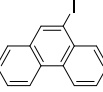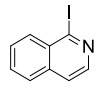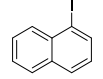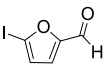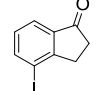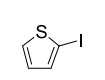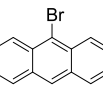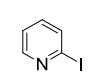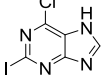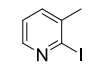
a) Yields reported according to the ratio between product and starting material in the GC-MS chromatogram. The two compounds were the only species present in it.

The coupling of aryl iodides bearing electro-withdrawing groups gave excellent results with CN and NO₂ as substituents (see Entries 1, 2 and 8). Good yields were also achieved for aryl iodides bearing esters, ketones and aldehydes. For these substrates, substitution in the *meta*-position generally gave better conversions than substitution in the *para*-position. The low isolated yields reported for the *meta*-substituted ketone and aldehyde are due to problems with the purification, where the starting material and product have similar R_f values (see Entries 5 and 9). In the case of the *para*-substituted ester, ketone and aldehyde (see Entries 6, 7 and 10) the products could not be obtained completely pure, and traces of starting material could be detected in the ¹H-NMR spectra even after several consecutive columns. Recrystallisation was also attempted, but in this case the starting material could also not be completely removed. In the case of 1-iodo-4-iodobenzene (see Entry 3) the product obtained was predominantly the disubstituted one. We therefore also performed an experiment using 8 equivalents of (CH₃)₄NSeCF₃ salt **346** in the hope of increasing the amount of disubstituted product. Instead of having a beneficial effect on the coupling, the increase of the number of equivalents instead resulted in a decrease in the yield from 40% to less than 10%. Purification of the product could not be achieved neither by chromatography on silica gel, nor by recrystallisation.

We then further expanded the scope of the reaction to include polyaromatic, heteroaromatic and other polycyclic compounds. The results are summarised in *Table 42*.

Table 42: SeCF$_3$ functionalisation of polyaromatic, heteroaromatic and polycyclic aryl halides, catalysed by Pd(I)-iodo dimer **193**.
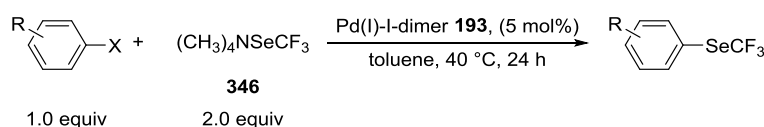
Entry	Aryl halide	GC-MS yields (%)[b]	isolated yield (%)	Entry	Aryl halide	GC-MS yields (%[b])	isolated yield (%)
1		99	68(85)[a]	7		99	94
2		99	85	8		0	-
3		99	55(99)[a]	9		0	-
4		99	93	10		0	-
5		95	84	11		0	-
6		0	-	12		0	-

a) The numbers in parenthesis refer to ^{19}F-NMR yields using as an internal standard 4,4'-difluorobiphenyl. b) Yields reported according to the ratio between product and starting material in the GC-MS chromatogram. The two compounds were the only species present in it.

The SeCF$_3$ functionalisation of polyaromatic compounds was achieved with good yields (see Entries 1-3), whilst no product formation was obtained when furanyl, thiophenyl and pyridinyl aryl halides were used as coupling partners (see Entries 8-12). Excellent yields were obtained in the presence of a cyclic ketone and indole (see Entries 4 and 7). We were pleased to obtain excellent results with 9-bromoanthracene (see Entry 5) because it represents the only successful example of coupling with an aryl bromide. To verify that the coupling is not due to a radical process, facilitated by the ease of homolytic cleavage of the C-Br bond, the reaction was repeated once in the absence of Pd(I)-iodo dimer **193** and once in the absence of light. In the first experiment no product was formed, excluding a radical

reaction initiated by the SeCF$_3$ salt **346**, whilst almost full conversion was reached in the second experiment, excluding the possibility of a radical reaction promoted by light.

The SeCF$_3$ functionalisation was shown to be tolerant to a large range of functional groups without the formation of any side product. The success obtain in the coupling of indoles led us to further explore the coupling of aryl iodides containing N-based substituents.

Table 43: SeCF$_3$ functionalisation of iodo-anilines catalysed by Pd(I)-iodo dimer **193**.
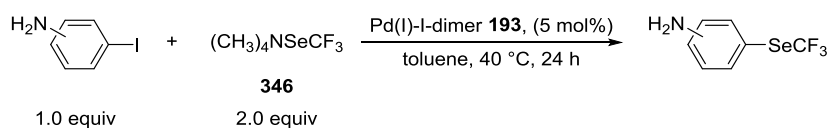
Entry	Aryl halide	Isolated yield (%)
1		73
2		77
3		81
4		62

To our surprise, the coupling with iodoanilines was very successful, with the products being obtained in good yield even in the case of *ortho*-substituted iodoaniline (see Entry 4). However, in these couplings the formation of small amounts of side-products was observed. Their nature is still unknown.

4.3.2 Use of other Pd-based precatalysts for the SeCF$_3$ functionalisation of aryl iodides

In the previous section we have shown that the use Pd(I)-iodo dimer **193** as precatalyst in combination with the (CH$_3$)$_4$NSeCF$_3$ salt **346** to generate the Pd(I)-SeCF$_3$ dimer **347** *in situ*, allowed the SeCF$_3$ functionalisation of aryl halides bearing a large number of substituents. As part of research into the SeCF$_3$ functionalisation, we also explored the effect of three commonly used Pd(0) complexes: Pd(PtBu$_3$)$_2$ **268**, Pd(PCy$_3$)$_2$ **270**, and

Pd(PPh$_3$)$_4$ **296**. We did not consider Pd(I)-bromo dimer **31** because, as shown in *Table 39* lower conversions were achieved when Pd(I)-bromo dimer **31** was used instead of its iodide analogue **193**. 1-Iodo-4cyanobenzene was used as test substrate and the results are summarised in *Table 44*.

Table 44: SeCF$_3$ functionalisation of 1-iodo-4cyanobenzene catalysed by different Pd(0) complexes.
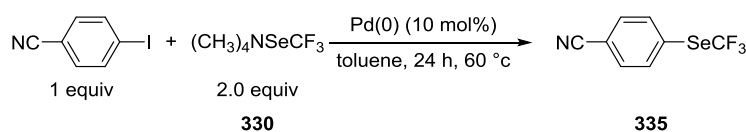
Entry	Catalyst	GC-MS yield (%)
1	Pd(I)-I-dimer **193**	99
2	Pd(P*t*Bu$_3$)$_2$ **268**	99
3	Pd(PCy$_3$)$_2$ **270**	4
4	Pd(PPh$_3$)$_4$ **296**	40

a) Yields reported according to the ratio between product and starting material in the GC-MS chromatogram. The two compounds were the only species present in it.

The results obtained showed that full conversion can also be achieved in the presence of Pd(P*t*Bu$_3$)$_2$ **268** (see Entry 2). The formation of Pd(I)-iodo dimer **193** from reaction of Pd(P*t*Bu$_3$)$_2$ **268** with aryl iodides was already observed (see *Figure 63* chapter 3), so in this case it is not possible to deduce whether a Pd(0)/Pd(II) catalytic cycle or a Pd(I) dimeric cycle is operating. The use of Pd(PCy$_3$)$_2$ **270** gave poor product formation (see Entry 3), whilst Pd(PPh$_3$)$_4$ **296** gave 40 % of conversion. We did not explore the mechanism of this transformation further because the yield obtained was not high enough to consider this Pd(0) complex as a good alternative catalyst/precatalyst for this type of functionalisation. As we have already shown that purification is very difficult for this transformation because of the similar R$_f$ of starting material and product, the presence of such a high concentration of remaining starting material would result in a low amount of isolated pure product.

4.4 Mechanistic proposal

After having successfully developed the SeCF$_3$ funcionalisation of aryl iodides, we wanted to investigate the possible mechanism of this transformation. Two mechanistic proposals were explored:

The first proposed mechanism involves a direct dimer catalysis where oxidative addition and reductive elimination occur on a single Pd-atom without destroying the dimeric structure. A similar dinuclear catalysis was recently reported by our group.[347] It was shown, through a combined computational and experimental study, that for Pd(I)-bromo dimer **31** and Pd(I)-iodo dimer **193** there is not only the possibility to act as precatalysts, but also the possibility to react as catalysts. Halide exchange was observed when dimer **31** was mixed with a series of aryl iodides, with concomitant formation of dimer **193**, as illustrated in *Scheme 136*.
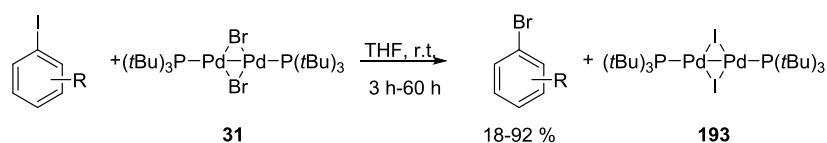
Scheme 136: Halogen exchange promoted by Pd(I) dimer **31**.[347]

The use of *n*-Bu$_4$NBr allowed the transformation to be catalytic in Pd. The salt is responsible for the exchange of one of the bridging iodides of dimer **193** to form the mixed bridged I-Br dimer **352**, responsible for the exchange with the aryl iodide, (*Scheme 137*).
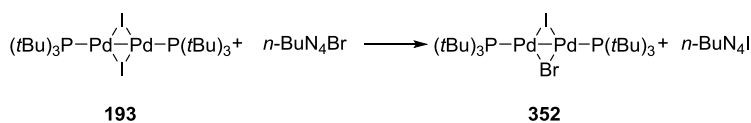
Scheme 137: Formation of the mixed Pd(I)-Br-I dimer **352** from dimer **193** and *n*-Bu$_4$NBr.[347]

Further kinetic studies employing one of the less reactive aryl iodides, 1-iodo-2-methoxynaphthalene, showed that the reaction is first order in both aryl iodide and Pd(I)-bromo dimer **31**, supporting the hypothesis of a direct involvement of the dimer in the catalytic cycle.[348] In addition the possibility to have assisted disproportionation of the Pd(I) dimer into Pd(0) and Pd(II), followed by oxidative addition of the aryl iodide onto the Pd(0), was excluded. In the presence of *n*-Bu$_4$NBr, it was found that the

preformed LPd(II)ArI complex only eliminates aryl bromides traces amounts. Computational studies helped to give an insight into the possible mechanism of the exchange. Two possible pathways for the exchange were studied using the CPCM (THF), M06L/6-311++G(d,p)//B3LYP/6–31G(d), and with SDD for Pd and I level of theory: *(i)* direct exchange on the dinuclear Pd(I) dimer; *(ii)* involvement of intermediate Pd(I) radicals, formed upon homolytic scission of the Pd-Pd bond. The transition state for the direct oxidative addition was located (see *Figure 68*) and pathway *(i)* resulted in being energetically-favoured in comparison to *(ii)*, $\Delta G^{\ddagger} = 14.8$ kcal/mol and 22.6 kcal/mol respectively. Moreover, the addition of a radical trap (cyclohexadiene or dihydroanthracene) to the reaction mixture did not change the outcome of the reaction, further indicating that the halide exchange does not involve a radical process.
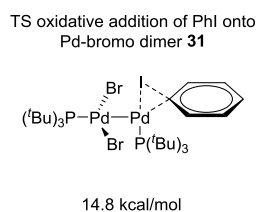
Figure 68: Located transition state for the direct oxidative addition of phenyl iodide onto Pd(I)-bromo dimer **31**, (The calculations were performed by Prof. Schoenebeck using CPCM (THF), M06L/6-311++G(d,p)//B3LYP/6–31G(d), and with SDD for Pd, I level of theory).[347]

In the case of our SeCF$_3$ reaction, the alternative mechanism would concern the disproportionation of the *in situ* formed Pd(I)-SeCF$_3$ dimer **347** into LPd(II)(SeCF$_3$)$_2$ and Pd(0)L, the latter of which undergoes oxidative addition with aryl iodides to form LPd(II)(Ar)(I) (**II**, *Scheme 138*). Subsequently, the iodide of complex **II** would be substituted by the SeCF$_3$ group present to form LPd(II)(Ar)(SeCF$_3$) (**III**, *Scheme 138*) that reductive eliminates the aryl-SeCF$_3$ product and regenerates the Pd(0) species, (*Scheme 138*.
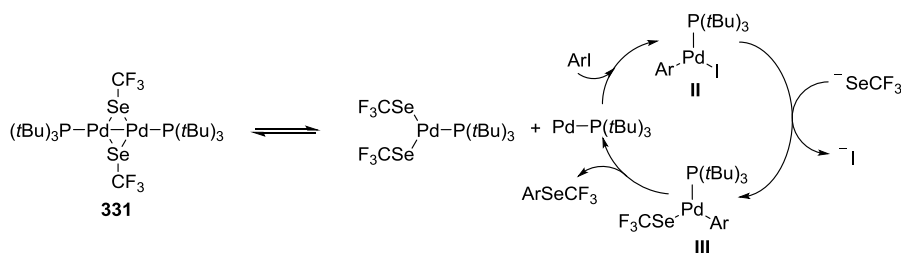
Scheme 138: One of the proposed mechanisms involving a Pd(0)/Pd(II) cycle.

The stoichiometric reaction of 1-iodo-4-nitrobenzene and $(CH_3)_4NSeCF_3$ salt **346** in the presence of Pd(I)-iodo dimer **193** as precatalyst (ratio 1:2:1 respectively) was monitored over time by ^{31}P-NMR and ^{19}F-NMR spectroscopy. The aim of the study was to identify some key intermediates that could allow us to rule out one of the two proposed mechanisms. In particular, we were looking for the presence of the two possible Pd(II) complexes **II** and **III** shown in *Scheme 138*, as their presence in the reaction mixture would eliminate a possible direct dimeric catalysis, (*Figure 69*).
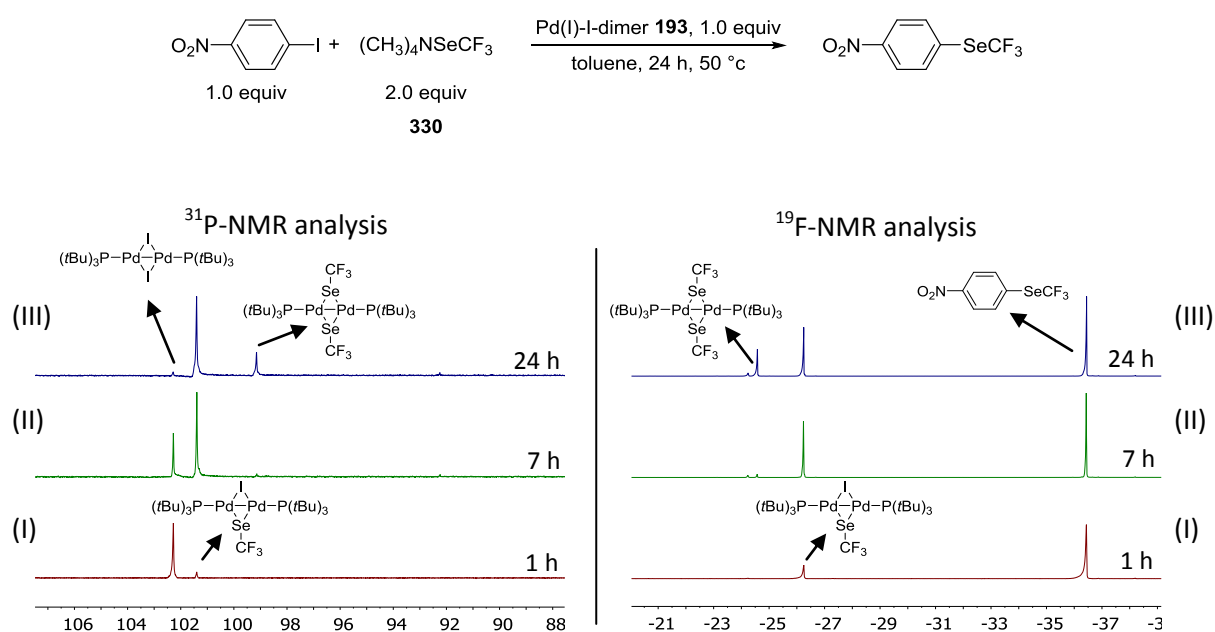
Figure 69: ^{31}P-NMR spectroscopic analysis of the reaction of Pd(I)-iodo dimer **193**, $(CH_3)_4NSeCF_3$ salt **346** and 1-iodo-4-nitrobenzene ratio (1:2:1) after 1 hour [(I), red], after 7 hours [(II), green] and after 24 hours [(III), blue] (left). ^{19}F-NMR spectroscopic analysis of the reaction of Pd(I)-iodo dimer **193**, $(CH_3)_4NSeCF_3$ salt **346** and 1-iodo-4-nitrobenzene (ratio 1:2:1) after 1 hour [(I), red], after 7 hours [(II), green] and after 24 hours [(III), blue] (right); (Chemical shifts in ppm referenced to trimethoxyphosphine oxide for ^{31}P and 4,4'-difluorobiphenyl for ^{19}F as internal standards).

The study in *Figure 69* did not show the formation of any additional intermediate in the course of the reaction. In the ^{31}P-NMR study, it is possible to observe Pd(I)-iodo dimer **193** disappearing over time to generate the mixed Pd(I)-I-SeCF_3 dimer **348**. After 24 hours the Pd(I)-iodo dimer **193** is fully converted into the mixed dimer **348** and in the Pd(I)-SeCF_3 dimer **347**. There is no evidence of other species that could be afforded to the two Pd(II) complexes **II** and **III**. The formation of the SeCF_3 dimer **347** is particularly slow, maybe due to the fact that the free I$^-$ present in solution can react either with the mixed dimer to reform the Pd(I)-iodo dimer **193**, or with the Pd(I)-SeCF_3 dimer **347** to regenerate the

mixed dimer **348**. Or alternatively, the aryl iodide react with the mixed Pd(I) dimer **348**, and the Pd(I) dimer **347** does not have the chance to form until all the aryl iodide is consumed. The only phosphine-containing compounds were represented by the three dimers. The ^{19}F-NMR study showed that together with the formation of the two dimers (mixed dimer **348** and Pd(I)-SeCF$_3$ dimer **347**), there is also the formation of the ArSeCF$_3$ product around −36 ppm. Also in this case there are no traces of other intermediates and the only fluorine-containing compounds were represented by the two Pd(I) dimers and by the product. These findings are in agreement with our proposed mechanism of direct dimer catalysis.

An additional spectroscopic experiment was performed in the presence of an aryl iodide bearing an electron-donating substituent (1-iodo-4-methylbenzene). As before the 1-iodo-4-nitrobenzene, the stoichiometric reaction of 1-iodo-4-methylbenzene and (CH$_3$)$_4$NSeCF$_3$ salt **346** in the presence of Pd(I)-iodo dimer **193** as precatalyst (ratio 1:2:1 respectively) was monitored by ^{31}P and ^{19}F-NMR spectroscopy over time, (*Figure 70*).
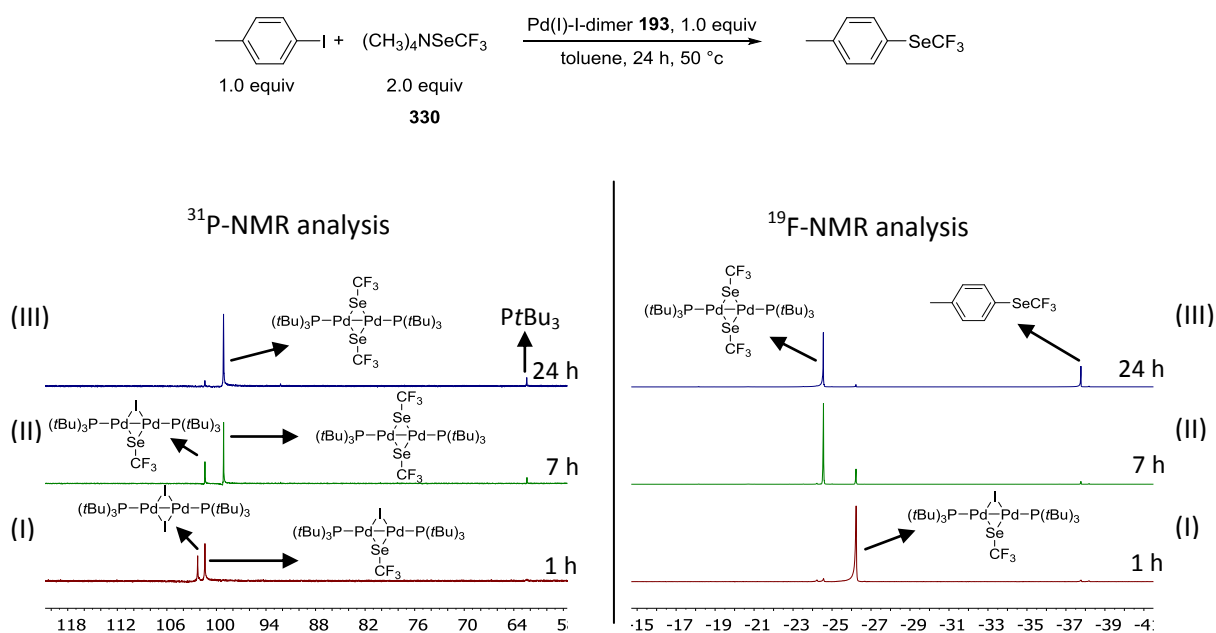
Figure 70: ^{31}P-NMR spectroscopic analysis of the reaction of Pd(I)-iodo dimer **193**, (CH$_3$)$_4$NSeCF$_3$ salt **346** and 1-iodo-4-methylbenzene ratio (1:2:1) after 1 hour [(I), red], after 7 hours [(II), green] and after 24 hours [(III), blue] (left). ^{19}F-NMR spectroscopic analysis of the reaction of Pd(I)-iodo dimer **193**, (CH$_3$)$_4$NSeCF$_3$ salt **346** and 1-iodo-4-methylbenzene ratio (1:2:1) after 1 hour [(I), red], after 7 hours [(II), green] and after 24 hours [(III), blue] (right); (Chemical shifts in ppm referenced to trimethoxyphosphine oxide for ^{31}P and 4,4'-difluorobiphenyl for ^{19}F as internal standards).

Also in this case the only species present in solution were represented by the three dimers and the product. The NMR spectra of the two nuclei did not show any trace of additional intermediates. The reaction profile appeared to be different from the one observed for 1-iodo-4-nitrobenzene. In this case product formation could only be observed after the formation of the Pd(I)-SeCF$_3$ dimer **347** and no product formation was detected after 7 hours when the major species in solution was represented by the mixed Pd(I)-I-SeCF$_3$ dimer **348**. Despite the slightly different profile, the result obtained from this study are also in agreement with direct dimer catalysis.

To support our mechanistic hypothesis of a direct involvement of the Pd(I)-SeCF$_3$ dimer **347** or the mixed Pd(I) dimer **348** in catalysis a computational study on the possible dimeric pathway was performed using DFT calculations using the CPCM (toluene) M06L/def2TZVP//B3LYP/6-31G(d) and LANL2DZ for Pd, I level of theory. The choice of using this method was dictated by the fact that in the case of halide exchange between Pd(I)-bromo dimer **31** and aryl iodides this method furnished results that were in very good agreement with the activation values obtained experimentally.[348]
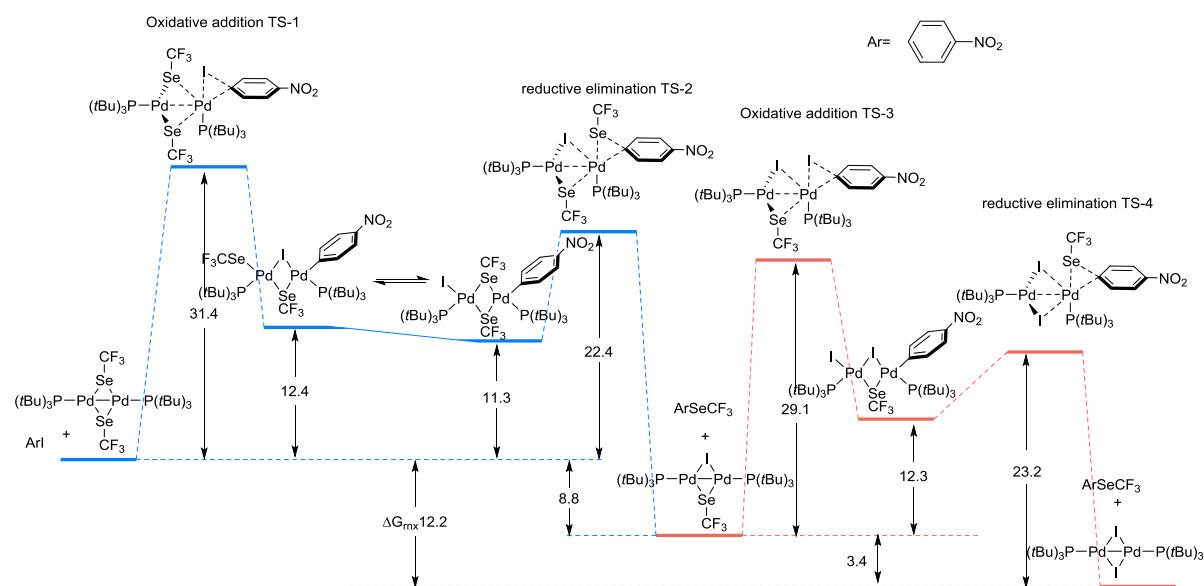
Figure 71: Calculated TSs for the oxidative addition of 1-iodo-4-nitrobenzene to Pd(I)-SeCF$_3$ dimer **347** and to the mixed Pd(I)-SeCF$_3$ dimer **348**.

In our study we considered both possible pathways, one concerning the Pd(I)-SeCF$_3$ dimer **347** and the other the mixed Pd(I)-I-SeCF$_3$ dimer **348**. In both cases TSs for the oxidative addition and also the reductive elimination were located, (*Figure 72*).

TS-1   TS-3

31.4 kcal/mol   29.1 kcal/mol
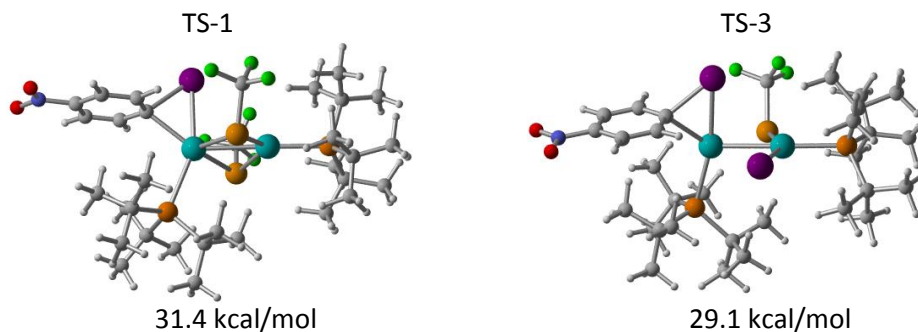
Figure 72: Located transition state for the direct oxidative addition of 1-iodo-4-nitrobenzene onto Pd(I)-SeCF$_3$ dimer **347** (left); located transition state for the direct oxidative addition of 1-iodo-4-nitrobenzene onto the mixed Pd(I)-I-SeCF$_3$ dimer **348** (right). (The calculations were performed using CPCM (toluene) M06L/def2TZVP//B3LYP/6-31G(d) and LANL2DZ for Pd,I level of theory).

Oxidative addition to Pd(I)-SeCF$_3$ dimer **347** was calculated to be 2 kcal/mol higher than oxidative addition to the mixed Pd(I)-I-SeCF$_3$ dimer **348**, in agreement with what was found experimentally using 1-iodo-4-nitrobenzene. Formation of the product could be observed after 1 hour of reaction and the only species present in solution and therefore responsible for the transformation was the mixed Pd(I)-I-SeCF$_3$ dimer **348**. However, the calculated values are considerably higher compared to what found for the halide exchange where the oxidative addition to the Pd(I)-bromo dimer **31** and to the mixed Pd-Br-I-dimer **350** was calculated to be 15 and 18 kcal/mol respectively. That could explain why higher temperatures (60 °C) were needed, although a computational method dependence could be not excluded.[348] Oxidative addition on the Pd(0)P*t*Bu$_3$ was calculated, but the energetic barriers are considerably higher compared to the energetic barriers of the dimeric oxidative addition (38 kcal/mol for the system Pd(0)P*t*Bu$_3$ + LPd(SeCF$_3$)$_2$ and 84 kcal/mol for the system Pd(0)P*t*Bu$_3$ + LPd(SeCF$_3$)I).

4.5 Conclusions

In this chapter we have synthesised and characterised, both spectroscopically and structurally, a new Pd-(I) dimer bearing two bridging SeCF$_3$ groups. This new Pd(I) dimer, which can be generated *in situ* from Pd(I)-iodo dimer **193** and (CH$_3$)$_4$NSeCF$_3$ salt **346**, was shown to be an efficient catalyst (or maybe precatalyst) for the SeCF$_3$ functionalisation of aryl iodides under mild reaction conditions. The reaction scope is broad and tolerant to a large number of functional groups, including non-protected aniline and amines. Two

possible mechanisms were proposed for the transformation: one concerning a direct dimer catalysis and the second one disproportionation of the dimer into a Pd(II) and a Pd(0) species. A combination of spectroscopic and computational studies were performed to gain more insight into the possible mechanism of this transformation. The stoichiometric spectroscopic study did not show any other intermediates than the three dimers. Computational studies performed using CPCM (toluene) M06L/def2TZVP//B3LYP/6-31G(d) and LANL2DZ for Pd,I level of theory, allowed us to locate the two transition states for the oxidative addition to Pd-SeCF$_3$ dimer **347** and to the mixed Pd-I-SeCF$_3$ dimer **348** (31.4 and 29.1 kcal/mol respectively). The results are in agreement with the spectroscopic findings of a functionalisation largely catalysed by the mixed dimer **348**.

Chapter 5. Conclusions

Chapter 5: Conclusions

The major focus of this work was driven by the study of the reactivity of Pd(I)-Pd(I) dimer bearing electron-rich ligands, such as PtBu$_3$, in cross-coupling reactions. Three particular aspects concerning [Pd(μ-X)PtBu$_3$]$_2$ (X= Br, I) were investigated: formation, possible mechanism of activation and possibility of direct dimer catalysis.

The studies on the metal additives effect on Pd(PtBu$_3$)$_2$ **268** showed that an oxidation reaction took place and Pd(0) is oxidised to Pd(I), whilst Cu(II) is reduced to Cu(I).
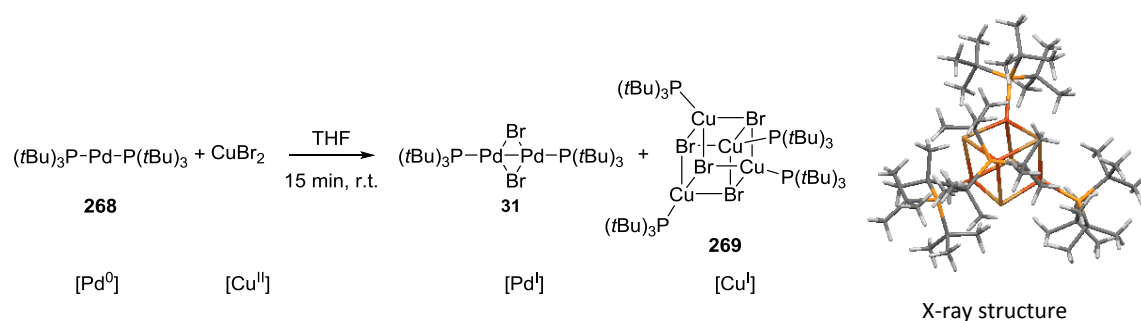
Scheme 139: Formation of Pd(I)-bromo-dimer **31** and Cu-cubane **269** from Pd(0) **268** and CuBr$_2$ (left). Crystal structure of Cu-cubane **269**.

The same redox reaction was observed in the case of CuI, but in this case the Pd(I)-iodo dimer **193** was formed.
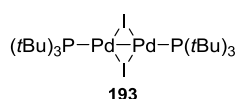
Figure 73: Pd(I)-iodo dimer **193**.

Further studies on the implications of this transformation in cross-coupling reactions showed that: *(i)* the use of Pd(I)-bromo dimer **31** and Pd(I)-iodo dimer **193** as precatalyst in the Sonogashira coupling of aryl chlorides and aryl alkynes did not give any product formation due to a fast oligomerization of the alkyne catalysed by both dimers. The oligomerization reaction was very slow in the presence of Pd(PtBu$_3$)$_2$ **268**, but became very fast when the Pd(0) complex **268** was used in combination with CuI and CuBr$_n$ (n= 1, 2)

salts. *(ii)* In Suzuki cross-coupling reactions, the formation *in situ* of Pd(I)-bromo dimer **31** from Pd(P*t*Bu$_3$)$_2$ **268** and CuBr$_n$ (n=1, 2) led to an increase of the rate of the reaction of chloroacetophenone **306** with 4-methoxyphenylboronic acid **312**. The yield increased from 11% to 45% (1 hour, ambient temperature, KF as base). On the contrary, the formation of Pd(I)-iodo dimer **193** *in situ* from Pd(P*t*Bu$_3$)$_2$ **268** and CuI, led to a decrease of the yield in the same transformation and conditions (from 11% to 5%).
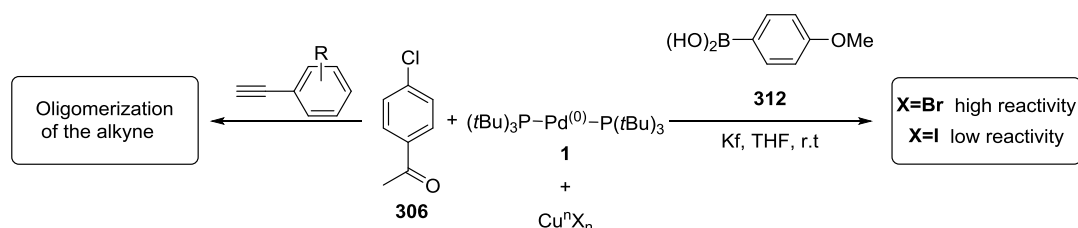
Scheme 140: Effect of copper additives on Pd(P*t*Bu$_3$)$_2$ **268** in: Sonogashira reactions (left); in Suzuki reactions (right).

The study was also extended to: *(i)* other oxidising salts and dimer formation was observed for all of the oxidising salts with a reduction potential higher than –0.26 eV (*E°*, 298 K, 100.325kPa (1 atm), [1 M], reference electrode: SHE) and with a bromide or an iodide counterion. Dimer formation was observed in the presence of AgBr, FeBr$_3$, AuBr$_3$ and AgI, these salts are generally used in substitution of Cu additives in cross-coupling reaction, especially Sonogashira coupling; *(ii)* to other Pd(0) systems. In the latter case a combination of spectroscopic and crystallographic studies allowed the identification of new Pd complexes in the oxidation state (I) and (II), as shown in *Figure 74*.
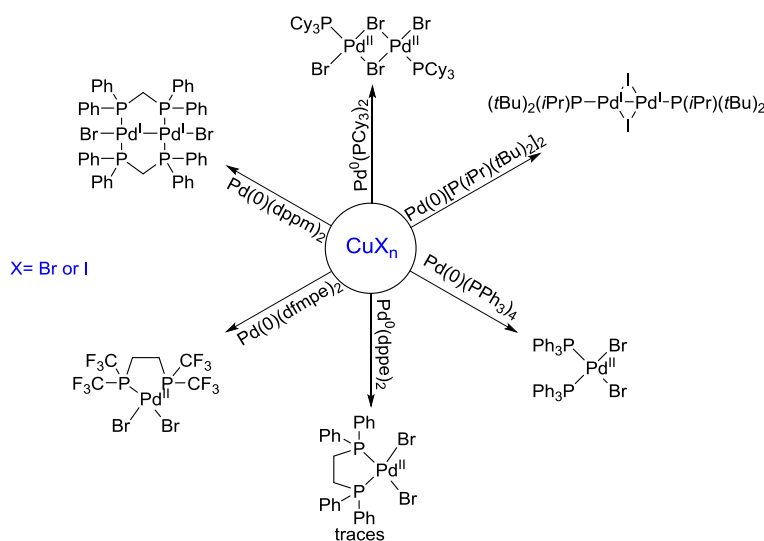
Figure 74: Reaction of CuBr$_2$ with different Pd(0) complexes.

Oxidation of Pd(0) to higher oxidation states of Pd (Pd(I) and Pd(II)) was observed for almost all of the Pd(0) complexes examined. In some cases the oxidation was complete and all the Pd(0) was converted to Pd(II) or Pd(I), in other cases, such as PPh_3 and dppe, oxidation products could be observed but the Pd(0) was still the main species in solution.

Subsequently, we studied the possible mechanism of activation of these $[Pd(\mu\text{-}X)PtBu_3]_2$ (X= Br, I). Despite the broad use of Pd(I)-bromo dimer **31** in cross-coupling reactions[168] little is known about the possible mechanism of its activation. In 2011, our group showed through a combination of experimental and computational studies, that the reactivity of Pd(I)-bromo dimer **31** is consistent with the one of the monoligated Pd(PtBu$_3$). The possibility of a nucleophile-assisted disproportionation was explored in this thesis and a possible activation mechanism was proposed:
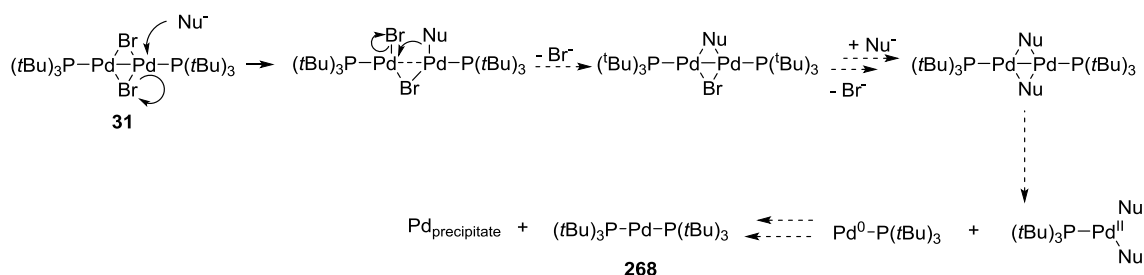
Scheme 141: Proposed activation mechanism of Pd(I)-bromo dimer **31** in the presence of charged nucleophiles.

We hypothesised that in the presence of an excess of nucleophile the two bridging bromine atoms could be substituted by two nucleophiles to generate a new Pd(I)-dimer. If the nucleophile is not good in stabilising the bridging structure, this dimer will undergo facile disproportionation to form the monoligated a Pd(II) species and monoligated Pd(PtBu$_3$), which is responsible for the catalysis. Release of one ligand from the Pd(II) complex and recombination with Pd(PtBu$_3$) will form the Pd(PtBu$_3$)$_2$ **268**, that was observed under Pd(I)-bromo dimer **31** catalysis. Phosphine exchange was hypothesised in the case of P-based nucleophiles as shown in *Scheme 142*.
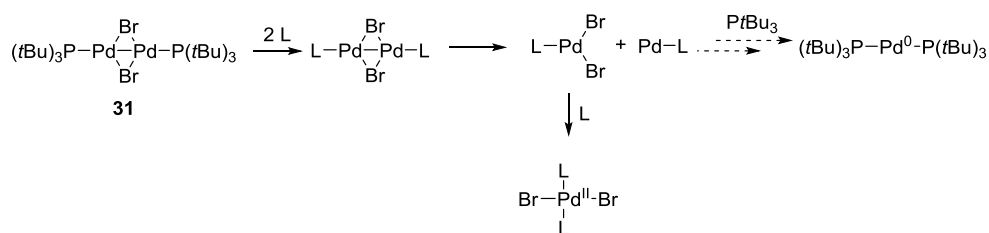
Scheme 142: Proposed activation mechanism in the presence of neutral nucleophiles.

We tested several nucleophiles in the presence of Pd(I)-bromo dimer **31** with an increasing N value (nucleophilic power) according to the Mayr's classification.[337,338] In the case of Pd(I)-bromo dimer **31** we observed formation of Pd(PtBu$_3$)$_2$ **268** in the presence of all of the nucleophiles with an N value higher than 10.5. In two case (PCy$_3$ and PEt$_3$) we were also able to identify the formation of a Pd(II) species. In the case of PEt$_3$ the reaction of Pd(I)-bromo dimer **31** with PEt$_3$ led to the formation of Pd(II)Br$_2$(PEt$_3$)$_2$ **326**. The complex was isolated and analysed by X-ray diffraction, as illustrated in *Figure 75*.
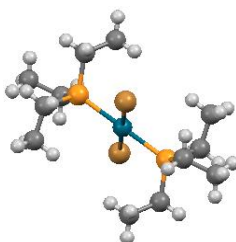
Figure 75: Crystal structure of Pd(II)Br$_2$(PEt$_3$)$_2$ **326**.

The same study was performed with Pd(I)-iodo dimer **193** both to support our mechanistic proposal and to activate this stable dimer towards cross-coupling reactions. The higher stability of Pd(I)-iodo dimer **193** compared to Pd(I)-bromo dimer **31** required a higher N value for its activation, which was shown to be 16.0. However, the use of P-containing nucleophile, such as PCy$_3$ and PEt$_3$, the N value required to observe activation is lower compared to other nucleophile. This phenomenon is probably due to the binding affinity for P-containing nucleophiles towards Pd. Once the minimum N value was identified, we decided to test Pd(I)-iodo dimer **31** as precatalyst in the Suzuki coupling of aryl halides in the presence of KOEt as base (N value=16.1). One of the advantages of the use of this

precatalyst is that dimer **193** is stable in solution even under aerobic conditions. This allowed us to use it under normal aerobic conditions.
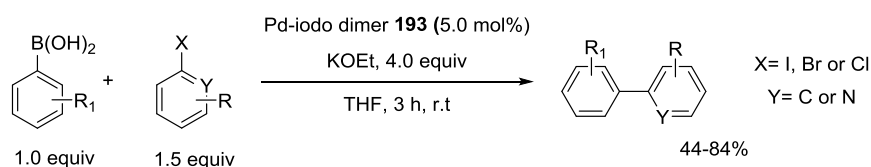
Scheme 143: Suzuki cross-coupling reactions catalysed by Pd(I)-iodo dimer **193** under both aerobic and anaerobic conditions.

The coupling of aryl iodides, bromides and chlorides gave from good to excellent yield both under aerobic and anaerobic conditions.[367]

In the last part of this thesis we have explored a potential direct use of dinuclear Pd(I) in catalysis. During this study a new Pd(I) dimer bearing $SeCF_3$ bridging groups, instead of the usual halide-bridges, was isolated and charatherised both by NMR spectroscopy and X-ray diffraction, see *Figure 76*.
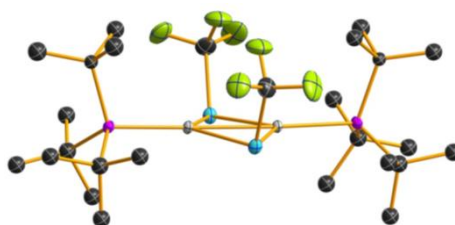
Figure 76: Crystal structure of the Pd(I)-SeCF$_3$ dimer **331**.

This novel Pd(I) dimer **331**, formed *in situ* from Pd(I)-iodo dimer **193** and $(CH_3)_4NSeCF_3$, was tested in the $SeCF_3$ functionalisation of aryl iodides, as illustrated in *Scheme 144*.
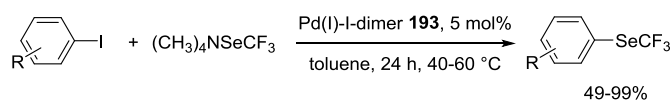
Scheme 144: Trifluoromethylselenolation of aryl iodides in the presence of a catalytic amount of Pd(I)-Iodo-dimer **193**.

The reaction in the presence of a catalytic amount of Pd(I)-iodo dimer **193** (5 mol%) allowed the functionalisation of aryl iodides bearing electron-withdrawing, electron-donating and electron-neutral substituents in good yields. A combined computational (DFT calculations using the CPCM (toluene) M06L/def2TZVP//B3LYP/6-31G(d) and LANL2DZ for Pd,I level of theory) and spectroscopic study was performed to investigate the possible mechanism of the transformation. Two possible scenarios were considered: *(i)* the first proposed mechanism involves a direct dimer catalysis where oxidative addition and reductive elimination occur on a single Pd-atom without destroying the dimeric structure; *(ii)* the alternative mechanistic proposal would concern the disproportionation of the *in situ* formed Pd(I)-SeCF$_3$ dimer **347** into LPd(II)(SeCF$_3$)$_2$ and Pd(0)L, the latter of which undergoes oxidative addition with aryl iodides to form LPd(II)(Ar)(I). Subsequently, the iodide would be substituted by the SeCF$_3$ group to form LPd(II)(Ar)(SeCF$_3$) that reductive eliminates the aryl-SeCF$_3$ product and regenerates the Pd(0) species. The combined studies did not exclude the possibility of having a direct dimer catalysis. In addition, the spectroscopic studies did not show traces of both the two intermediate Pd(II) complex LPd(II)(Ar)(I) and LPd(II)(Ar)(SeCF$_3$) which could form after disproportionation.[369]

In conclusion, the first part of my PhD research demonstrated that Pd(I)-bromo dimer **31** and Pd(I)-iodo dimer **193** can be readily formed from Pd(P*t*Bu$_3$)$_2$ **268** by reaction with appropriate oxidants. In turn, these dimers can be converted back to Pd(0) complex **268** by reaction with nucleophiles with an appropriate N value. In this context we were able to also activate the Pd(I)-iodo dimer **193**, which was usually non-reactive in the presence of weak nucleophiles/bases, such as KF. In the last part we have shown that the Pd(I) dimer **347**, formed *in situ* from Pd(I)-iodo dimer **193** and (CH$_3$)$_4$NSeCF$_3$ **346** , is a good catalyst/precatalyst in the SeCF$_3$ functionalisation of aryl iodides. Spectroscopic and computational studies did not exclude the possibility of a direct dimer catalysis.

Chapter 6. Experimental Part

Chapter 6: General Experimental Details

Reagents: Reagents were purchased from Acros, Aldrich, ABCR and Fluka, and used as received unless otherwise stated. Boronic acids were recrystallised in water and deoxygenated before their use. Se red was dried over P_2O_{10} prior to use.

Solvents: All reactions were performed in anhydrous solvents unless used in combination with H_2O. Toluene, acetonitrile, THF, hexane and DMF were purified by a solvent drying system from LC Technology Solutions Inc. SP-105 under an atmosphere of nitrogen. Anhydrous acetone was purchased from Acros and was deoxygenated with nitrogen prior to use. All other anhydrous solvents were purchased from Aldrich and used as received unless otherwise stated. Extraction solvents and chromatography eluents were technical grade and distilled prior to use. Benzene was purchased and used as received.

Experimental Techniques: Reactions were carried out in oven-dried glassware under an inert atmosphere of nitrogen, unless otherwise stated. Reaction temperatures other than room temperature were recorded as aluminum heating block, or bath temperatures. Flash column chromatography was performed on silica gel, particle size 0.040-0.063 mm, 230-400 mesh (purchased from Aldrich). Analytical thin-layer chromatography (TLC) was performed on aluminum sheets coated with SiO_2 60 F254 (purchased from Macherey-Nagel) which were visualised by ultraviolet light (254 and 350 nm) and/or chemical staining using potassium permanganate, and vanillin.

Characterisation: Infrared (IR) spectra were recorded on a Perkin-Elmer Spectrum One FTIR Spectrometer and the spectra were measured neat or as liquid film (film) using a Perkin-Elmer FT-IR Spectrum 100 device. The selected absorption bands are reported in wavenumbers (cm^{-1}). ^1H NMR, ^{13}C NMR, ^{19}F NMR and ^{31}P NMR spectra were recorded with either Varian Gemini 300, Varian Mercury 300, Bruker ARX 300, Bruker DRX 400, Bruker AV 400, Bruker DRX 500 or Varian VNMRS 600 spectrometers at 300, 400, 500 MHz or 600 (^1H NMR); 100, 125 or 151 MHz (^{13}C NMR); 282, 376 or 564 MHz (^{19}F NMR) and 121, 161 or 243 (^{31}P NMR). Chemical shifts (δ) are quoted in parts per million (ppm) and are referenced to the residual solvent peak for ^1H and ^{13}C NMR. Trimethoxyphosphine oxide or triphenylphosphine oxide were used as internal standard for ^{31}P NMR and 4,4'-difluorobiphenyl in the case of ^{19}F NMR. Coupling constants (J) are quoted in Hertz (Hz). The resonance multiplicity is described as s (singlet), d (doublet), t (triplet), q (quartet), quint. (quintet), hept. (heptet), m (multiplet), dd (doublet of doublets) and br. (broad). ^{31}P and ^{13}C and ^{19}F NMR spectra were obtained with proton decoupling. All NMR spectra were acquired at room temperature, unless otherwise stated. High-resolution mass spectra (HRMS) were performed by the MS service at the Laboratory for Organic Chemistry (ETH Zurich) and MS service of Institute of Organic Chemistry (RWTH Aachen).

All cross-coupling reactions were monitored using an Agilent Technologies 5975 series MSD mass spectrometer coupled with an Agilent Technologies 7820A gas chromatograph equipped with an Agilent 19091s-433 HP-SMS column (30 m × 0.250 μm × 0.25 μm).

GC-MS Conditions: Front inlet mode: split; temperature: 250 °C; pressure: 1.1066 psi; total flow 50.474 mL/min; split ratio: 100:1; split flow: 50 mL/min; run time: 18.667 min; oven program: 50 °C for 2 min then 15 °C/min to 300 °C for 0 min; flow 0.5 mL/min.

Calibrated GC-MS analyses were achieved using a calibration curve generated using the supplied GC-MS software ("ChemStation"). 1,3,5-tri-*t*-butylbenzene was used as an internal standard.

X-ray structure determinations were performed by the crystallographic centre of the Laboratory for Organic Chemistry at ETH Zurich (Dr. B. Schweizer, Dr M. D.Wörle, Dr N. Trapp and M. Solar).

6.2 General experimental procedures

General procedure A for the reaction of Pd(PtBu$_3$)$_2$ 268 with metal additives M^{n}X$_n$ (c.f Chapter 2)

In a dry reaction vessel equipped with a stirring bar Pd(P*t*Bu$_3$)$_2$ **268** (0.04 mmol, 20.4 mg) and M^{n}X$_n$ (0.04 mmol) were mixed in 1 mL of anhydrous and deoxygenated THF. The reaction was then stirred at room temperature and was analysed by ^{31}P NMR spectroscopy at various time points.

General procedure B for the reaction of Pd(0) complexes with metal additives M^{n}X$_n$ (c.f Chapter 2)

In a dry reaction vessel equipped with a stirring bar Pd(0)L$_n$ (n= 2 or 4) (0.1 mmol) and M^{n}X$_n$ (0.1 mmol) were mixed in 1 mL of anhydrous and deoxygenated THF. The reaction was then stirred at room temperature and was analysed by ^{31}P NMR spectroscopy at various time points.

General procedure C for the Sonogashira reaction of 4-chloroacetophenone 306 and aryl alkynes (c.f. Chapter 2)

Inside the glovebox 4-chloroacetophenone **306** (0.4 mmol, 1 equiv), Pd-catalyst (0.02 mmol, 5 mol % for Pd(P*t*Bu$_3$)$_2$ **268** or 0.01 mmol, 2.5 mol% for Pd(I) dimers), M^{n}X$_n$ (0.02 mmol, 5 mol %), NH(*i*Pr)$_2$ (0.25 mL, 1.8 mmol, 4.5 equiv) and 1 mL of dry and deoxygenated solvent (dioxane, CH$_3$CN or THF) were added in a dry reaction vessel equipped with a stirring bar. Then the alkyne (0.4 mmol, 1.0 equiv) was added. The temperature was increased to 50 °C and the reaction mixture was stirred at this temperature for 4 hours. The mixture was subsequently diluted with Et$_2$O and filtered through silica using Et$_2$O as eluent. After solvent removal, the residue was analysed by calibrated ^{1}H-NMR analysis and calibrated GC-MS (with 1,3,5-tri-*t*-butylbenzene as internal standard).

General procedure D for Suzuki cross-coupling reaction of 4-chloroacetophenone 306 with 4-methoxyphenylboronic acid 312 in presence of metal additives (c.f. Chapter 3)

In a dry reaction vessel equipped with a stirring bar were added 4-chloroacetophenone **306** (68.0 mg, 0.44 mmol, 1.0 equiv), boronic acid (70.0 mg, 0.46 mmol, 1.05 equiv), KF (73.9 mg, 1.32 mmol, 3 equiv), Pd(PtBu$_3$)$_2$ **268** (11.2 mg, 0.022 mmol, 5mol%) and M^{n}X$_n$ (0.022 mmol, 5 mol%). 1 mL of dry and deoxygenated THF (1.0 mL, THF/H$_2$O 80:1) and deoxygenated water (10 mg, 0.50 mmol), were subsequently added to the reaction mixture, and then stirred at room temperature for 1 h. The mixture was diluted with Et$_2$O (150 mL) and filtered through a short pad of silica gel and concentrated under reduced pressure. The residue was analyzed by ^{1}H NMR spectroscopy (with 1,4-dioxane as internal standard).

General procedure E for the reaction of Pd(I) dimers with different nucleophiles (c.f. Chapter 3).

Inside the glovebox: Pd(I)-dimer (0.026 mmol, 1.0 equiv), nucleophile (0.52 mmol, 20.0 equiv), internal standard (0.09 mmol, 3.5 equiv) and dry THF (2.0 ml, previously deoxygenated for 30 min) were added in a dry reaction vessel equipped with a stirring bar. The reaction was stirred at room temperature and was analyzed by ^{31}P-NMR spectroscopy at various time points.

General procedure F for the Suzuki cross-coupling reactions catalysed by Pd(I)-iodo dimer 193 (c.f. Chapter 3).

Inside the glovebox: aryl halide (0.5 mmol, 1.0 equiv), boronic acid (0.75 mmol, 1.5 equiv) and KOEt (168.3 mg, 2.0 mmol, 4 equiv) were added in a dry reaction vessel equipped with a stirring bar.

Then Pd(I)-iodo-dimer **193** (21.8 mg, 0.025 mmol, 5.0 mol%) and dry THF (1.5 ml, previously deoxygenated for 30 min) were added to the reaction mixture. The reaction was stirred at room temperature for 3 h. The mixture was subsequently diluted with Et$_2$O and filtered through silica using Et$_2$O as eluent. The product was purified by chromatography on silica gel using as eluent mixture a gradient of pentane:EtOAc from 100:0 to 95:5.

Outside the glovebox: aryl halide (0.5 mmol, 1.0 equiv), boronic acid (0.75 mmol, 1.5 equiv) and KOEt (168.3 mg, 2.0 mmol, 4 equiv) were added in a reaction vessel equipped with a stirring bar.

Then Pd(I)-iodo-dimer **193** (21.8 mg, 0.025 mmol, 5.0 mol%) and dry THF (1.5 ml) were added to the reaction mixture. In this case all the reagents were not degassed prior to use. The reaction was stirred at room temperature for 3 h. The mixture was subsequently diluted with Et$_2$O and filtered through silica using Et$_2$O as eluent. The product was purified by chromatography on silica gel using as eluent mixture a gradient of pentane:EtOAc from 100:0 to 95:5.

General procedure G for the synthesis of aryltrifluoromethylselenides bearing electron-neutral and electron-donating groups (c.f. Chapter 4).

Inside a glovebox, aryl halide (0.2 mmol, 1.0 equiv), $(CH_3)_4NSeCF_3$ (89.2 mg, 0.4 mmol, 2.0 equiv) and Pd(I)-iodo-dimer **193** (8.7 mg, 0.01 mmol, 5 mol%) were added in a dry reaction vessel with dark glass wall equipped with a stirring bar. Then dry toluene (1.0 mL, previously deoxygenated for 30 min) was added to the reaction mixture. The reaction was stirred in the glovebox for 24 h at 40 °C. The flask was removed from the glovebox and the mixture was subsequently diluted with Et_2O and filtered through a short pad of silica gel using Et_2O as eluent. The product was purified by flash column chromatography using the indicated eluent mixture.

General procedure H for the synthesis of aryltrifluoromethylselenides bearing electron-withdrawing groups (c.f. Chapter 4).

Inside a glovebox, aryl halide (0.2 mmol, 1.0 equiv), $(CH_3)_4NSeCF_3$ (89.2 mg, 0.4 mmol, 2.0 equiv) and Pd(I)-iodo-dimer **193** (8.7 mg, 0.01 mmol, 5 mol%) were added in a dry reaction vessel with dark glass wall equipped with a stirring bar. Then dry toluene (1.0 mL, previously deoxygenated for 30 min) was added to the reaction mixture. The reaction was stirred in the glovebox for 24 h at 60 °C. The flask was removed from the glovebox and the mixture was subsequently diluted with Et_2O and filtered through a short pad silica gel using Et_2O as eluent. The product was purified by flash column chromatography using the indicated eluent mixture.

6.3 Characterising data for compounds

6.3.1 Experimental details for the reactions reported in Chapter 2

Bis(tri-*tert*-butylphosphine)palladium(0), Pd(P*t*Bu$_3$)$_2$ **268**[370]
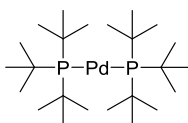
268

Inside the glove box, tris(dibenzylideneacetone)dipalladium(0) (1.1 g, 1.1 mmol, 1.0 equiv), tri-*tert*-butylphosphine (1.0 g, 4.9 mmol, 4.2 equiv) and DMF (25 mL) were added to a dry reaction vessel equipped with a stirring bar. The reaction was stirred at room temperature for 3 h. The reaction mixture was filtered through sinter funnel n°4 and the yellowish precipitate obtained was further washed with DMF to remove the excess of dba, and then dissolved in hexane. The hexane solution was filtered and the solvent removed under reduced pressure. The product was obtaine as an off-white solid in 80% of yield (899 mg): δ_H (C$_6$D$_6$, 300 MHz) 1.48-1.56 (54H, m, C*H*$_3$); δ_P (C$_6$D$_6$, 126 MHz) 85.2. This is consistent with the data reported previously.[370]

Tetra(tri-*tert*-butylphosphine)copperbromide cubane, Cu-cubane **269**

The general procedure A was followed for the synthesis of the Cu-cubane **269**. The solvent was removed under reduced pressure and the solid obtained was dissolved in 10 mL of toluene and then 20 mL of dry acetone were layered on it. The mixture was left at $-35°C$ for 24 h. Colorless crystals of the Cu-cubane **269** were obtained: δ_P (THF, 126 MHz) 57.1. This is consistent with the data reported previously.[259]

(X-Ray diffraction data and structure, see page 299)

Bis(tri-cyclohexylphosphine)palladium(0), Pd(PCy$_3$)$_2$ **270**

In a dry reaction vessel equipped with a stirring bar Pd(Me)$_2$(tmeda) (500 mg, 2.0 mmol, 1.0 equiv), PCy$_3$ (1110 mg, 4.0 mmol, 2.0 equiv) and 20 mL of dry and deoxygenated toluene were mixed. The reaction was left under stir for 1 h at room temperature. The solvent was removed under reduced pressure and the solid obtained was dissolved in hexane. The solution was left to stir for another 15 min and a white precipitate started forming during this time. The solvent was removed by decantation. The solid obtained was washed with additional hexane and subsequently dried under reduced pressure yielding the product as a white solid in 60% yield (799 mg): δ_H (C$_6$D$_6$, 300 MHz) 2.40 (12 H, bd, $J =$ 13.1 Hz, CH_2), 2.0-1.85 (24 H, m, CH_2), 1.63-1.29 (24 H, m, CH_2), 1.09-1.05 (6 H, m, CH_2); δ_P (C$_6$D$_6$, 126 MHz) 39.1. This is consistent with the data reported previously.[262]

Bis(tri-cyclohexylphosphine)(dibenzylideneacetone)palladium(0), Pd(PCy$_3$)$_2$(dba) **271**

In a dry reaction vessel equipped with a stirring bar tris(dibenzylideneacetone)dipalladium(0) (100 mg, 0.1 mmol, 1 equiv), PCy$_3$ (120.6 mg, 0.4 mmol, 4.0 equiv) and 10 mL of dry and deoxygenated THF were mixed. The reaction was left under stir for 1 h at room temperature. The solvent was removed under reduced

pressure and the sticky precipitate obtained was washed with hexane to remove the excess of dba. The orange solid was then dissolved in the smallest amount of acetone and hexane was layered on top. The mixture was left at −35 °C for 2 days. Orange crystals formed, which were suitable for X-ray analysis: δ_P (THF, 126 MHz) 44.8.

(X-Ray diffraction data and structure, see page 305)

Bromo-(tri-cyclohexylphosphine)dipalladium(II), [PdBr$_2$(PCy$_3$)]$_2$ **272**

$$Cy_3P \diagdown \diagup Br \diagdown \diagup Br$$
$$Pd \quad Pd$$
$$Br \diagup \diagdown Br \diagdown PCy_3$$

272
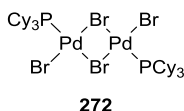
The general procedure B was followed for the synthesis of [PdBr$_2$(PCy$_3$)]$_2$ **272**. The THF was removed under reduced pressure and the solid obtained was washed with hexane to remove the unreacted Pd(PCy$_3$)$_3$ **270**. The dark brown solid obtained was then dissolved in CH$_2$Cl$_2$, filtered through sinter funnel n°4 (to remove the Pd-black formed) and left at −35°C for one week. Orange crystals were obtained, which were suitable for X-ray analysis: δ_P (THF, 126 MHz) 25.0.

(X-Ray diffraction data and structure, see page 318)

Iodo-(tri-cyclohexylphosphine)dicopper(I), [CuI(PCy$_3$)]$_2$ **274**

$$Cy_3P{-}Cu \diagup \diagdown Cu{-}PCy_3$$

274
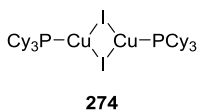
The general procedure B was followed for the synthesis of [CuI(PCy$_3$)]$_2$ **274**. The THF was evaporated under reduced pressure and the solid obtained dissolved in CH$_2$Cl$_2$ and filtered through sinter funnel n°4 to remove the Pd-black formed during the reaction. Hexane was layered on top of CH$_2$Cl$_2$ and the solution was left at −35°C for 1 week. Light orange/brown crystals were obtained, which were suitable for X-ray analysis.

(X-Ray diffraction data and structure, see page 324)

Iodo-(di-*tert*-butyl-*iso*-propylphosphine)dipalladium(I), Pd(I)-iodo dimer **278**

$$(tBu)_2(iPr)P{-}Pd \diagup \diagdown Pd{-}P(iPr)(tBu)_2$$

278
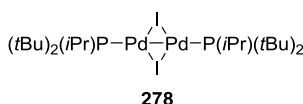
The general procedure B was followed for the synthesis of Pd(I)-iodo dimer **278**. After 4 h of reaction, the THF solution was filtered through sinter funnel n°4 and the solvent removed under reduced pressure. The solid obtained was dissolved in 5 mL of toluene and 10 mL of acetone were layered on top of it. The solution was left at −35°C for 1 day,

yielding dark purple crystals of Pd(I)-iodo dimer **278** in 65% yield (55 mg): δ_P (THF, 126 MHz) 88.9.

(X-Ray diffraction data and structure, see page 330)

Bis(1,1-Bis(diphenylphosphino)methane)palladium(0), Pd(dppm)$_2$ **279**
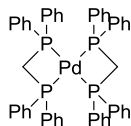
279

In a dry reaction vessel equipped with a stirring bar Pd(Me)$_2$(tmeda) (500 mg, 2.0 mmol, 1.0 equiv), dppm (1537 mg, 4.0 mmol, 2.0 equiv) and 20 mL of dry and deoxygenated toluene were mixed. The reaction was left under stir for 1 h at room temperature. The solvent was removed under reduced pressure and the solid obtained was dissolved in hexane and left at −35°C for 18 h. The complex was obtained as light yellow solid in 50 yield (870 mg): δ_H (CH$_2$Cl$_2$, 300 MHz) 7.40-7.18 (24 H, m, ArC*H*), 7.02-1.97 (8 H, m, ArC*H*), 6.85-6.80 (8 H, m, ArC*H*), 2.97 (4 H, bs, PC*H*$_2$P); δ_P (CH$_2$Cl$_2$, 126 MHz) 12.4.

Bis[l,2-bis(diphenylphosphino)ethane]palladium(0), Pd(dppe)$_2$ **283**.[274]
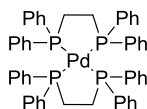
283

In a dry reaction vessel equipped with a stirring bar tris(dibenzylideneacetone)dipalladium(0) chloroform adduct (207 mg, 0.2 mmol, 1.0 equiv), and 10 mL of dry and deoxygenated benzene were mixed. Dppe was subsequently added to the benzene solution and the mixture was left under stir at room temperature for 1 h. The solvent was removed under reduced pressure and then acetone was added. The solution was left at −35°C for 1 h and then the solution was filtered through sinter funnel n°4. The yellow solid obtained was washed with acetone (2x50 mL) and then dried. The Pd(0) complex was obtained in 70% yield: δ_P (THF, 126 MHz) 30.6. This is consistent with the data reported previously.[274,275]

Bis-[1,2,3,4,5-Pentaphenyl-1′-(di-*tert*-butylphosphino)ferrocene]palladium(0), Pd(Qphos)$_2$ **292**

211

Pd(dba)$_2$ (287 g, 0.5 mml, 1.0 equiv), Qphos **291** (189.5, 0.75 mmol, 1.5 equiv) and toluene 15 mL were added to a dry reaction vessel equipped with a stirring bar. The temperature was raised at 40°C and the solution was left under stir at this temperature for 1 h. The reaction was filtered through sinter funnel n°4 and the toluene removed under reduced pressure. The red solid obtained was dissolved in hexane and the solution was left at −35°C for one day. The hexane was decanted and the solid dried, yielding the product as a red solid in 65% (665 mg) yield: δ$_P$ (THF, 126 MHz) 60.8. This is consistent with the data reported previously.[279]

Bis-[(2-Biphenyl)dicyclohexylphosphine]palladium(0), Pd(Cy-JohnPhos)$_2$ 305.

In a dry reaction vessel equipped with a stirring bar Pd(Me)$_2$(tmeda) (100 mg, 0.4 mmol, 1.0 equiv), Cy-JohnPhos **304** (280.4 mg, 0.8 mmol, 2.0 equiv) and 5 mL of dry and deoxygenated toluene were mixed. The reaction was left under stir for 1 h at room temperature. The solvent was removed under reduced pressure, the solid obtained was dissolved in hexane and the solution was left at −35°C for 12 h. The solution was filtered on sinter funnel n°4 and the off-yellow solid was washed with additional cold hexane. The product was obtained as a pale yellow solid in 56 % yield (181 mg): δ$_P$ (THF, 126 MHz) 29.6.

Bromo-(tri-*tert*-butylphosphine)palladium-copper dimer, Pd-Cu dimer **316**.

The general procedure A was followed for the synthesis of the Pd-Cu dimer **316**. The solvent was removed under reduced pressure and the solid obtained was dissolved in 10 mL of toluene and then 20 mL of dry acetone were layered on it. The mixture was left at −35°C for 24 h. Dark green crystals that may presumably belong to the Pd-Cu dimer **316** were obtained.

(X-Ray diffraction data and structure, see page 335)

Tetra(tri-*tert*-butylphosphine)silverbromide cubane, Ag-cubane **317**

The general procedure A was followed for the synthesis of the Ag-cubane **317**. The solvent was removed under reduced pressure and the solid obtained was dissolved in 10 mL of toluene and then 20 mL of dry acetone were layered on it. The mixture was left at −35°C for several days. Colorless crystals of the Ag-cubane **317** were obtained. The ^{31}P NMR analysis of the reaction mixture did not show any peak that could be assigned to the Ag-cubane also when the reaction was performed on a bigger scale.

(X-Ray diffraction data and structure, see page 344)

6.3.2 Experimental details for the reactions reported in Chapter 3

Bromo(tri-*tert*-butylphosphine)palladium(I) dimer**,** Pd(I)-bromo dimer **31**
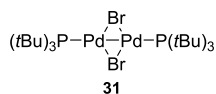
Tris(dibenzylideneacetone)dipalladium(0) (1.1 g, 1.2 mmol, 1.0 equiv), tri-*tert*-butylphosphine (1.0 g, 4.8 mmol, 4.0 equiv) and THF (30 mL) were added to a dry reaction vessel equipped with a stirring bar. The reaction mixture was stirred for 1 h at room temperature. Palladium(II) bromide (0.64 g, 2.4 mmol, 2.0 equiv.) was added and the reaction was then stirred at room temperature for an additional hour. The mixture was filtered through sinter funnel n°4, the volume of the THF was reduced to a half under reduced pressure and anhydrous acetone was added (25 mL). The solution was left for 12 h at −35°C for recrystallisation. The solution was filtered and the crystals obtained were washed with additional acetone and dried under reduced pressure. The product was obtained as a dark green solid in 53% yield (0.98 g,): δ_H (C$_6$D$_6$, 300 MHz) 1.30-1.40 (54 H, m, C*H*$_3$); δ_P (C$_6$D$_6$, 126 MHz) 87.1;. This is consistent with the data reported previously.[169]

Iodo(tri-*tert*-butylphosphine)palladium(I) dimer**,** Pd(I)-iodo dimer **193**
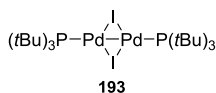
Tris(dibenzylideneacetone)dipalladium(0) (1.1 g, 1.2 mmol, 1.0 equiv), tri-*tert*-butylphosphine (1.0 g, 4.8 mmol, 4.0 equiv) and THF (30 mL) were added to a dry reaction vessel equipped with a stirring bar. The reaction mixture was stirred for 1 h at room temperature. Palladium(II) iodide (0.86 g, 2.4 mmol, 2.0 equiv.) was added and the

reaction was then stirred at room temperature for additional 3 hours. The mixture was filtered through sinter funnel n°4, the volume of the THF was reduced to a half under reduced pressure and anhydrous acetone was added (25 mL). The solution was left for 12 h at −35°C for recrystallisation. The solution was filtered and the crystals obtained were washed with additional acetone and dried under reduced pressure. The product was obtained as a dark purple solid in 57% yield (1.2 g,): δ_H (C_6D_6, 300 MHz) 1.20-1.30 (54 H, m, CH_3); δ_P (C_6D_6, 126 MHz) 102.5. This is consistent with the data reported previously.[170]

Bromo(tri-ethylphosphine)palladium(II), PEt$_2$PdBr$_2$ **326**

326
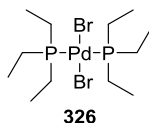
In a dry reaction vessel equipped with a stirring bar Pd(I)-bromo dimer **31** (50 mg, 0.065 mmol, 1.0 equiv), PEt$_3$ (15.2 mg, 0.130 mmol, 2.0 equiv) and THF 5 mL were mixed. The reaction was left under stir for 1 h and the THF removed under reduced pressure. The yellow solid obtained was washed with *n*-hexane to remove the Pd(PtBu$_3$)$_2$ **268** formed in the reaction mixture, the solid obtained was dissolved in CH$_2$Cl$_2$ and left at −35°C for one week. Yellow crystals suitable for X-ray analysis were formed. δ_P (THF, 126 MHz) 15.1.

(X-Ray diffraction data and structure, see page 351)

4-Cyano-4'-methoxybiphenyl, *Table 36* Entry 1
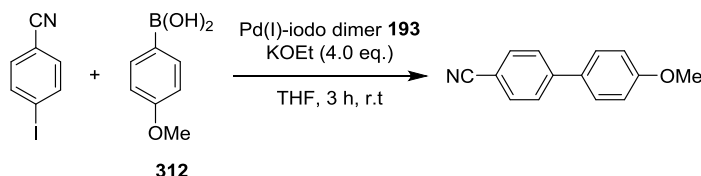
312

The general procedure F was followed for the synthesis of 4-cyano-4'-methoxybiphenyl. The compound was obtained as an off-white solid in 78% (82 mg) yield when the reaction was performed insiede the glovebox with fully degassed reagents; 76% (80 mg) yield was instead obtained when the reaction was performed outside the glovebox under normal aerobic conditions. δ_H (600 MHz, CDCl$_3$) 7.68 (2 H, d, *J* =8.4 Hz, Ar-*H*), 7.63 (2 H, d, *J* =8.4 Hz, Ar-*H*), 7.53 (2 H, d, *J* =8.6 Hz, Ar-*H*), 7.00 (2 H, d, *J* =8.6 Hz, Ar-*H*), 3.86 (3 H, s, OCH_3); δ_C (151 MHz, CDCl$_3$) 160.2 (*C*), 145.2 (*C*), 132.5 (*C*H), 131.5 (*C*), 128.3 (*C*H), 127.1 (*C*H), 119.1 (*C*), 114.6 (*C*H), 110.1 (*C*), 55.4 (O*C*H$_3$); *m/z* (EI) 209 (M, 100%), 194 (32), 166 (32), 140 (24), 113 (5). This is consistent with the data reported previously.[371]

4-Nitro-2′-methylbiphenyl, *Table 36* Entry 2
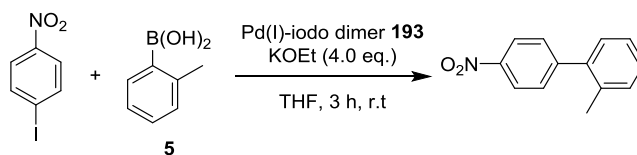
The general procedure F was followed for the synthesis of 4-nitro-2′-methylbiphenyl. The compound was obtained as an off-white solid in 66% (70 mg) yield when the reaction was performed insiede the glovebox with fully degassed reagents; 71% (75 mg) yield was instead obtained when the reaction was performed outside the glovebox under normal aerobic conditions. δ_H (600 MHz, CDCl$_3$) 8.28 (2 H, d, J =8.7 Hz, Ar-*H*), 7.50 (2 H, d, J =8.7 Hz, Ar-*H*), 7.35-7.29 (3 H, m, Ar-*H*), 7.24-7.22 (1 H, m, Ar-*H*), 2.29 (3 H, s, C*H*$_3$); δ_C (151 MHz, CDCl$_3$) 148.8 (*C*), 146.8 (*C*), 139.8 (*C*), 135.0 (*C*), 130.7 (*C*H), 130.1 (*C*H), 129.4 (*C*H), 128.5 (*C*H), 126.1 (*C*H), 123.4 (*C*H), 20.3 (*C*H$_3$); *m/z* (EI) 213 (M, 100%), 183 (6), 165 (79). This is consistent with the data reported previously.[370]

2-Methyl-4'-methoxylbiphenyl, *Table 36* Entry 3
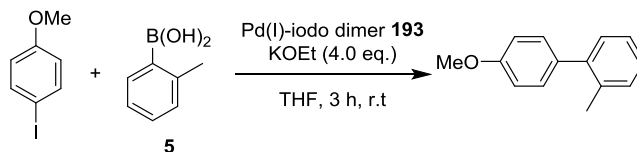
The general procedure F was followed for the synthesis of 2-methyl-4'-methoxylbiphenyl. The compound was obtained as a yellow oil in 53% (52 mg) yield when the reaction was performed insiede the glovebox with fully degassed reagents; 54% (53 mg) yield was instead obtained when the reaction was performed outside the glovebox under normal aerobic conditions. δ_H (600 MHz, CDCl$_3$) 7.26-7.22 (6 H, m, Ar-*H*), 6.98 (2 H, d, J =8.6 Hz, Ar-*H*), 3.85 (3 H, s, OC*H*$_3$), 2.28 (3 H, s, C*H*$_3$); δ_C (151 MHz, CDCl$_3$) 158.5 (*C*), 141.5 (*C*), 135.5 (*C*), 134.3 (*C*), 130.3 (*C*H), 130.2 (*C*H), 129.9 (*C*H), 127.0 (*C*H), 125.8 (*C*H), 113.5 (*C*H), 55.3 (*C*H$_3$), 20.6 (*C*H$_3$). *m/z* (EI) 198 (M, 100%), 183 (20), 164 (20), 153 (20), 128 (17). This is consistent with the data reported previously.[30]

4-Methyl-4'-methoxybiphenyl, *Table 36* Entry 4
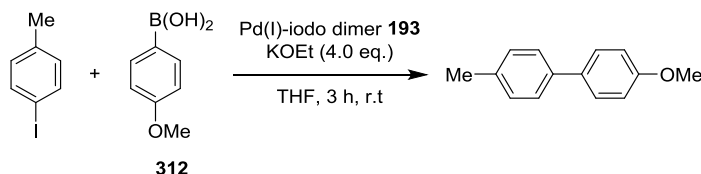
The general procedure F was followed for the synthesis of 4-methyl-4'-methoxylbiphenyl. The compound was obtained as a colorless oil in 43% (42 mg) yield when the reaction was performed insiede the glovebox with fully degassed reagents; 43% (42 mg) yield was

instead obtained when the reaction was performed outside the glovebox under normal aerobic conditions. δ_H (600 MHz, CDCl$_3$) 7.53 (2 H, d, J =8.7 Hz, Ar-*H*), 7.47 (2 H, d, J =8.0 Hz, Ar-*H*), 7.24 (2 H, d, J =8.0 Hz, Ar-*H*), 6.99 (2 H, d, J =8.7 Hz, Ar-*H*), 3.86 (3 H, s, OC*H*$_3$), 2.40 (3 H, s, C*H*$_3$); δ_C (151 MHz, CDCl$_3$) 158.9 (*C*), 138.0 (*C*), 136.3 (*C*), 133.7 (*C*), 129.4 (*C*H), 127.9 (*C*H), 126.6 (*C*H), 114.1 (*C*H), 55.3 (*C*H$_3$), 21.1 (*C*H$_3$). *m/z* (EI) 198 (M, 100%), 183 (45), 164 (55), 155 (34), 128 (17), 99 (6), 63 (5). This is consistent with the data reported previously.[372]

4-Fluorobiphenyl, *Table 36* Entry 5
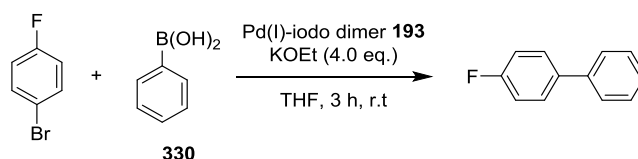
The general procedure F was followed for the synthesis of 4-methyl-4'-methoxylbiphenyl. The product was obtained as a white solid in 76% (65 mg) yield when the reaction was performed insiede the glovebox with fully degassed reagents; 82% (71 mg) yield was instead obtained when the reaction was performed outside the glovebox under normal aerobic conditions. δ_H (600 MHz, CDCl$_3$) 7.56-7.53 (4 H, m, Ar-*H*), 7.44 (2 H, dd, J = 7.5, 7.5 Hz, Ar-*H*), 7.36-7.34 (1 H, m, Ar-*H*), 7.15-7.12 (2 H, m, Ar-*H*); δ_C (151 MHz, CDCl$_3$) 162.4 (1 C, d, J^1 = 246.1 Hz, *C*F), 140.2 (*C*), 137.3 (*C*), 128.8 (*C*H), 128.6 (*C*H), 127.2 (*C*H), 127.0 (*C*H), 115.5 (*C*H); δ_F (450 MHz, CDCl$_3$): δ -115.9. *m/z* (EI) 172 (M, 100%), 154 (18), 133 (5), 115 (2), 85 (5), 63 (2). This is consistent with the data reported previously.[373]

4-Acetyl-4'-methoxybiphenyl, *Table 36* Entry 6
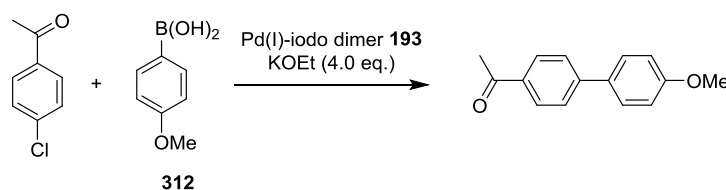
The general procedure F was followed for the synthesis of 4-methyl-4'-methoxylbiphenyl. The product was obtained as a white solid in 44% (50 mg) yield when the reaction was performed insiede the glovebox with fully degassed reagents; 45% (50 mg) yield was instead obtained when the reaction was performed outside the glovebox under normal aerobic conditions. δ_H (600 MHz, CDCl$_3$) 8.01 (2 H, d, J =8.3 Hz, Ar-*H*), 7.65 (2 H, d, J =8.3 Hz, Ar-*H*), 7.58 (2 H, d, J =8.7 Hz, Ar-*H*), 7.00 (2 H, d, J =8.7 Hz, Ar-*H*), 3.87 (3 H, s, OC*H*$_3$), 2.63 (3 H, s, COC*H*$_3$); δ_C (151 MHz, CDCl$_3$) 197.7 (*C*), 160.0 (*C*), 145.4 (*C*), 135.3 (*C*), 132.2 (*C*), 129.0 (*C*H), 128.4 (*C*H), 126.6 (*C*H), 114.4 (*C*H), 55.4 (O*C*H$_3$), 26.6 (CO*C*H$_3$); *m/z* (EI) 226 (69), 211 (M, 100%), 193 (5), 168 (22), 139 (29), 105 (9), 63.1 (5). This is consistent with the data reported previously.[374]

2-Methyl-6-(2-tolyl)pyridine**,** *Table 36* Entry 7
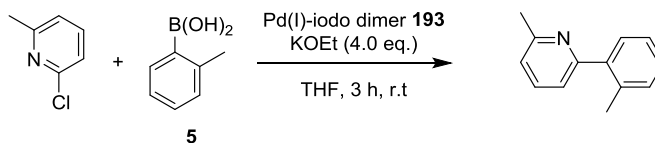
The general procedure F was followed for the synthesis of 2-methyl-6-(2-tolyl)pyridine. The product was obtained as a light yellow oil in 82% (75 mg) yield when the reaction was performed insiede the glovebox with fully degassed reagents; 84% (77 mg) yield was instead obtained when the reaction was performed outside the glovebox under normal aerobic conditions. δ_H (600 MHz, CDCl$_3$) 7.64-7.60 (1 H, m, Ar-*H*), 7.37 (1 H, d, *J* =7.8 Hz, Ar-*H*), 7.29-7.24 (3 H, m, Ar-*H*), 7.18 (1 H, d, *J* =7.6 Hz, Ar-*H*), 7.10 (1 H, d, *J* =7.7 Hz, Ar-*H*), 2.63 (3 H, s, C*H*$_3$), 2.36 (3 H, s, C*H*$_3$); δ_C (151 MHz, CDCl$_3$) 159.5 (*C*), 157.8 (*C*), 140.7 (*C*), 136.3 (*C*H), 135.7 (*C*), 130.6 (*C*H), 129.5 (*C*H), 128.0 (*C*H), 125.8 (*C*H), 121.0 (*C*H), 120.9 (*C*H), 24.7 (*C*H$_3$), 20.2 (*C*H$_3$). *m/z* (EI): 183 (55), 182 (M, 100), 167 (17), 115 (4). This is consistent with the data reported previously.[375]

4-Cyano-4'-methoxybiphenyl, *Table 36* Entry 8
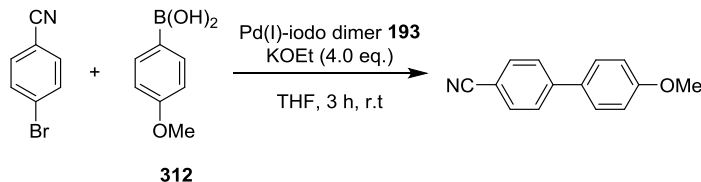
The general procedure F was followed for the synthesis of 4-cyano-4'-methoxybiphenyl. The compound was obtained as an off-white solid in 72% (75 mg) yield when the reaction was performed insiede the glovebox with fully degassed reagents; 70% (70 mg) yield was instead obtained when the reaction was performed outside the glovebox under normal aerobic conditions. δ_H (600 MHz, CDCl$_3$) 7.68 (2 H, d, *J* =8.4 Hz, Ar-*H*), 7.63 (2 H, d, *J* =8.4 Hz, Ar-*H*), 7.53 (2 H, d, *J* =8.6 Hz, Ar-*H*), 7.00 (2 H, d, *J* =8.6 Hz, Ar-*H*), 3.86 (3 H, s, OC*H*$_3$); δ_C (151 MHz, CDCl$_3$) 160.2 (*C*), 145.2 (*C*), 132.5 (*C*H), 131.5 (*C*), 128.3 (*C*H), 127.1 (*C*H), 119.1 (*C*), 114.6 (*C*H), 110.1 (*C*), 55.4 (O*C*H$_3$); *m/z* (EI) 209 (M, 100%), 194 (32), 166 (32), 140 (24), 113 (5). This is consistent with the data reported previously.[371]

6.3.3 Experimental details for the reactions reported in Chapter 4

Conversion of grey selenium to red selenium

Grey selenium (1.70 g, 21.5 mmol, 1.0 equiv) was added to conc. sulfuric acid (100 mL) and the reaction mixture stirred at 180 °C for 2 h. The reaction mixture was filtered through a sintered funnel directly onto ice (250 mL) and the resulting solution left to recrystallize at 4 °C overnight. The mixture was then filtered and the filtrate washed with additional water (3x20 mL) and with acetone (3x20 mL). The red solid obtained was then dried overnight on P_2O_5 to give 1.65 g (97% yield) of Se_8. This is consistent with the data reported previously.[376]

Tetramethyl ammoniumtrifluoromethyselenol, $(CH_3)_4NSeCF_3$ **346**.

$$(CH_3)_4NSeCF_3$$
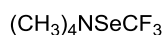
346

Trifluoromethyl(trimethyl)silane (3.25 g, 22.9 mmol, 8.5 equiv) was added to activated molecular sieves (20 g) in anhydrous dimethoxyethane (30 mL), inside a glovebox. The reaction mixture was taken out of the glovebox and stirred at −60 °C for 15 min before red selenium (S_8, 1.70 g, 2.69 mmol, 1.0 equiv) was added and the reaction mixture stirred at the same temperature for a further 15 min. Tetramethylammonium fluoride (2.03 g, 21.8 mmol, 8.1 equiv) was then added and stirred for 1 h at −60 °C. The reaction mixture was brought to room temperature and stirred for a further 24 h. The reaction mixture was transferred to the glovebox and the solvent decanted. The residue was washed with anhydrous acetonitrile (3 x 25 mL). The filtrate was collected and the solvent evaporated to give the product **346** (2.92 g, 78%) as a light brown solid. δ_H (300 MHz, $(CD_3)_2CO$) 3.20 (12 H, s, N-CH_3), δ_F (319 MHz, $(CD_3)_2CO$) -6.57. This is consistent with the data reported previously.[357]

Trifluoromethylselenol(tri-*tert*-butylphosphine)palladium(I) dimer, Pd(I)-SeCF$_3$ dimer **347**
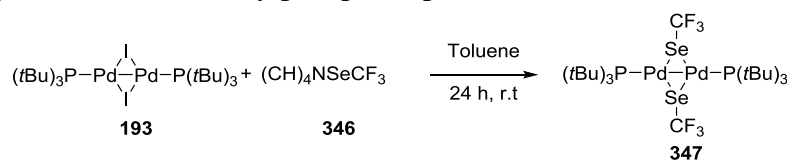
Pd(I)-iodo-dimer **193** (60 mg, 0.07 mmol, 1.0 equiv), $(CH_3)_4NSeCF_3$ **346** (30.7 mg, 0.14 mmol, 2.0 equiv) and dry toluene (5.0 ml, previously deoxygenated for 30 min) were added in a dry reaction vessel with dark glass wall equipped with a stirring bar. The reaction was stirred for 24 h at room temperature, then filtered and the solvent evaporated to give 51 mg of Pd(I)-SeCF$_3$ dimer **347** as a dark brown solid in 80% yield. δ_P (243 MHz, toluene) 99.1. δ_F (564 MHz, toluene) −24.6.

4-[(Trifluoromethyl)seleno]biphenyl**,** *Table 40* Entry 1
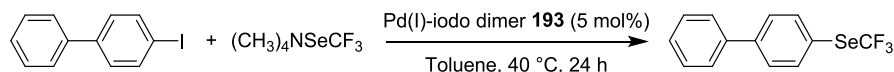
The general procedure G was followed for the synthesis of 4-[(trifluoromethyl)seleno]biphenyl. The residue was purified by flash chromatography on silica gel using pure hexane as eluent, to afford 4-[(trifluoromethyl)seleno]biphenyl as a white solid in 96% yield (58 mg): δ_H (600 MHz, CDCl$_3$) 7.81 (2 H, d, J =8.2 Hz, Ar-*H*), 7.62-7.58 (4 H, m, Ar-*H*), 7.48-7-46 (2 H, m, Ar-*H*), 7.37-7.40 (1 H, m, Ar-*H*). δ_C (151 MHz, CDCl$_3$) 143.32 (*C*), 139.78 (*C*), 137.41 (*C*H), 128.93 (*C*H), 128.24 (*C*H), 128.04 (*C*H), 127.19 (*C*H), 122.52 (1 C, q, J^1_{C-F} = 332.8 Hz, *C*F$_3$), 121.22 (*C*). δ_F (564 MHz, CDCl$_3$) −36.07. *m/z* (EI) 302 (100%, M+), 233.0 (97), 152.0 (80). This is consistent with the data reported previously.[377]

1-Methyl-4-[(trifluoromethyl)seleno]benzene, *Table 40* Entry 2
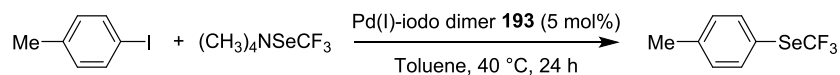
The general procedure G was followed for the synthesis of 1-methyl-4-[(trifluoromethyl)seleno]benzene. The residue was purified by flash chromatography on silica gel using pure pentane as eluent, to afford 1-methyl-4-[(trifluoromethyl)seleno]benzene as a colorless oil in 84% (40 mg) yield. δ_H (600 MHz, CDCl$_3$) 7.62 (2 H, d, J = 8.0 Hz, Ar-*H*), 7.20 (2 H, d, J = 8.0 Hz, Ar-*H*), 2.39 (3 H, s, C*H*$_3$). δ_C (151 MHz, CDCl$_3$) 140.74 (*C*), 137.08 (*C*H), 130.36 (*C*H), 122.52 (1 C, q, J^1_{C-F} = 332.8 Hz, *C*F$_3$), 118.97 (*C*), 21.33 (*C*H$_3$). δ_F (564 MHz, CDCl$_3$) −36.55. *m/z* (EI): 240.0 (100%, M+), 170.0 (96), 141.0 (22), 91.0 (59). This is consistent with the data reported previously.[377]

1-Methoxy-4-[(trifluoromethyl)seleno]benzene, *Table 40* Entry 3
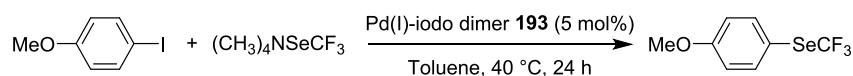
The general procedure G was followed for the synthesis of 1-methoxy-4-[(trifluoromethyl)seleno]benzene. The residue was purified by flash chromatography on silica gel using pure pentane as eluent, to afford

1-methoxy-4-[(trifluoromethyl)seleno]benzene as a colorless oil in 88% (45 mg) yield. δ_H (600 MHz, CDCl$_3$) 7.65 (2 H, d, J = 8.6 Hz, Ar-H), 6.90 (2 H, d, J = 8.6 Hz, Ar-H), 3.83 (3 H, s, OCH_3). δ_C (151 MHz, CDCl$_3$) 161.39 (*C*), 138.93 (*CH*), 122.46 (1 C, q, J^1_{C-F} = 332.8 Hz, *CF$_3$*), 115.15 (*CH*), 112.87 (*C*), 55.35 (O*CH$_3$*). δ_F (564 MHz, CDCl$_3$) −37.20. *m/z* (EI): 256.0 (81%, M+), 187.0 (100), 157.0 (19). This is consistent with the data reported previously.[377]

1-*tert*-Butyl-4-[(trifluoromethyl)seleno]benzene, *Table 40* Entry 4
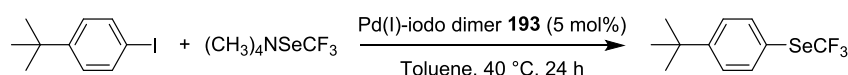
The general procedure G was followed for the synthesis of 1-*tert*-butyl-4-[(trifluoromethyl)seleno]benzene. The residue was purified by flash chromatography on silica gel using pure hexane as eluent, to afford 1-*tert*-butyl-4-[(trifluoromethyl)seleno]benzene as a colorless oil in 80% (45 mg) yield. δ_H (600 MHz, CDCl$_3$) 7.65 (2 H, d, J = 8.5 Hz, Ar-H), 7.40 (2H, d, J = 8.5 Hz, Ar-H), 1.33 (9 H, s, CCH_3). δ_C (151 MHz, CDCl$_3$) 153.75 (*C*), 136.80 (*CH*), 126.68 (*CH*), 122.54 (1 C, d, J^1_{C-F} = 333.0 Hz, *CF$_3$*), 119.07 (*C*), 34.8 (*C*), 31.15 (*C*(CH$_3$)$_3$). δ_F (564 MHz, CDCl$_3$) −36.31. *m/z* (EI): 282 (41%, M+), 267.0 (100) , 198.0 (18), 118 (26). This is consistent with the data reported previously.[377]

2-[(Trifluoromethyl)seleno]biphenyl, *Table 40* Entry 5
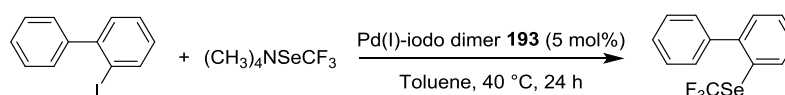
The general procedure G was followed for the synthesis of 2-[(trifluoromethyl)seleno]biphenyl. The residue was purified by flash chromatography on silica gel using as eluent a mixture of hexane/Et$_2$O (95:5), to afford 2-[(trifluoromethyl)seleno]biphenyl as a white solid in 99% (60 mg) yield. δ_H (600 MHz, CDCl$_3$) 7.89 (1 H, d, J = 7.9 Hz, Ar-H), 7.51-7.48 (1 H, m, Ar-H), 7.47–7.41 (4 H, m, Ar-H), 7.39–7.36 (1 H, m, Ar-H), 7.31–7.28 (2 H, m, Ar-H). δ_C (151 MHz, CDCl$_3$) 147.04 (*C*), 141.45 (*C*), 136.80 (*CH*), 130.78 (*CH*), 129.88 (*CH*), 129.37 (*CH*), 128.31 (*CH*), 127.99 (*CH*), 127.75 (*CH*), 123.36 (*C*), 122.49 (1 C, q, J^1_{C-F} = 333.1 Hz, *CF$_3$*). δ_F (564 MHz, CDCl$_3$) −35.46. *m/z* (EI): 302.0 (57%, M+), 233.0 (100), 152.0 (57). This is consistent with the data reported previously.[378]

1-[4-(Trifluoromethyl)selenophenyl]pyrrole, *Table 40* Entry 6
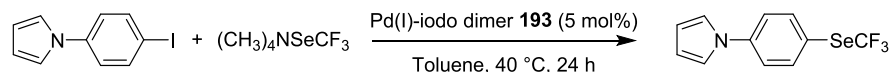
The general procedure G was followed for the synthesis of *1-[4-(trifluoromethyl)selenophenyl]pyrrole*. The residue was purified by flash chromatography on silica gel using as eluent pure pentane, to afford *1-[4-(trifluoromethyl)selenophenyl]pyrrole* as an off-white solid in 83% (49 mg) yield. δ_H (600 MHz, CDCl$_3$) 7.79 (2 H, d, J = 8.6 Hz, Ar-*H*), 7.41 (2 H, d, J = 8.6 Hz, Ar-*H*), 7.13–7.10 (2 H, m, NC-*H*), 6.38-6.36 (2 H, m, NCH*C-H*). δ_C (151 MHz, CDCl$_3$) 142.29 (*C*), 138.60 (*CH*), 122.41 (1 C, q, $J^1_{C\text{-}F}$ = 333.1 Hz, *C*F$_3$), 120.89 (*CH*), 119.04 (*CH*), 118.53 (*C*), 111.36 (*CH*). δ_F (564 MHz, CDCl$_3$) –36.37. IR: ν_{max}/cm^{-1} 3146, 1904, 1593, 1539, 1502, 1325, 1089, 914, 819, 719. *m/z* (EI): 291.0 (96%, M$^+$), 222.0 (100), 192 (21), 141.0 (27), 115.0 (37). HRMS(ESI): Calculated for [M+H]$^+$ C$_{11}$H$_9$NF$_3$Se: 291.98468; Found: 291.98456.

1-Morpholino-4-[(trifluoromethyl)seleno]benzene, *Table 40* Entry 7
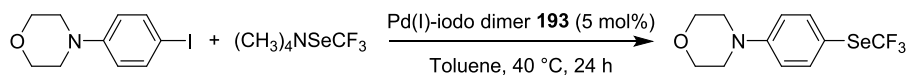
The general procedure G was followed for the synthesis of *1-morpholino-4-[(trifluoromethyl)seleno]benzene*. The residue was purified by flash chromatography on silica gel using as eluent a gradient mixture of hexane/Et$_2$O (from pure hexane to 9:1), to afford *1-morpholino-4-[(trifluoromethyl)seleno]benzene* as a yellow oil in 80% (50 mg) yiled. δ_H (600 MHz, CDCl$_3$) 7.61 (2 H, d, J = 8.9 Hz, Ar-*H*), 6.86 (2 H, d, J = 8.9 Hz, Ar-*H*), 3.87–3.84 (4 H, m, OC*H*$_2$CH$_2$), 3.24–3.21 (4 H, m, NC*H*$_2$CH$_2$). δ_C (151 MHz, CDCl$_3$) 152.49 (*C*), 138.55 (*CH*), 122.49 (1 C, q, $J^1_{C\text{-}F}$ = 333.2 Hz, *C*F$_3$), 115.54 (*CH*), 110.98 (*C*), 66.65 (O*C*H$_2$), 48.05 (N*C*H$_2$) . δ_F (564 MHz, CDCl$_3$) –37.34. IR: ν_{max}/cm^{-1} 3846, 3454, 2964, 2846, 1740, 1586, 1367, 1231, 1102, 927, 815, 735. *m/z* (EI): 311.0 (93%, M+), 242.0 (100), 184.0 (73). HRMS(ESI): Calculated for [M+H]$^+$ C$_{11}$H$_{13}$ONF$_3$Se: 312.01090; Found: 312.01096.

1-n-Butyl-4-[(trifluoromethyl)seleno]benzene, *Table 40* Entry 9
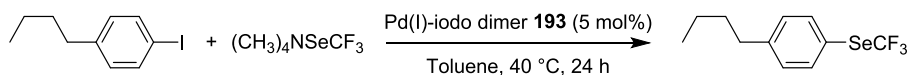
The general procedure G was followed for the synthesis of *1-n-butyl-4-[(trifluoromethyl)seleno]benzene*. The residue was purified by flash chromatography on silica gel using pure hexane as eluent, to afford *1-tert-butyl-4-[(trifluoromethyl)seleno]benzene* as a colorless oil in 75% (42 mg) yield. δ_H (600 MHz, CDCl$_3$) 7.64 (2 H, d, $J = 8.1$ Hz, Ar-*H*), 7.20 (2 H, d, $J = 8.1$ Hz, Ar-*H*), 2.64 (2 H, t, $J = 7.8$, Ar-C*H$_2$*CH$_2$), 1.63–1.59 (2 H, m, Ar-CH$_2$C*H$_2$*), 1.39–1.34 (2 H, m, CH$_2$C*H$_2$*CH$_3$), 0.94 (3 H, t, $J = 7.4$ Hz, CH$_2$CH$_2$C*H$_3$*). δ_C (151 MHz, CDCl$_3$) 145.64 (*C*), 137.06 (*C*H), 129.70 (*C*H), 122.54 (1 C, q, $J^1_{C\text{-}F} = 332.7$ Hz, *C*F$_3$), 119.16 (*C*), 35.40 (Ar-*C*H$_2$CH$_2$), 33.34 (Ar-CH$_2$*C*H$_2$), 22.32 (*C*H$_2$CH$_3$), 13.89 (CH$_2$*C*H$_3$). δ_F (564 MHz, CDCl$_3$) –36.46. IR: v_{max}/cm^{-1} 2933, 2865, 2325, 1740, 1457, 1369, 1099, 818, 737. *m/z* (EI): 282 (68%, M+), 238.9 (100), 169.9 (46), 91 (24). HRMS(ESI): Calculated for [M+Na]$^+$ C$_{15}$H$_{10}$F$_3$SeNa: 305.00268; Found: 305.00266.

1-Methoxy-2-[(trifluoromethyl)seleno]benzene, *Table 40* Entry 10
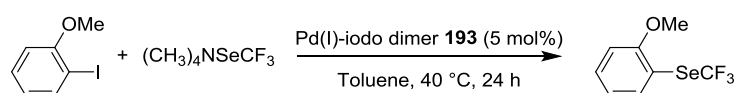
The general procedure G was followed for the synthesis of 1-methoxy-2-[(trifluoromethyl)seleno]benzene. The residue was purified by flash chromatography on silica gel using pure pentane as eluent, to afford 2-methoxy-4-[(trifluoromethyl)seleno]benzene as yellow oil in 59% (30 mg) yield. δ_H (600 MHz, CDCl$_3$) 7.67 (1 H, d, $J = 7.8$ Hz, Ar-*H*), 7.44–7.39 (1 H, m, Ar-*H*), 6.96 (2 H, m, Ar-*H*), 3.89 (3 H, s, OC*H$_3$*). δ_C (151 MHz, CDCl$_3$) 159.03 (*C*), 137.27 (*C*H), 131.79 (*C*H), 122.51 (1 C, q, $J^1_{C\text{-}F} = 333.1$ Hz, *C*F$_3$), 121.61 (*C*H), 112.38 (*C*), 111.34 (*C*H), 56.05 (O*C*H$_3$). δ_F (564 MHz, CDCl$_3$) –35.26. *m/z* (EI): 256.0 (100%, M+), 187.0 (13), 157 (44). This is consistent with the data reported previously.[365]

1-Cyano-4-[(trifluoromethyl)seleno]benzene, *Table 41* Entry 1
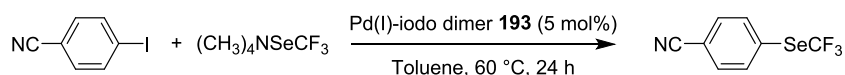
The general procedure H was followed for the synthesis of 1-cyano-4-[(trifluoromethyl)seleno]benzene. The residue was purified by flash chromatography on silica gel using as eluent a mixture of pentane/Et$_2$O (from 95:5 to 80:20), to afford 1-cyano-4-[(trifluoromethyl)seleno]benzene as a white solid in 99% (50 mg) yield. δ_H (600 MHz, CDCl$_3$) 7.85 (2 H, d, $J = 8.3$ Hz, Ar-*H*), 7.68 (2 H, d, $J = 8.3$ Hz, Ar-*H*), δ_C (151 MHz, CDCl$_3$) 136.88 (*C*H), 132.87 (*C*H), 128.42 (*C*), 122.20 (1 C, q, $J^1_{C\text{-}F} = 333.1$ Hz, CF$_3$), 117.73 (*C*N), 114.23 (*C*). δ_F (564 MHz, CDCl$_3$) –34.89. *m/z* (EI): 250.9 (64%, M+), 181.9 (100), 152.0 (18). This is consistent with the data reported previously.[377]

1-Nitro-4-[(trifluoromethyl)seleno]benzene, *Table 41* Entry 2
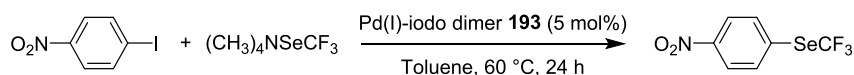
The general procedure H was followed for the synthesis of 1-nitro-4-[(trifluoromethyl)seleno]benzene. The residue was purified by flash chromatography on silica gel using as eluent a mixture pentane/Et$_2$O (99:1), to afford 1-nitro-4-[(trifluoromethyl)seleno]benzene as a light yellow oil in 84% yield (45 mg). δ_H (600 MHz, CDCl$_3$) 8.23 (2 H, d, J = 8.8 Hz, Ar-H), 7.91 (2 H, d, J = 8.8 Hz, Ar-H). δ_C (151 MHz, CDCl$_3$) 148.95 (C), 137.02 (CH), 130.44 (C), 124.35 (CH), 122.16 (1 C, q, $J^1_{C\text{-}F}$ = 333.0 Hz, CF$_3$). δ_F (564 MHz, CDCl$_3$) −34.73. *m/z* (EI): 270.9 (100 %, M+), 240.9 (17), 172.0 (34), 145.0 (60). This is consistent with the data reported previously.[377]

1-Acetyl-3-[(trifluoromethyl)seleno]benzene, Table 41 Entry 5
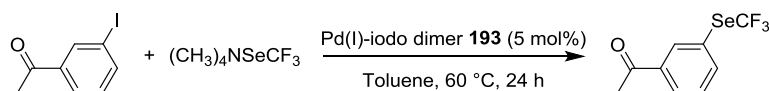
The general procedure H was followed for the synthesis of *1-acetyl-3-[(trifluoromethyl)seleno]benzene*. The residue was purified by flash chromatography on silica gel using as eluent a mixture of pentane/Et$_2$O (99:1), to afford *1-acetyl-3-[(trifluoromethyl)seleno]benzene* as an orange oil (26 mg, 48%) yield. δ_H (600 MHz, CDCl$_3$) 8.31 (1H, s, Ar-H), 8.05 (1 H, d, J= 7.8 Hz, Ar-H), 7.94 (1 H, d, J = 7.8 Hz, Ar-H), 7.52-7.50 (1 H, m, Ar-H), 2.63 (3 H, s, O=CCH_3). δ_C (151 MHz, CDCl$_3$) 196.73 (O=CCH$_3$), 141.22 (CH), 138.21 (C), 136.71 (CH), 130.03 (CH), 129.84 (CH), 123.17 (C), 122.37 (1 C, q, $J^1_{C\text{-}F}$ =332.8 Hz, CF$_3$), 26.64 (O=CCH$_3$). δ_F (564 MHz, CDCl$_3$) −35.75. IR: ν_{max}/cm^{-1} 3364, 2921, 2331, 1908, 1688, 1570, 1415, 1357, 1250, 1096, 792, 737, 685. *m/z* (EI): 269.9 (50%, M+), 252.9 (100), 184.0 (88), 144.9 (31). HRMS(ESI): Calculated for [M+H]$^+$ C$_9$H$_8$OF$_3$Se: 268.96870; Found: 268.96869.

1-Cyano-3-[(trifluoromethyl)seleno]benzene, *Table 41* Entry 8
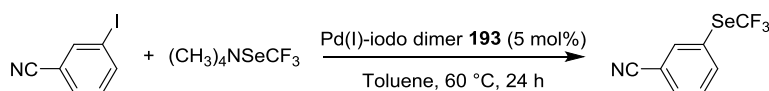
The general procedure H was followed for the synthesis of 1-cyano-3-[(trifluoromethyl)seleno]benzene. The residue was purified by flash chromatography on silica gel using as eluent a mixture of pentane/Et$_2$O (from 95:5 to 80:20), to afford

1-cyano-3-[(trifluoromethyl)seleno]benzene as an orange oil in 90% (45 mg) yield. δ_H 8.04 (1 H, s, Ar-*H*), 7.98 (1 H, d, *J* = 7.8 Hz, Ar-*H*), 7.77 (1 H, d, *J* = 8.8 Hz, Ar-*H*), 7.54-752 (1 H, m, Ar-*H*). δ_C (151 MHz, CDCl$_3$) 141.04 (*C*H), 139.96 (*C*H), 133.78 (*C*H), 130.27 (*C*H), 123.77 (*C*), 122.15 (1 C, q, J^1_{C-F} = 332.9 Hz, *C*F$_3$), 117.35 (*C*N), 114.03 (*C*). δ_F (564 MHz, CDCl$_3$) −35.43. *m/z* (EI): 250.9 (82%, M+), 181.9 (100), 152.0 (27). This is consistent with the data reported previously.[365]

3-[(Trifluoromethyl)seleno]benzaldehyde, *Table 41* Entry 9
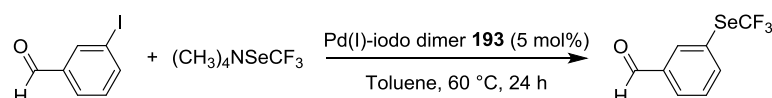
The general procedure H was followed for the synthesis of *3-[(trifluoromethyl)seleno]benzaldehyde*. The residue was purified by flash chromatography on silica gel using as eluent a mixture of pentane/Et$_2$O (99:1), to afford *3-[(trifluoromethyl)seleno]benzaldehyde* as a light yellow oil in 49% (25 mg) yield. δ_H (600 MHz, CDCl$_3$) 10.04 (1 H, s, O=C*H*), 8.24 (1 H, s, Ar-*H*), 8.03–7.93 (2 H, m, Ar-*H*), 7.59-7-56 (1 H, m, Ar-*H*). δ_C (151 MHz, CDCl$_3$) 190.85 (O=*C*H), 142.46 (*C*H), 137.95 (*C*H), 137.40 (*C*), 131.20 (*C*H), 130.27 (*C*H), 123.69 (*C*), 122.33 (1 C, q, J^1_{C-F} =332.9 Hz, *C*F$_3$). δ_F (564 MHz, CDCl$_3$) −35.60. IR: v_{max}/cm^{-1} 3855, 2310, 2095, 1699, 1578, 1093, 797, 745, 681. *m/z* (EI): 253.9 (100%, M+), 184.9 (35), 155.0 (22). HRMS(ESI): Calculated for [M+H]$^+$ C$_8$H$_6$OF$_3$Se: 254.95305; Found: 254.95302.

2-[(Trifluoromethyl)seleno]naphthalene, *Table 42* Entry 1
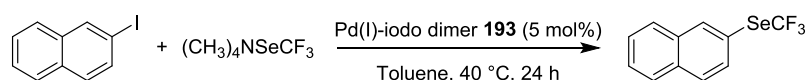
The general procedure G was followed for the synthesis of *2-[(trifluoromethyl)seleno]naphthalene*. The residue was purified by flash chromatography on silica gel using pure hexane as eluent, to afford *2-[(trifluoromethyl)seleno]benzen*e as a colorless oil in 68% (35 mg) yield. δ_H (600 MHz, CDCl$_3$) 8.29 (1H, s, Ar-*H*), 7.89-7.83 (3 H, m, Ar-*H*), 7.78-7.77 (1 H, m, Ar-*H*), 7.60–7.53 (2 H, m, Ar-*H*). δ_C (151 MHz, CDCl$_3$) 137.49 (*C*H), 133.61 (*C*), 133.57(*C*), 132.77 (*C*H), 129.15 (*C*H), 128.07 (*C*H), 127.80 (*C*H), 127.66 (*C*H), 126.90 (*C*H), 122.59 (1 C, q, J^1_{C-F} = 333.1 Hz, *C*F$_3$), 119.69 (*C*). δ_F (564 MHz, CDCl$_3$) −35.84. IR: v_{max}/cm^{-1} 3844, 3452, 3055, 2314, 2104, 1714, 1358, 1094, 854, 812, 740. *m/z* (EI): 275.9 (85%, M+), 207.0 (100), 115.0 (85). HRMS (atmospheric pressure chemical ionization (APCI)): Calculated for [M+H]$^+$ C$_{11}$H$_8$F$_3$Se: 276.97378; Found: 276.97372.

9-[(Trifluoromethyl)seleno]phenanthrene, *Table 42* Entry 2
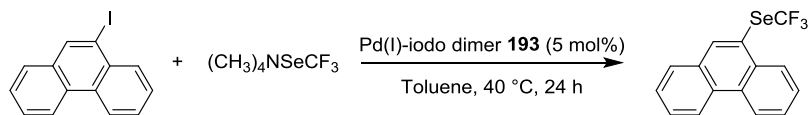
The general procedure G was followed for the synthesis of *9-[(trifluoromethyl)seleno]phenanthrene*. The residue was purified by 2 consecutive recrystallizations in warm hexane. The resulting solids were combined to afford *9-[(trifluoromethyl)seleno]phenanthrene* as an orange solid in 85% (55 mg) yield. δ_H (600 MHz, CDCl$_3$) 8.75–8.71 (2 H, m, Ar-*H*), 8.61–8.58 (1 H, m, Ar-*H*), 8.43 (1 H, s, Ar-*H*), 7.93 (1 H, d, *J* = 7.9 Hz, Ar-*H*), 7.78–7.70 (3 H, m, Ar-*H*), 7.66-7.65 (1 H, m, Ar-*H*). δ_C (151 MHz, CDCl$_3$) 140.63 (*CH*), 132.63 (*C*), 131.68 (*C*), 131.31 (*C*), 130.96 (*C*), 129.17 (*CH*), 129.12 (*CH*), 128.58 (*CH*), 127.51 (*CH*), 127.39 (*CH*), 127.23 (*CH*), 122.98 (*CH*), 122.74 (*CH*), 122.24 (1 C, q, $J^1_{C\text{-}F}$=356.5 Hz, *CF$_3$*), 121.8 (*C*). δ_F (564 MHz, CDCl$_3$) −35.28. IR: ν_{max}/cm^{-1} 3845, 3456, 3015, 1739, 1366, 1218, 1094, 889, 855, 749. *m/z* (EI): 326.0 (91%, M+), 257.0 (100), 165.0 (77). HRMS: (ESI): Calculated for [M]$^+$ C$_{15}$H$_9$F$_3$Se: 325.98161; Found: 325.98201.

1-[(Trifluoromethyl)seleno]naphthalene, *Table 42* Entry 3
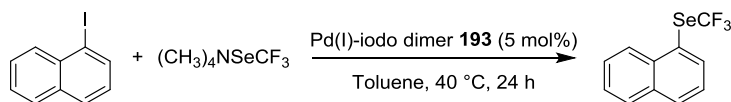
The general procedure G was followed for the synthesis of 1-[(Trifluoromethyl)seleno]naphthalene. The residue was purified by flash chromatography on silica gel using pure pentane as eluent, to afford 1-[(trifluoromethyl)seleno]naphthalene as a light yellow oil in 55% (30 mg) yield. δ_H (600 MHz, CDCl$_3$) 8.49 (1 H, d, *J* = 8.5 Hz, Ar-*H*), 8.08 (1 H, d, *J* = 7.1 Hz, Ar-*H*), 8.00 (1 H, d, *J* = 8.2 Hz, Ar-*H*), 7.88 (1 H, d, *J* = 8.2 Hz, Ar-*H*), 7.65–7.61 (1 H, m, Ar-*H*), 7.59–7.55 (1 H, m, Ar-*H*), 7.49-7.47 (1 H, m, Ar-*H*). δ_C (151 MHz, CDCl$_3$) 138.46 (*CH*), 135.29 (*C*), 134.18 (*C*), 131.97 (*CH*), 128.59 (*CH*), 128.12 (*CH*), 127.60 (*CH*), 126.68 (*CH*), 125.76 (*CH*), 122.52 (1 C, q, $J^1_{C\text{-}F}$ =334.0 Hz, *CF$_3$*), 122.08 (*C*). δ_F (564 MHz, CDCl$_3$) −35.44. *m/z* (EI): 276.0 (86%, M+), 207.0 (100), 115.0 (57). This is consistent with the data reported previously.[376]

4-[(Trifluoromethyl)seleno]-1-indanone, *Table 42* Entry 4
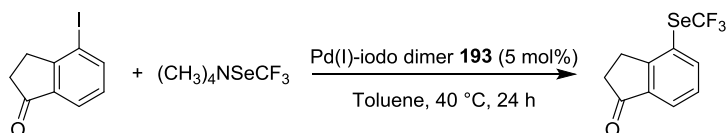
The general procedure G was followed for the synthesis of *4-[(trifluoromethyl)seleno]-1-indanone*. The residue was purified by flash chromatography on silica gel using as eluent mixture hexane/Et$_2$O (95:5), to afford *4-[(trifluoromethyl)seleno]1-indanone* as yellow oil in 93% (52 mg) yield. δ_H (600 MHz, CDCl$_3$) 8.01 (1 H, d, *J* = 7.5 Hz, Ar-*H*), 7.89 (1 H, d, *J* = 7.6 Hz, Ar-*H*), 7.44-7.42 (1 H, m, Ar-*H*), 3.28-3.24 (2 H, m, C=OCH$_2$C*H*$_2$), 2.77–2.73 (2 H, m, C=OC*H*$_2$CH$_2$). δ_C (151 MHz, CDCl$_3$) 206.03 (*C*=O), 160.03 (*C*), 144.08 (*C*H), 138.53 (*C*), 128.78 (*C*H), 126.37 (*C*H), 122.45 (1 C, q, $J^1_{C\text{-}F}$ = 333.3 Hz, *C*F$_3$), 121.68 (*C*), 36.15 (C=O*C*H$_2$CH$_2$), 27.47 (C=OCH$_2$*C*H$_2$). δ_F (564 MHz, CDCl$_3$) –34.75. IR: v_{max}/cm^{-1} 3853, 3403, 2952, 1712, 1586, 1366, 1218, 1092, 788, 737, 686. *m/z* (EI): 280.0 (96%, M+), 211.0 (92), 183.0 (71), 102.0 (100), 77 (29). HRMS(ESI): Calculated for [M+Na]$^+$ C$_{10}$H$_7$ONaF$_3$Se: 302.95064; Found: 302.95062.

9-[(Trifluoromethyl)seleno]anthracene, *Table 42* Entry 5
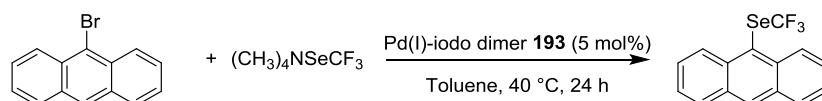
The general procedure G was followed for the synthesis of *9-[(trifluoromethyl)seleno]anthracene*. The residue was purified by recrystallization in warm hexane. The solution was kept and the solvent removed under reduced pressure to afford *9-[(trifluoromethyl)seleno]anthracene* as a bright yellow solid in 84% (55 mg) yield. δ_H (600 MHz, CDCl$_3$) 8.88 (2 H, d, *J* = 8.9 Hz, Ar-*H*), 8.65 (1 H, s, Ar-*H*), 8.04 (2 H, d, *J* = 8.4 Hz, Ar-*H*), 7.68-7.62 (2 H, m, Ar-*H*), 7.58-7.50 (2 H, m, Ar-*H*). δ_C (151 MHz, CDCl$_3$) 135.90 (*C*), 132.17 (*C*H), 131.75 (*C*), 129.02 (*C*H), 128.90 (*C*H), 127.66 (*C*H), 125.59 (*C*H), 120.63 (1 C, q, $J^1_{C\text{-}F}$ =260.5 Hz, *C*), 120.55 (*C*). δ_F (564 MHz, CDCl$_3$) –34.58. IR: v_{max}/cm^{-1} 3847, 3456, 3015, 1739, 1439, 1368, 1218, 1087, 897, 844, 773, 727. *m/z* (EI): 326.0 (60%, M+), 257.0 (100), 165.0 (53). HRMS(ESI): Calculated for [M+H]$^+$ C$_{15}$H$_{10}$F$_3$Se: 326.98943; Found: 326.98856.

5-[(Trifluoromethyl)seleno]indole, *Table 42* Entry 7
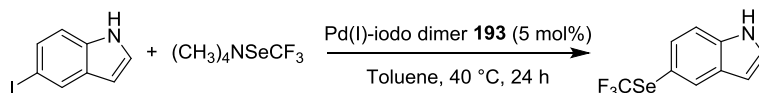
The general procedure G was followed for the synthesis of *5-[(Trifluoromethyl)seleno]indole*. The residue was purified by flash chromatography on silica gel using as eluent a gradient mixture of pentane/Et$_2$O (from pure pentane to 1:1), to afford *5-[(trifluoromethyl)seleno]indole* as a yellow oil 94% (50 mg) yield. δ_H (600 MHz, CDCl$_3$) 8.29 (1 H, s, N-*H*), 8.07 (1 H, s, Ar-*H*), 7.54 (1 H, d, *J* = 8.4 Hz, Ar-*H*), 7.40 (1 H,

d, J = 8.4 Hz), 7.28–7.26 (1 H, m, Ar-H), 6.61–6.59 (1 H, m, Ar-H). δ_C (151 MHz, CDCl$_3$) 136.42 (C), 130.81 (CH), 130.54 (CH), 128.92 (C), 125.37 (CH), 122.69 (1 C, q, $J^1_{C\text{-}F}$ = 333.5 Hz, CF_3), 112.48 (C), 112.00 (CH), 103.08 (CH). δ_F (564 MHz, CDCl$_3$) −37.25. IR: v_{max}/cm^{-1} 3379, 1721, 1602, 1451, 1410, 1313, 1083, 882, 803, 762, 726, 664. m/z (EI): 265.0 (72%, M+), 196.0 (100), 166.0 (21). HRMS(ESI): Calculated for [M+H]$^+$ C$_9$H$_7$NF$_3$Se: 265.96903; Found: 265.96902.

1-Amino-4-[(trifluoromethyl)seleno]benzene, *Table 43* Entry 1
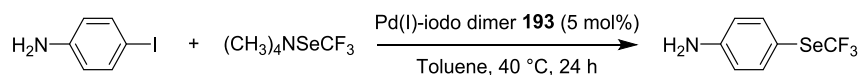
The general procedure G was followed for the synthesis of *1-amino-4-[(trifluoromethyl)seleno]benzene*. The residue was purified by flash chromatography on silica gel using as eluent a gradient of pentane/Et$_2$O (from pure pentane to 1:1), to afford *1-amino-4[(trifluoromethyl)seleno]benzene* as a yellow oil in 73% (35 mg) yield. δ_H (600 MHz, toluene-d_8) 7.28 (2 H, d, J=8.5 Hz, Ar-H), 5.94 (2 H, d, J=8.5 Hz, Ar-H), 2.75 (2 H, s, NH_2). δ_C (151 MHz, toluene-d_8) 153.80 (C), 143.66 (C), 142.08 (CH), 128.04 (1 C, q, $J^1_{C\text{-}F}$ = 333.4 Hz, CF_3), 120.00 (CH). δ_F (564 MHz, toluene-d_8) −32.82. IR: v_{max}/cm^{-1} 3457, 3005, 2318, 2093, 1740, 1366, 1216, 898, 777. m/z (EI): 240.9 (67%, M+), 171.9 (100), 142.0 (22), 80.0 (50), 57 (100). HRMS(ESI): Calculated for [M+H]$^+$ C$_7$H$_7$NF$_3$Se: 241.96903; Found: 241.96904

1-Amino-2-fluoro-4-[(trifluoromethyl)seleno]benzene, *Table 43* Entry 2
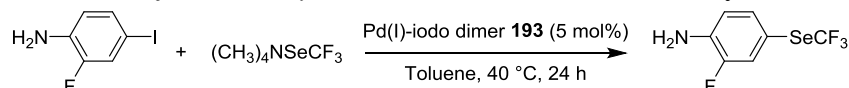
The general procedure G was followed for the synthesis of *1-amino-2-fluoro-4[(trifluoromethyl)seleno]benzene*. The residue was purified by flash chromatography on silica gel using as eluent a gradient mixture of pentane/Et$_2$O (from pure pentane to 1:1), to afford *1-amino-2-fluoro-4[(trifluoromethyl)seleno]benzene* as a yellow oil in 95% (45 mg) yield. δ_H (600 MHz, toluene-d_8) 7.15–7.11 (1 H, m, Ar-H), 7.00 (1 H, d, J = 8.2 Hz, Ar-H), 5.90–5.83 (1 H, m, Ar-H), 2.94 (2 H, s, NH_2). δ_C (151 MHz, toluene-d_8) 151.20 (C), 149.59 (C), 137.23 (C), 134.14 (CH), 123.89 (1 C, d, $J^3_{C\text{-}F}$ =19.2 Hz, CF), 122.6 (1 C, q, $J^1_{C\text{-}F}$ = 333.6 Hz CF_3), 116.28 (CH). δ_F (564 MHz, toluene-d_8) −37.6 (3 F, s, CF_3), −134.15 (1 F, t, J^3 = 9.8 Hz, CF). IR: v_{max}/cm^{-1} 3855, 3400, 2307, 1623, 1500, 1297, 1204, 1091, 879, 812, 734, 675. m/z (EI): 258.9 (74%, M+), 189.9 (100), 160.0 (24), 98.0 (34). HRMS(ESI): Calculated for [M+H]$^+$ C$_7$H$_6$NF$_4$Se: 259.95961; Found: 259.95959.

1-Amino-3-[(trifluoromethyl)seleno]benzene, *Table 43* Entry 3
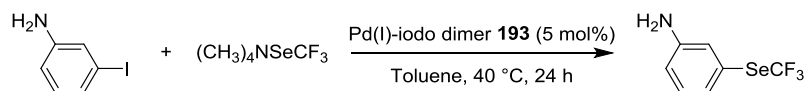
The general procedure G was followed for the synthesis of *1-amino-3-[(trifluoromethyl)seleno]benzene*. The residue was purified by flash chromatography on silica gel using as eluent a mixture of pentane/EtOAc (95:5), to afford *1-amino-3-[(trifluoromethyl)seleno]benzene* as a colorless oil in 81% (39 mg) yield. δ_H (600 MHz, C_6D_6) 6.97 (1 H, d, J = 7.6 Hz, Ar-*H*), 6.77-6.75 (1 H, m, Ar-*H*), 6.63 (1 H, s, Ar-*H*), 6.09 (1 H, d, J = 8.1 Hz, Ar-*H*), 2.63 (2 H, s, NH$_2$). δ_C (151 MHz, C_6D_6) 147.58 (*C*), 129.87 (*C*H), 125.95 (*C*H), 123.14 (1 C, q, J^1_{C-F} = 332.6 Hz *C*F$_3$), 122.73 (*C*), 122.38 (*C*H), 116.14 (*C*H). δ_F (564 MHz, C_6D_6) −36.01. IR: v_{max}/cm^{-1} 3476, 3373, 1721, 1620, 1591, 1479, 1265, 1093, 862, 775, 736, 681. *m/z* (EI): 241.0 (100%, M+), 172.0 (72), 142.0 (22), 80.1 (56). HRMS(ESI): Calculated for [M+H]$^+$ $C_7H_7NF_3Se$: 241.96903; Found: 241.96844.

1-Amino-2-[(trifluoromethyl)seleno]benzene, *Table 43* Entry 4
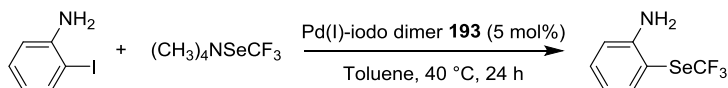
The general procedure G was followed for the synthesis of *1-amino-2-[(trifluoromethyl)seleno]benzene*. The residue was purified by flash chromatography on silica gel using as eluent a mixture of pentane/EtOAc (95:5), to afford *1-amino-2-[(trifluoromethyl)seleno]benzene* as an off-white solid in 62% (30 mg) yield. δ_H (600 MHz, C_6D_6) 7.42 (1 H, d, J = 9.1 Hz, Ar-*H*), 6.89-6.88 (1 H, m, Ar-*H*), 6.35-6.33 (1 H, m, Ar-*H*), 6.18 (1 H, d, J = 9.3 Hz, Ar-*H*), 3.62 (2 H, s, N*H*$_2$). δ_C (151 MHz, C_6D_6) 149.70 (*C*), 139.77 (*C*H), 132.46 (*C*H), 122.82 (1 C, q, J^1_{C-F} =334.9 Hz, *C*F$_3$), 118.24 (*C*H), 114.81 (*C*H), 106.14 (*C*). δ_F (564 MHz, C_6D_6) −35.94. IR: v_{max}/cm^{-1} 3456, 3336, 2925, 1612, 1475, 1309, 1092, 853, 803, 751. *m/z* (EI): 241.0 (74%, M+), 172.0 (100), 144.9 (21), 91 (37). HRMS(ESI): Calculated for [M+H]$^+$ $C_7H_7NF_3Se$: 241.96903; Found: 241.96901

6.4 NMR Investigation

6.4.1 NMR investigations for the reactions reported in Chapter 2

- Reaction between Pd(P*t*Bu$_3$)$_2$ **268** and CuBr$_2$
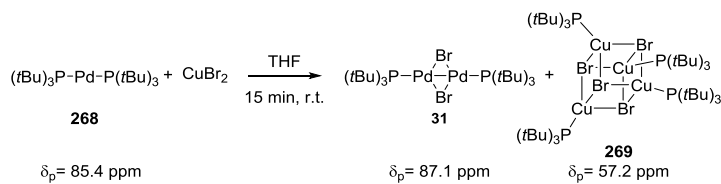
The general procedure A was followed for the formation of Pd(I)-bromo dimer **31** and Cu-cubane **269**. A ^{31}P-NMR spectrum was recorded after 15 min of reaction.
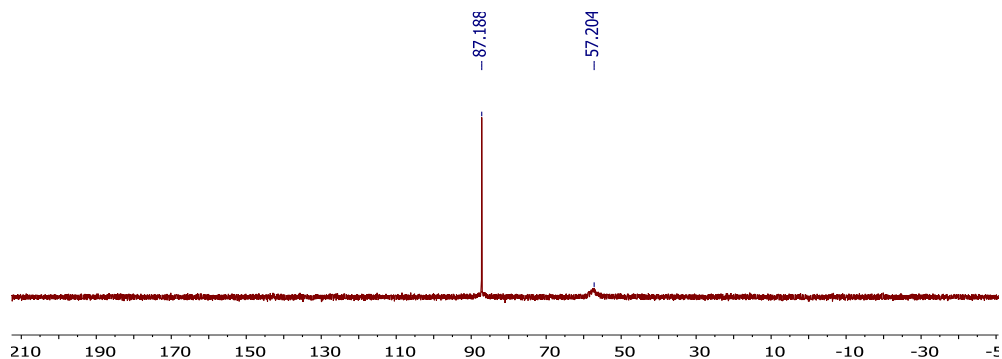
- Reaction between Pd(P*t*Bu$_3$)$_2$ **268** and CuBr

The general procedure A was followed for this study. The reaction was followed by ^{31}P-NMR spectroscopy over time. Time points were taken after: 15 min, 30 min and 60 min.

30 min

87.048
85.406

−3.050

i.s

210 190 170 150 130 110 90 70 50 30 10 -10 -30 -5

60 min

87.057
85.411

−3.050

i.s

210 190 170 150 130 110 90 70 50 30 10 -10 -30 -5

- Reaction between Pd(P*t*Bu$_3$)$_2$ **268** and CuI

(*t*Bu)$_3$P–Pd–P(*t*Bu)$_3$ + CuI $\xrightarrow[\text{15 min, r.t.}]{\text{THF}}$ (*t*Bu)$_3$P–Pd–Pd–P(*t*Bu)$_3$

268   **193**

δ_p= 85.4 ppm δ_p= 102.8 ppm
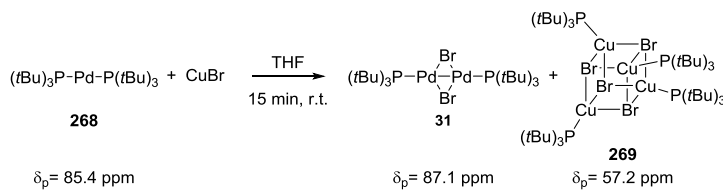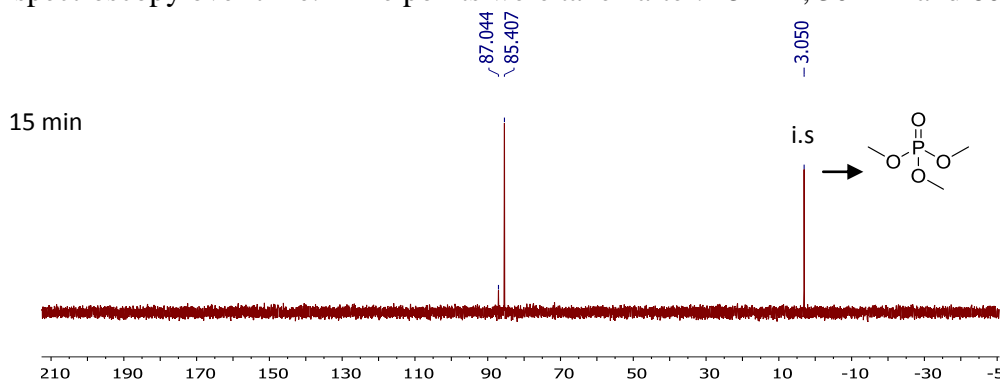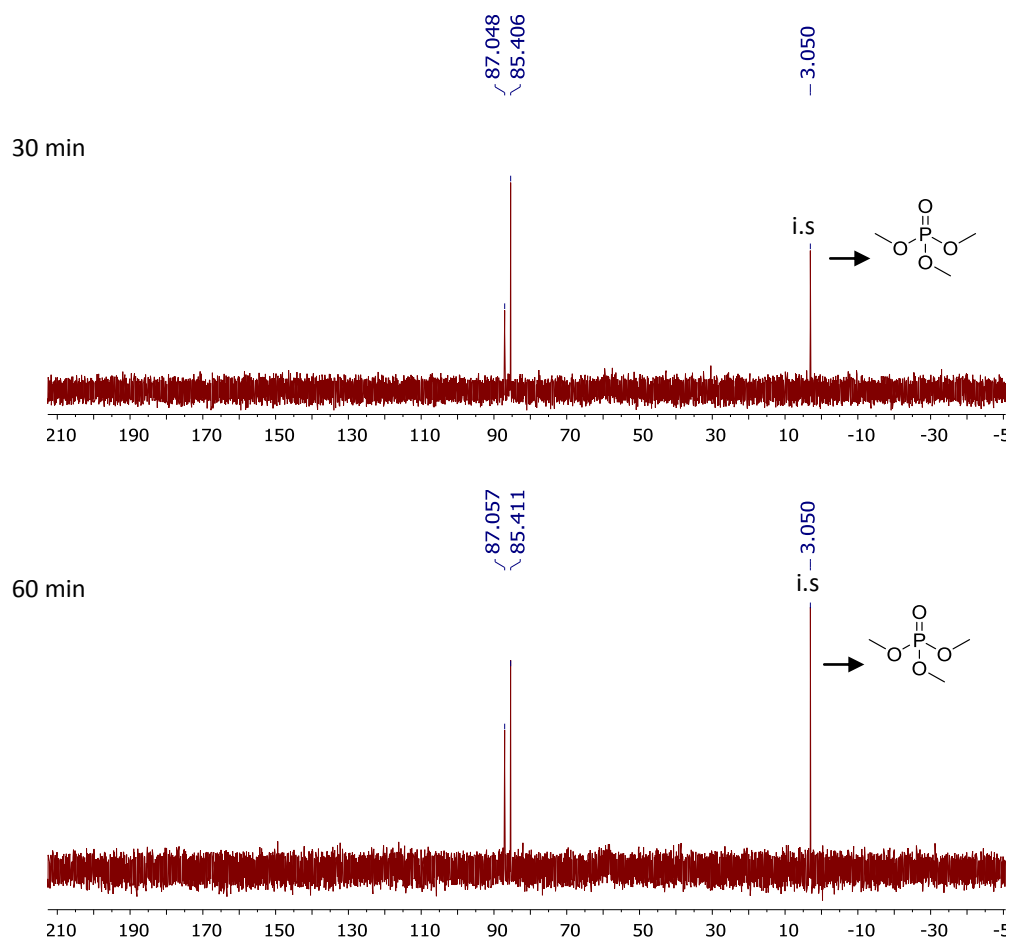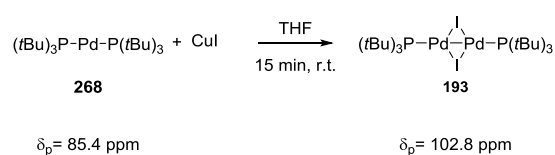
The general procedure A was followed for this study. The reaction was followed by ^{31}P-NMR spectroscopy over time. Time points were taken after: 15 min, 30 min, 60 min and 180 min.
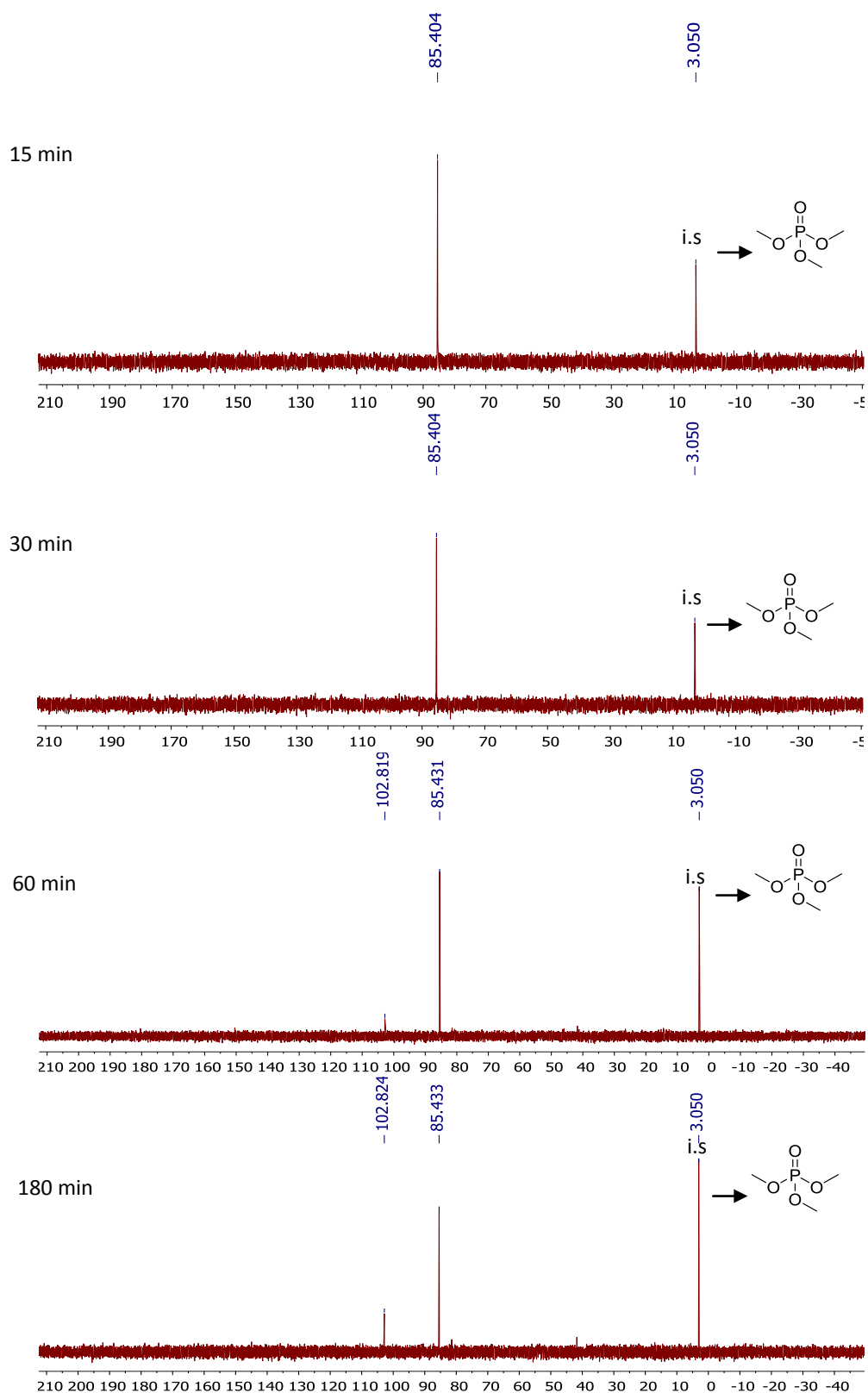
- **Reaction between Pd(PCy$_3$)$_2$ 270 and CuBr$_2$**
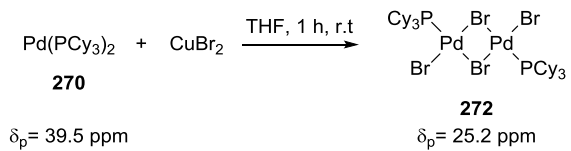
δ$_p$= 39.5 ppm

δ$_p$= 25.2 ppm

The general procedure B was followed for this study. The reaction was followed by ^{31}P-NMR spectroscopy over time. Time points were taken after: 15 min, 30 min and 60 min.

15 min

30 min

60 min

- Reaction between Pd(PCy$_3$)$_2$ **270** and PdBr$_2$

Pd(PCy$_3$)$_2$ + PdBr$_2$ $\xrightarrow{\text{THF, r.t}}$

270

272

δ_p= 39.5 ppm

δ_p= 25.0 ppm
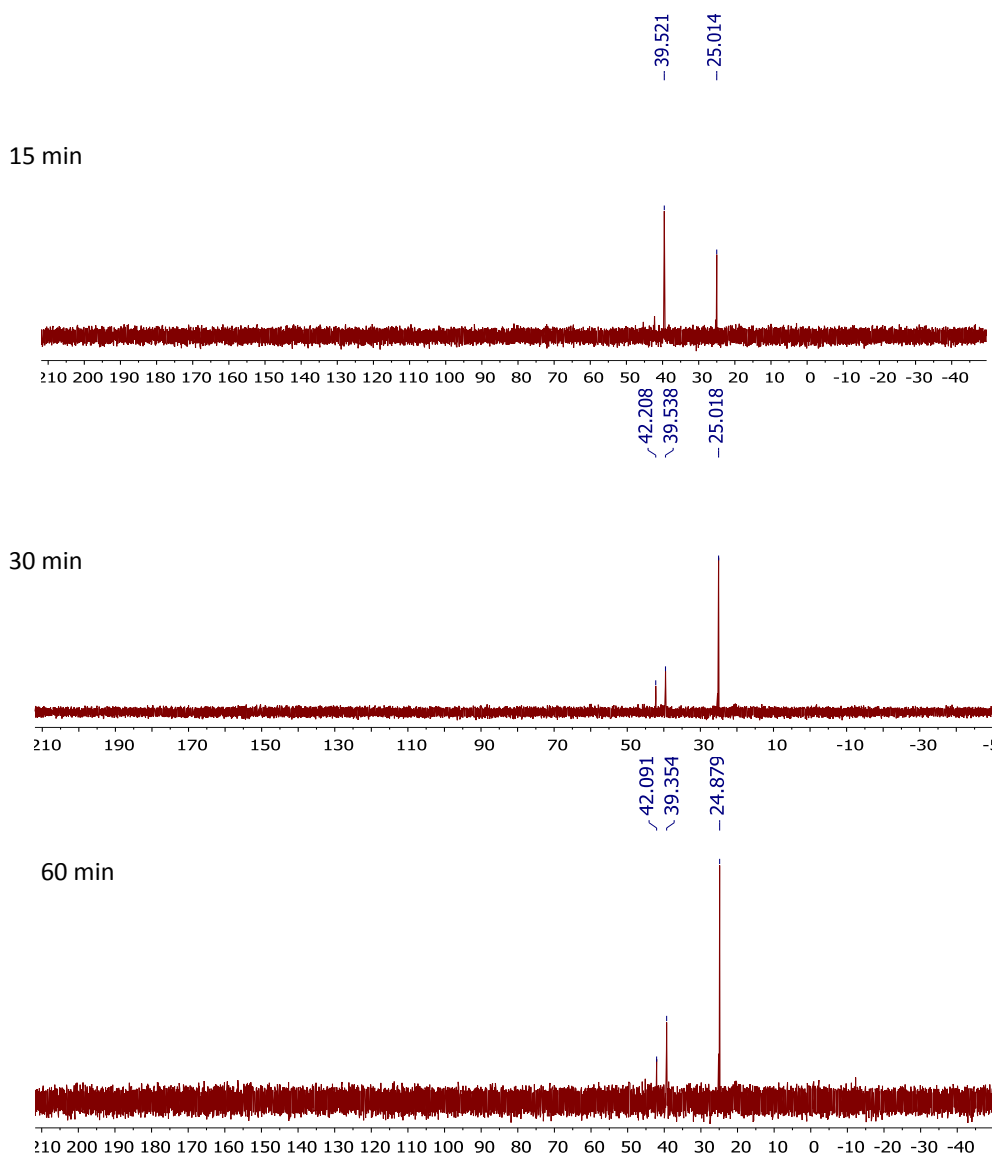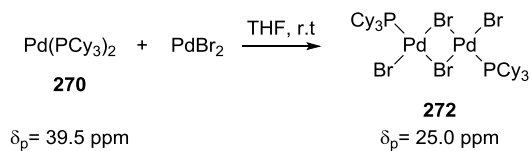
The general procedure B was followed for this study. The reaction was followed by ^{31}P-NMR spectroscopy over time. Time points were taken after: 20 min and 60 min
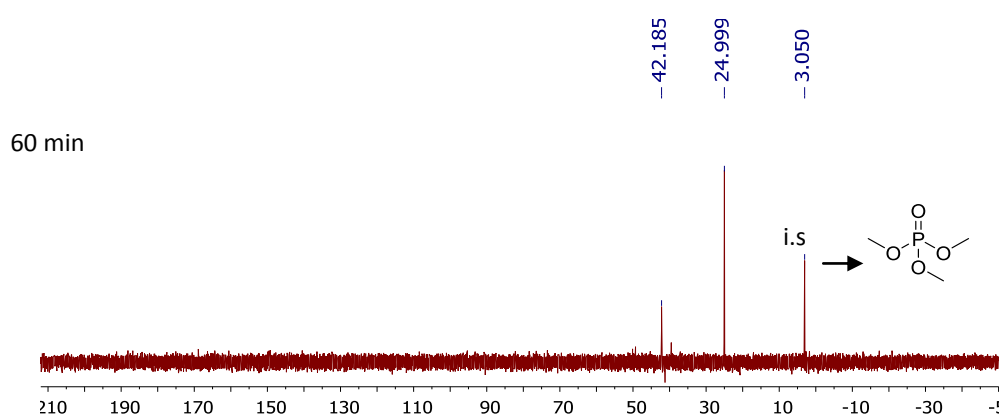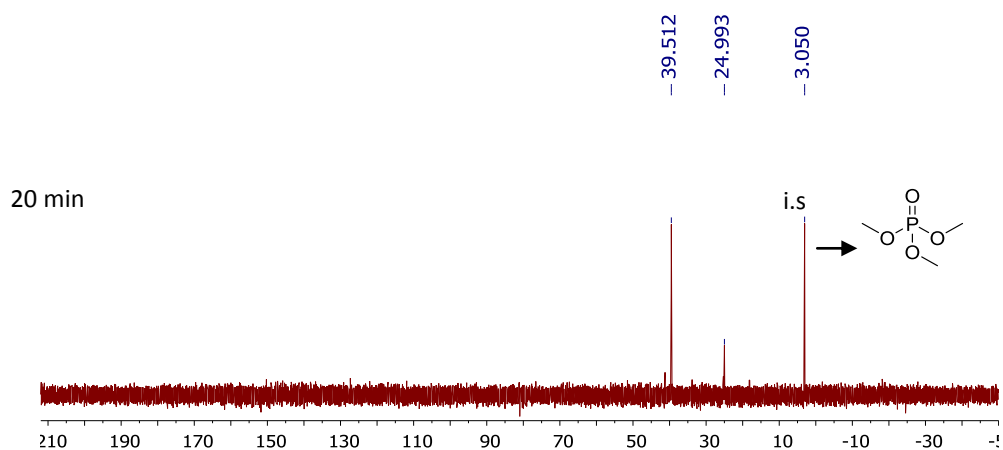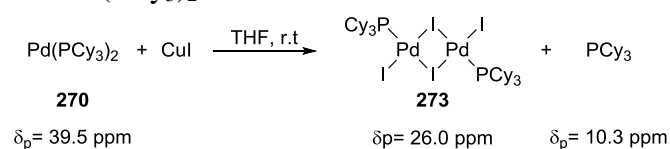
20 min

−39.512
−24.993
−3.050

i.s

60 min

−42.185
−24.999
−3.050

i.s

- Reaction between Pd(PCy$_3$)$_2$ **270** and CuI

Pd(PCy$_3$)$_2$ + CuI $\xrightarrow{\text{THF, r.t}}$ [Cy$_3$P–Pd(I)$_2$Pd–PCy$_3$] + PCy$_3$

270   **273**

δ_p= 39.5 ppm δ_p= 26.0 ppm δ_p= 10.3 ppm

The general procedure B was followed for this study. The reaction was followed by ^{31}P-NMR spectroscopy over time. Time points were taken after: 30 min and 90 min

45.087
39.326
26.041
−10.396

30 min

PCy$_3$

90 min

PCy$_3$
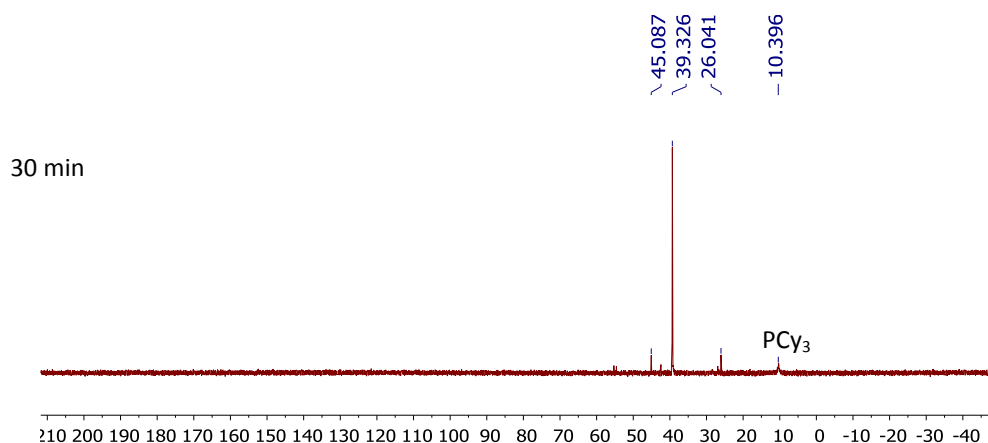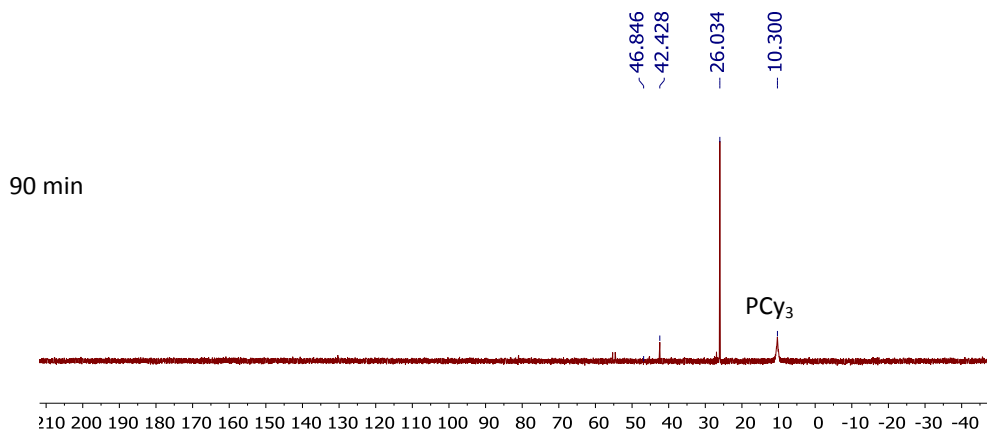
- Reaction between Pd[P(*i*Pr)(*t*Bu)$_2$]$_2$ **276** and PdBr$_2$

The general procedure B was followed for this study. A ^{31}P-NMR spectrum was recorded after 90 min of reaction
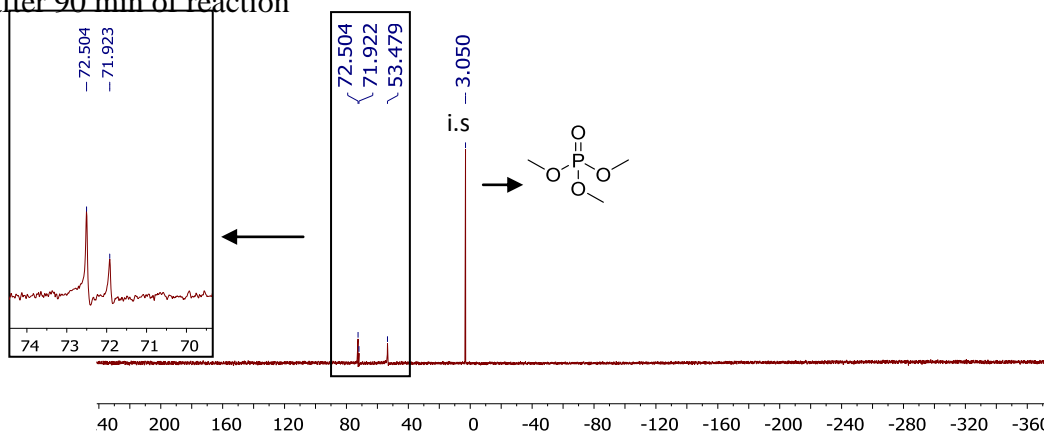
- Reaction between Pd[P(*i*Pr)(*t*Bu)$_2$]$_2$ **276** and PdI$_2$

The general procedure B was followed for this study. A ^{31}P-NMR spectrum was recorded after 90 min of reaction

- Reaction between Pd(dppm)$_2$ **279** and CuBr$_2$

Pd(dppm)$_2$ + CuBr$_2$ $\xrightarrow{\text{THF, r.t}}$	**29**	+ [CuBr$_2$(dppm)]
279		
δ_p =12.4 ppm	δ_p = -5.4 ppm	δ_p = -16.2 ppm
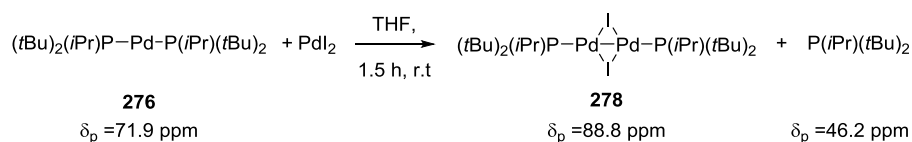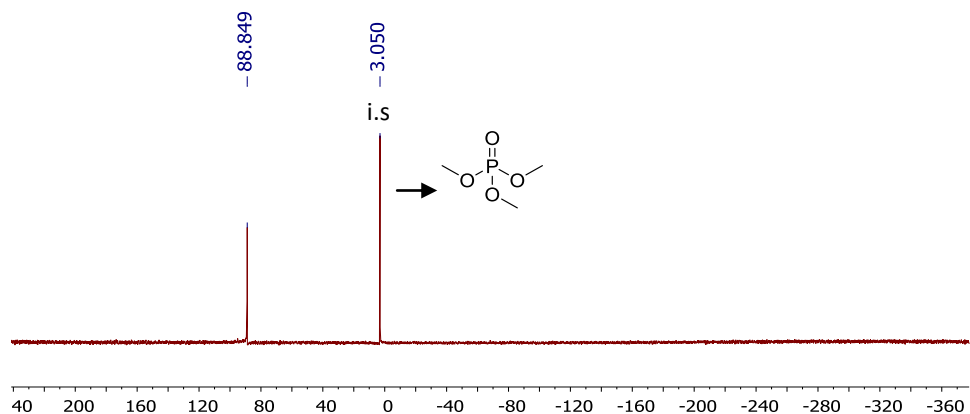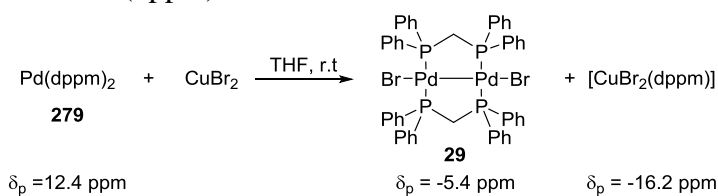
The general procedure B was followed for this study. A ^{31}P-NMR spectrum was recorded after 60 min of reaction.
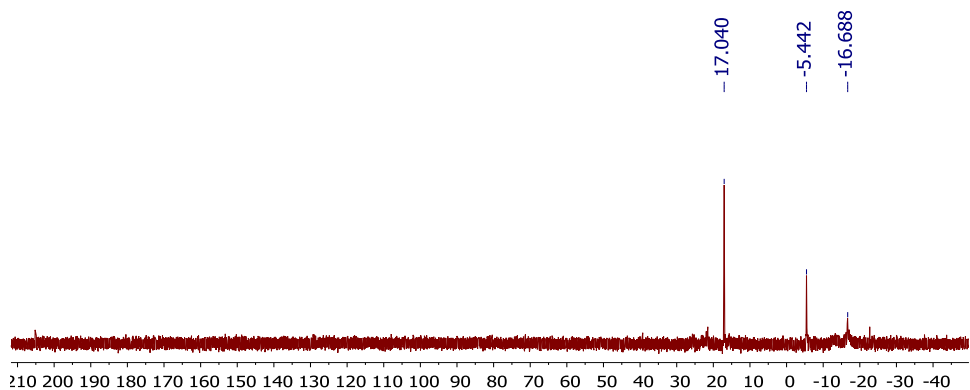
The species at 17.2 ppm was already present in trace amount in the ^{31}P-NMR of the Pd(dppm)$_2$ **279**.

- Reaction between Pd(dppm)$_2$ **279** and CuI

Pd(dppm)$_2$ + CuI $\xrightarrow{\text{THF, r.t}}$	**281**	+ dppm	+ [CuI(dppm)]
279			
δ_p =12.4 ppm	δ_p =-8.4 ppm δ_p =-21.9 ppm		δ_p =-17.0 ppm
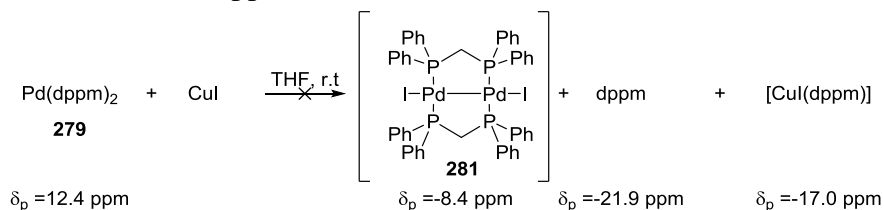
The general procedure B was followed for this study. A ^{31}P-NMR spectrum was recorded after 180 min of reaction.
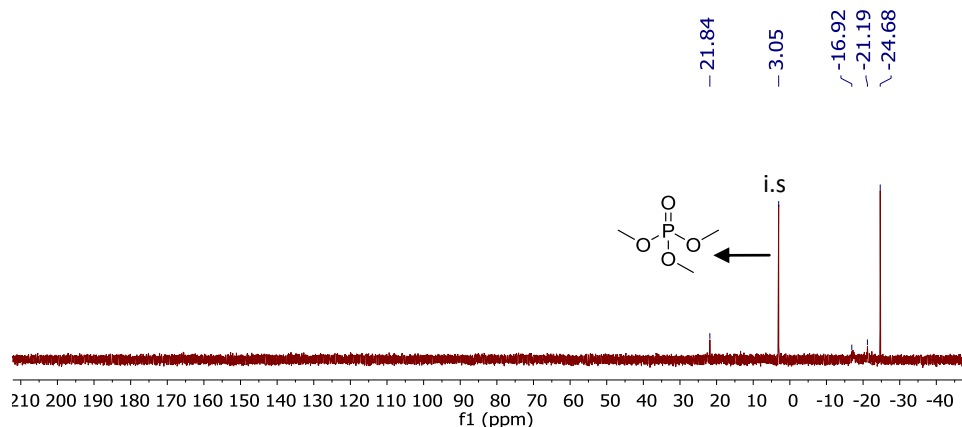
- Reaction between Pd(dppe)₂ **283** and CuBr₂
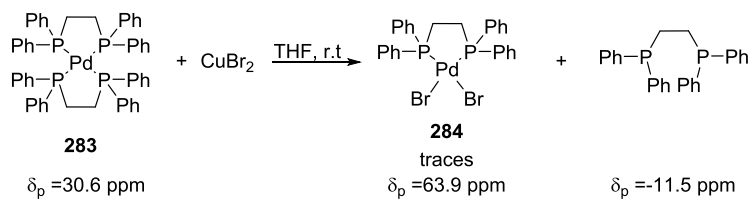
The general procedure B was followed for this study. The reaction was followed by ^{31}P-NMR spectroscopy over time. Time points were taken after: 15 min, 1h and 24 h.

−63.918
30.630
28.245
~ 3.050
~ −11.496

24 h

i.s

240 200 160 120 80 40 0 -40 -80 -120 -160 -200 -240 -280 -320 -360
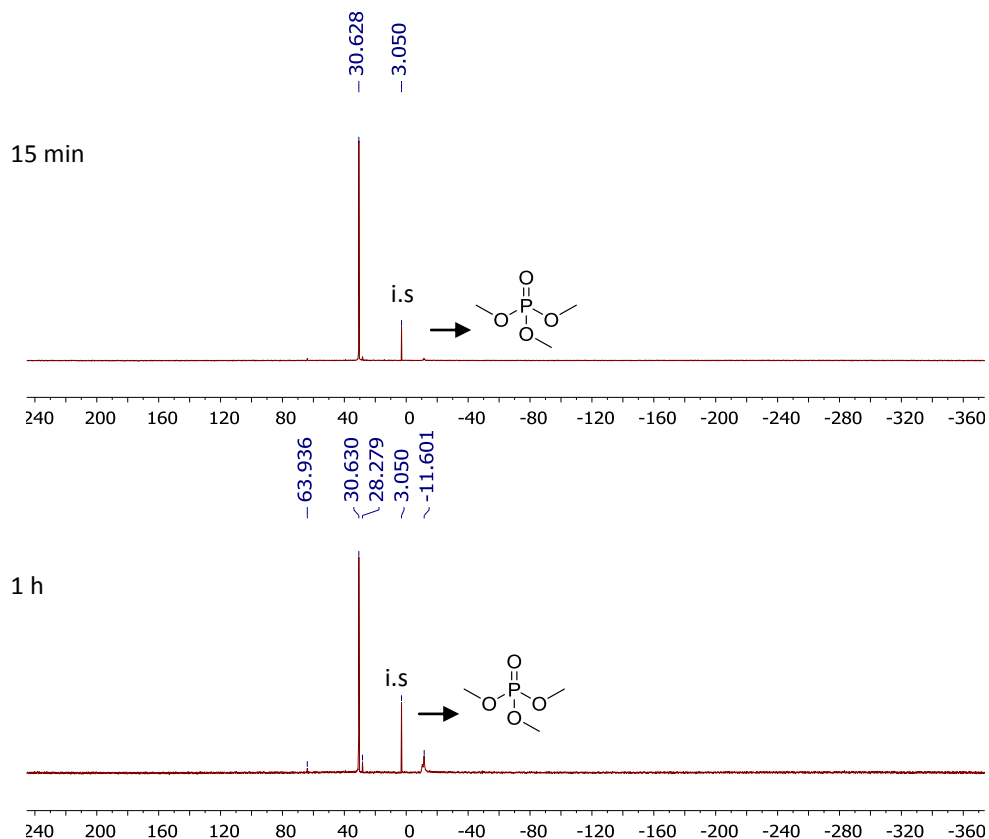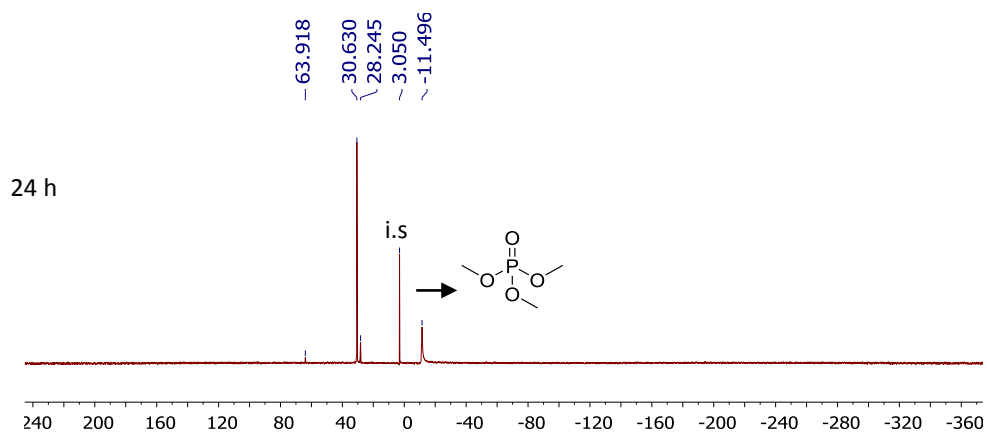
- Reaction between Pd(dfmpe)$_2$ **286** and CuBr$_2$
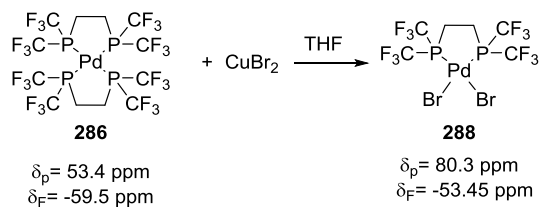
286

δ_p= 53.4 ppm
δ_F= -59.5 ppm

288

δ_p= 80.3 ppm
δ_F= -53.45 ppm

The general procedure B was followed for this study. The reaction was followed by ^{31}P-NMR spectroscopy over time. Time points were taken after: 1h and 6 h.

81.953
81.676
80.855
80.169
79.487
78.816
78.258
−53.344

1 h

210 190 170 150 130 110 90 70 50 30 10 -10 -30 -5

82.179
81.507
80.814
80.201
79.578
78.774
78.367
−53.306

6 h

210 190 170 150 130 110 90 70 50 30 10 -10 -30 -5

237
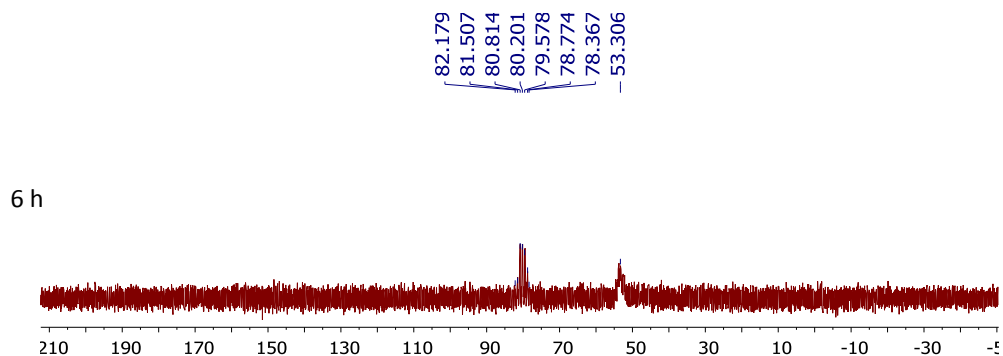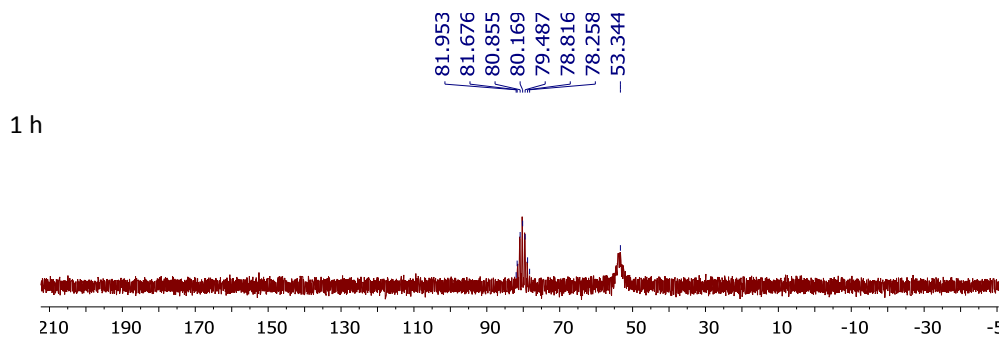
The general procedure B was followed for this study. The reaction was followed by ^{19}F-NMR spectroscopy over time. Time points were taken after: 1h and 6 h.

- Reaction between Pd(Qphos)$_2$ **292** and CuBr$_2$

The general procedure B was followed for this study. A ^{31}P-NMR spectrum was recorded after 15 min of reaction.

- Reaction between Pd(Qphos)$_2$ **292** and PdBr$_2$
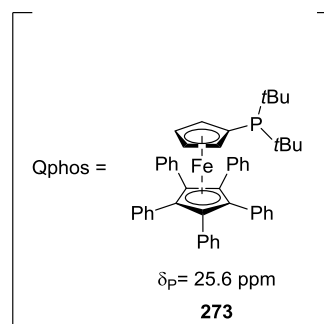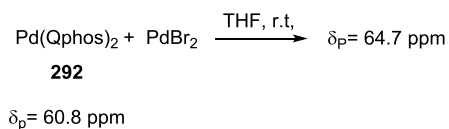
Pd(Qphos)$_2$ + PdBr$_2$ $\xrightarrow{\text{THF, r.t,}}$ δ_P= 64.7 ppm

292

δ_p= 60.8 ppm

Qphos =

δ_P= 25.6 ppm

273

The general procedure B was followed for this study. A ^{31}P-NMR spectrum was recorded after 4 h of reaction.

- Reaction between Pd(Qphos)$_2$ **292** and PdI$_2$

Pd(Qphos)$_2$ + PdI$_2$ $\xrightarrow{\text{THF, r.t,}}$ δ_P= 79.9 ppm

292

δ_p= 60.8 ppm

Qphos =

δ_P= 25.6 ppm

273

The general procedure B was followed for this study. A ^{31}P-NMR spectrum was recorded after 4 h of reaction.

- Reaction between Pd(PPh$_3$)$_4$ **296** and CuBr$_2$

Pd(PPh$_3$)$_4$ + CuBr$_2$ $\xrightarrow{\text{THF}}$ Pd(PPh$_3$)$_3$ + [Ph$_3$P,Br,Pd,Ph$_3$P,Br] + PPh$_3$ + (PPh$_3$)$_2$CuBr + [Ph$_3$P,Br,Cu,Cu—PPh$_3$,Ph$_3$P,Br]

296   **297**   **300a**
δ_P= 18.4 ppm δ_P= 22.7 ppm δ_P= 23.7 ppm δ_P= -5.3 ppm δ_P= 24.2 ppm δ_P= 10.3 ppm
δ_P= 9.9 ppm
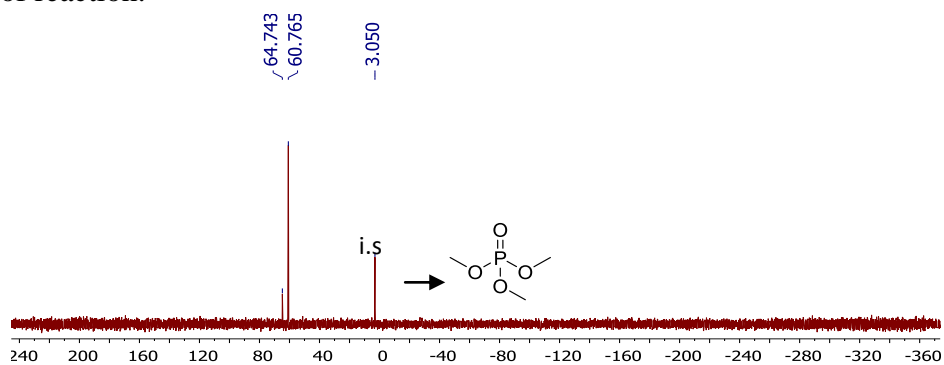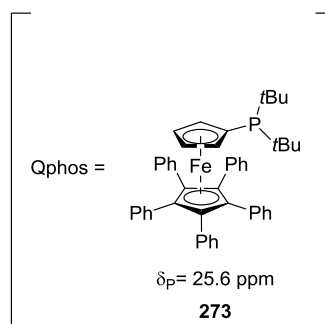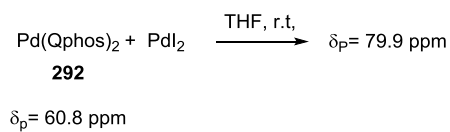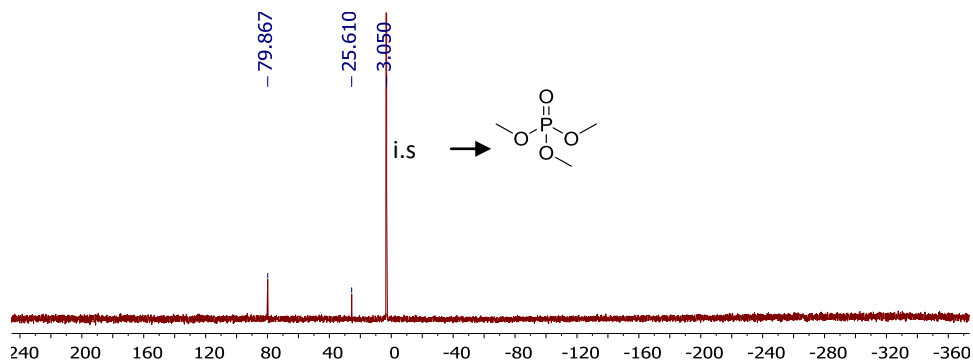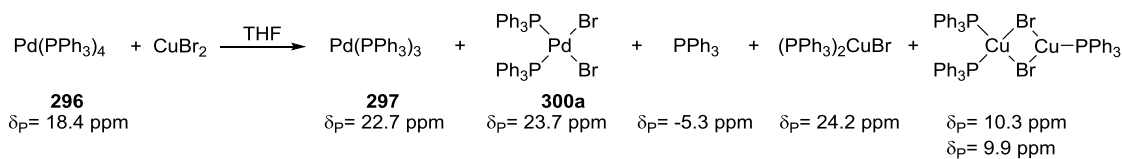
The general procedure B was followed for this study. The reaction was followed by ^{31}P-NMR spectroscopy over time. Time points were taken after: 15 min and 180 min.

15 min

180 min

- Reaction between Pd(PPh$_3$)$_4$ **296** and 2 equiv of CuBr
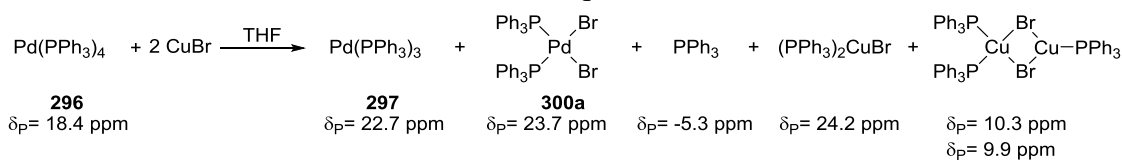
Pd(PPh$_3$)$_4$ + 2 CuBr $\xrightarrow{\text{THF}}$ Pd(PPh$_3$)$_3$ + [Ph$_3$P,Br,Pd,Ph$_3$P,Br] + PPh$_3$ + (PPh$_3$)$_2$CuBr + [Ph$_3$P,Br,Cu,Cu—PPh$_3$,Ph$_3$P,Br]

296   **297**   **300a**
δ_P= 18.4 ppm δ_P= 22.7 ppm δ_P= 23.7 ppm δ_P= -5.3 ppm δ_P= 24.2 ppm δ_P= 10.3 ppm
δ_P= 9.9 ppm

The general procedure B was followed for this study. A ^{31}P-NMR spectrum was recorded after 2 h of reaction.
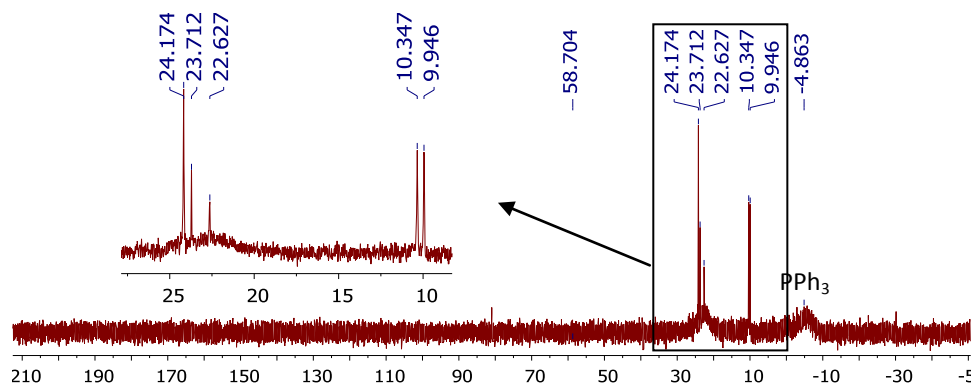
- Reaction between Pd(PPh$_3$)$_4$ **296** and CuI

The general procedure B was followed for this study. A ^{31}P-NMR spectrum was recorded after 2 h of reaction.

- Reaction between Pd(PtBu$_3$)$_2$ **268** and AgBr

δ_P= 85.4 ppm $\qquad\qquad\qquad\qquad\qquad$ δ_P= 87.1 ppm

The general procedure A was followed for this study. The reaction was followed by ^{31}P-NMR spectroscopy over time. Time points were taken after: 15 min, 1 h and 4 h

15 min

– 85.375

– 85.375

1 h

87.001
85.366

4 h

- Reaction between Pd(P*t*Bu₃)₂ **268** and AgI

(*t*Bu)₃P–Pd–P(*t*Bu)₃ + AgI $\xrightarrow{\text{THF}}$ (*t*Bu)₃P–Pd–Pd–P(*t*Bu)₃

268

193

δ_p= 85.4 ppm

δ_p= 102.9 ppm

The general procedure A was followed for this study. A ^{31}P-NMR spectrum was recorded after 2 h of reaction.

– 102.901

– 85.509

2 h

● Reaction between Pd(P*t*Bu$_3$)$_2$ **268** and AuBr$_3$

(*t*Bu)$_3$P-Pd-P(*t*Bu)$_3$ + AuBr$_3$ $\xrightarrow{\text{THF}}$ (*t*Bu)$_3$P—Pd$\overset{\text{Br}}{\underset{\text{Br}}{|}}$Pd—P(*t*Bu)$_3$ + (*t*Bu)$_3$P—AuBr$_3$ + [(*t*Bu)$_3$P-Au-P(*t*Bu)$_3$]$^+$ Br$^-$

268   **31**   **319**   **318**

δ$_P$= 85.4 ppm   δ$_P$= 87.1 ppm   δ$_P$= 94.3 ppm   δ$_P$= 97.3 ppm

The general procedure A was followed for this study. A ^{31}P-NMR spectrum was recorded after 15 min of reaction.

● Reaction between Pd(P*t*Bu$_3$)$_2$ **268** and Cu(OTf)$_2$

(*t*Bu)$_3$P-Pd-P(*t*Bu)$_3$ + Cu(OTf)$_2$ $\xrightarrow{\text{THF}}$ (*t*Bu)$_3$P-Pd$\overset{\text{OTf}}{\underset{\text{H}}{|}}$P(*t*Bu)$_3$

268   δ$_P$= 48.6 ppm   **176**
δ$_P$= 85.5 ppm   δ$_P$= -12.6 ppm

The general procedure A was followed for this study. A ^{31}P-NMR spectrum was recorded after 1 h of reaction.

● Reaction between Pd(P*t*Bu$_3$)$_2$ **268** and HOTf

(*t*Bu)$_3$P-Pd-P(*t*Bu)$_3$ + HOTf $\xrightarrow{\text{THF}}$ (*t*Bu)$_3$P-Pd$\overset{\text{OTf}}{\underset{\text{H}}{|}}$P(*t*Bu)$_3$

268
δ$_P$= 85.5 ppm   δ$_P$= 48.6 ppm

The general procedure A was followed for this study. A ^{31}P-NMR spectrum was recorded after 1 h of reaction.

243

- Reaction between Pd(P*t*Bu$_3$)$_2$ **268** and SnBr$_2$

$$(t\text{Bu})_3\text{P-Pd-P}(t\text{Bu})_3 \ + \ \text{SnBr}_2 \ \xrightarrow{\text{THF}}$$

268

δ_P= 85.4 ppm

The general procedure A was followed for this study. A ^{31}P-NMR spectrum was recorded after 15 min of reaction.

- Reaction between Pd(P*t*Bu$_3$)$_2$ **268** and CuCl$_2$

$$(t\text{Bu})_3\text{P-Pd-P}(t\text{Bu})_3 \ + \ \text{CuCl}_2 \ \xrightarrow{\text{THF}} \ (t\text{Bu})_3\text{P-Pd-P}(t\text{Bu})_3 \ + \ \left[(t\text{Bu})_2\text{P-Pd}\begin{smallmatrix}\text{Cl}\\\\\text{Cl}\end{smallmatrix}\text{Pd-P}(t\text{Bu})_2 \right] \ + \ \text{P}(t\text{Bu})_3$$

268		**176**	
δ_P= 85.4 ppm	δ_P= 82.8 ppm	δ_P= -10.1 ppm	δ_P= 63.5 ppm

The general procedure A was followed for this study. A ^{31}P-NMR spectrum was recorded after 30 min of reaction.

- Reaction between Pd(P*t*Bu$_3$)$_2$ **268** and CuF$_2$

$$(t\text{Bu})_3\text{P-Pd-P}(t\text{Bu})_3 \ + \ \text{CuF}_2 \quad \xrightarrow{\text{THF}}$$

268

δ_P= 85.4 ppm

The general procedure A was followed for this study. A ^{31}P-NMR spectrum was recorded after 30 min of reaction

- Reaction between Pd(P*t*Bu$_3$)$_2$ **268** and Ag$_2$O

$$(t\text{Bu})_3\text{P-Pd-P}(t\text{Bu})_3 \ + \ \text{Ag}_2\text{O} \quad \xrightarrow{\text{THF}}$$

268

δ_P= 85.4 ppm

The general procedure A was followed for this study. A ^{31}P-NMR spectrum was recorded after 1 h of reaction

- Reaction between Pd(P*t*Bu$_3$)$_2$ **268** and AgBr

(*t*Bu)$_3$P–Pd–P(*t*Bu)$_3$ + FeBr$_3$ $\xrightarrow{\text{THF}}$ (*t*Bu)$_3$P–Pd(Br)(Br)–Pd–P(*t*Bu)$_3$

268 **31**

δ_P= 85.4 ppm δ_P= 87.1 ppm

The general procedure A was followed for this study. The reaction was followed by ^{31}P-NMR spectroscopy over time. Time points were taken after: 10 min and 2 h.
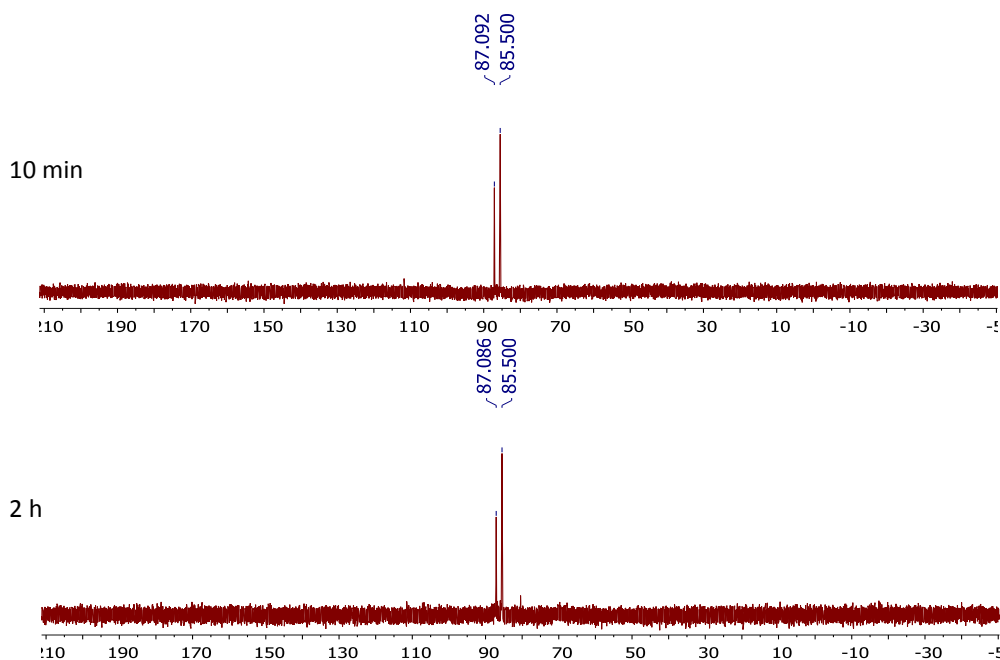
- Reaction between Pd(P*t*Bu$_3$)$_2$ **268** and AgF
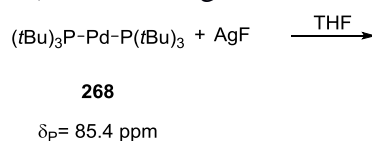
(*t*Bu)$_3$P–Pd–P(*t*Bu)$_3$ + AgF $\xrightarrow{\text{THF}}$

268

δ_P= 85.4 ppm

The general procedure A was followed for this study. A ^{31}P-NMR spectrum was recorded after 1 h of reaction

246

−85.399
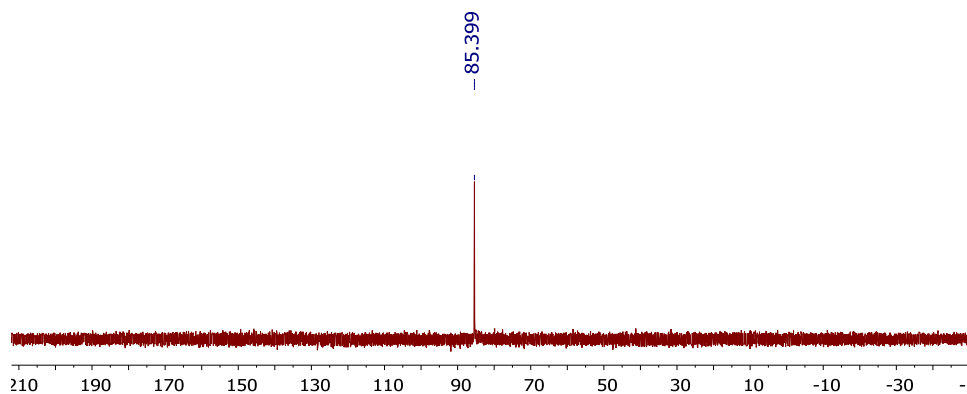
6.4.3 NMR investigations for the reactions reported in Chapter 3

- Reaction between Pd(I)-bromo dimer **31** (1 equiv) and KF (20 equiv) , *Table 21* Entry 1
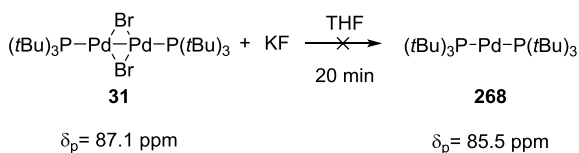
$(t\text{Bu})_3\text{P}-\text{Pd}\overset{\text{Br}}{\underset{\text{Br}}{-}}\text{Pd}-\text{P}(t\text{Bu})_3$ + KF $\xrightarrow[\text{20 min}]{\text{THF}}$ $(t\text{Bu})_3\text{P}-\text{Pd}-\text{P}(t\text{Bu})_3$

31   **268**

δ_p= 87.1 ppm δ_p= 85.5 ppm

The general procedure E was followed in this study. The ^{31}P-NMR spectrum was recorded after 20 min of reaction.

−87.07   −3.05

i.s

0.157   1.000
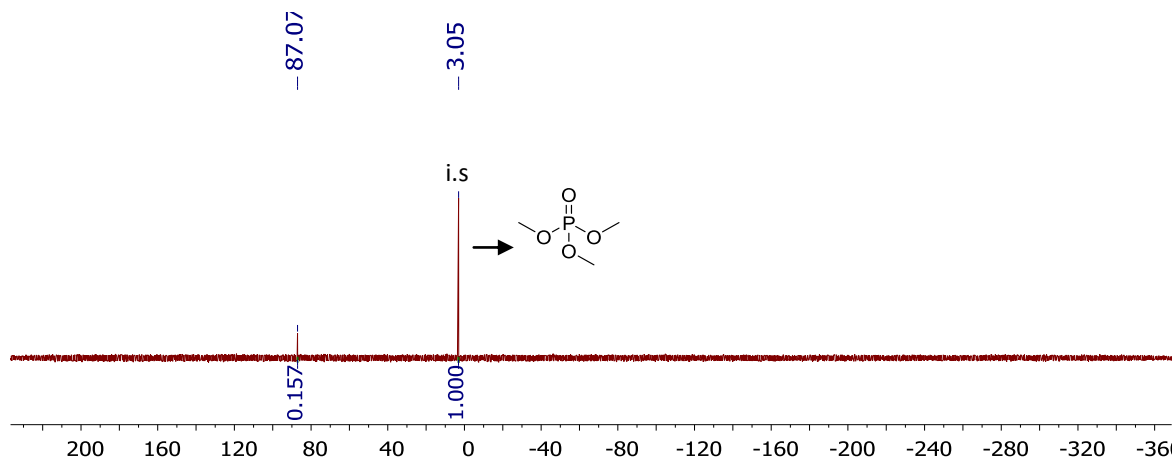
- Reaction between Pd(I)-bromo dimer **31** (1 equiv) and Hantzsch ester **327** (20 equiv), *Table 21* Entry 2
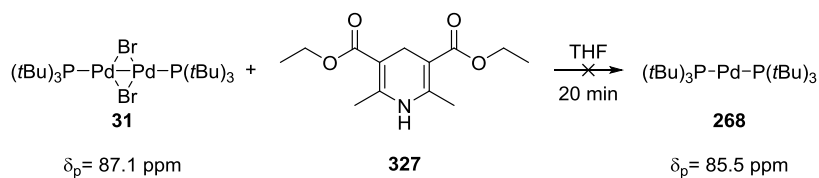
$(t\text{Bu})_3\text{P}-\text{Pd}\overset{\text{Br}}{\underset{\text{Br}}{-}}\text{Pd}-\text{P}(t\text{Bu})_3$ + [327] $\xrightarrow[\text{20 min}]{\text{THF}}$ $(t\text{Bu})_3\text{P}-\text{Pd}-\text{P}(t\text{Bu})_3$

31   **327**   **268**

δ_p= 87.1 ppm δ_p= 85.5 ppm

247

The general procedure E was followed in this study. The ^{31}P-NMR spectrum was recorded after 20 min of reaction.
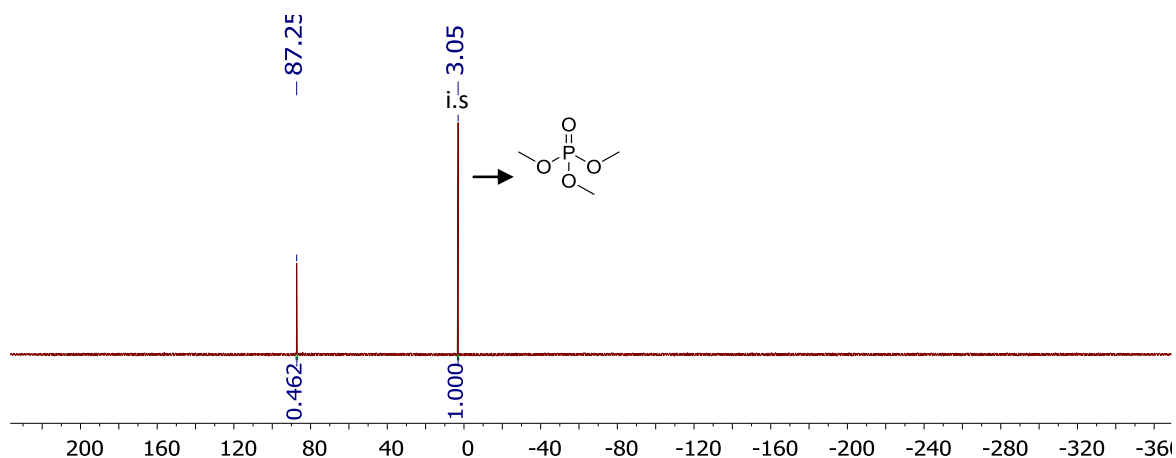
- Reaction between Pd(I)-bromo dimer **31** (1 equiv) and KOH (20 equiv), *Table 21* Entry 3
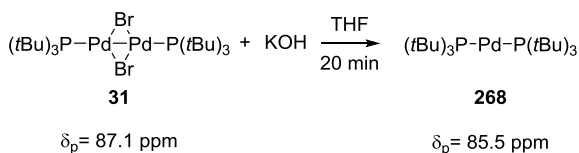
The general procedure E was followed in this study. The ^{31}P-NMR spectrum was recorded after 20 min of reaction.
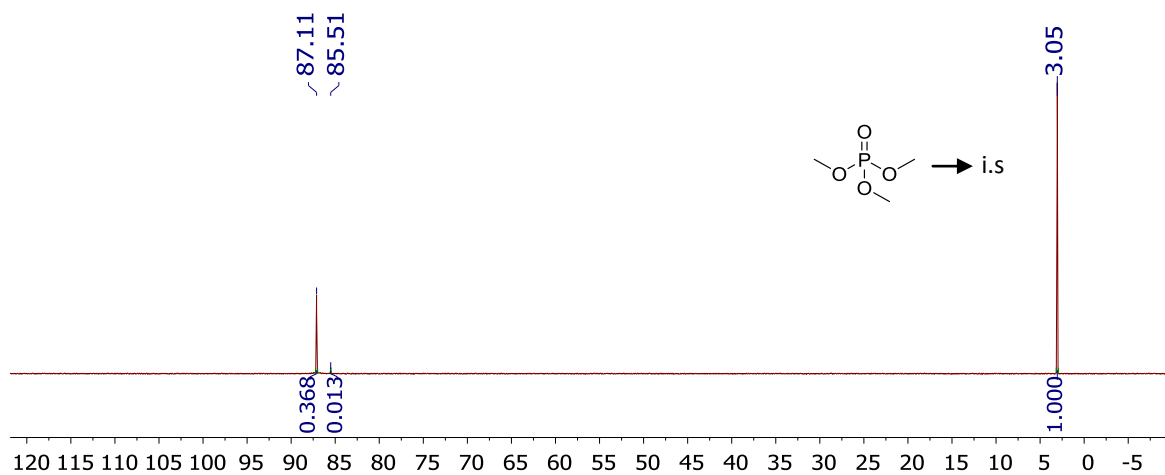
- Reaction between Pd(I)-bromo dimer **31** (1 equiv) and PCy$_3$ (20 equiv), *Table 21* Entry 4
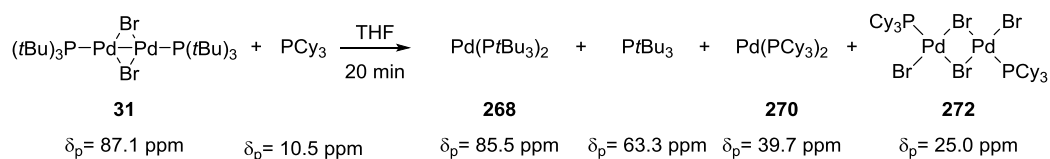
31

δ_p= 87.1 ppm δ_p= 10.5 ppm δ_p= 85.5 ppm δ_p= 63.3 ppm δ_p= 39.7 ppm δ_p= 25.0 ppm

The general procedure E was followed in this study. The ^{31}P-NMR spectrum was recorded after 20 min of reaction.
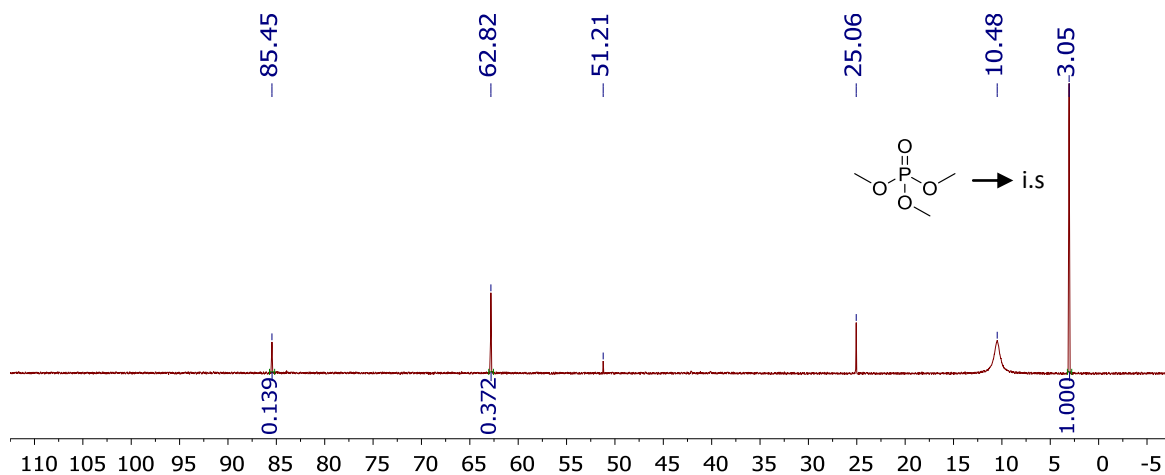
- Reaction between Pd(I)-bromo dimer **31** (1 equiv) and 1-Pyrrolidino-1-cyclopentene **328** (20 equiv), *Table 21* Entry 5
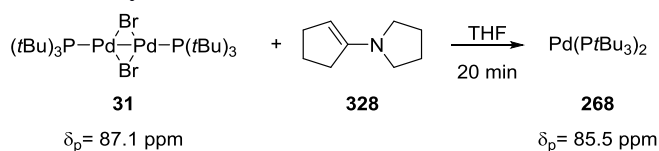
31   **328**   **268**

δ_p= 87.1 ppm δ_p= 85.5 ppm

The general procedure E was followed in this study. The ^{31}P-NMR spectrum was recorded after 20 min of reaction.
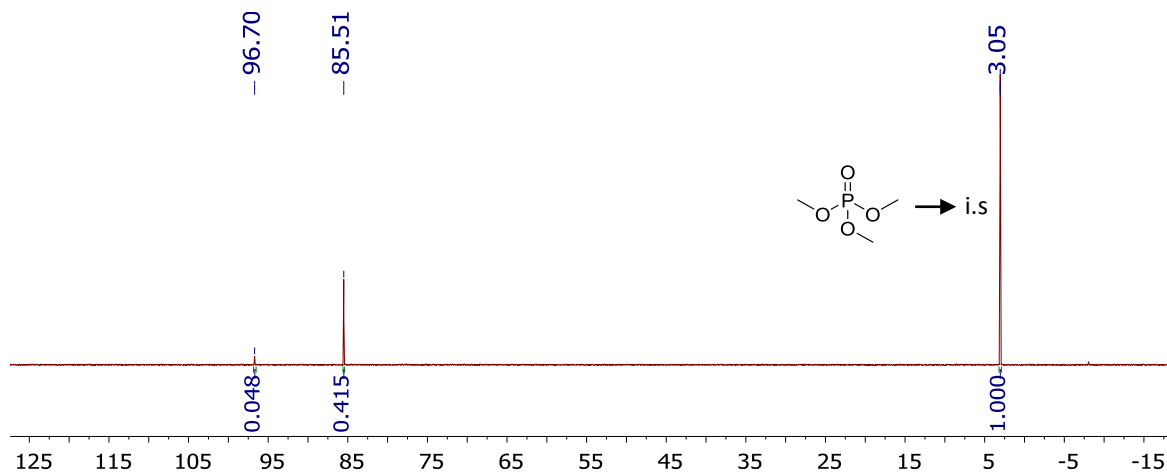
- Reaction between Pd(I)-bromo dimer **31** (1 equiv) and PEt$_3$ (20 equiv), *Table 21* Entry 6
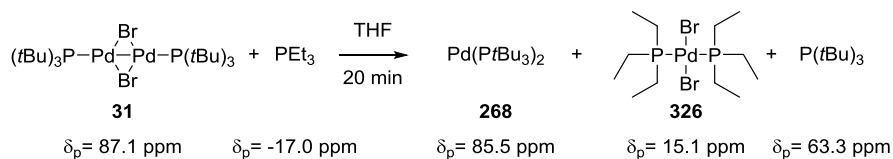
The general procedure E was followed in this study. The ^{31}P-NMR spectrum was recorded after 20 min of reaction.
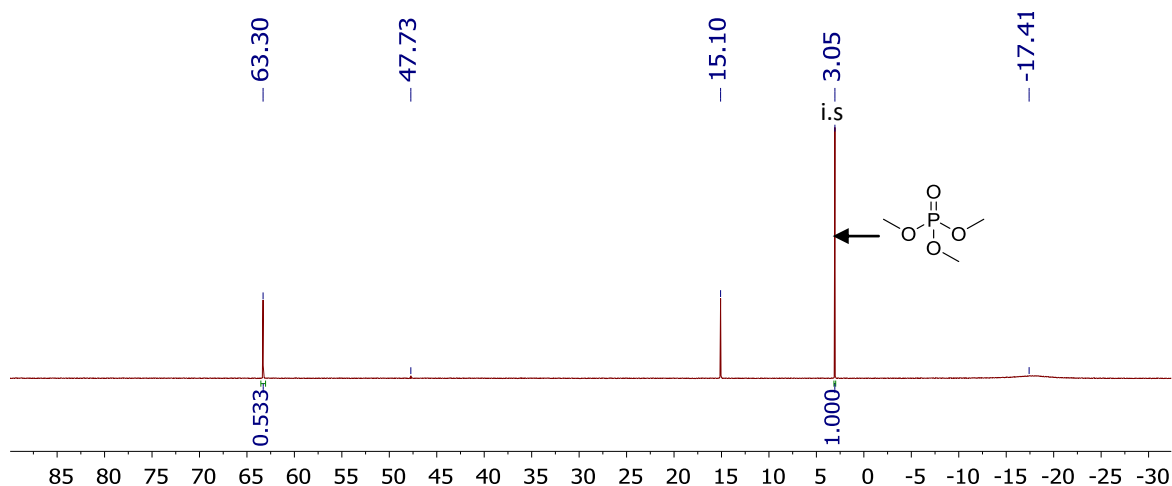
- Reaction between Pd(I)-bromo dimer **31** (1 equiv) and KOEt (20 equiv), *Table 21* Entry 7
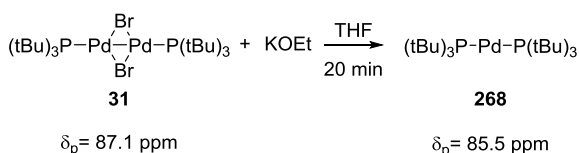
The general procedure E was followed in this study. The ^{31}P-NMR spectrum was recorded after 20 min of reaction.
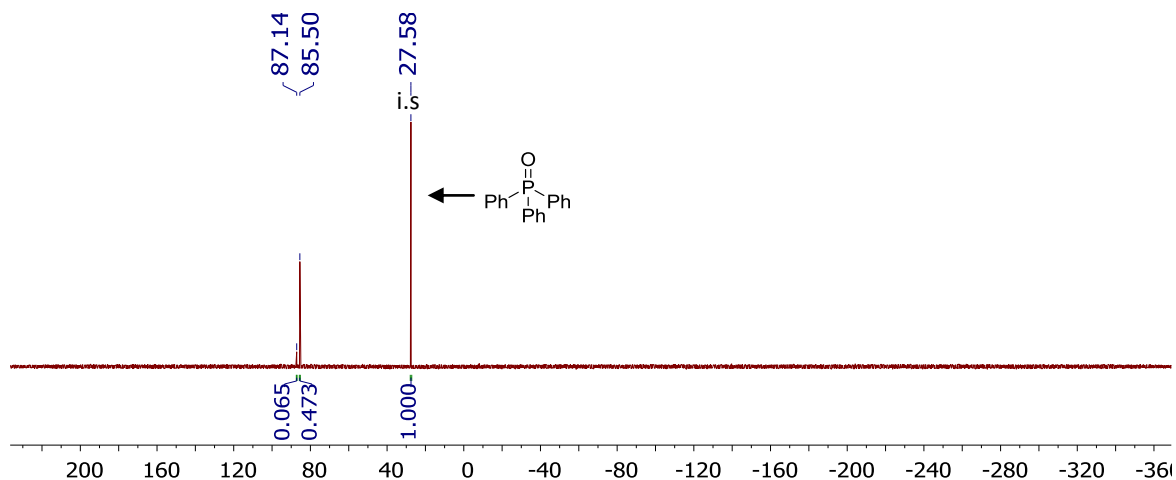
- Reaction between Pd(I)-bromo dimer **31** (1 equiv) and hppH **325** (20 equiv), *Table 21* Entry 8
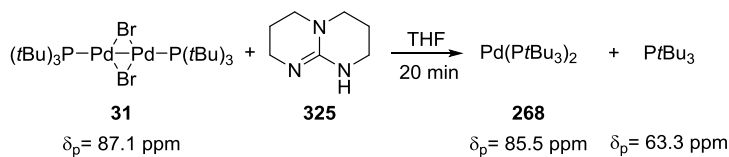
31
δ_p= 87.1 ppm

325

268
δ_p= 85.5 ppm δ_p= 63.3 ppm

The general procedure E was followed in this study. The ^{31}P-NMR spectrum was recorded after 20 min of reaction.
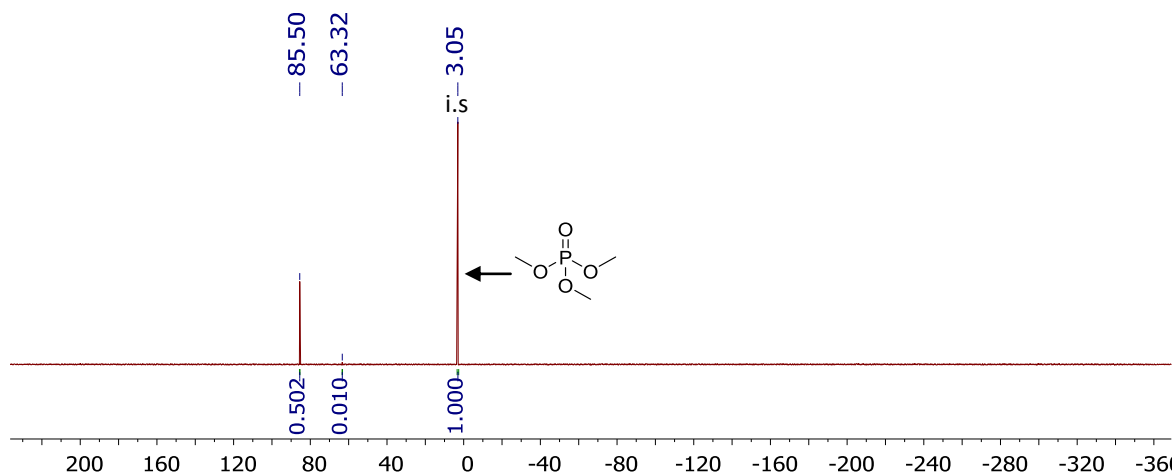
- Reaction between Pd(I)-bromo dimer **31** (1 equiv) and KO*t*Bu (20 equiv), *Table 21* Entry 9
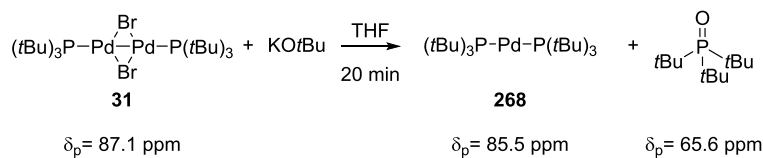
31
δ_p= 87.1 ppm

268
δ_p= 85.5 ppm

δ_p= 65.6 ppm

The general procedure E was followed in this study. The ^{31}P-NMR spectrum was recorded after 20 min of reaction.
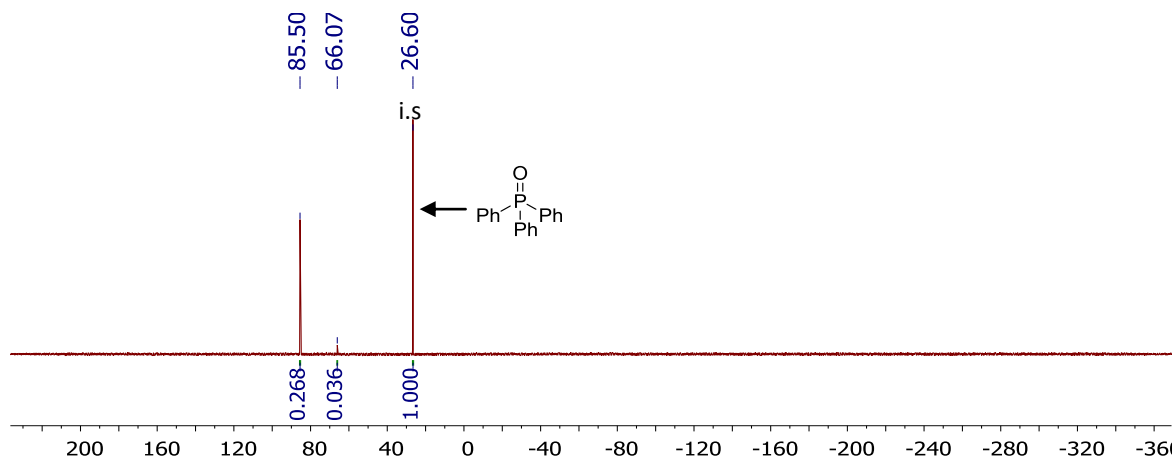
- Reaction between Pd(I)-iodo dimer **193** (1 equiv) and KF (20 equiv), *Table 22* Entry 1
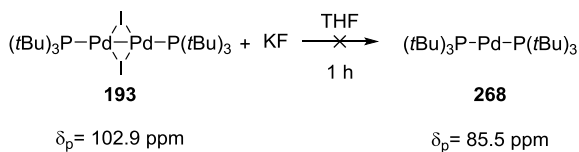
$(t\text{Bu})_3\text{P}-\text{Pd}\overset{\text{I}}{\underset{\text{I}}{-}}\text{Pd}-\text{P}(t\text{Bu})_3$ + KF $\xrightarrow[\text{1 h}]{\text{THF}}$ $(t\text{Bu})_3\text{P}-\text{Pd}-\text{P}(t\text{Bu})_3$

193   **268**

δ_p= 102.9 ppm δ_p= 85.5 ppm

The general procedure E was followed in this study. The ^{31}P-NMR spectrum was recorded after 1 h of reaction.
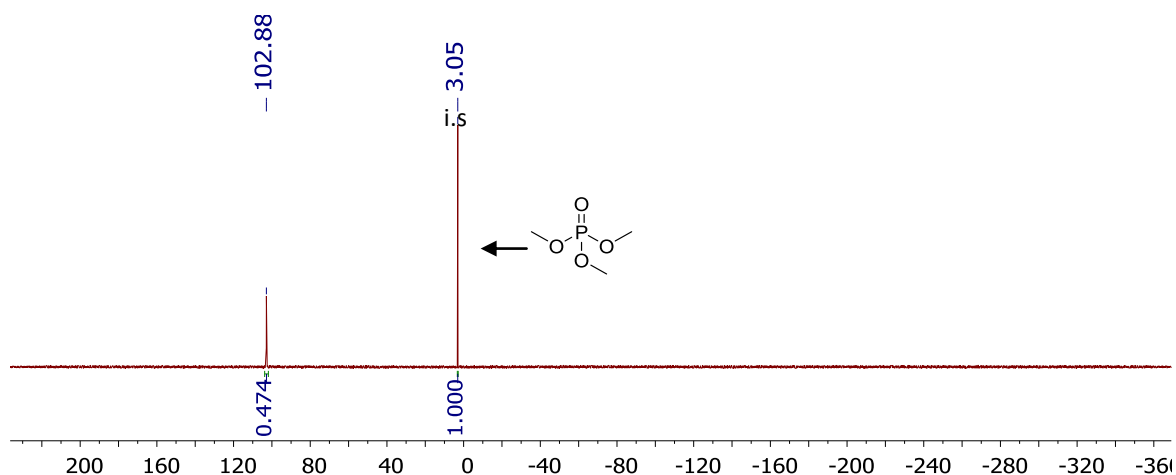
- Reaction between Pd(I)-iodo dimer **193** (1 equiv) and Hantzsch ester **327** (20 equiv), *Table 22* Entry 2
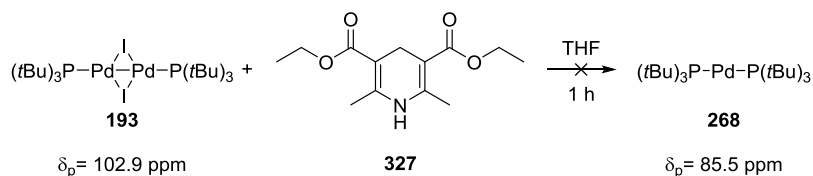
$(t\text{Bu})_3\text{P}-\text{Pd}\overset{\text{I}}{\underset{\text{I}}{-}}\text{Pd}-\text{P}(t\text{Bu})_3$ + [Hantzsch ester 327] $\xrightarrow[\text{1 h}]{\text{THF}}$ $(t\text{Bu})_3\text{P}-\text{Pd}-\text{P}(t\text{Bu})_3$

193   **327**   **268**

δ_p= 102.9 ppm δ_p= 85.5 ppm

The general procedure E was followed in this study. The ^{31}P-NMR spectrum was recorded after 1 h of reaction.
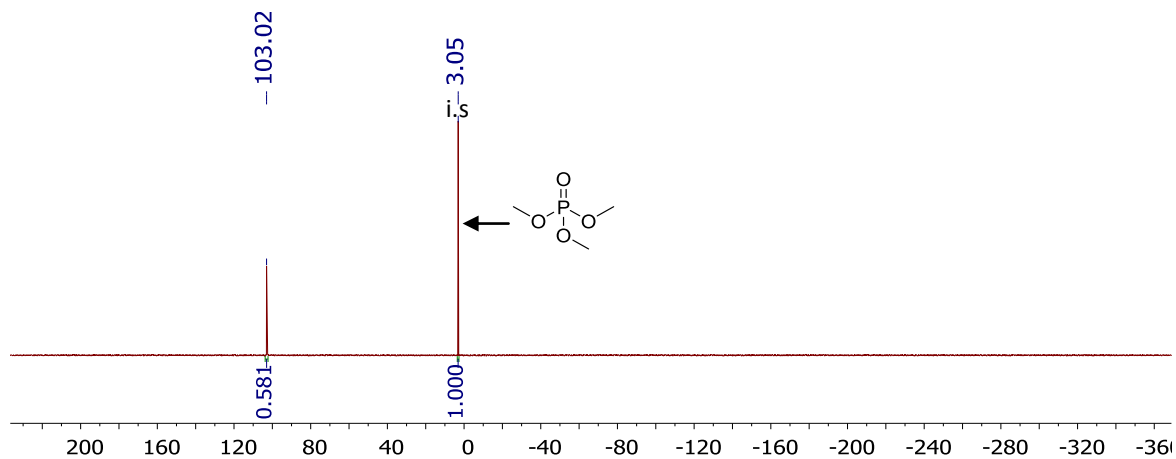
- Reaction between Pd(I)-iodo dimer **193** (1 equiv) and KOH (20 equiv), *Table 22* Entry 3
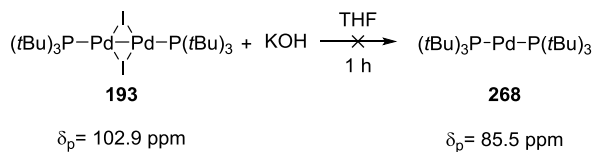
252

$$(tBu)_3P{-}Pd{-}Pd{-}P(tBu)_3 \ + \ KOH \ \xrightarrow[\text{1 h}]{\text{THF}} \ (tBu)_3P\text{-}Pd\text{-}P(tBu)_3$$

193   **268**

δ_p= 102.9 ppm δ_p= 85.5 ppm

The general procedure E was followed in this study. The ^{31}P-NMR spectrum was recorded after 1 h of reaction.
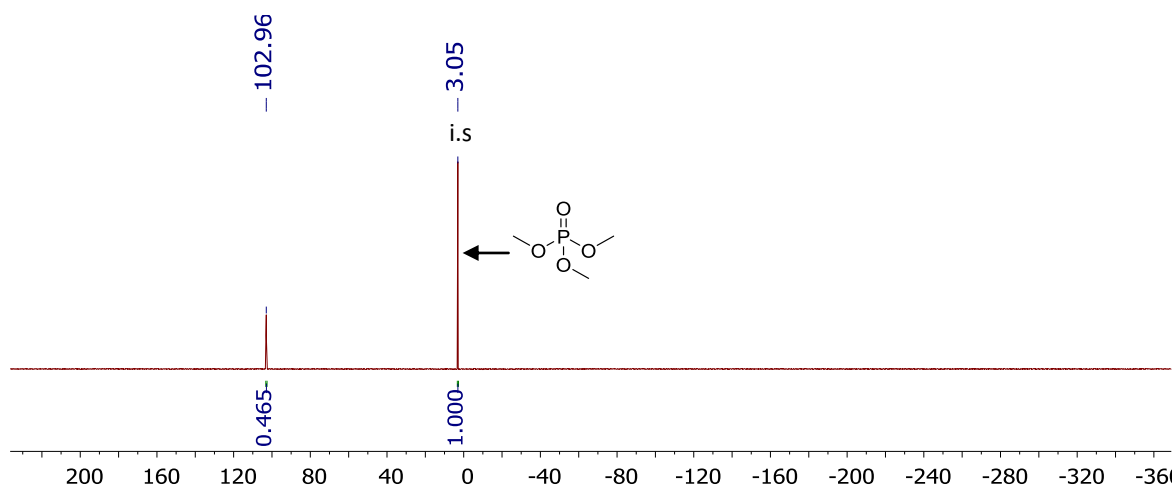
- Reaction between Pd(I)-iodo dimer **193** (1 equiv) and PCy$_3$ (20 equiv), *Table 22* Entry 4
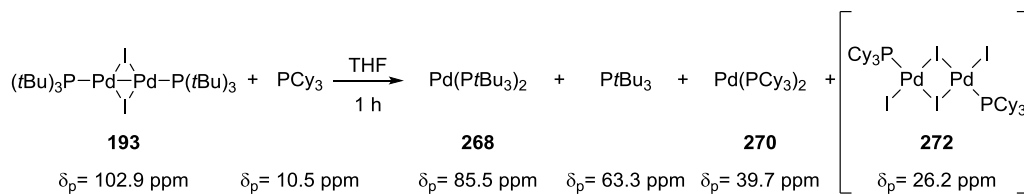
$(tBu)_3P{-}Pd{-}Pd{-}P(tBu)_3$ + PCy$_3$ $\xrightarrow[\text{1 h}]{\text{THF}}$ Pd(PtBu$_3$)$_2$ + PtBu$_3$ + Pd(PCy$_3$)$_2$ + [...]

193   **268**   **270**   **272**

δ_p= 102.9 ppm δ_p= 10.5 ppm δ_p= 85.5 ppm δ_p= 63.3 ppm δ_p= 39.7 ppm δ_p= 26.2 ppm

The general procedure E was followed in this study. The ^{31}P-NMR spectrum was recorded after 1 h of reaction.
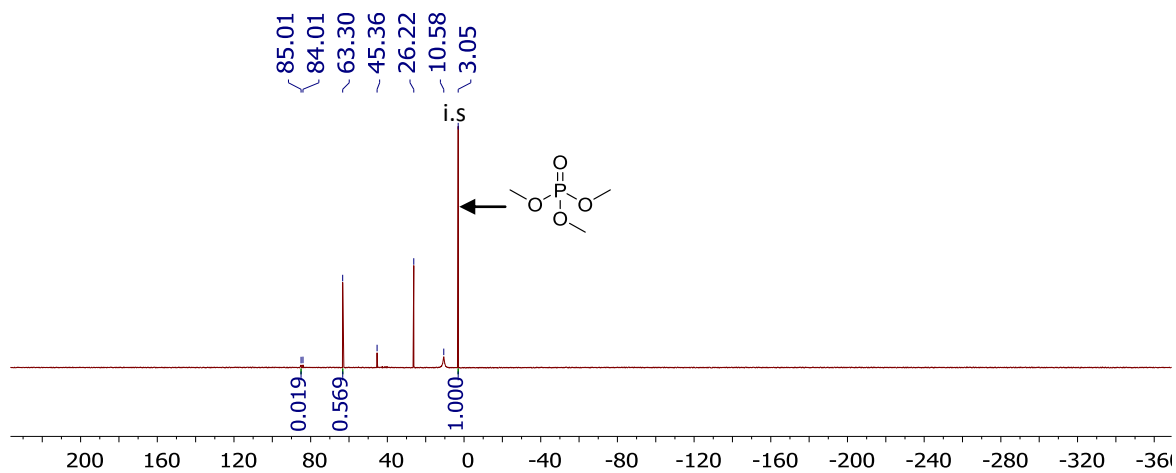
- Reaction between Pd(I)-iodo dimer **193** (1 equiv) and 1-Pyrrolidino-1-cyclopentene **328** (20 equiv), *Table 22* Entry 5
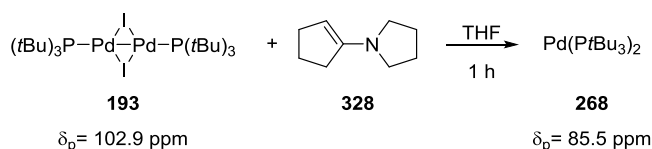
$(tBu)_3P-Pd-Pd-P(tBu)_3$ + [cyclopentenyl-pyrrolidine] $\xrightarrow[\text{1 h}]{\text{THF}}$ $Pd(PtBu_3)_2$

193   **328**   **268**

δ_p= 102.9 ppm δ_p= 85.5 ppm

The general procedure E was followed in this study. The ^{31}P-NMR spectrum was recorded after 1 h of reaction.
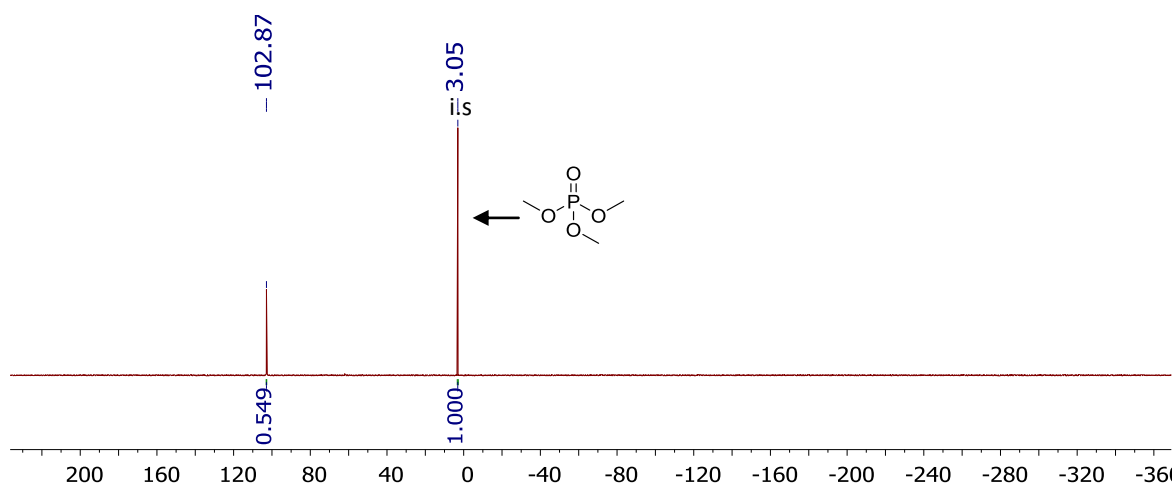
- Reaction between Pd(I)-iodo dimer **193** (1 equiv) and PEt$_3$ (20 equiv), *Table 22* Entry 6
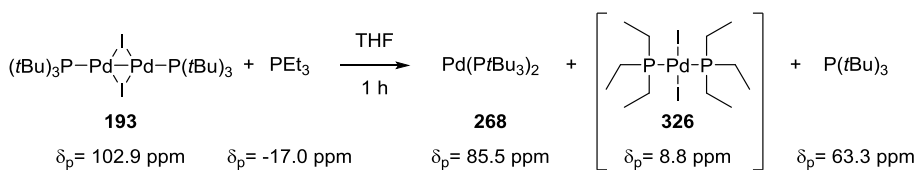
$(tBu)_3P-Pd-Pd-P(tBu)_3$ + PEt$_3$ $\xrightarrow[\text{1 h}]{\text{THF}}$ $Pd(PtBu_3)_2$ + [Et$_3$P-Pd-PEt$_3$] + P(tBu)$_3$

193   **268**   **326**

δ_p= 102.9 ppm δ_p= -17.0 ppm δ_p= 85.5 ppm δ_p= 8.8 ppm δ_p= 63.3 ppm

The general procedure E was followed in this study. The ^{31}P-NMR spectrum was recorded after 1 h of reaction.
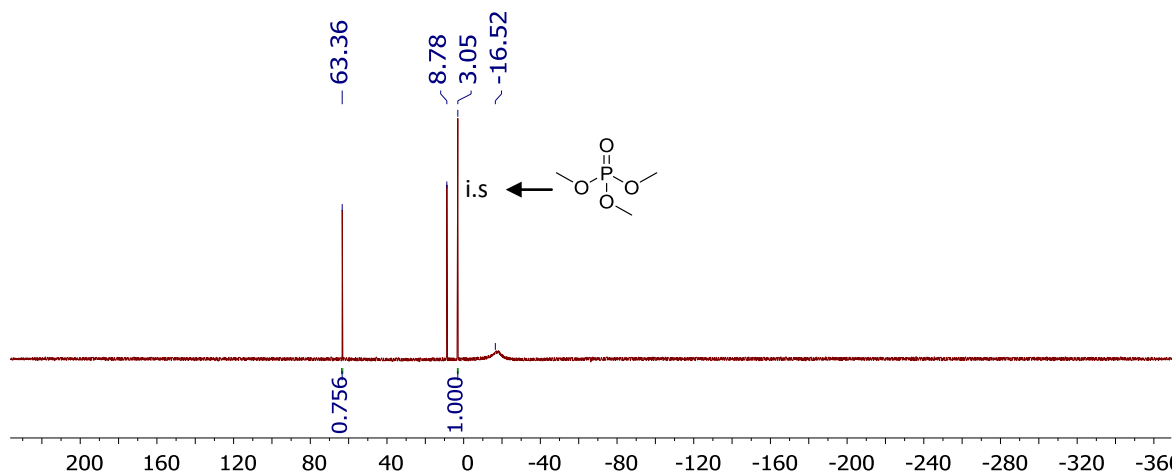
- Reaction between Pd(I)-iodo dimer **193** (1 equiv) and KOEt (20 equiv), *Table 22* Entry 7
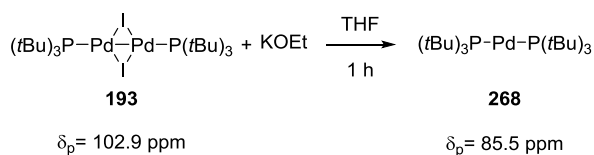
$(t\mathrm{Bu})_3\mathrm{P}-\mathrm{Pd}\overset{\mathrm{I}}{\underset{\mathrm{I}}{\cdot}}\mathrm{Pd}-\mathrm{P}(t\mathrm{Bu})_3$ + KOEt $\xrightarrow[\text{1 h}]{\text{THF}}$ $(t\mathrm{Bu})_3\mathrm{P}-\mathrm{Pd}-\mathrm{P}(t\mathrm{Bu})_3$

193   **268**

δ_p= 102.9 ppm δ_p= 85.5 ppm

The general procedure E was followed in this study. The ^{31}P-NMR spectrum was recorded after 1 h of reaction.
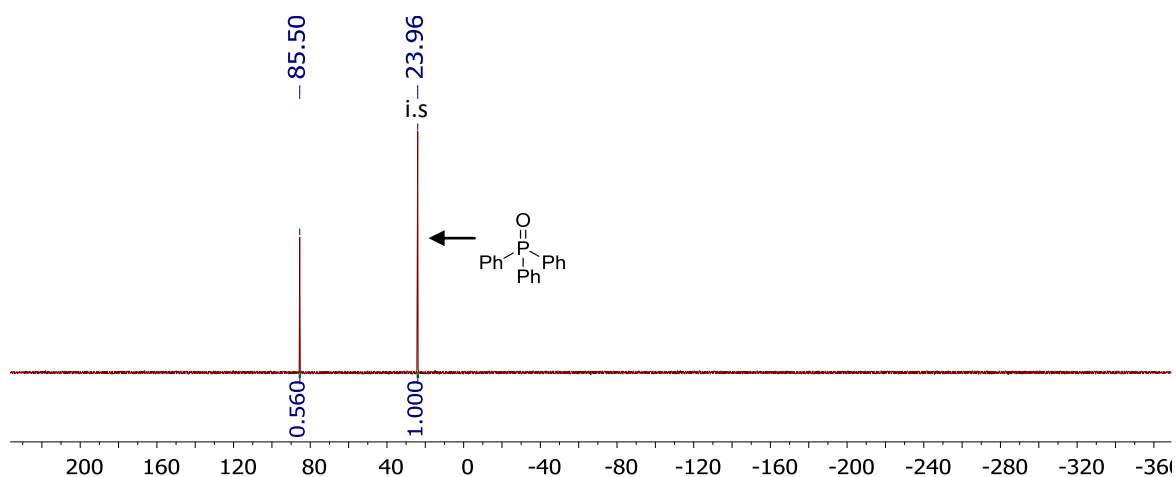
• Reaction between Pd(I)-iodo dimer **193** (1 equiv) and hppH **325** (20 equiv), *Table 22* Entry 8
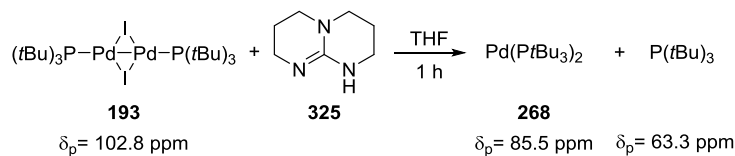
$(t\mathrm{Bu})_3\mathrm{P}-\mathrm{Pd}\overset{\mathrm{I}}{\underset{\mathrm{I}}{\cdot}}\mathrm{Pd}-\mathrm{P}(t\mathrm{Bu})_3$ + [hppH structure] $\xrightarrow[\text{1 h}]{\text{THF}}$ Pd(PtBu$_3$)$_2$ + P(tBu)$_3$

193   **325**   **268**

δ_p= 102.8 ppm δ_p= 85.5 ppm δ_p= 63.3 ppm

The general procedure E was followed in this study. The ^{31}P-NMR spectrum was recorded after 20 min of reaction.
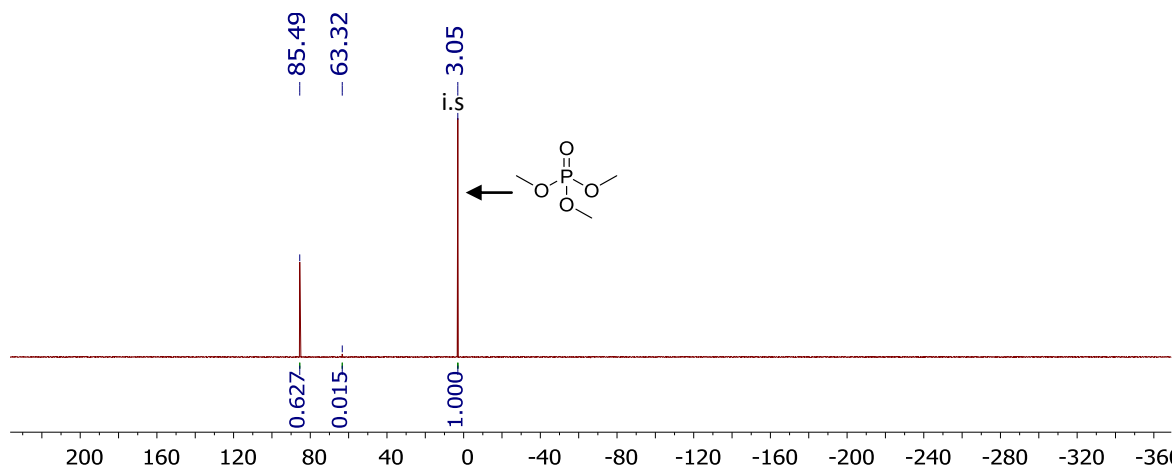
• Reaction between Pd-iodo dimer **193** and KOtBu, *Table 22* Entry 9
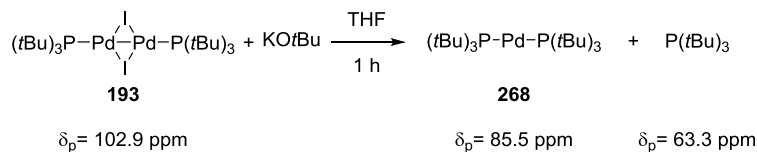
$(tBu)_3P-Pd-Pd-P(tBu)_3$ + KOtBu $\xrightarrow[\text{1 h}]{\text{THF}}$ $(tBu)_3P-Pd-P(tBu)_3$ + P$(tBu)_3$

193　　　　　　　　　　　　　　　　　　　　　**268**

δ_p= 102.9 ppm　　　　　　　　　　δ_p= 85.5 ppm　　　δ_p= 63.3 ppm

The general procedure E was followed in this study. The ^{31}P-NMR spectrum was recorded after 1 h of reaction.
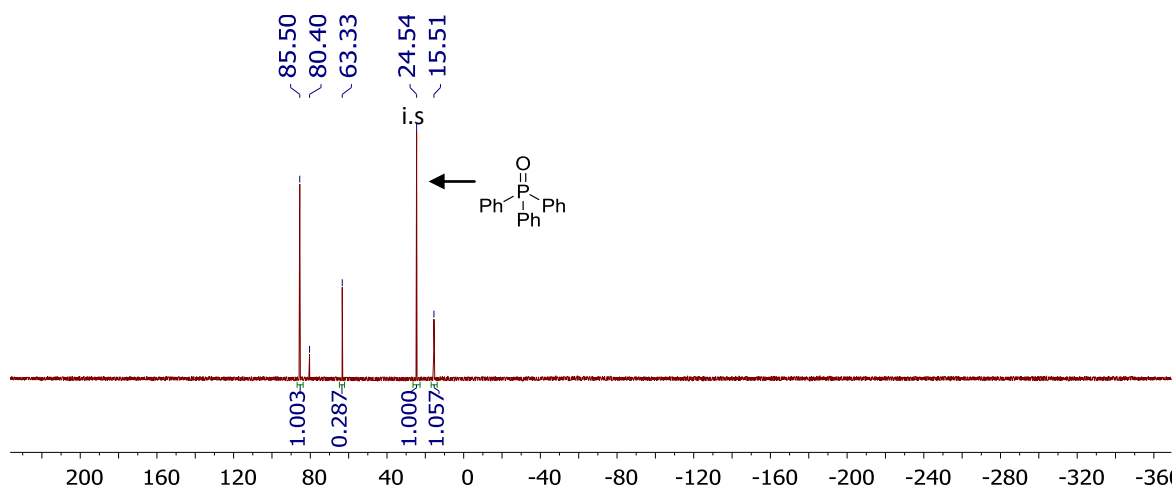
6.4.3 NMR investigations for the reactions reported in Chapter 4

- Reaction between Pd(I)-iodo dimer **193** and $(CH_3)_4NSeCF_3$ **346**.

$(tBu)_3P-Pd-Pd-P(tBu)_3$ + $(CH)_4NSeF_3$ $\xrightarrow[\text{24 h, r.t}]{\text{Toluene}}$ $(tBu)_3P-Pd-Pd-PH(tBu)_3$ + $(tBu)_3P-Pd-Pd-P(tBu)_3$ + P$(tBu)_3$

193　　　　　　**346**　　　　　　　　　　　　**348**　　　　　　　　**347**

δ_p= 102.3 ppm　　　　　　　　　　　　　δ_p= 101.4 ppm　　　δ_p= 99.1 ppm　　　δ_p= 62.4 ppm

　　　　　　　　　　　　　　　　　　　　　　δ_F= -26.2 ppm　　　δ_F= -24.5 ppm
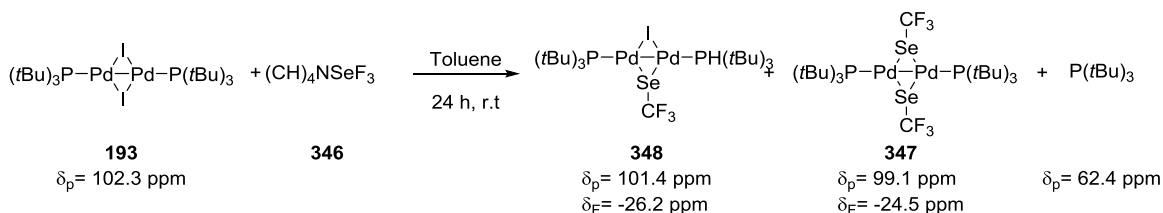
In A dry reaction vessel equipped with a stirring bar were added Pd(I)-iodo dimer **193** (20 mg, 0.023 mmol, 1 equiv) and $(CH_3)_4NSeCF_3$ **346** (10.3 mg, 0.046 mmol, 2 equiv) anf 2 mL of previously degassed dry toluene. The reaction was left under stir and it was analysed by ^{31}P and ^{19}F-NMR spectroscopy after 30 min, 2h, 5 h and 24 h.

^{31}P-NMR spectroscopy:

¹⁹F-NMR spectroscopy:

30 min

2 h

5 h

24 h

- Stoichiometric reaction between Pd(I)-iodo dimer **193**, $(CH_3)_4NSeCF_3$ **346** and 1-iodo-4-nitrobenzene
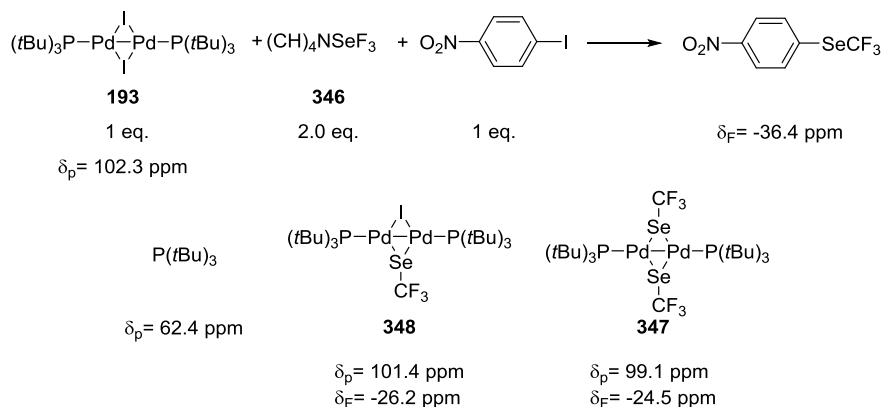
$(tBu)_3P-Pd-Pd-P(tBu)_3$ + $(CH_3)_4NSeF_3$ + O_2N—⟨C$_6$H$_4$⟩—I ⟶ O_2N—⟨C$_6$H$_4$⟩—$SeCF_3$

193 **346**

1 eq.   2.0 eq.   1 eq. δ_F= -36.4 ppm

δ_p= 102.3 ppm

$P(tBu)_3$

δ_p= 62.4 ppm

348

δ_p= 101.4 ppm
δ_F= -26.2 ppm

347

δ_p= 99.1 ppm
δ_F= -24.5 ppm

In a dry reaction vessel equipped with a stirring bar were added Pd(I)-iodo dimer **193** (50 mg, 0.06 mmol, 1.0 equiv), $(CH_3)_4NSeCF_3$ **346** (26.8 mg, 0.12, 2.0 equiv), 1-iodo-4-nitrobenzene (14.9 mg, 0.06 mmol, 1.0 equiv) and 2 mL of dry and degassed toluene. The reaction was left under stir at 50 °C and analysed by ^{31}P and ^{19}F-NMR spectroscopy after 1h, 7 h and 24 h.

^{31}P-NMR spectroscopy:
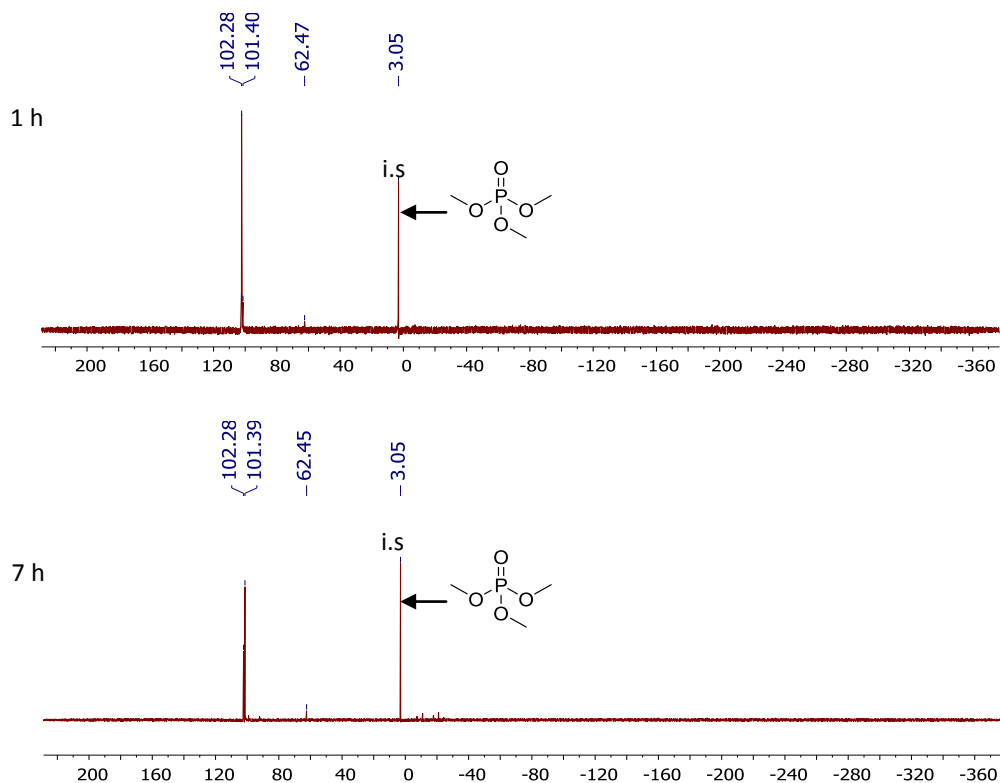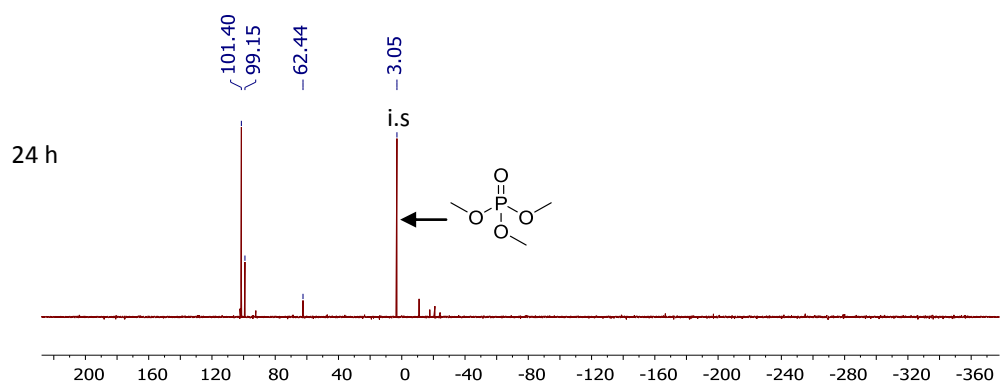
¹⁹F-NMR spectroscopy:
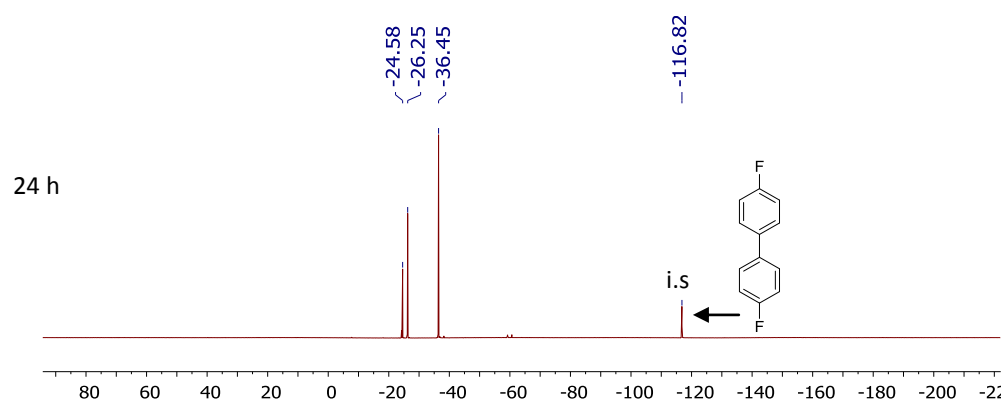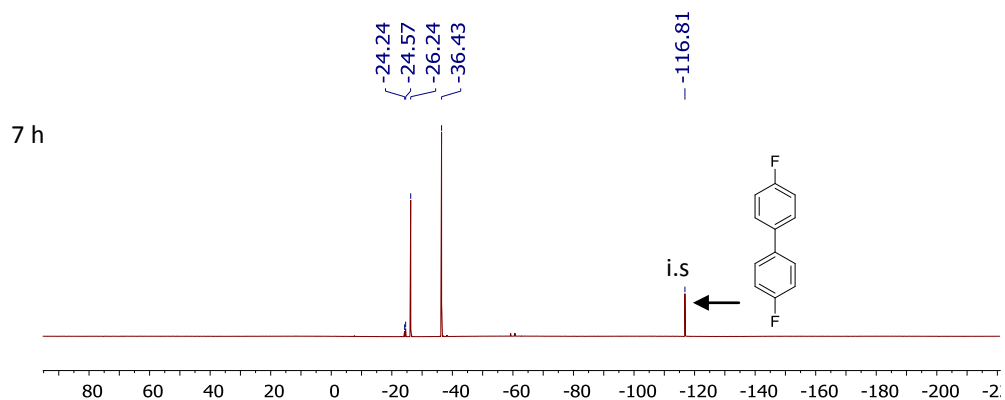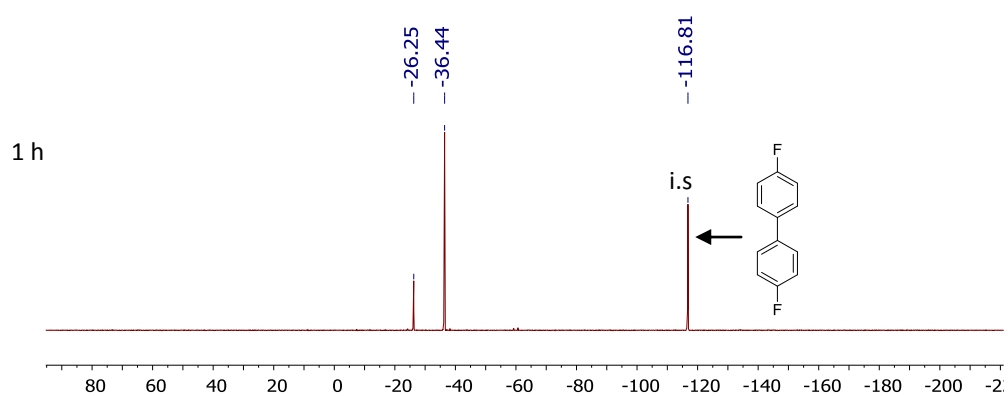
- Stoichiometric reaction between Pd-iodo dimer **193**, $(CH_3)_4NSeCF_3$ **346** and 1-iodo-4-methylbenzene.
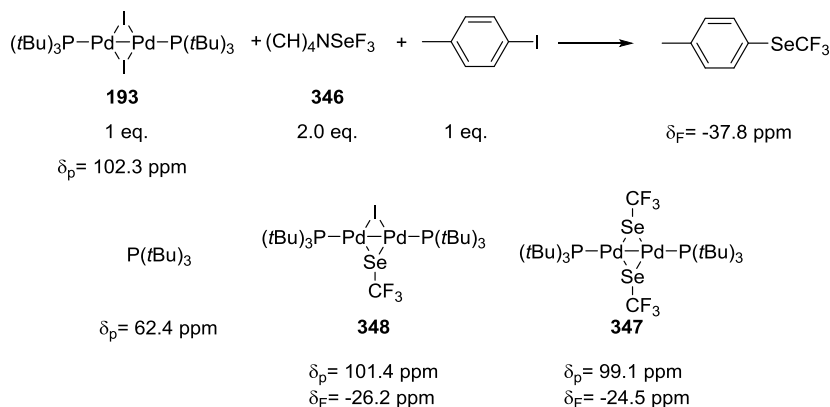
In a dry reaction vessel equipped with a stirring bar were added Pd(I)-iodo dimer **193** (50 mg, 0.06 mmol, 1.0 equiv), $(CH_3)_4NSeCF_3$ **346** (26.8 mg, 0.12, 2.0 equiv), 1-iodo-4-methylbenzene (13.1 mg, 0.06 mmol, 1.0 equiv) and 2 mL of dry and degassed toluene. The reaction was left under stir at 50 °C and analysed by ^{31}P and ^{19}F-NMR spectroscopy after 1h, 7 h and 24 h.

^{31}P-NMR spectroscopy:

24 h

101.37
99.14
−62.43
−3.05
i.s

¹⁹F-NMR spectroscopy:

1 h

−24.57
−26.24
−37.75
−116.81
i.s

7 h

−24.56
−26.23
−37.77
−116.81
i.s

f1 (ppm)

24 h

−24.546
−26.216
−37.760
−116.800
i.s

262
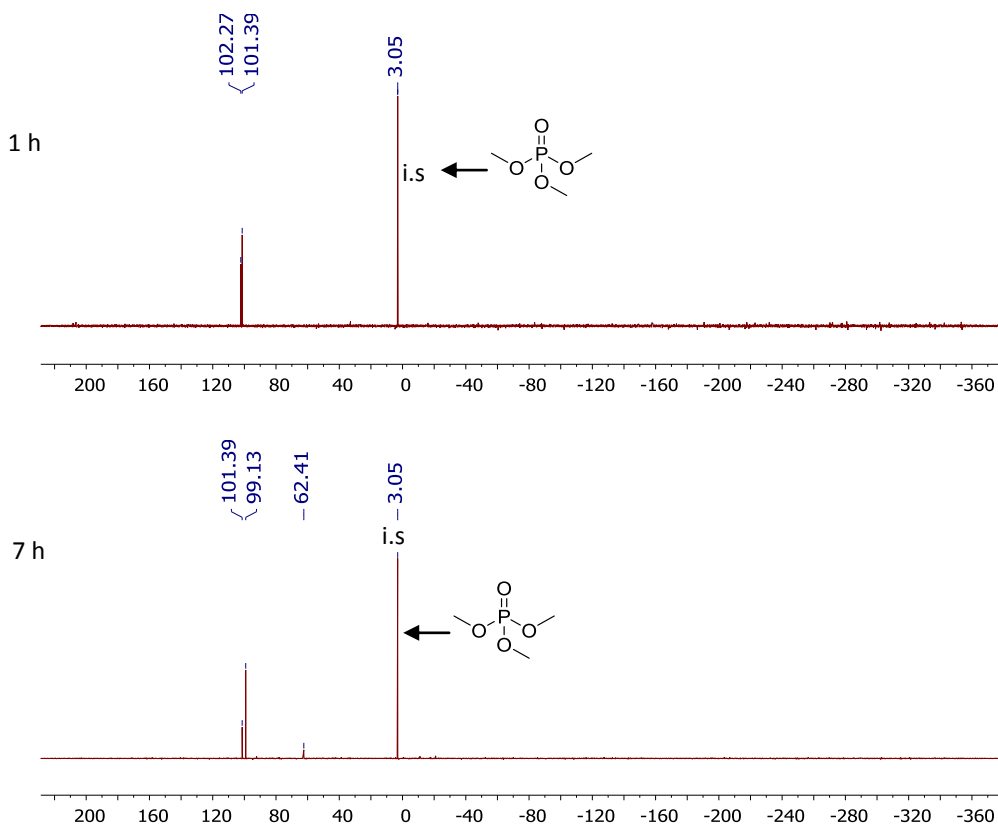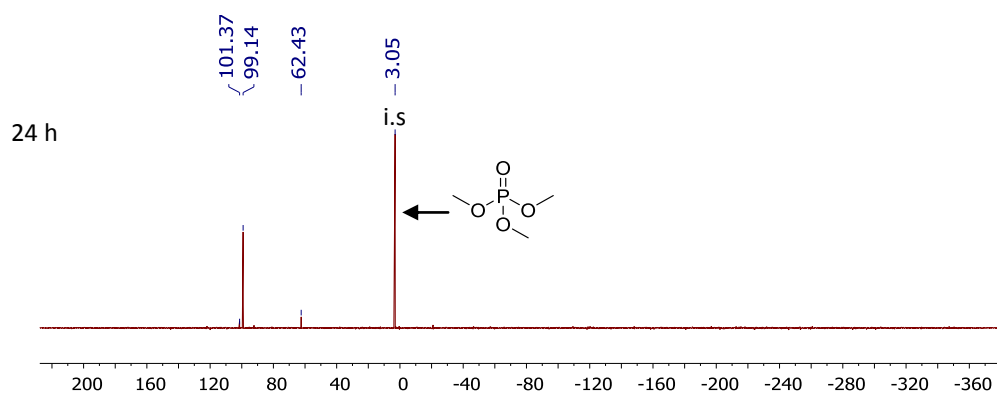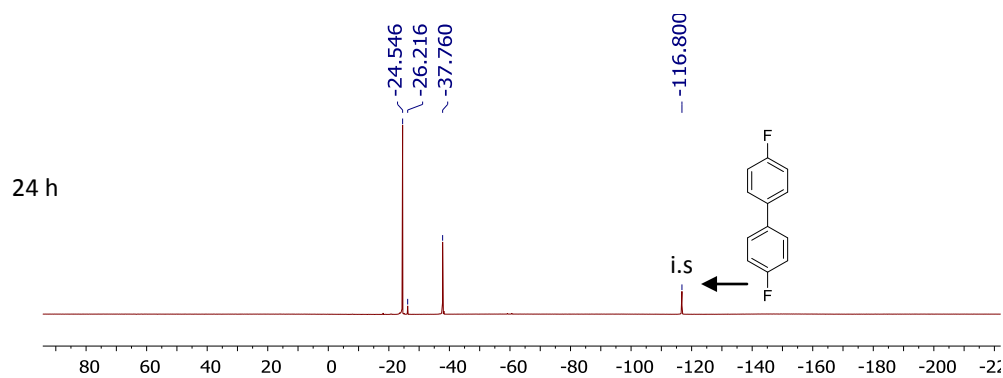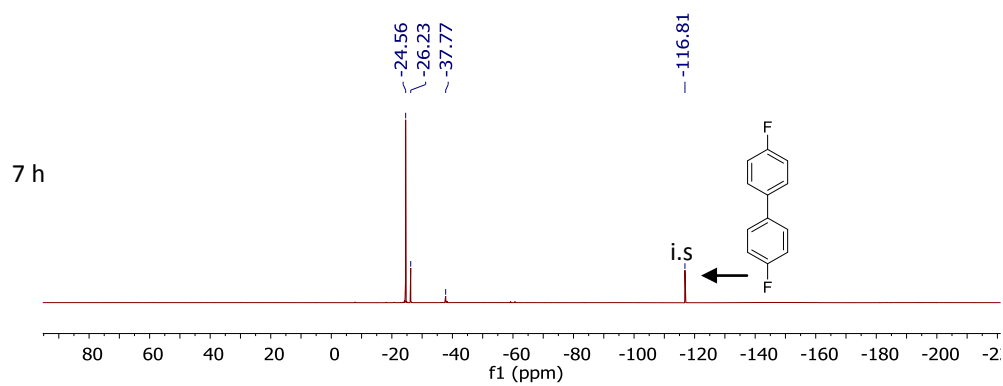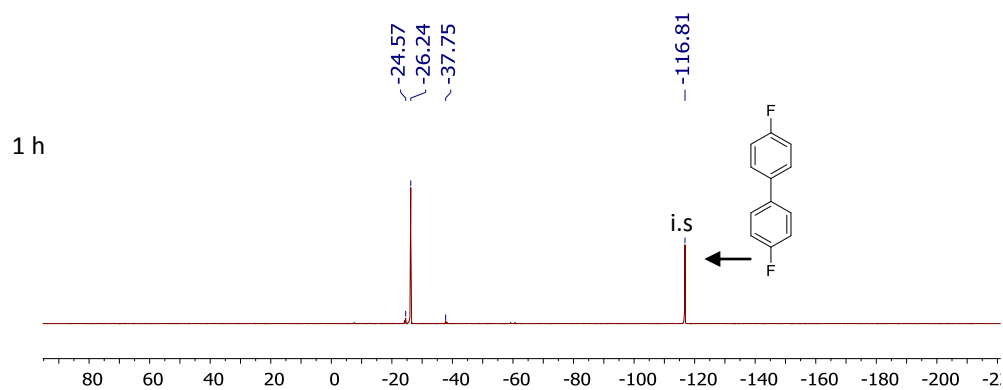
6.5 Computational details

All calculations were performed with the Gaussian 09 program package.[379] Structural optimizations and frequency calculations were performed with B3LYP along with 6-31G(d)[380] basis set on all atoms except Pd, I and the effective core potential (ECP) LANL2DZ on Pd and I atoms. Single point energy calculations were performed with M06L functional and 6-311++G(d,p) basis set and def2-TZVP for Pd, I. Solvent effects of toluene were taken into account using the CPCM solvation model. All energies are relative to 1M standard state.[381] Figures were made with CYLview.[382]

XYZ coordinates and Energies:
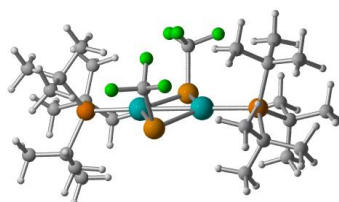
Pd	1.32873	0.03082	-0.3052	C	4.0996	-2.82274	-0.12089
P	3.71928	0.01564	-0.33762	H	3.05263	-2.86816	0.18631
C	4.37011	-1.66008	-1.10134	H	4.32941	-3.76419	-0.63696
C	4.48621	1.48518	-1.36282	H	4.72637	-2.78812	0.77287
C	4.33338	0.14793	1.50439	C	4.19589	1.60159	2.00889
Pd	-1.34627	0.01458	-0.28731	H	4.37032	1.60228	3.09294
P	-3.74226	0.00642	-0.32499	H	4.93128	2.27859	1.56801
C	-4.49324	1.80217	-0.49828	H	3.19619	2.00915	1.84001
C	-4.42286	-1.07543	-1.79801	C	3.36878	-0.69285	2.37428
C	-4.36012	-0.75795	1.35702	H	3.36372	-1.75386	2.12711
C	3.71634	2.78996	-1.05206	H	3.67364	-0.59878	3.4255
H	4.14345	3.59351	-1.66715	H	2.34185	-0.32511	2.28676
H	2.65687	2.70073	-1.30029	C	5.78558	-0.3088	1.75775
H	3.78699	3.10282	-0.01092	H	6.01857	-0.15833	2.8207
C	5.98916	1.73613	-1.11272	H	5.94085	-1.36857	1.54434
H	6.60706	0.85475	-1.29339	H	6.51564	0.2665	1.18203
H	6.33252	2.5237	-1.79716	C	-4.26138	2.58479	0.81334
H	6.1876	2.08851	-0.09741	H	-3.21067	2.58025	1.11377
C	4.27073	1.22505	-2.87037	H	-4.5452	3.63153	0.6425
H	4.89832	0.422	-3.26228	H	-4.86838	2.22177	1.64542
H	3.22387	0.99682	-3.09685	C	-5.99696	1.85379	-0.84219
H	4.53487	2.13785	-3.42003	H	-6.32201	2.9029	-0.83085
C	3.53627	-1.9792	-2.36691	H	-6.21039	1.46737	-1.84208
H	3.6609	-1.2504	-3.16768	H	-6.6197	1.31305	-0.12605
H	3.85917	-2.95386	-2.75686	C	-3.71469	2.57637	-1.58865
H	2.47179	-2.04959	-2.12877	H	-2.64983	2.63344	-1.35259
C	5.86734	-1.682	-1.47624	H	-3.8217	2.15116	-2.58639
H	6.12633	-2.69221	-1.82084	H	-4.10579	3.60195	-1.62669
H	6.10702	-0.99731	-2.2934	C	-3.4479	-0.20646	2.48015
H	6.52081	-1.44965	-0.632	H	-3.50517	0.87616	2.59621

H	-3.75621	-0.65774	3.43309
H	-2.40157	-0.47448	2.30559
C	-4.14901	-2.28833	1.35693
H	-3.12463	-2.56648	1.1005
H	-4.34073	-2.65657	2.37331
H	-4.83707	-2.81585	0.69198
C	-5.83575	-0.48451	1.71773
H	-6.06615	-1.00105	2.65934
H	-6.04452	0.57554	1.87799
H	-6.53218	-0.86057	0.96308
C	-5.90117	-1.50028	-1.67097
H	-6.18847	-2.04948	-2.57794
H	-6.07072	-2.17101	-0.82544
H	-6.58338	-0.65293	-1.57455
C	-3.55141	-2.34568	-1.92956
H	-3.58385	-2.9933	-1.05377
H	-3.91761	-2.92888	-2.78532

H	-2.50526	-2.09125	-2.11434
C	-4.24402	-0.3102	-3.1283
H	-4.4475	-1.00313	-3.95514
H	-4.93426	0.52907	-3.23672
H	-3.22021	0.05773	-3.2526
C	0.04918	-2.74927	1.50069
C	0.0506	2.73614	1.50834
F	-0.06763	-1.75255	2.40207
F	1.20363	-3.39847	1.77985
F	-0.9576	-3.61845	1.74322
F	1.16404	3.46834	1.74689
F	0.05857	1.71322	2.38623
F	-1.0084	3.51588	1.821
Se	-0.01497	2.17616	-0.37935
Se	0.01524	-2.14678	-0.3738

Zero-point correction=   0.778584
 Thermal correction to Energy=   0.831819
 Thermal correction to Enthalpy=   0.832763
 Thermal correction to Gibbs Free Energy=   0.694029
 Sum of electronic and zero-point Energies=   -7355.739204
 Sum of electronic and thermal Energies=   -7355.685968
 Sum of electronic and thermal Enthalpies=   -7355.685024
 Sum of electronic and thermal Free Energies=   -7355.823758

CPCM (Toluene) M06L/def2-TZVP   E(RM06L) = −7364.63341849

Oxidative addition TS-1
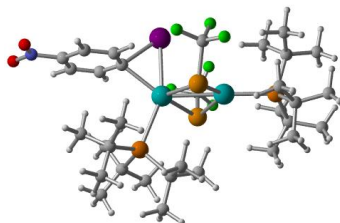
C	-5.52709	-1.93012	-0.10351
C	-3.75439	-1.30454	1.39679
C	-2.81127	-1.54469	0.37623
C	-3.2505	-2.01387	-0.87948
H	-2.52976	-2.26406	-1.64828
H	-3.42105	-1.01102	2.38522
C	-4.60666	-2.1912	-1.12288
C	-5.11029	-1.48714	1.1555
H	-4.96214	-2.54251	-2.08417
H	-5.84819	-1.30671	1.92816
Pd	-1.05472	-0.03599	0.24494
Pd	1.76094	0.00318	-0.08107
H	-4.25777	4.7546	2.00194
H	-3.58001	5.16784	0.42726
H	-4.41344	1.60354	1.62565
H	-2.84409	1.35892	2.40152
H	-3.97292	2.567	3.03878
C	-1.3879	5.10386	-1.1506
C	0.39169	3.50897	-0.40459
C	-0.64324	3.22817	-2.61981

I	-0.91645	-2.73027	1.22415
H	-2.21693	4.10095	3.08384
C	-1.79452	3.79808	2.11659
C	-2.938	3.21906	1.25455
H	-1.01812	3.05675	2.32191
H	-1.32908	4.68487	1.6814
P	-2.22691	2.36573	-0.36039
C	-3.97259	4.342	1.02463
C	-3.58435	2.11227	2.11745
C	-0.95202	3.62147	-1.15777
C	-3.69376	2.18339	-1.63753
H	-4.8898	3.98483	0.55223
H	7.01585	0.8115	0.66897
H	6.52394	2.23608	-0.26406
H	6.71407	2.34676	1.48092
H	3.02463	2.49422	1.15551
H	4.49378	3.35517	1.6295
H	4.09746	3.1743	-0.07896
H	5.05922	1.60832	3.05315
H	3.71914	0.55505	2.61503

C	-3.24782	1.17933	-2.72603	H	5.38944	-0.04897	2.56267
C	-4.91013	1.54682	-0.93228	H	4.00936	-1.67306	2.15912
C	-4.17291	3.47777	-2.32877	H	2.84396	-2.28412	0.98339
H	-2.34339	5.27282	-1.65035	H	4.23416	-3.2754	1.45504
H	-1.45155	5.52	-0.14316	H	5.13872	-2.45616	-1.98403
H	-0.6306	5.69007	-1.68933	H	4.73363	-3.67955	-0.7865
H	0.83048	2.51256	-0.52314	H	3.45687	-2.65916	-1.44226
H	1.09654	4.23292	-0.83628	H	6.50356	-2.83853	0.61021
H	0.31814	3.72296	0.66144	H	6.90381	-1.42322	-0.36369
H	0.21608	3.82172	-2.95989	H	6.49169	-1.24217	1.34952
H	-0.37081	2.1744	-2.72205	H	3.47389	2.3945	-2.12919
H	-1.46599	3.44105	-3.30473	H	5.19396	2.71345	-1.80717
H	-2.43303	1.54985	-3.34758	H	4.6605	2.30025	-3.43365
H	-2.93524	0.2289	-2.28946	H	6.36542	-0.84779	-2.45049
H	-4.10114	0.98041	-3.3882	H	6.45642	0.62615	-3.40746
H	-5.40875	2.22866	-0.2403	H	6.88227	0.66781	-1.69731
H	-5.64769	1.27002	-1.69649	H	3.82291	-1.21839	-3.11402
H	-4.64342	0.63836	-0.39284	H	2.81034	0.21941	-3.18104
H	-5.03564	3.23013	-2.96218	H	4.25582	0.10705	-4.19409
H	-4.50064	4.24393	-1.62257	C	1.00119	-0.24548	3.57707
H	-3.41624	3.91527	-2.98334	F	1.81444	0.35909	4.47445
P	4.11308	0.08672	-0.35039	F	-0.17235	-0.47591	4.18999
C	4.88321	1.35438	0.92328	F	1.56233	-1.43359	3.29188
C	4.75346	-1.70532	0.06541	C	0.56874	-2.32262	-2.6498
C	4.70952	0.57534	-2.14224	F	-0.61922	-2.83326	-3.04044
C	6.36943	1.69177	0.67017	F	1.40612	-2.40608	-3.7071
C	4.06804	2.66868	0.8859	F	1.06474	-3.13615	-1.69921
C	4.74974	0.81287	2.36336	Se	0.76312	0.94563	2.0145
C	3.90722	-2.24915	1.24036	Se	0.35738	-0.44266	-2.08289
C	4.50047	-2.66077	-1.12188	N	-6.94859	-2.12739	-0.35645
C	6.25009	-1.78496	0.43376	O	-7.28702	-2.5108	-1.48018
C	4.49701	2.0882	-2.36934	O	-7.7365	-1.89593	0.56561
C	6.19076	0.23004	-2.4187				
C	3.84215	-0.13382	-3.20586				

Zero-point correction=   0.871701
Thermal correction to Energy=   0.935861
Thermal correction to Enthalpy=   0.936805
Thermal correction to Gibbs Free Energy=   0.771542
Sum of electronic and zero-point Energies=   -7803.100237
Sum of electronic and thermal Energies=   -7803.036076
Sum of electronic and thermal Enthalpies=   -7803.035132
Sum of electronic and thermal Free Energies=   -7803.200395

CPCM (Toluene) M06L/def2-TZVP E= –8098.74306457
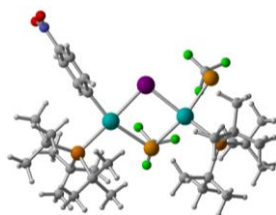
C	4.51465	4.16511	-1.76209	C	3.14033	1.92264	-0.77012
C	3.77299	2.80964	0.10824	C	3.16772	2.18455	-2.14637

H	2.64597	1.53188	-2.84085	C	-3.00934	-3.09959	-0.37615
H	3.72165	2.65268	1.18218	C	-5.27089	-1.10586	0.61186
C	3.85609	3.29903	-2.63822	C	-5.65613	-1.95007	-2.72372
C	4.46367	3.92138	-0.38848	C	-4.58735	0.30662	-2.83921
H	3.8699	3.49064	-3.70878	C	-3.2529	-1.6865	-3.39276
H	4.95397	4.60074	0.3051	C	-1.65558	-3.20403	-1.13773
H	4.72403	-3.44381	2.2174	C	-2.75582	-3.35048	1.12904
C	5.34931	-2.54973	2.24974	C	-3.89442	-4.25916	-0.89186
C	4.58859	-1.26512	1.85672	C	-6.20698	0.0412	0.16746
H	6.23081	-2.72653	1.63119	C	-6.14153	-2.373	0.75755
H	5.69548	-2.44021	3.2862	C	-4.71357	-0.7127	1.99923
P	3.92853	-1.208	0.02503	H	-5.59483	-3.00653	-2.45928
C	5.52426	-0.064	2.11702	H	-6.52	-1.5211	-2.21216
C	3.38027	-1.08915	2.8001	H	-5.86153	-1.89478	-3.80106
C	3.1798	-2.96512	-0.43352	H	-3.65346	0.87461	-2.83213
C	5.47719	-0.9436	-1.15856	H	-4.97313	0.3224	-3.86735
H	5.0853	0.88396	1.79461	H	-5.3072	0.82391	-2.20706
H	5.69892	0.00438	3.1985	H	-3.53187	-1.41324	-4.4183
H	6.50086	-0.17802	1.64132	H	-2.27919	-1.23049	-3.18707
H	3.74598	-1.05865	3.83531	H	-3.14476	-2.77188	-3.36881
H	2.8517	-0.15088	2.60674	H	-1.78571	-3.65771	-2.12276
H	2.6566	-1.89993	2.73532	H	-1.15905	-2.24425	-1.27779
C	2.23787	-2.76191	-1.64455	H	-0.96893	-3.84235	-0.57188
C	4.19787	-4.07127	-0.78788	H	-3.6846	-3.45702	1.69241
C	2.31858	-3.51898	0.72357	H	-2.20547	-4.29423	1.2329
C	6.03582	0.50064	-1.11223	H	-2.15562	-2.56842	1.59245
C	6.67384	-1.87361	-0.84365	H	-3.37548	-5.20001	-0.66274
C	5.03015	-1.16376	-2.62205	H	-4.87604	-4.30901	-0.41937
H	1.45512	-2.03053	-1.42803	H	-4.03158	-4.23216	-1.97497
H	2.76179	-2.43623	-2.54444	H	-5.67227	0.98258	0.03816
H	1.75046	-3.71844	-1.87491	H	-6.75705	-0.18601	-0.74876
H	4.89691	-4.27846	0.02679	H	-6.95308	0.18538	0.95997
H	3.63757	-4.9973	-0.97354	H	-5.61785	-3.20419	1.23309
H	4.7703	-3.86228	-1.69307	H	-6.99209	-2.12318	1.40525
H	1.80821	-4.42043	0.35872	H	-6.55272	-2.71871	-0.19451
H	2.91349	-3.82022	1.58749	H	-4.03555	-1.45562	2.42058
H	1.54573	-2.82503	1.05043	H	-4.18645	0.24205	1.96269
H	5.35766	1.21859	-1.56362	H	-5.55878	-0.60442	2.6921
H	6.28822	0.85031	-0.11349	C	-0.27211	-0.53981	2.5397
H	6.96305	0.50544	-1.70118	F	0.28215	-1.52764	3.28841
H	6.42213	-2.93018	-0.77106	F	0.33523	0.60558	2.90364
H	7.40591	-1.76806	-1.65531	F	-1.56347	-0.44312	2.93382
H	7.18172	-1.57753	0.07817	C	-3.46067	3.15992	1.01938
H	4.82911	-2.20878	-2.86478	F	-4.67874	3.69522	1.2718
H	4.14682	-0.56727	-2.86948	F	-3.15046	2.3709	2.0831
H	5.84206	-0.8322	-3.28203	F	-2.58457	4.18665	1.0425
Pd	2.01226	0.41609	-0.05537	Se	-3.50873	2.2649	-0.55192
Pd	-1.99278	0.45221	-0.10088	Se	-0.12788	-0.98136	0.65613
I	0.01581	2.3191	-0.22356	N	5.23658	5.3359	-2.2807
P	-3.7419	-1.29259	-0.59094	O	5.79017	6.05709	-1.4985
C	-4.35387	-1.1659	-2.44193	O	5.24315	5.52316	-3.46531

Zero-point correction=   0.874191 Thermal correction to Energy=   0.938224
Thermal correction to Enthalpy=   0.939169
Thermal correction to Gibbs Free Energy=   0.773638
Sum of electronic and zero-point Energies=   -7803.147126
Sum of electronic and thermal Energies=   -7803.083092
Sum of electronic and thermal Enthalpies=   -7803.082148
Sum of electronic and thermal Free Energies=   -7803.247679

CPCM (Toluene) M06L/def2-TZVP   E= –8098.77545865
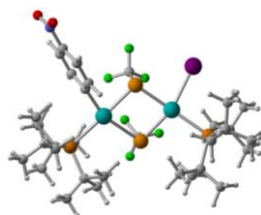
C	-4.57811	3.60734	1.07148
C	-3.79871	2.02068	-0.55649
C	-3.04022	1.3651	0.42691
C	-3.03765	1.88927	1.73357
H	-2.43248	1.42607	2.50824
H	-3.7849	1.67384	-1.58411
C	-3.80585	3.00343	2.06473
C	-4.57582	3.13492	-0.24023
H	-3.81572	3.40952	3.06932
H	-5.17169	3.6416	-0.99031
H	-4.19474	-4.60886	-1.58974
C	-4.8908	-3.78141	-1.73811
C	-4.23588	-2.39774	-1.53876
H	-5.75358	-3.94059	-1.08841
H	-5.24816	-3.84661	-2.77443
P	-3.56429	-2.03203	0.25262
C	-5.26953	-1.32284	-1.94242
C	-3.0553	-2.24995	-2.52326
C	-2.68328	-3.6498	0.93029
C	-5.10828	-1.72016	1.42512
H	-4.89971	-0.30814	-1.77323
H	-5.46813	-1.42598	-3.01692
H	-6.22573	-1.43869	-1.42751
H	-3.43064	-2.40153	-3.54409
H	-2.61796	-1.24862	-2.47617
H	-2.25681	-2.97315	-2.36166
C	-1.7525	-3.22552	2.09179
C	-3.61696	-4.77072	1.43738
C	-1.78537	-4.28663	-0.15442
C	-5.73113	-0.32286	1.19776
C	-6.25288	-2.74637	1.25464
C	-4.63891	-1.72396	2.89833
H	-1.01116	-2.494	1.76338
H	-2.28942	-2.80596	2.94348
H	-1.21048	-4.11143	2.44844
H	-4.30767	-5.12365	0.66782
H	-2.99128	-5.62562	1.72629
H	-4.19346	-4.49073	2.32056
H	-1.19746	-5.08342	0.31997
H	-2.35494	-4.74922	-0.96248
H	-1.07552	-3.58284	-0.58521
H	-5.06578	0.47305	1.52132
H	-6.02194	-0.12656	0.16768
H	-6.64043	-0.26398	1.81047
H	-5.94151	-3.78682	1.33635
H	-6.99266	-2.56416	2.04544
H	-6.77322	-2.61817	0.3021
H	-4.36339	-2.71364	3.26647
H	-3.7975	-1.04252	3.06032

H	-5.46878	-1.36901	3.52263
Pd	-1.80203	-0.17988	-0.00492
Pd	2.04591	0.48232	-0.01031
I	3.06894	3.03451	-0.3189
P	4.17513	-0.69194	0.80434
C	4.78757	0.0023	2.52688
C	3.85903	-2.61179	1.07658
C	5.6027	-0.48971	-0.51648
C	6.23007	-0.41611	2.8917
C	4.71711	1.54258	2.55335
C	3.83485	-0.48199	3.6422
C	2.5687	-2.80909	1.92896
C	3.65318	-3.27686	-0.3044
C	4.98358	-3.39609	1.79324
C	6.27264	0.89739	-0.40664
C	6.72828	-1.54283	-0.43405
C	4.93673	-0.55673	-1.91016
H	6.39321	-1.4938	2.8646
H	6.97515	0.05717	2.24881
H	6.43375	-0.07946	3.91694
H	3.69302	1.90409	2.44627
H	5.09516	1.87977	3.52797
H	5.31677	2.02287	1.7816
H	4.06792	0.07715	4.55706
H	2.78529	-0.2866	3.40001
H	3.94969	-1.54164	3.87536
H	2.81126	-3.0025	2.97647
H	1.89154	-1.9548	1.90354
H	2.01129	-3.67517	1.5573
H	4.57741	-3.3305	-0.88224
H	3.3134	-4.30806	-0.14515
H	2.89876	-2.77412	-0.90704
H	4.68938	-4.45434	1.81664
H	5.94909	-3.34046	1.28861
H	5.11533	-3.08456	2.83137
H	5.55384	1.71532	-0.4612
H	6.87226	1.00964	0.49923
H	6.95636	1.00454	-1.25902
H	6.39138	-2.55685	-0.65569
H	7.48505	-1.28796	-1.18748
H	7.23036	-1.54795	0.53712
H	4.45123	-1.51275	-2.11072
H	4.19182	0.23517	-2.03158
H	5.71087	-0.41012	-2.67496
C	0.6327	-1.63183	-2.39108
F	0.30446	-2.88862	-2.77567
F	-0.18331	-0.79461	-3.04964
F	1.88646	-1.39948	-2.82643
C	-0.31459	2.17666	-2.15398

F	-0.43117	3.50608	-2.26785	Se	0.51533	-1.52592	-0.42013
F	0.7341	1.78191	-2.88186	N	-5.40239	4.76961	1.41342
F	-1.42326	1.62745	-2.69563	O	-6.07373	5.2824	0.51627
Se	-0.13845	1.70651	-0.21495	O	-5.38173	5.16514	2.58052

Zero-point correction= 0.873799
Thermal correction to Energy= 0.937945
Thermal correction to Enthalpy= 0.938889
Thermal correction to Gibbs Free Energy= 0.773820
Sum of electronic and zero-point Energies= -7803.156801
Sum of electronic and thermal Energies= -7803.092655
Sum of electronic and thermal Enthalpies= -7803.091711
Sum of electronic and thermal Free Energies= -7803.256780

CPCM (Toluene) M06L/def2-TZVP E= −8098.77744341

Reductive elimination TS-2
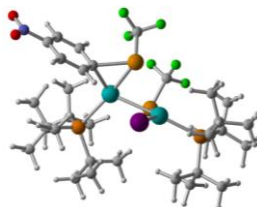
C	-5.3492	-1.86415	-1.20794	C	-3.3118	2.13339	-2.17519
C	-3.69038	-1.68308	0.52497	C	-4.89666	1.81088	-0.29329
C	-2.71445	-1.34471	-0.44132	C	-4.21648	4.12034	-0.94887
C	-3.07918	-1.33891	-1.80712	H	-2.2697	5.58555	0.14592
H	-2.31972	-1.15571	-2.55951	H	-1.33918	5.29694	1.62142
H	-3.42557	-1.75988	1.57191	H	-0.54708	5.95903	0.19523
C	-4.38968	-1.57849	-2.18777	H	0.83383	2.54254	0.1543
C	-5.00701	-1.92279	0.14317	H	1.16805	4.26282	0.38738
H	-4.68319	-1.5608	-3.23053	H	0.44614	3.32806	1.69689
H	-5.76825	-2.16128	0.87648	H	0.18495	4.57483	-1.68196
Pd	-1.25606	0.01367	0.40196	H	-0.46263	2.95285	-1.95209
Pd	1.57104	-0.06145	-0.24314	H	-1.52429	4.37828	-2.04288
H	-2.0065	2.90932	4.24097	H	-2.62822	2.79208	-2.70951
C	-1.6358	2.94021	3.20794	H	-2.85181	1.14653	-2.11955
C	-2.8299	2.6889	2.25962	H	-4.21883	2.04199	-2.78703
H	-0.87107	2.1658	3.11433	H	-5.35139	2.18902	0.62517
H	-1.16843	3.9173	3.06696	H	-5.67563	1.8318	-1.06584
P	-2.19798	2.42478	0.42838	H	-4.61719	0.76713	-0.14019
C	-3.85486	3.82245	2.47082	H	-5.10246	4.09947	-1.5979
C	-3.45471	1.35216	2.72436	H	-4.51655	4.58498	-0.00738
C	-0.91812	3.8395	0.01678	H	-3.48581	4.76987	-1.43524
C	-3.71016	2.67212	-0.77968	P	4.02456	0.07045	-0.54263
H	-4.80342	3.63762	1.96207	C	5.0692	-0.19931	1.10118
H	-4.07784	3.8935	3.54406	C	4.49453	-1.40016	-1.7712
H	-3.48081	4.79862	2.1527	C	4.56034	1.77084	-1.32762
H	-4.32159	1.04694	2.13686	C	6.59278	0.0122	0.93526
H	-2.71623	0.54353	2.68622	C	4.63242	0.76116	2.22917
H	-3.78052	1.45773	3.76795	C	4.80231	-1.63724	1.59588
C	-1.3082	5.2418	0.53146	C	3.58834	-2.60489	-1.42111
C	0.45298	3.46057	0.61498	C	4.22089	-1.03296	-3.24589
C	-0.68548	3.92821	-1.50874	C	5.97141	-1.85364	-1.71025

C	4.53158	2.87788	-0.25079		H	5.3801	2.82606	0.43481
C	5.96712	1.7526	-1.96657		H	4.59016	3.84798	-0.76037
C	3.53616	2.18361	-2.40491		H	6.02801	1.0882	-2.83023
H	7.04931	-0.58243	0.14677		H	6.19196	2.76582	-2.32535
H	6.83876	1.06294	0.76434		H	6.75578	1.47553	-1.2653
H	7.07047	-0.27649	1.88071		H	3.46685	1.48039	-3.23398
H	3.5582	0.7559	2.39816		H	2.53441	2.29647	-1.98477
H	5.11664	0.42962	3.15633		H	3.84658	3.15379	-2.81501
H	4.94529	1.79027	2.0539		C	1.35868	-1.15014	3.20684
H	5.22065	-1.74204	2.60428		F	2.47046	-1.05889	3.97239
H	3.73652	-1.85936	1.66173		F	0.32502	-1.33709	4.04845
H	5.27841	-2.39525	0.97175		F	1.49222	-2.27001	2.46489
H	3.74626	-2.98557	-0.41042		I	0.61384	-0.13431	-2.83412
H	2.52953	-2.35664	-1.53075		C	-1.13749	-3.46367	1.36947
H	3.81334	-3.42074	-2.12053		F	-2.19251	-4.24237	1.07116
H	4.92126	-0.29092	-3.63501		F	-0.10281	-4.27515	1.63849
H	4.35819	-1.94453	-3.84151		F	-1.44408	-2.77796	2.48492
H	3.20331	-0.68866	-3.423		Se	1.0965	0.48024	2.13681
H	6.10693	-2.63462	-2.46947		Se	-0.65131	-2.30666	-0.18284
H	6.67235	-1.04944	-1.95044		N	-6.72771	-2.11845	-1.60804
H	6.25554	-2.29297	-0.75333		O	-7.54949	-2.36859	-0.72142
H	3.60691	2.87011	0.33407		O	-6.99734	-2.06393	-2.81133

Zero-point correction=   0.872768 (Hartree/Particle)
Thermal correction to Energy=   0.936594
Thermal correction to Enthalpy=   0.937538
Thermal correction to Gibbs Free Energy=   0.773798
Sum of electronic and zero-point Energies=   -7803.117174
Sum of electronic and thermal Energies=   -7803.053348
Sum of electronic and thermal Enthalpies=   -7803.052404
Sum of electronic and thermal Free Energies=   -7803.216144

CPCM (Toluene) M06L/def2-TZVP   E= −8098.75964695
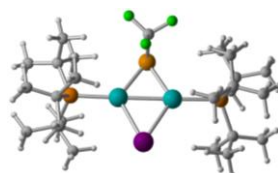
Pd	1.34376	-0.03885	0.17621		C	4.09769	-1.96052	-1.88509
P	3.73383	-0.00429	0.184		H	4.78447	-2.60183	-1.32795
C	4.43984	-1.32452	1.43159		H	3.07042	-2.26556	-1.6677
C	4.31931	-0.45547	-1.61936		H	4.27655	-2.14827	-2.95179
C	4.47424	1.73784	0.65776		C	3.5646	-2.59763	1.3579
Pd	-1.33825	-0.05405	0.17189		H	3.57952	-3.08247	0.38233
P	-3.72693	-0.01131	0.18253		H	3.94521	-3.32031	2.0924
C	-4.32842	0.4071	-1.62081		H	2.52193	-2.38058	1.60445
C	-4.40167	-1.77466	0.68008		C	5.91391	-1.71971	1.20063
C	-4.47719	1.29706	1.419		H	6.22012	-2.41329	1.99563
C	3.39191	0.28854	-2.61144		H	6.06324	-2.23881	0.25067
H	3.65563	-0.01794	-3.63276		H	6.59465	-0.86622	1.23304
H	2.34232	0.02756	-2.44095		C	4.28992	-0.80238	2.87803
H	3.4821	1.37388	-2.56079		H	3.27122	-0.45699	3.08232
C	5.78927	-0.11954	-1.94257		H	4.50103	-1.63096	3.56638
H	6.49317	-0.61996	-1.27265		H	4.98936	0.00075	3.11962
H	6.01092	-0.46084	-2.96272		C	4.2143	2.7391	-0.49015
H	5.99378	0.95306	-1.91368		H	4.49147	3.74151	-0.13857

H	4.81289	2.53739	-1.38076		C	-4.28356	0.80144	2.86984
H	3.15955	2.7771	-0.7723		H	-3.24503	0.51466	3.06525
C	3.70979	2.29548	1.88241		H	-4.53012	1.62595	3.5512
H	3.86104	1.71375	2.79161		H	-4.93462	-0.03533	3.13105
H	4.07495	3.31191	2.08114		C	-5.97108	1.61822	1.1975
H	2.63635	2.35608	1.69153		H	-6.30427	2.30034	1.99135
C	5.98507	1.74737	0.97839		H	-6.14884	2.12659	0.24649
H	6.29466	2.78493	1.16307		H	-6.61122	0.73455	1.23749
H	6.22625	1.17979	1.88034		C	-5.89811	-1.83106	1.05398
H	6.60052	1.36659	0.15979		H	-6.16784	-2.87668	1.25464
C	-4.12935	1.91316	-1.89844		H	-6.12979	-1.26423	1.95844
H	-3.11615	2.24596	-1.65992		H	-6.54904	-1.47605	0.25079
H	-4.29033	2.08844	-2.97014		C	-3.56279	-2.28754	1.87649
H	-4.84175	2.54408	-1.36143		H	-3.68898	-1.6924	2.78104
C	-5.79498	0.04412	-1.92985		H	-3.88215	-3.31205	2.11059
H	-6.02728	0.36358	-2.95482		H	-2.49682	-2.3167	1.63234
H	-5.98217	-1.03108	-1.88104		C	-4.15922	-2.77947	-0.46837
H	-6.50399	0.5442	-1.26556		H	-4.38433	-3.78614	-0.09273
C	-3.40072	-0.33546	-2.61272		H	-4.80663	-2.60869	-1.33135
H	-2.35024	-0.07671	-2.44496		H	-3.11794	-2.78141	-0.80092
H	-3.48942	-1.42059	-2.5592		C	-0.04981	2.92958	-0.68369
H	-3.66778	-0.0314	-3.63385		F	0.94513	3.8448	-0.63002
C	-3.67401	2.61475	1.32332		F	0.08619	2.27591	-1.85661
H	-3.71359	3.08439	0.34184		F	-1.21243	3.62048	-0.7541
H	-4.09817	3.32523	2.0457		I	0.01825	-2.38455	-0.59352
H	-2.62381	2.46153	1.57865		Se	-0.01866	1.85454	0.78459

Zero-point correction=   0.763861
Thermal correction to Energy=   0.813950
Thermal correction to Enthalpy=   0.814894
Thermal correction to Gibbs Free Energy=   0.681246
Sum of electronic and zero-point Energies=   -4630.596233
Sum of electronic and thermal Energies=   -4630.546143
Sum of electronic and thermal Enthalpies=   -4630.545199
Sum of electronic and thermal Free Energies=   -4630.678847

CPCM (Toluene) M06L/def2-TZVP   E= −4923.31654158

Oxidative addition TS-3
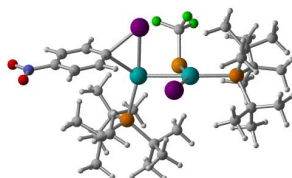
C	-5.48847	-1.88502	-0.71973		Pd	-1.21394	-0.09163	0.48568
C	-3.79165	-1.79593	0.98121		Pd	1.50467	-0.051	-0.16946
C	-2.80231	-1.79244	-0.02508		I	-0.87375	-2.85882	0.56204
C	-3.17438	-1.88041	-1.38217		H	-2.10634	3.21048	3.93862
H	-2.40905	-1.93046	-2.14919		C	-1.67624	3.12731	2.93169
H	-3.5078	-1.79983	2.02744		C	-2.81788	2.78426	1.94829
C	-4.51767	-1.9095	-1.72811		H	-0.91515	2.34359	2.96556
C	-5.13703	-1.8267	0.63042		H	-1.19257	4.08184	2.71369
H	-4.82856	-1.96237	-2.76456		P	-2.08833	2.30659	0.19733
H	-5.91475	-1.82297	1.38469		C	-3.82851	3.95032	1.96529

C	-3.49913	1.52254	2.5295	C	4.09717	-1.95267	-2.62678
C	-0.7854	3.67857	-0.29178	C	5.93481	-2.08569	-0.96019
C	-3.53217	2.41853	-1.11104	C	4.44165	2.79079	-1.29764
H	-4.73652	3.73483	1.39846	C	5.88947	1.10626	-2.46259
H	-4.13507	4.13058	3.00479	C	3.48217	1.37058	-3.06625
H	-3.40397	4.88323	1.58758	H	6.97918	-0.07794	0.30093
H	-4.34373	1.16937	1.93728	H	6.65453	1.66399	0.31424
H	-2.78054	0.70048	2.62424	H	6.96064	0.8116	1.82051
H	-3.87423	1.75646	3.53518	H	3.3736	1.58918	2.10652
C	-1.21561	5.13006	0.01655	H	5.00234	1.86895	2.71798
C	0.54326	3.40175	0.44281	H	4.49498	2.63183	1.21596
C	-0.45198	3.58324	-1.79814	H	5.27502	-0.39249	3.0416
C	-3.07521	1.66784	-2.3837	H	3.79655	-0.96556	2.27847
C	-4.7608	1.65519	-0.57624	H	5.3655	-1.60321	1.7667
C	-3.99324	3.83584	-1.51242	H	3.72212	-2.67174	0.74501
H	-2.16417	5.4037	-0.44835	H	2.51933	-2.60928	-0.54786
H	-1.28948	5.32974	1.08815	H	3.864	-3.759	-0.64223
H	-0.44948	5.80936	-0.38171	H	4.74249	-1.38606	-3.3018
H	0.96872	2.4438	0.12501	H	4.25641	-3.01564	-2.85027
H	1.26006	4.18957	0.1728	H	3.0552	-1.72686	-2.85813
H	0.45904	3.39736	1.52953	H	6.09096	-3.09534	-1.36173
H	0.41583	4.22706	-1.9955	H	6.59557	-1.41423	-1.51436
H	-0.18371	2.56677	-2.10037	H	6.2551	-2.10657	0.08222
H	-1.26095	3.93918	-2.43887	H	3.49525	3.00643	-0.7927
H	-2.25417	2.15817	-2.9054	H	5.26363	2.98915	-0.60761
H	-2.76125	0.64737	-2.15713	H	4.5402	3.50216	-2.12738
H	-3.92323	1.61567	-3.07988	H	5.93836	0.19007	-3.05411
H	-5.26908	2.17512	0.2386	H	6.13476	1.93566	-3.139
H	-5.48728	1.55096	-1.3922	H	6.66997	1.06645	-1.70284
H	-4.50168	0.65093	-0.2403	H	3.37328	0.40302	-3.55353
H	-4.84925	3.73741	-2.19373	H	2.48877	1.69575	-2.75396
H	-4.32385	4.43579	-0.66148	H	3.85252	2.08293	-3.8156
H	-3.22489	4.39601	-2.05004	C	1.30452	-1.21188	3.28816
P	3.93495	0.05871	-0.53551	F	2.16838	-1.00858	4.30734
C	4.96893	0.46677	1.08949	F	0.14025	-1.60396	3.84159
C	4.43992	-1.73584	-1.13681	F	1.78498	-2.25666	2.57499
C	4.47646	1.3642	-1.889	I	0.48193	-0.57151	-2.66108
C	6.47441	0.72379	0.84014	Se	1.07856	0.43787	2.23425
C	4.41166	1.7197	1.80444	N	-6.89992	-1.92891	-1.08621
C	4.83539	-0.7042	2.08601	O	-7.73231	-1.91327	-0.17505
C	3.58361	-2.74291	-0.33404	O	-7.18132	-1.97454	-2.28679

Zero-point correction=   0.857994 (Hartree/Particle)
Thermal correction to Energy=   0.917714
Thermal correction to Enthalpy=   0.918658
Thermal correction to Gibbs Free Energy=   0.763198
Sum of electronic and zero-point Energies=   -5077.962895
Sum of electronic and thermal Energies=   -5077.903176
Sum of electronic and thermal Enthalpies=   -5077.902231
Sum of electronic and thermal Free Energies=   -5078.057692

CPCM (Toluene) M06L/def2-TZVP   E= −5657.43446942
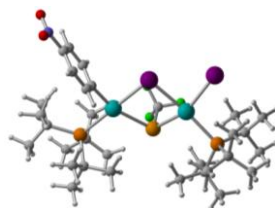
C	-4.79106	-4.37566	-0.58237
C	-3.93974	-2.61515	0.85369
C	-3.2888	-2.0256	-0.23725
C	-3.36814	-2.6359	-1.49547
H	-2.8412	-2.2137	-2.34677
H	-3.86056	-2.17655	1.84514
C	-4.12095	-3.80241	-1.66572
C	-4.69211	-3.78325	0.67814
H	-4.176	-4.26554	-2.6483
H	-5.19462	-4.23026	1.53297
Pd	-2.08791	-0.44572	0.09312
Pd	1.93228	-0.48792	0.0602
I	-0.09323	-2.35294	0.11238
H	-2.41367	4.00772	2.01205
C	-2.51177	3.43068	1.08356
C	-3.78478	2.56321	1.19684
H	-1.60297	2.84028	0.97459
H	-2.56429	4.1511	0.26381
P	-3.88331	1.26196	-0.26717
C	-4.97112	3.54444	1.3147
C	-3.66807	1.7587	2.5136
C	-3.42256	2.15211	-1.93895
C	-5.77172	0.71975	-0.39318
H	-5.92138	3.05617	1.53461
H	-4.76234	4.22586	2.15004
H	-5.09625	4.16178	0.42082
H	-4.5553	1.16262	2.73125
H	-2.80603	1.08926	2.50723
H	-3.53425	2.46342	3.34459
C	-4.0275	3.5587	-2.13655
C	-1.88368	2.26604	-2.0231
C	-3.84864	1.26689	-3.13145
C	-5.96946	-0.5279	-1.28786
C	-6.28372	0.3041	1.00536
C	-6.69792	1.82268	-0.95923
H	-5.11808	3.5638	-2.10992
H	-3.66483	4.2793	-1.4007
H	-3.72427	3.92987	-3.1248
H	-1.41203	1.27841	-1.99709
H	-1.62193	2.73802	-2.9797
H	-1.45015	2.87119	-1.22702
H	-3.39609	1.67685	-4.04359
H	-3.49635	0.23611	-3.02441
H	-4.92934	1.25383	-3.28735
H	-5.49814	-0.45754	-2.26632
H	-5.61044	-1.4323	-0.8053
H	-7.04909	-0.64512	-1.45244
H	-6.40279	1.14155	1.69457
H	-7.2741	-0.15294	0.88116
H	-5.63774	-0.44701	1.46792
H	-7.73659	1.491	-0.8291

H	-6.60245	2.78898	-0.4651
H	-6.54699	1.9685	-2.03197
P	3.73258	1.22904	-0.38969
C	3.02514	3.05437	-0.21296
C	5.20514	1.03114	0.88714
C	4.42476	1.08276	-2.2103
C	3.96028	4.19704	-0.67745
C	1.72007	3.19919	-1.04877
C	2.69429	3.30933	1.27654
C	4.57627	0.60276	2.23304
C	6.18332	-0.08881	0.46861
C	6.0577	2.30084	1.10253
C	3.35993	1.59229	-3.2069
C	5.73581	1.8672	-2.44942
C	4.67649	-0.39304	-2.57811
H	4.91855	4.22628	-0.15863
H	4.14753	4.17114	-1.75307
H	3.44935	5.1472	-0.46959
H	1.20021	2.25775	-1.21805
H	1.02547	3.86112	-0.52057
H	1.92069	3.64968	-2.02335
H	2.16483	4.26747	1.35302
H	2.04733	2.54485	1.70319
H	3.59018	3.38852	1.89428
H	3.85679	1.32404	2.62362
H	4.0722	-0.36283	2.14222
H	5.37913	0.49698	2.97474
H	6.78165	0.17382	-0.40652
H	6.88386	-0.24243	1.30008
H	5.68322	-1.03953	0.28728
H	6.87157	2.04357	1.7929
H	6.52144	2.66019	0.17979
H	5.50682	3.12412	1.55949
H	2.37894	1.13981	-3.03011
H	3.25306	2.6781	-3.19902
H	3.67492	1.30602	-4.21825
H	6.58166	1.44594	-1.90242
H	5.98149	1.79916	-3.51759
H	5.66414	2.92656	-2.20081
H	5.40357	-0.88705	-1.93518
H	3.75657	-0.97912	-2.5459
H	5.0648	-0.42235	-3.60516
C	0.09435	0.7007	2.55968
F	-0.30999	1.82678	3.19848
F	-0.72094	-0.28836	2.9828
F	1.33153	0.41633	3.02163
I	3.52061	-2.73993	-0.06607
Se	0.06886	0.99823	0.6428
N	-5.57959	-5.6029	-0.76404
O	-6.14122	-6.06624	0.18901
O	-5.6298	-6.09181	-1.85805

Zero-point correction=   0.859066 (Hartree/Particle)
Thermal correction to Energy=   0.919127
Thermal correction to Enthalpy=   0.920071
Thermal correction to Gibbs Free Energy= 0.763086
Sum of electronic and zero-point Energies=   -5078.010152
Sum of electronic and thermal Energies=   -5077.950091
Sum of electronic and thermal Enthalpies=   -5077.949147
Sum of electronic and thermal Free Energies= -5078.106132

CPCM (Toluene) M06L/def2-TZVP E= −5657.46095586

Reductive elimination TS-4
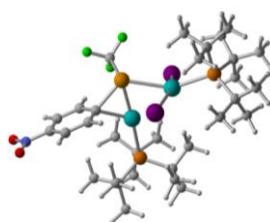
C	4.92657	-2.98712	0.28896	H	2.08386	5.51413	0.36322
C	3.49328	-1.70976	-1.15858	H	1.43195	5.64728	1.99347
C	2.60465	-1.48768	-0.08545	H	-0.21008	2.5161	0.84895
C	2.88548	-2.07311	1.17006	H	-0.4376	4.20181	1.33953
H	2.18132	-1.95919	1.98803	H	0.14742	3.82309	-0.28246
H	3.28197	-1.30113	-2.13853	H	0.70176	3.70845	3.29466
C	4.04649	-2.80941	1.36098	H	1.21328	2.06756	2.89127
C	4.65817	-2.44888	-0.96922	H	2.40605	3.28489	3.40609
H	4.27932	-3.25274	2.32173	H	3.35906	1.46035	3.31916
H	5.35886	-2.61052	-1.77971	H	3.54097	0.1274	2.17476
Pd	1.47223	0.35398	-0.23175	H	4.94299	0.7343	3.06261
Pd	-1.72267	-0.41743	-0.03231	H	5.85554	1.94751	-0.21671
H	2.37479	4.16476	-2.99901	H	6.23801	0.96579	1.19284
C	2.07928	3.85197	-1.98897	H	5.00456	0.41234	0.05706
C	3.30469	3.19994	-1.31065	H	5.94179	2.95552	2.56667
H	1.24738	3.15014	-2.0948	H	5.30439	4.02063	1.31273
H	1.72521	4.74439	-1.46874	H	4.38379	3.74129	2.79883
P	2.76956	2.35911	0.36304	P	-4.22561	0.00747	0.27766
C	4.41779	4.26178	-1.19983	C	-5.08502	0.76437	-1.31886
C	3.7672	2.07906	-2.27359	C	-4.87642	-1.8345	0.4914
C	1.63433	3.59317	1.35477	C	-4.81336	1.071	1.80461
C	4.36784	2.01807	1.42409	C	-6.61626	0.96635	-1.23626
H	5.37043	3.84141	-0.86994	C	-4.48868	2.1615	-1.64196
H	4.58681	4.69713	-2.19386	C	-4.78856	-0.17831	-2.50843
H	4.15423	5.0821	-0.52727	C	-4.00526	-2.75244	-0.39992
H	4.64375	1.5345	-1.92102	C	-4.6923	-2.33059	1.94207
H	2.96262	1.35715	-2.44804	C	-6.35843	-2.05268	0.11769
H	4.02684	2.53253	-3.23952	C	-4.63053	2.57229	1.49044
C	2.10918	5.06157	1.3573	C	-6.28408	0.83177	2.21222
C	0.20763	3.52436	0.7635	C	-3.91526	0.78011	3.02305
C	1.49908	3.12183	2.82014	H	-7.17973	0.05501	-1.04068
C	4.01276	1.03177	2.56061	H	-6.89457	1.7139	-0.48997
C	5.41691	1.29959	0.5455	H	-6.94962	1.35357	-2.20866
C	5.02341	3.26656	2.05086	H	-3.43732	2.26183	-1.38151
H	3.1176	5.18171	1.75967	H	-4.56623	2.33361	-2.72211

H	-5.04579	2.96102	-1.15085
H	-5.13813	0.30634	-3.42859
H	-3.72048	-0.3745	-2.62867
H	-5.31675	-1.13126	-2.42899
H	-4.02473	-2.48025	-1.45637
H	-2.96285	-2.75576	-0.06679
H	-4.38279	-3.78025	-0.31401
H	-5.37407	-1.85114	2.64788
H	-4.9196	-3.40473	1.95853
H	-3.66916	-2.21182	2.30074
H	-6.61791	-3.09192	0.35884
H	-7.0391	-1.41042	0.68214
H	-6.55295	-1.91821	-0.94797
H	-3.6402	2.79384	1.08019
H	-5.38774	2.95795	0.80628
H	-4.73043	3.13092	2.4297

H	-6.45713	-0.18173	2.57896
H	-6.52666	1.51691	3.03557
H	-6.99421	1.02896	1.40748
H	-3.94017	-0.2589	3.34872
H	-2.87372	1.03983	2.82497
H	-4.2667	1.39888	3.85974
I	-0.9848	-1.32309	2.52321
C	0.52186	-2.24806	-2.49633
F	1.20171	-3.40397	-2.61431
F	-0.70318	-2.43631	-3.00108
F	1.15707	-1.32769	-3.23277
Se	0.38708	-1.84416	-0.51787
N	6.1518	-3.76058	0.48831
O	6.90915	-3.89552	-0.47538
O	6.35817	-4.22946	1.6096
I	-1.07268	1.10418	-2.24815

Zero-point correction=   0.857053
Thermal correction to Energy=   0.917178
Thermal correction to Enthalpy=   0.918122
Thermal correction to Gibbs Free Energy=   0.760092
Sum of electronic and zero-point Energies=   -5077.984099
Sum of electronic and thermal Energies=   -5077.923973
Sum of electronic and thermal Enthalpies=   -5077.923029
Sum of electronic and thermal Free Energies=   -5078.081060

CPCM (Toluene) M06L/def2-TZVP   E= –5657.44595524
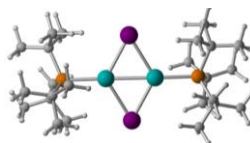
Pd	-1.35737	0.00807	-0.09646
P	-3.68354	0.00095	-0.01956
C	-4.10187	-0.47459	1.79097
C	-4.4456	1.72342	-0.39164
C	-4.50976	-1.27405	-1.19268
Pd	1.35719	0.00918	0.09595
P	3.68336	0.00142	0.01988
C	4.44509	1.72433	0.39081
C	4.50918	-1.27216	1.19466
C	4.10272	-0.476	-1.78991
C	-3.7773	2.29958	-1.64883
H	-4.1153	3.33737	-1.77872
H	-2.68497	2.31418	-1.55187
H	-4.02906	1.76154	-2.56505
C	-5.96473	1.73557	-0.5843
H	-6.50967	1.32074	0.27028
H	-6.29735	2.77642	-0.70734
H	-6.28209	1.19502	-1.48203
C	-4.09387	2.68675	0.74693
C	-3.63755	-2.53477	-1.24787
H	-3.49264	-3.02127	-0.28042
H	-4.119	-3.2629	-1.91626
H	-2.64537	-2.30922	-1.65349
C	-5.9386	-1.66855	-0.81012

H	-4.62542	2.46666	1.67805
H	-3.01583	2.70324	0.95131
H	-4.38329	3.70243	0.44411
C	-3.09779	0.24001	2.71038
H	-3.16972	1.32945	2.68514
H	-3.28283	-0.07941	3.74623
H	-2.06472	-0.03068	2.45255
C	-5.52578	-0.15692	2.25287
H	-5.65728	-0.53189	3.27829
H	-5.73275	0.9179	2.28066
H	-6.29389	-0.63359	1.63447
C	-3.84239	-1.97199	1.99023
H	-2.83523	-2.25567	1.65673
H	-3.90743	-2.19511	3.06423
H	-4.57212	-2.61253	1.48494
C	-4.51435	-0.72236	-2.62235
H	-4.7963	-1.53469	-3.30664
H	-5.23425	0.08753	-2.77345
H	-3.52071	-0.36999	-2.92599
H	3.28394	-0.08369	-3.7459
H	2.06564	-0.0331	-2.45249
C	3.84396	-1.97374	-1.98786
H	2.83644	-2.25737	-1.65541
H	3.91046	-2.19796	-3.06153

H	-6.34034	-2.3413	-1.58162
H	-5.98398	-2.21245	0.13904
H	-6.61816	-0.81303	-0.74062
C	4.0937	2.68666	-0.74872
H	3.01574	2.70278	-0.95362
H	4.38279	3.70265	-0.44665
H	4.62572	2.46588	-1.6794
C	5.96411	1.73667	0.58424
H	6.29675	2.77762	0.70637
H	6.28091	1.19702	1.48272
H	6.50948	1.32085	-0.26957
C	3.77634	2.30146	1.64731
H	2.68399	2.31524	1.55038
H	4.02853	1.76461	2.56411
H	4.11363	3.33963	1.77604
C	3.09876	0.23722	-2.71053
H	3.17067	1.32669	-2.68687
I	-0.00104	2.41646	-0.00077
I	0.00135	-2.39524	-0.00039

H	4.57319	-2.61358	-1.48092
C	5.52672	-0.15834	-2.25162
H	5.65867	-0.53434	-3.27659
H	5.73336	0.91652	-2.28049
H	6.29478	-0.63411	-1.63247
C	5.93815	-1.66692	0.81291
H	6.33968	-2.33899	1.58511
H	5.98397	-2.21159	-0.13578
H	6.6176	-0.81135	0.743
C	3.63684	-2.53275	1.25088
H	3.49156	-3.01979	0.28376
H	4.11829	-3.26054	1.91963
H	2.64476	-2.30674	1.65652
C	4.51335	-0.71895	2.62375
H	4.79539	-1.5305	3.30894
H	5.23304	0.09127	2.77415
H	3.51957	-0.36655	2.92686

Zero-point correction=   0.749548 (Hartree/Particle)
Thermal correction to Energy=   0.795414
Thermal correction to Enthalpy=   0.796359
Thermal correction to Gibbs Free Energy=   0.671948
Sum of electronic and zero-point Energies=   -1905.447012
Sum of electronic and thermal Energies=   -1905.401146
Sum of electronic and thermal Enthalpies=   -1905.400201
Sum of electronic and thermal Free Energies=   -1905.524612

CPCM (Toluene) M06L/def2-TZVP   E= −2481.9943046
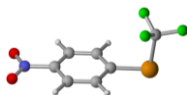
C	-1.88459	0.92191	-0.7194
C	-0.52521	0.66144	-0.86954
C	0.03589	-0.487	-0.29496
C	-0.76957	-1.38666	0.41386
C	-2.1351	-1.14563	0.5505
C	-2.66853	0.00972	-0.01514
H	-2.34361	1.80514	-1.14616
H	0.09792	1.34914	-1.42902
H	-0.32846	-2.26917	0.86468

H	-2.78071	-1.82522	1.09288
Se	1.90469	-0.90229	-0.53016
C	2.62089	0.67055	0.42977
F	3.95577	0.54423	0.4643
F	2.32359	1.82906	-0.18637
F	2.16356	0.75652	1.6851
N	-4.11049	0.27582	0.13418
O	-4.77937	-0.54968	0.75341
O	-4.55312	1.30631	-0.37018

Zero-point correction=   0.108144 (Hartree/Particle)
Thermal correction to Energy=   0.120706
Thermal correction to Enthalpy=   0.121651
Thermal correction to Gibbs Free Energy=   0.065355
Sum of electronic and zero-point Energies=   -3172.573379
Sum of electronic and thermal Energies=   -3172.560817
Sum of electronic and thermal Enthalpies=   -3172.559873
Sum of electronic and thermal Free Energies=   -3172.616169

CPCM (Toluene) M06L/def2-TZVP   E= -3175.46881270
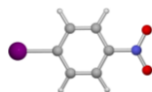
C	0.20301	3.15038	0.	Se	4.23571	4.35827	0.00112
C	1.59817	3.15038	0.	C	6.1757	4.35841	0.00224
C	2.29571	4.35813	0.	F	6.62511	5.23223	0.92796
C	1.59805	5.56664	-0.0012	F	6.62563	3.12007	0.29649
C	0.20323	5.56656	-0.00168	F	6.62638	4.72303	-1.21696
C	-0.49437	4.35835	-0.00068	N	-1.96437	4.3586	-0.00092
H	-0.34675	2.19806	0.00045	O	-2.53451	5.41376	-0.00151
H	2.14768	2.19786	0.00132	O	-2.53485	3.30362	-0.00052
H	2.14825	6.51878	-0.00126				
H	-0.3469	6.51884	-0.00263				

Zero-point correction=   0.092939 (Hartree/Particle)
Thermal correction to Energy=   0.101337
Thermal correction to Enthalpy=   0.102281
Thermal correction to Gibbs Free Energy= 0.057001
Sum of electronic and zero-point Energies=   -447.424527
Sum of electronic and thermal Energies=   -447.416128
Sum of electronic and thermal Enthalpies=   -447.415184
Sum of electronic and thermal Free Energies= -447.460465

CPCM (Toluene) M06L/def2-TZVP   E= -734,142214775
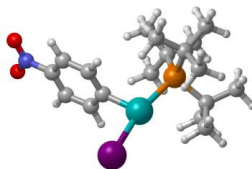
C	-4.72489	-3.10234	-0.61978	H	-4.01872	5.14733	0.9741
C	-3.26759	-2.49708	1.22246	H	-4.64626	1.40695	1.58913
C	-2.17941	-2.4578	0.33437	H	-3.07762	1.13076	2.36232
C	-2.34869	-2.79705	-1.0185	H	-4.2952	2.14978	3.15382
H	-1.4938	-2.83703	-1.68321	C	-1.79955	5.48823	-0.51832
H	-3.11873	-2.30866	2.27933	C	0.07407	3.94885	0.08818
C	-3.62861	-3.09254	-1.48876	C	-0.84834	3.88472	-2.19128
C	-4.53942	-2.80465	0.73231	C	-3.26455	1.70043	-2.71655
H	-3.76245	-3.33589	-2.53971	C	-5.00904	1.65777	-0.96608
H	-5.3822	-2.82555	1.41873	C	-4.40292	3.83141	-2.03045
Pd	-1.38753	0.32986	0.22522	H	-2.74812	5.65256	-1.03238
I	0.36774	-1.76836	1.3254	H	-1.93213	5.74887	0.5342
H	-2.64958	3.74982	3.50681	H	-1.07495	6.20141	-0.93482
C	-2.18458	3.64398	2.5176	H	0.58137	3.00053	-0.12041
C	-3.26498	3.14469	1.5313	H	0.74199	4.7617	-0.22858
H	-1.35897	2.93366	2.61941	H	-0.05044	4.02964	1.16752
H	-1.77986	4.62319	2.25165	H	-0.02743	4.58042	-2.41131
P	-2.43576	2.61381	-0.15654	H	-0.48937	2.87499	-2.41165
C	-4.36758	4.21954	1.43313	H	-1.65942	4.12441	-2.88134
C	-3.86036	1.87478	2.18311	H	-2.49524	2.24129	-3.2672
C	-1.24305	4.05973	-0.70719	H	-2.84303	0.74386	-2.40148
C	-3.834	2.49254	-1.51631	H	-4.08436	1.49435	-3.4181
H	-5.24421	3.87453	0.87991	H	-5.58145	2.18068	-0.19612
H	-4.70715	4.46636	2.44839	H	-5.70041	1.44749	-1.79257

H	-4.67913	0.69795	-0.56647	N	-6.06156 -3.45127 -1.12225	
H	-5.20579	3.61358	-2.74803	O	-6.20136 -3.62045 -2.30134	
H	-4.83674	4.44264	-1.2354	O	-6.9589 -3.55284 -0.33303	
H	-3.65992	4.43272	-2.55858			

Zero-point correction=   0.466084 (Hartree/Particle)
Thermal correction to Energy=   0.495739
Thermal correction to Enthalpy=   0.496683
Thermal correction to Gibbs Free Energy=   0.404610
Sum of electronic and zero-point Energies=   -1388.703927
Sum of electronic and thermal Energies=   -1388.674273
Sum of electronic and thermal Enthalpies=   -1388.673328
Sum of electronic and thermal Free Energies=   -1388.765401

CPCM (Toluene) M06L/def2-TZVP E= -1677.19718512
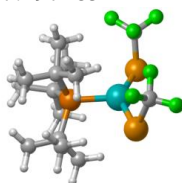
Pd	1.20786 -0.01398 0.0092	H	5.03698 -1.42534 -2.36615
P	3.63376 0.57374 -0.30268	H	4.87744 -2.89042 -1.40366
C	4.32092 1.7426 1.12779	H	3.43454 -1.9988 -1.8659
C	4.60436 -1.11744 -0.21982	H	6.5402 -2.009 0.0681
C	4.08047 1.4564 -2.00195	H	6.65571 -0.4011 -0.6426
C	5.71912 2.34268 0.8495	H	6.3176 -0.59344 1.08561
C	3.34411 2.91929 1.35438	H	2.5638 3.0094 -1.64697
C	4.40848 0.97162 2.46252	H	4.22107 3.55883 -1.31157
C	3.93151 -1.99056 0.86137	H	3.68258 3.3376 -2.97303
C	4.46971 -1.88195 -1.55253	H	5.92961 0.41393 -2.59341
C	6.11263 -0.998 0.09349	H	5.75231 2.04572 -3.22444
C	3.60988 2.92659 -1.95795	H	6.23366 1.80692 -1.54733
C	5.5912 1.42016 -2.33658	H	3.4791 -0.25778 -3.28331
C	3.33793 0.8171 -3.1929	H	2.26586 1.00133 -3.14913
H	6.48254 1.59083 0.6428	H	3.7252 1.28053 -4.11057
H	5.71487 3.0702 0.03532	C	1.06849 -0.69599 3.4565
H	6.03186 2.88143 1.75338	F	1.89372 -0.32376 4.47144
H	2.36364 2.56737 1.67092	F	-0.09074 -1.06763 4.04385
H	3.74729 3.5395 2.16621	F	1.61631 -1.81284 2.9204
H	3.22832 3.56281 0.48293	C	0.8344 -2.10535 -2.75838
H	4.67168 1.69267 3.24734	F	-0.22782 -2.72332 -3.33898
H	3.45852 0.52574 2.74933	F	1.80805 -2.08776 -3.71078
H	5.18289 0.20265 2.46396	F	1.28395 -2.93465 -1.78725
H	3.95566 -1.54861 1.85674	Se	0.83158 0.65805 2.28608
H	2.88784 -2.19809 0.61063	Se	0.36689 -0.46425 -2.18889
H	4.46208 -2.95105 0.90977		

Zero-point correction=   0.404909 (Hartree/Particle)
Thermal correction to Energy=   0.437329
Thermal correction to Enthalpy=   0.438273
Thermal correction to Gibbs Free Energy=   0.340756
Sum of electronic and zero-point Energies=   -6414.384543
Sum of electronic and thermal Energies=   -6414.352123
Sum of electronic and thermal Enthalpies=   -6414.351178

Sum of electronic and thermal Free Energies=   -6414.448696

CPCM (Toluene) M06L/def2-TZVP E= -6421.50967531
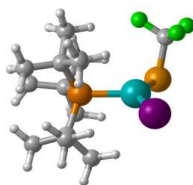
Pd	-0.50996	-0.06202	-0.6838	H	-0.6254	0.86983	2.08323
P	1.66248	0.29064	0.13006	H	0.25868	1.54221	3.45802
C	2.4013	1.91163	-0.69592	H	2.20185	-1.47032	2.74116
C	1.53561	0.52276	2.05546	H	1.0645	-0.64138	3.79796
C	2.88816	-1.18918	-0.26591	H	0.47433	-1.39578	2.31794
C	3.93971	2.02704	-0.59407	H	2.64274	1.21767	3.765
C	2.00127	1.91638	-2.19079	H	3.70384	0.62047	2.49116
C	1.81575	3.19316	-0.064	H	2.93749	2.20947	2.34249
C	0.29349	1.38284	2.37242	H	2.25741	-1.235	-2.37249
C	1.31074	-0.83921	2.74716	H	3.8023	-0.38994	-2.12579
C	2.78662	1.18206	2.67756	H	3.72422	-2.14414	-2.00522
C	3.17968	-1.21811	-1.78306	H	4.08288	-1.3171	1.58034
C	4.22058	-1.09013	0.51995	H	4.89914	-1.85347	0.11879
C	2.28282	-2.5681	0.07223	H	4.72785	-0.1305	0.43562
H	4.29467	2.02789	0.43964	H	1.92819	-2.66176	1.09585
H	4.47132	1.25119	-1.14689	H	1.46058	-2.82585	-0.59382
H	4.22925	2.98859	-1.03614	H	3.07442	-3.31495	-0.07211
H	0.91642	1.92329	-2.32008	C	-1.50483	-3.05102	0.57871
H	2.39768	2.83068	-2.65045	F	-2.52584	-3.91896	0.4771
H	2.40022	1.06806	-2.74781	F	-0.49478	-3.69466	1.21269
H	2.17181	4.04496	-0.65755	F	-1.89637	-2.0577	1.41085
H	0.72556	3.21478	-0.09099	Se	-0.98854	-2.40578	-1.20401
H	2.15217	3.35673	0.96148	I	-1.58598	2.30307	-0.93006
H	0.29961	2.36168	1.89483				

Zero-point correction=   0.390081 (Hartree/Particle)
Thermal correction to Energy=   0.418426
Thermal correction to Enthalpy=   0.419370
Thermal correction to Gibbs Free Energy=   0.330931
Sum of electronic and zero-point Energies=   -3689.250448
Sum of electronic and thermal Energies=   -3689.222102
Sum of electronic and thermal Enthalpies=   -3689.221158
Sum of electronic and thermal Free Energies=   -3689.309598

CPCM (Toluene) M06L/def2-TZVP E= -3980.19584564

Appendix

NMR spectra

1-[4-(Trifluoromethyl)selenophenyl]pyrrole

^{1}H NMR Spectrum (CDCl$_3$, 600 MHz):
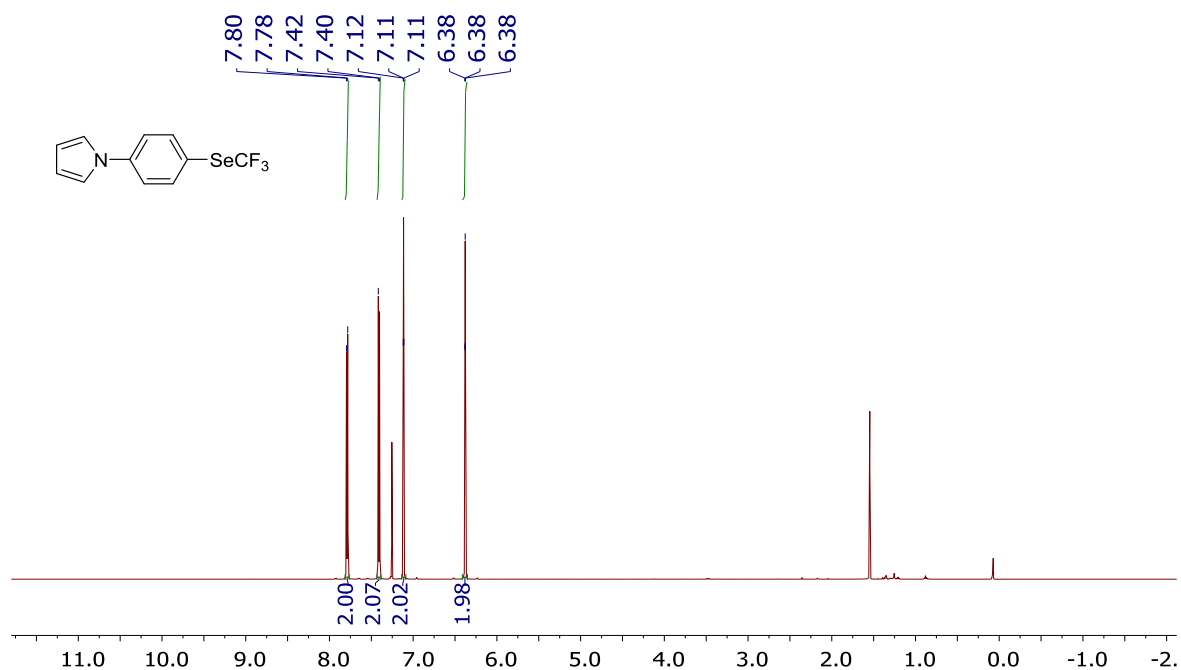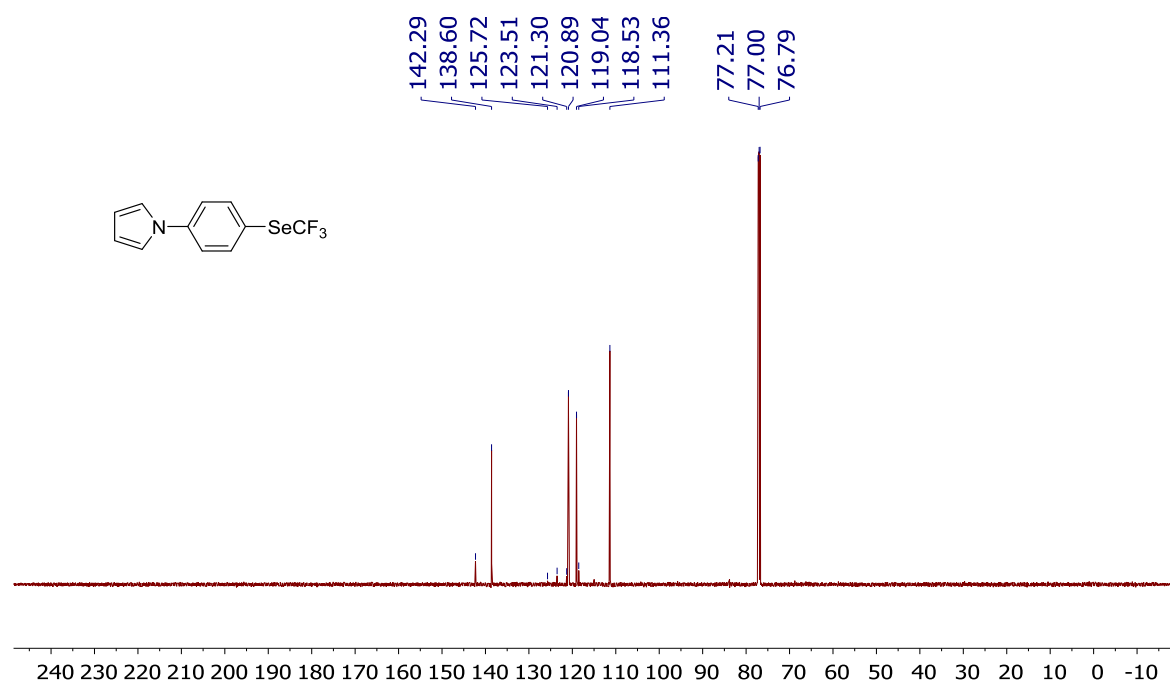
7.80 7.78 7.42 7.40 7.12 7.11 7.11 6.38 6.38 6.38

2.00 2.07 2.02 1.98

11.0 10.0 9.0 8.0 7.0 6.0 5.0 4.0 3.0 2.0 1.0 0.0 -1.0 -2.

^{13}C NMR Spectrum (CDCl$_3$, 151 MHz):

142.29 138.60 125.72 123.51 121.30 120.89 119.04 118.53 111.36

77.21 77.00 76.79

240 230 220 210 200 190 180 170 160 150 140 130 120 110 100 90 80 70 60 50 40 30 20 10 0 -10

279

^{19}F NMR Spectrum (CDCl$_3$, 564 MHz):

-36.37

1-Morpholino-4-[(trifluoromethyl)seleno]benzene

^{1}H NMR Spectrum (CDCl$_3$, 600 MHz):

7.61
7.60
7.26
6.87
6.85
3.86
3.85
3.85
3.23
3.22
3.22

0.93 1.01 2.00 2.00
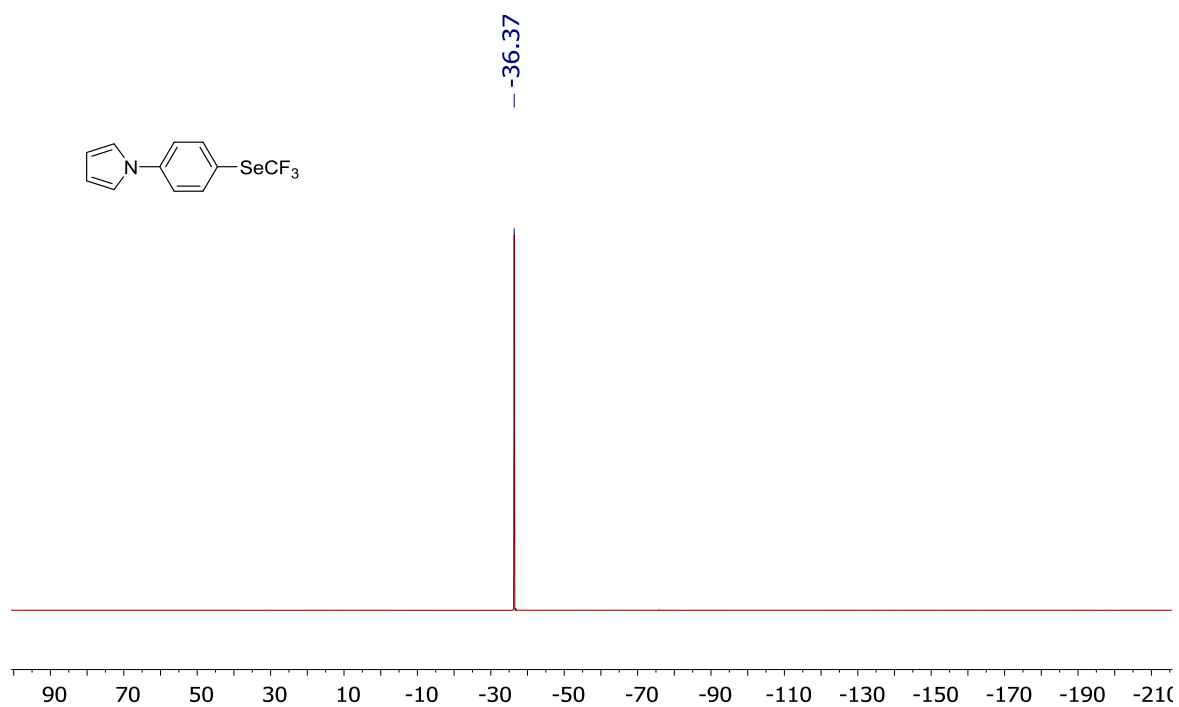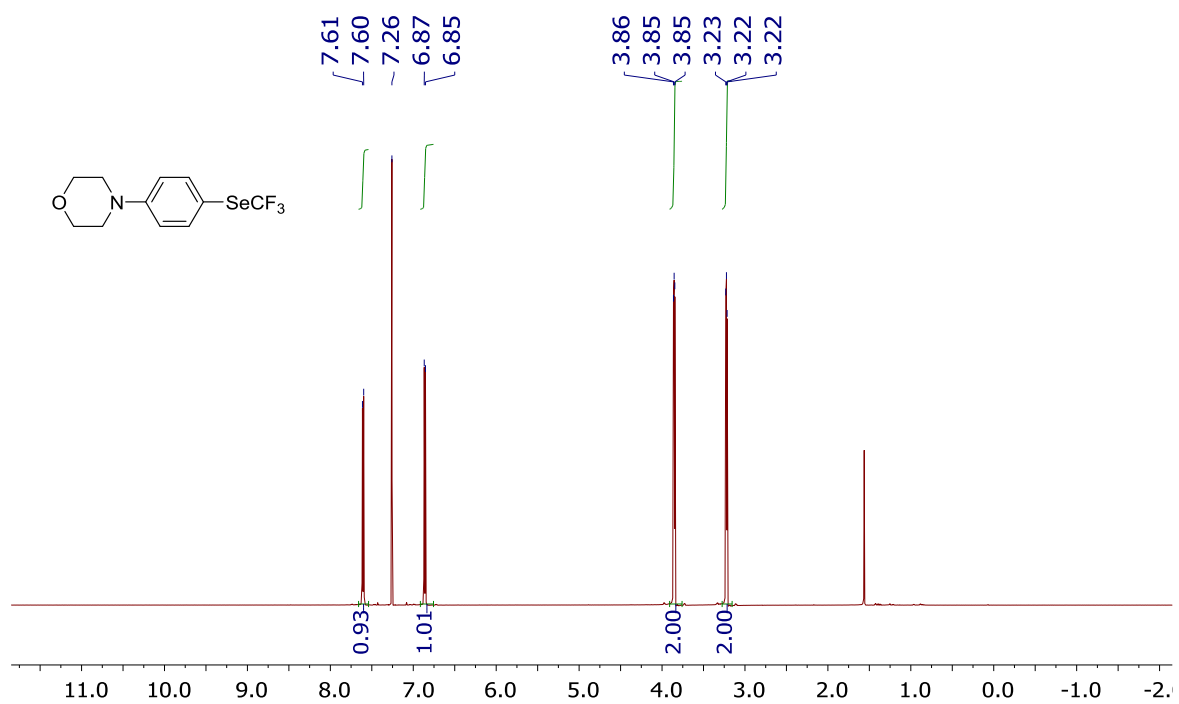
¹³C NMR Spectrum (CDCl₃, 151 MHz):
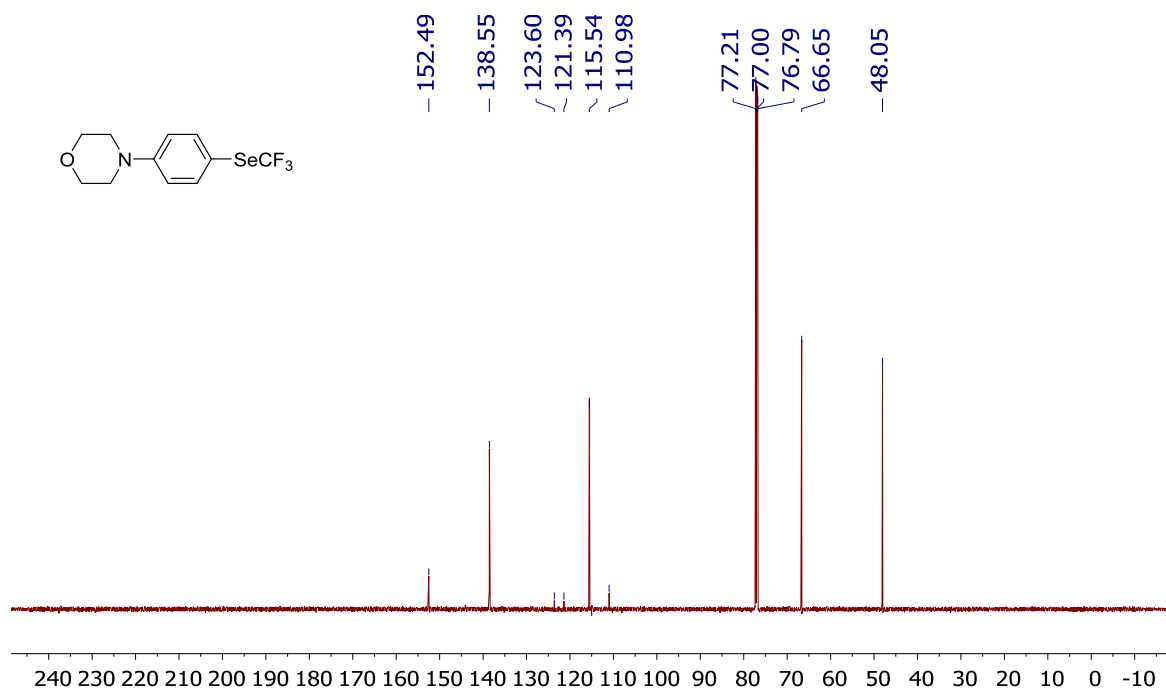
¹⁹F NMR Spectrum (CDCl₃, 564 MHz):

1-n-Butyl-4-[(trifluoromethyl)seleno]benzene
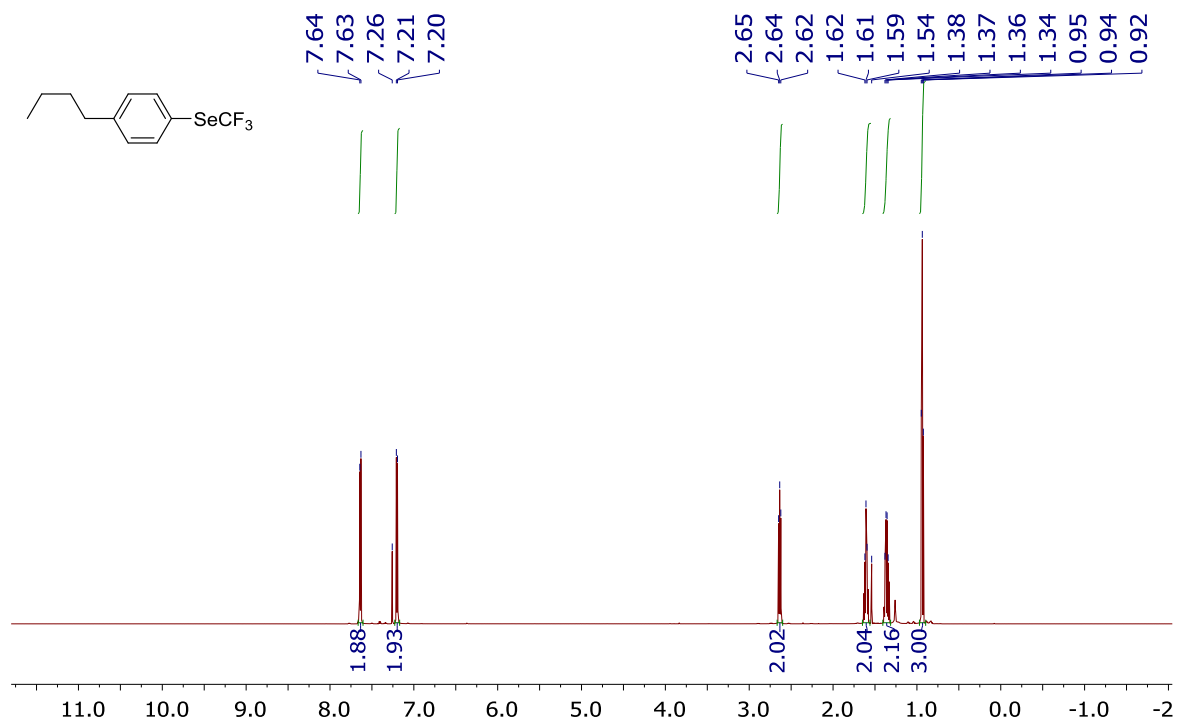
^{1}H NMR Spectrum (CDCl$_3$, 600 MHz):

7.64
7.63
7.26
7.21
7.20
2.65
2.64
2.62
1.62
1.61
1.59
1.54
1.38
1.37
1.36
1.34
0.95
0.94
0.92

1.88
1.93
2.02
2.04
2.16
3.00

11.0 10.0 9.0 8.0 7.0 6.0 5.0 4.0 3.0 2.0 1.0 0.0 -1.0 -2

^{13}C NMR Spectrum (CDCl$_3$, 151 MHz):

145.64
137.06
129.70
123.64
121.44
119.16
77.20 CDCl3
76.99 CDCl3
76.78 CDCl3
35.40
33.34
22.32
13.89

240 230 220 210 200 190 180 170 160 150 140 130 120 110 100 90 80 70 60 50 40 30 20 10 0 -10

^{19}F NMR Spectrum (CDCl$_3$, 564 MHz):

−36.46

1-Acetyl-3-[(trifluoromethyl)seleno]benzene

^{1}H NMR Spectrum (CDCl$_3$, 600 MHz):

8.312
8.057
8.044
7.943
7.930
7.526
7.514
7.501

2.627

0.93
0.95
0.97
0.98

3.00

¹³C NMR Spectrum (CDCl$_3$, 151 MHz)

— 196.735

141.216
138.214
136.712
130.030
129.843
125.678
123.472
123.173
121.266
119.060

77.205
76.994
76.782

— 26.639

240 230 220 210 200 190 180 170 160 150 140 130 120 110 100 90 80 70 60 50 40 30 20 10 0 -10

¹⁹F NMR Spectrum (CDCl$_3$, 564 MHz):

— -35.747

90 70 50 30 10 -10 -30 -50 -70 -90 -110 -130 -150 -170 -190 -210
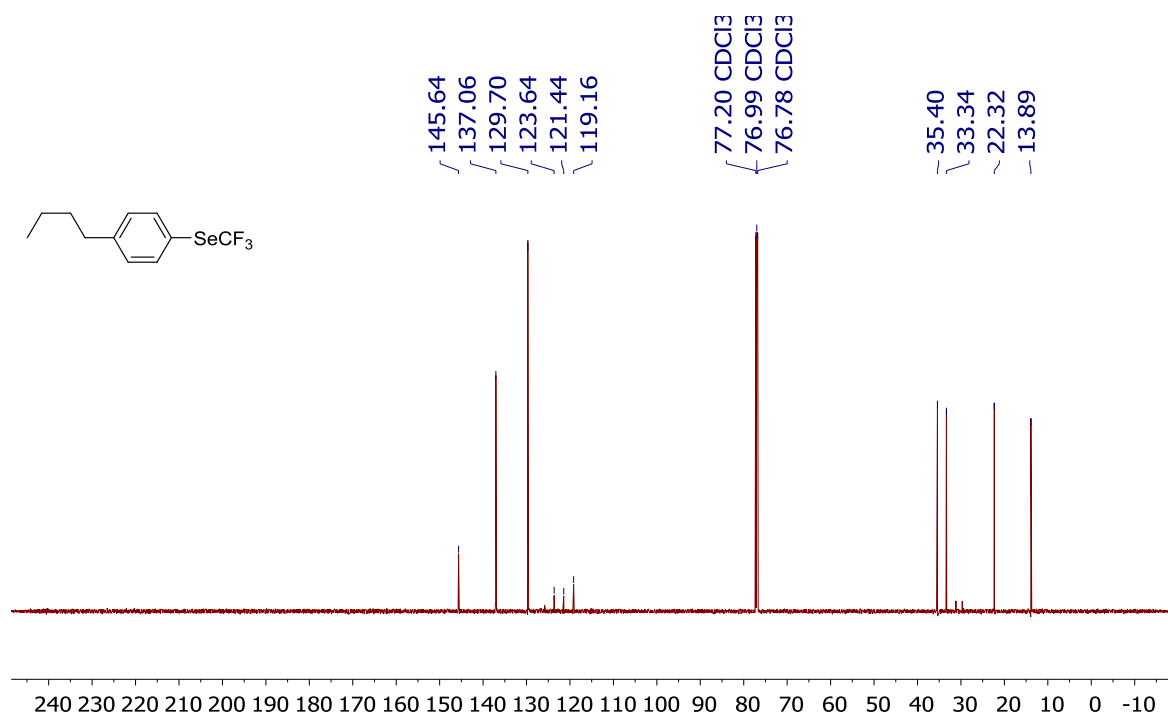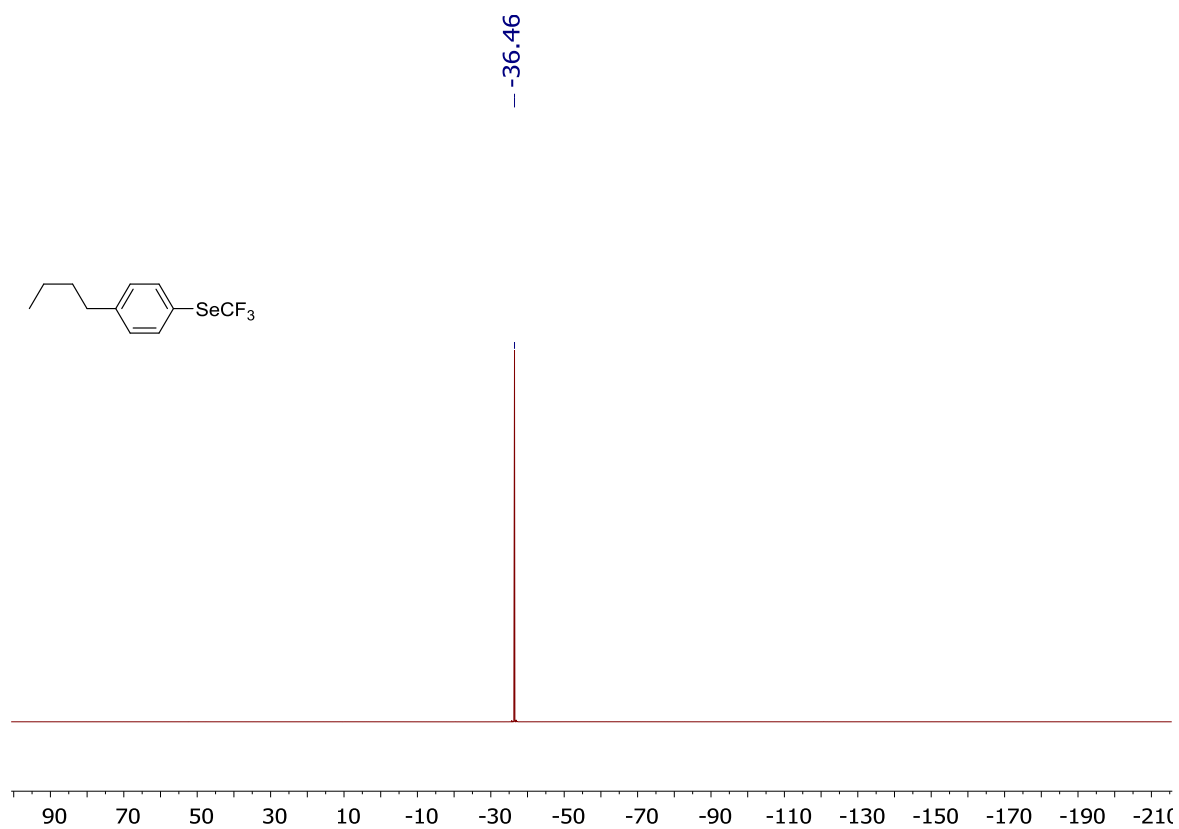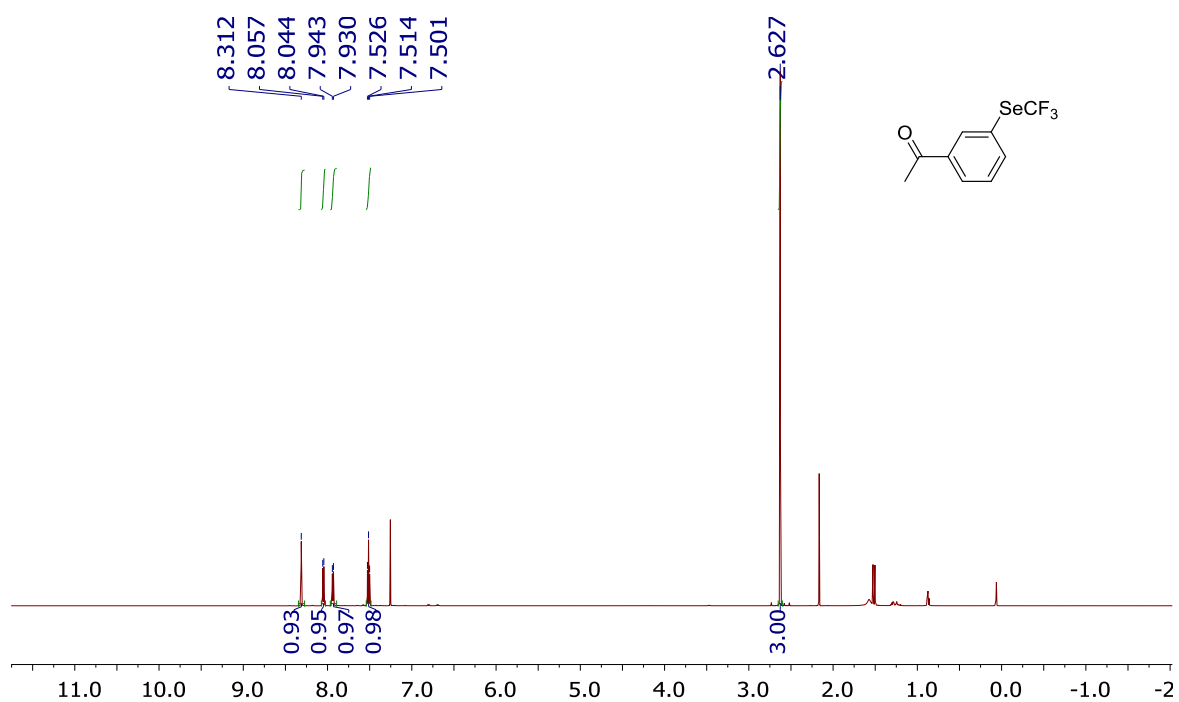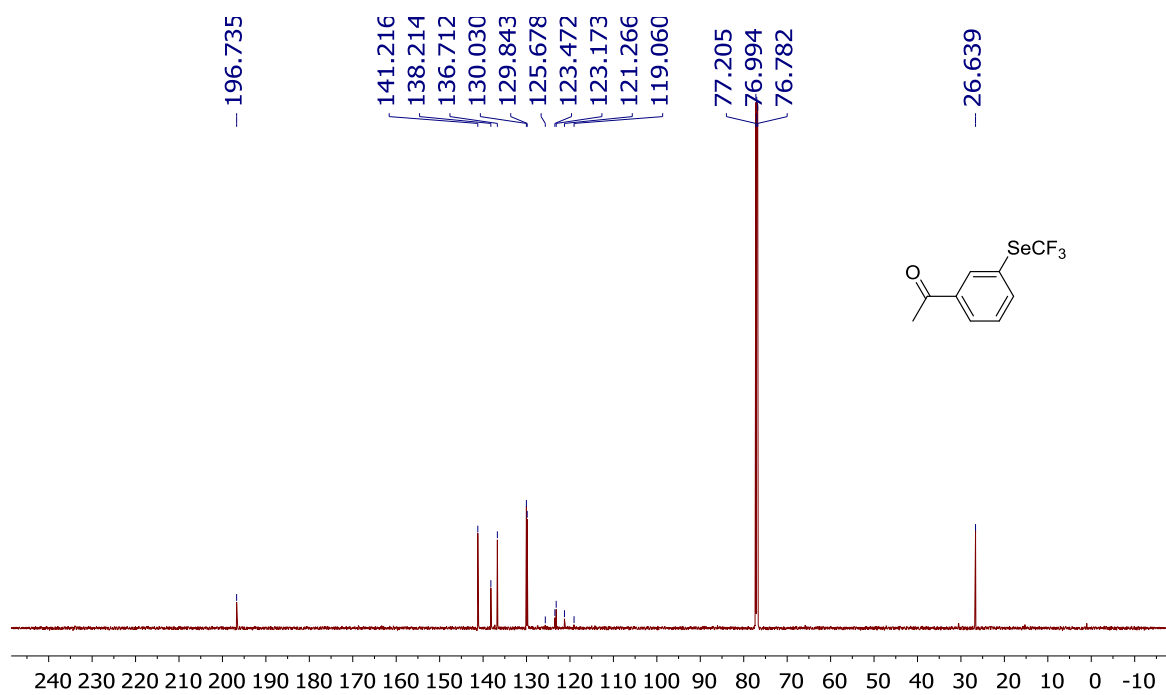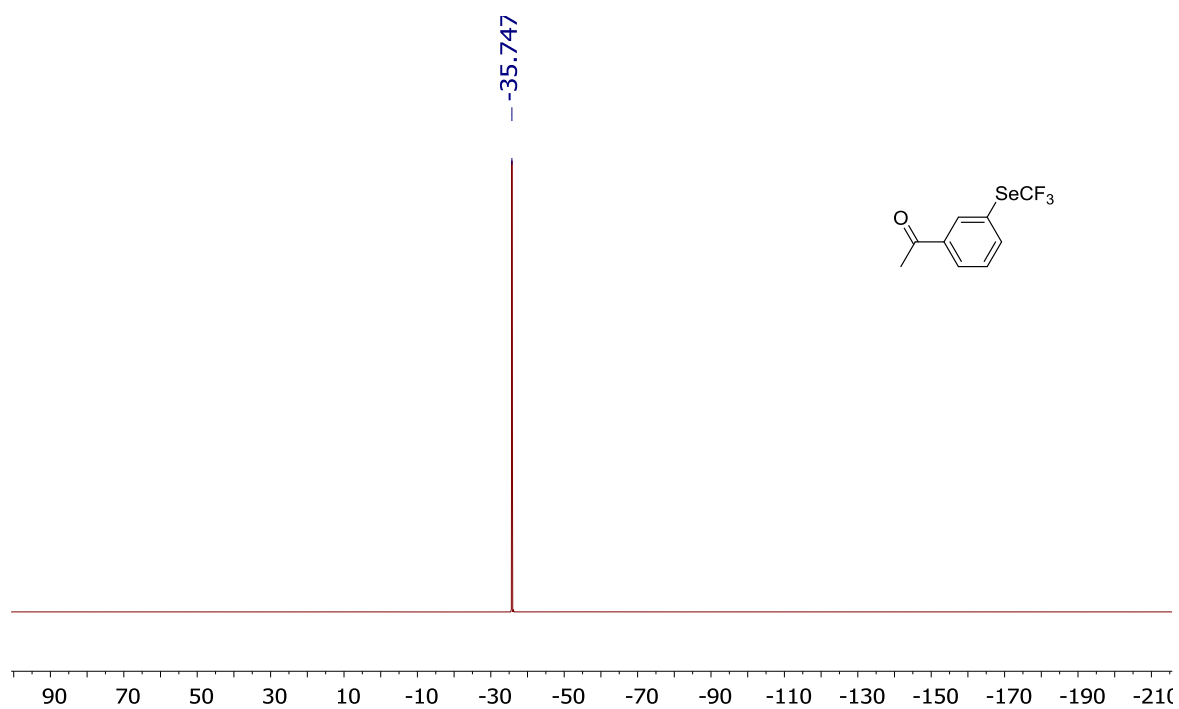
3-[(Trifluoromethyl)seleno]benzaldehyde

¹H NMR Spectrum (CDCl₃, 600 MHz):
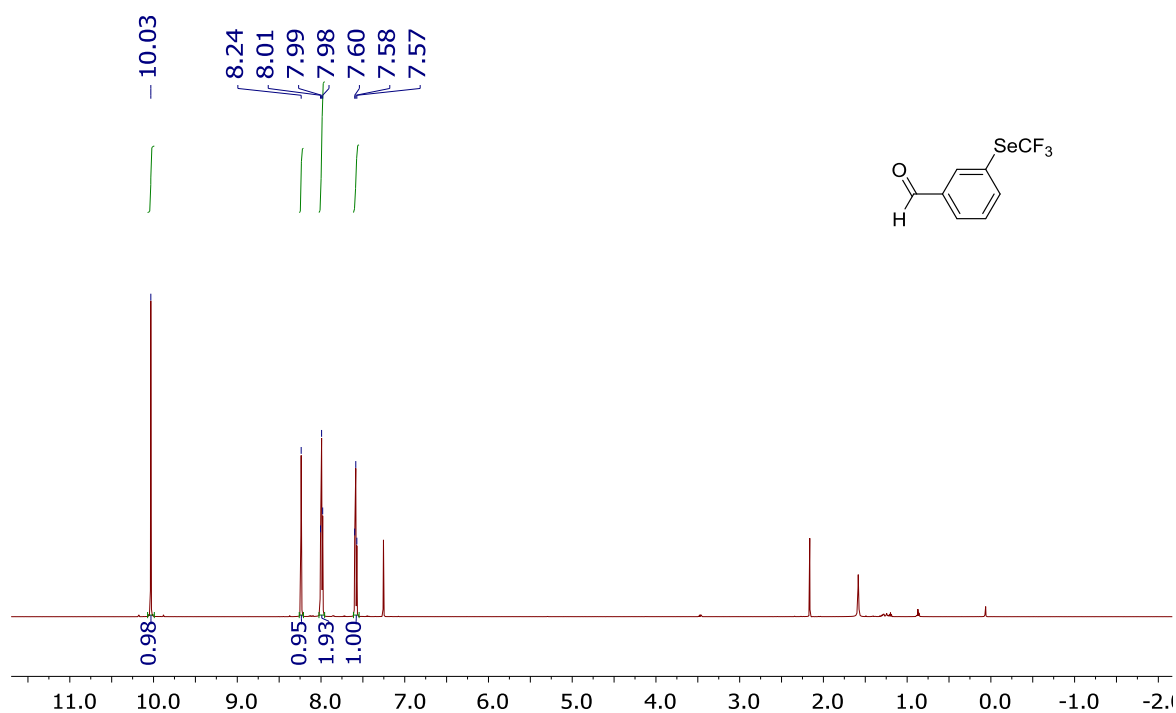
¹³C NMR Spectrum (CDCl₃, 151 MHz)

¹⁹F NMR Spectrum (CDCl₃, 564 MHz):

^{19}F NMR Spectrum (CDCl$_3$, 564 MHz):

−35.61
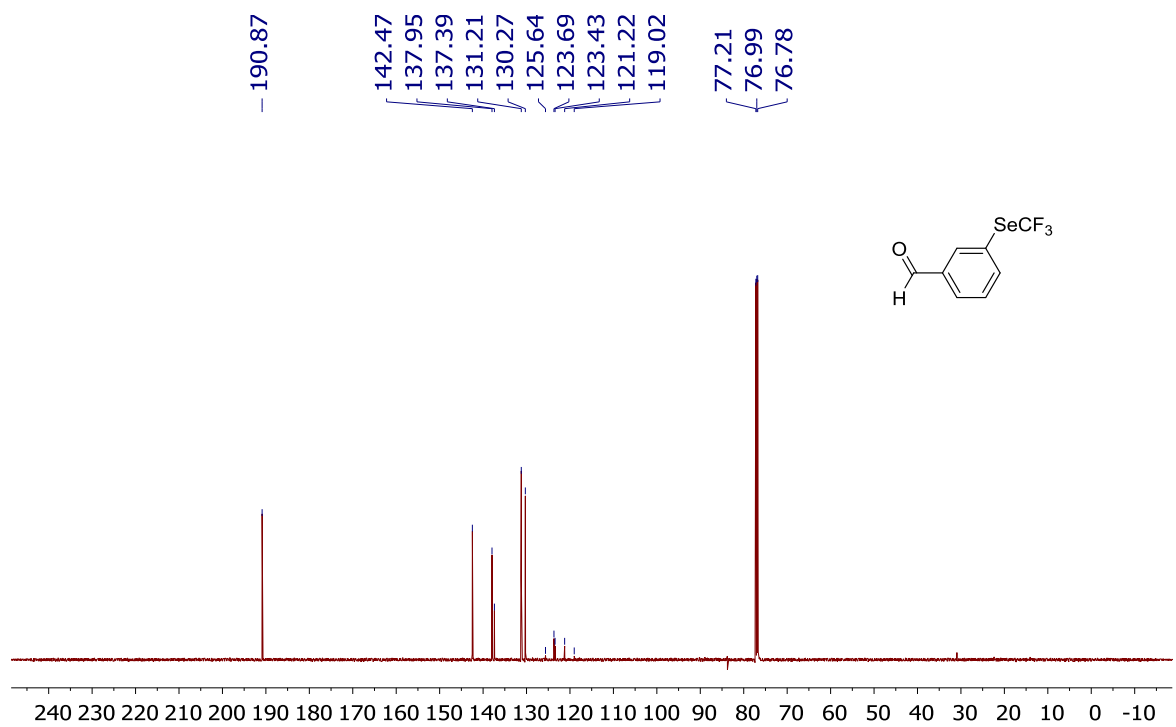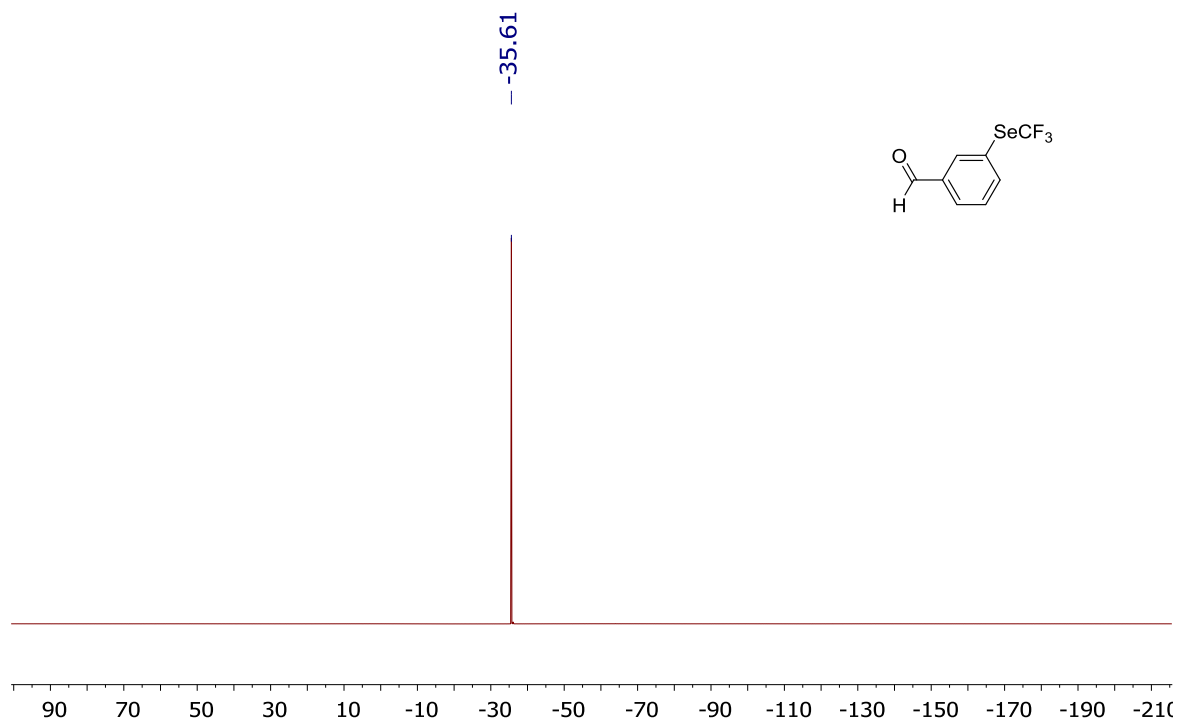
2-[(Trifluoromethyl)seleno]naphthalene

^{1}H NMR Spectrum (CDCl$_3$, 600 MHz):
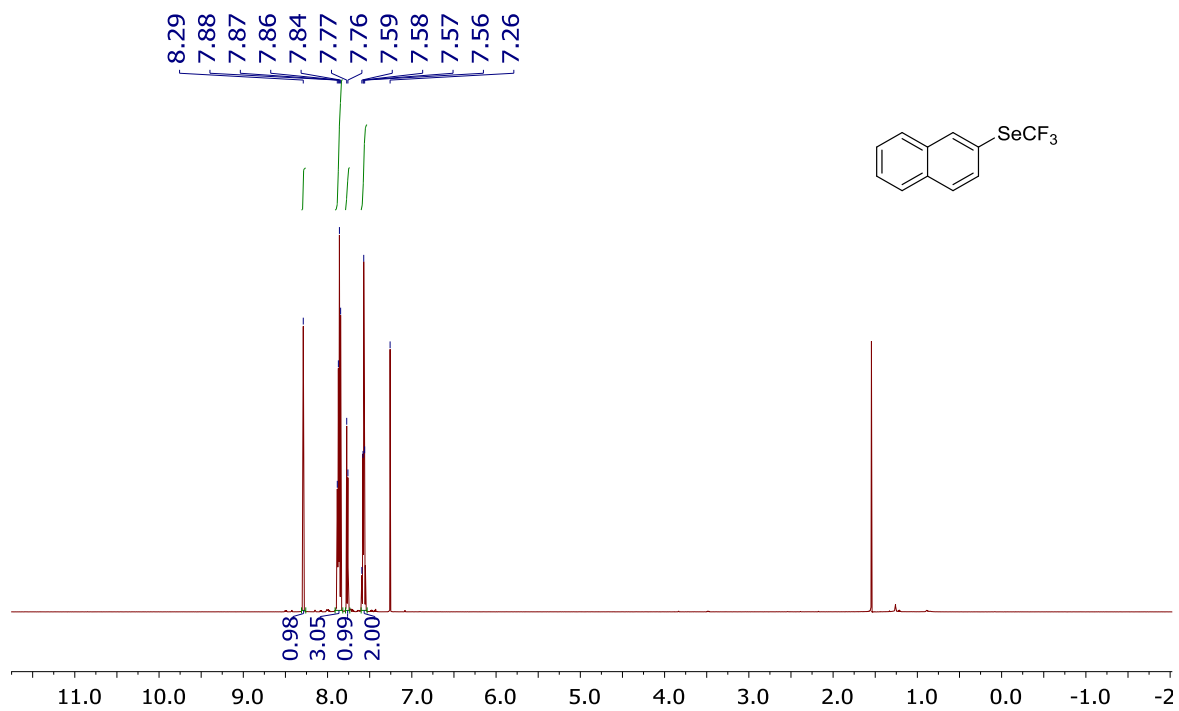
8.29 7.88 7.87 7.86 7.84 7.77 7.76 7.59 7.58 7.57 7.56 7.26

0.98 3.05 0.99 2.00

^{13}C NMR Spectrum (CDCl$_3$, 151 MHz)

137.49
133.57
132.77
129.15
128.07
127.80
127.66
126.90
123.70
121.49
119.69
77.21
77.00
76.79

^{19}F NMR Spectrum (CDCl$_3$, 564 MHz):

−35.84
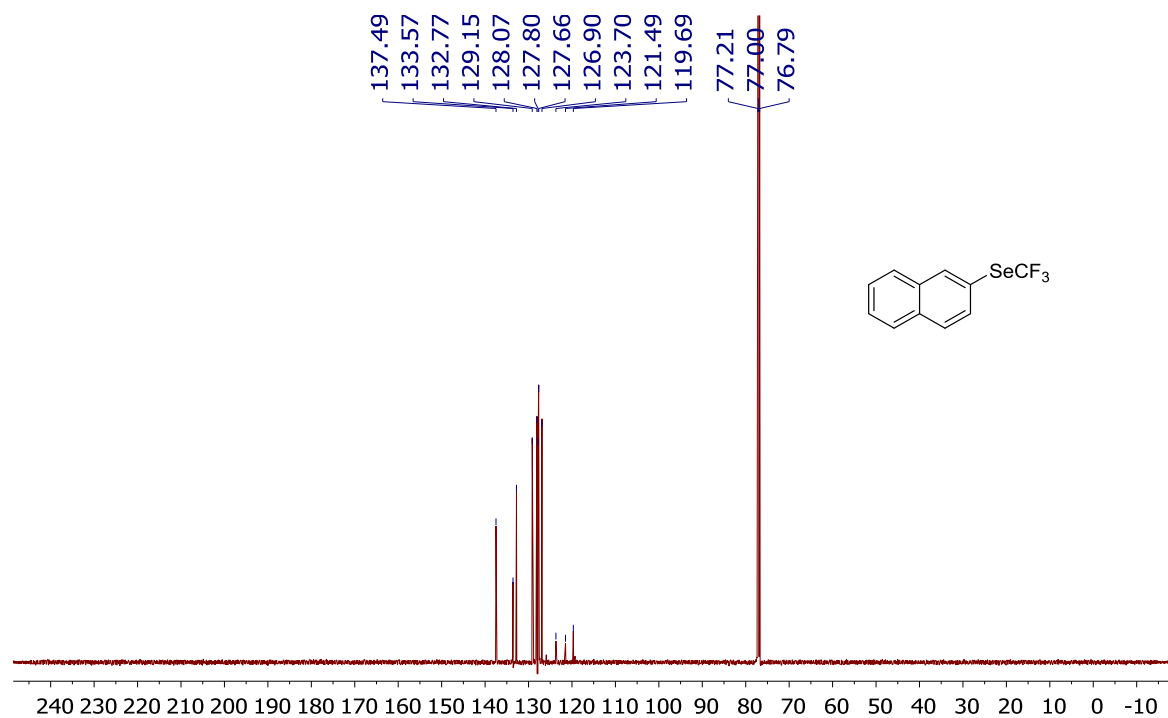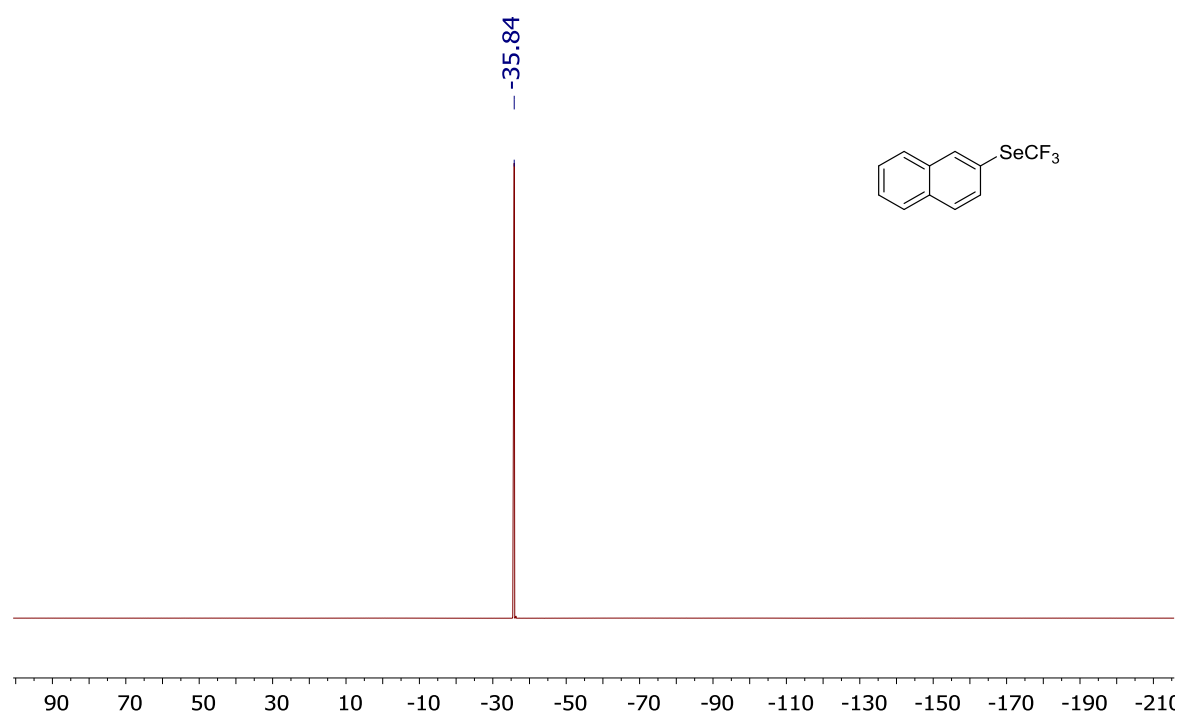
9-[(Trifluoromethyl)seleno]phenanthrene

^{1}H NMR Spectrum (CDCl$_3$, 600 MHz):
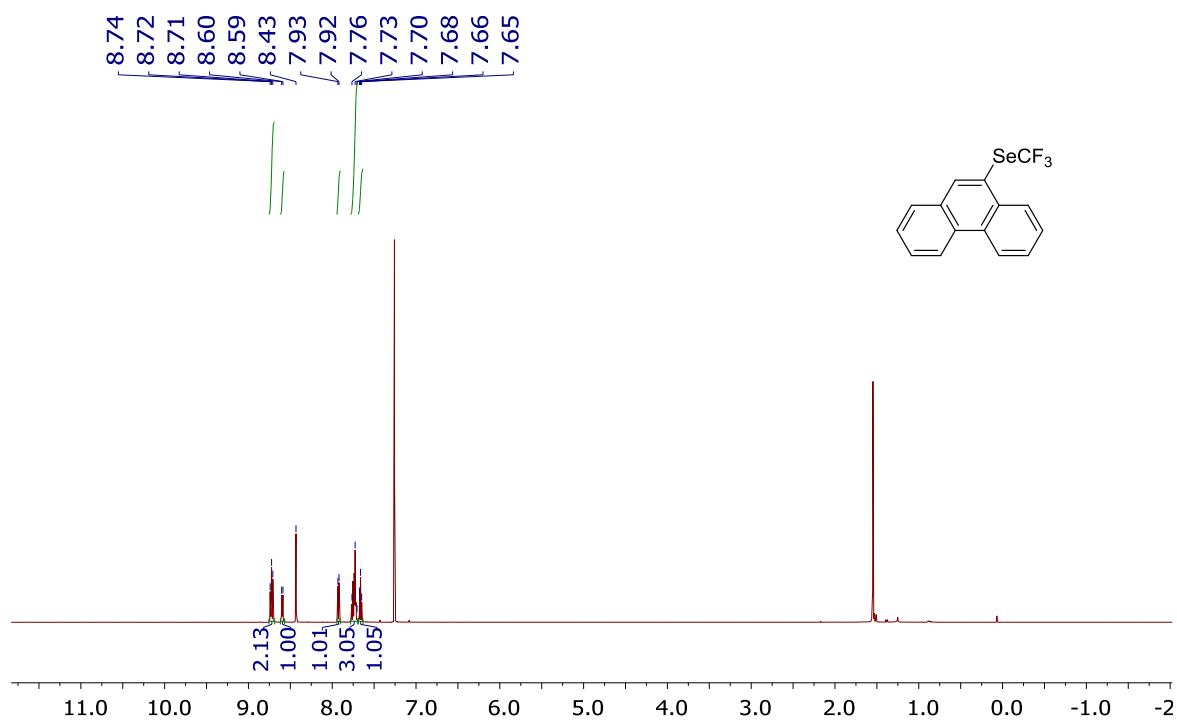
^{13}C NMR Spectrum (CDCl$_3$, 151 MHz)

¹⁹F NMR Spectrum (CDCl₃, 564 MHz):

^{19}F NMR Spectrum (CDCl$_3$, 564 MHz):

−35.28
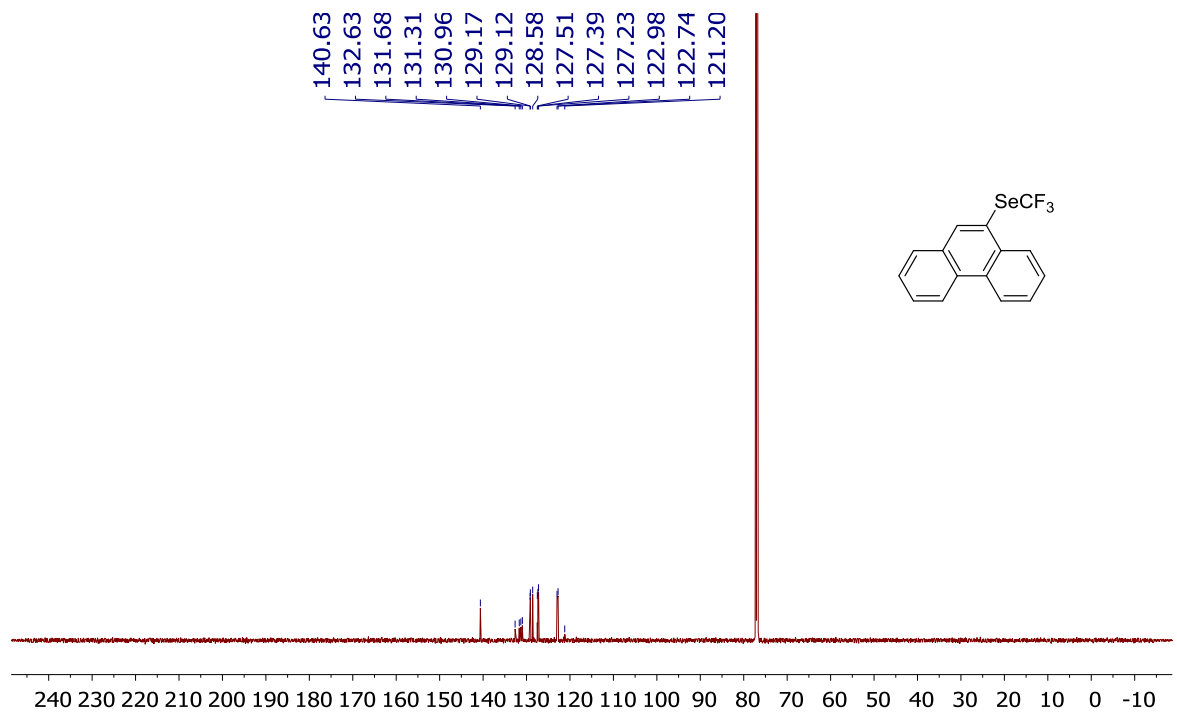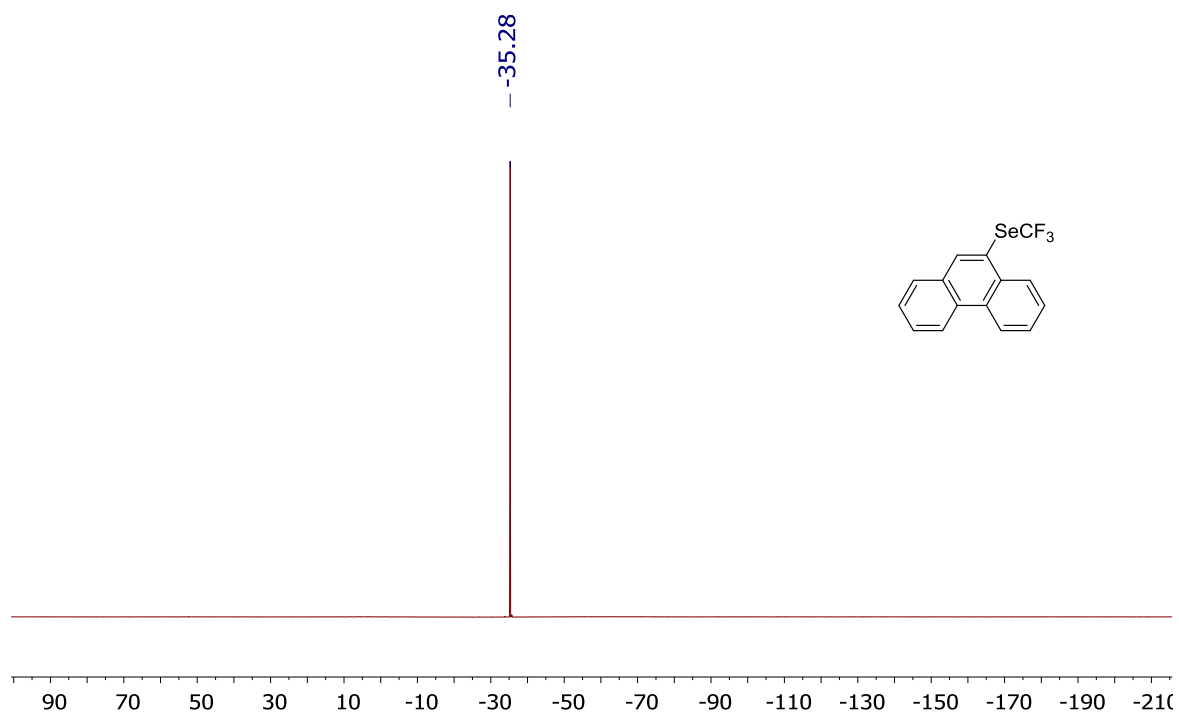
4-[(Trifluoromethyl)seleno]-1-indanone

^{1}H NMR Spectrum (CDCl$_3$, 600 MHz):
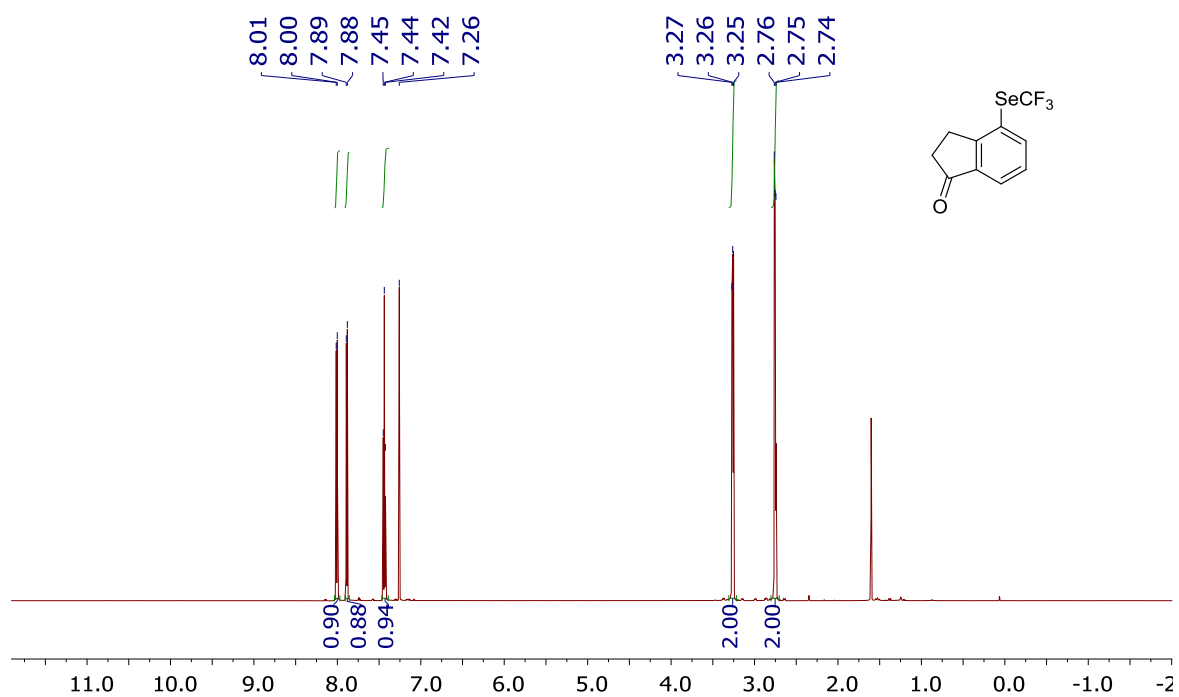
8.01
8.00
7.89
7.88
7.45
7.44
7.42
7.26

3.27
3.26
3.25
2.76
2.75
2.74

0.90
0.88
0.94

2.00
2.00

^{13}C NMR Spectrum (CDCl$_3$, 151 MHz):
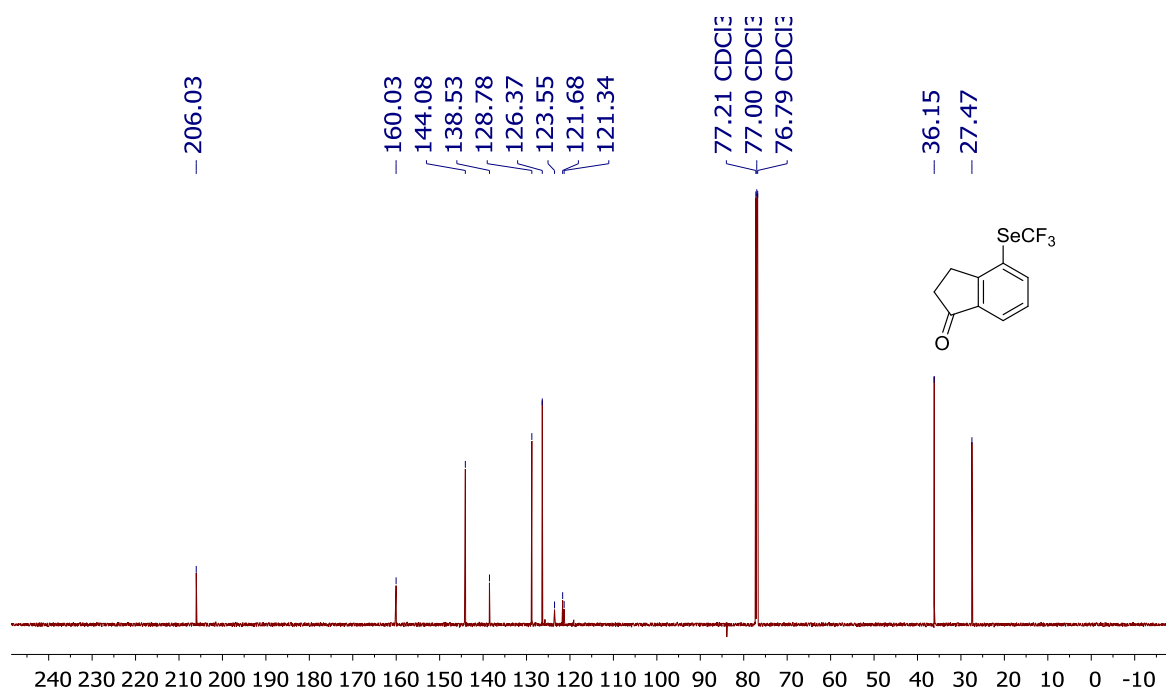
^{19}F NMR Spectrum (CDCl$_3$, 564 MHz):
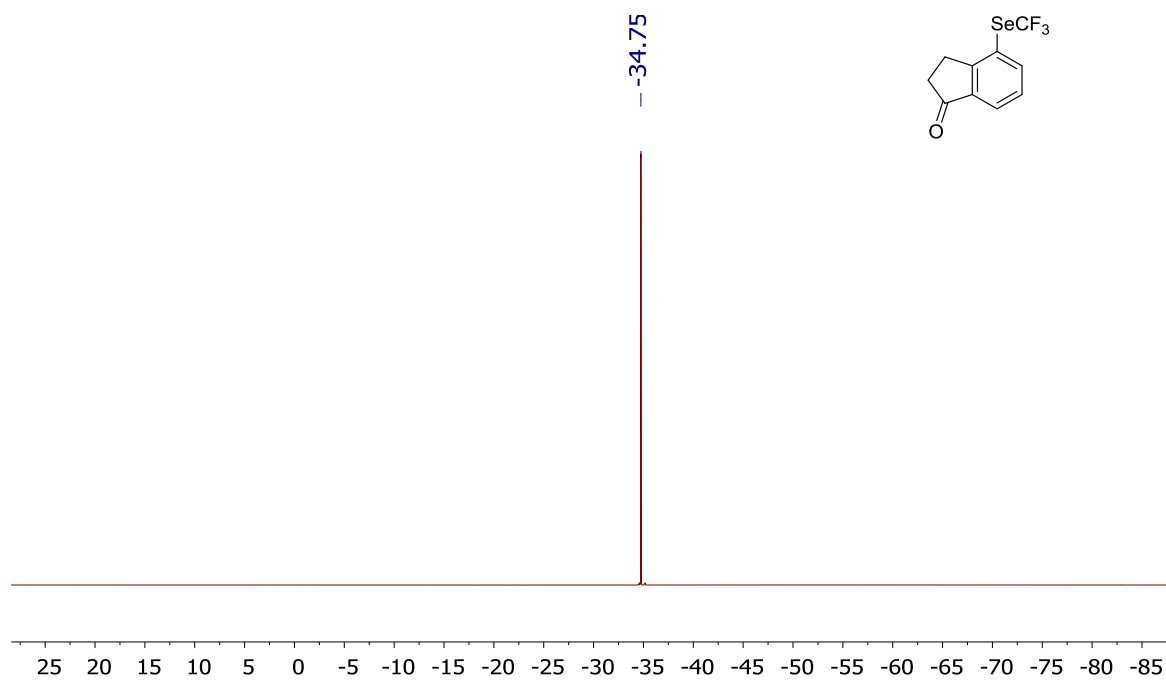
9-[(Trifluoromethyl)seleno]anthracene

^{1}H NMR Spectrum (CDCl$_3$, 600 MHz):
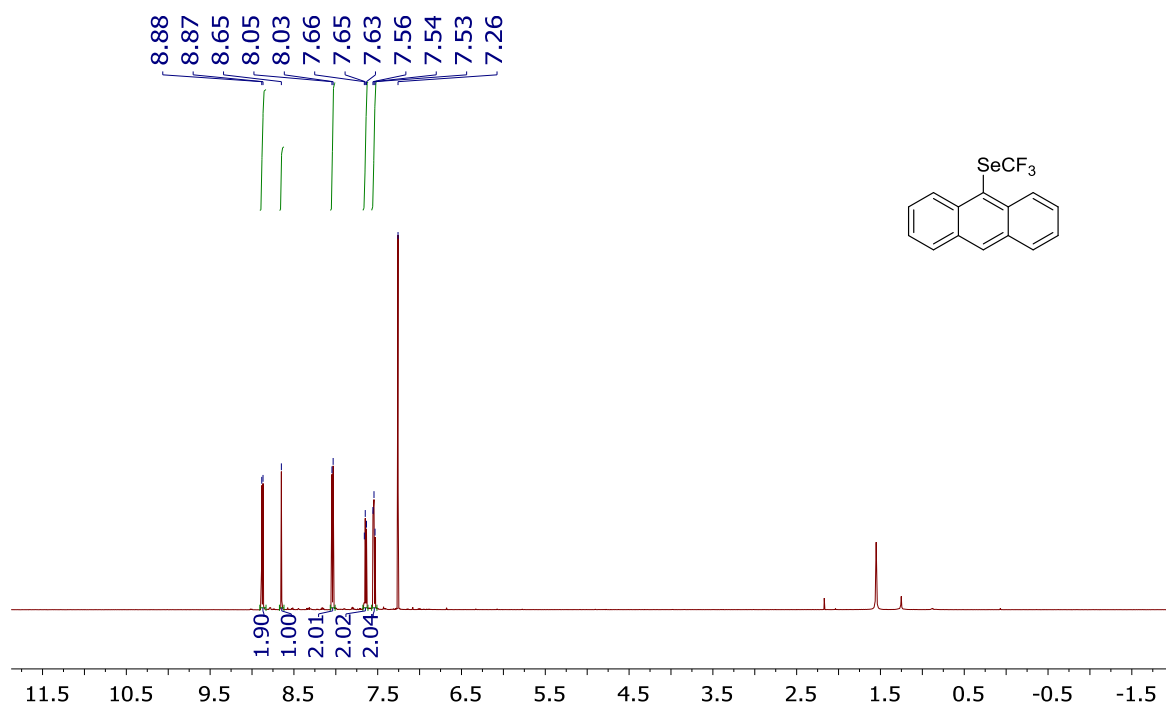
^{13}C NMR Spectrum (CDCl$_3$, 151 MHz):

^{19}F NMR Spectrum (CDCl$_3$, 564 MHz):

-34.579

SeCF$_3$
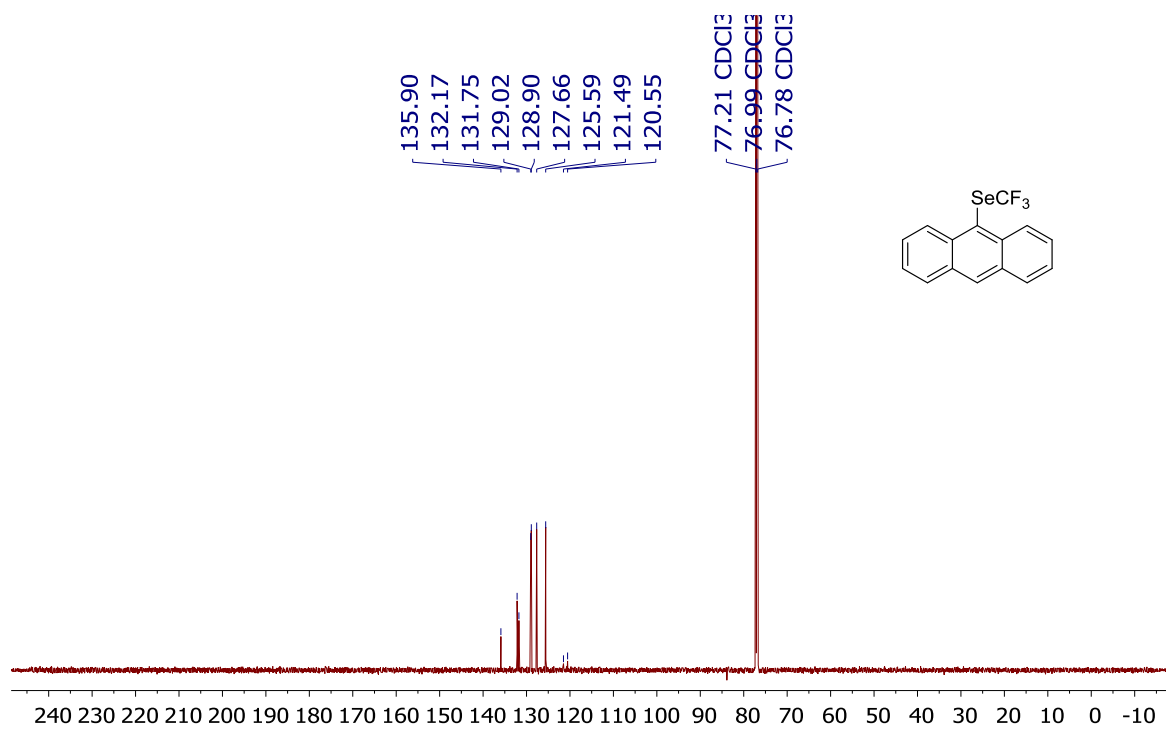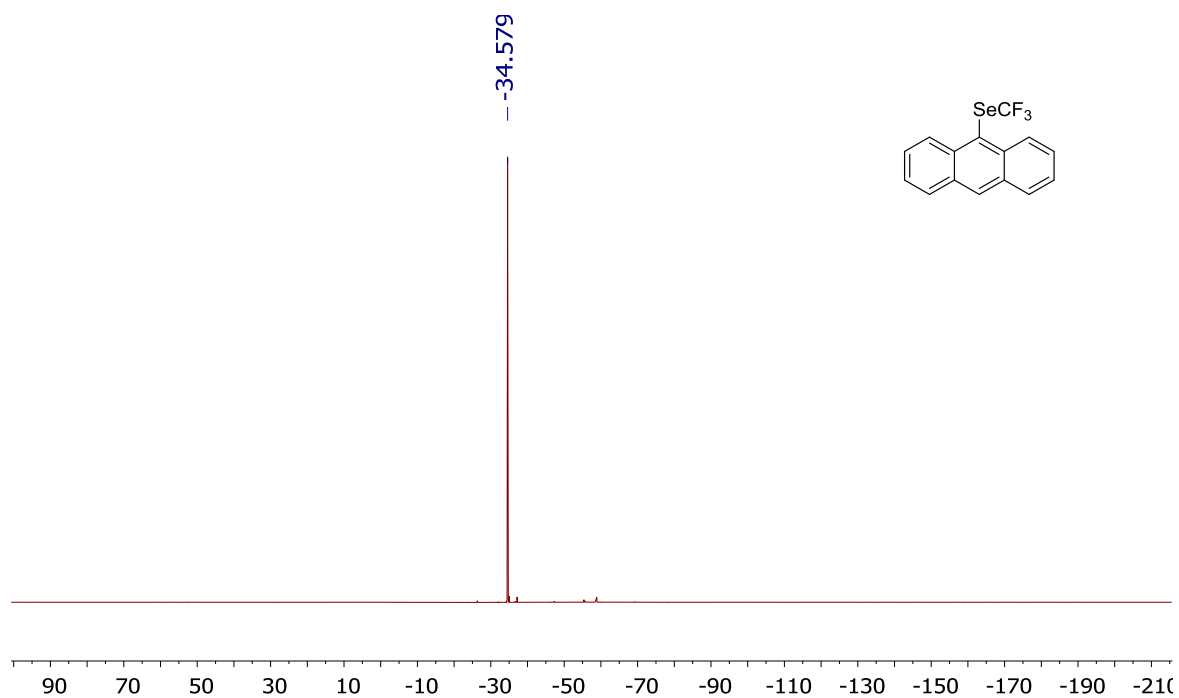
5-[(Trifluoromethyl)seleno]indole

^{1}H NMR Spectrum (CDCl$_3$, 600 MHz):

8.29
8.07
7.55
7.55
7.54
7.54
7.41
7.39
7.28
7.27
7.27
7.25
6.60
6.60

F$_3$CSe

1.00
1.01
1.02
1.04
0.99
1.00
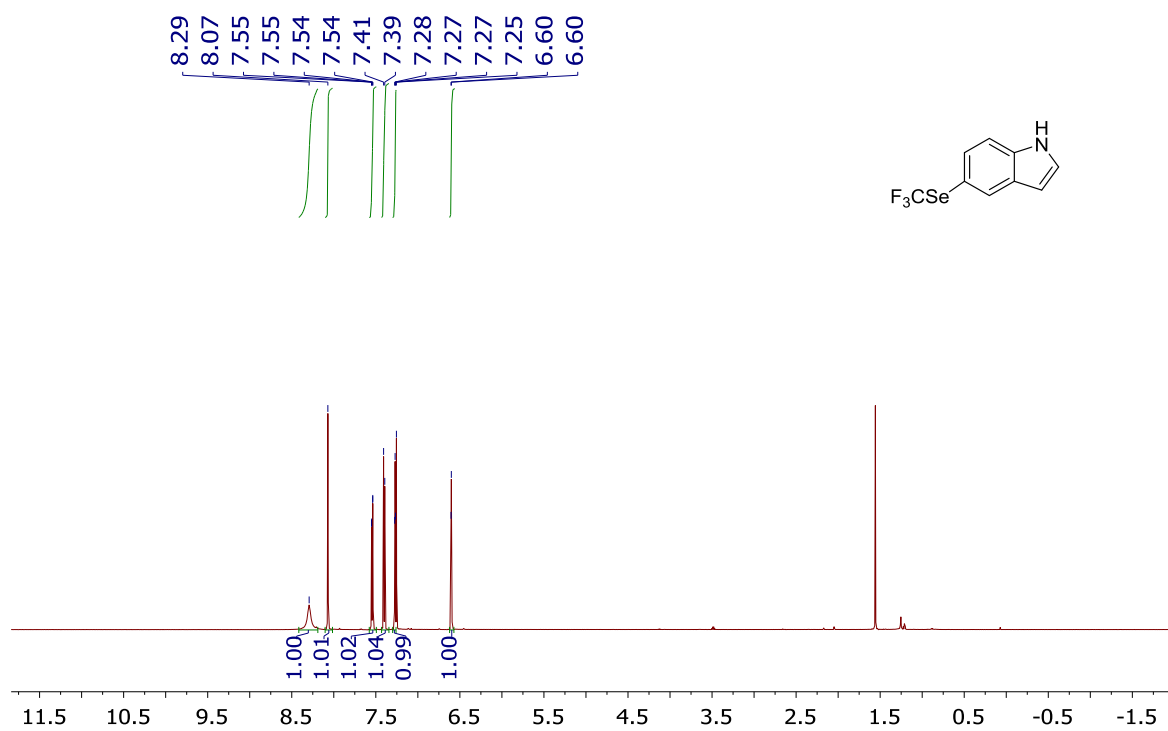
^{13}C NMR Spectrum (CDCl$_3$, 151 MHz):
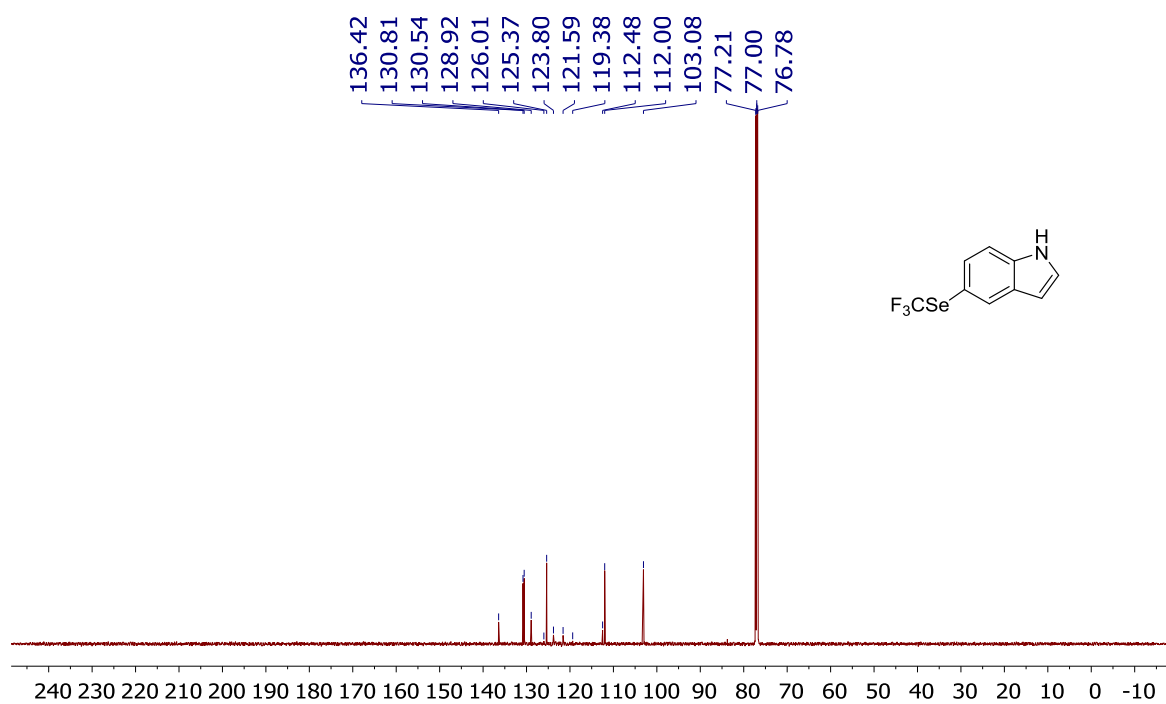
^{19}F NMR Spectrum (CDCl$_3$, 564 MHz):

1-Amino-4-[(trifluoromethyl)seleno]benzene
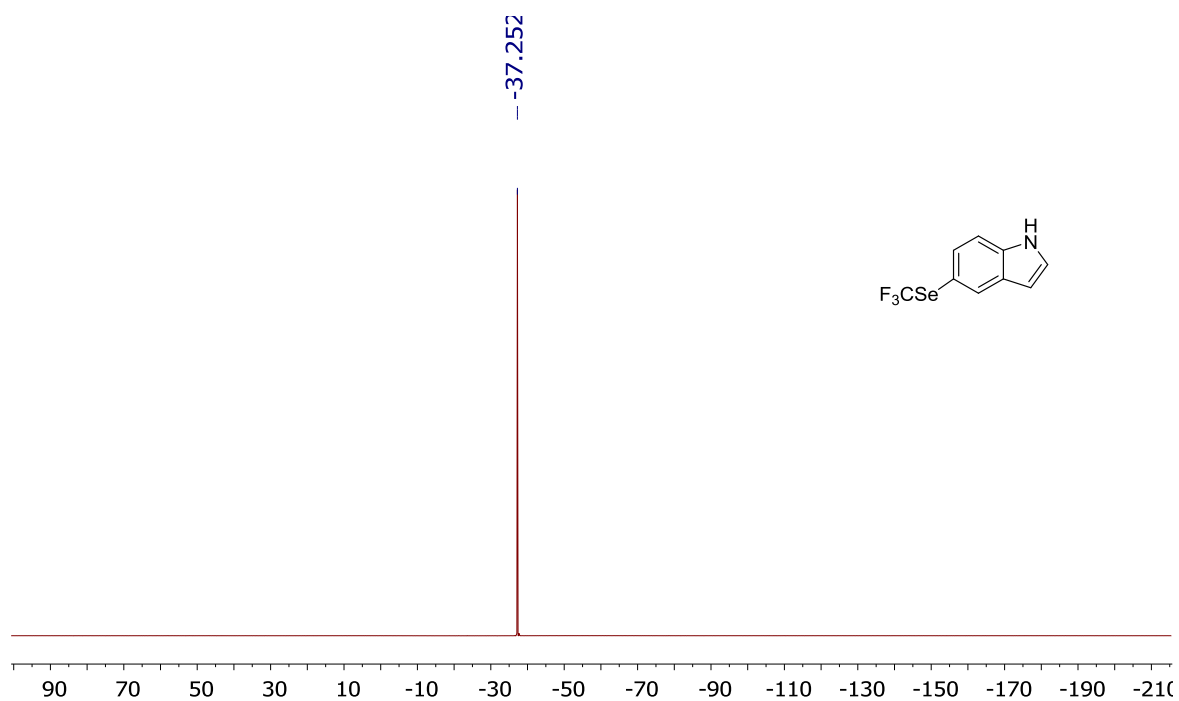
¹H NMR Spectrum (Toluene-*d₈*, 600 MHz):

¹³C NMR Spectrum (Toluene-*d₈*, 151 MHz):
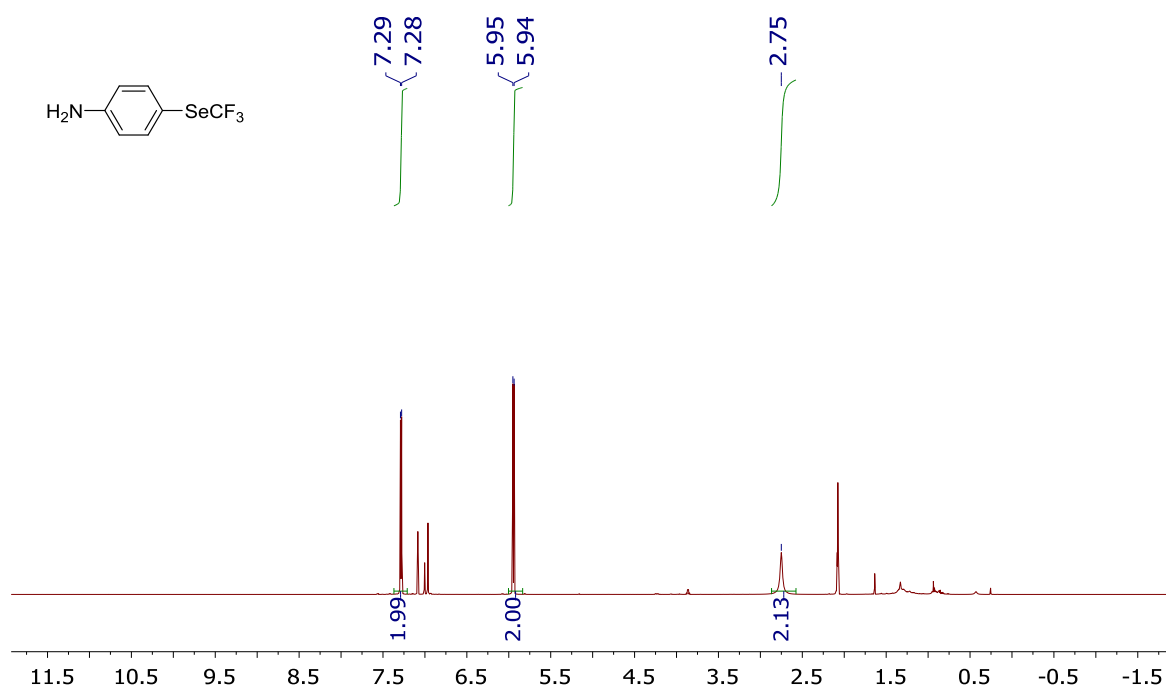
¹⁹F NMR Spectrum (Toluene-*d₈*, 564 MHz):
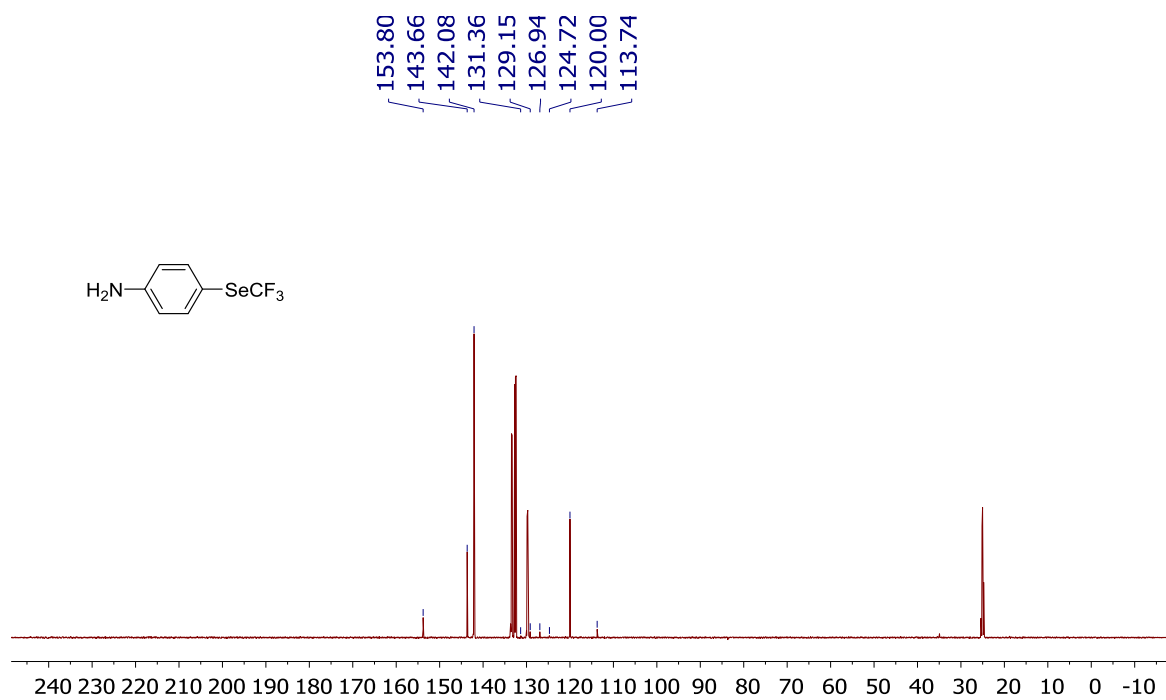
^{19}F NMR Spectrum (Toluene-d_8, 564 MHz):

1-Amino-2-fluoro-4-[(trifluoromethyl)seleno]benzene
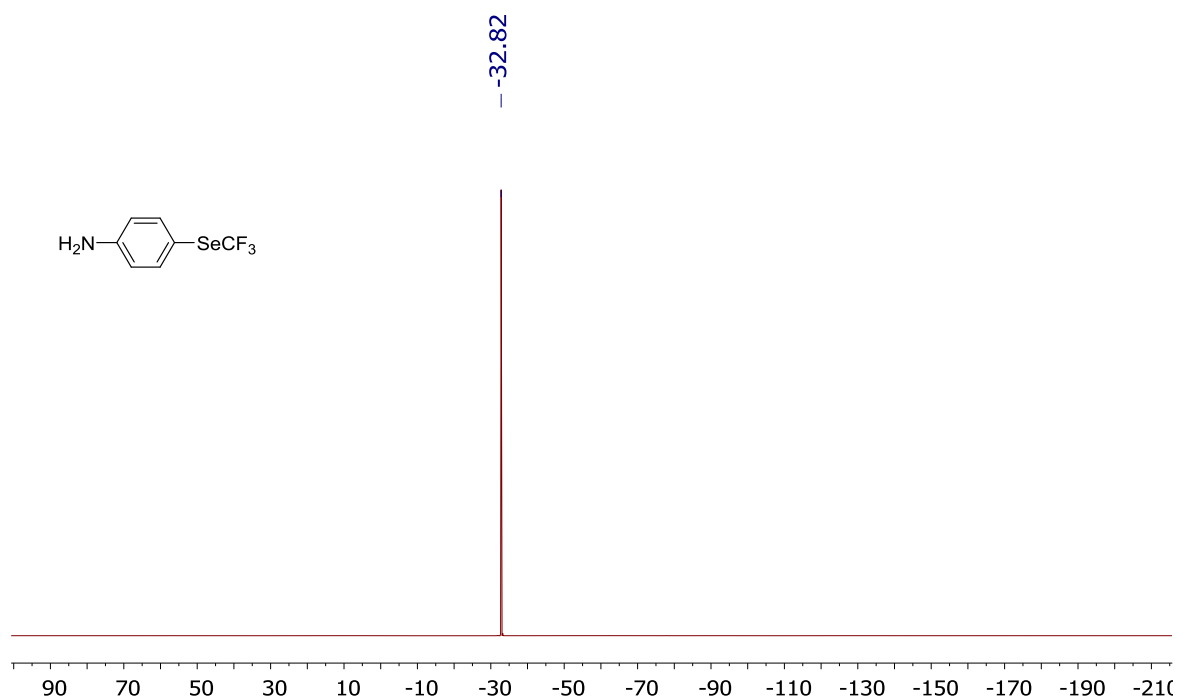
^{1}H NMR Spectrum (Toluene-d_8, 600 MHz):

¹³C NMR Spectrum (Toluene-*d₈*, 151 MHz):
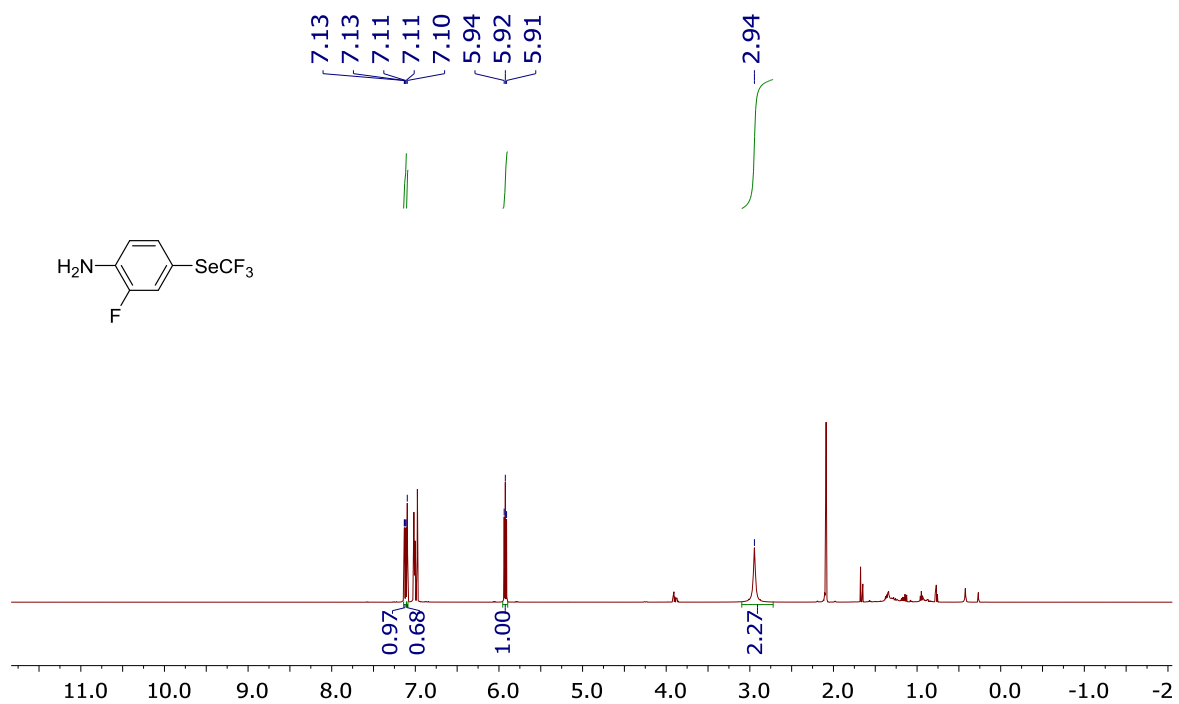
^{13}C NMR Spectrum (Toluene-d_8, 151 MHz):
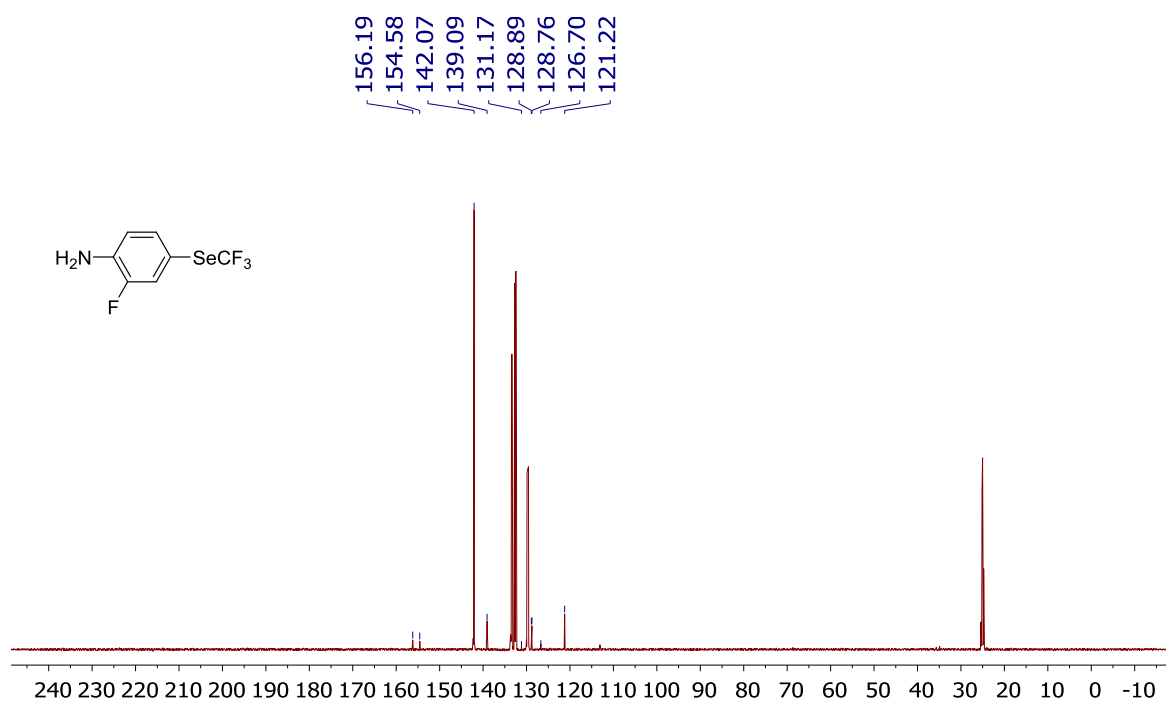
^{19}F NMR Spectrum (Toluene-d_8, 564 MHz):
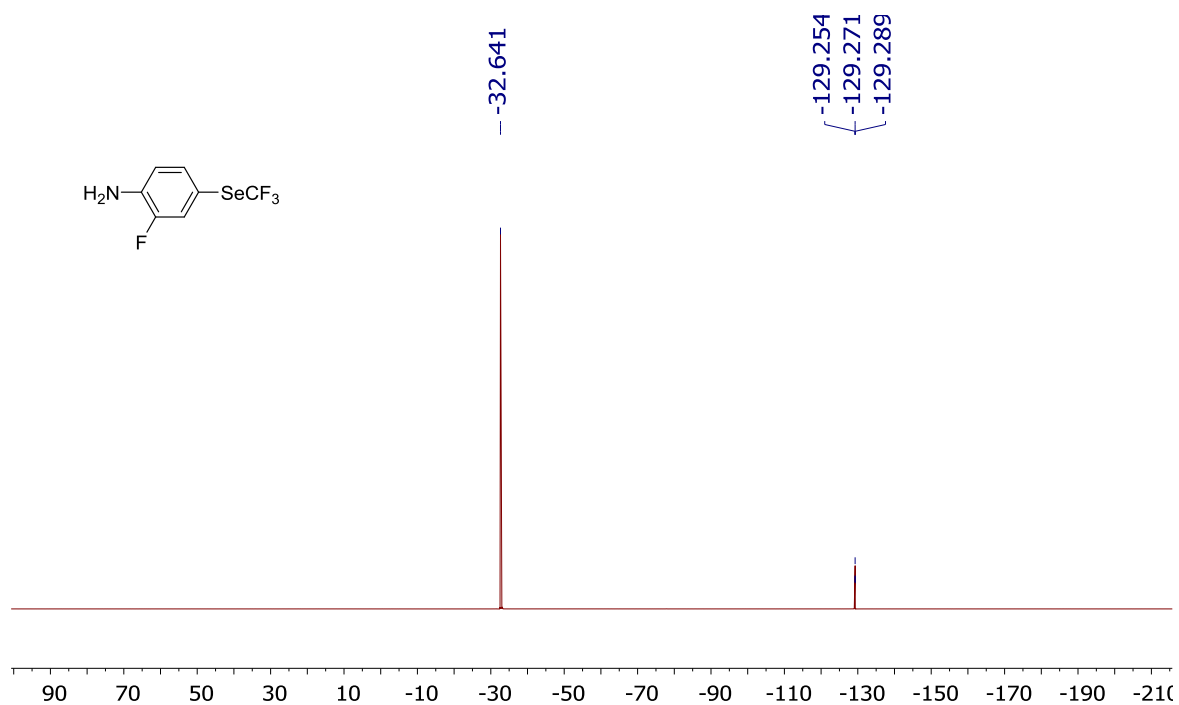
1-Amino-3-[(trifluoromethyl)seleno]benzene

^{1}H NMR Spectrum (Benzene-d_6, 600 MHz):
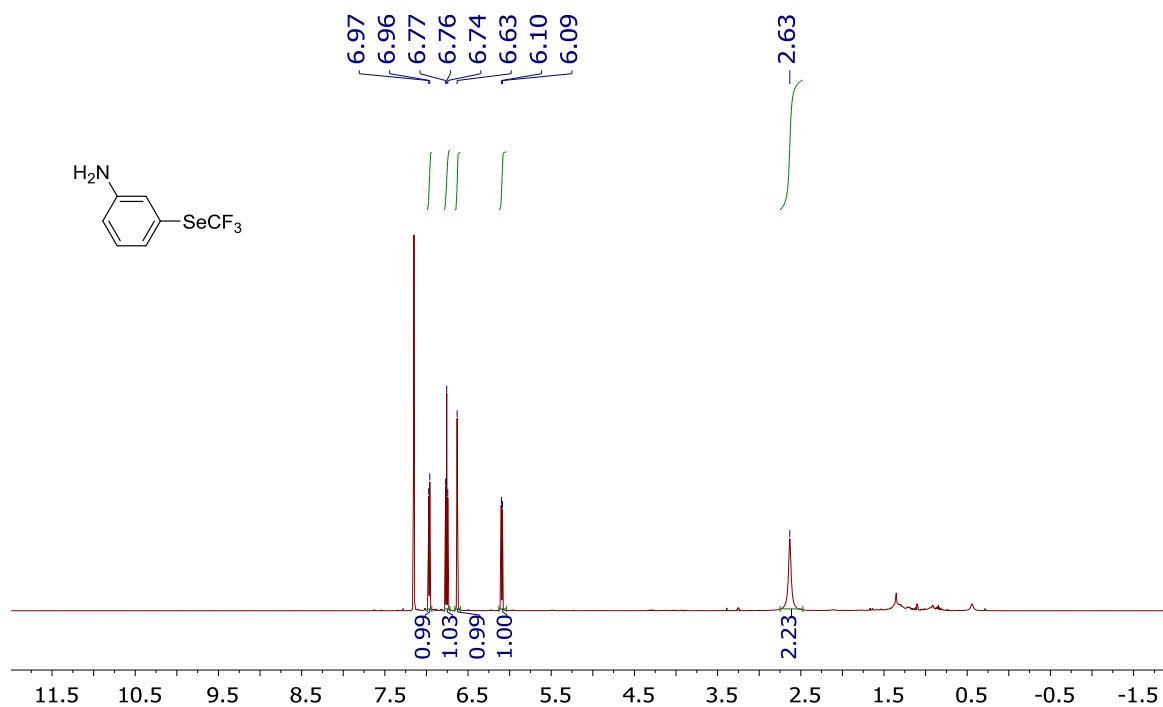
^{13}C NMR Spectrum (Benzene-d_6, 600 MHz):

^{19}F NMR Spectrum (Benzene-d_6, 600 MHz):

1-Amino-2-[(trifluoromethyl)seleno]benzene

^{1}H NMR Spectrum (Benzene-d_6, 600 MHz):

^{13}C NMR Spectrum (Benzene-*d$_6$*, 600 MHz):

149.704
139.766
132.464
126.154
123.933
121.713
119.493
118.237
114.806
106.136

240 230 220 210 200 190 180 170 160 150 140 130 120 110 100 90 80 70 60 50 40 30 20 10 0 -10

^{19}F NMR Spectrum (Benzene-*d$_6$*, 600 MHz):

−35.94

90 70 50 30 10 -10 -30 -50 -70 -90 -110 -130 -150 -170 -190 -210
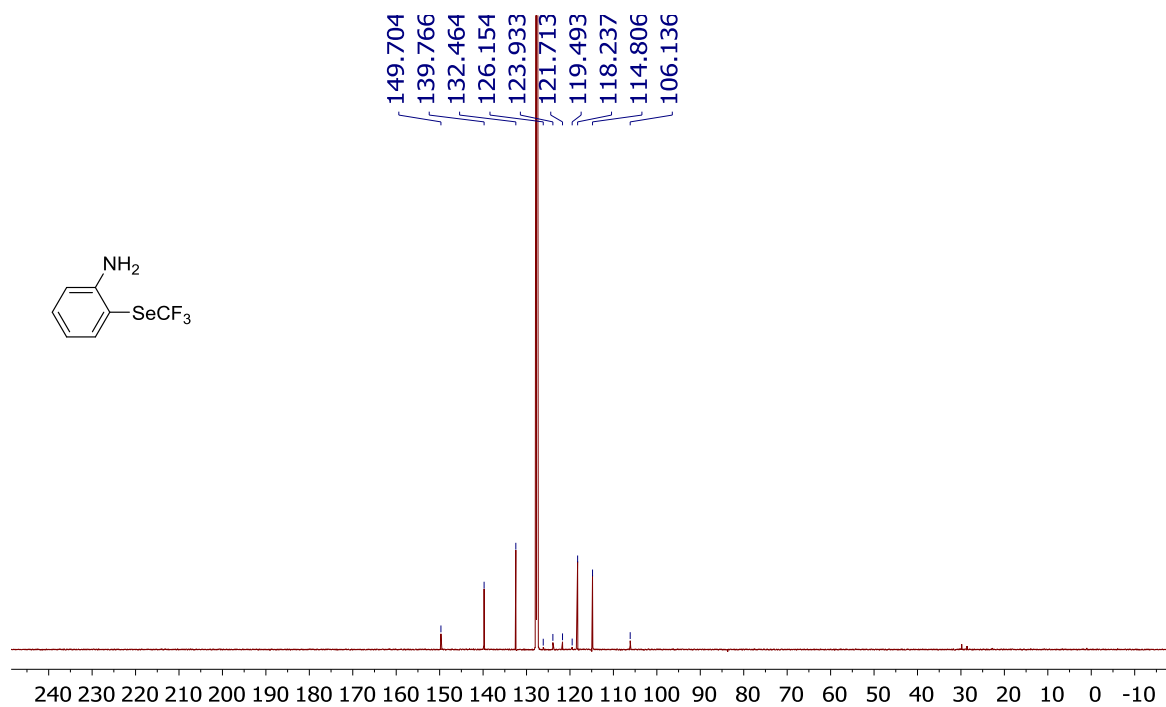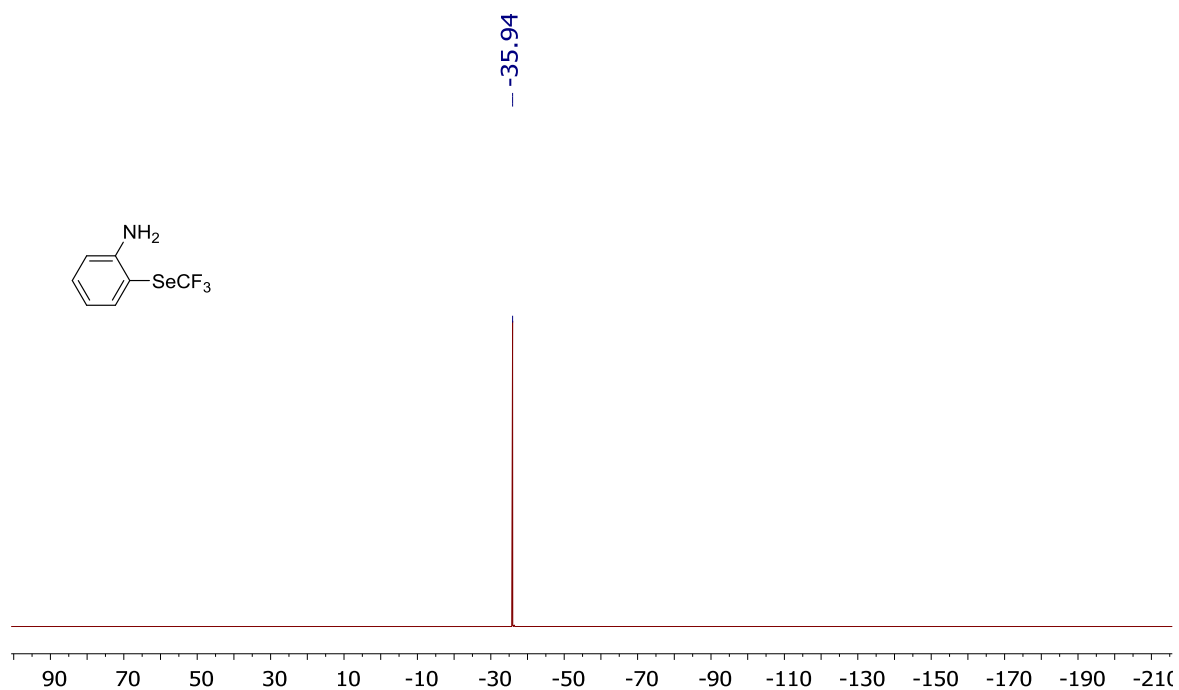
X-ray crystallographic data

Tetra(tri-*tert*-butylphosphine)copperbromide cubane, Cu-cubane **269**
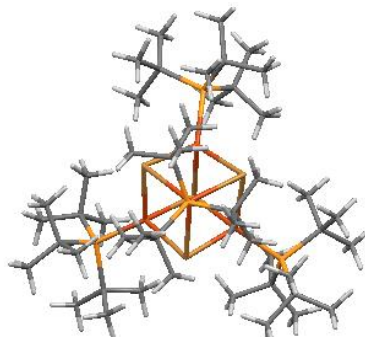
A clear pale yellow prism-like specimen of $C_{55}H_{116}Br_4Cu_4P_4$, approximate dimensions 0.190 mm x 0.240 mm x 0.360 mm, was used for the X-ray crystallographic analysis. The X-ray intensity data were measured on a Bruker Nonius APEX-II system equipped with a graphite monochromator.

The total exposure time was 2.45 hours. The frames were integrated with the Bruker SAINT software package using a narrow frame algorithm. The integration of the data using a trigonal unit cell yielded a total of 47527 reflections to a maximum θ angle of 33.45° (0.64 Å resolution), of which 7860 were independent (average redundancy 6.047, completeness = 91.5%, R_{int} = 3.75%, R_{sig} = 3.77%) and 5945(75.64%) were greater than $2\sigma(F^2)$. The final cell constants of <u>a</u> = 13.8200(9) Å, <u>b</u> = 13.8200(9) Å, <u>c</u> = 59.646(4) Å, volume = 9865.7(11) Å^3, are based upon the refinement of the XYZ-centroids of 9996 reflections above 20 $\sigma(I)$ with 5.869° < 2θ < 64.13°. Data were corrected for absorption effects using the multi-scan method (SADABS). The ratio of minimum to maximum apparent transmission was 0.778. The calculated minimum and maximum transmission coefficients (based on crystal size) are 0.3389 and 0.5294.

The structure was solved and refined using the [OLEX2](#) and Bruker SHELXTL Software Package, using the space group R -3, with Z = 6 for the formula unit, $C_{55}H_{116}Br_4Cu_4P_4$. Structure contains a disordered toluene molecule located close to a three-fold axis. The final anisotropic full-matrix least-squares refinement on F^2 with 377 variables converged at R1 = 2.83%, for the observed data and wR2 =5.47% for all data. The goodness-of-fit was 1.130. The largest peak in the final difference electron density synthesis was 0.458 e$^-$/Å^3 and the largest hole was -0.566 e$^-$/Å^3 with an RMS deviation of 0.085 e$^-$/Å^3. On the basis of the final model, the calculated density was 1.490 g/cm^3 and F(000), 4572 e$^-$.

Table 1. Sample and crystal data for sb261011.		
Identification code	sb261011	
Chemical formula	$C_{55}H_{116}Br_4Cu_4P_4$	
Formula weight	1475.16	
Temperature	100(2) K	
Wavelength	0.71073 Å	
Crystal size	0.190 x 0.240 x 0.360 mm	
Crystal habit	clear pale yellow prism	
Crystal system	trigonal	
Space group	R -3	
Unit cell dimensions	a = 13.8200(9) Å	α = 90°
	b = 13.8200(9) Å	β = 90°
	c = 59.646(4) Å	γ = 120°
Volume	9865.7(11) Å^3	
Z	6	
Density (calculated)	1.490 Mg/cm^3	
Absorption coefficient	3.835 mm^{-1}	
F(000)	4572	

Appendix

<table>
<tr><td colspan="2" align="center">Table 2. Data collection and structure refinement for sb261011.</td></tr>
<tr><td>Diffractometer</td><td>Bruker Nonius APEX-II</td></tr>
<tr><td>Theta range for data collection</td><td>1.02 to 33.45°</td></tr>
<tr><td>Index ranges</td><td>-20<=h<=20, -15<=k<=20, -90<=l<=85</td></tr>
<tr><td>Reflections collected</td><td>47527</td></tr>
<tr><td>Independent reflections</td><td>7860 [R(int) = 0.0375]</td></tr>
<tr><td>Coverage of independent reflections</td><td>91.5%</td></tr>
<tr><td>Absorption correction</td><td>multi-scan</td></tr>
<tr><td>Max. and min. transmission</td><td>0.5294 and 0.3389</td></tr>
<tr><td>Structure solution technique</td><td>direct methods</td></tr>
<tr><td>Structure solution program</td><td>SHELXS-97 (Sheldrick, 2008)</td></tr>
<tr><td>Refinement method</td><td>Full-matrix least-squares on F^2</td></tr>
<tr><td>Refinement program</td><td>SHELXL-97 (Sheldrick, 2008)</td></tr>
<tr><td>Function minimized</td><td>$\Sigma\ w(F_o^2 - F_c^2)^2$</td></tr>
<tr><td>Data / restraints / parameters</td><td>7860 / 3 / 377</td></tr>
<tr><td>Goodness-of-fit on F^2</td><td>1.130</td></tr>
<tr><td>Δ/σ_{max}</td><td>0.004</td></tr>
<tr><td>Final R indices</td><td>5945 data; I>2σ(I)   R1 = 0.0283, wR2 = 0.0508</td></tr>
<tr><td></td><td>all data   R1 = 0.0502, wR2 = 0.0547</td></tr>
<tr><td>Weighting scheme</td><td>w=1/[σ²(F_o^2)+(0.0200P)²+0.0000P]
where P=(F_o^2+2F_c^2)/3</td></tr>
<tr><td>Largest diff. peak and hole</td><td>0.458 and -0.566 eÅ⁻³</td></tr>
<tr><td>R.M.S. deviation from mean</td><td>0.085 eÅ⁻³</td></tr>
</table>

Table 3. Atomic coordinates and equivalent isotropic atomic displacement parameters (Å^2) for sb261011.
U(eq) is defined as one third of the trace of the orthogonalized U$_{ij}$ tensor.

	x/a	y/b	z/c	U(eq)
Br1	0.3333	0.6667	0.454963(4)	0.01398(5)
Br2	0.490012(11)	0.828612(11)	0.403029(2)	0.01383(4)
Cu3	0.3333	0.6667	0.38115(5)	0.01696(7)
Cu4	0.479973(14)	0.673079(14)	0.427723(3)	0.01658(5)
P5	0.3333	0.6667	0.343956(10)	0.01313(12)
P6	0.63170(3)	0.67483(3)	0.440519(6)	0.01212(7)
C7	0.48240(12)	0.46613(13)	0.45797(3)	0.0200(3)
C8	0.59925(11)	0.52692(11)	0.44724(2)	0.0152(3)
C9	0.13758(14)	0.46302(13)	0.34796(3)	0.0219(3)
C10	0.18806(11)	0.56626(12)	0.33279(2)	0.0167(3)
C11	0.18065(14)	0.53055(14)	0.30832(3)	0.0226(3)
C12	0.69366(13)	0.69348(14)	0.39595(3)	0.0208(3)
C13	0.80399(13)	0.79848(14)	0.47408(3)	0.0213(3)
C14	0.68208(13)	0.51697(13)	0.46255(3)	0.0208(3)
C15	0.79864(13)	0.86365(13)	0.41768(3)	0.0212(3)
C16	0.58739(13)	0.46295(13)	0.42545(3)	0.0205(3)
C18	0.84324(12)	0.71117(14)	0.42221(3)	0.0209(3)
C19	0.67139(15)	0.86551(13)	0.46371(3)	0.0217(3)
C20	0.68368(12)	0.76168(12)	0.46713(2)	0.0167(3)
C21	0.60573(14)	0.69854(14)	0.48673(3)	0.0211(3)
C22	0.74857(11)	0.73657(11)	0.41896(2)	0.0156(3)
C1	0.11258(13)	0.61705(14)	0.33607(3)	0.0216(3)
C31	0.4864(6)	0.3173(8)	0.3662(2)	0.060(3)
C32	0.6005(4)	0.3359(6)	0.36532(10)	0.0262(15)
C33	0.6861(7)	0.4460(5)	0.36313(17)	0.044(2)
C34	0.7967(5)	0.4706(7)	0.36246(14)	0.062(3)
C35	0.8216(4)	0.3851(11)	0.36397(11)	0.081(4)
C36	0.7360(8)	0.2750(9)	0.36616(16)	0.065(4)

C37	0.6255(6)	0.2504(5)	0.36683(11)	0.058(4)

Table 4. Bond lengths (Å) for sb261011.

Br1-Cu4	2.5642(3)	Br1-Cu4#1	2.5643(3)
Br1-Cu4#2	2.5643(3)	Br2-Cu4	2.5516(2)
Br2-Cu3	2.5602(2)	Br2-Cu4#1	2.5812(3)
Cu3-P5	2.2185(7)	Cu3-Br2#1	2.5602(2)
Cu3-Br2#2	2.5602(2)	Cu4-P6	2.2202(4)
Cu4-Br2#2	2.5813(3)	P5-C10	1.9010(14)
P5-C10#2	1.9010(14)	P5-C10#1	1.9010(14)
P6-C22	1.9006(14)	P6-C20	1.9009(14)
P6-C8	1.9035(14)	C7-C8	1.538(2)
C7-H7A	0.942(16)	C7-H7B	0.967(16)
C7-H7C	0.967(17)	C8-C14	1.524(2)
C8-C16	1.534(2)	C9-C10	1.531(2)
C9-H9A	0.961(17)	C9-H9B	0.944(17)
C9-H9C	0.973(17)	C10-C11	1.528(2)
C10-C1	1.533(2)	C11-H11A	0.943(19)
C11-H11B	0.955(17)	C11-H11C	0.972(17)
C12-C22	1.537(2)	C12-H12A	0.954(17)
C12-H12B	0.997(18)	C12-H12C	0.916(16)
C13-C20	1.533(2)	C13-H13A	0.931(16)
C13-H13B	0.989(17)	C13-H13C	0.950(17)
C14-H14A	0.914(16)	C14-H14B	1.012(17)
C14-H14C	0.946(17)	C15-C22	1.534(2)
C15-H15A	0.980(16)	C15-H15B	0.961(17)
C15-H15C	0.946(16)	C16-H16A	0.964(16)
C16-H16B	0.970(19)	C16-H16C	0.965(17)
C18-C22	1.527(2)	C18-H18A	0.977(16)
C18-H18B	0.930(17)	C18-H18C	0.953(17)
C19-C20	1.540(2)	C19-H19A	0.958(17)
C19-H19B	0.990(18)	C19-H19C	0.952(17)
C20-C21	1.533(2)	C21-H21A	0.951(17)
C21-H21B	0.952(16)	C21-H21C	0.952(18)
C1-H1A	0.923(16)	C1-H1B	0.960(16)
C1-H1C	0.964(18)	C31-C32	1.466(6)
C31-H31A	1.0831	C31-H31B	1.0831
C31-H31C	1.0831	C32-C37	1.3899
C32-C33	1.3899	C33-C34	1.3899
C33-H33	0.9502	C34-C35	1.39
C34-H34	0.9499	C35-C36	1.3899
C35-H35	1.0078	C36-C37	1.3902
C36-H36	0.95	C37-H37	1.1346

Symmetry transformations used to generate equivalent atoms:

#1	x-y+1, -y+1, z
#2	-x, y+1, z

Table 5. Bond angles (°) for sb261011.

Cu4-Br1-Cu4#1	84.129(9)	Cu4-Br1-Cu4#2	84.128(9)
Cu4#1-Br1-Cu4#2	84.126(9)	Cu4-Br2-Cu3	83.790(8)
Cu4-Br2-Cu4#1	84.041(9)	Cu3-Br2-Cu4#1	83.194(8)
P5-Cu3-Br2	120.646(7)	P5-Cu3-Br2#1	120.647(7)
Br2-Cu3-Br2#1	96.329(9)	P5-Cu3-Br2#2	120.647(7)
Br2-Cu3-Br2#2	96.329(9)	Br2#1-Cu3-Br2#2	96.328(9)
P6-Cu4-Br2	122.413(12)	P6-Cu4-Br1	120.554(13)

Br2-Cu4-Br1	95.970(8)	P6-Cu4-Br2#2	120.269(12)
Br2-Cu4-Br2#2	96.017(9)	Br1-Cu4-Br2#2	95.238(8)
C10-P5-C10#2	108.42(5)	C10-P5-C10#1	108.42(5)
C10#2-P5-C10#1	108.42(5)	C10-P5-Cu3	110.50(5)
C10#2-P5-Cu3	110.50(5)	C10#1-P5-Cu3	110.50(5)
C22-P6-C20	108.26(6)	C22-P6-C8	108.39(6)
C20-P6-C8	108.31(6)	C22-P6-Cu4	110.99(4)
C20-P6-Cu4	110.52(4)	C8-P6-Cu4	110.27(4)
C8-C7-H7A	111.6(10)	C8-C7-H7B	108.7(9)
H7A-C7-H7B	110.7(13)	C8-C7-H7C	115.2(10)
H7A-C7-H7C	107.3(14)	H7B-C7-H7C	103.0(13)
C14-C8-C16	108.93(12)	C14-C8-C7	109.40(12)
C16-C8-C7	104.91(12)	C14-C8-P6	116.03(10)
C16-C8-P6	109.91(10)	C7-C8-P6	107.06(9)
C10-C9-H9A	115.6(10)	C10-C9-H9B	109.0(10)
H9A-C9-H9B	106.0(14)	C10-C9-H9C	111.4(9)
H9A-C9-H9C	107.1(14)	H9B-C9-H9C	107.3(14)
C11-C10-C9	109.73(13)	C11-C10-C1	108.57(12)
C9-C10-C1	104.71(12)	C11-C10-P5	116.50(10)
C9-C10-P5	107.22(10)	C1-C10-P5	109.46(10)
C10-C11-H11A	110.2(11)	C10-C11-H11B	115.3(10)
H11A-C11-H11B	104.7(14)	C10-C11-H11C	114.1(10)
H11A-C11-H11C	108.5(14)	H11B-C11-H11C	103.5(14)
C22-C12-H12A	107.6(10)	C22-C12-H12B	109.7(10)
H12A-C12-H12B	108.9(14)	C22-C12-H12C	111.9(10)
H12A-C12-H12C	108.8(14)	H12B-C12-H12C	109.9(14)
C20-C13-H13A	110.4(10)	C20-C13-H13B	113.0(10)
H13A-C13-H13B	106.8(14)	C20-C13-H13C	112.6(10)
H13A-C13-H13C	107.6(14)	H13B-C13-H13C	106.0(13)
C8-C14-H14A	113.7(10)	C8-C14-H14B	114.1(9)
H14A-C14-H14B	106.9(14)	C8-C14-H14C	111.8(10)
H14A-C14-H14C	104.5(14)	H14B-C14-H14C	105.0(14)
C22-C15-H15A	112.4(9)	C22-C15-H15B	106.5(10)
H15A-C15-H15B	109.7(13)	C22-C15-H15C	110.0(10)
H15A-C15-H15C	107.6(13)	H15B-C15-H15C	110.7(14)
C8-C16-H16A	112.7(9)	C8-C16-H16B	107.8(11)
H16A-C16-H16B	103.7(14)	C8-C16-H16C	114.6(10)
H16A-C16-H16C	106.7(13)	H16B-C16-H16C	110.9(14)
C22-C18-H18A	113.3(9)	C22-C18-H18B	110.1(10)
H18A-C18-H18B	109.0(14)	C22-C18-H18C	114.7(10)
H18A-C18-H18C	103.0(13)	H18B-C18-H18C	106.2(14)
C20-C19-H19A	107.5(10)	C20-C19-H19B	110.7(10)
H19A-C19-H19B	106.7(14)	C20-C19-H19C	114.1(10)
H19A-C19-H19C	108.2(15)	H19B-C19-H19C	109.4(14)
C21-C20-C13	108.63(12)	C21-C20-C19	104.95(12)
C13-C20-C19	109.47(13)	C21-C20-P6	109.96(10)
C13-C20-P6	116.11(10)	C19-C20-P6	107.14(10)
C20-C21-H21A	114.2(10)	C20-C21-H21B	112.1(9)
H21A-C21-H21B	105.7(13)	C20-C21-H21C	108.1(11)
H21A-C21-H21C	105.8(14)	H21B-C21-H21C	110.8(14)
C18-C22-C15	108.75(12)	C18-C22-C12	109.77(12)
C15-C22-C12	104.59(12)	C18-C22-P6	116.37(10)
C15-C22-P6	110.07(10)	C12-C22-P6	106.62(9)
C10-C1-H1A	112.3(10)	C10-C1-H1B	111.8(9)
H1A-C1-H1B	108.3(13)	C10-C1-H1C	108.5(10)
H1A-C1-H1C	106.3(14)	H1B-C1-H1C	109.4(14)

C37-C32-C33	120.0	C37-C32-C31	123.4(7)
C33-C32-C31	116.6(7)	C32-C33-C34	120.0
C33-C34-C35	120.0	C36-C35-C34	120.0
C35-C36-C37	120.0	C32-C37-C36	120.0

Symmetry transformations used to generate equivalent atoms:

| #1 | x-y+1, -y+1, z |
| #2 | -x, y+1, z |

Table 6. Torsion angles (°) for sb261011.

Cu4-Br2-Cu3-P5	-137.678(5)	Cu4#1-Br2-Cu3-P5	137.611(5)
Cu4-Br2-Cu3-Br2#1	90.880(8)	Cu4#1-Br2-Cu3-Br2#1	6.169(7)
Cu4-Br2-Cu3-Br2#2	-6.237(7)	Cu4#1-Br2-Cu3-Br2#2	-90.948(8)
Cu3-Br2-Cu4-P6	138.042(15)	Cu4#1-Br2-Cu4-P6	-138.188(14)
Cu3-Br2-Cu4-Br1	-89.748(8)	Cu4#1-Br2-Cu4-Br1	-5.977(7)
Cu3-Br2-Cu4-Br2#2	6.182(7)	Cu4#1-Br2-Cu4-Br2#2	89.953(8)
Cu4#1-Br1-Cu4-P6	139.454(15)	Cu4#2-Br1-Cu4-P6	-135.874(15)
Cu4#1-Br1-Cu4-Br2	6.016(7)	Cu4#2-Br1-Cu4-Br2	90.688(5)
Cu4#1-Br1-Cu4-Br2#2	-90.612(5)	Cu4#2-Br1-Cu4-Br2#2	-5.940(7)
Br2-Cu3-P5-C10	-160.81(5)	Br2#1-Cu3-P5-C10	-40.81(5)
Br2#2-Cu3-P5-C10	79.19(5)	Br2-Cu3-P5-C10#2	-40.81(5)
Br2#1-Cu3-P5-C10#2	79.19(5)	Br2#2-Cu3-P5-C10#2	-160.81(5)
Br2-Cu3-P5-C10#1	79.19(5)	Br2#1-Cu3-P5-C10#1	-160.81(5)
Br2#2-Cu3-P5-C10#1	-40.81(5)	Br2-Cu4-P6-C22	-36.10(5)
Br1-Cu4-P6-C22	-157.29(5)	Br2#2-Cu4-P6-C22	84.85(5)
Br2-Cu4-P6-C20	84.04(5)	Br1-Cu4-P6-C20	-37.15(5)
Br2#2-Cu4-P6-C20	-155.01(5)	Br2-Cu4-P6-C8	-156.23(5)
Br1-Cu4-P6-C8	82.57(5)	Br2#2-Cu4-P6-C8	-35.28(5)
C22-P6-C8-C14	76.39(12)	C20-P6-C8-C14	-40.86(13)
Cu4-P6-C8-C14	-161.91(10)	C22-P6-C8-C16	-47.73(11)
C20-P6-C8-C16	-164.98(10)	Cu4-P6-C8-C16	73.96(10)
C22-P6-C8-C7	-161.15(10)	C20-P6-C8-C7	81.60(11)
Cu4-P6-C8-C7	-39.46(11)	C10#2-P5-C10-C11	76.33(10)
C10#1-P5-C10-C11	-41.19(12)	Cu3-P5-C10-C11	-162.43(10)
C10#2-P5-C10-C9	-160.34(10)	C10#1-P5-C10-C9	82.15(14)
Cu3-P5-C10-C9	-39.09(11)	C10#2-P5-C10-C1	-47.29(14)
C10#1-P5-C10-C1	-164.80(8)	Cu3-P5-C10-C1	73.96(10)
C22-P6-C20-C21	-165.06(10)	C8-P6-C20-C21	-47.72(11)
Cu4-P6-C20-C21	73.18(10)	C22-P6-C20-C13	-41.24(13)
C8-P6-C20-C13	76.10(12)	Cu4-P6-C20-C13	-163.00(10)
C22-P6-C20-C19	81.41(11)	C8-P6-C20-C19	-161.25(10)
Cu4-P6-C20-C19	-40.35(11)	C20-P6-C22-C18	76.62(12)
C8-P6-C22-C18	-40.66(13)	Cu4-P6-C22-C18	-161.91(10)
C20-P6-C22-C15	-47.67(11)	C8-P6-C22-C15	-164.95(10)
Cu4-P6-C22-C15	73.80(10)	C20-P6-C22-C12	-160.56(10)
C8-P6-C22-C12	82.16(11)	Cu4-P6-C22-C12	-39.09(11)
C37-C32-C33-C34	-0.1	C31-C32-C33-C34	179.2(8)
C32-C33-C34-C35	0.1	C33-C34-C35-C36	0
C34-C35-C36-C37	0	C33-C32-C37-C36	0
C31-C32-C37-C36	-179.2(8)	C35-C36-C37-C32	0

Symmetry transformations used to generate equivalent atoms:

| #1 | x-y+1, -y+1, z |
| #2 | -x, y+1, z |

Table 7. Anisotropic atomic displacement parameters ($\mathring{A}^2$) for sb261011.
The anisotropic atomic displacement factor exponent takes the form: $-2\pi^2[\,h^2\,a^{*2}\,U_{11} + ... + 2\,h\,k$
$a^*\,b^*\,U_{12}\,]$

	U_{11}	U_{22}	U_{33}	U_{23}	U_{13}	U_{12}
Br1	0.01358(7)	0.01358(7)	0.01477(12)	0	0	0.00679(4)
Br2	0.01379(7)	0.01318(7)	0.01464(7)	0.00033(5)	-0.00018(5)	0.00683(5)
Cu3	0.01949(10)	0.01949(10)	0.01190(15)	0	0	0.00975(5)
Cu4	0.01387(9)	0.01877(9)	0.01910(10)	0.00076(7)	-0.00198(7)	0.00967(7)
P5	0.01361(18)	0.01361(18)	0.0122(3)	0	0	0.00680(9)
P6	0.01158(16)	0.01153(16)	0.01363(17)	0.00108(13)	0.00607(14)	
C7	0.0166(7)	0.0161(7)	0.0259(9)	0.0057(6)	0.0035(6)	0.0072(6)
C8	0.0140(7)	0.0125(6)	0.0203(7)	0.0020(5)	0.0009(5)	0.0074(5)
C9	0.0177(8)	0.0174(7)	0.0251(9)	0.0011(6)	-0.0005(6)	0.0046(6)
C10	0.0149(7)	0.0165(7)	0.0166(7)	-0.0002(6)	-0.0031(6)	0.0063(6)
C11	0.0226(8)	0.0241(8)	0.0190(8)	-0.0032(7)	-0.0048(6)	0.0102(7)
C12	0.0192(8)	0.0251(8)	0.0158(8)	0.0015(6)	0.0015(6)	0.0092(7)
C13	0.0217(8)	0.0221(8)	0.0204(8)	-0.0037(7)	-0.0066(6)	0.0113(7)
C14	0.0196(8)	0.0185(8)	0.0279(9)	0.0045(6)	-0.0007(6)	0.0123(6)
C15	0.0188(8)	0.0176(7)	0.0218(8)	0.0050(6)	0.0016(6)	0.0050(6)
C16	0.0176(7)	0.0150(7)	0.0284(9)	-0.0007(6)	0.0008(7)	0.0079(6)
C18	0.0129(7)	0.0230(8)	0.0254(9)	0.0033(7)	0.0042(6)	0.0080(6)
C19	0.0281(9)	0.0185(8)	0.0222(8)	-0.0043(6)	-0.0062(7)	0.0144(7)
C20	0.0202(7)	0.0181(7)	0.0152(7)	-0.0024(6)	-0.0038(6)	0.0120(6)
C21	0.0251(8)	0.0256(8)	0.0165(8)	-0.0019(6)	-0.0017(6)	0.0157(7)
C22	0.0122(6)	0.0161(7)	0.0157(7)	0.0015(5)	0.0003(5)	0.0050(6)
C1	0.0168(7)	0.0247(8)	0.0236(9)	0.0006(7)	-0.0011(6)	0.0106(7)
C31	0.045(5)	0.089(7)	0.060(6)	-0.003(4)	-0.007(4)	0.044(4)
C32	0.023(4)	0.033(4)	0.022(3)	0.002(3)	0.000(3)	0.013(4)
C33	0.039(5)	0.055(5)	0.037(5)	-0.002(4)	0.004(4)	0.023(4)
C34	0.026(5)	0.071(9)	0.052(5)	0.005(6)	0.009(4)	-0.003(6)
C35	0.042(5)	0.160(12)	0.042(4)	0.041(6)	0.008(4)	0.052(7)
C36	0.073(8)	0.075(10)	0.047(6)	0.019(7)	0.012(6)	0.036(8)
C37	0.083(9)	0.084(9)	0.043(5)	0.012(5)	0.010(6)	0.069(8)

Symmetry transformations used to generate equivalent atoms:

#1	x-y+1, -y+1, z
#2	-x, y+1, z

Table 8. Hydrogen atomic coordinates and isotropic atomic displacement
parameters ($\mathring{A}^2$) for sb261011.

	x/a	y/b	z/c	U(eq)
H18A	0.8796(13)	0.7347(13)	0.4368(3)	0.019(4)
H15A	0.8418(13)	0.9018(12)	0.4311(3)	0.017(4)
H7A	0.4283(13)	0.4675(13)	0.4486(3)	0.024(4)
H13A	0.8208(13)	0.8359(13)	0.4878(3)	0.022(4)
H12A	0.7505(14)	0.7283(13)	0.3848(3)	0.026(4)
H1A	0.1318(13)	0.6772(13)	0.3267(3)	0.019(4)
H9A	0.1726(14)	0.4181(14)	0.3472(3)	0.031(5)
H1B	0.1143(13)	0.6409(12)	0.3512(3)	0.016(4)
H18B	0.8966(14)	0.7454(14)	0.4110(3)	0.027(5)
H13B	0.8175(13)	0.7351(14)	0.4759(3)	0.027(5)
H12B	0.6357(15)	0.7151(14)	0.3934(3)	0.039(5)
H19A	0.6899(14)	0.9055(14)	0.4776(3)	0.029(5)
H15B	0.8467(14)	0.8884(14)	0.4048(3)	0.027(5)
H7B	0.4632(13)	0.3900(13)	0.4613(3)	0.022(4)

	x/a	y/b	z/c	U(eq)
H16A	0.5337(13)	0.4641(13)	0.4153(3)	0.020(4)
H7C	0.4767(14)	0.4944(13)	0.4724(3)	0.026(5)
H9B	0.0622(15)	0.4155(14)	0.3439(3)	0.029(5)
H19B	0.5928(16)	0.8434(14)	0.4604(3)	0.037(5)
H13C	0.8574(13)	0.8471(13)	0.4634(3)	0.021(4)
H12C	0.6623(13)	0.6176(14)	0.3947(3)	0.023(4)
H11A	0.1053(16)	0.4855(14)	0.3040(3)	0.034(5)
H14A	0.7535(14)	0.5520(13)	0.4571(3)	0.023(4)
H14B	0.6857(13)	0.5462(14)	0.4783(3)	0.026(4)
H18C	0.8208(13)	0.6338(15)	0.4217(3)	0.028(5)
H21A	0.6082(13)	0.6339(14)	0.4913(3)	0.025(4)
H9C	0.1384(13)	0.4832(13)	0.3636(3)	0.022(4)
H14C	0.6637(14)	0.4417(15)	0.4645(3)	0.027(5)
H15C	0.7410(13)	0.8812(13)	0.4162(3)	0.022(4)
H1C	0.0372(15)	0.5615(15)	0.3322(3)	0.032(5)
H11B	0.2110(14)	0.5901(14)	0.2977(3)	0.024(4)
H19C	0.7187(14)	0.9150(14)	0.4524(3)	0.028(5)
H16B	0.5552(15)	0.3845(16)	0.4292(3)	0.039(5)
H21B	0.5296(14)	0.6732(12)	0.4832(3)	0.018(4)
H11C	0.2199(14)	0.4902(13)	0.3051(3)	0.027(5)
H21C	0.6290(14)	0.7469(14)	0.4994(3)	0.029(5)
H16C	0.6559(14)	0.4894(13)	0.4171(3)	0.027(5)
H31A	0.4863	0.3853	0.3752	0.09
H31B	0.4326	0.2392	0.3747	0.09
H31C	0.4561	0.3138	0.3493	0.09
H33	0.6691	0.5045	0.3621	0.053
H34	0.8552	0.5459	0.3610	0.074
H35	0.9010	0.4013	0.3626	0.097
H36	0.7530	0.2165	0.3672	0.078
H37	0.5591	0.1607	0.3704	0.069

Bis(tri-cyclohexylphosphine)(dibenzylideneacetone)palladium(0), Pd(PCy$_3$)$_2$(dba) **271**
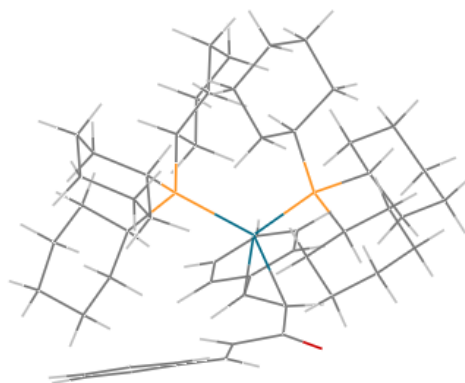
A orange plate-like specimen of C$_{62}$H$_{101}$OP$_2$Pd, approximate dimensions 0.010 mm x 0.070 mm x 0.130 mm, was used for the X-ray crystallographic analysis. The X-ray intensity data were measured on a Bruker Kappa Apex-II Duo system equipped with a graphite monochromator.

Table 1: Data collection details for sb021412.

Axis	dx/mm	2θ/°	ω/°	φ/°	χ/°	Width/°	Frames	Time/s	Wavelength/Å	Voltage/kV	Current/mA	Temperature/K
Omega	40.036	-25.50	-195.19	-212.94	99.74	0.50	66	85.00	0.71073	50	30.0	99.99
Omega	40.036	-23.00	-116.64	-99.03	36.31	0.50	200	85.00	0.71073	50	30.0	99.99
Omega	40.036	19.50	-77.69	-235.39	43.60	0.50	156	85.00	0.71073	50	30.0	99.99
Omega	40.036	22.00	16.16	-63.12	-35.57	0.50	187	85.00	0.71073	50	30.0	99.99
Omega	40.036	27.00	-46.18	63.17	97.52	0.50	150	85.00	0.71073	50	30.0	99.99

A total of 759 frames were collected. The total exposure time was 17.92 hours. The frames were integrated with the Bruker SAINT software package using a narrow-frame algorithm. The integration of the data using a triclinic unit cell yielded a total of 21435 reflections to a maximum θ angle of 27.58° (0.77 Å resolution), of which 12657 were independent (average redundancy 1.694, completeness $= 97.5\%$, $R_{int} = 7.60\%$, $R_{sig} = 16.65\%$) and 7759 (61.30%) were greater than $2\sigma(F^2)$. The final cell constants of $\underline{a}$ = 10.4527(4) Å, $\underline{b}$ = 16.2269(9) Å, $\underline{c}$ = 18.3209(9) Å, α = 70.007(3)°, β = 74.851(3)°, γ = 79.631(3)°, volume = 2804.6(2) Å^3, are based upon the refinement of the XYZ-centroids of 2804 reflections above 20 σ(I) with 4.755° $< 2\theta < 52.84°$. Data were corrected for absorption effects using the multi-scan method (SADABS). The ratio of minimum to maximum apparent transmission was 0.768.

The structure was solved and refined using the **OLEX2** and Bruker SHELXTL Software Package, using the space group P -1, with Z = 2 for the formula unit, $C_{62}H_{101}OP_2Pd$. The final anisotropic full-matrix least-squares refinement on F^2 with 598 variables converged at R1 = 8.07%, for the observed data and wR2 = 12.68% for all data. The goodness-of-fit was 1.222. The largest peak in the final difference electron density synthesis was 1.813 e$^-$/Å^3 and the largest hole was -1.659 e$^-$/Å^3 with an RMS deviation of 0.123 e$^-$/Å^3. On the basis of the final model, the calculated density was 1.221 g/cm^3 and F(000),1114 e$^-$.

Table 2. Sample and crystal data for sb021412.

Identification code	sb021412	
Chemical formula	$C_{62}H_{101}OP_2Pd$	
Formula weight	1030.77	
Temperature	293(2) K	
Wavelength	0.71073 Å	
Crystal size	0.010 x 0.070 x 0.130 mm	
Crystal habit	orange plate	
Crystal system	Triclinic	
Space group	P -1	
Unit cell dimensions	a = 10.4527(4) Å	α = 70.007(3)°
	b = 16.2269(9) Å	β = 74.851(3)°
	c = 18.3209(9) Å	γ = 79.631(3)°
Volume	2804.6(2) Å^3	
Z	2	
Density (calculated)	1.221 Mg/cm^3	
Absorption coefficient	0.427 mm^{-1}	
F(000)	1114	

Table 3. Data collection and structure refinement for sb021412.

Diffractometer	Bruker Kappa Apex-II Duo
Theta range for data collection	2.03 to 27.58°
Index ranges	-13<=h<=13, -20<=k<=21, -22<=l<=23
Reflections collected	21435
Independent reflections	12657 [R(int) = 0.0760]
Coverage of independent reflections	97.5%
Absorption correction	multi-scan

Structure solution technique	direct methods
Structure solution program	SHELXS-97 (Sheldrick, 2008)
Refinement method	Full-matrix least-squares on F^2
Refinement program	SHELXL-97 (Sheldrick, 2008)
Function minimized	$\Sigma\, w(F_o^2 - F_c^2)^2$
Data / restraints / parameters	12657 / 0 / 598
Goodness-of-fit on F^2	1.222
Δ/σ_{max}	0.058
Final R indices	7759 data; I>2σ(I) R1 = 0.0807, wR2 = 0.1152
	all data R1 = 0.1451, wR2 = 0.1268
Weighting scheme	$w=1/[\sigma^2(F_o^2)+(0.0100P)^2+0.0000P]$ where $P=(F_o^2+2F_c^2)/3$
Largest diff. peak and hole	1.813 and -1.659 eÅ^{-3}
R.M.S. deviation from mean	0.123 eÅ^{-3}

Table 4. Atomic coordinates and equivalent isotropic atomic displacement parameters (Å^2) for sb021412.

U(eq) is defined as one third of the trace of the orthogonalized U_{ij} tensor.

	x/a	y/b	z/c	U(eq)
Pd1	0.51975(4)	0.15007(3)	0.24172(2)	0.01604(11)
P1	0.28853(12)	0.18667(9)	0.27601(7)	0.0167(3)
P2	0.61468(12)	0.19736(9)	0.10343(7)	0.0164(3)
O39	0.8587(3)	0.1770(3)	0.2565(2)	0.0296(10)
C1	0.2387(5)	0.3051(3)	0.2323(3)	0.0173(11)
C2	0.0937(5)	0.3383(3)	0.2582(3)	0.0218(12)
C3	0.0639(5)	0.4347(3)	0.2106(3)	0.0286(13)
C4	0.1549(5)	0.4941(4)	0.2168(3)	0.0300(14)
C5	0.3017(5)	0.4606(4)	0.1916(3)	0.0293(14)
C6	0.3317(5)	0.3644(3)	0.2387(3)	0.0241(13)
C7	0.2230(5)	0.1569(4)	0.3856(3)	0.0200(12)
C8	0.0740(4)	0.1474(3)	0.4207(3)	0.0203(12)
C9	0.0490(5)	0.1056(4)	0.5118(3)	0.0274(13)
C10	0.1024(5)	0.1577(4)	0.5506(3)	0.0309(14)
C11	0.2491(5)	0.1716(4)	0.5134(3)	0.0306(14)
C12	0.2706(5)	0.2132(4)	0.4234(3)	0.0257(13)
C13	0.1819(5)	0.1283(3)	0.2474(3)	0.0173(12)
C14	0.2023(5)	0.1498(3)	0.1579(3)	0.0180(11)
C15	0.1179(5)	0.0987(3)	0.1359(3)	0.0230(12)
C16	0.1437(5)	0.9999(3)	0.1748(3)	0.0239(13)
C17	0.1195(5)	0.9787(4)	0.2654(3)	0.0264(13)
C18	0.2068(5)	0.0292(3)	0.2862(3)	0.0206(12)
C19	0.5009(5)	0.2613(3)	0.0351(3)	0.0198(12)
C20	0.5276(5)	0.2546(4)	0.9503(3)	0.0283(14)
C21	0.4039(5)	0.2955(4)	0.9153(3)	0.0346(15)
C22	0.3646(5)	0.3899(4)	0.9143(3)	0.0346(15)
C23	0.3477(5)	0.4002(4)	0.9953(3)	0.0285(14)
C24	0.4705(5)	0.3579(3)	0.0308(3)	0.0215(12)
C25	0.6788(4)	0.0996(3)	0.0684(3)	0.0181(12)
C26	0.8009(5)	0.0471(3)	0.0990(3)	0.0205(12)
C27	0.8457(5)	0.9645(3)	0.0734(3)	0.0241(13)
C28	0.7322(5)	0.9051(3)	0.0996(3)	0.0241(13)
C29	0.6128(5)	0.9565(4)	0.0672(3)	0.0252(13)
C30	0.5666(5)	0.0390(3)	0.0929(3)	0.0215(12)
C31	0.7646(4)	0.2552(3)	0.0757(3)	0.0161(11)
C32	0.8423(5)	0.2767(4)	0.9884(3)	0.0220(12)

	x/a	y/b	z/c	U(eq)
C33	0.9740(5)	0.3130(4)	0.9774(3)	0.0242(13)
C34	0.9533(5)	0.3914(3)	0.0065(3)	0.0231(12)
C35	0.8751(5)	0.3707(3)	0.0937(3)	0.0218(12)
C36	0.7435(5)	0.3361(3)	0.1037(3)	0.0204(12)
C37	0.6793(5)	0.0888(3)	0.3032(3)	0.0188(12)
C38	0.7426(5)	0.1652(4)	0.2954(3)	0.0236(13)
C40	0.6639(5)	0.2326(4)	0.3307(3)	0.0225(13)
C41	0.6983(5)	0.3134(4)	0.3120(3)	0.0241(13)
C42	0.6219(5)	0.3850(4)	0.3391(3)	0.0279(13)
C43	0.6449(6)	0.4721(4)	0.2960(4)	0.0460(17)
C44	0.5725(7)	0.5427(5)	0.3177(4)	0.057(2)
C45	0.4714(7)	0.5271(5)	0.3874(4)	0.058(2)
C46	0.4491(6)	0.4415(5)	0.4311(4)	0.0431(17)
C47	0.5202(5)	0.3715(4)	0.4085(3)	0.0326(15)
C48	0.5556(5)	0.0654(4)	0.3548(3)	0.0227(12)
C49	0.5101(5)	0.9786(4)	0.3737(3)	0.0227(12)
C50	0.5543(5)	0.9268(4)	0.3233(3)	0.0300(14)
C51	0.5040(5)	0.8472(4)	0.3404(3)	0.0349(15)
C52	0.4068(6)	0.8180(4)	0.4091(4)	0.0399(16)
C53	0.3656(5)	0.8669(4)	0.4598(3)	0.0345(15)
C54	0.4151(5)	0.9457(4)	0.4437(3)	0.0284(14)
C55	0.2090(9)	0.3336(6)	0.6393(5)	0.093(3)
C56	0.1791(9)	0.2758(9)	0.7176(5)	0.149(6)
C57	0.0479(8)	0.2709(6)	0.7629(5)	0.075(3)
C58	0.9398(7)	0.2627(5)	0.7307(4)	0.062(2)
C59	0.8050(8)	0.2626(6)	0.7781(5)	0.094(3)
C60	0.6954(7)	0.2545(6)	0.7429(5)	0.084(3)
C61	0.0579(5)	0.5256(4)	0.4918(4)	0.0404(16)
C62	0.0472(6)	0.5789(4)	0.5462(4)	0.0450(17)
C63	0.1648(6)	0.6328(5)	0.5260(4)	0.057(2)

Table 5. Bond lengths (Å) for sb021412.

Pd1-C48	2.143(5)	Pd1-C37	2.158(5)
Pd1-P1	2.3524(13)	Pd1-P2	2.3713(13)
P1-C1	1.847(5)	P1-C13	1.854(5)
P1-C7	1.864(5)	P2-C31	1.839(4)
P2-C25	1.863(5)	P2-C19	1.872(5)
O39-C38	1.247(5)	C1-C2	1.522(6)
C1-C6	1.535(6)	C1-H1	1.09
C2-C3	1.529(7)	C2-H2A	1.09
C2-H2B	1.09	C3-C4	1.519(6)
C3-H3A	1.09	C3-H3B	1.09
C4-C5	1.538(7)	C4-H4A	1.09
C4-H4B	1.09	C5-C6	1.525(7)
C5-H5A	1.09	C5-H5B	1.09
C6-H6A	1.09	C6-H6B	1.09
C7-C12	1.528(6)	C7-C8	1.536(6)
C7-H7	1.09	C8-C9	1.542(6)
C8-H8A	1.09	C8-H8B	1.09
C9-C10	1.523(7)	C9-H9A	1.09
C9-H9B	1.09	C10-C11	1.530(6)
C10-H10A	1.09	C10-H10B	1.09
C11-C12	1.525(7)	C11-H11A	1.09
C11-H11B	1.09	C12-H12A	1.09
C12-H12B	1.09	C13-C14	1.519(6)

C13-C18	1.525(7)	C13-H13	1.09
C14-C15	1.518(6)	C14-H14A	1.09
C14-H14B	1.09	C15-C16	1.522(7)
C15-H15A	1.09	C15-H15B	1.09
C16-C17	1.535(7)	C16-H16A	1.09
C16-H16B	1.09	C17-C18	1.522(6)
C17-H17A	1.09	C17-H17B	1.09
C18-H18A	1.09	C18-H18B	1.09
C19-C24	1.521(7)	C19-C20	1.542(7)
C19-H19	1.09	C20-C21	1.536(7)
C20-H20A	1.09	C20-H20B	1.09
C21-C22	1.507(8)	C21-H21A	1.09
C21-H21B	1.09	C22-C23	1.513(7)
C22-H22A	1.09	C22-H22B	1.09
C23-C24	1.534(6)	C23-H23A	1.09
C23-H23B	1.09	C24-H24A	1.09
C24-H24B	1.09	C25-C26	1.525(7)
C25-C30	1.543(6)	C25-H25	1.09
C26-C27	1.524(7)	C26-H26A	1.09
C26-H26B	1.09	C27-C28	1.537(6)
C27-H27A	1.09	C27-H27B	1.09
C28-C29	1.510(7)	C28-H28A	1.09
C28-H28B	1.09	C29-C30	1.525(7)
C29-H29A	1.09	C29-H29B	1.09
C30-H30A	1.09	C30-H30B	1.09
C31-C36	1.526(6)	C31-C32	1.543(6)
C31-H31	1.09	C32-C33	1.533(6)
C32-H32A	1.09	C32-H32B	1.09
C33-C34	1.502(7)	C33-H33A	1.09
C33-H33B	1.09	C34-C35	1.543(6)
C34-H34A	1.09	C34-H34B	1.09
C35-C36	1.523(6)	C35-H35A	1.09
C35-H35B	1.09	C36-H36A	1.09
C36-H36B	1.09	C37-C48	1.415(6)
C37-C38	1.457(7)	C37-H37	1.09
C38-C40	1.474(7)	C40-C41	1.327(7)
C40-H40	1.08	C41-C42	1.445(7)
C41-H41	1.08	C42-C43	1.392(8)
C42-C47	1.408(7)	C43-C44	1.374(9)
C43-H43	1.08	C44-C45	1.408(9)
C44-H44	1.08	C45-C46	1.372(9)
C45-H45	1.08	C46-C47	1.369(8)
C46-H46	1.08	C47-H47	1.08
C48-C49	1.467(7)	C48-H48	1.09
C49-C50	1.394(7)	C49-C54	1.405(7)
C50-C51	1.387(7)	C50-H50	1.08
C51-C52	1.393(8)	C51-H51	1.08
C52-C53	1.360(8)	C52-H52	1.08
C53-C54	1.375(7)	C53-H53	1.08
C54-H54	1.08	C55-C56	1.410(11)
C55-H55A	1.0899	C55-H55B	1.0899
C55-H55C	1.0899	C56-C57	1.404(10)
C56-H56A	1.09	C56-H56B	1.09
C57-C58	1.450(8)	C57-H57A	1.09
C57-H57B	1.09	C58-C59	1.448(9)
C58-H58A	1.09	C58-H58B	1.09

C59-C60	1.498(9)	C59-H59A	1.09
C59-H59B	1.09	C60-H60A	1.0899
C60-H60B	1.0899	C60-H60C	1.0899
C61-C62	1.500(7)	C61-C61#1	1.500(10)
C61-H61A	1.09	C61-H61B	1.09
C62-C63	1.530(7)	C62-H62A	1.09
C62-H62B	1.09	C63-H63A	1.0899
C63-H63B	1.0899	C63-H63C	1.0899

Symmetry transformations used to generate equivalent atoms:

#1   -x, -y+1, -z+1

Table 6. Bond angles (°) for sb021412.

C48-Pd1-C37	38.41(16)	C48-Pd1-P1	100.32(13)
C37-Pd1-P1	137.20(13)	C48-Pd1-P2	143.82(14)
C37-Pd1-P2	107.80(12)	P1-Pd1-P2	114.89(5)
C1-P1-C13	105.2(2)	C1-P1-C7	107.7(2)
C13-P1-C7	101.2(2)	C1-P1-Pd1	112.68(15)
C13-P1-Pd1	116.31(17)	C7-P1-Pd1	112.67(16)
C31-P2-C25	102.3(2)	C31-P2-C19	108.6(2)
C25-P2-C19	102.3(2)	C31-P2-Pd1	114.82(15)
C25-P2-Pd1	109.57(16)	C19-P2-Pd1	117.43(15)
C2-C1-C6	110.5(4)	C2-C1-P1	117.2(3)
C6-C1-P1	112.6(3)	C2-C1-H1	105.1
C6-C1-H1	105.1	P1-C1-H1	105.1
C1-C2-C3	111.2(4)	C1-C2-H2A	109.4
C3-C2-H2A	109.4	C1-C2-H2B	109.4
C3-C2-H2B	109.4	H2A-C2-H2B	108.0
C4-C3-C2	112.1(4)	C4-C3-H3A	109.2
C2-C3-H3A	109.2	C4-C3-H3B	109.2
C2-C3-H3B	109.2	H3A-C3-H3B	107.9
C3-C4-C5	110.4(5)	C3-C4-H4A	109.6
C5-C4-H4A	109.6	C3-C4-H4B	109.6
C5-C4-H4B	109.6	H4A-C4-H4B	108.1
C6-C5-C4	111.6(4)	C6-C5-H5A	109.3
C4-C5-H5A	109.3	C6-C5-H5B	109.3
C4-C5-H5B	109.3	H5A-C5-H5B	108.0
C5-C6-C1	111.6(4)	C5-C6-H6A	109.3
C1-C6-H6A	109.3	C5-C6-H6B	109.3
C1-C6-H6B	109.3	H6A-C6-H6B	108.0
C12-C7-C8	109.3(4)	C12-C7-P1	112.8(3)
C8-C7-P1	120.2(3)	C12-C7-H7	104.3
C8-C7-H7	104.3	P1-C7-H7	104.3
C9-C8-C7	110.3(4)	C9-C8-H8A	109.6
C7-C8-H8A	109.6	C9-C8-H8B	109.6
C7-C8-H8B	109.6	H8A-C8-H8B	108.1
C10-C9-C8	111.8(4)	C10-C9-H9A	109.3
C8-C9-H9A	109.3	C10-C9-H9B	109.3
C8-C9-H9B	109.3	H9A-C9-H9B	107.9
C9-C10-C11	111.7(4)	C9-C10-H10A	109.3
C11-C10-H10A	109.3	C9-C10-H10B	109.3
C11-C10-H10B	109.3	H10A-C10-H10B	107.9
C12-C11-C10	110.8(4)	C12-C11-H11A	109.5
C10-C11-H11A	109.5	C12-C11-H11B	109.5
C10-C11-H11B	109.5	H11A-C11-H11B	108.1
C11-C12-C7	111.3(4)	C11-C12-H12A	109.4
C7-C12-H12A	109.4	C11-C12-H12B	109.4

C7-C12-H12B	109.4	H12A-C12-H12B	108.0
C14-C13-C18	110.2(4)	C14-C13-P1	113.0(3)
C18-C13-P1	109.7(3)	C14-C13-H13	107.9
C18-C13-H13	107.9	P1-C13-H13	107.9
C15-C14-C13	112.1(4)	C15-C14-H14A	109.2
C13-C14-H14A	109.2	C15-C14-H14B	109.2
C13-C14-H14B	109.2	H14A-C14-H14B	107.9
C14-C15-C16	111.5(4)	C14-C15-H15A	109.3
C16-C15-H15A	109.3	C14-C15-H15B	109.3
C16-C15-H15B	109.3	H15A-C15-H15B	108.0
C15-C16-C17	110.0(4)	C15-C16-H16A	109.7
C17-C16-H16A	109.7	C15-C16-H16B	109.7
C17-C16-H16B	109.7	H16A-C16-H16B	108.2
C18-C17-C16	110.4(4)	C18-C17-H17A	109.6
C16-C17-H17A	109.6	C18-C17-H17B	109.6
C16-C17-H17B	109.6	H17A-C17-H17B	108.1
C17-C18-C13	111.5(4)	C17-C18-H18A	109.3
C13-C18-H18A	109.3	C17-C18-H18B	109.3
C13-C18-H18B	109.3	H18A-C18-H18B	108.0
C24-C19-C20	108.8(4)	C24-C19-P2	113.5(3)
C20-C19-P2	120.4(4)	C24-C19-H19	104.0
C20-C19-H19	104.0	P2-C19-H19	104.0
C21-C20-C19	109.0(4)	C21-C20-H20A	109.9
C19-C20-H20A	109.9	C21-C20-H20B	109.9
C19-C20-H20B	109.9	H20A-C20-H20B	108.3
C22-C21-C20	112.6(4)	C22-C21-H21A	109.1
C20-C21-H21A	109.1	C22-C21-H21B	109.1
C20-C21-H21B	109.1	H21A-C21-H21B	107.8
C21-C22-C23	112.1(5)	C21-C22-H22A	109.2
C23-C22-H22A	109.2	C21-C22-H22B	109.2
C23-C22-H22B	109.2	H22A-C22-H22B	107.9
C22-C23-C24	111.2(4)	C22-C23-H23A	109.4
C24-C23-H23A	109.4	C22-C23-H23B	109.4
C24-C23-H23B	109.4	H23A-C23-H23B	108.0
C19-C24-C23	111.3(4)	C19-C24-H24A	109.4
C23-C24-H24A	109.4	C19-C24-H24B	109.4
C23-C24-H24B	109.4	H24A-C24-H24B	108.0
C26-C25-C30	109.8(4)	C26-C25-P2	113.8(3)
C30-C25-P2	109.3(3)	C26-C25-H25	107.9
C30-C25-H25	107.9	P2-C25-H25	107.9
C27-C26-C25	112.4(4)	C27-C26-H26A	109.1
C25-C26-H26A	109.1	C27-C26-H26B	109.1
C25-C26-H26B	109.1	H26A-C26-H26B	107.8
C26-C27-C28	111.4(4)	C26-C27-H27A	109.3
C28-C27-H27A	109.3	C26-C27-H27B	109.3
C28-C27-H27B	109.3	H27A-C27-H27B	108.0
C29-C28-C27	109.9(4)	C29-C28-H28A	109.7
C27-C28-H28A	109.7	C29-C28-H28B	109.7
C27-C28-H28B	109.7	H28A-C28-H28B	108.2
C28-C29-C30	111.6(4)	C28-C29-H29A	109.3
C30-C29-H29A	109.3	C28-C29-H29B	109.3
C30-C29-H29B	109.3	H29A-C29-H29B	108.0
C29-C30-C25	112.2(4)	C29-C30-H30A	109.2
C25-C30-H30A	109.2	C29-C30-H30B	109.2
C25-C30-H30B	109.2	H30A-C30-H30B	107.9
C36-C31-C32	110.4(4)	C36-C31-P2	113.8(3)

C32-C31-P2	117.5(3)	C36-C31-H31	104.5
C32-C31-H31	104.5	P2-C31-H31	104.5
C33-C32-C31	111.2(4)	C33-C32-H32A	109.4
C31-C32-H32A	109.4	C33-C32-H32B	109.4
C31-C32-H32B	109.4	H32A-C32-H32B	108.0
C34-C33-C32	111.9(4)	C34-C33-H33A	109.2
C32-C33-H33A	109.2	C34-C33-H33B	109.2
C32-C33-H33B	109.2	H33A-C33-H33B	107.9
C33-C34-C35	111.7(4)	C33-C34-H34A	109.3
C35-C34-H34A	109.3	C33-C34-H34B	109.3
C35-C34-H34B	109.3	H34A-C34-H34B	107.9
C36-C35-C34	110.7(4)	C36-C35-H35A	109.5
C34-C35-H35A	109.5	C36-C35-H35B	109.5
C34-C35-H35B	109.5	H35A-C35-H35B	108.1
C35-C36-C31	111.6(4)	C35-C36-H36A	109.3
C31-C36-H36A	109.3	C35-C36-H36B	109.3
C31-C36-H36B	109.3	H36A-C36-H36B	108.0
C48-C37-C38	124.4(5)	C48-C37-Pd1	70.2(3)
C38-C37-Pd1	101.4(3)	C48-C37-H37	116.3
C38-C37-H37	116.3	Pd1-C37-H37	116.3
O39-C38-C37	121.7(5)	O39-C38-C40	119.5(5)
C37-C38-C40	118.6(5)	C41-C40-C38	123.8(5)
C41-C40-H40	118.1	C38-C40-H40	118.1
C40-C41-C42	127.1(5)	C40-C41-H41	116.5
C42-C41-H41	116.5	C43-C42-C47	116.6(6)
C43-C42-C41	120.7(5)	C47-C42-C41	122.7(5)
C44-C43-C42	123.0(6)	C44-C43-H43	118.5
C42-C43-H43	118.5	C43-C44-C45	119.1(7)
C43-C44-H44	120.5	C45-C44-H44	120.5
C46-C45-C44	118.4(6)	C46-C45-H45	120.8
C44-C45-H45	120.8	C47-C46-C45	122.2(6)
C47-C46-H46	118.9	C45-C46-H46	118.9
C46-C47-C42	120.6(6)	C46-C47-H47	119.7
C42-C47-H47	119.7	C37-C48-C49	122.0(5)
C37-C48-Pd1	71.4(3)	C49-C48-Pd1	110.7(3)
C37-C48-H48	115.0	C49-C48-H48	115.0
Pd1-C48-H48	115.0	C50-C49-C54	117.2(5)
C50-C49-C48	122.6(5)	C54-C49-C48	120.1(5)
C51-C50-C49	121.4(5)	C51-C50-H50	119.3
C49-C50-H50	119.3	C52-C51-C50	119.8(6)
C52-C51-H51	120.1	C50-C51-H51	120.1
C53-C52-C51	119.2(6)	C53-C52-H52	120.4
C51-C52-H52	120.4	C52-C53-C54	121.6(5)
C52-C53-H53	119.2	C54-C53-H53	119.2
C53-C54-C49	120.8(5)	C53-C54-H54	119.6
C49-C54-H54	119.6	C56-C55-H55A	109.5
C56-C55-H55B	109.5	H55A-C55-H55B	109.5
C56-C55-H55C	109.5	H55A-C55-H55C	109.5
H55B-C55-H55C	109.5	C55-C56-C57	121.8(9)
C55-C56-H56A	106.9	C57-C56-H56A	106.9
C55-C56-H56B	106.9	C57-C56-H56B	106.9
H56A-C56-H56B	106.7	C56-C57-C58	121.5(8)
C56-C57-H57A	107.0	C58-C57-H57A	107.0
C56-C57-H57B	106.9	C58-C57-H57B	106.9
H57A-C57-H57B	106.7	C59-C58-C57	119.5(7)
C59-C58-H58A	107.4	C57-C58-H58A	107.4

C59-C58-H58B	107.4	C57-C58-H58B	107.4
H58A-C58-H58B	107.0	C58-C59-C60	118.2(7)
C58-C59-H59A	107.8	C60-C59-H59A	107.8
C58-C59-H59B	107.8	C60-C59-H59B	107.8
H59A-C59-H59B	107.1	C59-C60-H60A	109.5
C59-C60-H60B	109.5	H60A-C60-H60B	109.5
C59-C60-H60C	109.5	H60A-C60-H60C	109.5
H60B-C60-H60C	109.5	C62-C61-C61#1	115.7(6)
C62-C61-H61A	108.4	C61#1-C61-H61A	108.4
C62-C61-H61B	108.4	C61#1-C61-H61B	108.4
H61A-C61-H61B	107.4	C61-C62-C63	114.3(5)
C61-C62-H62A	108.7	C63-C62-H62A	108.7
C61-C62-H62B	108.7	C63-C62-H62B	108.7
H62A-C62-H62B	107.6	C62-C63-H63A	109.5
C62-C63-H63B	109.5	H63A-C63-H63B	109.5
C62-C63-H63C	109.5	H63A-C63-H63C	109.5
H63B-C63-H63C	109.5		

Symmetry transformations used to generate equivalent atoms:

#1   -x, -y+1, -z+1

Table 7. Torsion angles (°) for sb021412.

C48-Pd1-P1-C1	136.0(2)	C37-Pd1-P1-C1	123.3(3)
P2-Pd1-P1-C1	-52.52(17)	C48-Pd1-P1-C13	-102.4(2)
C37-Pd1-P1-C13	-115.1(3)	P2-Pd1-P1-C13	69.06(18)
C48-Pd1-P1-C7	13.8(2)	C37-Pd1-P1-C7	1.2(3)
P2-Pd1-P1-C7	-174.69(18)	C48-Pd1-P2-C31	-63.0(3)
C37-Pd1-P2-C31	-45.8(2)	P1-Pd1-P2-C31	131.24(19)
C48-Pd1-P2-C25	51.4(3)	C37-Pd1-P2-C25	68.6(2)
P1-Pd1-P2-C25	-114.32(16)	C48-Pd1-P2-C19	167.5(3)
C37-Pd1-P2-C19	-175.3(2)	P1-Pd1-P2-C19	1.72(19)
C13-P1-C1-C2	59.2(4)	C7-P1-C1-C2	-48.2(4)
Pd1-P1-C1-C2	-173.1(3)	C13-P1-C1-C6	-171.0(3)
C7-P1-C1-C6	81.6(4)	Pd1-P1-C1-C6	-43.3(4)
C6-C1-C2-C3	55.5(5)	P1-C1-C2-C3	-173.7(3)
C1-C2-C3-C4	-56.4(6)	C2-C3-C4-C5	55.2(6)
C3-C4-C5-C6	-54.6(6)	C4-C5-C6-C1	55.3(6)
C2-C1-C6-C5	-55.5(5)	P1-C1-C6-C5	171.4(4)
C1-P1-C7-C12	-56.5(4)	C13-P1-C7-C12	-166.6(4)
Pd1-P1-C7-C12	68.5(4)	C1-P1-C7-C8	74.8(4)
C13-P1-C7-C8	-35.4(5)	Pd1-P1-C7-C8	-160.3(4)
C12-C7-C8-C9	-58.1(6)	P1-C7-C8-C9	169.2(4)
C7-C8-C9-C10	55.8(6)	C8-C9-C10-C11	-53.5(6)
C9-C10-C11-C12	53.8(6)	C10-C11-C12-C7	-57.3(6)
C8-C7-C12-C11	59.5(6)	P1-C7-C12-C11	-164.0(4)
C1-P1-C13-C14	61.1(4)	C7-P1-C13-C14	173.2(4)
Pd1-P1-C13-C14	-64.4(4)	C1-P1-C13-C18	-175.4(3)
C7-P1-C13-C18	-63.3(4)	Pd1-P1-C13-C18	59.1(4)
C18-C13-C14-C15	54.7(5)	P1-C13-C14-C15	177.8(4)
C13-C14-C15-C16	-55.7(6)	C14-C15-C16-C17	56.1(5)
C15-C16-C17-C18	-57.0(6)	C16-C17-C18-C13	57.5(6)
C14-C13-C18-C17	-55.8(5)	P1-C13-C18-C17	179.1(3)
C31-P2-C19-C24	-52.8(4)	C25-P2-C19-C24	-160.4(3)
Pd1-P2-C19-C24	79.6(3)	C31-P2-C19-C20	78.9(4)
C25-P2-C19-C20	-28.8(4)	Pd1-P2-C19-C20	-148.8(3)
C24-C19-C20-C21	-59.5(5)	P2-C19-C20-C21	167.0(4)

C19-C20-C21-C22	57.1(6)	C20-C21-C22-C23	-53.5(6)
C21-C22-C23-C24	51.9(6)	C20-C19-C24-C23	59.9(5)
P2-C19-C24-C23	-163.0(3)	C22-C23-C24-C19	-55.9(6)
C31-P2-C25-C26	52.7(4)	C19-P2-C25-C26	165.1(3)
Pd1-P2-C25-C26	-69.6(3)	C31-P2-C25-C30	175.8(3)
C19-P2-C25-C30	-71.8(4)	Pd1-P2-C25-C30	53.5(3)
C30-C25-C26-C27	53.6(5)	P2-C25-C26-C27	176.5(3)
C25-C26-C27-C28	-56.0(6)	C26-C27-C28-C29	56.3(6)
C27-C28-C29-C30	-56.5(5)	C28-C29-C30-C25	56.3(6)
C26-C25-C30-C29	-53.6(5)	P2-C25-C30-C29	-179.1(3)
C25-P2-C31-C36	-175.4(3)	C19-P2-C31-C36	77.0(4)
Pd1-P2-C31-C36	-56.8(4)	C25-P2-C31-C32	53.3(4)
C19-P2-C31-C32	-54.3(4)	Pd1-P2-C31-C32	171.9(3)
C36-C31-C32-C33	55.1(6)	P2-C31-C32-C33	-172.1(4)
C31-C32-C33-C34	-54.8(6)	C32-C33-C34-C35	54.6(6)
C33-C34-C35-C36	-55.1(6)	C34-C35-C36-C31	56.2(6)
C32-C31-C36-C35	-56.4(5)	P2-C31-C36-C35	168.9(3)
P1-Pd1-C37-C48	20.3(4)	P2-Pd1-C37-C48	-163.7(3)
C48-Pd1-C37-C38	-122.6(5)	P1-Pd1-C37-C38	-102.3(3)
P2-Pd1-C37-C38	73.7(3)	C48-C37-C38-O39	171.1(5)
Pd1-C37-C38-O39	-115.1(5)	C48-C37-C38-C40	-12.5(7)
Pd1-C37-C38-C40	61.2(5)	O39-C38-C40-C41	13.0(8)
C37-C38-C40-C41	-163.4(5)	C38-C40-C41-C42	174.8(5)
C40-C41-C42-C43	-157.6(5)	C40-C41-C42-C47	21.3(8)
C47-C42-C43-C44	-0.9(9)	C41-C42-C43-C44	178.0(6)
C42-C43-C44-C45	1.0(10)	C43-C44-C45-C46	0.1(10)
C44-C45-C46-C47	-1.1(10)	C45-C46-C47-C42	1.1(9)
C43-C42-C47-C46	-0.1(8)	C41-C42-C47-C46	-179.0(5)
C38-C37-C48-C49	-166.2(5)	Pd1-C37-C48-C49	103.3(4)
C38-C37-C48-Pd1	90.5(5)	P1-Pd1-C48-C37	-166.1(3)
P2-Pd1-C48-C37	27.0(4)	C37-Pd1-C48-C49	-118.1(5)
P1-Pd1-C48-C49	75.8(4)	P2-Pd1-C48-C49	-91.1(4)
C37-C48-C49-C50	-24.8(7)	Pd1-C48-C49-C50	55.7(6)
C37-C48-C49-C54	157.2(5)	Pd1-C48-C49-C54	-122.3(4)
C54-C49-C50-C51	1.8(8)	C48-C49-C50-C51	-176.3(5)
C49-C50-C51-C52	0.2(9)	C50-C51-C52-C53	-2.0(9)
C51-C52-C53-C54	1.7(9)	C52-C53-C54-C49	0.3(9)
C50-C49-C54-C53	-2.1(8)	C48-C49-C54-C53	176.0(5)
C55-C56-C57-C58	48.4(17)	C56-C57-C58-C59	-176.7(10)
C57-C58-C59-C60	179.6(8)	C61#1-C61-C62-C63	-178.0(7)

Symmetry transformations used to generate equivalent atoms:

#1   -x, -y+1, -z+1

Table 8. Anisotropic atomic displacement parameters (Å^2) for sb021412.
The anisotropic atomic displacement factor exponent takes the form: $-2\pi^2[\,h^2\,a^{*2}\,U_{11} + ... + 2\,h\,k\,a^*\,b^*\,U_{12}\,]$

	U_{11}	U_{22}	U_{33}	U_{23}	U_{13}	U_{12}
Pd1	0.0131(2)	0.0242(3)	0.00872(18)	-0.00347(17)	-0.00016(15)	-0.00297(17)
P1	0.0141(7)	0.0224(8)	0.0113(6)	-0.0024(6)	-0.0010(5)	-0.0046(6)
P2	0.0156(7)	0.0203(8)	0.0117(6)	-0.0018(6)	-0.0025(5)	-0.0051(6)

	U₁₁	U₂₂	U₃₃	U₂₃	U₁₃	U₁₂
O39	0.015(2)	0.049(3)	0.025(2)	-0.013(2)	0.0002(16)	-0.0060(19)
C1	0.018(3)	0.018(3)	0.015(2)	-0.006(2)	-0.002(2)	0.000(2)
C2	0.019(3)	0.021(3)	0.023(3)	-0.004(2)	-0.004(2)	-0.002(2)
C3	0.023(3)	0.022(4)	0.033(3)	-0.005(3)	0.000(3)	0.001(2)
C4	0.036(3)	0.020(3)	0.027(3)	-0.004(3)	0.002(3)	-0.004(3)
C5	0.029(3)	0.026(4)	0.036(3)	-0.016(3)	-0.002(3)	-0.005(3)
C6	0.023(3)	0.030(4)	0.021(3)	-0.009(3)	-0.005(2)	-0.007(3)
C7	0.018(3)	0.028(3)	0.008(2)	-0.001(2)	0.003(2)	-0.006(2)
C8	0.015(3)	0.028(3)	0.014(2)	-0.004(2)	0.005(2)	-0.006(2)
C9	0.024(3)	0.039(4)	0.015(3)	-0.007(3)	0.004(2)	-0.007(3)
C10	0.033(3)	0.038(4)	0.017(3)	-0.005(3)	0.002(2)	-0.007(3)
C11	0.031(3)	0.044(4)	0.019(3)	-0.012(3)	-0.004(2)	-0.005(3)
C12	0.019(3)	0.033(4)	0.017(3)	0.000(3)	0.001(2)	-0.005(3)
C13	0.013(3)	0.024(3)	0.013(2)	-0.005(2)	-0.003(2)	-0.002(2)
C14	0.015(3)	0.026(3)	0.014(2)	-0.007(2)	-0.003(2)	0.000(2)
C15	0.024(3)	0.028(4)	0.015(3)	-0.004(2)	-0.006(2)	-0.001(2)
C16	0.031(3)	0.022(3)	0.025(3)	-0.012(3)	-0.010(2)	-0.002(3)
C17	0.028(3)	0.024(3)	0.023(3)	0.004(3)	-0.008(2)	-0.009(3)
C18	0.018(3)	0.026(3)	0.014(3)	0.001(2)	-0.006(2)	-0.004(2)
C19	0.013(3)	0.028(3)	0.014(3)	-0.001(2)	0.000(2)	-0.006(2)
C20	0.036(3)	0.030(4)	0.023(3)	-0.008(3)	-0.014(3)	-0.004(3)
C21	0.040(4)	0.041(4)	0.023(3)	-0.003(3)	-0.015(3)	-0.005(3)
C22	0.032(3)	0.039(4)	0.027(3)	0.007(3)	-0.016(3)	-0.008(3)
C23	0.025(3)	0.029(4)	0.024(3)	-0.001(3)	-0.008(2)	0.002(3)
C24	0.019(3)	0.023(3)	0.017(3)	-0.002(2)	-0.001(2)	-0.001(2)
C25	0.017(3)	0.024(3)	0.015(2)	-0.008(2)	0.000(2)	-0.008(2)
C26	0.022(3)	0.025(3)	0.016(3)	-0.008(2)	0.001(2)	-0.008(2)
C27	0.020(3)	0.027(4)	0.025(3)	-0.013(3)	0.001(2)	0.000(2)
C28	0.027(3)	0.020(3)	0.027(3)	-0.010(3)	-0.002(2)	-0.008(2)
C29	0.023(3)	0.028(4)	0.026(3)	-0.009(3)	-0.004(2)	-0.010(3)
C30	0.016(3)	0.031(4)	0.019(3)	-0.007(3)	-0.005(2)	-0.007(2)
C31	0.013(3)	0.021(3)	0.012(2)	-0.003(2)	-0.002(2)	-0.003(2)
C32	0.015(3)	0.032(4)	0.017(3)	-0.005(2)	0.002(2)	-0.007(2)
C33	0.015(3)	0.032(4)	0.020(3)	-0.007(3)	0.005(2)	-0.006(2)
C34	0.018(3)	0.025(3)	0.023(3)	-0.001(3)	-0.004(2)	-0.008(2)
C35	0.024(3)	0.023(3)	0.020(3)	-0.005(2)	-0.006(2)	-0.007(2)
C36	0.018(3)	0.025(3)	0.015(3)	-0.004(2)	-0.002(2)	-0.002(2)
C37	0.016(3)	0.031(3)	0.007(2)	-0.001(2)	-0.004(2)	-0.003(2)
C38	0.020(3)	0.036(4)	0.016(3)	-0.005(3)	-0.013(2)	0.004(3)
C40	0.018(3)	0.040(4)	0.009(2)	-0.008(3)	0.001(2)	-0.006(3)
C41	0.018(3)	0.039(4)	0.016(3)	-0.009(3)	-0.004(2)	-0.002(3)
C42	0.026(3)	0.037(4)	0.020(3)	-0.009(3)	-0.005(2)	0.000(3)
C43	0.054(4)	0.045(5)	0.031(4)	-0.009(3)	-0.004(3)	0.002(4)
C44	0.079(5)	0.036(5)	0.034(4)	-0.004(3)	0.005(4)	0.005(4)
C45	0.068(5)	0.043(5)	0.052(5)	-0.021(4)	-0.006(4)	0.021(4)
C46	0.036(4)	0.049(5)	0.040(4)	-0.021(4)	0.001(3)	0.008(3)
C47	0.030(3)	0.042(4)	0.027(3)	-0.013(3)	-0.006(3)	-0.003(3)
C48	0.018(3)	0.032(4)	0.014(3)	-0.001(2)	-0.008(2)	0.001(2)
C49	0.027(3)	0.024(3)	0.013(3)	0.000(2)	-0.005(2)	0.000(2)
C50	0.033(3)	0.028(4)	0.025(3)	-0.005(3)	-0.008(3)	0.000(3)
C51	0.037(4)	0.035(4)	0.033(3)	-0.006(3)	-0.016(3)	0.000(3)
C52	0.042(4)	0.037(4)	0.034(4)	0.008(3)	-0.015(3)	-0.015(3)
C53	0.029(3)	0.049(4)	0.023(3)	0.001(3)	-0.012(3)	-0.011(3)
C54	0.023(3)	0.038(4)	0.019(3)	-0.002(3)	-0.010(2)	0.002(3)
C55	0.115(8)	0.078(8)	0.065(6)	-0.008(5)	-0.012(5)	0.002(6)

	U_{11}	U_{22}	U_{33}	U_{23}	U_{13}	U_{12}
C56	0.067(7)	0.257(16)	0.060(6)	0.009(8)	0.012(5)	-0.009(8)
C57	0.073(6)	0.089(7)	0.064(6)	-0.022(5)	-0.009(5)	-0.019(5)
C58	0.057(5)	0.082(7)	0.051(5)	-0.028(4)	-0.005(4)	-0.008(4)
C59	0.084(7)	0.135(10)	0.087(7)	-0.068(7)	0.007(5)	-0.045(6)
C60	0.072(6)	0.124(9)	0.069(6)	-0.058(6)	-0.028(5)	0.029(5)
C61	0.028(4)	0.045(5)	0.041(4)	-0.011(3)	-0.001(3)	0.000(3)
C62	0.037(4)	0.052(5)	0.047(4)	-0.024(4)	-0.001(3)	-0.001(3)
C63	0.045(4)	0.062(6)	0.072(5)	-0.032(4)	-0.014(4)	0.000(4)

Table 9. Hydrogen atomic coordinates and isotropic atomic displacement parameters (Å^2) for sb021412.

	x/a	y/b	z/c	U(eq)
H1	0.2535	0.3154	0.1688	0.021
H2A	0.0720	0.3318	0.3213	0.026
H2B	0.0294	0.2979	0.2497	0.026
H3A	0.0760	0.4399	0.1483	0.034
H3B	-0.0393	0.4569	0.2324	0.034
H4A	0.1347	0.4952	0.2779	0.036
H4B	0.1351	0.5611	0.1787	0.036
H5A	0.3246	0.4674	0.1284	0.035
H5B	0.3652	0.5009	0.2008	0.035
H6A	0.3202	0.3589	0.3011	0.029
H6B	0.4347	0.3421	0.2165	0.029
H7	0.2717	0.0911	0.4090	0.024
H8A	0.0175	0.2120	0.4060	0.024
H8B	0.0400	0.1061	0.3949	0.024
H9A	-0.0577	0.1027	0.5360	0.033
H9B	0.0971	0.0383	0.5262	0.033
H10A	0.0913	0.1226	0.6140	0.037
H10B	0.0439	0.2216	0.5441	0.037
H11A	0.2810	0.2143	0.5387	0.037
H11B	0.3096	0.1084	0.5273	0.037
H12A	0.3761	0.2205	0.3982	0.031
H12B	0.2163	0.2786	0.4097	0.031
H13	0.0783	0.1488	0.2704	0.021
H14A	0.1769	0.2202	0.1317	0.022
H14B	0.3070	0.1343	0.1330	0.022
H15A	0.1404	0.1134	0.0715	0.028
H15B	0.0129	0.1197	0.1548	0.028
H16A	0.2462	-0.0226	0.1517	0.029
H16B	0.0777	-0.0346	0.1607	0.029
H17A	0.0150	-0.0036	0.2890	0.032
H17B	0.1419	-0.0919	0.2926	0.032
H18A	0.3112	0.0076	0.2664	0.025
H18B	0.1863	0.0146	0.3506	0.025
H19	0.4059	0.2339	0.0644	0.024
H20A	0.6133	0.2895	-0.0869	0.034
H20B	0.5495	0.1857	-0.0478	0.034
H21A	0.4237	0.2926	-0.1452	0.042
H21B	0.3209	0.2567	-0.0497	0.042
H22A	0.2714	0.4132	-0.1058	0.042
H22B	0.4408	0.4306	-0.1280	0.042
H23A	0.2600	0.3695	0.0351	0.034
H23B	0.3320	0.4701	-0.0099	0.034
H24A	0.5562	0.3932	-0.0057	0.026
H24B	0.4529	0.3633	0.0904	0.026

	x/a	y/b	z/c	U(eq)
H25	0.7064	0.1228	0.0036	0.022
H26A	0.8824	0.0889	0.0768	0.025
H26B	0.7781	0.0282	0.1637	0.025
H27A	0.9296	-0.0722	0.0995	0.029
H27B	0.8791	-0.0165	0.0089	0.029
H28A	0.7655	-0.1514	0.0778	0.029
H28B	0.7048	-0.1192	0.1644	0.029
H29A	0.5316	-0.0854	0.0883	0.03
H29B	0.6383	-0.0246	0.0025	0.03
H30A	0.5314	0.0196	0.1573	0.026
H30B	0.4834	0.0755	0.0661	0.026
H31	0.8333	0.2089	0.1097	0.019
H32A	0.8626	0.2172	-0.0293	0.026
H32B	0.7816	0.3252	-0.0499	0.026
H33A	1.0396	0.2615	0.0098	0.029
H33B	1.0228	0.3319	-0.0855	0.029
H34A	0.8990	0.4461	-0.0310	0.028
H34B	1.0499	0.4117	0.0018	0.028
H35A	0.9345	0.3216	0.1324	0.026
H35B	0.8559	0.4303	0.1113	0.026
H36A	0.6802	0.3877	0.0697	0.024
H36B	0.6925	0.3188	0.1662	0.024
H37	0.7443	0.0363	0.2837	0.023
H40	0.5729	0.2154	0.3742	0.027
H41	0.7939	0.3270	0.2723	0.029
H43	0.7233	0.4847	0.2429	0.055
H44	0.5929	0.6092	0.2819	0.068
H45	0.4127	0.5813	0.4061	0.069
H46	0.3728	0.4290	0.4852	0.052
H47	0.4980	0.3053	0.4442	0.039
H48	0.5239	0.0949	0.4027	0.027
H50	0.6294	-0.0510	0.2697	0.036
H51	0.5401	-0.1920	0.3005	0.042
H52	0.3647	-0.2429	0.4221	0.048
H53	0.2923	-0.1567	0.5139	0.041
H54	0.3806	-0.0173	0.4854	0.034
H55A	0.3050	0.3105	0.6079	0.139
H55B	0.2133	0.3995	0.6410	0.139
H55C	0.1319	0.3355	0.6084	0.139
H56A	0.2372	0.2917	0.7516	0.179
H56B	0.2173	0.2096	0.7148	0.179
H57A	0.0206	0.3298	0.7817	0.091
H57B	0.0504	0.2149	0.8166	0.091
H58A	-0.0601	0.3165	0.6752	0.075
H58B	-0.0367	0.2016	0.7153	0.075
H59A	-0.2190	0.3234	0.7937	0.113
H59B	-0.1959	0.2083	0.8333	0.113
H60A	-0.3057	0.3078	0.6871	0.125
H60B	-0.3999	0.2587	0.7843	0.125
H60C	-0.2881	0.1913	0.7316	0.125
H61A	0.1476	0.4795	0.4955	0.049
H61B	0.0705	0.5700	0.4309	0.049
H62A	0.0387	0.5346	0.6069	0.054
H62B	-0.0439	0.6237	0.5441	0.054
H63A	0.1629	0.6860	0.4704	0.085

	x/a	y/b	z/c	U(eq)
H63B	0.2578	0.5903	0.5197	0.085
H63C	0.1575	0.6605	0.5736	0.085

Bromo-(tri-cyclohexylphosphine)dipalladium(II), [PdBr$_2$(PCy$_3$)]$_2$ **272**
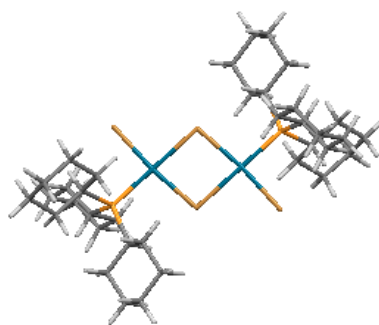
A clear orange needle-like specimen of C$_{38}$H$_{70}$Br$_2$Cl$_4$P$_2$Pd$_2$, approximate dimensions 0.010 mm x 0.020 mm x 0.080 mm, was used for the X-ray crystallographic analysis. The X-ray intensity data were measured on a Bruker Kappa Apex-II Duo system equipped with a graphite monochromator.

Table 1: Data collection details for sb171012.

Axis	dx/mm	2θ/°	ω/°	φ/°	χ/°	Width/°	Frames	Time/s	Wavelength/Å	Voltage/kV	Current/mA	Temperature/K
Phi	36.908	-17.00	-37.66	-334.67	21.36	0.50	704	60.00	0.71073	50	30.0	100.01
Omega	36.908	8.00	-235.99	-187.45	-99.15	0.50	90	60.00	0.71073	50	30.0	100.01

A total of 794 frames were collected. The total exposure time was 13.23 hours. The frames were integrated with the Bruker SAINT software package using a narrow frame algorithm. The integration of the data using a monoclinic unit cell yielded a total of 20522 reflections to a maximum θ angle of 27.57° (0.77 Å resolution), of which 5394 were independent (average redundancy 3.805, completeness = 99.7%, R_{int} = 10.30%, R_{sig} = 12.64%) and 3242 (60.10%) were greater than $2\sigma(F^2)$. The final cell constants of $\underline{a}$ = 12.318(2) Å, $\underline{b}$ = 8.7051(11) Å, $\underline{c}$ = 22.366(3) Å, β = 102.867(7)°, volume = 2338.1(6) Å^3, are based upon the refinement of the XYZ-centroids of 1913 reflections above 20 σ(I) with 5.038° < 2θ < 44.42°. Data were corrected for absorption effects using the multi-scan method (SADABS). The ratio of minimum to maximum apparent transmission was 0.893. The calculated minimum and maximum transmission coefficients (based on crystal size) are 0.9092 and 0.9880.

The structure was solved and refined using the [OLEX2](#) and Bruker SHELXTL Software Package, using the space group P 1 21/c 1, with Z = 1 for the formula unit, C$_{38}$H$_{70}$Br$_2$Cl$_4$P$_2$Pd. The final anisotropic full-matrix least-squares refinement on F^2 with 226 variables converged at R1 = 5.34%, for the observed data and wR2 = 6.31% for all data. The goodness-of-fit was 1.057. The largest peak in the final difference electron density synthesis was 0.818 e$^-$/Å^3 and the largest hole was -0.797 e$^-$/Å^3 with an RMS deviation of 0.183 e$^-$/Å^3. On the basis of the final model, the calculated density was 0.708 g/cm^3 and F(000), 512 e$^-$.

Table 2. Sample and crystal data for sb171012.

Identification code	sb171012
Chemical formula	C$_{38}$H$_{70}$Br$_4$Cl$_4$P$_2$Pd$_2$
Formula weight	1263.18

Temperature	100(2) K	
Wavelength	0.71073 Å	
Crystal size	0.010 x 0.020 x 0.080 mm	
Crystal habit	clear orange needle	
Crystal system	monoclinic	
Space group	P 1 21/c 1	
Unit cell dimensions	a = 12.318(2) Å	α = 90°
	b = 8.7051(11) Å	β = 102.867(7)°
	c = 22.366(3) Å	γ = 90°
Volume	2338.1(6) Å^3	
Z	2	
Density (calculated)	1.798 g/cm^3	
Absorption coefficient	4.51 mm^{-1}	
F(000)	1256	

Table 3. Data collection and structure refinement for sb171012.

Diffractometer	Bruker Nonius APEX-II
Theta range for data collection	2.23 to 27.57°
Index ranges	-16<=h<=16, -11<=k<=9, -26<=l<=29
Reflections collected	20522
Independent reflections	5394 [R(int) = 0.1030]
Coverage of independent reflections	99.7%
Absorption correction	multi-scan
Max. and min. transmission	0.9880 and 0.9092
Structure solution technique	direct methods
Structure solution program	SHELXS-97 (Sheldrick, 2008)
Refinement method	Full-matrix least-squares on F^2
Refinement program	SHELXL-97 (Sheldrick, 2008)
Function minimized	$\Sigma\ w(F_o^2 - F_c^2)^2$
Data / restraints / parameters	5394 / 0 / 226
Goodness-of-fit on F^2	1.057
Δ/σ_{max}	0.001
Final R indices	3242 data; I>2σ(I) R1 = 0.0534, wR2 = 0.0545
	all data R1 = 0.1177, wR2 = 0.0631
Weighting scheme	w=1/[σ^2(F$_o^2$)+(0.0003P)^2+0.0000P] where P=(F$_o^2$+2F$_c^2$)/3
Largest diff. peak and hole	0.818 and -0.797 eÅ^{-3}
R.M.S. deviation from mean	0.183 eÅ^{-3}

Table 4. Atomic coordinates and equivalent isotropic atomic displacement parameters (Å^2) for sb171012.

U(eq) is defined as one third of the trace of the orthogonalized U$_{ij}$ tensor.

	x/a	y/b	z/c	U(eq)
Pd1	0.13586(4)	0.45916(5)	0.48288(2)	0.01459(11)
Br1	0.96165(5)	0.32032(6)	0.47673(3)	0.01959(15)
Br2	0.30284(5)	0.61433(6)	0.50314(3)	0.02141(16)
P1	0.22007(12)	0.26905(15)	0.44194(6)	0.0143(4)
C1	0.1185(4)	0.1296(5)	0.4004(2)	0.0122(12)
C2	0.1631(4)	0.9713(5)	0.3864(2)	0.0178(13)
C3	0.0657(5)	0.8661(6)	0.3588(2)	0.0220(15)
C4	0.9929(5)	0.9354(6)	0.3011(2)	0.0243(15)
C5	0.9499(4)	0.0936(6)	0.3145(2)	0.0223(15)
C6	0.0465(4)	0.1994(6)	0.3416(2)	0.0167(13)
C7	0.3035(4)	0.3503(5)	0.3910(2)	0.0141(13)
C8	0.3543(5)	0.2324(6)	0.3549(3)	0.0244(15)

	x/a	y/b	z/c	U(eq)
C9	0.4365(5)	0.3099(6)	0.3230(3)	0.0293(16)
C10	0.3787(5)	0.4393(6)	0.2815(3)	0.0318(16)
C11	0.3270(5)	0.5526(6)	0.3174(3)	0.0259(15)
C12	0.2459(4)	0.4767(6)	0.3495(2)	0.0204(14)
C13	0.3131(4)	0.1557(5)	0.5013(2)	0.0138(13)
C14	0.2529(4)	0.1102(6)	0.5511(2)	0.0175(13)
C15	0.3264(5)	0.0126(6)	0.6012(2)	0.0220(15)
C16	0.4360(5)	0.0914(6)	0.6275(2)	0.0215(15)
C17	0.4950(5)	0.1289(6)	0.5768(2)	0.0214(14)
C18	0.4241(4)	0.2329(6)	0.5289(2)	0.0182(14)
Cl1	0.85834(15)	0.59831(18)	0.34024(8)	0.0446(5)
Cl2	0.67994(15)	0.41998(19)	0.26740(7)	0.0487(5)
C19	0.7600(5)	0.4549(7)	0.3395(3)	0.0456(19)

Table 5. Bond lengths (Å) for sb171012.

Pd1-P1	2.2530(15)	Pd1-Br2	2.4177(8)
Pd1-Br1	2.4399(8)	Pd1-Br1#1	2.5352(7)
Br1-Pd1#1	2.5352(7)	P1-C13	1.836(5)
P1-C7	1.838(5)	P1-C1	1.839(5)
C1-C6	1.538(6)	C1-C2	1.541(6)
C1-H1	1.09	C2-C3	1.526(6)
C2-H2A	1.09	C2-H2B	1.09
C3-C4	1.523(6)	C3-H3A	1.09
C3-H3B	1.09	C4-C5	1.529(7)
C4-H4A	1.09	C4-H4B	1.09
C5-C6	1.520(6)	C5-H5A	1.09
C5-H5B	1.09	C6-H6A	1.09
C6-H6B	1.09	C7-C12	1.511(6)
C7-C8	1.523(6)	C7-H7	1.09
C8-C9	1.520(7)	C8-H8A	1.09
C8-H8B	1.09	C9-C10	1.530(7)
C9-H9A	1.09	C9-H9B	1.09
C10-C11	1.499(7)	C10-H10A	1.09
C10-H10B	1.09	C11-C12	1.507(7)
C11-H11A	1.09	C11-H11B	1.09
C12-H12A	1.09	C12-H12B	1.09
C13-C14	1.521(7)	C13-C18	1.524(7)
C13-H13	1.09	C14-C15	1.531(6)
C14-H14A	1.09	C14-H14B	1.09
C15-C16	1.512(7)	C15-H15A	1.09
C15-H15B	1.09	C16-C17	1.511(7)
C16-H16A	1.09	C16-H16B	1.09
C17-C18	1.522(6)	C17-H17A	1.09
C17-H17B	1.09	C18-H18A	1.09
C18-H18B	1.09	Cl1-C19	1.737(6)
Cl2-C19	1.720(6)	C19-H19A	1.09
C19-H19B	1.09		

Symmetry transformations used to generate equivalent atoms:

#1   -x, -y+1, -z+1

Table 6. Bond angles (°) for sb171012.

P1-Pd1-Br2	92.13(4)	P1-Pd1-Br1	95.28(4)
Br2-Pd1-Br1	171.17(3)	P1-Pd1-Br1#1	176.91(5)
Br2-Pd1-Br1#1	87.76(2)	Br1-Pd1-Br1#1	85.10(2)
Pd1-Br1-Pd1#1	94.90(2)	C13-P1-C7	108.0(2)

C13-P1-C1	104.8(2)	C7-P1-C1	110.7(2)
C13-P1-Pd1	111.75(17)	C7-P1-Pd1	109.93(16)
C1-P1-Pd1	111.52(17)	C6-C1-C2	110.1(4)
C6-C1-P1	111.6(3)	C2-C1-P1	117.4(3)
C6-C1-H1	105.6	C2-C1-H1	105.6
P1-C1-H1	105.6	C3-C2-C1	109.6(4)
C3-C2-H2A	109.7	C1-C2-H2A	109.7
C3-C2-H2B	109.7	C1-C2-H2B	109.7
H2A-C2-H2B	108.2	C4-C3-C2	111.5(4)
C4-C3-H3A	109.3	C2-C3-H3A	109.3
C4-C3-H3B	109.3	C2-C3-H3B	109.3
H3A-C3-H3B	108.0	C3-C4-C5	110.8(4)
C3-C4-H4A	109.5	C5-C4-H4A	109.5
C3-C4-H4B	109.5	C5-C4-H4B	109.5
H4A-C4-H4B	108.1	C6-C5-C4	110.5(4)
C6-C5-H5A	109.5	C4-C5-H5A	109.5
C6-C5-H5B	109.5	C4-C5-H5B	109.5
H5A-C5-H5B	108.1	C5-C6-C1	110.7(4)
C5-C6-H6A	109.5	C1-C6-H6A	109.5
C5-C6-H6B	109.5	C1-C6-H6B	109.5
H6A-C6-H6B	108.1	C12-C7-C8	111.0(4)
C12-C7-P1	114.2(4)	C8-C7-P1	114.9(3)
C12-C7-H7	105.2	C8-C7-H7	105.2
P1-C7-H7	105.2	C9-C8-C7	110.1(4)
C9-C8-H8A	109.6	C7-C8-H8A	109.6
C9-C8-H8B	109.6	C7-C8-H8B	109.6
H8A-C8-H8B	108.1	C8-C9-C10	110.1(5)
C8-C9-H9A	109.6	C10-C9-H9A	109.6
C8-C9-H9B	109.6	C10-C9-H9B	109.6
H9A-C9-H9B	108.2	C11-C10-C9	110.8(5)
C11-C10-H10A	109.5	C9-C10-H10A	109.5
C11-C10-H10B	109.5	C9-C10-H10B	109.5
H10A-C10-H10B	108.1	C10-C11-C12	111.8(5)
C10-C11-H11A	109.3	C12-C11-H11A	109.3
C10-C11-H11B	109.3	C12-C11-H11B	109.3
H11A-C11-H11B	107.9	C11-C12-C7	110.0(5)
C11-C12-H12A	109.7	C7-C12-H12A	109.7
C11-C12-H12B	109.7	C7-C12-H12B	109.7
H12A-C12-H12B	108.2	C14-C13-C18	110.9(4)
C14-C13-P1	110.0(4)	C18-C13-P1	114.5(3)
C14-C13-H13	107.0	C18-C13-H13	107.0
P1-C13-H13	107.0	C13-C14-C15	112.1(4)
C13-C14-H14A	109.2	C15-C14-H14A	109.2
C13-C14-H14B	109.2	C15-C14-H14B	109.2
H14A-C14-H14B	107.9	C16-C15-C14	111.3(4)
C16-C15-H15A	109.4	C14-C15-H15A	109.4
C16-C15-H15B	109.4	C14-C15-H15B	109.4
H15A-C15-H15B	108.0	C17-C16-C15	110.1(5)
C17-C16-H16A	109.6	C15-C16-H16A	109.6
C17-C16-H16B	109.6	C15-C16-H16B	109.6
H16A-C16-H16B	108.2	C16-C17-C18	111.2(5)
C16-C17-H17A	109.4	C18-C17-H17A	109.4
C16-C17-H17B	109.4	C18-C17-H17B	109.4
H17A-C17-H17B	108.0	C17-C18-C13	110.2(4)
C17-C18-H18A	109.6	C13-C18-H18A	109.6
C17-C18-H18B	109.6	C13-C18-H18B	109.6

H18A-C18-H18B	108.1	Cl2-C19-Cl1	112.8(3)
Cl2-C19-H19A	109.0	Cl1-C19-H19A	109.0
Cl2-C19-H19B	109.0	Cl1-C19-H19B	109.0
H19A-C19-H19B	107.8		

Symmetry transformations used to generate equivalent atoms:

#1   -x, -y+1, -z+1

Table 7. Torsion angles (°) for sb171012.

P1-Pd1-Br1-Pd1#1	-176.92(4)	Br2-Pd1-Br1-Pd1#1	36.21(18)
Br1#1-Pd1-Br1-Pd1#1	0	Br2-Pd1-P1-C13	76.47(18)
Br1-Pd1-P1-C13	-98.72(18)	Br1#1-Pd1-P1-C13	164.4(8)
Br2-Pd1-P1-C7	-43.50(18)	Br1-Pd1-P1-C7	141.32(18)
Br1#1-Pd1-P1-C7	44.4(9)	Br2-Pd1-P1-C1	-166.61(18)
Br1-Pd1-P1-C1	18.20(18)	Br1#1-Pd1-P1-C1	-78.7(9)
C13-P1-C1-C6	-169.8(4)	C7-P1-C1-C6	-53.6(4)
Pd1-P1-C1-C6	69.1(4)	C13-P1-C1-C2	-41.4(4)
C7-P1-C1-C2	74.8(4)	Pd1-P1-C1-C2	-162.5(3)
C6-C1-C2-C3	-57.4(6)	P1-C1-C2-C3	173.4(4)
C1-C2-C3-C4	57.2(6)	C2-C3-C4-C5	-56.8(6)
C3-C4-C5-C6	56.5(6)	C4-C5-C6-C1	-57.5(6)
C2-C1-C6-C5	58.3(6)	P1-C1-C6-C5	-169.6(4)
C13-P1-C7-C12	-165.8(4)	C1-P1-C7-C12	80.0(4)
Pd1-P1-C7-C12	-43.6(4)	C13-P1-C7-C8	64.3(4)
C1-P1-C7-C8	-49.9(4)	Pd1-P1-C7-C8	-173.5(3)
C12-C7-C8-C9	58.1(6)	P1-C7-C8-C9	-170.5(4)
C7-C8-C9-C10	-56.7(6)	C8-C9-C10-C11	56.2(6)
C9-C10-C11-C12	-56.7(7)	C10-C11-C12-C7	57.0(6)
C8-C7-C12-C11	-57.4(6)	P1-C7-C12-C11	170.8(4)
C7-P1-C13-C14	169.7(3)	C1-P1-C13-C14	-72.2(4)
Pd1-P1-C13-C14	48.7(4)	C7-P1-C13-C18	44.0(4)
C1-P1-C13-C18	162.0(4)	Pd1-P1-C13-C18	-77.0(4)
C18-C13-C14-C15	-53.4(6)	P1-C13-C14-C15	178.9(3)
C13-C14-C15-C16	53.9(6)	C14-C15-C16-C17	-56.0(6)
C15-C16-C17-C18	59.0(6)	C16-C17-C18-C13	-58.8(6)
C14-C13-C18-C17	55.4(6)	P1-C13-C18-C17	-179.4(3)

Symmetry transformations used to generate equivalent atoms:

   #1   -x, -y+1, -z+1

Table 8. Anisotropic atomic displacement parameters (Å^2) for sb171012.
The anisotropic atomic displacement factor exponent takes the form: $-2\pi^2[h^2 a^{*2} U_{11} + ... + 2 h k a^* b^* U_{12}]$

	U_{11}	U_{22}	U_{33}	U_{23}	U_{13}	U_{12}
Pd1	0.0127(2)	0.0166(2)	0.0146(2)	-0.0030(2)	0.00332(19)	0.0009(2)
Br1	0.0157(3)	0.0187(3)	0.0258(4)	-0.0076(3)	0.0074(3)	-0.0007(3)
Br2	0.0174(4)	0.0213(3)	0.0265(4)	-0.0068(3)	0.0069(3)	-0.0033(3)
P1	0.0141(9)	0.0161(8)	0.0120(9)	-0.0009(7)	0.0018(7)	0.0029(6)
C1	0.011(3)	0.015(3)	0.011(3)	0.000(2)	0.003(2)	0.002(2)
C2	0.017(3)	0.016(3)	0.019(3)	-0.002(3)	0.002(3)	0.003(3)
C3	0.030(4)	0.013(3)	0.022(4)	-0.006(3)	0.003(3)	-0.002(3)
C4	0.031(4)	0.028(4)	0.013(3)	0.002(3)	0.002(3)	-0.007(3)
C5	0.023(4)	0.026(3)	0.014(3)	0.000(3)	-0.006(3)	-0.002(3)

	U₁₁	U₂₂	U₃₃	U₂₃	U₁₃	U₁₂
C6	0.021(4)	0.017(3)	0.011(3)	-0.001(3)	0.000(3)	0.001(3)
C7	0.019(3)	0.017(3)	0.009(3)	0.005(2)	0.009(3)	0.000(2)
C8	0.032(4)	0.022(3)	0.022(4)	0.000(3)	0.014(3)	0.006(3)
C9	0.036(4)	0.031(4)	0.028(4)	-0.001(3)	0.025(3)	0.006(3)
C10	0.045(5)	0.032(4)	0.022(4)	0.012(3)	0.018(3)	-0.003(3)
C11	0.030(4)	0.025(4)	0.023(4)	0.006(3)	0.007(3)	0.005(3)
C12	0.023(4)	0.022(3)	0.016(3)	0.004(3)	0.006(3)	0.000(3)
C13	0.017(3)	0.012(3)	0.012(3)	-0.002(2)	0.004(3)	0.003(2)
C14	0.012(3)	0.024(3)	0.016(3)	0.000(3)	0.003(3)	0.003(3)
C15	0.026(4)	0.027(4)	0.016(3)	0.008(3)	0.009(3)	0.003(3)
C16	0.030(4)	0.022(3)	0.010(3)	0.000(3)	-0.001(3)	0.004(3)
C17	0.025(4)	0.023(3)	0.017(3)	0.001(3)	0.004(3)	0.000(3)
C18	0.017(4)	0.022(3)	0.016(3)	0.008(3)	0.006(3)	0.002(3)
Cl1	0.0532(13)	0.0405(10)	0.0435(11)	-0.0099(9)	0.0178(10)	-0.0183(9)
Cl2	0.0485(13)	0.0652(13)	0.0289(10)	-0.0026(9)	0.0013(9)	-0.0182(10)
C19	0.046(5)	0.057(5)	0.030(4)	0.007(4)	0.001(4)	-0.024(4)

Table 9. Hydrogen atomic coordinates and isotropic atomic displacement parameters (Å^2) for sb171012.

	x/a	y/b	z/c	U(eq)
H1	0.0615	0.1068	0.4303	0.015
H2A	0.2173	-0.0155	0.3544	0.021
H2B	0.2116	-0.0793	0.4285	0.021
H3A	0.0978	-0.2445	0.3476	0.026
H3B	0.0155	-0.1538	0.3925	0.026
H4A	-0.0774	-0.1405	0.2837	0.029
H4B	0.0410	-0.0541	0.2658	0.029
H5A	-0.0986	0.1433	0.2722	0.027
H5B	-0.1044	0.0818	0.3466	0.027
H6A	0.0143	0.3104	0.3521	0.02
H6B	0.0974	0.2178	0.3082	0.02
H7	0.3742	0.4056	0.4214	0.017
H8A	0.3969	0.1439	0.3860	0.029
H8B	0.2885	0.1775	0.3210	0.029
H9A	0.4695	0.2257	0.2957	0.035
H9B	0.5058	0.3566	0.3572	0.035
H10A	0.4393	0.4979	0.2607	0.038
H10B	0.3145	0.3910	0.2448	0.038
H11A	0.2838	0.6409	0.2865	0.031
H11B	0.3924	0.6085	0.3513	0.031
H12A	0.1766	0.4288	0.3156	0.024
H12B	0.2126	0.5616	0.3764	0.024
H13	0.3319	0.0499	0.4796	0.017
H14A	0.1781	0.0456	0.5305	0.021
H14B	0.2273	0.2137	0.5717	0.021
H15A	0.2826	-0.0082	0.6378	0.026
H15B	0.3422	-0.0982	0.5820	0.026
H16A	0.4211	0.1967	0.6507	0.026
H16B	0.4883	0.0164	0.6610	0.026
H17A	0.5132	0.0229	0.5551	0.026
H17B	0.5737	0.1857	0.5963	0.026
H18A	0.4682	0.2573	0.4928	0.022
H18B	0.4092	0.3415	0.5500	0.022
H19A	-0.1975	-0.6507	0.3576	0.055
H19B	-0.2943	-0.5119	0.3698	0.055

Iodo-(tri-cyclohexylphosphine)dicopper(I), [CuI(PCy$_3$)]$_2$ **274**
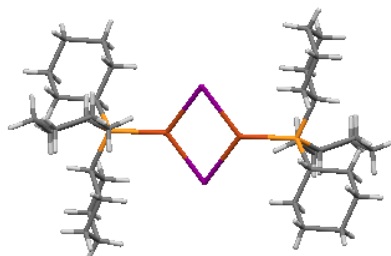
A clear pale bronze prism-like specimen of C$_{36}$H$_{66}$Cu$_2$I$_2$P$_2$, approximate dimensions 0.080 mm x 0.100 mm x 0.160 mm, was used for the X-ray crystallographic analysis. The X-ray intensity data were measured on a Bruker Kappa Apex-II Duo system equipped with a graphite monochromator.

Table 1: Data collection details for sb260612.

Axis	dx/mm	2θ/°	ω/°	φ/°	χ/°	Width/ °	Frames	Time/s	Wavelength/ Å	Voltage/kV	Current/mA	Temperature/K
Phi	40.031	-28.00	302.71	-339.77	19.47	0.50	713	50.00	0.71073	50	30.0	100.00
Omega	40.031	-25.50	-195.51	-212.94	99.74	0.50	64	50.00	0.71073	50	30.0	100.00
Omega	40.031	12.00	-59.12	-57.89	43.60	0.50	73	50.00	0.71073	50	30.0	100.00
Phi	40.031	14.50	3.21	43.05	78.01	0.50	207	50.00	0.71073	50	30.0	100.00
Phi	40.031	24.50	21.61	73.17	97.52	0.50	357	50.00	0.71073	50	30.0	100.00

A total of 1414 frames were collected. The total exposure time was 19.64 hours. The frames were integrated with the Bruker SAINT software package using a narrow-frame algorithm. The integration of the data using a triclinic unit cell yielded a total of 12302 reflections to a maximum θ angle of 27.50° (0.77 Å resolution), of which 4370 were independent (average redundancy 2.815, completeness = 98.8%, R$_{int}$= 1.65%, R$_{sig}$ = 2.10%) and 3922 (89.75%) were greater than 2σ(F^2). The final cell constants of $\underline{a}$ = 8.7822(3) Å, $\underline{b}$ = 9.7307(3) Å, $\underline{c}$ = 12.7606(4) Å, α = 96.4840(10)°, β = 94.1570(10)°, γ = 116.6860(10)°, volume = 958.72(5) Å^3, are based upon the refinement of the XYZ-centroids of 7394 reflections above 20 σ(I) with 4.748° < 2θ < 54.99°. Data were corrected for absorption effects using the multi-scan method (SADABS). The ratio of minimum to maximum apparent transmission was 0.910. The calculated minimum and maximum transmission coefficients (based on crystal size) are 0.6605 and 0.8055.

The structure was solved and refined using the Bruker SHELXTL Software Package, using the space group P -1, with Z = 1 for the formula unit, C$_{36}$H$_{66}$Cu$_2$I$_2$P$_2$. The final anisotropic full-matrix least-squares refinement on F^2 with 322 variables converged at R1 = 1.95%, for the observed data and wR2 = 5.04% for all data. The goodness-of-fit was 1.231. The largest peak in the final difference electron density synthesis was 0.725 e$^-$/Å^3 and the largest hole was -0.416 e$^-$/Å^3 with an RMS deviation of 0.073 e$^-$/Å^3. On the basis of the final model, the calculated density was 1.631 g/cm^3 and F(000), 476 e$^-$

Table 2. Sample and crystal data for sb260612.

Identification code	sb260612
Chemical formula	C$_{36}$H$_{66}$Cu$_2$I$_2$P$_2$

Formula weight	941.71	
Temperature	100(2) K	
Wavelength	0.71073 Å	
Crystal size	0.080 x 0.100 x 0.160 mm	
Crystal habit	clear pale bronze prism	
Crystal system	Triclinic	
Space group	P -1	
Unit cell dimensions	a = 8.7822(3) Å	$\alpha = 96.4840(10)°$
	b = 9.7307(3) Å	$\beta = 94.1570(10)°$
	c = 12.7606(4) Å	$\gamma = 116.6860(10)°$
Volume	958.72(5) Å^3	
Z	1	
Density (calculated)	1.631 g/cm^3	
Absorption coefficient	2.826 mm^{-1}	
F(000)	476	

Table 3. Data collection and structure refinement for sb260612.

Diffractometer	Bruker Kappa Apex-II Duo
Theta range for data collection	2.37 to 27.50°
Index ranges	-11<=h<=11, -12<=k<=12, -16<=l<=16
Reflections collected	12302
Independent reflections	4370 [R(int) = 0.0165]
Coverage of independent reflections	98.8%
Absorption correction	multi-scan
Max. and min. transmission	0.8055 and 0.6605
Structure solution technique	direct methods
Structure solution program	SHELXS-97 (Sheldrick, 2008)
Refinement method	Full-matrix least-squares on F^2
Refinement program	SHELXL-97 (Sheldrick, 2008)
Function minimized	$\Sigma\ w(F_o^2 - F_c^2)^2$
Data / restraints / parameters	4370 / 0 / 322
Goodness-of-fit on F^2	1.231
Δ/σ_{max}	0.001
Final R indices	3922 data; I>2σ(I) R1 = 0.0195, wR2 = 0.0490
	all data R1 = 0.0238, wR2 = 0.0504
Weighting scheme	$w=1/[\sigma^2(F_o^2)+(0.0250P)^2+0.0000P]$ where $P=(F_o^2+2F_c^2)/3$
Largest diff. peak and hole	0.725 and -0.416 eÅ^{-3}
R.M.S. deviation from mean	0.073 eÅ^{-3}

Table 4. Atomic coordinates and equivalent isotropic atomic displacement parameters (Å^2) for sb260612.

U(eq) is defined as one third of the trace of the orthogonalized U$_{ij}$ tensor.

	x/a	y/b	z/c	U(eq)
I1	0.152617(16)	0.433148(17)	0.40649(10)	0.02224(5)
Cu1	0.14725(3)	0.59105(3)	0.580732(18)	0.01430(6)
P1	0.37098(6)	0.71483(5)	0.70831(4)	0.01106(10)
C1	0.5492(2)	0.8889(2)	0.67160(15)	0.0144(4)
C2	0.6000(3)	0.8486(2)	0.56423(16)	0.0175(4)
C3	0.7346(3)	0.9955(3)	0.52920(18)	0.0218(4)
C4	0.8912(3)	0.0840(3)	0.6134(2)	0.0307(6)
C5	0.8401(3)	0.1245(3)	0.71934(19)	0.0334(6)
C6	0.7076(3)	0.9769(3)	0.75540(17)	0.0233(5)
C7	0.4671(2)	0.5886(2)	0.74470(15)	0.0124(4)

C8	0.3321(3)	0.4160(2)	0.71808(17)	0.0168(4)
C9	0.4102(3)	0.3083(2)	0.73752(17)	0.0198(4)
C10	0.5021(3)	0.3474(2)	0.85057(17)	0.0211(4)
C11	0.6371(3)	0.5171(2)	0.87602(16)	0.0168(4)
C12	0.5585(3)	0.6259(2)	0.85819(16)	0.0138(4)
C13	0.3176(2)	0.7885(2)	0.83301(15)	0.0125(4)
C14	0.2692(3)	0.9179(2)	0.81457(16)	0.0156(4)
C15	0.2188(3)	0.9786(2)	0.91492(17)	0.0184(4)
C16	0.0745(3)	0.8485(2)	0.95625(18)	0.0185(4)
C17	0.1221(3)	0.7198(2)	0.97538(16)	0.0162(4)
C18	0.1698(2)	0.6573(2)	0.87425(16)	0.0139(4)

Table 5. Bond lengths (Å) for sb260612.

I1-Cu1#1	2.5556(3)	I1-Cu1	2.5720(3)
Cu1-P1	2.2202(5)	Cu1-I1#1	2.5556(3)
Cu1-Cu1#1	2.8915(5)	P1-C13	1.8487(19)
P1-C7	1.8548(19)	P1-C1	1.855(2)
C1-C6	1.523(3)	C1-C2	1.535(3)
C1-H1	0.93(2)	C2-C3	1.531(3)
C2-H2A	0.91(2)	C2-H2B	0.93(2)
C3-C4	1.517(3)	C3-H3A	0.87(2)
C3-H3B	0.84(3)	C4-C5	1.520(4)
C4-H4A	0.92(3)	C4-H4B	0.88(3)
C5-C6	1.534(3)	C5-H5A	0.92(3)
C5-H5B	0.97(3)	C6-H6A	0.94(2)
C6-H6B	0.90(3)	C7-C12	1.525(3)
C7-C8	1.538(3)	C7-H7	0.91(2)
C8-C9	1.520(3)	C8-H8A	0.96(2)
C8-H8B	0.90(2)	C9-C10	1.519(3)
C9-H9A	0.91(2)	C9-H9B	0.90(3)
C10-C11	1.517(3)	C10-H10A	0.83(3)
C10-H10B	0.90(2)	C11-C12	1.529(3)
C11-H11A	0.92(2)	C11-H11B	0.98(2)
C12-H12A	0.85(2)	C12-H12B	0.92(2)
C13-C14	1.534(3)	C13-C18	1.535(3)
C13-H13	0.88(2)	C14-C15	1.527(3)
C14-H14A	0.95(2)	C14-H14B	0.93(3)
C15-C16	1.514(3)	C15-H15A	0.89(2)
C15-H15B	0.96(3)	C16-C17	1.525(3)
C16-H16A	0.90(2)	C16-H16B	0.88(2)
C17-C18	1.530(3)	C17-H17A	0.88(2)
C17-H17B	0.90(3)	C18-H18A	0.95(2)
C18-H18B	0.88(2)		

Symmetry transformations used to generate equivalent atoms:
#1   -x, -y+1, -z+1

Table 6. Bond angles (°) for sb260612.

Cu1#1-I1-Cu1	68.652(9)	P1-Cu1-I1#1	124.963(15)
P1-Cu1-I1	123.495(15)	I1#1-Cu1-I1	111.350(9)
P1-Cu1-Cu1#1	175.86(2)	I1#1-Cu1-Cu1#1	55.945(8)
I1-Cu1-Cu1#1	55.405(8)	C13-P1-C7	106.36(8)
C13-P1-C1	104.77(9)	C7-P1-C1	105.75(9)
C13-P1-Cu1	113.47(6)	C7-P1-Cu1	112.24(6)
C1-P1-Cu1	113.55(6)	C6-C1-C2	110.63(17)

C6-C1-P1	115.87(14)	C2-C1-P1	111.07(13)
C6-C1-H1	110.0(14)	C2-C1-H1	105.9(14)
P1-C1-H1	102.6(14)	C3-C2-C1	110.78(17)
C3-C2-H2A	108.7(14)	C1-C2-H2A	112.0(14)
C3-C2-H2B	109.9(14)	C1-C2-H2B	108.3(14)
H2A-C2-H2B	107.2(19)	C4-C3-C2	111.71(19)
C4-C3-H3A	105.3(16)	C2-C3-H3A	112.4(15)
C4-C3-H3B	106.9(18)	C2-C3-H3B	114.8(17)
H3A-C3-H3B	105.(2)	C3-C4-C5	111.0(2)
C3-C4-H4A	106.0(16)	C5-C4-H4A	110.5(16)
C3-C4-H4B	112.5(19)	C5-C4-H4B	103.1(18)
H4A-C4-H4B	114.(2)	C4-C5-C6	110.7(2)
C4-C5-H5A	109.4(18)	C6-C5-H5A	103.5(18)
C4-C5-H5B	108.3(16)	C6-C5-H5B	109.2(16)
H5A-C5-H5B	116.(2)	C1-C6-C5	111.05(18)
C1-C6-H6A	111.2(14)	C5-C6-H6A	106.3(14)
C1-C6-H6B	110.9(16)	C5-C6-H6B	112.2(16)
H6A-C6-H6B	105.(2)	C12-C7-C8	110.52(16)
C12-C7-P1	116.80(13)	C8-C7-P1	110.30(13)
C12-C7-H7	109.2(14)	C8-C7-H7	106.5(14)
P1-C7-H7	102.8(14)	C9-C8-C7	111.78(16)
C9-C8-H8A	107.7(13)	C7-C8-H8A	110.1(14)
C9-C8-H8B	105.3(15)	C7-C8-H8B	108.3(15)
H8A-C8-H8B	114.(2)	C10-C9-C8	111.57(17)
C10-C9-H9A	109.2(14)	C8-C9-H9A	109.8(13)
C10-C9-H9B	109.7(17)	C8-C9-H9B	110.1(17)
H9A-C9-H9B	106.(2)	C11-C10-C9	111.02(17)
C11-C10-H10A	98.(2)	C9-C10-H10A	113.(2)
C11-C10-H10B	109.4(14)	C9-C10-H10B	110.4(15)
H10A-C10-H10B	114.(2)	C10-C11-C12	111.34(17)
C10-C11-H11A	106.4(14)	C12-C11-H11A	112.3(14)
C10-C11-H11B	109.5(13)	C12-C11-H11B	110.9(12)
H11A-C11-H11B	106.1(18)	C7-C12-C11	111.28(16)
C7-C12-H12A	107.8(15)	C11-C12-H12A	111.0(15)
C7-C12-H12B	109.8(14)	C11-C12-H12B	109.1(14)
H12A-C12-H12B	107.8(19)	C14-C13-C18	109.95(15)
C14-C13-P1	109.85(13)	C18-C13-P1	111.38(13)
C14-C13-H13	110.4(14)	C18-C13-H13	109.0(14)
P1-C13-H13	106.3(14)	C15-C14-C13	111.52(17)
C15-C14-H14A	106.9(13)	C13-C14-H14A	110.5(13)
C15-C14-H14B	110.8(15)	C13-C14-H14B	110.9(15)
H14A-C14-H14B	106.(2)	C16-C15-C14	111.72(17)
C16-C15-H15A	106.1(14)	C14-C15-H15A	111.1(13)
C16-C15-H15B	107.8(16)	C14-C15-H15B	111.0(16)
H15A-C15-H15B	109.(2)	C15-C16-C17	110.95(17)
C15-C16-H16A	109.3(13)	C17-C16-H16A	113.0(13)
C15-C16-H16B	109.4(15)	C17-C16-H16B	108.4(15)
H16A-C16-H16B	106.(2)	C16-C17-C18	111.01(17)
C16-C17-H17A	110.8(14)	C18-C17-H17A	110.5(14)
C16-C17-H17B	111.0(15)	C18-C17-H17B	111.4(15)
H17A-C17-H17B	102.(2)	C17-C18-C13	111.19(16)
C17-C18-H18A	107.9(12)	C13-C18-H18A	110.5(13)
C17-C18-H18B	109.6(14)	C13-C18-H18B	110.3(13)
H18A-C18-H18B	107.3(18)		

Symmetry transformations used to generate equivalent atoms:

 #1   -x, -y+1, -z+1

Table 7. Torsion angles (°) for sb260612.

Cu1#1-I1-Cu1-P1	175.18(2)	Cu1#1-I1-Cu1-I1#1	0
I1#1-Cu1-P1-C13	4.70(7)	I1-Cu1-P1-C13	-169.82(7)
Cu1#1-Cu1-P1-C13	-96.6(3)	I1#1-Cu1-P1-C7	125.33(6)
I1-Cu1-P1-C7	-49.19(7)	Cu1#1-Cu1-P1-C7	24.1(3)
I1#1-Cu1-P1-C1	-114.79(7)	I1-Cu1-P1-C1	70.69(7)
Cu1#1-Cu1-P1-C1	143.9(3)	C13-P1-C1-C6	56.71(17)
C7-P1-C1-C6	-55.44(17)	Cu1-P1-C1-C6	-178.94(14)
C13-P1-C1-C2	-175.96(14)	C7-P1-C1-C2	71.88(16)
Cu1-P1-C1-C2	-51.62(15)	C6-C1-C2-C3	-55.4(2)
P1-C1-C2-C3	174.44(15)	C1-C2-C3-C4	55.4(3)
C2-C3-C4-C5	-56.0(3)	C3-C4-C5-C6	56.4(3)
C2-C1-C6-C5	56.5(3)	P1-C1-C6-C5	-175.92(17)
C4-C5-C6-C1	-57.1(3)	C13-P1-C7-C12	-27.62(16)
C1-P1-C7-C12	83.41(15)	Cu1-P1-C7-C12	-152.27(12)
C13-P1-C7-C8	99.64(14)	C1-P1-C7-C8	-149.33(13)
Cu1-P1-C7-C8	-25.01(14)	C12-C7-C8-C9	-54.5(2)
P1-C7-C8-C9	174.86(14)	C7-C8-C9-C10	54.9(2)
C8-C9-C10-C11	-55.4(2)	C9-C10-C11-C12	56.0(2)
C8-C7-C12-C11	55.0(2)	P1-C7-C12-C11	-177.89(13)
C10-C11-C12-C7	-56.4(2)	C7-P1-C13-C14	169.34(13)
C1-P1-C13-C14	57.63(15)	Cu1-P1-C13-C14	-66.76(14)
C7-P1-C13-C18	-68.59(15)	C1-P1-C13-C18	179.69(13)
Cu1-P1-C13-C18	55.30(14)	C18-C13-C14-C15	55.3(2)
P1-C13-C14-C15	178.24(14)	C13-C14-C15-C16	-55.6(2)
C14-C15-C16-C17	55.4(2)	C15-C16-C17-C18	-56.0(2)
C16-C17-C18-C13	56.8(2)	C14-C13-C18-C17	-56.1(2)
P1-C13-C18-C17	-178.11(13)		

Symmetry transformations used to generate equivalent atoms:

#1   -x, -y+1, -z+1

Table 8. Anisotropic atomic displacement parameters (Å^2) for sb260612.
The anisotropic atomic displacement factor exponent takes the form: $-2\pi^2[h^2 a^{*2} U_{11} + ... + 2 h k a^* b^* U_{12}]$

	U_{11}	U_{22}	U_{33}	U_{23}	U_{13}	U_{12}
I1	0.01524(7)	0.03529(9)	0.01557(8)	-0.00425(5)	0.00004(5)	0.01331(6)
Cu1	0.01241(12)	0.01622(13)	0.01290(12)	0.00183(9)	0.00013(9)	0.00579(10)
P1	0.0103(2)	0.0112(2)	0.0108(2)	0.00174(17)	0.00132(17)	0.00417(18)
C1	0.0143(9)	0.0133(9)	0.0152(10)	0.0040(7)	0.0034(7)	0.0055(8)
C2	0.0170(10)	0.0195(11)	0.0156(10)	0.0039(8)	0.0047(8)	0.0074(9)
C3	0.0201(11)	0.0254(12)	0.0173(11)	0.0069(9)	0.0068(9)	0.0070(9)
C4	0.0154(10)	0.0349(14)	0.0276(13)	0.0138(11)	0.0040(9)	-0.0030(10)
C5	0.0252(12)	0.0269(13)	0.0216(12)	0.0049(10)	-0.0024(10)	-0.0103(10)
C6	0.0207(11)	0.0218(11)	0.0139(10)	0.0036(8)	0.0005(8)	-0.0018(9)
C7	0.0119(9)	0.0123(9)	0.0124(9)	0.0018(7)	0.0024(7)	0.0051(7)
C8	0.0148(9)	0.0153(10)	0.0147(10)	0.0005(8)	-0.0032(8)	0.0032(8)
C9	0.0245(11)	0.0106(10)	0.0214(11)	0.0015(8)	-0.0003(9)	0.0062(9)
C10	0.0255(11)	0.0185(11)	0.0210(11)	0.0045(8)	-0.0011(9)	0.0119(9)
C11	0.0144(9)	0.0204(10)	0.0154(10)	0.0032(8)	-0.0010(8)	0.0083(8)
C12	0.0125(9)	0.0129(10)	0.0141(9)	0.0018(7)	0.0014(7)	0.0044(8)
C13	0.0102(9)	0.0137(9)	0.0123(9)	0.0009(7)	0.0015(7)	0.0047(7)
C14	0.0165(10)	0.0131(10)	0.0185(10)	0.0034(8)	0.0055(8)	0.0074(8)

	U₁₁	U₂₂	U₃₃	U₂₃	U₁₃	U₁₂
C15	0.0202(10)	0.0139(10)	0.0214(11)	0.0006(8)	0.0052(9)	0.0083(8)
C16	0.0176(10)	0.0208(11)	0.0200(11)	0.0011(8)	0.0071(9)	0.0114(9)
C17	0.0143(9)	0.0183(10)	0.0167(10)	0.0042(8)	0.0046(8)	0.0073(8)
C18	0.0131(9)	0.0133(10)	0.0165(10)	0.0031(7)	0.0036(8)	0.0067(8)

Table 9. Hydrogen atomic coordinates and isotropic atomic displacement parameters ($Å^2$) for sb260612.

	x/a	y/b	z/c	U(eq)
H12A	0.485(3)	0.618(2)	0.9005(18)	0.013(5)
H18A	0.070(3)	0.609(2)	0.8222(17)	0.011(5)
H15A	0.307(3)	1.022(2)	0.9677(18)	0.011(5)
H11A	0.720(3)	0.528(2)	0.8334(18)	0.017(6)
H6A	0.764(3)	0.916(3)	0.7669(18)	0.020(6)
H18B	0.199(3)	0.584(2)	0.8873(17)	0.009(5)
H1	0.497(3)	0.952(3)	0.6597(18)	0.017(6)
H13	0.411(3)	0.826(2)	0.8799(18)	0.014(5)
H14A	0.173(3)	0.880(2)	0.7607(18)	0.012(5)
H17A	0.207(3)	0.753(3)	1.0282(19)	0.015(5)
H3A	0.696(3)	1.061(3)	0.5189(18)	0.014(6)
H7	0.545(3)	0.603(2)	0.6984(18)	0.016(5)
H16A	-0.024(3)	0.814(2)	0.9108(18)	0.012(5)
H10A	0.567(4)	0.307(3)	0.859(2)	0.042(8)
H9A	0.486(3)	0.316(2)	0.6911(17)	0.009(5)
H2A	0.508(3)	0.801(3)	0.5122(19)	0.016(6)
H9B	0.328(3)	0.209(3)	0.725(2)	0.031(7)
H2B	0.644(3)	0.780(3)	0.5718(18)	0.019(6)
H8A	0.283(3)	0.391(3)	0.6445(19)	0.019(6)
H8B	0.254(3)	0.398(3)	0.7632(19)	0.020(6)
H12B	0.644(3)	0.728(3)	0.8717(17)	0.015(5)
H11B	0.693(3)	0.540(2)	0.9495(19)	0.015(5)
H17B	0.036(3)	0.642(3)	1.001(2)	0.025(6)
H6B	0.678(3)	0.998(3)	0.819(2)	0.028(7)
H10B	0.427(3)	0.328(3)	0.8974(18)	0.016(6)
H15B	0.181(3)	1.054(3)	0.901(2)	0.035(7)
H4A	0.961(3)	1.173(3)	0.588(2)	0.029(6)
H14B	0.359(3)	0.999(3)	0.790(2)	0.028(6)
H3B	0.771(3)	0.980(3)	0.472(2)	0.025(6)
H16B	0.055(3)	0.886(3)	1.0173(19)	0.019(6)
H5A	0.933(4)	1.162(3)	0.772(2)	0.041(8)
H5B	0.790(3)	1.194(3)	0.710(2)	0.033(7)
H4B	0.942(4)	1.027(3)	0.629(2)	0.035(8)

Iodo-(di-*tert*-butyl-*iso*-propylphosphine)dipalladium(I), Pd[P(*i*Pr)(*t*Bu)₂]₂ **276**
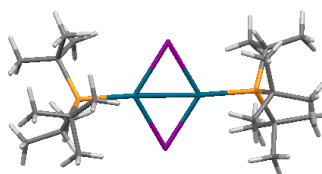
Experimental

Single crystals of $C_{22}H_{50}I_2P_2Pd_2$ were prepared by recrystallization from a toleune/acetone 1:2 mixture at -35 °C over a period of 15 days. A suitable crystal was selected and measured on on a Bruker APEX-II CCD diffractometer. The crystal was kept at 100.1 K during data collection. Using Olex2[6], the structure was solved with the XT[i] structure solution program using Direct Methods and refined with the XL[2] refinement package using Least Squares minimisation.

Crystal structure determination of mo_sb080714_0m

Crystal Data for mo_sb080714_0m (M =843.16 g/mol): triclinic, space group P-1 (no. 2), a = 10.4969(10) Å, b = 11.1685(11) Å, c = 12.5738(12) Å, α = 84.7690(10)°, β = 86.613(2)°, γ = 87.770(2)°, V = 1464.5(2) Å^3, Z = 2, T = 100.01 K, μ(MoKα) = 3.453 mm^{-1}, $Dcalc$ = 1.912 g/cm^3, ? reflections measured (4.682° $\leq$ 2Θ $\leq$ 60.934°), 8807 unique (R_{int} = ?, R_{sigma} = 0.0279) which were used in all calculations. The final R_1 was 0.0243 (I > 2σ(I)) and wR_2 was 0.0601 (all data).

Refinement model description

Number of restraints - 0, number of constraints - unknown.

Details:

1. Fixed Uiso
At 1.2 times of:
All C(H) groups
At 1.5 times of:
 All C(H,H,H) groups
2.a Ternary CH refined with riding coordinates:
 C1(H1), C12(H12)
2.b Idealised Me refined as rotating group:
 C2(H2A,H2B,H2C), C3(H3A,H3B,H3C), C5(H5A,H5B,H5C), C6(H6A,H6B,H6C), C7(H7A,
 H7B,H7C), C9(H9A,H9B,H9C), C10(H10A,H10B,H10C), C11(H11A,H11B,H11C), C13(H13A,
 H13B,H13C), C14(H14A,H14B,H14C), C16(H16A,H16B,H16C), 17(H17A,H17B,H17C),
 C18(H18A,H18B,H18C), C20(H20A,H20B,H20C), C21(H21A,H21B,H21C), C22(H22A,H22B, H22C)

Table 1 Crystal data and structure refinement

Empirical formula	$C_{22}H_{50}P_2Pd_2I_2$
Formula weight	843.16
Temperature/K	100.01
Crystal system	triclinic
Space group	P-1
a/Å	10.4969(10)
b/Å	11.1685(11)
c/Å	12.5738(12)
α/°	84.7690(10)
β/°	86.613(2)
γ/°	87.770(2)
Volume/Å^3	1464.5(2)
Z	2
ρ$_{calc}$g/cm^3	1.912
μ/mm^{-1}	3.453
F(000)	820.0
Crystal size/mm^3	? × ? × ?
Radiation	MoKα (λ = 0.71073)
2Θ range for data collection/°	4.682 to 60.934
Index ranges	? ≤ h ≤ ?, ? ≤ k ≤ ?, ? ≤ l ≤ ?
Reflections collected	?
Independent reflections	8807 [R_{int} = 0.0244, R_{sigma} = 0.0279]

Data/restraints/parameters	8807/0/269
Goodness-of-fit on F^2	1.050
Final R indexes [I>=2σ (I)]	$R_1 = 0.0243$, $wR_2 = 0.0572$
Final R indexes [all data]	$R_1 = 0.0341$, $wR_2 = 0.0601$
Largest diff. peak/hole / e Å^{-3}	1.02/-1.22

Table 2 Fractional Atomic Coordinates (×10^4) and Equivalent Isotropic Displacement Parameters (Å^2×10^3)

Atom	x	y	z	U(eq)
I1	6150.3(2)	3409.2(2)	2642.1(2)	15.09(4)
I2	2989.6(2)	805.7(2)	2532.1(2)	15.05(4)
Pd1	5405.0(2)	1198.1(2)	2613.3(2)	10.83(4)
Pd2	3728.8(2)	3031.8(2)	2522.5(2)	10.88(4)
P1	6797.5(6)	-432.2(5)	2603.3(4)	10.47(11)
P2	2400.8(6)	4715.3(5)	2412.5(4)	10.40(11)
C1	5982(2)	-1804(2)	3231.0(17)	13.6(4)
C2	5554(3)	-1672(2)	4404.8(19)	21.6(5)
C3	6619(3)	-3054(2)	3129(2)	20.1(5)
C4	8287(2)	-205(2)	3320.3(19)	16.5(5)
C5	7878(3)	391(2)	4353.5(19)	22.9(5)
C6	9122(3)	691(2)	2627(2)	22.8(5)
C7	9073(3)	-1359(2)	3614(2)	26.5(6)
C8	7192(2)	-724(2)	1154.1(17)	14.8(4)
C9	7373(3)	498(2)	497.0(19)	20.8(5)
C10	6010(2)	-1273(2)	752.0(18)	18.3(5)
C11	8367(3)	-1549(2)	935(2)	21.3(5)
C12	2994(2)	5813(2)	3293.7(18)	16.5(5)
C13	2393(3)	7094(2)	3285(2)	27.1(6)
C14	3086(3)	5258(3)	4453(2)	25.2(6)
C15	674(2)	4376(2)	2807.0(18)	14.9(4)
C16	128(2)	3726(2)	1921(2)	19.6(5)
C17	-190(3)	5461(2)	3035(2)	23.0(5)
C18	654(3)	3495(2)	3827.4(19)	20.9(5)
C19	2556(2)	5478(2)	1002.5(17)	14.4(4)
C20	3840(2)	6096(2)	871.8(19)	20.3(5)
C21	2620(3)	4488(2)	216.1(18)	19.8(5)
C22	1500(3)	6410(2)	681.8(19)	19.5(5)

Table 3 Anisotropic Displacement Parameters (Å^2×10^3)

Atom	U$_{11}$	U$_{22}$	U$_{33}$	U$_{23}$	U$_{13}$	U$_{12}$
I1	13.03(8)	10.84(7)	21.36(8)	-1.10(5)	-1.05(5)	-0.42(5)
I2	13.29(8)	12.29(8)	19.81(8)	-2.38(5)	-1.40(5)	-0.46(6)
Pd1	11.00(8)	7.60(8)	13.75(8)	-1.09(6)	-1.47(6)	3.02(6)
Pd2	10.66(8)	8.05(8)	13.52(8)	-0.42(6)	-0.48(6)	3.14(6)
P1	10.9(3)	7.7(3)	12.8(3)	-1.39(19)	-1.94(19)	1.8(2)
P2	10.7(3)	8.2(3)	12.1(3)	-0.65(19)	-1.01(19)	1.9(2)
C1	13.8(11)	10.4(11)	16.3(10)	-0.3(8)	-1.7(8)	0.4(8)
C2	25.1(14)	21.4(13)	17.4(11)	1.3(9)	0.2(9)	1(1)
C3	24.8(14)	11.5(12)	23.5(12)	0.5(9)	-1.3(10)	1.8(10)
C4	16.0(12)	12.3(11)	22.0(11)	-4.3(9)	-7.1(9)	3.5(9)
C5	28.0(15)	21.1(13)	21.2(12)	-5(1)	-11.2(10)	1.6(11)
C6	17.1(13)	18.0(13)	34.7(14)	-7.2(10)	-2.7(10)	-3.1(10)
C7	24.5(15)	17.2(13)	39.9(15)	-4.9(11)	-18.8(12)	6.1(11)
C8	17.0(12)	13.8(11)	13.8(10)	-2.4(8)	0.0(8)	-0.2(9)
C9	27.1(14)	18.4(13)	16.3(11)	-0.5(9)	2.1(9)	-1.5(10)
C10	22.9(13)	18.7(12)	13.8(11)	-3.1(9)	-2.0(9)	-0.9(10)
C11	21.3(13)	17.8(13)	25.2(13)	-7.0(9)	1.9(10)	2.5(10)
C12	17.6(12)	13.1(11)	19.4(11)	-3.3(8)	-3.2(9)	2.0(9)
C13	29.4(16)	14.8(13)	39.6(16)	-12.2(11)	-9.2(12)	4.2(11)
C14	30.7(15)	27.3(15)	18.7(12)	-5.4(10)	-4.7(10)	-0.7(11)
C15	12.9(11)	12.5(11)	18.3(11)	0.5(8)	2.2(8)	2.9(9)

C16	14.1(12)	18.7(13)	26.2(12)	-1.4(9)	-2.2(9)	-3.4(9)
C17	17.7(13)	18.6(13)	31.3(14)	-2.5(10)	5.9(10)	5.4(10)
C18	23.1(14)	17.1(12)	20.6(12)	1.4(9)	8.6(9)	-0.3(10)
C19	17.0(12)	12.0(11)	13.6(10)	0.6(8)	0.3(8)	0.2(9)
C20	19.6(13)	19.3(13)	21.0(12)	3.7(9)	0.7(9)	-2.9(10)
C21	24.3(14)	20.2(13)	14.8(11)	-1.6(9)	0.2(9)	0.6(10)
C22	22.5(13)	13.9(12)	21.0(12)	4.3(9)	-3.9(9)	2(1)

Table 4 Bond Lengths

Atom	Atom	Length/Å	Atom	Atom	Length/Å
I1	Pd1	2.6232(3)	C4	C5	1.544(3)
I1	Pd2	2.6079(3)	C4	C6	1.533(4)
I2	Pd1	2.5992(3)	C4	C7	1.531(3)
I2	Pd2	2.6320(3)	C8	C9	1.542(3)
Pd1	Pd2	2.6465(3)	C8	C10	1.537(3)
Pd1	P1	2.2907(6)	C8	C11	1.537(3)
Pd2	P2	2.2954(6)	C12	C13	1.540(3)
P1	C1	1.872(2)	C12	C14	1.538(3)
P1	C4	1.887(2)	C15	C16	1.533(3)
P1	C8	1.899(2)	C15	C17	1.523(3)
P2	C12	1.873(2)	C15	C18	1.544(3)
P2	C15	1.894(2)	C19	C20	1.531(3)
P2	C19	1.897(2)	C19	C21	1.547(3)
C1	C2	1.536(3)	C19	C22	1.536(3)
C1	C3	1.538(3)			

Table 5 Bond Angles

Atom	Atom	Atom	Angle/°	Atom	Atom	Atom	Angle/°
Pd2	I1	Pd1	60.782(7)	C3	C1	P1	119.72(17)
Pd1	I2	Pd2	60.779(6)	C5	C4	P1	107.71(17)
I1	Pd1	Pd2	59.322(9)	C6	C4	P1	108.88(16)
I2	Pd1	I1	119.534(8)	C6	C4	C5	106.7(2)
I2	Pd1	Pd2	60.222(8)	C7	C4	P1	114.71(17)
P1	Pd1	I1	123.021(18)	C7	C4	C5	108.9(2)
P1	Pd1	I2	117.417(17)	C7	C4	C6	109.6(2)
P1	Pd1	Pd2	176.417(16)	C9	C8	P1	108.23(16)
I1	Pd2	I2	118.884(8)	C10	C8	P1	106.95(16)
I1	Pd2	Pd1	59.895(8)	C10	C8	C9	106.83(19)
I2	Pd2	Pd1	58.999(9)	C10	C8	C11	109.1(2)
P2	Pd2	I1	115.971(17)	C11	C8	P1	116.53(16)
P2	Pd2	I2	125.145(18)	C11	C8	C9	108.8(2)
P2	Pd2	Pd1	175.714(17)	C13	C12	P2	120.31(17)
C1	P1	Pd1	109.63(7)	C14	C12	P2	111.70(18)
C1	P1	C4	109.82(11)	C14	C12	C13	109.9(2)
C1	P1	C8	105.75(10)	C16	C15	P2	108.65(15)
C4	P1	Pd1	112.34(7)	C16	C15	C18	107.4(2)
C4	P1	C8	111.41(11)	C17	C15	P2	115.48(18)
C8	P1	Pd1	107.67(8)	C17	C15	C16	109.3(2)
C12	P2	Pd2	108.19(8)	C17	C15	C18	107.98(19)
C12	P2	C15	110.15(11)	C18	C15	P2	107.72(16)
C12	P2	C19	105.62(11)	C20	C19	P2	107.64(16)
C15	P2	Pd2	112.98(7)	C20	C19	C21	107.0(2)
C15	P2	C19	110.62(11)	C20	C19	C22	108.5(2)
C19	P2	Pd2	108.99(7)	C21	C19	P2	107.90(16)
C2	C1	P1	111.54(16)	C22	C19	P2	116.59(16)
C2	C1	C3	109.68(19)	C22	C19	C21	108.82(19)

Table 6 Torsion Angles

A	B	C	D	Angle/°	A	B	C	D	Angle/°
Pd1	P1	C1	C2	-61.85(17)	C4	P1	C8	C9	-82.39(19)
Pd1	P1	C1	C3	168.19(16)	C4	P1	C8	C10	162.84(15)
Pd1	P1	C4	C5	42.42(18)	C4	P1	C8	C11	40.6(2)
Pd1	P1	C4	C6	-72.96(17)	C8	P1	C1	C2	-177.65(17)
Pd1	P1	C4	C7	163.80(17)	C8	P1	C1	C3	52.4(2)
Pd1	P1	C8	C9	41.20(18)	C8	P1	C4	C5	163.32(16)
Pd1	P1	C8	C10	-73.57(16)	C8	P1	C4	C6	47.94(19)
Pd1	P1	C8	C11	164.19(17)	C8	P1	C4	C7	-75.3(2)
Pd2	P2	C12	C13	172.65(19)	C12	P2	C15	C16	166.70(16)
Pd2	P2	C12	C14	-56.22(19)	C12	P2	C15	C17	43.5(2)
Pd2	P2	C15	C16	-72.18(16)	C12	P2	C15	C18	-77.26(18)
Pd2	P2	C15	C17	164.60(15)	C12	P2	C19	C20	42.17(18)
Pd2	P2	C15	C18	43.86(17)	C12	P2	C19	C21	157.29(17)
Pd2	P2	C19	C20	-73.87(16)	C12	P2	C19	C22	-80.0(2)
Pd2	P2	C19	C21	41.24(18)	C15	P2	C12	C13	-63.4(2)
Pd2	P2	C19	C22	163.99(16)	C15	P2	C12	C14	67.7(2)
C1	P1	C4	C5	-79.86(18)	C15	P2	C19	C20	161.34(16)
C1	P1	C4	C6	164.75(16)	C15	P2	C19	C21	-83.55(18)
C1	P1	C4	C7	41.5(2)	C15	P2	C19	C22	39.2(2)
C1	P1	C8	C9	158.34(17)	C19	P2	C12	C13	56.1(2)
C1	P1	C8	C10	43.57(18)	C19	P2	C12	C14	-172.81(18)
C1	P1	C8	C11	-78.7(2)	C19	P2	C15	C16	50.32(18)
C4	P1	C1	C2	62.03(19)	C19	P2	C15	C17	-72.9(2)
C4	P1	C1	C3	-67.9(2)	C19	P2	C15	C18	166.35(15)

Table 7 Hydrogen Atom Coordinates (Å×10⁴) and Isotropic Displacement Parameters (Å²×10³)

Atom	x	y	z	U(eq)
H1	5170	-1817	2854	16
H2A	4912	-2268	4643	32
H2B	5184	-861	4472	32
H2C	6292	-1803	4849	32
H3A	7411	-3120	3508	30
H3B	6814	-3166	2371	30
H3C	6038	-3674	3441	30
H5A	8632	495	4755	34
H5B	7278	-122	4793	34
H5C	7464	1178	4168	34
H6A	8595	1391	2374	34
H6B	9508	304	2011	34
H6C	9797	952	3051	34
H7A	9277	-1779	2971	40
H7B	8580	-1882	4141	40
H7C	9866	-1155	3919	40
H9A	7484	373	-265	31
H9B	8130	873	720	31
H9C	6619	1024	618	31
H10A	6110	-1294	-26	28
H10B	5248	-783	935	28
H10C	5919	-2094	1090	28
H11A	8256	-2333	1341	32
H11B	9132	-1183	1156	32
H11C	8463	-1656	170	32
H12	3900	5935	3029	20
H13A	1518	7056	3600	41
H13B	2382	7458	2546	41
H13C	2898	7581	3702	41
H14A	3654	5731	4828	38

H14B	3428	4429	4452	38
H14C	2235	5260	4818	38
H16A	-733	3464	2151	29
H16B	679	3024	1777	29
H16C	90	4275	1269	29
H17A	-113	6076	2429	34
H17B	66	5791	3683	34
H17C	-1077	5214	3139	34
H18A	-226	3266	4026	31
H18B	996	3885	4412	31
H18C	1180	2774	3692	31
H20A	4030	6349	114	30
H20B	4513	5532	1134	30
H20C	3797	6801	1284	30
H21A	1808	4076	270	30
H21B	3314	3906	396	30
H21C	2777	4854	-516	30
H22A	1446	7038	1180	29
H22B	681	6014	706	29
H22C	1700	6773	-45	29

Bromo-(tri-*tert*-butylphosphine)palladium-copper dimer, Pd-Cu dimer **316**.
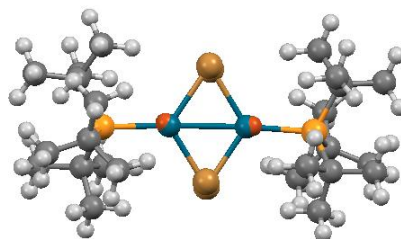
A clear green-black plate-like specimen of $C_{24}H_{54}Br_2Cu_{0.74}P_2Pd_{1.26}$, approximate dimensions 0.030 mm x 0.120 mm x 0.160 mm, was used for the X-ray crystallographic analysis. The X-ray intensity data were measured on a Bruker Kappa Apex-II Duo system equipped with a graphite monochromator.

Table 1: Data collection details for sb032211.

Axis	dx/mm	2θ/°	ω/°	φ/°	χ/°	Width/°	Frames	Time/s	Wavelength/Å	Voltage/ kV	Current/ mA	Temperature/K
Omega	40.071	2.00	-91.79	-199.22	19.47	0.50	216	10.00	0.71073	50	30.0	99.98
Phi	40.071	17.00	94.92	-334.13	-20.60	0.50	669	10.00	0.71073	50	30.0	99.98

A total of 885 frames were collected. The total exposure time was 2.46 hours. The frames were integrated with the Bruker SAINT software package using a narrow-frame algorithm. The integration of the data using a monoclinic unit cell yielded a total of 25829 reflections to a maximum θ angle of 27.55° (0.77 Å resolution), of which 6879 were independent (average redundancy 3.755, completeness = 98.1%, $R_{int} = 2.27\%$, $R_{sig} = 2.62\%$) and 4863 (70.69%) were greater than $2\sigma(F^2)$. The final cell constants of $\underline{a} = 13.1303(3)$ Å, $\underline{b} = 14.4066(4)$ Å, $\underline{c} = 16.0589(4)$ Å, $\beta = 92.1480(10)°$, volume = 3035.61(13) Å^3, are

based upon the refinement of the XYZ-centroids of 7858 reflections above 20 σ(I) with 4.966° < 2θ < 54.97°. Data were corrected for absorption effects using the multi-scan method (SADABS). The ratio of minimum to maximum apparent transmission was 0.797.

The structure was solved and refined using the OLEX2 and Bruker SHELXTL Software Package, using the space group P 1 21/n 1, with Z = 4 for the formula unit, $C_{24}H_{54}Br_2Cu_{0.74}P_2Pd_{1.26}$. The final anisotropic full-matrix least-squares refinement on F^2 with 326 variables converged at R1 = 3.26%, for the observed data and wR2 = 8.76% for all data. The goodness-of-fit was 1.414. The largest peak in the final difference electron density synthesis was 0.420 e$^-$/Å^3 and the largest hole was -0.604 e$^-$/Å^3 with an RMS deviation of 0.081 e$^-$/Å^3. On the basis of the final model, the calculated density was 1.631 g/cm^3 and F(000), 1510 e$^-$

Table 2. Sample and crystal data for sb032211.

Identification code	sb032211	
Chemical formula	$C_{24}H_{54}Br_2Cu_{0.74}P_2Pd_{1.26}$	
Formula weight	745.41	
Temperature	100(2) K	
Wavelength	0.71073 Å	
Crystal size	0.030 x 0.120 x 0.160 mm	
Crystal habit	clear green-black plate	
Crystal system	monoclinic	
Space group	P 1 21/n 1	
Unit cell dimensions	a = 13.1303(3) Å	α = 90°
	b = 14.4066(4) Å	β = 92.1480(10)°
	c = 16.0589(4) Å	γ = 90°
Volume	3035.61(13) Å^3	
Z	4	
Density (calculated)	1.631 Mg/cm^3	
Absorption coefficient	4.013 mm^{-1}	
F(000)	1510	

Table 3. Data collection and structure refinement for sb032211.

Diffractometer	Bruker Kappa Apex-II Duo
Theta range for data collection	1.90 to 27.55°
Index ranges	-15<=h<=17, -17<=k<=18, -20<=l<=20
Reflections collected	25829
Independent reflections	6879 [R(int) = 0.0227]
Coverage of independent reflections	98.1%
Absorption correction	multi-scan
Structure solution technique	direct methods
Structure solution program	SHELXS-97 (Sheldrick, 2008)
Refinement method	Full-matrix least-squares on F^2
Refinement program	SHELXL-97 (Sheldrick, 2008)
Function minimized	$\Sigma\ w(F_o^2 - F_c^2)^2$
Data / restraints / parameters	6879 / 0 / 326
Goodness-of-fit on F^2	1.414
Δ/σ$_{max}$	0.006
Final R indices	4863 data; I>2σ(I)　　R1 = 0.0326, wR2 = 0.0799
	all data　　R1 = 0.0560, wR2 = 0.0876
Weighting scheme	w=1/[σ^2(F$_o^2$)+(0.0300P)^2+0.0000P] where P=(F$_o^2$+2F$_c^2$)/3
Largest diff. peak and hole	0.420 and -0.604 eÅ^{-3}
R.M.S. deviation from mean	0.081 eÅ^{-3}

**Table 4. Atomic coordinates and equivalent isotropic atomic
displacement parameters (Å^2) for sb032211.**

U(eq) is defined as one third of the trace of the orthogonalized U$_{ij}$ tensor.

	x/a	y/b	z/c	U(eq)
Pd1	0.5832(2)	0.49584(12)	0.29944(12)	0.0123(2)
Pd2	0.41207(15)	0.50433(13)	0.20466(14)	0.0121(3)
Br3	0.5042(3)	0.3570(2)	0.2330(2)	0.0234(3)
Br3A	0.5002(5)	0.3651(4)	0.2456(4)	0.0495(17)
Br4	0.4942(2)	0.64332(14)	0.26888(16)	0.0248(3)
Br4A	0.5025(4)	0.6326(3)	0.2515(3)	0.0476(13)
Cu1	0.5973(6)	0.4938(4)	0.3023(4)	0.0321(19)
Cu2	0.4056(5)	0.4991(4)	0.1977(4)	0.0365(19)
P5	0.73505(6)	0.49821(5)	0.38003(4)	0.01810(19)
P18	0.26344(6)	0.51779(5)	0.12255(4)	0.01761(18)
C6	0.8044(2)	0.3824(2)	0.38043(18)	0.0300(7)
C7	0.7271(3)	0.3034(2)	0.3919(2)	0.0430(9)
C8	0.8474(3)	0.3669(2)	0.29392(19)	0.0451(10)
C9	0.8918(2)	0.3706(2)	0.44660(19)	0.0382(8)
C10	0.8209(2)	0.5907(2)	0.33447(16)	0.0247(7)
C11	0.9335(2)	0.5866(2)	0.36305(17)	0.0325(8)
C12	0.7798(2)	0.6868(2)	0.35496(18)	0.0293(7)
C13	0.8115(2)	0.5832(2)	0.23821(16)	0.0333(8)
C14	0.7082(2)	0.5322(2)	0.49181(16)	0.0263(7)
C15	0.6627(2)	0.4469(2)	0.53570(18)	0.0395(9)
C16	0.8000(2)	0.5657(2)	0.54519(16)	0.0302(7)
C17	0.6233(2)	0.6067(2)	0.48975(17)	0.0345(8)
C19	0.1848(2)	0.40647(19)	0.11911(17)	0.0245(7)
C20	0.1353(2)	0.3935(2)	0.20363(17)	0.0326(8)
C21	0.2565(2)	0.3229(2)	0.10972(18)	0.0339(8)
C22	0.1011(2)	0.4005(2)	0.04972(18)	0.0321(7)
C23	0.2979(2)	0.5510(2)	0.01240(16)	0.0262(7)
C24	0.3407(3)	0.4642(2)	0.96912(18)	0.0363(8)
C25	0.3864(2)	0.6211(2)	0.01770(18)	0.0352(8)
C26	0.2115(2)	0.5898(2)	0.95592(17)	0.0318(7)
C27	0.1826(2)	0.61467(19)	0.16685(16)	0.0216(6)
C28	0.1872(2)	0.6056(2)	0.26297(15)	0.0264(7)
C29	0.2313(2)	0.70947(19)	0.14867(17)	0.0258(7)
C30	0.0713(2)	0.6178(2)	0.13467(17)	0.0282(7)

	x/a	y/b	z/c	U(eq)
C6	0.8044(2)	0.3824(2)	0.38043(18)	0.0300(7)
C7	0.7271(3)	0.3034(2)	0.3919(2)	0.0430(9)
C8	0.8474(3)	0.3669(2)	0.29392(19)	0.0451(10)
C9	0.8918(2)	0.3706(2)	0.44660(19)	0.0382(8)
C10	0.8209(2)	0.5907(2)	0.33447(16)	0.0247(7)
C11	0.9335(2)	0.5866(2)	0.36305(17)	0.0325(8)
C12	0.7798(2)	0.6868(2)	0.35496(18)	0.0293(7)
C13	0.8115(2)	0.5832(2)	0.23821(16)	0.0333(8)
C14	0.7082(2)	0.5322(2)	0.49181(16)	0.0263(7)
C15	0.6627(2)	0.4469(2)	0.53570(18)	0.0395(9)
C16	0.8000(2)	0.5657(2)	0.54519(16)	0.0302(7)
C17	0.6233(2)	0.6067(2)	0.48975(17)	0.0345(8)
C19	0.1848(2)	0.40647(19)	0.11911(17)	0.0245(7)
C20	0.1353(2)	0.3935(2)	0.20363(17)	0.0326(8)
C21	0.2565(2)	0.3229(2)	0.10972(18)	0.0339(8)
C22	0.1011(2)	0.4005(2)	0.04972(18)	0.0321(7)
C23	0.2979(2)	0.5510(2)	0.01240(16)	0.0262(7)
C24	0.3407(3)	0.4642(2)	0.96912(18)	0.0363(8)
C25	0.3864(2)	0.6211(2)	0.01770(18)	0.0352(8)
C26	0.2115(2)	0.5898(2)	0.95592(17)	0.0318(7)
C27	0.1826(2)	0.61467(19)	0.16685(16)	0.0216(6)
C28	0.1872(2)	0.6056(2)	0.26297(15)	0.0264(7)
C29	0.2313(2)	0.70947(19)	0.14867(17)	0.0258(7)
C30	0.0713(2)	0.6178(2)	0.13467(17)	0.0282(7)

Table 5. Bond lengths (Å) for sb032211.

Pd1-P5	2.337(3)	Pd1-Br4	2.465(3)
Pd1-Br3	2.477(4)	Pd1-Pd2	2.669(4)
Pd2-P18	2.322(2)	Pd2-Br3	2.477(4)
Pd2-Br4	2.480(3)	Br3A-Cu2	2.406(9)
Br3A-Cu1	2.409(9)	Br4A-Cu2	2.446(7)
Br4A-Cu1	2.478(8)	Cu1-P5	2.159(7)
Cu1-Cu2	2.975(9)	Cu2-P18	2.201(6)
P5-C6	1.900(3)	P5-C14	1.906(3)
P5-C10	1.909(3)	P18-C23	1.903(3)
P18-C19	1.907(3)	P18-C27	1.907(3)
C6-C8	1.535(4)	C6-C7	1.540(4)
C6-C9	1.544(4)	C7-H7A	1.0899
C7-H7B	1.0899	C7-H7C	1.0899
C8-H8A	1.0899	C8-H8B	1.0899
C8-H8C	1.0899	C9-H9A	1.0899
C9-H9B	1.0899	C9-H9C	1.0899
C10-C12	1.526(4)	C10-C11	1.533(4)
C10-C13	1.550(4)	C11-H11A	1.0899
C11-H11B	1.0899	C11-H11C	1.0899
C12-H12A	1.0899	C12-H12B	1.0899
C12-H12C	1.0899	C13-H13A	1.0899
C13-H13B	1.0899	C13-H13C	1.0899
C14-C16	1.531(4)	C14-C15	1.547(4)
C14-C17	1.548(4)	C15-H15A	1.0899
C15-H15B	1.0899	C15-H15C	1.0899
C16-H16A	1.0899	C16-H16B	1.0899
C16-H16C	1.0899	C17-H17A	1.0899
C17-H17B	1.0899	C17-H17C	1.0899
C19-C20	1.538(4)	C19-C22	1.538(4)

C19-C21	1.539(4)	C20-H20A	1.0899
C20-H20B	1.0899	C20-H20C	1.0899
C21-H21A	1.0899	C21-H21B	1.0899
C21-H21C	1.0899	C22-H22A	1.0899
C22-H22B	1.0899	C22-H22C	1.0899
C23-C26	1.530(4)	C23-C25	1.539(4)
C23-C24	1.548(4)	C24-H24A	1.0899
C24-H24B	1.0899	C24-H24C	1.0899
C25-H25A	1.0899	C25-H25B	1.0899
C25-H25C	1.0899	C26-H26A	1.0899
C26-H26B	1.0899	C26-H26C	1.0899
C27-C30	1.533(4)	C27-C29	1.540(4)
C27-C28	1.548(3)	C28-H28A	1.0899
C28-H28B	1.0899	C28-H28C	1.0899
C29-H29A	1.0899	C29-H29B	1.0899
C29-H29C	1.0899	C30-H30A	1.0899
C30-H30B	1.0899	C30-H30C	1.0899

Table 6. Bond angles (°) for sb032211.

P5-Pd1-Br4	119.08(11)	P5-Pd1-Br3	125.82(12)
Br4-Pd1-Br3	115.01(16)	P5-Pd1-Pd2	176.34(8)
Br4-Pd1-Pd2	57.61(9)	Br3-Pd1-Pd2	57.41(11)
P18-Pd2-Br3	124.76(13)	P18-Pd2-Br4	120.78(10)
Br3-Pd2-Br4	114.45(14)	P18-Pd2-Pd1	177.84(9)
Br3-Pd2-Pd1	57.39(10)	Br4-Pd2-Pd1	57.07(8)
Pd1-Br3-Pd2	65.19(12)	Cu2-Br3A-Cu1	76.3(3)
Pd1-Br4-Pd2	65.32(10)	Cu2-Br4A-Cu1	74.3(3)
P5-Cu1-Br3A	131.4(3)	P5-Cu1-Br4A	124.5(3)
Br3A-Cu1-Br4A	104.1(3)	P5-Cu1-Cu2	176.7(3)
Br3A-Cu1-Cu2	51.8(2)	Br4A-Cu1-Cu2	52.3(2)
P18-Cu2-Br3A	133.7(3)	P18-Cu2-Br4A	121.1(3)
Br3A-Cu2-Br4A	105.2(3)	P18-Cu2-Cu1	174.4(3)
Br3A-Cu2-Cu1	51.9(2)	Br4A-Cu2-Cu1	53.32(19)
C6-P5-C14	109.12(13)	C6-P5-C10	108.93(13)
C14-P5-C10	108.32(13)	C6-P5-Cu1	111.52(18)
C14-P5-Cu1	111.82(19)	C10-P5-Cu1	107.02(17)
C6-P5-Pd1	112.83(11)	C14-P5-Pd1	109.96(11)
C10-P5-Pd1	107.57(10)	Cu1-P5-Pd1	1.9(2)
C23-P18-C19	109.39(13)	C23-P18-C27	108.50(12)
C19-P18-C27	108.56(13)	C23-P18-Cu2	108.32(18)
C19-P18-Cu2	111.09(18)	C27-P18-Cu2	110.93(17)
C23-P18-Pd2	108.96(11)	C19-P18-Pd2	112.87(10)
C27-P18-Pd2	108.47(10)	Cu2-P18-Pd2	2.5(2)
C8-C6-C7	105.5(3)	C8-C6-C9	108.5(3)
C7-C6-C9	108.2(2)	C8-C6-P5	108.5(2)
C7-C6-P5	109.3(2)	C9-C6-P5	116.3(2)
C6-C7-H7A	109.5	C6-C7-H7B	109.5
H7A-C7-H7B	109.5	C6-C7-H7C	109.5
H7A-C7-H7C	109.5	H7B-C7-H7C	109.5
C6-C8-H8A	109.5	C6-C8-H8B	109.5
H8A-C8-H8B	109.5	C6-C8-H8C	109.5
H8A-C8-H8C	109.5	H8B-C8-H8C	109.5
C6-C9-H9A	109.5	C6-C9-H9B	109.5
H9A-C9-H9B	109.5	C6-C9-H9C	109.5
H9A-C9-H9C	109.5	H9B-C9-H9C	109.5
C12-C10-C11	108.4(2)	C12-C10-C13	105.2(2)

C11-C10-C13	109.6(2)	C12-C10-P5	109.39(18)
C11-C10-P5	115.8(2)	C13-C10-P5	107.9(2)
C10-C11-H11A	109.5	C10-C11-H11B	109.5
H11A-C11-H11B	109.5	C10-C11-H11C	109.5
H11A-C11-H11C	109.5	H11B-C11-H11C	109.5
C10-C12-H12A	109.5	C10-C12-H12B	109.5
H12A-C12-H12B	109.5	C10-C12-H12C	109.5
H12A-C12-H12C	109.5	H12B-C12-H12C	109.5
C10-C13-H13A	109.5	C10-C13-H13B	109.5
H13A-C13-H13B	109.5	C10-C13-H13C	109.5
H13A-C13-H13C	109.5	H13B-C13-H13C	109.5
C16-C14-C15	107.8(2)	C16-C14-C17	110.1(3)
C15-C14-C17	105.7(2)	C16-C14-P5	116.04(19)
C15-C14-P5	108.3(2)	C17-C14-P5	108.45(19)
C14-C15-H15A	109.5	C14-C15-H15B	109.5
H15A-C15-H15B	109.5	C14-C15-H15C	109.5
H15A-C15-H15C	109.5	H15B-C15-H15C	109.5
C14-C16-H16A	109.5	C14-C16-H16B	109.5
H16A-C16-H16B	109.5	C14-C16-H16C	109.5
H16A-C16-H16C	109.5	H16B-C16-H16C	109.5
C14-C17-H17A	109.5	C14-C17-H17B	109.5
H17A-C17-H17B	109.5	C14-C17-H17C	109.5
H17A-C17-H17C	109.5	H17B-C17-H17C	109.5
C20-C19-C22	108.6(2)	C20-C19-C21	105.7(2)
C22-C19-C21	108.0(2)	C20-C19-P18	108.85(19)
C22-C19-P18	116.04(19)	C21-C19-P18	109.2(2)
C19-C20-H20A	109.5	C19-C20-H20B	109.5
H20A-C20-H20B	109.5	C19-C20-H20C	109.5
H20A-C20-H20C	109.5	H20B-C20-H20C	109.5
C19-C21-H21A	109.5	C19-C21-H21B	109.5
H21A-C21-H21B	109.5	C19-C21-H21C	109.5
H21A-C21-H21C	109.5	H21B-C21-H21C	109.5
C19-C22-H22A	109.5	C19-C22-H22B	109.5
H22A-C22-H22B	109.5	C19-C22-H22C	109.5
H22A-C22-H22C	109.5	H22B-C22-H22C	109.5
C26-C23-C25	109.6(2)	C26-C23-C24	107.6(2)
C25-C23-C24	105.6(2)	C26-C23-P18	116.49(19)
C25-C23-P18	108.59(19)	C24-C23-P18	108.5(2)
C23-C24-H24A	109.5	C23-C24-H24B	109.5
H24A-C24-H24B	109.5	C23-C24-H24C	109.5
H24A-C24-H24C	109.5	H24B-C24-H24C	109.5
C23-C25-H25A	109.5	C23-C25-H25B	109.5
H25A-C25-H25B	109.5	C23-C25-H25C	109.5
H25A-C25-H25C	109.5	H25B-C25-H25C	109.5
C23-C26-H26A	109.5	C23-C26-H26B	109.5
H26A-C26-H26B	109.5	C23-C26-H26C	109.5
H26A-C26-H26C	109.5	H26B-C26-H26C	109.5
C30-C27-C29	107.9(2)	C30-C27-C28	109.8(2)
C29-C27-C28	105.2(2)	C30-C27-P18	115.63(19)
C29-C27-P18	109.74(18)	C28-C27-P18	108.01(19)
C27-C28-H28A	109.5	C27-C28-H28B	109.5
H28A-C28-H28B	109.5	C27-C28-H28C	109.5
H28A-C28-H28C	109.5	H28B-C28-H28C	109.5
C27-C29-H29A	109.5	C27-C29-H29B	109.5
H29A-C29-H29B	109.5	C27-C29-H29C	109.5
H29A-C29-H29C	109.5	H29B-C29-H29C	109.5

C27-C30-H30A	109.5	C27-C30-H30B	109.5
H30A-C30-H30B	109.5	C27-C30-H30C	109.5
H30A-C30-H30C	109.5	H30B-C30-H30C	109.5

Table 7. Torsion angles (°) for sb032211.

P5-Pd1-Pd2-P18	-21.(4)	Br4-Pd1-Pd2-P18	5.(3)
Br3-Pd1-Pd2-P18	-174.(3)	P5-Pd1-Pd2-Br3	152.8(17)
Br4-Pd1-Pd2-Br3	178.55(14)	P5-Pd1-Pd2-Br4	-25.7(17)
Br3-Pd1-Pd2-Br4	-178.55(14)	P5-Pd1-Br3-Pd2	-177.94(13)
Br4-Pd1-Br3-Pd2	-1.35(13)	P18-Pd2-Br3-Pd1	179.71(12)
Br4-Pd2-Br3-Pd1	1.34(13)	P5-Pd1-Br4-Pd2	178.18(12)
Br3-Pd1-Br4-Pd2	1.35(13)	P18-Pd2-Br4-Pd1	-179.78(12)
Br3-Pd2-Br4-Pd1	-1.35(13)	Cu2-Br3A-Cu1-P5	178.8(4)
Cu2-Br3A-Cu1-Br4A	-1.0(3)	Cu2-Br4A-Cu1-P5	-178.9(4)
Cu2-Br4A-Cu1-Br3A	0.9(3)	Cu1-Br3A-Cu2-P18	-179.1(4)
Cu1-Br3A-Cu2-Br4A	1.0(3)	Cu1-Br4A-Cu2-P18	179.1(3)
Cu1-Br4A-Cu2-Br3A	-0.9(3)	P5-Cu1-Cu2-P18	8.(8)
Br3A-Cu1-Cu2-P18	173.(3)	Br4A-Cu1-Cu2-P18	-8.(3)
P5-Cu1-Cu2-Br3A	-165.(5)	Br4A-Cu1-Cu2-Br3A	178.8(3)
P5-Cu1-Cu2-Br4A	16.(5)	Br3A-Cu1-Cu2-Br4A	-178.8(3)
Br3A-Cu1-P5-C6	16.3(5)	Br4A-Cu1-P5-C6	-163.9(3)
Cu2-Cu1-P5-C6	-180.(100)	Br3A-Cu1-P5-C14	-106.2(4)
Br4A-Cu1-P5-C14	73.6(4)	Cu2-Cu1-P5-C14	58.(5)
Br3A-Cu1-P5-C10	135.4(4)	Br4A-Cu1-P5-C10	-44.9(4)
Cu2-Cu1-P5-C10	-61.(5)	Br3A-Cu1-P5-Pd1	-118.(6)
Br4A-Cu1-P5-Pd1	62.(5)	Cu2-Cu1-P5-Pd1	47.(5)
Br4-Pd1-P5-C6	-169.54(13)	Br3-Pd1-P5-C6	6.92(18)
Pd2-Pd1-P5-C6	-144.7(17)	Br4-Pd1-P5-C14	68.38(15)
Br3-Pd1-P5-C14	-115.16(17)	Pd2-Pd1-P5-C14	93.2(17)
Br4-Pd1-P5-C10	-49.38(15)	Br3-Pd1-P5-C10	127.08(15)
Pd2-Pd1-P5-C10	-24.6(17)	Br4-Pd1-P5-Cu1	-123.(6)
Br3-Pd1-P5-Cu1	54.(5)	Pd2-Pd1-P5-Cu1	-98.(6)
Br3A-Cu2-P18-C23	-102.1(4)	Br4A-Cu2-P18-C23	77.9(3)
Cu1-Cu2-P18-C23	86.(3)	Br3A-Cu2-P18-C19	18.1(5)
Br4A-Cu2-P18-C19	-161.9(3)	Cu1-Cu2-P18-C19	-154.(3)
Br3A-Cu2-P18-C27	138.9(4)	Br4A-Cu2-P18-C27	-41.1(3)
Cu1-Cu2-P18-C27	-33.(3)	Br3A-Cu2-P18-Pd2	153.(5)
Br4A-Cu2-P18-Pd2	-27.(4)	Cu1-Cu2-P18-Pd2	-19.(2)
Br3-Pd2-P18-C23	-95.18(16)	Br4-Pd2-P18-C23	83.09(15)
Pd1-Pd2-P18-C23	78.(3)	Br3-Pd2-P18-C19	26.55(17)
Br4-Pd2-P18-C19	-155.18(13)	Pd1-Pd2-P18-C19	-160.(3)
Br3-Pd2-P18-C27	146.90(15)	Br4-Pd2-P18-C27	-34.84(15)
Pd1-Pd2-P18-C27	-40.(3)	Br3-Pd2-P18-Cu2	-19.(4)
Br4-Pd2-P18-Cu2	159.(5)	Pd1-Pd2-P18-Cu2	154.(7)
C14-P5-C6-C8	-166.9(2)	C10-P5-C6-C8	-48.8(3)
Cu1-P5-C6-C8	69.1(3)	Pd1-P5-C6-C8	70.5(2)
C14-P5-C6-C7	78.5(2)	C10-P5-C6-C7	-163.4(2)
Cu1-P5-C6-C7	-45.5(3)	Pd1-P5-C6-C7	-44.0(2)
C14-P5-C6-C9	-44.3(3)	C10-P5-C6-C9	73.7(2)
Cu1-P5-C6-C9	-168.4(3)	Pd1-P5-C6-C9	-166.9(2)
C6-P5-C10-C12	-164.79(19)	C14-P5-C10-C12	-46.2(2)
Cu1-P5-C10-C12	74.5(3)	Pd1-P5-C10-C12	72.6(2)
C6-P5-C10-C11	-42.0(2)	C14-P5-C10-C11	76.5(2)
Cu1-P5-C10-C11	-162.7(2)	Pd1-P5-C10-C11	-164.63(19)
C6-P5-C10-C13	81.2(2)	C14-P5-C10-C13	-160.20(19)
Cu1-P5-C10-C13	-39.5(3)	Pd1-P5-C10-C13	-41.4(2)

C6-P5-C14-C16	73.9(3)	C10-P5-C14-C16	-44.6(3)
Cu1-P5-C14-C16	-162.3(3)	Pd1-P5-C14-C16	-161.9(2)
C6-P5-C14-C15	-47.4(2)	C10-P5-C14-C15	-165.8(2)
Cu1-P5-C14-C15	76.5(3)	Pd1-P5-C14-C15	76.9(2)
C6-P5-C14-C17	-161.6(2)	C10-P5-C14-C17	80.0(2)
Cu1-P5-C14-C17	-37.7(3)	Pd1-P5-C14-C17	-37.3(2)
C23-P18-C19-C20	-166.06(19)	C27-P18-C19-C20	-47.8(2)
Cu2-P18-C19-C20	74.4(3)	Pd2-P18-C19-C20	72.5(2)
C23-P18-C19-C22	-43.3(2)	C27-P18-C19-C22	74.9(2)
Cu2-P18-C19-C22	-162.8(2)	Pd2-P18-C19-C22	-164.79(19)
C23-P18-C19-C21	79.0(2)	C27-P18-C19-C21	-162.81(18)
Cu2-P18-C19-C21	-40.6(3)	Pd2-P18-C19-C21	-42.5(2)
C19-P18-C23-C26	73.0(3)	C27-P18-C23-C26	-45.3(3)
Cu2-P18-C23-C26	-165.8(3)	Pd2-P18-C23-C26	-163.2(2)
C19-P18-C23-C25	-162.8(2)	C27-P18-C23-C25	79.0(2)
Cu2-P18-C23-C25	-41.6(3)	Pd2-P18-C23-C25	-39.0(2)
C19-P18-C23-C24	-48.5(2)	C27-P18-C23-C24	-166.8(2)
Cu2-P18-C23-C24	72.7(3)	Pd2-P18-C23-C24	75.3(2)
C23-P18-C27-C30	76.4(2)	C19-P18-C27-C30	-42.4(2)
Cu2-P18-C27-C30	-164.7(2)	Pd2-P18-C27-C30	-165.37(18)
C23-P18-C27-C29	-45.9(2)	C19-P18-C27-C29	-164.70(18)
Cu2-P18-C27-C29	73.0(2)	Pd2-P18-C27-C29	72.32(19)
C23-P18-C27-C28	-160.12(18)	C19-P18-C27-C28	81.1(2)
Cu2-P18-C27-C28	-41.2(3)	Pd2-P18-C27-C28	-41.9(2)

Table 8. Anisotropic atomic displacement parameters (Å^2) for sb032211.
The anisotropic atomic displacement factor exponent takes the form: $-2\pi^2[\,h^2\,a^{*2}\,U_{11} + ... + 2\,h\,k\,a^*\,b^*\,U_{12}\,]$

	U_{11}	U_{22}	U_{33}	U_{23}	U_{13}	U_{12}
Pd1	0.0123(5)	0.0113(5)	0.0130(4)	0.0007(3)	-0.0014(3)	-0.0002(3)
Pd2	0.0115(5)	0.0108(4)	0.0139(4)	-0.0002(3)	-0.0013(3)	-0.0008(3)
Br3	0.0178(6)	0.0167(6)	0.0350(5)	-0.0037(5)	-0.0108(4)	0.0020(4)
Br3A	0.0383(19)	0.0381(18)	0.070(3)	-0.0072(13)	-0.0276(17)	0.0000(11)
Br4	0.0192(5)	0.0175(5)	0.0366(8)	0.0045(5)	-0.0112(5)	-0.0024(4)
Br4A	0.0322(13)	0.0583(18)	0.051(2)	-0.0043(10)	-0.0172(12)	-0.0021(10)
Cu1	0.028(3)	0.040(2)	0.0283(19)	-0.0080(12)	0.0049(14)	-0.0101(13)
Cu2	0.039(3)	0.040(3)	0.031(2)	0.0084(14)	0.0082(16)	0.0079(16)
P5	0.0180(4)	0.0209(4)	0.0152(4)	-0.0001(3)	-0.0012(3)	-0.0002(3)
P18	0.0175(4)	0.0200(4)	0.0152(3)	0.0007(3)	-0.0009(3)	0.0010(3)
C6	0.0352(19)	0.0226(17)	0.0314(16)	-0.0005(13)	-0.0105(14)	0.0080(15)
C7	0.054(2)	0.0228(18)	0.050(2)	0.0054(15)	-0.0267(18)	-0.0021(17)
C8	0.056(2)	0.040(2)	0.0390(19)	-0.0109(16)	-0.0068(17)	0.0288(19)
C9	0.041(2)	0.031(2)	0.0412(18)	0.0012(14)	-0.0150(16)	0.0112(16)
C10	0.0231(16)	0.0314(18)	0.0196(14)	0.0041(12)	0.0022(12)	-0.0039(14)
C11	0.0215(17)	0.044(2)	0.0316(16)	0.0038(14)	-0.0008(13)	-0.0067(15)
C12	0.0301(18)	0.0218(17)	0.0355(16)	0.0041(13)	-0.0041(14)	-0.0074(14)
C13	0.0325(18)	0.047(2)	0.0204(14)	0.0073(14)	0.0057(13)	0.0013(16)
C14	0.0268(17)	0.0380(18)	0.0143(13)	-0.0027(13)	0.0017(12)	-0.0045(15)
C15	0.038(2)	0.056(2)	0.0243(16)	0.0085(15)	0.0024(14)	-0.0195(18)
C16	0.0310(18)	0.040(2)	0.0188(14)	-0.0048(13)	-0.0064(13)	-0.0046(15)
C17	0.0245(17)	0.057(2)	0.0222(15)	-0.0100(15)	0.0024(13)	0.0049(17)
C19	0.0276(17)	0.0198(16)	0.0253(15)	-0.0001(12)	-0.0098(13)	-0.0041(14)
C20	0.0389(19)	0.0303(18)	0.0281(16)	0.0041(13)	-0.0066(14)	-0.0160(16)
C21	0.044(2)	0.0183(17)	0.0384(17)	-0.0015(13)	-0.0157(15)	0.0008(16)
C22	0.0318(18)	0.0285(18)	0.0350(17)	-0.0036(14)	-0.0138(14)	-0.0020(15)
C23	0.0285(17)	0.0320(19)	0.0182(14)	0.0048(12)	0.0019(12)	0.0036(15)

	U_{11}	U_{22}	U_{33}	U_{23}	U_{13}	U_{12}
C24	0.039(2)	0.045(2)	0.0254(16)	-0.0041(15)	0.0093(15)	0.0157(18)
C25	0.0285(18)	0.051(2)	0.0266(16)	0.0116(14)	0.0076(14)	-0.0016(17)
C26	0.0358(18)	0.039(2)	0.0204(14)	0.0060(13)	-0.0053(13)	0.0057(16)
C27	0.0186(15)	0.0255(16)	0.0204(14)	-0.0027(12)	-0.0013(12)	0.0007(13)
C28	0.0252(16)	0.0349(18)	0.0193(14)	-0.0069(12)	0.0026(12)	-0.0026(15)
C29	0.0257(17)	0.0219(17)	0.0293(15)	-0.0014(12)	-0.0040(13)	0.0024(14)
C30	0.0177(15)	0.0367(19)	0.0299(16)	-0.0033(13)	-0.0048(13)	0.0040(14)

Table 9. Hydrogen atomic coordinates and isotropic atomic displacement parameters (Å^2) for sb032211.

	x/a	y/b	z/c	U(eq)
H7A	0.6999	0.3054	0.4552	0.064
H7B	0.7638	0.2369	0.3811	0.064
H7C	0.6629	0.3122	0.3476	0.064
H8A	0.7875	0.3788	0.2462	0.068
H8B	0.8751	0.2959	0.2893	0.068
H8C	0.9100	0.4151	0.2848	0.068
H9A	0.9453	0.4281	0.4419	0.057
H9B	0.9313	0.3054	0.4360	0.057
H9C	0.8606	0.3701	0.5085	0.057
H11A	0.9398	0.5897	0.4309	0.049
H11B	0.9739	0.6453	0.3370	0.049
H11C	0.9669	0.5220	0.3417	0.049
H12A	0.6984	0.6894	0.3394	0.044
H12B	0.8190	0.7390	0.3189	0.044
H12C	0.7927	0.7006	0.4212	0.044
H13A	0.8411	0.5163	0.2187	0.05
H13B	0.8550	0.6388	0.2104	0.05
H13C	0.7316	0.5891	0.2179	0.05
H15A	0.6029	0.4164	0.4956	0.059
H15B	0.6307	0.4686	0.5943	0.059
H15C	0.7224	0.3957	0.5482	0.059
H16A	0.8595	0.5130	0.5458	0.045
H16B	0.7768	0.5783	0.6087	0.045
H16C	0.8292	0.6299	0.5191	0.045
H17A	0.6522	0.6706	0.4631	0.052
H17B	0.5996	0.6200	0.5530	0.052
H17C	0.5583	0.5820	0.4518	0.052
H20A	0.1935	0.3992	0.2536	0.049
H20B	0.0998	0.3252	0.2058	0.049
H20C	0.0777	0.4469	0.2114	0.049
H21A	0.2906	0.3255	0.0489	0.051
H21B	0.2132	0.2587	0.1151	0.051
H21C	0.3164	0.3252	0.1585	0.051
H22A	0.0497	0.4596	0.0545	0.048
H22B	0.0583	0.3363	0.0564	0.048
H22C	0.1359	0.4016	-0.0108	0.048
H24A	0.3973	0.4308	0.0105	0.054
H24B	0.3763	0.4848	-0.0883	0.054
H24C	0.2789	0.4157	-0.0454	0.054
H25A	0.3584	0.6878	0.0392	0.053
H25B	0.4178	0.6294	-0.0437	0.053
H25C	0.4455	0.5956	0.0613	0.053
H26A	0.1505	0.5387	-0.0503	0.048
H26B	0.2404	0.6051	-0.1053	0.048

	x/a	y/b	z/c	U(eq)
H26C	0.1821	0.6532	-0.0168	0.048
H28A	0.1525	0.5402	0.2808	0.04
H28B	0.1459	0.6631	0.2901	0.04
H28C	0.2664	0.6072	0.2857	0.04
H29A	0.3122	0.7074	0.1665	0.039
H29B	0.1941	0.7632	0.1843	0.039
H29C	0.2221	0.7248	0.0824	0.039
H30A	0.0686	0.6241	0.0670	0.042
H30B	0.0333	0.6773	0.1617	0.042
H30C	0.0328	0.5541	0.1524	0.042

Tetra(tri-*tert*-butylphosphine)silverbromide cubane, Ag-cubane **317**
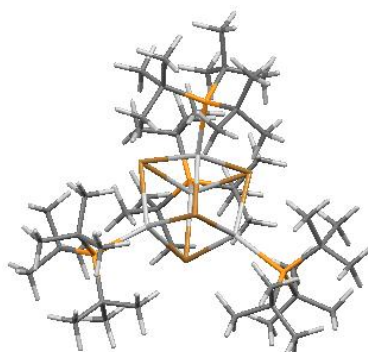
A clear pale bronze prism-like specimen of $C_{55}H_{116}Ag_4Br_4P_4$, approximate dimensions 0.030 mm x 0.160 mm x 0.200 mm, was used for the X-ray crystallographic analysis. The X-ray intensity data were measured on a Bruker Kappa Apex-II Duo system equipped with a graphite monochromator.

Table 1: Data collection details for sb150312.

Axis	dx/mm	2θ/°	ω/°	φ/°	χ/°	Width/°	Frames	Time/s	Wavelength/Å	Voltage/kV	Current/mA	Temperature/K
Phi	68.730	31.53	0.00	-273.75	-23.00	0.50	725	10.00	0.71073	50	30.0	100.02
Omega	68.730	-31.63	-58.52	97.34	-55.58	0.50	332	10.00	0.71073	50	30.0	100.02
Omega	68.730	-31.63	-60.91	-45.53	-49.82	0.50	260	10.00	0.71073	50	30.0	100.02
Omega	68.730	31.63	3.26	76.49	-52.08	0.50	331	10.00	0.71073	50	30.0	100.02
Omega	68.730	-31.63	-38.86	63.21	69.21	0.50	61	10.00	0.71073	50	30.0	100.02
Omega	68.730	-31.63	-62.25	-112.12	-47.34	0.50	330	10.00	0.71073	50	30.0	100.02
Omega	68.730	-31.63	-53.60	136.28	63.94	0.50	93	10.00	0.71073	50	30.0	100.02
Omega	68.730	31.63	-82.09	-127.96	35.97	0.50	162	10.00	0.71073	50	30.0	100.02
Omega	68.730	-31.63	-43.80	169.27	-77.44	0.50	101	10.00	0.71073	50	30.0	100.02
Omega	68.730	31.63	-11.21	-109.55	-33.93	0.50	341	10.00	0.71073	50	30.0	100.02
Omega	68.730	31.63	-10.47	-223.16	-34.44	0.50	340	10.00	0.71073	50	30.0	100.02
Omega	68.730	-31.63	-53.95	126.46	-54.17	0.50	271	10.00	0.71073	50	30.0	100.02
Omega	68.730	31.63	16.75	-164.43	-32.63	0.50	274	10.00	0.71073	50	30.0	100.02
Omega	68.730	31.63	4.85	-251.06	-55.84	0.50	302	10.00	0.71073	50	30.0	100.02
Phi	68.730	-14.37	0.00	-273.75	-23.00	0.50	725	10.00	0.71073	50	30.0	100.02
Omega	68.730	-31.63	-57.93	-59.10	-57.34	0.50	323	10.00	0.71073	50	30.0	100.02
Omega	68.730	31.63	15.19	-76.40	-39.61	0.50	294	10.00	0.71073	50	30.0	100.02

Axis	dx/mm	2θ/°	ω/°	φ/°	χ/°	Width/°	Frames	Time/s	Wavelength/Å	Voltage/kV	Current/mA	Temperature/K
Omega	68.730	31.63	-3.45	-11.77	-32.44	0.50	314	10.00	0.71073	50	30.0	100.02

A total of 5579 frames were collected. The total exposure time was 15.50 hours. The frames were integrated with the Bruker SAINT software package using a narrow-frame algorithm. The integration of the data using a trigonal unit cell yielded a total of 120779 reflections to a maximum θ angle of 27.58° (0.77 Å resolution), of which 5243 were independent (average redundancy 23.036, completeness = 99.6%, R_{int} = 4.32%, R_{sig} = 1.12%) and 4871 (92.90%) were greater than $2\sigma(F^2)$. The final cell constants of $\underline{a}$ = 13.9482(4) Å, $\underline{b}$ = 13.9482(4) Å, $\underline{c}$ = 60.5717(13) Å, volume = 10205.6(5) Å^3, are based upon the refinement of the XYZ-centroids of 9853 reflections above 20 σ(I) with 5.84° < 2θ < 54.95°. Data were corrected for absorption effects using the multi-scan method (SADABS). The ratio of minimum to maximum apparent transmission was 0.851. The calculated minimum and maximum transmission coefficients (based on crystal size) are 0.5322 and 0.8994.

The structure was solved and refined using the Bruker SHELXTL Software Package, using the space group R-3, with Z = 6 for the formula unit, $C_{55}H_{116}Ag_4Br_4P_4$. The final anisotropic full-matrix least-squares refinement on F^2 with 213 variables converged at R1 = 2.36%, for the observed data and wR2 = 5.56% for all data. The goodness-of-fit was 2.717. The largest peak in the final difference electron density synthesis was 0.979 e$^-$/Å^3 and the largest hole was -0.453 e$^-$/Å^3 with an RMS deviation of 0.075 e$^-$/Å^3. On the basis of the final model, the calculated density was 1.613 g/cm^3 and F(000), 5004 e$^-$

Table 2. Sample and crystal data for sb150312●

Identification code	sb150312	
Chemical formula	$C_{55}H_{116}Ag_4Br_4P_4$	
Formula weight	1652.48	
Temperature	100(2) K	
Wavelength	0.71073 Å	
Crystal size	0.030 x 0.160 x 0.200 mm	
Crystal habit	clear pale bronze prism	
Crystal system	Trigonal	
Space group	R -3	
Unit cell dimensions	a = 13.9482(4) Å	α = 90°
	b = 13.9482(4) Å	β = 90°
	c = 60.5717(13) Å	γ = 120°
Volume	10205.6(5) Å^3	
Z	6	
Density (calculated)	1.613 Mg/cm^3	
Absorption coefficient	3.609 mm^{-1}	
F(000)	5004	

Table 3. Data collection and structure refinement for sb150312●

Diffractometer	Bruker Kappa Apex-II Duo
Theta range for data collection	1.72 to 27.58°
Index ranges	-18<=h<=18, -18<=k<=18, -78<=l<=78
Reflections collected	120779
Independent reflections	5243 [R(int) = 0.0432]
Coverage of independent reflections	99.6%
Absorption correction	multi-scan
Max. and min. transmission	0.8994 and 0.5322
Structure solution technique	direct methods

Appendix

Structure solution program	SHELXS-97 (Sheldrick, 2008)
Refinement method	Full-matrix least-squares on F^2
Refinement program	SHELXL-97 (Sheldrick, 2008)
Function minimized	$\Sigma\, w(F_o^2 - F_c^2)^2$
Data / restraints / parameters	5243 / 7 / 213
Goodness-of-fit on F^2	2.717
Δ/σ_{max}	0.003
Final R indices	4871 data; I>2σ(I) R1 = 0.0236, wR2 = 0.0553
	all data R1 = 0.0267, wR2 = 0.0556
Weighting scheme	$w=1/[\sigma^2(F_o^2)+(0.0100P)^2+0.0000P]$ where $P=(F_o^2+2F_c^2)/3$
Largest diff. peak and hole	0.979 and -0.453 eÅ^{-3}
R.M.S. deviation from mean	0.075 eÅ^{-3}

Table 4. Atomic coordinates and equivalent isotropic atomic displacement parameters (Å^2) for sb150312.

U(eq) is defined as one third of the trace of the orthogonalized U_{ij} tensor.

	x/a	y/b	z/c	U(eq)
Ag1	0.6667	0.3333	0.118604(5)	0.02375(8)
Ag2	0.519281(14)	0.325961(15)	0.072531(3)	0.02391(6)
Br1	0.492341(19)	0.152117(18)	0.09837(4)	0.01991(6)
Br2	0.6667	0.3333	0.040984(7)	0.02116(9)
P1	0.6667	0.3333	0.158656(16)	0.01557(19)
P2	0.35534(5)	0.32382(5)	0.058572(9)	0.01579(12)
C1	0.62821(18)	0.19010(18)	0.16920(4)	0.0191(5)
C2	0.6575(2)	0.1834(2)	0.19337(4)	0.0261(5)
C3	0.6843(2)	0.14356(19)	0.15405(4)	0.0244(5)
C4	0.50329(19)	0.11169(19)	0.16594(4)	0.0251(5)
C5	0.30229(19)	0.23178(18)	0.03311(4)	0.0199(5)
C6	0.3789(2)	0.2915(2)	0.01333(4)	0.0252(5)
C7	0.3148(2)	0.12970(19)	0.03731(4)	0.0271(5)
C8	0.1823(2)	0.1948(2)	0.02642(4)	0.0263(5)
C9	0.24294(19)	0.26807(19)	0.08048(4)	0.0215(5)
C10	0.1928(2)	0.1412(2)	0.08247(4)	0.0271(5)
C11	0.14833(19)	0.2933(2)	0.07716(4)	0.0264(5)
C12	0.2993(2)	0.3150(2)	0.10296(4)	0.0279(6)
C13	0.39135(18)	0.47028(17)	0.05075(4)	0.0188(5)
C14	0.50675(19)	0.52690(19)	0.03984(4)	0.0237(5)
C15	0.4057(2)	0.53734(19)	0.07197(4)	0.0243(5)
C16	0.3082(2)	0.4791(2)	0.03556(4)	0.0245(5)
C21	0.1661(4)	0.6068(8)	0.1353(2)	0.074(3)
C22	0.3590(4)	0.7408(4)	0.13392(10)	0.0674(16)
C23	0.2976(5)	0.5453(4)	0.13489(11)	0.085(2)
C24	0.5015(5)	0.6791(8)	0.1337(7)	0.123(14)
C24A	0.4902(5)	0.6766(7)	0.1366(6)	0.084(8)

Table 5. Bond lengths (Å) for sb150312.

Ag1-P1	2.4260(10)	Ag1-Br1#1	2.7671(3)
Ag1-Br1#4	2.7671(3)	Ag1-Br1	2.7672(3)
Ag2-P2	2.4242(6)	Ag2-Br1	2.7494(3)
Ag2-Br2	2.7707(3)	Ag2-Br1#4	2.7833(3)
Br1-Ag2#1	2.7832(3)	Br2-Ag2#1	2.7708(3)
Br2-Ag2#4	2.7708(3)	P1-C1#1	1.901(2)
P1-C1	1.901(2)	P1-C1#4	1.901(2)
P2-C9	1.898(2)	P2-C13	1.904(2)
P2-C5	1.904(2)	C1-C2	1.536(3)

C1-C4	1.538(3)	C1-C3	1.544(3)
C2-H2A	1.0899	C2-H2B	1.0899
C2-H2C	1.0899	C3-H3A	1.0899
C3-H3B	1.0899	C3-H3C	1.0899
C4-H4A	1.0899	C4-H4B	1.0899
C4-H4C	1.0899	C5-C8	1.540(3)
C5-C7	1.540(3)	C5-C6	1.543(3)
C6-H6A	1.0899	C6-H6B	1.0899
C6-H6C	1.0899	C7-H7A	1.0899
C7-H7B	1.0899	C7-H7C	1.0899
C8-H8A	1.0899	C8-H8B	1.0899
C8-H8C	1.0899	C9-C11	1.540(3)
C9-C12	1.545(3)	C9-C10	1.548(3)
C10-H10A	1.0899	C10-H10B	1.0899
C10-H10C	1.0899	C11-H11A	1.0899
C11-H11B	1.0899	C11-H11C	1.0899
C12-H12A	1.0899	C12-H12B	1.0899
C12-H12C	1.0899	C13-C16	1.533(3)
C13-C15	1.542(3)	C13-C14	1.543(3)
C14-H14A	1.0899	C14-H14B	1.0899
C14-H14C	1.0899	C15-H15A	1.0899
C15-H15B	1.0899	C15-H15C	1.0899
C16-H16A	1.0899	C16-H16B	1.0899
C16-H16C	1.0899	C21-C22#2	1.229(7)
C21-C23#3	1.247(8)	C21-C24#3	1.601(11)
C22-C21#3	1.229(8)	C22-C23#2	1.263(7)
C22-C23#3	1.368(7)	C22-C24#2	1.478(8)
C22-C22#2	1.576(8)	C22-C22#3	1.576(8)
C23-C21#2	1.247(8)	C23-C22#3	1.263(7)
C23-C22#2	1.368(7)	C23-C24#3	1.463(9)
C24-C23#2	1.463(9)	C24-C22#3	1.478(8)
C24-C21#2	1.601(11)		

Symmetry transformations used to generate equivalent atoms:

#1   x-y+1, -y, z

#2   x-y+1, -y+1, z

#3   -x, y+1, z

#4   -x+1, y+1, z

Table 6. Bond angles (°) for sb150312.

P1-Ag1-Br1#1	116.286(7)	P1-Ag1-Br1#4	116.286(7)
Br1#1-Ag1-Br1#4	101.878(9)	P1-Ag1-Br1	116.290(7)
Br1#1-Ag1-Br1	101.875(9)	Br1#4-Ag1-Br1	101.875(9)
P2-Ag2-Br1	118.396(16)	P2-Ag2-Br2	115.958(16)
Br1-Ag2-Br2	101.362(8)	P2-Ag2-Br1#4	115.959(16)
Br1-Ag2-Br1#4	101.915(11)	Br2-Ag2-Br1#4	100.518(8)
Ag2-Br1-Ag1	77.076(8)	Ag2-Br1-Ag2#1	77.819(9)
Ag1-Br1-Ag2#1	76.520(8)	Ag2-Br2-Ag2#1	77.673(11)
Ag2-Br2-Ag2#4	77.672(11)	Ag2#1-Br2-Ag2#4	77.671(11)
C1#1-P1-C1	109.32(7)	C1#1-P1-C1#4	109.32(7)
C1-P1-C1#4	109.32(7)	C1#1-P1-Ag1	109.62(7)
C1-P1-Ag1	109.62(7)	C1#4-P1-Ag1	109.62(7)
C9-P2-C13	109.52(10)	C9-P2-C5	109.10(10)
C13-P2-C5	109.09(10)	C9-P2-Ag2	110.00(7)
C13-P2-Ag2	109.41(7)	C5-P2-Ag2	109.70(7)

C2-C1-C4	108.66(18)	C2-C1-C3	109.58(19)
C4-C1-C3	104.89(18)	C2-C1-P1	116.13(16)
C4-C1-P1	109.16(15)	C3-C1-P1	107.83(15)
C1-C2-H2A	109.5	C1-C2-H2B	109.5
H2A-C2-H2B	109.5	C1-C2-H2C	109.5
H2A-C2-H2C	109.5	H2B-C2-H2C	109.5
C1-C3-H3A	109.5	C1-C3-H3B	109.5
H3A-C3-H3B	109.5	C1-C3-H3C	109.5
H3A-C3-H3C	109.5	H3B-C3-H3C	109.5
C1-C4-H4A	109.5	C1-C4-H4B	109.5
H4A-C4-H4B	109.5	C1-C4-H4C	109.5
H4A-C4-H4C	109.5	H4B-C4-H4C	109.5
C8-C5-C7	109.94(19)	C8-C5-C6	108.65(19)
C7-C5-C6	105.06(19)	C8-C5-P2	115.46(16)
C7-C5-P2	107.71(15)	C6-C5-P2	109.51(15)
C5-C6-H6A	109.5	C5-C6-H6B	109.5
H6A-C6-H6B	109.5	C5-C6-H6C	109.5
H6A-C6-H6C	109.5	H6B-C6-H6C	109.5
C5-C7-H7A	109.5	C5-C7-H7B	109.5
H7A-C7-H7B	109.5	C5-C7-H7C	109.5
H7A-C7-H7C	109.5	H7B-C7-H7C	109.5
C5-C8-H8A	109.5	C5-C8-H8B	109.5
H8A-C8-H8B	109.5	C5-C8-H8C	109.5
H8A-C8-H8C	109.5	H8B-C8-H8C	109.5
C11-C9-C12	109.3(2)	C11-C9-C10	108.82(19)
C12-C9-C10	105.02(19)	C11-C9-P2	116.22(16)
C12-C9-P2	107.53(16)	C10-C9-P2	109.33(16)
C9-C10-H10A	109.5	C9-C10-H10B	109.5
H10A-C10-H10B	109.5	C9-C10-H10C	109.5
H10A-C10-H10C	109.5	H10B-C10-H10C	109.5
C9-C11-H11A	109.5	C9-C11-H11B	109.5
H11A-C11-H11B	109.5	C9-C11-H11C	109.5
H11A-C11-H11C	109.5	H11B-C11-H11C	109.5
C9-C12-H12A	109.5	C9-C12-H12B	109.5
H12A-C12-H12B	109.5	C9-C12-H12C	109.5
H12A-C12-H12C	109.5	H12B-C12-H12C	109.5
C16-C13-C15	108.99(19)	C16-C13-C14	109.82(19)
C15-C13-C14	105.11(18)	C16-C13-P2	115.56(15)
C15-C13-P2	109.16(15)	C14-C13-P2	107.69(15)
C13-C14-H14A	109.5	C13-C14-H14B	109.5
H14A-C14-H14B	109.5	C13-C14-H14C	109.5
H14A-C14-H14C	109.5	H14B-C14-H14C	109.5
C13-C15-H15A	109.5	C13-C15-H15B	109.5
H15A-C15-H15B	109.5	C13-C15-H15C	109.5
H15A-C15-H15C	109.5	H15B-C15-H15C	109.5
C13-C16-H16A	109.5	C13-C16-H16B	109.5
H16A-C16-H16B	109.5	C13-C16-H16C	109.5
H16A-C16-H16C	109.5	H16B-C16-H16C	109.5
C22#2-C21-C23#3	61.4(3)	C22#2-C21-C24#3	61.3(5)
C23#3-C21-C24#3	122.6(6)	C21#3-C22-C23#2	60.0(3)
C21#3-C22-C23#3	133.0(6)	C23#2-C22-C23#3	165.5(7)
C21#3-C22-C24#2	71.8(7)	C23#2-C22-C24#2	131.8(6)
C23#3-C22-C24#2	61.7(3)	C21#3-C22-C22#2	174.6(6)
C23#2-C22-C22#2	116.3(5)	C23#3-C22-C22#2	50.2(4)
C24#2-C22-C22#2	111.8(5)	C21#3-C22-C22#3	116.3(5)
C23#2-C22-C22#3	56.3(5)	C23#3-C22-C22#3	110.2(4)

C24#2-C22-C22#3	171.8(5)	C22#2-C22-C22#3	60.0010(10)
C21#2-C23-C22#3	58.6(3)	C21#2-C23-C22#2	132.1(7)
C22#3-C23-C22#2	73.4(6)	C21#2-C23-C24#3	165.0(7)
C22#3-C23-C24#3	136.1(7)	C22#2-C23-C24#3	62.8(3)
C23#2-C24-C22#3	55.4(2)	C23#2-C24-C21#2	102.0(5)
C22#3-C24-C21#2	46.9(4)		

Symmetry transformations used to generate equivalent atoms:

#1   x-y+1, -y, z

#2   x-y+1, -y+1, z

#3   -x, y+1, z

#4   -x+1, y+1, z

Table 7. Torsion angles (°) for sb150312.

P2-Ag2-Br1-Ag1	-140.834(18)	Br2-Ag2-Br1-Ag1	91.130(8)
Br1#2-Ag2-Br1-Ag1	-12.326(8)	P2-Ag2-Br1-Ag2#1	140.419(17)
Br2-Ag2-Br1-Ag2#1	12.383(9)	Br1#2-Ag2-Br1-Ag2#1	-91.073(8)
P1-Ag1-Br1-Ag2	139.887(5)	Br1#1-Ag1-Br1-Ag2	-92.622(8)
Br1#2-Ag1-Br1-Ag2	12.397(9)	P1-Ag1-Br1-Ag2#1	-139.762(5)
Br1#1-Ag1-Br1-Ag2#1	-12.271(9)	Br1#2-Ag1-Br1-Ag2#1	92.748(8)
P2-Ag2-Br2-Ag2#1	-142.039(18)	Br1-Ag2-Br2-Ag2#1	-12.446(8)
Br1#2-Ag2-Br2-Ag2#1	92.120(6)	P2-Ag2-Br2-Ag2#2	138.095(18)
Br1-Ag2-Br2-Ag2#2	-92.312(6)	Br1#2-Ag2-Br2-Ag2#2	12.254(8)
Br1#1-Ag1-P1-C1#1	43.04(7)	Br1#2-Ag1-P1-C1#1	-76.96(7)
Br1-Ag1-P1-C1#1	163.04(7)	Br1#1-Ag1-P1-C1	-76.96(7)
Br1#2-Ag1-P1-C1	163.04(7)	Br1-Ag1-P1-C1	43.04(7)
Br1#1-Ag1-P1-C1#2	163.04(7)	Br1#2-Ag1-P1-C1#2	43.04(7)
Br1-Ag1-P1-C1#2	-76.96(7)	Br1-Ag2-P2-C9	39.00(8)
Br2-Ag2-P2-C9	159.81(8)	Br1#2-Ag2-P2-C9	-82.62(8)
Br1-Ag2-P2-C13	159.35(7)	Br2-Ag2-P2-C13	-79.84(8)
Br1#2-Ag2-P2-C13	37.73(8)	Br1-Ag2-P2-C5	-81.01(8)
Br2-Ag2-P2-C5	39.81(8)	Br1#2-Ag2-P2-C5	157.38(7)
C1#1-P1-C1-C2	42.15(19)	C1#2-P1-C1-C2	-77.49(15)
Ag1-P1-C1-C2	162.33(14)	C1#1-P1-C1-C4	165.36(12)
C1#2-P1-C1-C4	45.7(2)	Ag1-P1-C1-C4	-74.46(16)
C1#1-P1-C1-C3	-81.2(2)	C1#2-P1-C1-C3	159.15(15)
Ag1-P1-C1-C3	38.97(16)	C9-P2-C5-C8	42.31(19)
C13-P2-C5-C8	-77.29(19)	Ag2-P2-C5-C8	162.87(15)
C9-P2-C5-C7	-80.95(18)	C13-P2-C5-C7	159.44(16)
Ag2-P2-C5-C7	39.60(17)	C9-P2-C5-C6	165.31(15)
C13-P2-C5-C6	45.70(18)	Ag2-P2-C5-C6	-74.14(16)
C13-P2-C9-C11	41.9(2)	C5-P2-C9-C11	-77.41(19)
Ag2-P2-C9-C11	162.21(15)	C13-P2-C9-C12	-80.95(18)
C5-P2-C9-C12	159.71(16)	Ag2-P2-C9-C12	39.34(17)
C13-P2-C9-C10	165.55(16)	C5-P2-C9-C10	46.21(18)
Ag2-P2-C9-C10	-74.16(16)	C9-P2-C13-C16	-76.77(19)
C5-P2-C13-C16	42.6(2)	Ag2-P2-C13-C16	162.59(15)
C9-P2-C13-C15	46.45(18)	C5-P2-C13-C15	165.80(15)
Ag2-P2-C13-C15	-74.19(15)	C9-P2-C13-C14	160.06(15)
C5-P2-C13-C14	-80.59(17)	Ag2-P2-C13-C14	39.42(16)

Symmetry transformations used to generate equivalent atoms:

#1   x-y+1, -y, z

#2   -x+1, y+1, z

349

Table 8. Anisotropic atomic displacement parameters (Å^2) for sb150312.
The anisotropic atomic displacement factor exponent takes the form: $-2\pi^2[\, h^2\, a^{*2}\, U_{11} + ... + 2\, h\, k\, a^*\, b^*\, U_{12}\,]$

	U$_{11}$	U$_{22}$	U$_{33}$	U$_{23}$	U$_{13}$	U$_{12}$
Ag1	0.02698(11)	0.02698(11)	0.01731(15)	0	0	0.01349(5)
Ag2	0.01984(10)	0.02624(10)	0.02848(10)	0.00108(7)	-0.00377(7)	0.01364(8)
Br1	0.02069(12)	0.01907(11)	0.02091(11)	-0.00019(9)	-0.00101(9)	0.01063(9)
Br2	0.01941(12)	0.01941(12)	0.0247(2)	0	0	0.00971(6)
P1	0.0155(3)	0.0155(3)	0.0157(5)	0	0	0.00775(14)
P2	0.0144(3)	0.0149(3)	0.0179(3)	0.0020(2)	-0.0004(2)	0.0072(2)
C1	0.0191(11)	0.0161(11)	0.0223(11)	0.0024(9)	0.0010(9)	0.0090(9)
C2	0.0287(13)	0.0257(13)	0.0246(12)	0.0073(10)	0.0019(10)	0.0142(11)
C3	0.0280(13)	0.0197(12)	0.0300(13)	-0.0014(10)	0.0013(10)	0.0152(11)
C4	0.0221(12)	0.0178(11)	0.0315(13)	0.0016(10)	0.0009(10)	0.0070(10)
C5	0.0219(12)	0.0171(11)	0.0205(11)	-0.0022(9)	-0.0038(9)	0.0097(10)
C6	0.0319(13)	0.0273(13)	0.0198(11)	-0.0006(10)	0.0023(10)	0.0173(11)
C7	0.0341(14)	0.0202(12)	0.0292(13)	-0.0030(10)	-0.0037(11)	0.0153(11)
C8	0.0257(13)	0.0233(12)	0.0270(13)	-0.0023(10)	-0.0082(10)	0.0102(11)
C9	0.0194(11)	0.0217(12)	0.0204(11)	0.0029(9)	0.0024(9)	0.0081(10)
C10	0.0249(12)	0.0232(12)	0.0280(13)	0.0089(10)	0.0031(10)	0.0081(10)
C11	0.0166(11)	0.0305(14)	0.0298(13)	0.0023(11)	0.0030(10)	0.0101(10)
C12	0.0259(13)	0.0345(14)	0.0199(12)	0.0032(10)	0.0011(10)	0.0126(11)
C13	0.0181(11)	0.0131(10)	0.0249(12)	0.0032(9)	0.0012(9)	0.0075(9)
C14	0.0190(12)	0.0167(11)	0.0314(13)	0.0060(10)	0.0055(10)	0.0058(10)
C15	0.0236(12)	0.0176(11)	0.0315(13)	-0.0027(10)	-0.0009(10)	0.0101(10)
C16	0.0253(12)	0.0217(12)	0.0310(13)	0.0042(10)	-0.0017(10)	0.0152(11)

Table 9. Hydrogen atomic coordinates and isotropic atomic displacement parameters (Å^2) for sb150312.

	x/a	y/b	z/c	U(eq)
H2A	0.7472	0.2261	0.1952	0.039
H2B	0.6225	0.0969	0.1981	0.039
H2C	0.6235	0.2224	0.2039	0.039
H3A	0.6612	0.1458	0.1369	0.037
H3B	0.6574	0.0584	0.1587	0.037
H3C	0.7739	0.1937	0.1558	0.037
H4A	0.4574	0.1361	0.1769	0.038
H4B	0.4828	0.0271	0.1697	0.038
H4C	0.4811	0.1163	0.1489	0.038
H6A	0.3727	0.3641	0.0090	0.038
H6B	0.3539	0.2355	-0.0008	0.038
H6C	0.4641	0.3172	0.0178	0.038
H7A	0.4011	0.1564	0.0409	0.041
H7B	0.2887	0.0771	0.0227	0.041
H7C	0.2634	0.0833	0.0513	0.041
H8A	0.1263	0.1457	0.0397	0.039
H8B	0.1613	0.1451	0.0114	0.039
H8C	0.1742	0.2675	0.0234	0.039
H10A	0.1476	0.1014	0.0674	0.041
H10B	0.1364	0.1106	0.0965	0.041
H10C	0.2591	0.1224	0.0849	0.041
H11A	0.1814	0.3825	0.0779	0.04
H11B	0.0868	0.2532	0.0901	0.04
H11C	0.1098	0.2622	0.0611	0.04
H12A	0.3613	0.2908	0.1060	0.042

	x/a	y/b	z/c	U(eq)
H12B	0.2373	0.2823	0.1160	0.042
H12C	0.3392	0.4050	0.1027	0.042
H14A	0.5662	0.5235	0.0510	0.036
H14B	0.5325	0.6130	0.0363	0.036
H14C	0.5031	0.4842	0.0245	0.036
H15A	0.3257	0.5056	0.0801	0.036
H15B	0.4386	0.6242	0.0677	0.036
H15C	0.4629	0.5296	0.0831	0.036
H16A	0.3066	0.4423	0.0196	0.037
H16B	0.3329	0.5660	0.0333	0.037
H16C	0.2260	0.4354	0.0430	0.037

Bromo(tri-ethylphosphine)palladium(II), PEt$_2$PdBr$_2$ **326**
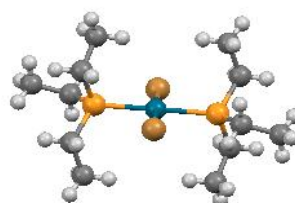
Table 1 Crystal data and structure refinement for sb260413_0ma

Identification code	sb260413_0ma
Empirical formula	C$_{12}$H$_{30}$Br$_2$P$_2$Pd
Formula weight	502.52
Temperature/K	100.15
Crystal system	monoclinic
Space group	P2$_1$/c
a/Å	7.2221(10)
b/Å	11.5769(15)
c/Å	13.2152(13)
α/°	90.00
β/°	122.447(6)
γ/°	90.00
Volume/Å^3	932.4(2)
Z	2
ρ$_{calc}$mg/mm^3	1.790
m/mm^{-1}	5.435
F(000)	496.0
Crystal size/mm^3	0.28 × 0.18 × 0.03
2Θ range for data collection	5.08 to 55.32°
Index ranges	-9 ≤ h ≤ 7, -15 ≤ k ≤ 14, -14 ≤ l ≤ 17
Reflections collected	6412
Independent reflections	2130[R(int) = 0.0235]
Data/restraints/parameters	2130/0/82
Goodness-of-fit on F^2	1.034
Final R indexes [I>=2σ (I)]	R$_1$ = 0.0183, wR$_2$ = 0.0415
Final R indexes [all data]	R$_1$ = 0.0222, wR$_2$ = 0.0426
Largest diff. peak/hole / e Å^{-3}	0.45/-0.64

Table 2 Fractional Atomic Coordinates (×10^4) and Equivalent Isotropic Displacement Parameters (Å^2×10^3) for sb260413_0ma. U$_{eq}$ is defined as 1/3 of of the trace of the orthogonalised U$_{IJ}$ tensor.

Atom	x	y	Z	U(eq)
Pd1	10000	0	10000	11.07(6)
Br2	11171.3(3)	-478.84(19)	12043.25(17)	18.74(6)

P1	8202.0(8)	-1753.0(5)	9260.6(4)	13.62(11)
C1	7254(4)	-3931.9(19)	9882.7(19)	23.2(5)
C2	8008(3)	-2695.7(18)	10307.2(18)	18.3(4)
C3	5404(3)	-1629.5(19)	7980.2(19)	22.0(5)
C4	4020(4)	-773(2)	8179(2)	31.4(6)
C5	9609(3)	-2603.4(18)	8716.4(18)	18.9(4)
C6	11965(3)	-2878(2)	9720.6(19)	23.4(5)

Table 3 Anisotropic Displacement Parameters ($Å^2 \times 10^3$) for sb260413_0ma. The Anisotropic displacement factor exponent takes the form: $-2\pi^2[h^2a^{*2}U_{11}+...+2hka \times b \times U_{12}]$

Atom	U_{11}	U_{22}	U_{33}	U_{23}	U_{13}	U_{12}
Pd1	11.19(10)	11.71(11)	9.59(10)	0.29(7)	5.09(8)	0.36(8)
Br2	23.13(12)	19.40(12)	11.33(10)	0.85(7)	7.67(9)	-3.10(8)
P1	13.3(2)	13.5(3)	12.2(2)	-0.28(18)	5.5(2)	-0.51(19)
C1	24.8(11)	17.3(12)	25.0(11)	1.7(9)	11.6(9)	-3.0(9)
C2	21(1)	16.5(11)	17.7(10)	0.6(8)	10.5(9)	-1.8(8)
C3	15.6(10)	20.8(12)	20.9(11)	3.0(9)	4.0(9)	-2.7(8)
C4	17.3(11)	34.2(15)	37.6(14)	8.4(11)	11.5(11)	4.9(10)
C5	22.0(11)	16.1(11)	19.3(10)	-3.7(8)	11.6(9)	0.2(8)
C6	21.8(11)	20.8(12)	27.4(12)	-3.2(9)	13(1)	3.2(9)

Table 4 Bond Lengths for sb260413_0ma.

Atom	Atom	Length/Å	Atom	Atom	Length/Å
Pd1	Br2	2.4214(3)	P1	C3	1.816(2)
Pd1	Br2[1]	2.4214(3)	P1	C5	1.818(2)
Pd1	P1[1]	2.3234(6)	C1	C2	1.527(3)
Pd1	P1	2.3234(6)	C3	C4	1.527(3)
P1	C2	1.825(2)	C5	C6	1.528(3)

[1]2-X,-Y,2-Z

Table 5 Bond Angles for sb260413_0ma.

Atom	Atom	Atom	Angle/°	Atom	Atom	Atom	Angle/°
Br2	Pd1	Br2[1]	180.0	C3	P1	C2	104.70(10)
P1	Pd1	Br2	92.926(14)	C3	P1	C5	104.65(10)
P1[1]	Pd1	Br2	87.075(14)	C5	P1	Pd1	109.54(7)
P1[1]	Pd1	Br2[1]	92.924(14)	C5	P1	C2	105.21(10)
P1	Pd1	Br2[1]	87.075(14)	C1	C2	P1	116.06(14)
P1	Pd1	P1[1]	179.999(12)	C4	C3	P1	113.24(15)
C2	P1	Pd1	117.15(7)	C6	C5	P1	111.56(14)
C3	P1	Pd1	114.49(8)				

[1]2-X,-Y,2-Z

Table 6 Hydrogen Atom Coordinates ($Å \times 10^4$) and Isotropic Displacement Parameters ($Å^2 \times 10^3$) for sb260413_0ma.

Atom	x	y	Z	U(eq)
H1A	5833	-3918	9119	35
H1B	7109	-4346	10483	35
H1C	8337	-4324	9773	35
H2A	9468	-2727	11063	22
H2B	6979	-2340	10494	22
H3A	5436	-1383	7273	26

H3B	4698	-2399	7802	26
H4A	2526	-756	7467	47
H4B	4671	-1	8320	47
H4C	3975	-1013	8877	47
H5A	8800	-3334	8368	23
H5B	9624	-2171	8074	23
H6A	11950	-3386	10310	35
H6B	12733	-2159	10113	35
H6C	12722	-3265	9383	35

Single crystals of $C_{12}H_{30}Br_2P_2Pd$ **[sb260413_0ma]** were crystallised from CH_2Cl_2 at -35°C. A suitable crystal was selected and **[tip-mounted]** on a **ETH_LOC_ApexIINonius_Mo** diffractometer. The crystal was kept at 100.15 K during data collection. Using Olex2 [1], the structure was solved with the XS [2] structure solution program using Direct Methods and refined with the XL [3] refinement package using Least Squares minimisation.

1. O. V. Dolomanov, L. J. Bourhis, R. J. Gildea, J. A. K. Howard and H. Puschmann, OLEX2: a complete structure solution, refinement and analysis program. J. Appl. Cryst. (2009). 42, 339-341.
2. SHELXS-97 (Sheldrick, 2008)
3. SHELXL-97 (Sheldrick, 2008)

Crystal structure determination of [sb260413_0ma]

Crystal Data for $C_{12}H_{30}Br_2P_2Pd$ (M =502.52): monoclinic, space group P2$_1$/c (no. 14), a = 7.2221(10) Å, b = 11.5769(15) Å, c = 13.2152(13) Å, β = 122.447(6)°, V = 932.4(2) Å^3, Z = 2, T = 100.15 K, μ(MoKα) = 5.435 mm^{-1}, $Dcalc$ = 1.790 g/mm^3, 6412 reflections measured (5.08 ≤ 2Θ ≤ 55.32), 2130 unique (R_{int} = 0.0235) which were used in all calculations. The final R_1 was 0.0183 (>2sigma(I)) and wR_2 was 0.0426 (all data).

Trifluoromethylselenol(tri-*tert*-butylphosphine)palladium(I) dimer**, Pd(I)-SeCF$_3$ dimer 347**
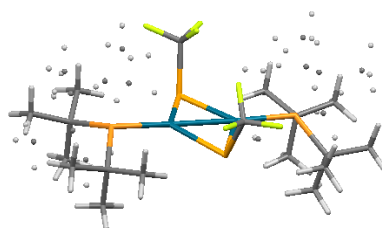
Table 2 Fractional Atomic Coordinates (×10^4) and Equivalent Isotropic Displacement Parameters (Å^2×10^3) for sb070714. U$_{eq}$ is defined as 1/3 of the trace of the orthogonalised U$_{IJ}$ tensor.

Atom	x	y	z	U(eq)
Pd1	5639.8(2)	5000	3287.0(2)	10.83(4)
Pd2	3963.7(2)	5000	2330.0(2)	11.65(5)
Se1	4755.5(2)	6333.4(2)	2863.5(2)	15.80(5)
P2	2485.8(5)	5000	1459.0(4)	14.39(11)
P1	7164.3(5)	5000	4100.2(4)	17.72(13)
F2	5909.7(13)	6200.3(12)	1592.5(9)	45.7(4)
F3	4902.8(13)	7280.8(10)	1525.3(9)	42.1(4)
F1	6274.3(13)	7296.2(11)	2332.6(10)	52.4(5)
C13A	8463(3)	3992(3)	5203(3)	24.7(3)
C17A	2391(3)	3134(3)	1563(3)	24.8(3)
C6	2869(2)	4894(3)	417.4(16)	15.9(6)
C11	7348(3)	3114(3)	4167(3)	24.7(3)

C14A	1702(4)	3941(3)	1530(3)	24.8(3)
C10	7252(4)	3879(3)	4701(3)	24.7(3)
C1	5503.9(18)	6793.0(15)	2030.3(14)	30.7(4)
C2	8242(2)	5097(3)	3439.2(16)	15.4(6)
C15A	849(3)	3810(3)	821(2)	24.8(3)
C9	2027(3)	4619(3)	-215(3)	29.3(8)
C8	3782(3)	4294(3)	444(3)	25.8(8)
C7	3283(4)	5788(3)	154(3)	29.7(9)
C12A	6656(3)	4252(3)	5478(2)	24.7(3)
C16	1641(3)	3991(3)	2575(2)	24.8(3)
C12	6199(3)	3737(3)	5030(2)	24.7(3)
C13	8094(3)	3850(3)	5388(3)	24.7(3)
C11A	7008(3)	3292(3)	4400(3)	24.7(3)
C10A	7345(4)	4122(3)	4814(3)	24.7(3)
C5	9272(3)	5419(3)	3822(2)	24.1(7)
C4	8408(3)	4163(3)	3137(3)	27.7(8)
C3	7898(3)	5619(3)	2703(2)	22.5(7)
C16A	1174(3)	3962(3)	2279(2)	24.8(3)
C15	543(3)	4082(3)	1287(2)	24.8(3)
C14	1642(4)	4072(3)	1658(3)	24.8(3)
C17	2164(3)	3251(3)	1438(3)	24.8(3)

Table 3 Anisotropic Displacement Parameters (Å^2×10^3) for sb070714. The Anisotropic displacement factor exponent takes the form: -2π^2[h^{2}a*^{2}U$_{11}$+2hka*b*U$_{12}$+…].

Atom	U_{11}	U_{22}	U_{33}	U_{23}	U_{13}	U_{12}
Pd1	9.46(8)	12.03(8)	10.73(8)	0	-0.30(5)	0
Pd2	10.70(8)	12.82(8)	10.93(8)	0	-1.24(6)	0
Se1	17.24(9)	11.11(8)	18.65(9)	-1.08(6)	-0.06(6)	0.62(6)
P2	12.1(3)	20.7(3)	10.0(2)	0	-1.0(2)	0
P1	9.2(2)	31.3(4)	12.4(3)	0	-0.2(2)	0
F2	47.7(9)	54.2(10)	39.7(8)	1.0(7)	25.8(7)	-1.7(8)
F3	53.8(9)	36.2(8)	35.6(7)	18.9(6)	0.8(7)	-7.3(7)
F1	47.6(9)	50.8(10)	57.2(10)	15.1(8)	-2.8(8)	-34.6(8)
C1	32.6(11)	27.2(10)	32.5(11)	5.2(8)	4.4(9)	-10.3(9)

Table 4 Bond Lengths for sb070714.

Atom	Atom	Length/Å	Atom	Atom	Length/Å
Pd1	Pd2	2.6073(3)	F1	C1	1.341(3)
Pd1	Se1[1]	2.4479(2)	C13A	C10A	1.564(6)
Pd1	Se1	2.4480(2)	C17A	C14A	1.545(7)
Pd1	P1	2.3202(7)	C6	C9	1.527(5)
Pd2	Se1	2.4512(2)	C6	C8	1.518(5)
Pd2	Se1[1]	2.4512(2)	C6	C7	1.574(6)
Pd2	P2	2.3243(6)	C11	C10	1.510(6)
Se1	C1	1.947(2)	C14A	C15A	1.577(7)
P2	C6	1.904(3)	C14A	C16A	1.516(6)
P2	C14A[1]	1.953(5)	C10	C12	1.564(6)
P2	C14A	1.953(6)	C10	C13	1.529(6)
P2	C14[1]	1.873(6)	C2	C5	1.528(5)
P2	C14	1.873(6)	C2	C4	1.561(6)
P1	C10	2.018(5)	C2	C3	1.525(5)
P1	C10[1]	2.018(5)	C12A	C10A	1.537(6)
P1	C2	1.908(3)	C16	C14	1.570(6)
P1	C10A	1.827(5)	C11A	C10A	1.515(6)
P1	C10A[1]	1.827(5)	C15	C14	1.519(7)
F2	C1	1.332(3)	C14	C17	1.514(7)
F3	C1	1.343(3)			

[1]+X,1-Y,+Z

Table 5 Bond Angles for sb070714.

Atom	Atom	Atom	Angle/°	Atom	Atom	Atom	Angle/°
Se1	Pd1	Pd2	57.907(6)	C7	C6	P2	108.9(3)
Se1[1]	Pd1	Pd2	57.907(6)	C17A	C14A	P2	111.9(4)

Se1[1]	Pd1	Se1	115.523(11)	C17A C14A C15A		107.0(4)
P1	Pd1	Pd2	177.971(18)	C15A C14A P2		113.6(3)
P1	Pd1	Se1	122.185(6)	C16A C14A P2		109.0(3)
P1	Pd1	Se1[1]	122.185(6)	C16A C14A C17A		107.8(4)
Se1[1]	Pd2	Pd1	57.786(6)	C16A C14A C15A		107.4(4)
Se1	Pd2	Pd1	57.786(6)	C11 C10 P1		112.1(3)
Se1[1]	Pd2	Se1	115.284(11)	C11 C10 C12		103.8(4)
P2	Pd2	Pd1	179.032(17)	C11 C10 C13		109.8(4)
P2	Pd2	Se1[1]	122.263(6)	C12 C10 P1		107.3(3)
P2	Pd2	Se1	122.263(6)	C13 C10 P1		114.4(3)
Pd1	Se1	Pd2	64.307(8)	C13 C10 C12		108.7(4)
C1	Se1	Pd1	105.33(7)	F2 C1 Se1		114.77(15)
C1	Se1	Pd2	105.45(7)	F2 C1 F3		105.92(19)
C6	P2	Pd2	108.16(9)	F2 C1 F1		106.7(2)
C14A	P2	Pd2	111.94(16)	F3 C1 Se1		111.47(16)
C14A[1]	P2	Pd2	111.94(16)	F1 C1 Se1		110.65(16)
C14A[1]	P2	C14A	114.8(3)	F1 C1 F3		106.91(19)
C14[1]	P2	Pd2	110.96(17)	C5 C2 P1		117.0(2)
C14	P2	Pd2	110.96(17)	C5 C2 C4		107.3(3)
C14[1]	P2	C6	117.10(18)	C4 C2 P1		105.1(3)
C14	P2	C6	108.83(18)	C3 C2 P1		110.7(2)
C14	P2	C14[1]	100.6(3)	C3 C2 C5		110.7(3)
C10	P1	Pd1	107.72(13)	C3 C2 C4		105.1(3)
C10[1]	P1	Pd1	107.72(13)	C13A C10A P1		115.6(3)
C10[1]	P1	C10	119.3(3)	C12A C10A P1		110.3(3)
C2	P1	Pd1	107.29(8)	C12A C10A C13A		107.8(4)
C2	P1	C10	111.18(19)	C11A C10A P1		108.2(3)
C2	P1	C10[1]	103.04(19)	C11A C10A C13A		107.8(4)
C10A[1]	P1	Pd1	116.37(14)	C11A C10A C12A		106.7(4)
C10A	P1	Pd1	116.37(14)	C16 C14 P2		107.7(3)
C10A[1]	P1	C10A	96.5(3)	C15 C14 P2		118.3(4)
C9	C6	P2	116.2(2)	C15 C14 C16		108.6(4)
C9	C6	C7	107.0(3)	C17 C14 P2		108.0(3)
C8	C6	P2	108.1(2)	C17 C14 C16		103.1(4)
C8	C6	C9	111.4(3)	C17 C14 C15		110.0(4)
C8	C6	C7	104.7(3)			

[1]+X,1-Y,+Z

Table 6 Torsion Angles for sb070714.

A	B	C	D	Angle/°	A	B	C	D	Angle/°
C10A_b[1]	P1	C10A_b	C11A_b	167.76(19)	C14A	P2	C14	C17	29.4(17)
Pd1	P1	C10A	C13A	165.0(3)	C10	P1	C10A	C13A	120.8(13)
Pd1	P1	C10A	C12A	-72.4(3)	C10[1]	P1	C10A	C13A	-73.8(3)
Pd1	P1	C10A	C11A	44.0(3)	C10[1]	P1	C10A	C12A	48.8(3)
Pd2	P2	C14	C16	42.1(3)	C10	P1	C10A	C12A	-116.7(13)
Pd2	P2	C14	C15	165.6(3)	C10[1]	P1	C10A	C11A	165.2(3)
Pd2	P2	C14	C17	-68.6(3)	C10	P1	C10A	C11A	-0.2(10)
C6	P2	C14	C16	161.0(3)	C2	P1	C10A	C13A	39.7(4)
C6	P2	C14	C15	-75.5(3)	C2	P1	C10A	C12A	162.3(3)
C6	P2	C14	C17	50.3(4)	C2	P1	C10A	C11A	-81.3(3)
C14A[1]	P2	C14	C16	-80.9(3)	C10A[1]	P1	C10A	C13A	-71.2(4)
C14A	P2	C14	C16	140(2)	C10A[1]	P1	C10A	C12A	51.3(4)
C14A	P2	C14	C15	-96(2)	C14[1]	P2	C14	C16	-75.3(4)
C14A[1]	P2	C14	C15	42.6(4)	C14[1]	P2	C14	C15	48.1(4)
C14A[1]	P2	C14	C17	168.3(4)	C14[1]	P2	C14	C17	173.9(2)

[1]+X,1-Y,+Z

Table 7 Hydrogen Atom Coordinates (Å×10⁴) and Isotropic Displacement Parameters (Å²×10³) for sb070714.

Atom	x	y	z	U(eq)
H13A	8920	3910	4791	37
H13B	8491	3484	5545	37
H13C	8677	4502	5517	37

H17A	2705	3083	1068	37
H17B	1980	2620	1637	37
H17C	2927	3187	2003	37
H11A	6789	3122	3742	37
H11B	7316	2581	4472	37
H11C	8003	3142	3943	37
H15A	410	4320	768	37
H15B	438	3303	920	37
H15C	1171	3725	333	37
H9A	1772	4049	-84	44
H9B	2302	4593	-727	44
H9C	1468	5037	-240	44
H8A	4317	4498	843	39
H8B	4045	4286	-72	39
H8C	3573	3712	580	39
H7A	2711	6188	40	45
H7B	3633	5710	-321	45
H7C	3762	6023	577	45
H12A	6921	4728	5817	37
H12B	6646	3724	5790	37
H12C	5962	4389	5250	37
H16A	2346	3985	2823	37
H16B	1300	3455	2701	37
H16C	1277	4483	2774	37
H12D	6046	4233	5353	37
H12E	6229	3214	5353	37
H12F	5664	3676	4590	37
H13D	8762	3886	5184	37
H13E	8047	3309	5678	37
H13F	8013	4337	5742	37
H11D	6308	3356	4151	37
H11E	7034	2822	4785	37
H11F	7463	3160	3997	37
H5A	9214	6027	3965	36
H5B	9787	5356	3451	36
H5C	9475	5080	4297	36
H4A	8677	3799	3579	42
H4B	8894	4176	2740	42
H4C	7755	3929	2902	42
H3A	7274	5366	2436	34
H3B	8436	5612	2346	34
H3C	7763	6214	2852	34
H16D	1666	4133	2722	37
H16E	904	3389	2379	37
H16F	613	4378	2219	37
H15D	174	4555	1511	37
H15E	214	3534	1392	37
H15F	531	4164	716	37
H17D	2164	3222	865	37
H17E	1796	2753	1621	37
H17F	2868	3246	1687	37

Table 8 Atomic Occupancy for sb070714.

Atom	*Occupancy*	Atom	*Occupancy*	Atom	*Occupancy*
C13A	0.5	H13A	0.5	H13B	0.5
H13C	0.5	C17A	0.5	H17A	0.5
H17B	0.5	H17C	0.5	C6	0.5
C11	0.5	H11A	0.5	H11B	0.5
H11C	0.5	C14A	0.5	C10	0.5
C2	0.5	C15A	0.5	H15A	0.5
H15B	0.5	H15C	0.5	C9	0.5
H9A	0.5	H9B	0.5	H9C	0.5
C8	0.5	H8A	0.5	H8B	0.5
H8C	0.5	C7	0.5	H7A	0.5

H7B	0.5	H7C	0.5	C12A	0.5
H12A	0.5	H12B	0.5	H12C	0.5
C16	0.5	H16A	0.5	H16B	0.5
H16C	0.5	C12	0.5	H12D	0.5
H12E	0.5	H12F	0.5	C13	0.5
H13D	0.5	H13E	0.5	H13F	0.5
C11A	0.5	H11D	0.5	H11E	0.5
H11F	0.5	C10A	0.5	C5	0.5
H5A	0.5	H5B	0.5	H5C	0.5
C4	0.5	H4A	0.5	H4B	0.5
H4C	0.5	C3	0.5	H3A	0.5
H3B	0.5	H3C	0.5	C16A	0.5
H16D	0.5	H16E	0.5	H16F	0.5
C15	0.5	H15D	0.5	H15E	0.5
H15F	0.5	C14	0.5	C17	0.5
H17D	0.5	H17E	0.5	H17F	0.5

Experimental

Single crystals of $C_{26}H_{54}F_6P_2Pd_2Se_2$ **[sb070714]** were **[crystallized from a toluene/acetone mixture]**. A suitable crystal was selected and **[tip-mounted]** on a **Bruker SMART Platform** diffractometer. The crystal was kept at 100 K during data collection. Using Olex2 [1], the structure was solved with the Superflip [2] structure solution program using Charge Flipping and refined with the ShelXL [3] refinement package using Least Squares minimisation.

1.   Dolomanov, O.V., Bourhis, L.J, Gildea, R.J, Howard, J.A.K. & Puschmann, H. (2009), J. Appl. Cryst. 42, 339-341.
2.   Palatinus, L. & Chapuis, G. (2007). J. Appl. Cryst., 40, 786-790; Palatinus, L. & van der Lee, A. (2008). J. Appl. Cryst. 41, 975-984; Palatinus, L., Prathapa, S. J. & van Smaalen, S. (2012). J. Appl. Cryst. 45, 575-580.
3.   Sheldrick, G.M. (2008). Acta Cryst. A64, 112-122.

Crystal structure determination of [sb070714]

Crystal Data for $C_{26}H_{54}F_6P_2Pd_2Se_2$ (M =913.35 g/mol): monoclinic, space group I2/m (no. 12), a = 13.1716(9) Å, b = 15.5289(11) Å, c = 17.0646(17) Å, β = 95.9150(10)°, V = 3471.8(5) Å^3, Z = 4, T = 100 K, μ(MoKα) = 3.272 mm^{-1}, $Dcalc$ = 1.747 g/cm^3, 23136 reflections measured (3.554° ≤ 2Θ ≤ 64.826°), 5968 unique (R_{int} = 0.0203, R_{sigma} = 0.0192) which were used in all calculations. The final R_1 was 0.0265 (I > 2σ(I)) and wR_2 was 0.0624 (all data).

Refinement model description

Number of restraints - 0, number of constraints - unknown.
Details:
1. Fixed Uiso
 At 1.5 times of:
  All C(H,H,H) groups
2. Uiso/Uaniso restraints and constraints
Uiso(C13A) = Uiso(C11) = Uiso(C10) = Uiso(C12A) = Uiso(C12) = Uiso(C13) =
Uiso(C11A) = Uiso(C10A)
Uiso(C17A) = Uiso(C14A) = Uiso(C15A) = Uiso(C16) = Uiso(C16A) = Uiso(C15) =
Uiso(C14) = Uiso(C17)
3. Others
 Fixed Sof: C13A(0.5) H13A(0.5) H13B(0.5) H13C(0.5) C17A(0.5) H17A(0.5)
 H17B(0.5) H17C(0.5) C6(0.5) C11(0.5) H11A(0.5) H11B(0.5) H11C(0.5) C14A(0.5)
 C10(0.5) C2(0.5) C15A(0.5) H15A(0.5) H15B(0.5) H15C(0.5) C9(0.5) H9A(0.5)
 H9B(0.5) H9C(0.5) C8(0.5) H8A(0.5) H8B(0.5) H8C(0.5) C7(0.5) H7A(0.5) H7B(0.5)
 H7C(0.5) C12A(0.5) H12A(0.5) H12B(0.5) H12C(0.5) C16(0.5) H16A(0.5) H16B(0.5)
 H16C(0.5) C12(0.5) H12D(0.5) H12E(0.5) H12F(0.5) C13(0.5) H13D(0.5) H13E(0.5)
 H13F(0.5) C11A(0.5) H11D(0.5) H11E(0.5) H11F(0.5) C10A(0.5) C5(0.5) H5A(0.5)
 H5B(0.5) H5C(0.5) C4(0.5) H4A(0.5) H4B(0.5) H4C(0.5) C3(0.5) H3A(0.5) H3B(0.5)
 H3C(0.5) C16A(0.5) H16D(0.5) H16E(0.5) H16F(0.5) C15(0.5) H15D(0.5) H15E(0.5)

H15F(0.5) C14(0.5) C17(0.5) H17D(0.5) H17E(0.5) H17F(0.5)
4.a Idealised Me refined as rotating group:
C13A(H13A,H13B,H13C), C17A(H17A,H17B,H17C), C11(H11A,H11B,H11C), C15A(H15A,
H15B,H15C), C9(H9A,H9B,H9C), C8(H8A,H8B,H8C), C7(H7A,H7B,H7C), C12A(H12A,H12B,
H12C), C16(H16A,H16B,H16C), C12(H12D,H12E,H12F), C13(H13D,H13E,H13F),
C11A(H11D,H11E,H11F), C5(H5A,H5B,H5C), C4(H4A,H4B,H4C), C3(H3A,H3B,H3C),
C16A(H16D,H16E,H16F), C15(H15D,H15E,H15F), C17(H17D,H17E,H17F)

References

(1) Natta, G.; Pino, P.; Corradini, P.; Danusso, F.; Mantica, E.; Mazzanti, G.; Moraglio, G.: Crystalline High Polymers Of A-Olefins. *J. Am. Chem. Soc.* **1955**, *77*, 1708-1710.

(2) Hill, A. F.: In *Organotrasition metal chemistry*; Wiley-InterScience, Ed., 2002; Vol. 7; pp 122-148.

(3) http://www.nobelprize.org/nobel_prizes/chemistry/laureates/1963/.

(4) Smidt, J.; Hafner, W.; Jira, R.; Sedlmeier, J.; Sieber, R.; Rüttinger, R.; Kojer, H.: Katalytische Umsetzungen von Olefinen an Platinmetall-Verbindungen Das Consortium-Verfahren zur Herstellung von Acetaldehyd. *Angewandte Chemie* **1959**, *71*, 176-182.

(5) Smidt, J.; Hafner, W.; Jira, R.; Sieber; R.; Sedlmeier; J.; Sieber; R.; Rüttinger, R.; Kojer, H.: The Oxidation of Olefins with Palladium Chloride Catalysts. *Angewandte Chemie International Edition in English* **1962**, *1*, 80-88. *Angewandte Chemie,* **1962**, *71*, 176-182.

(6) Nicolaou, K. C.; Bulger, P. G.; Sarlah, D.: Palladium-Catalyzed Cross-Coupling Reactions in Total Synthesis. *Ang. Chem. Int. Ed.* **2005**, *44*, 4442. *Angewandte Chemie,* **2005**, *117*, 4516-4563.

(7) Negishi, E. I.: *Handbook of Organopalladium Chemistry for Organic Synthesis*; Wiley-Interscience: New-York, 2002.

(8) de Mejiere, A.; Diederich, F.: *Metal Catalyzed Cross-Coupling Reactions*; Wiley: New York, **2004**.

(9) Bolm, C.: Cross-Coupling Reactions. *J. Org. Chem* **2012**, *77*, 5221.

(10) Dumrath, A.; Lübbe., C.; Beller, M.: Palladium-Catalyzed Cross-Coupling Reactions – Industrial Applications. In *Palladium-Catalyzed Coupling Reactions: Practical Aspects and Future Developments, First Edition*; Wiley-VCH Verlag GmbH & Co. KGaA, **2013**; pp 445.

(11) http://www.nobelprize.org/nobel_prizes/chemistry/laureates/2010/.

(12) C. C. C. Johansson Seechurn, M. O. K., T. J. Colacot, V. Snieckus: Palladium-Catalyzed Cross-Coupling: A Historical Contextual Perspective to the 2010 Nobel Prize. *Ang. Chem. Int. Ed.* **2012**, *51*, 5062.

13) Low, J. J.; Gottard, W. A.: Theoretical Studies of Oxidative Addition and Reductive Elimination. 3.
C-H and C-C Reductive Coupling from Palladium and Platinum Bis(phosphine) Complexes. *J. Am. Chem. Soc* **1986**, *108*, 6115. 124: 5150–5174

(14) García-Melcho, M.; Braga, A. A.; Lledós, A.; Ujaque, G.; Maseras, F.: Computational Perspective on Pd-Catalyzed C–C Cross-Coupling Reaction Mechanisms. *Accounts of Chemical Research* **2013**, *46*, 2626-2634

(15) Xue, L.; Lin, Z.: Theoretical aspects of palladium-catalysed carbon-carbon cross-coupling reactions. *Chemical Society Reviews* **2010**, *39*, 1692-1705

(16) Bonney, K. J.; Schoenebeck, F.: Experiment and computation: a combined approach to study the reactivity of palladium complexes in oxidation states 0 to iv. *Chemical Society Reviews* **2014**, *43*, 6609-6638.

(17) Colacot, T. J.: *New Trends in Cross-Coupling : Theory and Applications*; Royal Society Of Chemistry, **2015**.

(18) Amatore, C.; Pflüger, F.: Mechanism of oxidative addition of palladium(0) with aromatic iodides in toluene, monitored at ultramicroelectrodes. *Organometallics* **1990**, *9*, 2276.

(19) McMullin, C. L.; Jover, J.; Harvey, J. N.; Fey, N.: Accurate modelling of Pd(0) + PhX oxidative addition kinetics. *Dalton Trans.* **2010**, *39*, 10833–10836.

(20) Fauvarque, J.-F.; Pflüger, F.; Troupel, M.: Kinetics of oxidative addition of zerovalent palladium to aromatic iodides. *J. Organomet. Chem.* **1981**, *208*, 419.

(21) Musco, A.; Kuran, W.; Silvani, A.; Anker, M. W.: Tertiary phosphine palladium(0) complexes. *J. Chem. Soc., Chem. Commun.* **1973**, 938.

(22) Amatore, C.; Carre, E.; Jutand, A.; M'Barki, M. A.; Meyer, G.: Evidence for the Ligation of Palladium(0) Complexes by Acetate Ions: Consequences on the Mechanism of Their Oxidative Addition with Phenyl Iodide and PhPd(OAc)(PPh3)2 as Intermediate in the Heck Reaction. *Organometallics* **1995**, *14*, 5605.

(23) Schoenebeck, F.: Ligand, Additive, and Solvent Effects in Palladium Catalysis - Mechanistic Studies En Route to Catalyst Design. Understanding Organometallic Reaction Mechanisms and Catalysis. Wiley-VCH, **2014**; pp 69-92.

(24)   Barrios-Landeros, F.; Carrow, B. P.; Hartwig, J. F.: Effect of Ligand Steric Properties and Halide Identity on the Mechanism for Oxidative Addition of Haloarenes toTrialkylphosphine Pd(0) Complexes. *J. Am. Chem. Soc* **2009**, *131*, 8141

(25)   Proutiere, F.; Schoenebeck, F.: Solvent Effect on Palladium-Catalyzed Cross-Coupling Reactions and Implications on the Active Catalytic Species. *Angewandte Chemie International Edition* **2011**, *50*, 8192-8195. *Angew. Chem.*, **2011**, *123*, 8342–8345

(26)   Dai, X.; Chen., Y.; Garrell, S.; Liu, H.; Zhang, L.-K.; Palani, A.; Hughes, G.; Nargund, R.: Ligand-Dependent Site-Selective Suzuki Cross-Coupling of 3,5-Dichloropyridazines. / *J. Org. Chem.* **2013**, *78*, 7758.

(27)   Strotman, N. A.; Chobanian, H. R; He, J.; Guo, Y.; Dormer, P. G.; Jones, C. M.; Steves, J. E.: Catalyst-Controlled Regioselective Suzuki Couplings at Both Positions of Dihaloimidazoles, Dihalooxazoles, and Dihalothiazoles. *J. Org. Chem.* **2010**, *75*, 1733.

(28)   Kamikawa, T.; Hayashi, T.: Control of reactive site in palladium-catalyzed Grignard cross-coupling of arenes containing both bromide and triflate. *Tetrahedron Lett.* **1997**, *38*, 7087-7090.

(29)   Littke, A. F.; Dai, C.; Fu, G. C.: Versatile Catalysts for the Suzuki Cross-Coupling of Arylboronic Acids with Aryl and Vinyl Halides and Triflates under Mild Conditions. *J. Am. Chem. Soc.* **2000**, *122*, 4020-4028.

(30)   Espino, G.; Kurbangalieva, A.; Brown, J. M.: Aryl bromide/triflate selectivities reveal mechanistic divergence in palladium-catalysed couplings; the Suzuki-Miyaura anomaly. *Chemical Communications* **2007**, 1742-1744.

(31)   Schoenebeck, F.; Houk, K. N.: Ligand-Controlled Regioselectivity in Palladium-Catalyzed Cross Coupling Reactions. *J. Am. Chem. Soc.* **2010**, *132*, 2496-2497.

(32)   Proutière, F.: Reactivities of Palladium Complexes in Oxidation States Zero, One and Two - Fundamental Studies and Applications. *PhD Thesis,* ETH Zurich, **2014**

(33)   N. Miyaura, K. Y., A. Suzuki: A New Stereospecific Cross-Coupling By The Palladium-Catalyzed Reaction Of 1-Alkenylboranes With 1-Alkenyl Or 1-Alkynyl Halides. *Tetrahedron Lett.* **1979**, *36*, 3437.

(34)   King, A. Y.; Okukado, N.; Negishi, E. I: Highly general stereo-, regio-, and chemo-selective synthesis of terminal and internal conjugated enynes by the Pd-catalysed reaction of alkynylzinc reagents with alkenyl halides. *J. Chem. Soc., Chem. Commun.* **1977**, 683-684

(35)   Heck, R. F.; Nolley, J. P.: Palladium-Catalyzed Vinylic Hydrogen Substitution Reactions with Aryl, Benzyl, and Styryl Halides. *J. Org. Chem* **1972**, *14*, 2320.

(36)   Sonogashira, K.; Tohda., Y.; Hagihara, N.: A convenient synthesis of acetylenes: catalytic substitutions of acetylenic hidrogen with Bromoalkenes, Iodoarene and Bromopyridines. *Tetrahedron Letters* **1975**, *50*, 4467-4470.

(37)   Hatanaka, Y.; Hiyama, T.: Cross-coupling of organosilanes with organic halides mediated by a palladium catalyst and tris(diethylamino)sulfonium difluorotrimethylsilicate. *The Journal of Organic Chemistry* **1988**, *53*, 918-920

(38)   Hiyama, T.: How I came across the silicon-based cross-coupling reaction. *Journal of Organometallic Chemistry* **2002**, *653*, 58-61.

(38)   Hiyama, T.: How I came across the silicon-based cross-coupling reaction. *Journal of Organometallic Chemistry* **2002**, *653*, 58-61.

(39)   Guram, A. S.; Buchwald, S. L.: Palladium-Catalyzed Aromatic Aminations with in situ Generated Aminostannanes. *J. Am. Chem. Soc.* **1994**, *116*, 7901-7902.

(40)   Guram, A. S.; Rennels, R. A.; Buchwald, S. L.: A Simple Catalytic Method for the Conversion of Aryl Bromides to Arylamines. *Angewandte Chemie International Edition in English* **1995**, *34*, 1348-1350. *Angew. Chem.*, **1995**, *107*, 1456–1459

(41)   Hartwig, J. F.: Palladium-Catalyzed Amination of Aryl Halides: Mechanism and Rational Catalyst Design. *Synlett* **1997**, *1997*, 329-340.

(42)   Tamao, K.; Sumitani, K.; Kumada, M.: Selective carbon-carbon bond formation by cross-coupling of Grignard reagents with organic halides. Catalysis by nickel-phosphine complexes. *J. Am. Chem. Soc.* **1972**, *94*, 4374-4376.

(43)   Stille, J. K.: The Palladium-Catalyzed Cross-Coupling Reactions of Organotin Reagents with Organic Electrophiles [New Synthetic Methods (58)]. *Angewandte Chemie International Edition in English* **1986**, *25*, 508-524. *Angew. Chem.*, **1986**, *98*, 504–519

(44)   Milstein, D.; Stille, J. K.: Mild, selective, general method of ketone synthesis from acid chlorides and organotin compounds catalyzed by palladium. *The Journal of Organic Chemistry* **1979**, *44*, 1613-1618.

(45)   Miyaura, N.: Cross-coupling reaction of organoboron compounds via base-assisted transmetalation to palladium(II) complexes. *J. Organomet. Chem.* **2002**, *653*, 54.

(46)   Butters, M.; Harvey, J. N.; Jover, J.; Lennox, A. J. J.; Lloyd-Jones, G. C.; Murray, P. M.: Aryl Trifluoroborates in Suzuki–Miyaura Coupling: The Roles of Endogenous Aryl Boronic Acid and Fluoride. *Angewandte Chemie International Edition* **2010**, *49*, 5156-5160. *Angew. Chem.*, **2010**, *122*, 5282–5286

(47)   Amatore, C.; Jutand, A.; Le Duc, G.: Kinetic Data for the Transmetalation/Reductive Elimination in Palladium-Catalyzed Suzuki–Miyaura Reactions: Unexpected Triple Role of Hydroxide Ions Used as Base. *Chemistry – A European Journal* **2011**, *17*, 2492-2503.

(48)   Carrow, B. P.; Hartwig, J. F.: Distinguishing Between Pathways for Transmetalation in Suzuki−Miyaura Reactions. *J. Am. Chem. Soc.* **2011**, *133*, 2116-2119.

(49)   Lennox, A. J. J.; Lloyd-Jones, G. C.: Transmetalation in the Suzuki–Miyaura Coupling: The Fork in the Trail. *Angewandte Chemie International Edition* **2013**, *52*, 7362-7370. *Angew. Chem.*, **2013**, *125*, 7506–7515

(50)   Amatore, C.; Jutand, A.; Le Duc, G.: The Triple Role of Fluoride Ions in Palladium-Catalyzed Suzuki–Miyaura Reactions: Unprecedented Transmetalation from [ArPdFL$_2$] Complexes. *Angew. Chem. Int. Ed.,* **2011**, *51*, 1379. *Angew. Chem.*, **2011**, *124*, 1408–1411

(51)   Brown, J. M.; Guiry, P. J.: Bite angle dependence of the rate of reductive elimination from diphosphine palladium complexes. *Inorganica Chimica Acta* **1994**, *220*, 249-259.

(52)   Hartwig, J. F.: Electronic Effects on Reductive Elimination To Form Carbon−Carbon and Carbon−Heteroatom Bonds from Palladium(II) Complexes. *Inorganic Chemistry* **2007**, *46*, 1936-1947.

(53)   Albright, T. A.; Burdett, J. K.; Whangbo, M. H.: Orbital Interactions in Chemistry, Second Edition. Wiley & Sons, Inc, 2013; pp 503.

(54)   Moravskiy, A.; Stille, J. K.: Mechanisms of 1,1 -Reductive Elimination from Palladium: Elimination of Ethane from Dimethylpalladium(II) and Trimethylpalladium(IV). *J. Am. Chem. Soc.* **1981**, *103*, 4182-4186.

(55)   Perez-Rodrıguez, M.; Braga, A. A. C.; Garcia-Melchor, M.; Perez-Temprano, M. H.; Casares, J. A.; Ujaque, G.; de Lera, A. R.; Alvarez, R.; Maseras, F.; Espinet, P.: C-C Reductive Elimination in Palladium Complexes, and the Role of Coupling Additives. A DFT Study Supported by Experiment. *J. Am. Chem. Soc.,* **2009**, *131*, 3650.

(56)   Hartwig, J. F.: *Organotransition Metal Chemistry. From bond to catalysis*; University Science Book: Mill Valley, California, **2010**.

(57)   Driver, M. S.; Hartwig, J. F.: Carbon−Nitrogen-Bond-Forming Reductive Elimination of Arylamines from Palladium(II) Phosphine Complexes. *J. Am. Chem. Soc.* **1997**, *119*, 8232-8245.

(58)   Bryndza, H. E.; Tam, W.: Monomeric metal hydroxides, alkoxides, and amides of the late transition metals: synthesis, reactions, and thermochemistry. *Chem. Rev.* **1988**, *88*, 1163-1188.

(59)   Holland, P. L.; Andersen, R. A.; Bergman, R. G.: Application of the E-C Approach to Understanding the Bond Energies Thermodynamics of Late-Metal Amido, Aryloxo and Alkoxo Complexes: An Alternative to pπ/dπ Repulsion. *Comments on Inorganic Chemistry* **1999**, *21*, 115-129.

(60)   Fulton, J. R.; Holland, A. W.; Fox, D. J.; Bergman, R. G.: Formation, Reactivity, and Properties of Nondative Late Transition Metal−Oxygen and −Nitrogen Bonds. *Accounts of Chemical Research* **2001**, *35*, 44-56.

(61)   Mann, G.; Baranano, D.; Hartwig, J. F.; Rheingold, A. L.; Guzei, I. A.: Carbon−Sulfur Bond-Forming Reductive Elimination Involving sp-, sp2-, and sp3-Hybridized Carbon. Mechanism, Steric Effects, and Electronic Effects on Sulfide Formation. *J. Am. Chem. Soc.* **1998**, *120*, 9205-9219.

(62)   Widenhoefer, R. A.; Zhong, H. A.; Buchwald, S. L.: Direct Observation of C−O Reductive Elimination from Palladium Aryl Alkoxide Complexes To Form Aryl Ethers. *J. Am. Chem. Soc.* **1997**, *119*, 6787-6795.

(63)   Moiseev, I. I.; Stromnova, T. A.; Vargaftik, M. N.: Palladium clusters: stoichiometric and catalytic reactions. *J. Mol. Catal.* **1994**, *86*, 71.

(64)   Muetterties; E. L.; Rhodin; T. N.; Band; E.; Brucker; C. F.; Pretzers, W. R.: Clusters and surfaces. *Chem. Rev.* **1979**, *79*, 91.

(65)   Murahashi, T.; Kurosawa, H.: Organopalladium complexes containing palladium-palladium bonds. *Coord. Chem. Rev* **2002**, *231*, 207-228.

(66)   Doonan, D.J.; Balch, A.L.; Goldberg, S.Z.; Eisenberg, R.; Miller, J.S.: *J. Am. Chem. Soc.* **1975**, *97*, 1961.

(67)   Lin, W.; Wilson, S. R; Girolami, G. S.: Synthesis and X-ray Crystal Structure of the New Palladium(1) Dimer [Pd$_2$(PMe$_3$)$_6$][hfac]$_2$ and Its Conversion to [PdMe(PMe$_3$)$_3$][hfac] via Activation of Phosphorus-Carbon Bonds. *Inorg. Chem.* **1994**, *33*, 2265.

(68)   Murahashi, T.; Nagai, T.; Okuno, T.; Matsutani, T.; Kurosawa, H.: Synthesis and ligand substitution reactions of a homoleptic acetonitrile dipalladium() complex. *Chemical Communications* **2000**, 1689-1690.

(69)   Harvey, P. D.; Murtaza, Z.: Properties of PdI-PdI bonds. Theoretical and spectroscopic study of palladium $Pd_2(dmb)_2X_2$ complexes (dmb = 1,8-diisocyano-p-menthane; X = Cl, Br). *Inorganic Chemistry* **1993**, *32*, 4721-4729.

(70)   Fafard, C. M.; Adhikari, D.; Foxman, B. M.; Mindiola, D. J.; Ozerov, O. V.: Addition of Ammonia, Water, and Dihydrogen Across a Single Pd−Pd Bond. *J. Am. Chem. Soc.* **2007**, *129*, 10318-10319..

(71)   Huacuja, R.; Graham, D. J.; Fafard, C. M.; Chen, C.-H.; Foxman, B. M.; Herbert, D. E.; Alliger, G.; Thomas, C. M.; Ozerov, O. V.: Reactivity of a Pd(I)−Pd(I) Dimer with O2: Monohapto Pd Superoxide and Dipalladium Peroxide in Equilibrium. *J. Am. Chem. Soc.* **2011**, *133*, 3820-3823.

(72)   Tanase, T.; Fukushima, T.; Nomura, T.; Yamamoto, Y.; Kobayashi, K.: Synthesis and Characterization of Binuclear Palladium(I) Complexes of Isocyanides with Phenyl-Substituted Cyclopentadienyl and Tris(pyrazol-1-yl)borate Ligands. *Inorg. Chem.* **1994**, *33*, 32.

(73)   Murahashi, T.; Okuno, T.; Nagai, T.; Kurosawa, H.: Generation of Oligoene Species Capped by Palladium(II) Moieties from a Dinuclear Palladium(I) Complex and Alkyne. *Organometallics* **2002**, *21*, 3679-3682.

(74)   Sumino, S.; Fusano, A.; Fukuyama, T.; Ryu, I.: Carbonylation Reactions of Alkyl Iodides through the Interplay of Carbon Radicals and Pd Catalysts. *Accounts of Chemical Research* **2014**, *47*, 1563-1574.

(75)   Han, X.; Weng, Z.; Hor, T. S. A.: Suzuki coupling catalyzed by a homoleptic Pd(I)–Pd(I) solvento complex. *Journal of Organometallic Chemistry* **2007**, *692*, 5690-5696.

(76)   Gel'man, A. D.; Meilakh, E.: *DoRZady Akad. Nazth S.S.S.R* **1942**, *36*, 171.

(77)   Goggin, P. L.; Mink, J.: Palladium(I) Carbonyl Halide Complexes. *J. Chem. Soc. Dalton Trans* **1974**, 534.

(78)   Goggin, P. L.; Goodfellow, R. J.; Herbert, I. R.; Orpen, A. G.: Bridging by carbonyl vs. halide ligands: X-ray crystal structure of $[NBu_4n]_2[Pd_2Cl_4([small\ micro]-CO)_2]$. *Journal of the Chemical Society, Chemical Communications* **1981**, 1077-1079.

(79)   Tanase, T.; Fukushima, T.; Nomura, T.; Yamamoto, Y.; Kobayashi, K.: Synthesis and characterization of binuclear palladium(I) complexes of isocyanides with phenyl-substituted cyclopentadienyl and tris(pyrazol-1-yl)borate ligands. *Inorganic Chemistry* **1994**, *33*, 32-39.

(80)   Kuz'mina, L. G.; Struchkov, Y. T.: New Palladium Carbonyl Clusters : X-Ray Crystal Structure of $[Pd_4(Co)_4(oAc)_4](AcoH)$. *J. Chem. Soc. Chem. Commun.* **1978**, 27

(81)   Ragaini, F.; Larici, H.; Rimoldi, M.; Caselli, A.; Ferretti, F.; Macchi, P.; Casati, N.: Mapping Palladium Reduction by Carbon Monoxide in a Catalytically Relevant System. A Novel Palladium(I) Dimer. *Organometallics* **2011**, *30*, 2385.

(82)   Baig, S.; Richard, B.; Serp, P.; Mijoule, C.; Hussein, K.; Guihéry, N.; Barthelat, J.-C.; Kalck, P.: Synthesis and Theoretical Study of a Series of Dipalladium(I) Complexes Containing the $Pd_2(\mu-CO)_2$ Core. *Inorganic Chemistry* **2006**, *45*, 1935-1944.

(83)   Baig, S.; Richard, B.; Serp, P.; Mijoule, C.; Hussein, K.; Guihéry, N.; Barthelat, J.-C.; Kalck, P.: Synthesis and Theoretical Study of a Series of Dipalladium(I) Complexes Containing the $Pd_2(\mu-CO)_2$ Core. *Inorg. Chem.* **2006**, *45*, 1935.

(84)   Colton, R.; Farthing, R.; McCormick, M.: Carbonyl halides of the Group VIII transition metals. VI. Compounds of palladium(I). *Australian Journal of Chemistry* **1973**, *26*, 2607-2614.

(85)   Holloway, R. G.; Penfold, B. R.; Colton, R.; McCormick, M. J.: Crystal and molecular structure of bis-[small micro]-(bisdiphenylphosphinomethane)-dibromodipalladium(Pd-Pd), a compound containing palladium(I). *Journal of the Chemical Society, Chemical Communications* **1976**, 485-486.

(86)   Benner, L. S.; Balch, A. L.: Novel reactions of metal-metal bonds. Insertion of isocyanides and carbon monoxide into the palladium-palladium bond of some palladium(I) dimers. *J. Am. Chem. Soc.* **1978**, *100*, 6099-6106.

(87)   Bérubé, J.-F.; Gagnon, K.; Fortin, D.; Decken, A.; Harvey, P. D.: Solution and Solid-State Properties of Luminescent M−M Bond-Containing Coordination/Organometallic Polymers Using the RNC-$M_2(dppm)_2$-CNR Building Blocks (M = Pd, Pt; R = Aryl, Alkyl). *Inorganic Chemistry* **2006**, *45*, 2812-2823.

(88)   Espinet, P.; Fornies, J.; Fortuño, C.; Hidalgo, G.; Martinez, F.; Tomas, M.; Welch, A. J.: Syntheses and reactivity of pentachlorophenylpalladium(I) derivatives. Molecular structure of $Pd_2(\mu$-dppm$)_2(C_6Cl_5)_2$. *Journal of Organometallic Chemistry* **1986**, *317*, 105-119.

(89)   Usón, R.; Forniés, J.; Espinet, P.; Martinez, F.; Fortuño, C.; Menjón, B.: Synthesis of neutral and cationic pentafluorophenylpalladium(I) derivatives. Insertion versus coordination of isocyanides in binuclear palladium(I) complexes. *Journal of Organometallic Chemistry* **1983**, *256*, 365-373.

(90)   Besenyei, G.; Párkányi, L.; Gács-Baitz, E.; James, B. R.: Crystallographic characterization of the palladium(I) dimers, syn-Pd$_2$Cl$_2$(dppmMe)$_2$ and Pd$_2$Cl$_2$(dppm)$_2$; solution conformational behavior of syn- and anti-Pd$_2$Cl$_2$(dppmMe)$_2$ and their (μ-Se) adducts [dppmMe=μ-1,1-bis(diphenylphosphino)ethane, and dppm=μ-bis(diphenylphosphino)methane]. *Inorganica Chimica Acta* **2002**, *327*, 179-187.

(91)   Scott Browning, C.; Farrar, D. H.; Frankel, D. C.; Vittal, J. J.: Synthesis, characterization and reactivity of binuclear palladium(I)bis(diphenylphosphino)amine complexes. *Inorganica Chimica Acta* **1997**, *254*, 329-338.

(92)   Kullberg, M. L.; Lemke, F. R.; Powell, D. R.; Kubiak, C. P.: Palladium-palladium .sigma.-bonds supported by bis(dimethylphosphino)methane (dmpm). Synthetic, structural, and Raman studies of Pd$_2$X$_2$(dmpm)$_2$ (X = Cl, Br, OH). *Inorganic Chemistry* **1985**, *24*, 3589-3593.

(93)   Maisonnat, A.; Farr, J. P.; Balch, A. L.: Dinuclear palladium complexes of 2-diphenylphosphinopyridine. *Inorganica Chimica Acta* **1981**, *53*, L217-L218.

(94)   Farr, J. P.; Wood, F. E.; Balch, A. L.: Head-to-head and head-to-tail isomers of binuclear complexes of platinum(I) and palladium(I) involving 2-(diphenylphosphino)pyridine as a bridging ligand. *Inorganic Chemistry* **1983**, *22*, 3387-3393.

(95)   Párkányi, L.; Szalontai, G.; Besenyei, G.: Structural characterization of the head-to-head isomers of the [Pd$_2$(Ph$_2$Ppy)$_2$Cl$_2$] and [PtPd(Ph$_2$Ppy)$_2$I$_2$] complexes (Ph$_2$Ppy= 2-(diphenylphosphino)pyridine). *Inorganica Chimica Acta* **2006**, *359*, 2933-2941.

(96)   Suzuki, T.; Fujita, J.: Preparation and Characterization of Palladium(I) and Platinum(I) Dinuclear Complexes Bridged by 2-(Dimethylphosphino)pyridine. *Bull. Chem. Soc. Jpn.* **1992**, *65*, 1016-1025.

(97)   Suzuki, T.; Iitaka, N.; Kurachi, S.; Kita, M.; Kashiwabara, K.; Ohba, S.; Fujita, J.: Molecular Structures of HT-[MM′Cl$_2$(μ-Me$_2$Ppy)$_2$] (MM′ = Pd$_2$, PdPt, and Pt$_2$; Me$_2$Ppy = 2-(Dimethylphosphino)pyridine) and HT-[Pd$_2$Cl$_2$(μ-Ph$_2$Ppy)$_2$] (Ph$_2$Ppy = 2-(Diphenylphosphino)pyridine).Bull. Chem. Soc. Jpn. 1992, 65, 1817-1824.

(98)   Li, S.-L.; Zhang, Z.-Z.; Wu, B.-M.; Mak, T. C. W.: Reactivity of trans-(CO)$_3$Fe(Ph$_2$Ppym)$_2$ toward metal reagents: synthesis and crystal structures of [HgCl(Ph2Ppym)(μ-Cl)]2, trans-[(Ph$_2$Ppym)$_2$Rh(CO)Cl]·0.5 CH$_2$Cl$_2$, [PdCl(μ-Ph$_2$Ppym)]$_2$·CH$_2$Cl$_2$, cis-[(Ph$_2$Ppym)$_2$PdCl$_2$]·0.5CH$_2$Cl$_2$ and cis-[Fe(NCS)$_2${Ph$_2$P(O)pym}$_2$] (Ph$_2$Ppym = 2-(diphenylphosphino)pyrimidine). *Inorganica Chimica Acta* **1997**, *255*, 239-248.

(99)   Dervisi, A.; G. Edwards, P.; D. Newman, P.; P. Tooze, R.; J. Coles, S.; B. Hursthouse, M.: Palladium diphenyl-2-pyridylphosphine complexes. *Journal of the Chemical Society, Dalton Transactions* **1998**, 3771-3776.

(100)   Leoni, P.; Pasquali, M.; Pieri, G.; Englert, U.: Synthesis of mono-phosphido, mono-dppm bridged Pd(I) cationic dimers. Structure and fluxionality of [Pd$_2$(μ-PtBu$_2$)(μ-dppm)(η$_1$-dppm)$_2$]CF$_3$SO$_3$ (dppm = bis-diphenylphosphinomethane). *Journal of Organometallic Chemistry* **1996**, *514*, 243-255.

(101)   Usón, R.; Forniés, J.; Fernández Sanz, J.; Usón, M. A.; Usón, I.; Herrero, S.: Reactions of {[Pd(μ-SC$_6$F$_5$)(μ-dppm)Pd](μ-SC$_6$F$_5$)}$_4$·2O(C$_2$H$_5$)$_2$. Crystal Structures of the Complexes [(Ph$_3$P)Pd(μ-SC$_6$F$_5$)(μ-dppm)Pd(SC$_6$F$_5$)]·1.4CH$_2$Cl$_2$ and [(Ph$_3$P)Pd(μ-SC$_6$F$_5$)(μ-dppm)Pd(PPh$_3$)]SO$_3$CF$_3$·2CH$_2$Cl$_2$ and ab Initio MO Calculations on the Model Systems [(H$_3$P)Pd(μ-H$_2$PCH$_2$PH$_2$)(μ-SH)Pd(PH$_3$)]$^+$ and [(H$_3$P)Pd(μ-H$_2$PCH$_2$PH$_2$)Pd(PH$_3$)]$_2^+$. *Inorganic Chemistry* **1997**, *36*, 1912-1922.

(102)   Puddephatt, R. J.; Thomson, M. A.: Reactions of binuclear hydridoplatinum complexes with alkynes. *Inorganic Chemistry* **1982**, *21*, 725-730.

(103)   Puddephatt, R. J.: Chemistry of bis(diphenylphosphino)methane. *Chemical Society Reviews* **1983**, *12*, 99-127.

(104)   Olmstead, M. M.; Hope, H.; Benner, L. S.; Balch, A. L.: Insertion of isocyanides and carbon monoxide into metal-metal bonds. Preparation and structure of [Pd$_2$(CNCH$_3$)$_3$[(C$_6$H$_5$)$_2$PCH$_2$P(C$_6$H$_5$)$_2$]$_2$][PF$_6$]$_2$. *J. Am. Chem. Soc.* **1977**, *99*, 5502-5503.

(105)   Bondi, A.: van der Waals Volumes and Radii. *The Journal of Physical Chemistry* **1964**, *68*, 441-451.

(106)   Rattray, A. D.; Sutton, D.: An aryldiazenido complex of palladium: insertion of aryldiazonium cation into a PdI-PdI bond. *Inorganica Chimica Acta* **1978**, *27*, L85-L86.

(107)   Kikukawa, K.; Matsuda, T.: Reaction Of Diazonium Salts With Transition Metals. I. Arylation Of Olefins With Arenediazonium Salts Catalyzed By Zero Valent Palladium. *Chemistry Letters* **1977**, *6*, 159-162.

(108)   Balch, A. L.; Hunt, C. T.; Lee, C.-L.; Olmstead, M. M.; Farr, J. P.: Organo halide addition to tris(bis(diphenylphosphino)methane)dipalladium. Preparation of novel methylene- and phenylene-bridged complexes by two-center, three-fragment oxidative addition. *J. Am. Chem. Soc.* **1981**, *103*, 3764-3772.

(109)   Balch, A. L.; Benner, L. S.; Olmstead, M. M.: Novel reactions of metal-metal bonds. Addition of sulfur dioxide and sulfur to dichlorobis(bis(diphenylphosphino)methane)dipalladium and the oxidation of coordinated sulfide. *Inorganic Chemistry* **1979**, *18*, 2996-3003.

(110)   Lee, C.-L.; Besenyei, G.; James, B. R.; Nelson, D. A.; Lilga, M. A.: Quantitative recovery of dihydrogen from hydrogen sulphide using the complexes, [Pd$_2$X$_2$([small micro]-dppm)$_2$][X = Cl, Br, l; dppm = bis(diphenylphosphino)methane]. *Journal of the Chemical Society, Chemical Communications* **1985**, 1175-1176.

(111)   Besenyei, G.; Lee, C. L.; Gulinski, J.; Rettig, S. J.; James, B. R.; Nelson, D. A.; Lilga, M. A.: Reaction of hydrogen sulfide with dinuclear palladium(I) complexes containing bis(diphenylphosphino)methane (dpm) and conversion of bridged-sulfide derivatives to bridged-sulfoxide species. X-ray crystal structure of the dimetallic sulfoxide Pd$_2$Cl$_2$(.mu.-SO)(.μ.-dpm)$_2$ containing pyramidal sulfur. *Inorganic Chemistry* **1987**, *26*, 3622-3628.

(112)   Pamplin, C. B.; Rettig, S. J.; Patrick, B. O.; James, B. R.: Solution Behavior and Structural Diversity of Bis(dialkylphosphino)methane Complexes of Palladium. *Inorganic Chemistry* **2003**, *42*, 4117-4126.

(113)   Balch, A. L.; Chung-Li, L.; Lindsay, C. H.; Olmstead, M. M.: Insertion of acetylenes in the Pd-Pd bond of Pd$_2$ (Ph$_2$ PCH$_2$ PPh$_2$)$_2$ Cl$_2$. *Journal of Organometallic Chemistry* **1979**, *177*, C22-C26.

(114)   Lee, C.-L.; Hunt, C. T.; Balch, A. L.: Novel reactions of metal-metal bonds. Reactions of Pd$_2${C$_6$H$_5$)$_2$PCH$_2$P(C$_6$H$_5$)$_2$}$_2$Cl$_2$ with acetylenes, olefins, and isothiocyanates. *Inorganic Chemistry* **1981**, *20*, 2498-2504.

(115)   Kellenberger, B.; Young, S. J.; Stille, J. K.: Intramolecular reductive elimination of methane from a dinuclear palladium complex containing methyl and hydride on adjacent palladium centers. *J. Am. Chem. Soc.* **1985**, *107*, 6105-6107.

(116)   Hazari, N.; Hruszkewycz, D. P.; Wu, J.: Pd(I)-Bridging Allyl Dimers: A New System for the Catalytic Functionalization of Carbon Dioxide. *Synlett* **2011**, *2011*, 1793-1797.

(117)   Hruszkewycz, D. P.; Balcells, D.; Guard, L. M.; Hazari, N.; Tilset, M.: Insight into the Efficiency of Cinnamyl-Supported Precatalysts for the Suzuki–Miyaura Reaction: Observation of Pd(I) Dimers with Bridging Allyl Ligands During Catalysis. *J. Am. Chem. Soc.* **2014**, *136*, 7300-7316

(118)   Hruszkewycz, D. P.; Wu, J.; Green, J. C.; Hazari, N.; Schmeier, T. J.: Mechanistic Studies of the Insertion of CO$_2$ into Palladium(I) Bridging Allyl Dimers. *Organometallics* **2011**, *31*, 470-485.

(119)   Dau, P. D.; Hruszkewycz, D. P.; Huang, D.-L.; Chalkley, M. J.; Liu, H.-T.; Green, J. C.; Hazari, N.; Wang, L.-S.: Photoelectron Spectroscopy of Palladium(I) Dimers with Bridging Allyl Ligands. *Organometallics* **2012**, *31*, 8571-8576.

(120)   Allegra, G.; Immirzi, A.; Porri, L.: A New Type of Bis Arene-Metal Complex. *J. Am. Chem. Soc.* **1965**, *87*, 1394-1395.

(121)   Allegra, G.; Tettamanti Casagrande, G.; Immirzi, A.; Porri, L.; Vitulli, G.: Preparation and structure of two binuclear sandwich benzene-metal complexes of palladium. *J. Am. Chem. Soc.* **1970**, *92*, 289-293.

(122)   Werner, H.; Tune, D.; Parker, G.; Krüger, C.; Brauer, D. J.: Preparation and Structure of Novel Binuclear Palladium Complexes Containing a Metal-Metal Bond: μ-(η-C$_5$H$_5$)-μ-(η-C$_4$H$_7$)Pd$_2$L$_2$. *Angewandte Chemie International Edition in English* **1975**, *14*, 185-186. *Angew. Chem.*, **1975**, *87*, 205–206

(123)   Werner, H.; Kühn, A.; Tune, D. J.; Krüger, C.; Brauer, D. J.; Sekutowski, J. C.; Tsay, Y.-h.: Untersuchungen zur Reaktivität von Metall-π-Komplexen, XXII. Sandwichartig gebaute (Pd–Pd)-Zweikernkomplexe mit brückenbildenden Cyclopentadienyl- und Allyl-Liganden. *Chem. Ber.* **1977**, *110*, 1763-1775.

(124)   Werner, H.: Novel Types of Metal-Metal Bonded Complexes Containing Allyl and Cyclopentadienyl Bridging Ligands. In *Advances in Organometallic Chemistry*; Stone, F. G. A., Robert, W., Eds.; Academic Press, 1981; Vol. Volume 19; pp 155-182.

(125)   Powell, J.; Dowling, N. I.: Direct synthesis of pentaphenylcyclopentadienyl complexes of palladium. *Organometallics* **1983**, *2*, 1742-1748.

(126)   Norton, D. M.; Mitchell, E. A.; Botros, N. R.; Jessop, P. G.; Baird, M. C.: A Superior Precursor for Palladium(0)-Based Cross-Coupling and Other Catalytic Reactions. *The Journal of Organic Chemistry* **2009**, *74*, 6674-6680.

(127)   Werner, H.; Kühn, A.: A General Method for the Synthesis of Sandwich-Type Complexes with a Pd-Pd or Pt-Pt Bond. *Angewandte Chemie International Edition in English* **1977**, *16*, 412-413. *Angew. Chem.*, **1977**, *89*, 427–428

(128)   Chalkley, M. J.; Guard, L. M.; Hazari, N.; Hofmann, P.; Hruszkewycz, D. P.; Schmeier, T. J.; Takase, M. K.: Synthesis, Electronic Structure, and Reactivity of Palladium(I) Dimers with Bridging Allyl, Cyclopentadienyl, and Indenyl Ligands. *Organometallics* **2013**, *32*, 4223-4238.

(129)   Dai, W.; Chalkley, M. J.; Brudvig, G. W.; Hazari, N.; Melvin, P. R.; Pokhrel, R.; Takase, M. K.: Synthesis and Properties of NHC-Supported Palladium(I) Dimers with Bridging Allyl, Cyclopentadienyl, and Indenyl Ligands. *Organometallics* **2013**, *32*, 5114-5127.

(130)   Werner, H.; Kühn, A.: Untersuchungen zur reaktivität von metall-π-komplexen: XXX. (Pd-Pd)-Zweikernkomplexe mit zwei allylgruppen sowie mit einer allylgruppe und einem halogen als brückenliganden. *Journal of Organometallic Chemistry* **1979**, *179*, 439-445.

(131)   Hruszkewycz, D. P.; Wu, J.; Hazari, N.; Incarvito, C. D.: Palladium(I)-Bridging Allyl Dimers for the Catalytic Functionalization of CO_2. *J. Am. Chem. Soc.* **2011**, *133*, 3280-3283.

(132)   Felkin, H.; Kevin Turner, G.: Dimeric palladium (I) complexes containing the bridging cyclopentadienyl group. *Journal of Organometallic Chemistry* **1977**, *129*, 429-436.

(133)   Jolly, P. W.; Kruger, C.; Schick, K.-P.; Wilke, G. Z.: The Structure of [η_3-C_3H_5PdP(C_6H_5)]. *Naturforsch.,B: Anorg. Chem., Org. Chem.* **1980**, *35*, 926.

(134)   Henc, B.; Jolly, P. W.; Salz, R.; Stobbe, S.; Wilke, G.; Benn, R.; Mynott, R.; Seevogel, K.; Goddard, R.; Krüger, C.: Transition metal allyls : IV. The (η_3-allyl)$_2$ M complexes of nickel, palladium and platinum: reaction with tertiary phosphines. *Journal of Organometallic Chemistry* **1980**, *191*, 449-475.

(135)   Werner, H.; Kraus, H.-J.: Synthesis and Structural Dynamics of Bis(cyclopentadienyl)phosphanepalladium Complexes. *Angewandte Chemie International Edition in English* **1979**, *18*, 948-949. *Angew. Chem.*, **1979**, *91*, 1013–1014.

(136)   Werner, H.; Kraus, H.-J.: Di-[small micro]-(cyclopentadienyl)-bis(tri-isopropylphosphine)dipalladium(I). *Journal of the Chemical Society, Chemical Communications* **1979**, 814-815.

(137)   Werner, H.; Kraus, H.-J.; Schubert, U.; Ackermann, K.: Untersuchungen zur Reaktivität von Metall-π-Komplexen, XXXVI. Zweikernige Sandwichkomplexe mit Metall-Metall-Bindung: Synthese und Struktur von (μ-C_5H_5)2Pd$_2$(PR$_3$)$_2$. *Chem. Ber.* **1982**, *115*, 2905-2913.

(138)Tanase, T.; Nomura, T.; Fukushima, T.; Yamamoto, Y.; Kobayashi, K.: Studies on interactions of isocyanide with transition metal complexes. 36. Synthesis and characterization of a binuclear palladium(I) complex with bridging .eta.3-indenyl ligands, Pd$_2$(.mu.-.eta.3-indenyl)$_2$(isocyanide)$_2$, and its transformation to a tetranuclear palladium(I) cluster of isocyanides, Pd$_4$(.mu.-acetate)$_4$(.mu.-isocyanide)$_4$. *Inorganic Chemistry* **1993**, *32*, 4578-4584.

(139)   Dupont, J.; Pfeffer, M.; Rotteveel, M. A.; De Cian, A.; Fischer, J.: Reactivity of cyclopalladated compounds. 20. Isolation of a bis(.eta.4-arene)dipalladium(I) complex during the annelation of palladated aryl groups with diphenylacetylene. *Organometallics* **1989**, *8*, 1116-1118.

(140)   Gorlov, M.; Fischer, A.; Kloo, L.: Reaction between palladium(II) and gallium(III) halogenides in arenes: influence of halogen nature on the formation of binuclear palladium(I) clusters. *Journal of Organometallic Chemistry* **2004**, *689*, 489-492.

(141)   Gorlov, M.; Fischer, A.; Kloo, L.: Dimeric palladium and platinum complexes isolated in Lewis-acidic media. *Inorganica Chimica Acta* **2009**, *362*, 605-609.

(142)   Gorlov, M.; Fischer, A.; Kloo, L.: Binuclear palladium(I) and platinum(I) dimers stabilized by aromatic ligands: synthesis, structural characterization and reactivity with carbon monoxide. *Inorganica Chimica Acta* **2003**, *350*, 449-454.

(143)   Barder, T. E.: Synthesis, Structural, and Electron Topographical Analyses of a Dialkylbiaryl Phosphine/Arene-Ligated Palladium(I) Dimer: Enhanced Reactivity in Suzuki−Miyaura Coupling Reactions. *J. Am. Chem. Soc.* **2005**, *128*, 898-904.

(144)   Lin, S.; Herbert, D. E.; Velian, A.; Day, M. W.; Agapie, T.: Dipalladium(I) Terphenyl Diphosphine Complexes as Models for Two-Site Adsorption and Activation of Organic Molecules. *J. Am. Chem. Soc.* **2013**, *135*, 15830-15840

(145)   Murahashi, T.; Kimura, S.; Takase, K.; Ogoshi, S.; Yamamoto, K.: Bridging [small pi]-coordination of pyrrole and indole over a PdI-PdI bond. *Chemical Communications* **2013**, *49*, 4310-4312.

(146)   Werner, H.; Kraus, H.-J.; Thometzek, P.: Untersuchungen zur Reaktivität von Metall-π-Komplexen, XXXVII. Brückenaustauschreaktionen an zweikernigen μ-(Cyclopentadienyl)-dipalladium-Komplexen: Synthese sandwich-artiger heterometallischer Pd$_2$Cr- und Pd$_2$Mo-Cluster. *Chem. Ber.* **1982**, *115*, 2914-2926.

(147)   Kobayashi, Y.; Iitaka, Y.; Yamazaki, H.: The crystal and molecular structures of a novel μ-allyl palladium complex, μ-allyl-μ-iodo-bis(triphenylphosphinepalladium) benzene solvate. *Acta Crystallographica Section B* **1972**, *28*, 899-906.

(148)   Sieler, J.; Helms, M.; Gaube, W.; Svensson, A.; Lindqvist, O.: Darstellung und kristallstruktur von μ3-allyl-μ1-chlorobis(triphenylphosphin)dipalladium(I). *Journal of Organometallic Chemistry* **1987**, *320*, 129-136.

(149)   Weissman, H.; Shimon, L. J. W.; Milstein, D.: Unsaturated Pd(0), Pd(I), and Pd(II) Complexes of a New Methoxy-Substituted Benzyl Phosphine. Aryl−X (X = Cl, I) Oxidative Addition, C−O Cleavage, and Suzuki−Miyaura Coupling of Aryl Chlorides. *Organometallics* **2004**, *23*, 3931-3940.

(150)   Hill, L. L.; Crowell, J. L.; Tutwiler, S. L.; Massie, N. L.; Hines, C. C.; Griffin, S. T.; Rogers, R. D.; Shaughnessy, K. H.; Grasa, G. A.; Johansson Seechurn, C. C. C.; Li, H.; Colacot, T. J.; Chou, J.; Woltermann, C. J.: Synthesis and X-ray Structure Determination of Highly Active Pd(II), Pd(I), and Pd(0) Complexes of Di(tert-butyl)neopentylphosphine (DTBNpP) in the Arylation of Amines and Ketones. *The Journal of Organic Chemistry* **2010**, *75*, 6477-6488.

(151)   Kurosawa, H.; Hirako, K.; Natsume, S.; Ogoshi, S.; Kanehisa, N.; Kai, Y.; Sakaki, S.; Takeuchi, K.: New Insights into Structures, Stability, and Bonding of μ-Allyl Ligands Coordinated with Pd−Pd and Pd−Pt Fragments. *Organometallics* **1996**, *15*, 2089-2097.

(152)   Yamamoto, T.; Akimoto, M.; Yamamoto, A.: Oxidative Addition Of Allyl-Chalcogen (0, S, Se) Bonds To Palladium(0). Isolation Of The Oxidative Addition Products. *Chem. Lett* **1983**, 1725.

(153)   Osakada, K.; Chiba, T.; Nakamura, Y.; Yamamoto, T.; Yamamoto, A.: Steric effect of substituents in allylic groups in oxidative addition of allylic phenyl sulphides to a palladium(0) complex. C-S bond cleavage triggered by attack of Pd on the terminal carbon of the C=C double bond. *Journal of the Chemical Society, Chemical Communications* **1986**, 1589-1591.

(154)   Osakada, K.; Chiba, T.; Nakamura, Y.; Yamamoto, T.; Yamamoto, A.: Synthesis, characterization, and isomerization behavior of syn-(μ-.eta.3-1-methylallyl)(μ-benzenethiolato)bis(tricyclohexylphosphine)dipalladium(I), [(C$_6$H$_{11}$)$_3$P]$_2$Pd$_2$(syn-μ-.eta.3-CH$_2$CHCHCH$_3$)(μ-SC$_6$H$_5$) and its anti isomer. *Organometallics* **1989**, *8*, 2602-2605.

(155)   Osakada, K.; Ozawa, Y.; Yamamoto, A.: Preparation of (Me$_3$P)$_2$Pd$_2$(μ-η$_3$-C$_3$H$_5$)(μ-SPH) by reaction of Pd(O) complex with allyl phenyl sulfide. *Journal of Organometallic Chemistry* **1990**, *399*, 341-348.

(156)   Miyauchi, Y.; Watanabe, S.; Kuniyasu, H.; Kurosawa, H.: Ligand-Dependent Relative Stability Order in Allyl Sulfide/Palladium(0) Species vs (.eta.3-Allyl)palladium(II) Thiolate Species. *Organometallics* **1995**, *14*, 5450-5453.

(157)   Ducruix, A.; Felkin, H.; Pascard, C.; Turner, G. K.: Preparation and crystal structure of [small micro]-cyclopentadienyl-[small micro]-bromo-bis(tri-isopropylphosphinepalladium). *Journal of the Chemical Society, Chemical Communications* **1975**, 615-616.

(158)   Kühn, A.; Werner, H.: Untersuchungen zur reaktivität von metall-π-komplexen : XXIX. Synthesewege und reaktivität von (Pd-Pd)- und (Pt-Pt)-zweikernkomplexen des typs (μ-C$_5$H$_5$)(μ-allyl)M$_2$L$_2$. *Journal of Organometallic Chemistry* **1979**, *179*, 421-438.

(159)   Kuehn, A.; Burschka, C.; Werner, H.: Studies on the reactivity of metal π.-complexes. Part 35. Synthesis and molecular structure of C$_5$H$_5$(PPr-i$_3$)Pd(.eta.1,.eta.3-C$_3$H$_4$)Pd(PPr-i$_3$)Br: a compound formed through insertion of allene into a metal-metal bond. *Organometallics* **1982**, *1*, 496-499.

(160)   Sui-Seng, C.; Enright, G. D.; Zargarian, D.: New Palladium(II)−(η$_{3/5}$- or η1-Indenyl) and Dipalladium(I)−(μ,η$_3$-Indenyl) Complexes. *J. Am. Chem. Soc.* **2006**, *128*, 6508-6519.

(161)   Werner, H.; Kraus, H.-J.: Untersuchungen zur Reaktivität von Metall-π-Komplexen, XXXI. Zweikernige Palladium(I)-Komplexe mit brückenbildenden Carboxylat-Liganden. *Chem. Ber.* **1980**, *113*, 1072-1083.

(162)   Yamamoto, T.; Saito, O.; Yamamoto, A.: Oxidative addition of allyl acetate to palladium(0) complexes. *J. Am. Chem. Soc.* **1981**, *103*, 5600-5602.

(163)   Christmann, U.; Pantazis, D. A.; Benet-Buchholz, J.; McGrady, J. E.; Maseras, F.; Vilar, R.: Experimental and Theoretical Investigations of New Dinuclear Palladium Complexes as Precatalysts for the Amination of Aryl Chlorides. *J. Am. Chem. Soc.* **2006**, *128*, 6376-6390.

(164)   Denmark, S. E.; Baird, J. D.: Palladium-Catalyzed Cross-Coupling Reactions of Heterocyclic Silanolates with Substituted Aryl Iodides and Bromides. *Organic Letters* **2006**, *8*, 793-795.

(165)   Denmark, S. E.; Baird, J. D.; Regens, C. S.: Palladium-Catalyzed Cross-Coupling of Five-Membered Heterocyclic Silanolates. *The Journal of Organic Chemistry* **2008**, *73*, 1440-1455.

(166)   Elliott, E. L.; Ray, C. R.; Kraft, S.; Atkins, J. R.; Moore, J. S.: Solid-Phase Synthesis of m-Phenylene Ethynylene Heterosequence Oligomers. *The Journal of Organic Chemistry* **2006**, *71*, 5282-5290.

(167)   Finke, A. D.; Elleby, E. C.; Boyd, M. J.; Weissman, H.; Moore, J. S.: Zinc Chloride-Promoted Aryl Bromide−Alkyne Cross-Coupling Reactions at Room Temperature. *The Journal of Organic Chemistry* **2009**, *74*, 8897-8900.

(168)   Colacot, T. J.: A Highly Active Palladium(I) Dimer for Pharmaceutical Applications. *Platinum Metals Rev.,* **2009**, *53*, 183.

(169)   Vilar, R.; Mingos, D. M. P.; Cardin, C. J.: Synthesis and structural characterisation of [Pd$_2$([μ]-Br)$_2$(PBut$_3$)$_2$], an example of a palladium(I)-palladium(I) dimer. *Journal of the Chemical Society, Dalton Transactions* **1996**, 4313-4314.

(170)   Durà-Vilà, V.; P. Mingos, D. M.; Vilar, R.; White, A. J. P.; Williams, D. J.: Reactivity studies of [Pd$_2$(μ-X)$_2$(PtBu$_3$)$_2$] (X = Br, I) with CNR (R = 2,6-dimethylphenyl), H$_2$ and alkynes. *Journal of Organometallic Chemistry* **2000**, *600*, 198-205.

(171)   Stambuli, J. P.; Kuwano, R.; Hartwig, J. F.: Unparalleled Rates for the Activation of Aryl Chlorides and Bromides: Coupling with Amines and Boronic Acids in Minutes at Room Temperature. *Angewandte Chemie International Edition* **2002**, *41*, 4746-4748. *Angew. Chem.*, **2002**,*114*, 4940–4942.

(172)   Christmann, U.; Pantazis, D. A.; Benet-Buchholz, J.; McGrady, J. E.; Maseras, F.; Vilar, R.: Synthesis and Computational Studies of Palladium(I) Dimers Pd$_2$X$_2$(PtBu$_2$Ph)$_2$ (X = Br, I): Phenyl versus Halide Bridging Modes. *Organometallics* **2006**, *25*, 5990-5995.

(173)   Mingos, D. M. P.; Vilar, R.: Synthesis and reactivity of palladium cluster compounds. *Journal of Organometallic Chemistry* **1998**, *557*, 131-142.

(174)   Vilar, R.; E. Lawrence, S.; Menzer, S.; Michael P. Mingos, D.; J. Williams, D.: Synthesis and structural characterisation of tetranuclear palladium-cobalt clusters. *Journal of the Chemical Society, Dalton Transactions* **1997**, 3305-3310.

(175)   Dura-Vila, V.; Mingos, D. M. P.; Vilar, R.; White, A. J. P.; Williams, D. J.: Insertion of O$_2$ into a Pd(i)-Pd(i) dimer and subsequent C-O bond formation by activation of a C-H bond. *Chemical Communications* **2000**, 1525-1526.

(176)   Old, D. W.; Wolfe, J. P.; Buchwald, S. L.: A Highly Active Catalyst for Palladium-Catalyzed Cross-Coupling Reactions: Room-Temperature Suzuki Couplings and Amination of Unactivated Aryl Chlorides. *J. Am. Chem. Soc.* **1998**, *120*, 9722-9723.

(177)   Hamann, B. C.; Hartwig, J. F.: Sterically Hindered Chelating Alkyl Phosphines Provide Large Rate Accelerations in Palladium-Catalyzed Amination of Aryl Iodides, Bromides, and Chlorides, and the First Amination of Aryl Tosylates. *J. Am. Chem. Soc.* **1998**, *120*, 7369-7370.

(178)   Li, G. Y.; Zheng, G.; Noonan, A. F.: Highly Active, Air-Stable Versatile Palladium Catalysts for the C−C, C−N, and C−S Bond Formations via Cross-Coupling Reactions of Aryl Chlorides. *The Journal of Organic Chemistry* **2001**, *66*, 8677-8681.

(179)   Bei, X.; Turner, H. W.; Weinberg, W. H.; Guram, A. S.; Petersen, J. L.: Palladium/P,O-Ligand-Catalyzed Suzuki Cross-Coupling Reactions of Arylboronic Acids and Aryl Chlorides. Isolation and Structural Characterization of (P,O)-Pd(dba) Complex. *The Journal of Organic Chemistry* **1999**, *64*, 6797-6803.

(180)   Zapf, A.; Ehrentraut, A.; Beller, M.: A New Highly Efficient Catalyst System for the Coupling of Nonactivated and Deactivated Aryl Chlorides with Arylboronic Acids. *Angewandte Chemie International Edition* **2000**, *39*, 4153-4155. *Angew. Chem.*, **2000**, *112*, 4315–4317.

(181)   Reetz, M. T.; Lohmer, G.; Schwickardi, R.: A New Catalyst System for the Heck Reaction of Unreactive Aryl Halides. *Angewandte Chemie International Edition* **1998**, *37*, 481-483. Angew. Chem., **1998**, 110, 492–495

(182)   Navarro, O.; Kaur, H.; Mahjoor, P.; Nolan, S. P.: Cross-Coupling and Dehalogenation Reactions Catalyzed by (N-Heterocyclic carbene)Pd(allyl)Cl Complexes. *The Journal of Organic Chemistry* **2004**, *69*, 3173-3180.

(183)   Böhm, V. P. W.; Gstöttmayr, C. W. K.; Weskamp, T.; Herrmann, W. A.: N-Heterocyclic carbenes: Part 26. N-Heterocyclic carbene complexes of palladium(0): synthesis and application in the Suzuki cross-coupling reaction. *Journal of Organometallic Chemistry* **2000**, *595*, 186-190.

(184)   Prashad, M.; Mak, X. Y.; Liu, Y.; Repič, O.: Palladium-Catalyzed Amination of Aryl Bromides with Hindered N-Alkyl-Substituted Anilines Using a Palladium(I) Tri-tert-butylphosphine Bromide Dimer. *The Journal of Organic Chemistry* **2003**, *68*, 1163-1164.

(185)   Huang, J.; Bunel, E.; Faul, M. M.: Palladium-Catalyzed α-Vinylation of Carbonyl Compounds. *Organic Letters* **2007**, *9*, 4343-4346.

(186)   Hama, T.; Culkin, D. A.; Hartwig, J. F.: Palladium-Catalyzed Intermolecular α-Arylation of Zinc Amide Enolates under Mild Conditions. *J. Am. Chem. Soc.* **2006**, *128*, 4976-4985.

(187)   Hama, T.; Ge, S.; Hartwig, J. F.: Palladium-Catalyzed α-Arylation of Zinc Enolates of Esters: Reaction Conditions and Substrate Scope. *The Journal of Organic Chemistry* **2013**, *78*, 8250-8266.

(188)   Hama, T.; Hartwig, J. F.: Palladium-Catalyzed α-Arylation of Esters with Chloroarenes. *Organic Letters* **2008**, *10*, 1549-1552.

(189)   Hama, T.; Hartwig, J. F.: α-Arylation of Esters Catalyzed by the Pd(I) Dimer {[P(t-Bu)$_3$]PdBr}$_2$. *Organic Letters* **2008**, *10*, 1545-1548.

(190)   Eichman, C. C.; Stambuli, J. P.: Zinc-Mediated Palladium-Catalyzed Formation of Carbon−Sulfur Bonds. *The Journal of Organic Chemistry* **2009**, *74*, 4005-4008.

(191)   Ryberg, P.: Development of a Mild and Robust Method for Large-Scale Palladium-Catalysed Cyanation of Aryl Bromides: Importance of the Order of Addition. *Organic Process Research & Development* **2008**, *12*, 540-543.

(192)   Bercot, E. A.; Caille, S.; Bostick, T. M.; Ranganathan, K.; Jensen, R.; Faul, M. M.: Diastereoselective Palladium-Catalyzed α-Arylation of 4-Substituted Cyclohexyl Esters. *Organic Letters* **2008**, *10*, 5251-5254.

(193)   Mamone, P.; Grünberg, M. F.; Fromm, A.; Khan, B. A.; Gooßen, L. J.: [Pd(μ-Br)(PtBu$_3$)]$_2$ as a Highly Active Isomerization Catalyst: Synthesis of Enol Esters from Allylic Esters. *Organic Letters* **2012**, *14*, 3716-3719.

(194)   Buscemi, G.; Miller, P. W.; Kealey, S.; Gee, A. D.; Long, N. J.; Passchier, J.; Vilar, R.: Rapid carbonylative coupling reactions using palladium(i) dimers: applications to 11CO-radiolabelling for the synthesis of PET tracers. *Organic & Biomolecular Chemistry* **2011**, *9*, 3499-3503.

(195)   Dedieu, A.; Hoffmann, R.: Platinum(0)-platinum(0) dimers. Bonding relationships in a d10-d10 system. *J. Am. Chem. Soc.* **1978**, *100*, 2074-2079.

(196)   Stern, E. W.; Maples, P. K.: Homogeneous hydrogenation of unsaturated compounds catalyzed by Pd complexes: I. Scope and effect of variables. *Journal of Catalysis* **1972**, *27*, 120-133.

(197)   Kirss, R. U.; Eisenberg, R.: Di(phosphine)-bridged complexes of palladium. Parahydrogen-induced polarization in hydrogenation reactions and structure determination of tris(μ-bis(diphenylphosphino)methane)dipalladium, Pd$_2$(dppm)$_3$. *Inorganic Chemistry* **1989**, *28*, 3372-3378.

(198)   Lindsay, C. H.; Balch, A. L.: Halogen additions to bis(diphenylphosphino)methane complexes of palladium. Interrelationships of monomeric and dimeric complexes of palladium(II), palladium(I), and palladium(0). *Inorganic Chemistry* **1981**, *20*, 2267-2270.

(199)   Pan, Y.; Mague, J. T.; Fink, M. J.: Synthesis, structure, and unusual reactivity of a d10-d10 palladium(0) dimer. *J. Am. Chem. Soc.* **1993**, *115*, 3842-3843.

(200)   Reid, S. M.; Fink, M. J.: Reductive Routes to Dinuclear d10−d10 Palladium(0) Complexes and Their Redistribution Equilibria in Solution. *Organometallics* **2001**, *20*, 2959-2961.

(201)   Trebbe, R.; Goddard, R.; Rufińska, A.; Seevogel, K.; Pörschke, K.-R.: Preparation and Structural Characterization of the Palladium(0)−Carbonyl Complexes (R$_2$PC$_2$H$_4$PR$_2$)Pd(CO)$_2$ and {(R$_2$PC$_2$H$_4$PR$_2$)Pd}$_2$(μ-CO)†. *Organometallics* **1999**, *18*, 2466-2472.

(202)   Reid, S. M.; Mague, J. T.; Fink, M. J.: Facile Reductive Elimination of Ethane from Strained Dimethylpalladium(II) Complexes. *J. Am. Chem. Soc.* **2001**, *123*, 4081-4082.

(203)   Lumbreras Jr, E.; Sisler, E. M.; Shelby, Q. D.: Synthesis, X-ray crystal structure, and reactivity of Pd$_2$(μ-dotpm)$_2$ (dotpm=bis(di-ortho-tolylphosphino)methane). *Journal of Organometallic Chemistry* **2010**, *695*, 201-205.

(203)   Yamamoto, Y.; Ohno, T.; Itoh, K.: Dinuclear Palladium(0) and Platinum(0) Complexes with p-Benzoquinone and Norbornene Ligands. *Organometallics* **2003**, *22*, 2267-2272.

(204)   Yamamoto, Y.; Ohno, T.; Itoh, K.: Dinuclear Palladium(0) and Platinum(0) Complexes with p-Benzoquinone and Norbornene Ligands. *Organometallics* **2003**, *22*, 2267-2272

(205)   Cotton, F. A.; Matusz, M.; Poli, R.; Feng, X.: Dinuclear formamidinato complexes of nickel and palladium. *J. Am. Chem. Soc.* **1988**, *110*, 1144-1154.

(206)   Churchill M. R; Mason, R.: Molecular Structure Of Π-Alyll-Palladium Acetate. *Nature* **1964**, *204*, 777.

(207)   Corbett, M.; Hoskins, B.; McLeod, N.; O'Day, B.: Binuclear metal(II) complexes of 1,3-diphenyltriazene : The crystal and molecular structures of the nickel(II), palladium(II) and copper(II) derivatives. *Australian Journal of Chemistry* **1975**, *28*, 2377-2392.

(208)   Piovesana, O.; Bellitto, C.; Flamini, A.; Zanazzi, P. F.: Metal-metal interactions in one dimension. 1. Synthesis and structural and spectroscopic properties of dithioacetic acid derivatives of palladium(II). *Inorganic Chemistry* **1979**, *18*, 2258-2265.

(209)   Clegg, W.; Garner, C. D.; Al-Samman, M. H.: Preparation and structural characterization of dipalladium(II) tetrakis(6-methyl-2-oxypyridine), [Pd$_2$(mhp)$_4$]. *Inorganic Chemistry* **1982**, *21*, 1897-1901.

(210)   Hiraki, K.; Fuchita, Y.; Takechi, K.: Preparation and characterization of novel six-membered cyclopalladated complexes of 2-benzylpyridine. *Inorganic Chemistry* **1981**, *20*, 4316-4320.

(211)   Bercaw, J. E.; Durrell, A. C.; Gray, H. B.; Green, J. C.; Hazari, N.; Labinger, J. A.; Winkler, J. R.: Electronic Structures of PdII Dimers. *Inorganic Chemistry* **2010**, *49*, 1801-1810.

(212)   Xia, B.-H.; Che, C.-M.; Zhou, Z.-Y.: The Quest for PdII–PdII Interactions: Structural and Spectroscopic Studies and Ab Initio Calculations on Dinuclear [Pd$_2$(CN)$_4$(μ-diphosphane)$_2$] Complexes. *Chemistry – A European Journal* **2003**, *9*, 3055-3064.

(213)   Pan, Q.-J.; Zhang, H.-X.; Zhou, X.; Fu, H.-G.; Yu, H.-T.: Electronic Structures and Spectroscopic Properties of Mono- and Binuclear d8 Complexes: A Theoretical Exploration on Promising Phosphorescent Materials. *The Journal of Physical Chemistry A* **2006**, *111*, 287-294.

(214)   Marino, N.; Fazen, C. H.; Blakemore, J. D.; Incarvito, C. D.; Hazari, N.; Doyle, R. P.: Isostructural PdII and PtII Pyrophosphato Complexes: Polymorphism and Unusual Bond Character in d8−d8 Systems. *Inorganic Chemistry* **2011**, *50*, 2507-2520.

(215)   Luo, J.; Khusnutdinova, J. R.; Rath, N. P.; Mirica, L. M.: Unsupported d8-d8 interactions in cationic PdII and PtII complexes: evidence for a significant metal-metal bonding character. *Chemical Communications* **2012**, *48*, 1532-1534.

(216)   Weber, M.; Klein, J. E. M. N.; Miehlich, B.; Frey, W.; Peters, R.: Monomeric Ferrocene Bis-Imidazoline Bis-Palladacycles: Variation of Pd–Pd Distances by an Interplay of Metallophilic, Dispersive, and Coulombic Interactions. *Organometallics* **2013**, *32*, 5810-5817.

(217)   Powers, D. C.; Ritter, T.: 7.23 Oxidation of Carbon–Metal Bonds. In *Comprehensive Organic Synthesis II (Second Edition)*; Knochel, P., Ed.; Elsevier: Amsterdam, 2014; pp 719-743.

(218)   Yao, C. L.; He, L. P.; Korp, J. D.; Bear, J. L.: Dipalladium complexes with N,N'-diphenylbenzamidine bridging and chelating ligands. Synthesis and structural and electrochemical studies. *Inorganic Chemistry* **1988**, *27*, 4389-4395.

(219)   Cotton, F. A.; Gu, J.; Murillo, C. A.; Timmons, D. J.: The First Dinuclear Complex of Palladium(III). *J. Am. Chem. Soc.* **1998**, *120*, 13280-13281.

(220)   Powers, D. C.; Geibel, M. A. L.; Klein, J. E. M. N.; Ritter, T.: Bimetallic Palladium Catalysis: Direct Observation of Pd(III)−Pd(III) Intermediates. *J. Am. Chem. Soc.* **2009**, *131*, 17050-17051.

(221)   Powers, D. C.; Ritter, T.: Bimetallic Pd(III) complexes in palladium-catalysed carbon–heteroatom bond formation. *Nat Chem* **2009**, *1*, 302-309.

(222)   Cotton, F. A.; Koshevoy, I. O.; Lahuerta, P.; Murillo, C. A.; Sanaú, M.; Ubeda, M. A.; Zhao, Q.: High Yield Syntheses of Stable, Singly Bonded Pd$_2$6+ Compounds. *J. Am. Chem. Soc.* **2006**, *128*, 13674-13675.

(223)   Penno, D.; Lillo, V.; Koshevoy, I. O.; Sanaú, M.; Ubeda, M. A.; Lahuerta, P.; Fernández, E.: Multifaceted Palladium Catalysts Towards the Tandem Diboration–Arylation Reactions of Alkenes. *Chemistry – A European Journal* **2008**, *14*, 10648-10655.

(224)   Dick, A. R.; Hull, K. L.; Sanford, M. S.: A Highly Selective Catalytic Method for the Oxidative Functionalization of C−H Bonds. *J. Am. Chem. Soc.* **2004**, *126*, 2300-2301.

(225)   Powers, D. C.; Benitez, D.; Tkatchouk, E.; Goddard, W. A.; Ritter, T.: Bimetallic Reductive Elimination from Dinuclear Pd(III) Complexes. *J. Am. Chem. Soc.* **2010**, *132*, 14092-14103.

(226)   Powers, D. C.; Xiao, D. Y.; Geibel, M. A. L.; Ritter, T.: On the Mechanism of Palladium-Catalyzed Aromatic C−H Oxidation. *J. Am. Chem. Soc.* **2010**, *132*, 14530-14536.

(227)   Ariafard, A.; Hyland, C. J. T.; Canty, A. J.; Sharma, M.; Brookes, N. J.; Yates, B. F.: Ligand Effects in Bimetallic High Oxidation State Palladium Systems. *Inorganic Chemistry* **2010**, *49*, 11249-11253.

(228)   Gronowitz, S.; Björk, P.; Malm, J.; Hörnfeldt, A.-B.: The effect of some additives on the Stille Pd0-catalyzed cross-coupling reaction. *Journal of Organometallic Chemistry* **1993**, *460*, 127-129.

(229)   Saa, J. M.; Martorell, G.: Palladium-catalyzed cross-coupling synthesis of hindered biaryls and terphenyls. Cocatalysis by copper(I) salts. *The Journal of Organic Chemistry* **1993**, *58*, 1963-1966.

(230)   Farina, V.; Kapadia, S.; Krishnan, B.; Wang, C.; Liebeskind, L. S.: On the Nature of the "Copper Effect" in the Stille Cross-Coupling. *The Journal of Organic Chemistry* **1994**, *59*, 5905-5911.

(231)   Han, X.; Stoltz, B. M.; Corey, E. J.: Cuprous Chloride Accelerated Stille Reactions. A General and Effective Coupling System for Sterically Congested Substrates and for Enantioselective Synthesis. *J. Am. Chem. Soc.* **1999**, *121*, 7600-7605.

(232)   Espinet, P.; Echavarren, A. M.: The Mechanisms of the Stille Reaction. *Angewandte Chemie International Edition* **2004**, *43*, 4704-4734. *Angew. Chem.*, **2004**, *116*, 4808–4839.

(233)   Sonogashira, K.; Tohda, Y.; Hagihara, N.: A convenient synthesis of acetylenes: catalytic substitutions of acetylenic hydrogen with bromoalkenes, iodoarenes and bromopyridines. *Tetrahedron Lett.* **1975**, *16*, 4467-4470.

(234)   Liebeskind, L. S.; Srogl, J.: Thiol Ester−Boronic Acid Coupling. A Mechanistically Unprecedented and General Ketone Synthesis. *J. Am. Chem. Soc.* **2000**, *122*, 11260-11261.

(235)   Deng, J. Z.; Paone, D. V.; Ginnetti, A. T.; Kurihara, H.; Dreher, S. D.; Weissman, S. A.; Stauffer, S. R.; Burgey, C. S.: Copper-Facilitated Suzuki Reactions: Application to 2-Heterocyclic Boronates. *Organic Letters* **2008**, *11*, 345-347.

(236)   Casado, A. L.; Espinet, P.: Quantitative Evaluation of the Factors Contributing to the "Copper Effect" in the Stille Reaction. *Organometallics* **2003**, *22*, 1305-1309.

(237)   Meyer, N.; Schuh, E.; Mohr, F.: Silver and gold. *Annual Reports Section "A" (Inorganic Chemistry)* **2011**, *107*, 233-245.

(238)   Halbes-Letinois, U.; Weibel, J.-M.; Pale, P.: The organic chemistry of silver acetylides. *Chemical Society Reviews* **2007**, *36*, 759-769.

(239)   Negishi, E.-i.; Anastasia, L.: Palladium-Catalyzed Alkynylation. *Chem. Rev.* **2003**, *103*, 1979-2018.

(240)   Plenio, H.: Catalysts for the Sonogashira Coupling—The Crownless Again Shall Be King. *Angewandte Chemie International Edition* **2008**, *47*, 6954-6956. *Angew. Chem.*, **2008**,*120*, 7060–7063.

(241)   Pérez-Temprano, M. H.; Casares, J. A.; Espinet, P.: Bimetallic Catalysis using Transition and Group 11 Metals: An Emerging Tool for C-C Coupling and Other Reactions. *Chemistry – A European Journal* **2012**, *18*, 1864-1884.

(242)   Chinchilla, R.; Nájera, C.: The Sonogashira Reaction: A Booming Methodology in Synthetic Organic Chemistry†. *Chem. Rev.* **2007**, *107*, 874-922.

(243)   Long, N. J.; Williams, C. K.: Metal Alkynyl σ Complexes: Synthesis and Materials. *Angewandte Chemie International Edition* **2003**, *42*, 2586-2617. *Angew. Chem.*, **2003**, *115*, 2690–2722

(244)   an der Heiden, M. R.; Plenio, H.; Immel, S.; Burello, E.; Rothenberg, G.; Hoefsloot, H. C. J.: Insights into Sonogashira Cross-Coupling by High-Throughput Kinetics and Descriptor Modeling. *Chemistry – A European Journal* **2008**, *14*, 2857-2866.

(245)   Barrios-Landeros, F.; Hartwig, J. F.: Distinct Mechanisms for the Oxidative Addition of Chloro-, Bromo-, and Iodoarenes to a Bisphosphine Palladium(0) Complex with Hindered Ligands. *J. Am. Chem. Soc.* **2005**, *127*, 6944-6945.

(246)   Eberhard, M. R.; Wang, Z.; Jensen, C. M.: Investigations into the Pd-catalysed cross-coupling of phenylacetylene with aryl chlorides: simple one-pot procedure and the effect of ZnCl2 co-catalysis. *Chemical Communications* **2002**, 818-819.

(247)   Choudary, B. M.; Madhi, S.; Chowdari, N. S.; Kantam, M. L.; Sreedhar, B.: Layered Double Hydroxide Supported Nanopalladium Catalyst for Heck-, Suzuki-, Sonogashira-, and Stille-Type Coupling Reactions of Chloroarenes. *J. Am. Chem. Soc.* **2002**, *124*, 14127-14136.

(248)   Köllhofer, A.; Pullmann, T.; Plenio, H.: A Versatile Catalyst for the Sonogashira Coupling of Aryl Chlorides. *Angewandte Chemie International Edition* **2003**, *42*, 1056-1058. *Angew. Chem.*, **2003**, *115*, 1086–1088

(249)   Koellhofer, A.; Pullmann, T.; Plenio, H.: A Versatile Catalyst for the Sonogashira Coupling of Aryl Chlorides. *Angew. Chem. Int. Ed.* **2003**, *42*, 1056-1058. *Angew. Chem*, **2003**, *115,* 1086-1088.

(250)   Siemsen, P.; Livingston, R. C.; Diederich, F.: Acetylenic Coupling: A Powerful Tool in Molecular Construction. *Angewandte Chemie International Edition* **2000**, *39*, 2632-2657. *Angew. Chem.*, **2000**, *112*, 2740–2767.

(251)   Pal, M.; Parasuraman, K.; Gupta, S.; Yeleswarapu, K. R.: Regioselective Synthesis of 4-Substituted-1-Aryl-1-butanones Using a Sonogashira-Hydration Strategy: Copper-Free Palladium-Catalyzed Reaction of Terminal Alkynes with Aryl Bromides. *Synlett* **2002**, *2002*, 1976-1982.

(252)   Fukuyama, T.; Shinmen, M.; Nishitani, S.; Sato, M.; Ryu, I.: A Copper-Free Sonogashira Coupling Reaction in Ionic Liquids and Its Application to a Microflow System for Efficient Catalyst Recycling. *Organic Letters* **2002**, *4*, 1691-1694.

(253)   Mery, D.; Heuze, K.; Astruc, D.: A very efficient, copper-free palladium catalyst for the Sonogashira reaction with aryl halides. *Chemical Communications* **2003**, 1934-1935.

(254)   Böhm, Volker P. W.; Herrmann, Wolfgang A.: A Copper-Free Procedure for the Palladium-Catalyzed Sonogashira Reaction of Aryl Bromides with Terminal Alkynes at Room Temperature. *European Journal of Organic Chemistry* **2000**, *2000*, 3679-3681.

(255)   Faller, J. W.; Kultyshev, R. G.; Parr, J.: Alkynyl germatranes as alternative reagents for the preparation of biarylethynes. *Tetrahedron Lett.* **2003**, *44*, 451-453.

(256)   Huang, H.; Liu, H.; Jiang, H.; Chen, K.: Rapid and Efficient Pd-Catalyzed Sonogashira Coupling of Aryl Chlorides. *The Journal of Organic Chemistry* **2008**, *73*, 6037-6040.

(257)   Gelman, D.; Buchwald, S. L.: Efficient Palladium-Catalyzed Coupling of Aryl Chlorides and Tosylates with Terminal Alkynes: Use of a Copper Cocatalyst Inhibits the Reaction. *Angew. Chem. Int. Ed.*, **2003**, *42*, 5993–5996. *Angewandte Chemie* **2003**, *115*, 6175-6178.

(258)   Aufiero, M.; Proutiere, F.; Schoenebeck, F.: Redox Reactions in Palladium Catalysis: On the Accelerating and/or Inhibiting Effects of Copper and Silver Salt Additives in Cross-Coupling Chemistry Involving Electron-rich Phosphine Ligands. *Angew. Chem. Int. Ed.*, **2012**, 51, 7226–7230. *Angewandte Chemie* **2012**, *124*, 7338-7342.

(259)   Goel, R. G.; Beauchamp, A. L.: Preparation, characterization, and solution behavior of tri-tert-butylphosphine complexes of copper(I) halides and crystal structure of bromo(tri-tert-butylphosphine)copper(I) tetramer. *Inorganic Chemistry* **1983**, *22*, 395-400.

(260)   Amatore, C.; Broeker, G.; Jutand, A.; Khalil, F.: Identification of the Effective Palladium(0) Catalytic Species Generated in Situ from Mixtures of Pd(dba)₂ and Bidentate Phosphine Ligands. Determination of Their Rates and Mechanism in Oxidative Addition. *J. Am. Chem. Soc.* **1997**, *119*, 5176-5185.

(261)   Barrios-Landeros, F.; Carrow, B. P.; Hartwig, J. F.: Effect of Ligand Steric Properties and Halide Identity on the Mechanism for Oxidative Addition of Haloarenes to Trialkylphosphine Pd(0) Complexes. *J. Am. Chem. Soc.* **2009**, *131*, 8141-8154.

(262)   Tanabe, M.; Ishikawa, N.; Osakada, K.: Preparation and Structure of a New Dipalladium Complex with Bridging Diphenylgermyl Ligands. Diverse Reactivities of $Pd(PCy_3)_2$ and $Pt(PCy_3)_2$ toward Ph_2GeH_2. *Organometallics* **2005**, *25*, 796-798.

(263)   Huser, M.; Youinou, M.-T.; Osborn, J. A.: Chlorocarbon Activation: Catalytic Carbonylation of Dichloromethane and Chlorobenzene. *Angewandte Chemie International Edition in English* **1989**, *28*, 1386-1388. *Angew. Chem.*, **1989**, *101*, 1427–1430.

(264)   Majchrzak, M.; Kostera, S.; Kubicki, M.; Kownacki, I.: Synthesis of new styrylarenes via Suzuki-Miyaura coupling catalysed by highly active, well-defined palladium catalysts. *Dalton Transactions* **2013**, *42*, 15535-15539.

(265)   Bowmaker, G. A.; Boyd, S. E.; Hanna, J. V.; Hart, R. D.; Healy, P. C.; Skelton, B. W.; White, A. H.: Structural and spectroscopic studies on three-coordinate complexes of copper(i) halides with tricyclohexylphosphine. *Journal of the Chemical Society, Dalton Transactions* **2002**, 2722-2730.

(266)   Tolman, C. A.: Steric effects of phosphorus ligands in organometallic chemistry and homogeneous catalysis. *Chem. Rev.* **1977**, *77*, 313-348.

(267)   Maehara, S.; Iwazaki, H.: Process for Producing Tertiary Phosphine having Bulky Hydrocarbon Group Bonded. . In *Hokko Chemical Industry Co. Ltd.*; Patent, E., Ed., February 3, 2003; Vol. EP 1473297,.

(268)   Proutiere, F.; Lyngvi, E.; Aufiero, M.; Sanhueza, I. A.; Schoenebeck, F.: Combining the Reactivity Properties of PCy_3 and $PtBu_3$ into a Single Ligand, $P(iPr)(tBu)_2$. Reaction via Mono- or Bisphosphine Palladium(0) Centers and Palladium(I) Dimer Formation. *Organometallics* **2014**, *33*, 6879-6884.

(269)   Note: The assumption was done based on our experience with Pd-dimers **31** and **193** , usually the Pd(I) species are found down field compared to the analogue $Pd(0)L_2$ complex.

(270)   Denise, B.; Sneeden, R. P. A.: Hydrocondensation of CO_2. *Journal of Organometallic Chemistry* **1981**, *221*, 111-116.

(271)   Hunt, C. T.; Balch, A. L.: Scrambling of halide ligands between palladium(II) and between palladium(I) complexes of bis(diphenylphosphino)methane. Observation of unusual temperature-dependent phosphorus-31 NMR chemical shifts. *Inorganic Chemistry* **1982**, *21*, 1641-1644.

(272)   Lang, J.-P.; Tatsumi, K.: Low Temperature Solid-State Reactions of $(NH_4)_2[MS_4]$ (M = W, Mo) with $[Cu(CH_3CN)_4](PF_6)$ and CuBr in the Presence of Bis(diphenylphosphino)methane (dppm): Crystal Structures of $[MS_4Cu_4(dppm)_4](PF_6)_2$ (M = W, Mo), $[WS_4Cu_3(dppm)_3]X$ (X = PF_6, Br), $[Cu_3(dppm)_3Br_2]Br$, $[WS_4Cu_2(dppm)_3]$, and $[(n-Bu)_4N][WS_4Cu_3Br_2(dppm)_2]$. *Inorganic Chemistry* **1998**, *37*, 6308-6316.

(273)   Nicola, C. D.; Effendy; Fazaroh, F.; Pettinari, C.; Skelton, B. W.; Somers, N.; White, A. H.: Structural characterization of 1:1 adducts of silver(I) (pseudo-) halides (AgX, X = NCO, Cl, Br, I) with $Ph_2E(CH_2)EPh_2$ (E = P, As) (dp(p/a)m) and 4:3 adducts of copper(I) halide (CuX, X = Cl, Br, I), containing trinuclear cations, of the form $[X_2Ag_3(dppm)_3]X$ and $[X_2Cu_3(dppm)_3](CuX_2)$ and the novel neutral $[(OCN)_3Ag_3(dpam)_3]$ *Inorganica Chimica Acta* **2005**, *358*, 720-734.

(274)   Granberg, K. L.; Baeckvall, J. E.: Isomerization of (.pi.-allyl)palladium complexes via nucleophilic displacement by palladium(0). A common mechanism in palladium(0)-catalyzed allylic substitution. *J. Am. Chem. Soc.* **1992**, *114*, 6858-6863.

(275)   Mason, M. R.; Verkade, J. G.: Fluoride-induced reduction of palladium(II) and platinum(II) phosphine complexes. *Organometallics* **1992**, *11*, 2212-2220.

(276)   Kelly, P. F.; Slawin, A. M. Z.; Soriano-Rama, A.: Reaction of $(Me_3SiN_SN)_2S$ with palladium complexes; crystal structures of $[PPh_4]_2[Pd_2Br_4(S_3N_2)]$ and $[PPh_4][PdBr_2(S_2N_3)]$. *Journal of the Chemical Society, Dalton Transactions* **1996**, 53-59.

(277)   Nielsen, M. C.; Bonney, K. J.; Schoenebeck, F.: Computational Ligand Design for the Reductive Elimination of $ArCF_3$ from a Small Bite Angle PdII Complex: Remarkable Effect of a Perfluoroalkyl Phosphine. *Angewandte Chemie International Edition* **2014**, *53*, 5903-5906. *Angew. Chem.*, **2014**, *126*, 6013–6016

(278)   Mann, G.; Incarvito, C.; Rheingold, A. L.; Hartwig, J. F.: Palladium-Catalyzed C−O Coupling Involving Unactivated Aryl Halides. Sterically Induced Reductive Elimination To Form the C−O Bond in Diaryl Ethers. *J. Am. Chem. Soc.* **1999**, *121*, 3224-3225.

(279)   Shelby, Q.; Kataoka, N.; Mann, G.; Hartwig, J.: Unusual in Situ Ligand Modification to Generate a Catalyst for Room Temperature Aromatic C−O Bond Formation. *J. Am. Chem. Soc.* **2000**, *122*, 10718-10719.

(280)   Kataoka, N.; Shelby, Q.; Stambuli, J. P.; Hartwig, J. F.: Air Stable, Sterically Hindered Ferrocenyl Dialkylphosphines for Palladium-Catalyzed C−C, C−N, and C−O Bond-Forming Cross-Couplings. *The Journal of Organic Chemistry* **2002**, *67*, 5553-5566.

(281)   Wong, B.; Linghu, X.; Crawford, J. J.; Drobnick, J.; Lee, W.; Zhang, H.: A chemoselective Reformatsky–Negishi approach to α-haloaryl esters. *Tetrahedron* **2014**, *70*, 1508-1515.

(282)   Hama, T.; Liu, X.; Culkin, D. A.; Hartwig, J. F.: Palladium-Catalyzed α-Arylation of Esters and Amides under More Neutral Conditions. *J. Am. Chem. Soc.* **2003**, *125*, 11176-11177.

(283)   Stambuli, J. P.; Stauffer, S. R.; Shaughnessy, K. H.; Hartwig, J. F.: Screening of Homogeneous Catalysts by Fluorescence Resonance Energy Transfer. Identification of Catalysts for Room-Temperature Heck Reactions. *J. Am. Chem. Soc.* **2001**, *123*, 2677-2678.

(284)   Beare, N. A.; Hartwig, J. F.: Palladium-Catalyzed Arylation of Malonates and Cyanoesters Using Sterically Hindered Trialkyl- and Ferrocenyldialkylphosphine Ligands. *The Journal of Organic Chemistry* **2001**, *67*, 541-555.

(285)   Culkin, D. A.; Hartwig, J. F.: Palladium-Catalyzed α-Arylation of Carbonyl Compounds and Nitriles. *Accounts of Chemical Research* **2003**, *36*, 234-245.

(286)   Colacot, T. J.; Hosmane, N. S.: Organometallic Sandwich Compounds in Homogeneous Catalysis: An Overview. *Zeitschrift für anorganische und allgemeine Chemie* **2005**, *631*, 2659-2668.

(287)   Knowles, J. P.; Whiting, A.: The Heck-Mizoroki cross-coupling reaction: a mechanistic perspective. *Organic & Biomolecular Chemistry* **2007**, *5*, 31-44.

(288)   Tsuji, J.: Palladium Reagents and Catalysts,. Wiley: New York, 28 JAN 2005.

(289)   Leal, R. A.; Beaudry, D. R.; Alzghari, S. K.; Sarpong, R.: Synthesis of the Pentacyclic Skeleton of the Indole Alkaloid Arboflorine. *Organic Letters* **2012**, *14*, 5350-5353.

(290)   Bonaterra, M.; Rossi, R. A.; Martín, S. E.: Organoheteroatom Stannanes in Palladium-Catalyzed Cross-Coupling Reactions with 1-Naphthyl Triflate. *Organometallics* **2009**, *28*, 933-936.

(291)   Jutand, A.: Contribution of Electrochemistry to Organometallic Catalysis. *Chem. Rev.* **2008**, *108*, 2300-2347.

(292)   Ahlquist, M.; Fristrup, P.; Tanner, D.; Norrby, P.-O.: Theoretical Evidence for Low-Ligated Palladium(0): [Pd−L] as the Active Species in Oxidative Addition Reactions. *Organometallics* **2006**, *25*, 2066-2073.

(293)   Lam, K. C.; Marder, T. B.; Lin, Z.: DFT Studies on the Effect of the Nature of the Aryl Halide $Y−C_6H_4−X$ on the Mechanism of Its Oxidative Addition to $Pd0L$ versus $Pd0L_2$. *Organometallics* **2006**, *26*, 758-760.

(294)   Grushin, V. V.: Thermal Stability, Decomposition Paths, and Ph/Ph Exchange Reactions of $[(Ph_3P)_2Pd(Ph)X]$ (X = I, Br, Cl, F, and HF_2). *Organometallics* **2000**, *19*, 1888-1900.

(295)   Malatesia, L.; Angoletta, M.: 231. Palladium(0) compounds. Part II. Compounds with triarylphosphines, triaryl phosphites, and triarylarsines. *Journal of the Chemical Society (Resumed)* **1957**, 1186-1188.

(296)   Kuran, W.; Musco, A.: Synthesis and characterization of tertiary phosphine Pd(0) complexes. *Inorganica Chimica Acta* **1975**, *12*, 187-193.

(297)   Ioele, M.; Ortaggi, G.; Scarsella, M.; Sleiter, G.: A rapid and convenient synthesis of tetrakis(triphenylphosphine)palladium(O) and -platinum(O) complexes by phase-transfer catalysis. *Polyhedron* **1991**, *10*, 2475-2476.

(298)   Mann, B. E.; Musco, A.: Phosphorus-31 nuclear magnetic resonance spectroscopic characterisation of tertiary phosphine palladium(0) complexes: evidence for 14-electron complexes in solution. *Journal of the Chemical Society, Dalton Transactions* **1975**, 1673-1677.

(299)   Jutand, A.; Mosleh, A.: Rate and Mechanism of Oxidative Addition of Aryl Triflates to Zerovalent Palladium Complexes. Evidence for the Formation of Cationic (.sigma.-Aryl)palladium Complexes. *Organometallics* **1995**, *14*, 1810-1817.

(300)   Amatore, C.; Godin, B.; Jutand, A.; Ferber, B.; Top, S.; Jaouen, G.: Comparative Oxidative Addition of Transition-Metal Iodocyclopentadienyl Complexes (η_5-C_5H_4-I)MLn (M = Re, Mn, Fe) with a Palladium(0) Complex: Relevance to the Efficiency of Catalytic Reactions. *Organometallics* **2007**, *26*, 3887-3890.

(301)   Fitton, P.; Johnson, M. P.; McKeon, J. E.: Oxidative additions to palladium(0). *Chemical Communications (London)* **1968**, 6-7.

(302)   Fitton,   P.;   Rick,   E.   A.:   The   addition   of   aryl   halides   to tetrakis(triphenylphosphine)palladium(0). *Journal of Organometallic Chemistry* **1971**, *28*, 287-291.

(303)   Fauvarque, J.-F.; Pflüger, F.; Troupel, M.: Kinetics of oxidative addition of zerovalent palladium to aromatic iodides. *Journal of Organometallic Chemistry* **1981**, *208*, 419-427.

(304)   Amatore, C.; Azzabi, M.; Jutand, A.: Role and effects of halide ions on the rates and mechanisms of oxidative addition of iodobenzene to low-ligated zerovalent palladium complexes $Pd0(PPh_3)_2$. *J. Am. Chem. Soc.* **1991**, *113*, 8375-8384.

(305)   Amatore, C.; Jutand, A.; Mottier, L.: Formation of Anionic $PdX_3(PPh_3)−$ Complexes by Reaction of Halide Ions with $PdX_2(PPh_3)_2$. *European Journal of Inorganic Chemistry* **1999**, *1999*, 1081-1085.

(306)   Kagirov, R. M.; Voloshin, A. V.; Rizvanov, I. K.; Sinyashin, O. G.; Yakhvarov, D. G.: Activation and transformation of white phosphorus by palladium(ii) complexes. *Russ Chem Bull* **2010**, *59*, 1116-1118.

(307)   Bowmaker, G. A.; Skelton, B. W.; White, A. H.; Healy, P. C.: Synthesis and characterization of the novel copper(I) anion [Cu(PPh$_3$)Br$_2$]. *Journal of the Chemical Society, Dalton Transactions* **1988**, 2825-2830.

(308)   Kaye, S.; Fox, J. M.; Hicks, F. A.; Buchwald, S. L.: The Use of Catalytic Amounts of CuCl and Other Improvements in the Benzyne Route to Biphenyl-Based Phosphine Ligands. *Advanced Synthesis & Catalysis* **2001**, *343*, 789-794.

(309)   Martin, R.; Buchwald, S. L.: Palladium-Catalyzed Suzuki−Miyaura Cross-Coupling Reactions Employing Dialkylbiaryl Phosphine Ligands. *Accounts of Chemical Research* **2008**, *41*, 1461-1473.

(310)   Denmark, S. E.; Kallemeyn, J. M.: Stereospecific Palladium-Catalyzed Cross-Coupling of (E)- and (Z)-Alkenylsilanolates with Aryl Chlorides. *J. Am. Chem. Soc.* **2006**, *128*, 15958-15959.

(311)   Martín, R.; Buchwald, S. L.: A General Method for the Direct α-Arylation of Aldehydes with Aryl Bromides and Chlorides. *Angewandte Chemie International Edition* **2007**, *46*, 7236-7239. *Angew. Chem.*, **2007**, *119*, 7374–7377.

(312)   Ikawa, T.; Barder, T. E.; Biscoe, M. R.; Buchwald, S. L.: Pd-Catalyzed Amidations of Aryl Chlorides Using Monodentate Biaryl Phosphine Ligands: A Kinetic, Computational, and Synthetic Investigation. *J. Am. Chem. Soc.* **2007**, *129*, 13001-13007.

(313)   Anderson, K. W.; Ikawa, T.; Tundel, R. E.; Buchwald, S. L.: The Selective Reaction of Aryl Halides with KOH: Synthesis of Phenols, Aromatic Ethers, and Benzofurans. *J. Am. Chem. Soc.* **2006**, *128*, 10694-10695.

(314)   Teverovskiy, G.; Surry, D. S.; Buchwald, S. L.: Pd-Catalyzed Synthesis of Ar-SCF3 Compounds under Mild Conditions. *Angewandte Chemie International Edition* **2011**, *50*, 7312-7314. *Angew. Chem.*, **2011**, *123*, 7450–7452.

(315)   Note: The choice of this ligand was done only based on the availability of this ligand in our laboratory.

(316)   Shen, Q.; Ogata, T.; Hartwig, J. F.: Highly Reactive, General and Long-Lived Catalysts for Palladium-Catalyzed Amination of Heteroaryl and Aryl Chlorides, Bromides, and Iodides: Scope and Structure–Activity Relationships. *J. Am. Chem. Soc.* **2008**, *130*, 6586-6596.

(317)   Fors, B. P.; Davis, N. R.; Buchwald, S. L.: An Efficient Process for Pd-Catalyzed C−N Cross-Coupling Reactions of Aryl Iodides: Insight Into Controlling Factors. *J. Am. Chem. Soc.* **2009**, *131*, 5766-5768.

(318)   Söhnel, O.; Novotny, P.: *Densities of aqueous solutions of inorganic substances.*; Elsevier: Amsterdam, 1985.

(319)   Zalesskiy, S. S.; Ananikov, V. P.: Pd$_2$(dba)$_3$ as a Precursor of Soluble Metal Complexes and Nanoparticles: Determination of Palladium Active Species for Catalysis and Synthesis. *Organometallics* **2012**, *31*, 2302-2309.

(320)   Dillinger, S.; Bertus, P.; Pale, P.: First Evidence for the Use of Organosilver Compounds in Pd-Catalyzed Coupling Reactions; A Mechanistic Rationale for the Pd/Ag-Catalyzed Enyne Synthesis? *Organic Letters* **2001**, *3*, 1661-1664.

(321)   Weibel, J.-M.; Blanc, A.; Pale, P.: Coupling Reactions Promoted by Silver. In *Silver in Organic Chemistry*; John Wiley & Sons, Inc., 2010; pp 285-328.

(322)   Weibel, J.-M.; Blanc, A.; Pale, P.: Ag-Mediated Reactions: Coupling and Heterocyclization Reactions. *Chem. Rev.* **2008**, *108*, 3149-3173.

(323)   delPozo, J.; Casares, J. A.; Espinet, P.: The decisive role of ligand metathesis in Au/Pd bimetallic catalysis. *Chemical Communications* **2013**, *49*, 7246-7248.

(324)   Schneider, D.; Schuster, O.; Schmidbaur, H.: Bromination of (phosphine)gold(i) bromide complexes: stoichiometry and structure of products. *Dalton Transactions* **2005**, 1940-1947.

(325)   Haynes, W. M.: *Handbook of Chemistry and Physics*; 95th, 2014-2015 ed.; CRCnetBase, copyright Taylor & Francis Group, 2014-2015.

(326)   Buchwald, S. L.; Bolm, C.: On the Role of Metal Contaminants in Catalyses with FeCl$_3$. *Angewandte Chemie International Edition* **2009**, *48*, 5586-5587. *Angew. Chem.*, **2009**, *121*, 5694–5695

(327)   Thome, I.; Nijs, A.; Bolm, C.: Trace metal impurities in catalysis. *Chemical Society Reviews* **2012**, *41*, 979-987.

(328)   Alcazar-Roman, L. M.; Hartwig, J. F.: Mechanism of Aryl Chloride Amination: Base-Induced Oxidative Addition. *J. Am. Chem. Soc.* **2001**, *123*, 12905-12906.

(329)   Das, R. K.; Saha, B.; Rahaman, S. M. W.; Bera, J. K.: Bimetallic Catalysis Involving Dipalladium(I) and Diruthenium(I) Complexes. *Chemistry – A European Journal* **2010**, *16*, 14459-14468.

(330)   Proutiere, F.; Aufiero, M.; Schoenebeck, F.: Reactivity and Stability of Dinuclear Pd(I) Complexes: Studies on the Active Catalytic Species, Insights into Precatalyst Activation and Deactivation, and Application in Highly Selective Cross-Coupling Reactions. *J. Am. Chem. Soc.* **2011**, *134*, 606-612.

(331)   Christmann, U.; Vilar, R.: Monoligated Palladium Species as Catalysts in Cross-Coupling Reactions. *Angewandte Chemie International Edition* **2005**, *44*, 366-374. *Angew. Chem.*, **2005**, *117*, 370–378

(332)   Lee, C. L.; James, B. R.; Nelson, D. A.; Hallen, R. T.: Kinetics and thermodynamics of the reversible reaction between carbon monoxide and palladium(I) dimers containing bis(diphenylphosphino)methane. *Organometallics* **1984**, *3*, 1360-1364.

(333)   Hooper, M. W.; Utsunomiya, M.; Hartwig, J. F.: Scope and Mechanism of Palladium-Catalyzed Amination of Five-Membered Heterocyclic Halides. *The Journal of Organic Chemistry* **2003**, *68*, 2861-2873.

(334)   Jimeno, C.; Christmann, U.; Escudero-Adán, E. C.; Vilar, R.; Pericàs , M. A.: Studies on the Amination of Aryl Chlorides with a Monoligated Palladium Catalyst: Kinetic Evidence for a Cooperative Mechanism. *Chemistry – A European Journal* **2012**, *18*, 16510-16516.

(335)   Note: The dark green solution containing the dimer turned purple immedially after the addition of the KO*t*Bu. After few minutes the color change again from purple to brown, indicating that the Pd-bromo dimer **31** was not longer present in solution.

(336)   Note: In this case we had to use a different internal standard (triphenylphosphine oxide) because the trimethoxyphosphie oxide reacted with the two bases to give mixed alkoxydes phosphine oxides.

(337)   Kempf, B.; Mayr, H.: Rates and Equilibria of the Reactions of Tertiary Phosphanes and Phosphites with Benzhydrylium Ions. *Chemistry – A European Journal* **2005**, *11*, 917-927.

(338)   Phan, T. B.; Mayr, H.: Comparison of the nucleophilicities of alcohols and alkoxides. *Canadian Journal of Chemistry* **2005**, *83*, 1554-1560.

(339)   Richter, D.; Mayr, H.: Hydride-Donor Abilities of 1,4-Dihydropyridines: A Comparison with π Nucleophiles and Borohydride Anions. *Angewandte Chemie International Edition* **2009**, *48*, 1958-1961. *Angew. Chem.*, **2009**, 121, 1992–1995

(340)   Kempf, B.; Hampel, N.; Ofial, A. R.; Mayr, H.: Structure–Nucleophilicity Relationships for Enamines. *Chemistry – A European Journal* **2003**, *9*, 2209-2218.

(341)   Gilheany, D. G.: Ylides, phosphoniumNo d Orbitals but Walsh Diagrams and Maybe Banana Bonds: Chemical Bonding in Phosphines, Phosphine Oxides, and Phosphonium Ylides. *Chem. Rev.* **1994**, *94*, 1339-1374.

(342)   Roy, A. H.; Hartwig, J. F.: Directly Observed Reductive Elimination of Aryl Halides from Monomeric Arylpalladium(II) Halide Complexes. *J. Am. Chem. Soc.* **2003**, *125*, 13944-13945.

(343)   Moreno-Mañas, M.; Pérez, M.; Pleixats, R.: Palladium-Catalyzed Suzuki-Type Self-Coupling of Arylboronic Acids. A Mechanistic Study. *The Journal of Organic Chemistry* **1996**, *61*, 2346-2351.

(344)   Aramendía, M. A.; Lafont, F.; Moreno-Mañas, M.; Pleixats, R.; Roglans, A.: Electrospray Ionization Mass Spectrometry Detection of Intermediates in the Palladium-Catalyzed Oxidative Self-Coupling of Areneboronic Acids. *The Journal of Organic Chemistry* **1999**, *64*, 3592-3594.

(345)   Aufiero, M.; Sperger, T.; Tsang, A.; Schoenebeck, F.; Highly Efficient C-SeCF$_3$ Coupling of Aryl Iodides Enabled by an Air-Stable Dinuclear Pd(I) Catalyst, *Angewandte Chemie Inernational Edition* DOI: 10.1002/anie.201503388.

(346)   Holm, R. H.; Kennepohl, P.; Solomon, E. I.: Structural and Functional Aspects of Metal Sites in Biology, *Chem. Rev.* **1996**, *96*, 2239.

(347)   Bonney, K. J.; Proutiere, F.; Schoenebeck, F.: Dinuclear Pd(I) complexes-solely precatalysts? Demonstration of direct reactivity of a Pd(I) dimer with an aryl iodide. *Chemical Science* **2013**, *4*, 4434-4439.

(348)   Kalvet, I.; Bonney, K. J.; Schoenebeck, F.: Kinetic and Computational Studies on Pd(I) Dimer-Mediated Halogen Exchange of Aryl Iodides. *The Journal of Organic Chemistry* **2014,** 12041-12046.

(349)   Yin, G; Kalvet, I.; Schoenebeck, F.: Trifluoromethylthiolation of Aryl Iodides and Bromides Enabled by a Bench-Stable and Easy-To-Recover Dinuclear Pd(I) Catalyst. *Angewandte Chemie International Edition* **2015**, doi: 10.1002/anie.201501617. *Angew. Chem.*, **2015**, doi: 10.1002/ange.201501617.

(350)   Leroux, F.; Jeschke, P.; Schlosser, M.: α-Fluorinated Ethers, Thioethers, and Amines: Anomerically Biased Species. *Chem. Rev.* **2005**, *105*, 827-856.

(351)   Böhm, H.-J.; Banner, D.; Bendels, S.; Kansy, M.; Kuhn, B.; Müller, K.; Obst-Sander, U.; Stahl, M.: Fluorine in Medicinal Chemistry. *Chembiochem* **2004**, *5*, 637-643.

(352)   Chen, Q.; Xu, J.; Zhang, W.: The Reaction Of A,A,A-Trifluoromethoxybenzene With AlCl$_3$: A High Yield Preparation Of A,A,A-Trichloromethoxybenzene. *Synthetic Communications* **2002**, *32*, 799-801.

(353)   Feiring, A. E.: Chemistry in hydrogen fluoride. 7. A novel synthesis of aryl trifluoromethyl ethers. *The Journal of Organic Chemistry* **1979**, *44*, 2907-2910.

(354)   Manteau, B.; Pazenok, S.; Vors, J.-P.; Leroux, F. R.: New trends in the chemistry of α-fluorinated ethers, thioethers, amines and phosphines. *Journal of Fluorine Chemistry* **2010**, *131*, 140-158.

(355)   Kieltsch, I.; Eisenberger, P.; Togni, A.: Mild Electrophilic Trifluoromethylation of Carbon- and Sulfur-Centered Nucleophiles by a Hypervalent Iodine(III)–CF$_3$ Reagent. *Angew. Chem. Int. Ed*., **2007**, *46,* 754–757. *Angewandte Chemie* **2007**, *119*, 768-771.

(356)   Pooput, C.; Medebielle, M.; Dolbier, W. R.: A New and Efficient Method for the Synthesis of Trifluoromethylthio- and Selenoethers. *Organic Letters* **2003**, *6*, 301-303.

(357)   Tyrra, W.; Naumann, D.; Hoge, B.; Yagupolskii, Y. L.: Stable trifluoromethylselenates(0), [A]SeCF3—synthesis, characterizations and properties. *Journal of Fluorine Chemistry* **2003**, *123*, 183-187.

(358)   Hansch, C.; Leo, A.; Unger, S. H.; Kim, K. H.; Nikaitani, D.; Lien, E. J.: Aromatic substituent constants for structure-activity correlations. *J. Med. Chem.* **1973**, *16*, 1207-1216.

(359)   Hansch, C.; Leo, A.; Taft, R. W.: A survey of Hammett substituent constants and resonance and field parameters. *Chem. Rev.* **1991**, *91*, 165-195.

(360)   Ruppert, I.: Nucleophilic trifluoromethylation with the reagent combination (Et$_2$N)$_3$P/CF$_3$Br. *Journal of Fluorine Chemistry* **1985**, *29*, 98.

(361)   Kondratenko, N. V.; Kolomeytsev, A. A.; Popov, V.I.; Yagupolskii, L. M. : Synthesis and Reactions of Trifluoromethylthio(seleno)- and Pentafluorophenylthio(seleno)-copper. *Synthesis* **1985**, *6/7*, 667.

(362)   Teruo,   U.;   Sumi,   I.:   Power-variable   trifluoromethylating   agents, (trifluoromethyl)dibenzothio- and -selenophenium salt system. *Tetrahedron Lett.* **1990**, *31*, 3579-3582.

(363)   Billard, T.; Langlois, B. R.: A new simple access to trifluoromethyl thioethers or selenoethers from trifluoromethyl trimethylsilane and disulfides or diselenides. *Tetrahedron Lett.* **1996**, *37*, 6865-6868.

(364)   Billard, T.; Large, S.; Langlois, B. R.: Preparation of trifluoromethyl sulfides or selenides from trifluoromethyl trimethylsilane and thiocyanates or selenocyanates. *Tetrahedron Lett.* **1997**, *38*, 65-68

(365)   Chen, C.; Ouyang, L.; Lin, Q.; Liu, Y.; Hou, C.; Yuan, Y.; Weng, Z.: Synthesis of CuI Trifluoromethylselenates for Trifluoromethylselenolation of Aryl and Alkyl Halides. *Chemistry – A European Journal* **2014**, *20*, 657-661.

(366)   Chen, C.; Hou, C.; Wang, Y.; Hor, T. S. A.; Weng, Z.: Copper-Catalyzed Trifluoromethylselenolation of Aryl and Alkyl Halides: The Silver Effect in Transmetalation. *Organic Letters* **2013**, *16*, 524-527.

(367)   Sonoda, N.; Ogawa, A.: Benzeneselenol. In *Encyclopedia of Reagents for Organic Synthesis*; John Wiley & Sons, Ltd, 2001.

(368)   Kirij, N. V.; Tyrra, W.; Pantenburg, I.; Naumann, D.; Scherer, H.; Naumann, D.; Yagupolskii, Y. L.: Trifluoromethylselenato(0) and trifluoromethyltellurato(0) complexes of platinum(II). *Journal of Organometallic Chemistry* **2006**, *691*, 2679-2685.

(369)   Nishiyama, Y.; Tokunaga, K.; Sonoda, N.: New Synthetic Method of Diorganyl Selenides: Palladium-Catalyzed Reaction of PhSeSnBu$_3$ with Aryl and Alkyl Halides. *Organic Letters* **1999**, *1*, 1725-1727.

(370)   Dai, C.; Fu, G. C.: The First General Method for Palladium-Catalyzed Negishi Cross-Coupling of Aryl and Vinyl Chlorides: Use of Commercially Available Pd(P(t-Bu)3)2 as a Catalyst. *J. Am. Chem. Soc.* **2001**, *123*, 2719-2724.

(371)   Amatore, M.; Gosmini, C.: Efficient Cobalt-Catalyzed Formation of Unsymmetrical Biaryl Compounds and Its Application in the Synthesis of a Sartan Intermediate. *Angewandte Chemie International Edition* **2008**, *47*, 2089-2092. *Angew. Chem.,* **2008**, *120,* 2119–2122

(372)   Arvela, R. K.; Leadbeater, N. E.; Sangi, M. S.; Williams, V. A.; Granados, P.; Singer, R. D.: A Reassessment of the Transition-Metal Free Suzuki-Type Coupling Methodology. *The Journal of Organic Chemistry* **2004**, *70*, 161-168.

(373)   Li, J.-H.; Liu, W.-J.; Xie, Y.-X.: Recyclable and Reusable Pd(OAc)$_2$/DABCO/PEG-400 System for Suzuki−Miyaura Cross-Coupling Reaction. *The Journal of Organic Chemistry* **2005**, *70*, 5409-5412.

(374)   Bonin, H.; Leuma-Yona, R.; Marchiori, B.; Demonchaux, P.; Gras, E.: Highly practical boronic acid surrogates for the Suzuki–Miyaura cross-coupling. *Tetrahedron Lett.* **2011**, *52*, 1132-1135.

(375)   So, C. M.; Yeung, C. C.; Lau, C. P.; Kwong, F. Y.: A New Family of Tunable Indolylphosphine Ligands by One-Pot Assembly and Their Applications in Suzuki−Miyaura Coupling of Aryl Chlorides. *The Journal of Organic Chemistry* **2008**, *73*, 7803-7806.

(376)   Ebels, J.; Spirk, S.; Pietschnig, R: A Facile Lab Scale Synthesis of Red Selenium; *10th International Electronic Conference on Synthetic Organic Chemistry* (1-30 November) **2006**

(377)	Chen, C.; Hou, C.; Wang, Y.; Hor, A. T. S.; Wenig, Z.: Copper-Catalyzed Trifluoromethylselenolation of Aryl and Alkyl Halides: The Silver Effect in Transmetalation. *Org. Lett* 2014, *16*, 524.

(378)	Umemoto, T.; Ishihara S.: Power-variable electrophilic trifluoromethylating agents. S-, Se-, and Te-(trifluoromethyl)dibenzothio-, -seleno-, and -tellurophenium salt system. *J. Am. Chem. Soc* 1993, *115*, 2156.

(379)	Gaussian 09; Revision A.01; Frisch, M. J.; Trucks, G. W.; Schlegel, H. B.; Scuseria, G. E.; Robb, M. A.; Cheeseman, J. R.; Scalmani, G.; Barone, V.; Mennucci, B.; Petersson, G. A.; Nakatsuji, H.; Caricato, M.; Li, X. H.; A.;, H. P.; Izmaylov, F.; Bloino, J.; Zheng, G.; Sonnenberg, J. L.; Hada, M.; Ehara, M.; Toyota, K.; Fukuda, R.; Hasegawa, J.; Ishida, M.; Nakajima, T.; Honda, Y.; Kitao, O.; Nakai, H.; Vreven, T.; Montgomery Jr., J. A.; Peralta, J. E.; Ogliaro, F.; Bearpark, M.; Heyd, J. J.; Brothers, E.; Kudin, K. N.; Staroverov, V. N.; Kobayashi, R.; Normand, J.; Raghavachari, K.; Rendell, A.; Burant, J. C.; Iyengar, S. S.; Tomasi, J.; Cossi, M.; Rega, N.; Millam, J. M.; Klene, M.; Knox, J. E.; Cross, J. B.; Bakken, V.; Adamo, C.; Jaramillo, J.; Gomperts, R.; Stratmann, R. E.; Yazyev, O.; Austin, A. J.; Cammi, R.; Pomelli, C.; Ochterski, J. W.; Martin, R. L.; Morokuma, K.; Zakrzewski, V. G.; Voth, G. A.; Salvador, P.; Dannenberg, J. J.; Dapprich, S.; Daniels, A. D.; Farkas, O.; Foresman, J. B.; Ortiz, J. V.; Cioslowski, J.; Fox, D. J. G., Inc., : Wallingford CT. 2009.

(380)	Kohn, W.; Becke, A. D.; Parr, R. G.: Density Functional Theory of Electronic Structure. *The Journal of Physical Chemistry* **1996**, *100*, 12974-12980.

(381)	Cramer, C. J.: *Essentials of Computational Chemistry, Theories and Models*; Second edition ed.; John Wiley & Sons Ltd: West Sussex PO19 8SQ, England, 2004.

(382)	CYLview, b.; Legault, C. Y.: University of Sherbrooke. **2009**.

Curriculum Vitae

2011-2015	Laboratorium für Organische Chemie- ETHZ (Zurich, Switzerland) and Laboratory of Organic chemistry RWTH Aachen University (Aachen, Germany), PhD reasearch with Prof. Dr.Franziska Schoenebeck.
2010	University "La Sapienza" M. Sc. thesis with Prof. Dr. Luigi Mandolini. Rome, Italy.
2008-2010	University "La Sapienza" M. Sc. studies in Chemistry. Rome, Italy.
2008	University "La Sapienza" B. Sc. thesis with Prof. Dr. Luigi Mandolini. Rome, Italy.
2005-2008	University "La Sapienza" B. Sc. studies Organic Chemistry. Rome, Italy
2000-2005	Liceo Linguistico, P. E. Imbriani, high school. Avellino, Italy.
1986:	Born on May 5th in Avellino, Italy- Italian Nationality.

Zurich, 2015   Marialuisa Aufiero